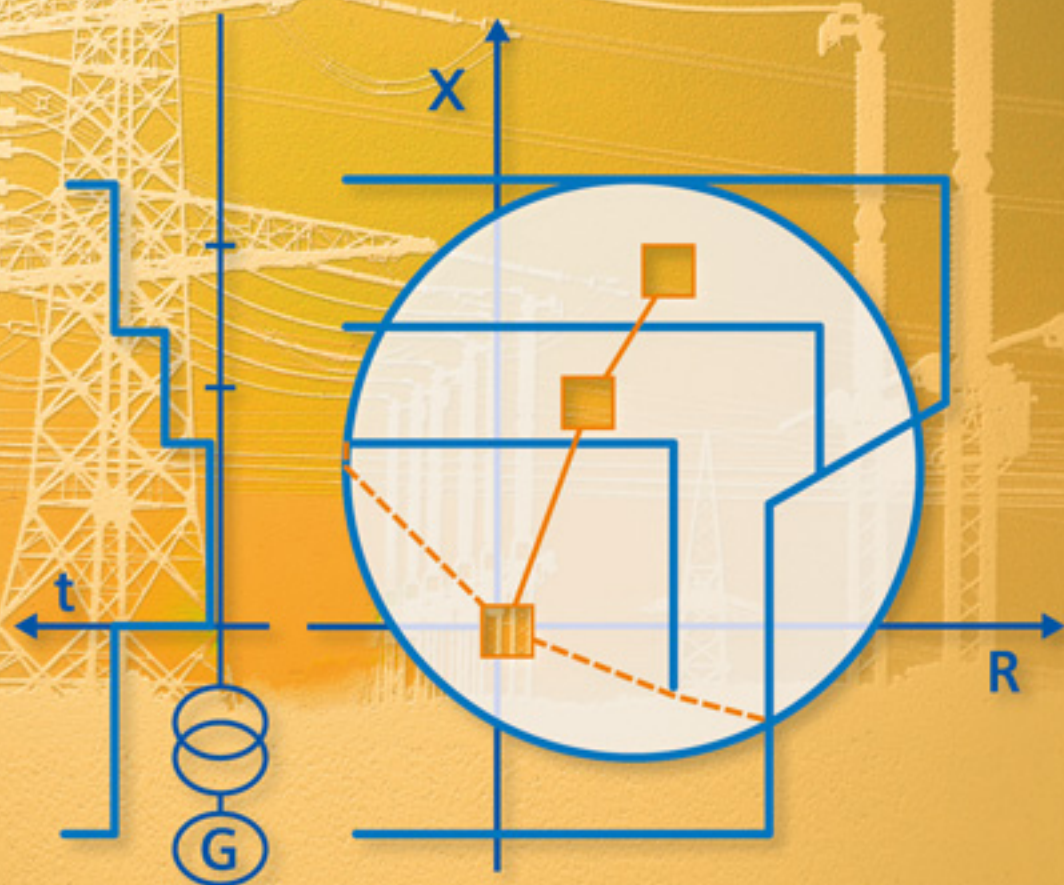


Gerhard Ziegler

# Numerical Distance Protection

Principles and Applications

**SIEMENS**



Fourth Edition

Ziegler Numerical Distance Protection



Gerhard Ziegler (Grad. Eng.), was born in 1939, and has been working in the area of power system protection with Siemens AG in Erlangen/Nuremberg, Germany for a period of 35 years.

He was active in the areas of product support, application and project planning, marketing and sales, on a world-wide basis. He retired in 2002 but continues to work as consultant. G. Ziegler has published numerous national and international contributions in the area of power system protection. He served in international organisations for many years.

From 1993 to 2001 he was the German delegate to the IEC TC95 (measuring relays and protection equipment). He is past chairman of the Study Committee 34 (protection and local control) and Honorary Member of CIGRE.

# Numerical Distance Protection

Principles and Applications

by Gerhard Ziegler

4th updated and enlarged edition, 2011

Publicis Publishing



[www.publicis.de/books](http://www.publicis.de/books)

Complete ebook edition of Gerhard Ziegler, “Numerical Distance Protection”,  
ISBN 978-3-89578-381-4 (Print edition)  
4th edition, 2011

ISBN 978-3-89678-667-9

Publisher: Publicis Publishing

© Publicis Erlangen, Zweigniederlassung der PWW GmbH

---

# Preface

to the First Edition

Distance protection provides short-circuit protection for universal application. It provides the basis for network protection in transmission systems and meshed distribution systems. While classic distance protection, based on electro-mechanical or static technology, are still in wide use, the state of the art today are multi-functional micro-processor devices. They communicate with centralised control systems and may be operated with personal computers locally or from remote. The basic operating principles of distance protection also apply to the new technology. Numerical signal processing, and intelligent evaluation algorithms facilitate measuring techniques with increased accuracy and protection functions with improved selectivity. The large degree of functional integration along with continuous self-monitoring results in the space-saving protection concepts, as well as economical maintenance strategies.

The book at hand initially covers the general principles of distance protection, thereby addressing the particular influence of numerical technology. The emphasis is placed on the practical application of numerical distance relays in power systems. The behaviour of the distance protection during varying fault and system conditions is extensively analysed. Procedures and equations for practical application are derived.

As the device design is manufacturer-specific, and subject to relatively rapid change, particular device configurations are only addressed in-so-far as this is necessary for general understanding. The Siemens device range 7SA is used as an illustrative example. The general statements however also apply to other manufacturers. Furthermore, reference is made to the documentation provided by the manufacturers.

Finally, the current practice in relation to distance protection application in utility and industrial systems is described. The choice of topics and examples is based on the authors extensive experience in the area of power system protection. The queries and problems experienced by users have therefore directly or indirectly contributed to this book.

This books is aimed at students and young engineers who wish to familiarise themselves with the subject of distance protection and its application as well as the experienced user, entering the area of numerical distance protection. Furthermore it serves as a reference guide for solving particular application problems.

Nuremberg, July 1999

Gerhard Ziegler

---

# Preface

to the fourth edition

The fourth edition of this book appears nearly 12 years after the first edition and about 3 years after the third edition.

Numerical relays have in the meantime developed into smart IEDs (Intelligent Electronic Devices) with many integrated functions. Local and remote communication via dedicated optic fibers and data networks is common state of the art. In total, the protection performance has improved considerably.

Digital protection technology has reached a widely mature state. The emphasis of development has since some years shifted more to communication and substation automation.

The function principles of numerical relays and their application in practice are well established and have not significantly changed in the recent years.

The contents of the third edition of this book could therefore be left without major changes. New sections about distance protection of cables and auto-transformers have been added.

The author hopes that the book will further be world-wide accepted with such great interest by beginners and experts in the field of protective relaying.

Nuremberg, December 2010

Gerhard Ziegler

---

# Contents

<b>1 Introduction</b>	11
<b>2 Definitions</b>	13
<b>3 Mode of Operation</b>	20
3.1 Fundamentals of distance protection	20
3.1.1 Concept	20
3.1.2 Relay impedance (secondary impedance)	21
3.1.3 Impedance diagram	22
3.1.4 Distance measurement	23
3.1.5 Directional fault discrimination	27
3.1.6 Starting (fault detection)	30
3.1.7 Distance zones (steps)	41
3.1.8 Zone- and timer-control	45
3.1.9 Switched and non-switched distance protection	47
3.1.10 Distance protection with signalling channels	50
3.1.11 Power swing blocking, power swing tripping (out of step protection)	62
3.1.12 Distance protection with automatic reclosure	67
3.1.13 Distance to fault locator	74
3.1.14 Grading chart	79
3.2 Numerical distance measurement	89
3.2.1 Definition of the fault loop	89
3.2.2 Determination of the loop impedance	94
3.2.3 Numerical impedance computation	98
3.3 Numerical direction determination (polarisation)	108
3.3.1 Direction determination with fault loop voltage (self polarisation)	108
3.3.2 Direction determination with healthy phase voltages (cross-polarisation)	110
3.3.3 Directional characteristic in the impedance plane	112
3.3.4 Selection of the cross polarisation voltage	114
3.3.5 Influence of load transfer	115
3.3.6 Implementation of voltage-memory(-ies)	118
3.3.7 Adaptive directional determination	119
3.4 Circular characteristics with numerical technology	120
3.4.1 MHO-circle	120
3.4.2 Polarised MHO-characteristic	122
3.4.3 Load influence on polarised MHO-circles	126
3.4.4 MHO-circle with voltage memory	129

3.5 Distance measurement, Influencing quantities	129
3.5.1 Fault resistance	129
3.5.2 Intermediate infeeds	150
3.5.3 Parallel lines	154
3.5.4 Distance protection for transformers	167
3.5.5 Non-symmetry of the line	181
3.5.6 Distance protection of HV cables	193
3.5.7 Series-compensation	200
<b>4 Device design</b>	<b>209</b>
4.1 Intelligent electronic devices (IEDs)	209
4.2 Mechanical design	211
4.3 Relay Communications	212
4.4 Integrated functions	214
4.5 Relay terminal connections	220
4.6 Relay operation	223
<b>5 Application</b>	<b>225</b>
5.1 General aspects	225
5.1.1 Application criteria	225
5.1.2 Shortest line length	226
5.1.3 Tripping time	227
5.1.4 Teleprotection, choice of technique	230
5.1.5 Instrument transformer requirements	232
5.2 Distance protection in the distribution system	262
5.2.1 General	262
5.2.2 Distance protection in isolated or compensated systems	270
5.2.3 Distance protection in distribution networks with low impedance star-point earthing	277
5.2.4 Distance protection in industrial networks	280
5.3 Distance protection in transmission networks	282
5.3.1 General aspects	282
5.3.2 Protection concepts	287
5.3.2.1 High-voltage overhead lines	287
5.3.2.2 EHV-line	289
5.3.2.3 1 1/2 circuit-breaker substations	292
5.3.2.4 Ring busbar	293
5.3.2.5 Double circuit line	293
5.3.2.6 Three-terminal line	294
5.3.2.7 Series-compensated lines	296
<b>6 Protection settings</b>	<b>299</b>
6.1 General aspects	300
6.2 Fault detection (3rd Zone)	300
6.2.1 Fault detection methods and setting philosophies	301
6.2.2 Security of the fault detection	302

6.2.3 Relay (Line) loadability .....	303
6.2.4 Phase-selectivity .....	304
6.2.5 Setting of the $U-I-\phi$ fault detection .....	306
6.2.6 Setting of the impedance fault detection .....	307
6.3 Setting of the distance zones .....	313
6.3.1 Reach (X-setting) and grading time .....	313
6.3.2 Arc compensation (R-setting) .....	318
6.3.3 Specifics for the zone settings in cable networks .....	322
6.3.4 Adjusting the zone reach in case of large R/X-setting .....	325
6.3.5 Grading of distance zones with different characteristics .....	326
6.3.6 Setting of the power swing blocking .....	328
<b>7 Calculation examples .....</b>	<b>333</b>
7.1 Double circuit lines in earthed systems .....	333
7.2 Three terminal line (teed feeders) .....	346
<b>8 Commissioning .....</b>	<b>356</b>
8.1 Testing of the protection system .....	356
8.2 Test with load .....	358
<b>9 Maintenance .....</b>	<b>361</b>
9.1 Self monitoring .....	361
9.2 Maintenance strategy .....	362
<b>10 Bibliography .....</b>	<b>364</b>
10.1 Technical papers .....	364
10.2 Books .....	371
<b>11 Appendix .....</b>	<b>372</b>
A.1 Distance measurement algorithms .....	372
A.1.1 Principle .....	372
A.1.2 Fourier analysis based technique .....	373
A.1.3 Transient behaviour .....	378
A.1.4 Practical application .....	379
A.1.5 Literature .....	380
A.2 Calculation with phasors and complex quantities .....	381
A.2.1 Definitions .....	381
A.2.2 Calculation with phasors and complex quantities .....	382
A.3 Fundamentals of symmetrical component analysis .....	385
A.3.1 Calculation procedure .....	385
A.3.2 Typical system component data .....	390
A.3.3 Equivalent circuits and formulas for network reduction .....	391
A.3.4 Equivalent circuits of transformers .....	393
A.4 Impedances of overhead lines and cables .....	397
A.4.1 Single line (transposed) .....	397
A.4.2 Double circuit line (transposed) .....	398

A.4.3 Bundle conductor ..... 399

A.4.4 Cable impedances ..... 400

A.5 Reach of back-up zones on parallel lines ..... 401

    A.5.1 Phase-to-phase faults ..... 401

    A.5.2 Phase-to-earth faults ..... 404

A.6 Tilting of the quadrilateral top line to avoid overreach ..... 412

**Index** ..... 417

---

# 1 Introduction

Distance protection is a universal short- circuit protection.

It's mode of operation is based on the measurement and evaluation of the short- circuit impedance, which in the classic case is proportional to the distance to the fault.

## **Area of application**

Distance protection forms the basis for network protection in transmission, as well as interconnected distribution networks.

Thereby it acts as the main protection for overhead lines and cables and in addition functions as backup protection for adjoining parts of the network, such as busbars, transformers and further feeders.

Distance protection is faster and more selective than overcurrent protection. It is also less susceptible to changes in the relative source impedances and system conditions.

A further advantage of numerical distance protection is the integrated fault location function.

Therefore it is also applied in radial networks.

Its tripping time is approximately one to two cycles (20 to 40 ms at 50 Hz) in the first zone for faults within the first 80 to 90% of the line length. In the second zone, for faults on the last 10 to 20% of the protected feeder, the tripping time is approximately 300 to 400 ms. Further zones acting as remote backup protection accordingly follow with longer set grading times.

With a communication channel between the two line-ends (pilot wire, power line carrier, radio link or optical fibre) the distance protection can be upgraded to a comparison protection scheme with absolute selectivity. It then facilitates fast tripping of short circuits on 100% of the line length similar to a differential protection scheme, whilst in addition providing remote backup protection for adjoining parts of the network.

The distance protection communication only requires a narrow band width channel, as no measured values, but only "GO/NO GO" signals are transmitted. These distance protection schemes with signal transmission appear in various forms, particularly in HV and EHV networks.

Finally the distance protection is also applied as backup protection for large generator and transformer blocks, where high pick-up sensitivity along with short tripping times are required.



### **Technical advances**

In 1920 distance protection was introduced and it has since then undergone continuous development – from induction disk measuring elements to moving coil technology, and further to analogue static relays with operational amplifiers. Hereby the accuracy and selectivity were approved upon substantially. The tripping time was also improved by a factor ten, from the original several hundred to the present few tens of milliseconds. A quantum leap in the development of distance protection was achieved roundabout 1985, when microprocessor technology was introduced [1.1-1.4].

The numerical devices are intelligent. They can store information and communicate with peripherals. These capabilities introduce fundamentally new concepts for the improvement of protection quality. For the application and management of protection fundamentally new aspects result. At the same time the further developments of distance protection correspond to the higher demands on protection systems, resulting from the growing complexity of the transmission and distribution networks and the increased utilisation of the plant. [1.9]

### **Numerical distance protection**

The discreet signal processing and the numerical mode of measurement allows a higher accuracy and shorter tripping times with exact filter algorithms and the application of adaptive processes. Intelligent evaluation routines furthermore allow improved selectivity, even during complex fault situations. Over and above this the cost/performance ratio was dramatically improved [1.5-1.8].

The modern devices are multifunctional and thereby can implement the protection functions as well as additional functions for other tasks such as e.g. operational measurements and disturbance recordings. Only one device for main and one device for backup protection (when applied) is therefore required at each line end. By means of the integrated self monitoring the transition from the expensive preventive maintenance to the more cost effective condition based maintenance and testing is achieved.

The numerical devices also allow for the operation with PC or the integration into network control systems, via serial interfaces. Thereby several new aspects arise for the configuration, installation, commissioning and maintenance.

---

## 2 Definitions

In this document the following terminology is used.

Where the definitions correspond to IEC60050-448: “International Electro-technical Vocabulary – Chapter 448: Power System Protection”, the relevant reference number is indicated [2.1]:

### *Distance protection*

A non-unit protection whose operation and selectivity depend on local measurement of electrical quantities from which the equivalent to the fault is evaluated by comparing with zone settings [448-14-01].

### *Static relay (protection)*

Analogue electronic relay generation using transistors, operational amplifiers and logic gates. In the US called solid-state relay (protection).

### *Numerical distance protection (relay)*

Fully digital distance protection utilising microprocessor technology with analogue to digital conversion of the measured values (current and voltage), computed (numerical) distance determination and digital processing logic. Sometimes the designation computer relay has also been used. The term “digital distance relay” was originally used to designate a previous generation relay with analogue measurement circuits and digital coincidence time measurement (angle measurement), using microprocessors. In the US, the term “digital distance protection” has always been used in the meaning of numerical protection. Nowadays, both terms are used in parallel.

### *Digital distance protection*

See “numerical distance protection”.

### *Distance zones*

The reaches of the measuring elements of distance protection, in a power system [448-14-02].

### *Under- and/or overreach*

Mode of operation of the distance protection where the fastest zone is set with a reach which is shorter (underreach), or longer (overreach) than the protected zone [448-14-05/07].

*Zone limit (cut-off distance, balance point, set point)*

Measured impedance corresponding to the zone end.

*Transient overreach*

Operation of a distance zone for a larger value of impedance than that for which it is adjusted to operate under steady state condition [15]. This tendency occurs with offset of the short circuit current initially after fault inception. Conventional relays used a “line replica” shunt in the current path to minimise this effect. Numerical relays avoid the overreach by digital filtering of the DC component and adaptive control of the zone reach.

*Impedance characteristic (relay)*

Distance zone characteristic with constant impedance reach (Circle in the impedance plane centred at the origin of the R-X diagram). When used as directional zone, a directional characteristic (e.g. straight line) must be added. When the circle is shifted in the R-X diagram, we get a modified or offset impedance-type characteristic.

*Impedance relay*

Originally this term designated a relay with impedance circle characteristic. Impedance however is a generic term including resistance and reactance alone or a combination of the two. In this sense, the term impedance relay is often used as generic term equivalent to distance relay.

*MHO (Admittance) characteristic (relay)*

Circle characteristic which passes through the origin of the R-X-diagram. It is therefore inherently directional. The name is due to the fact that the MHO circle corresponds to a straight line in the admittance ( $1/OHM$ ) plain.

*Polarisation*

Providing a relay with directional sensitivity.

*Cross polarisation*

Polarisation of a relay for directionality using some portion of the healthy (unfaulted) phase voltage(s). In many cases *quadrature polarisation* is used. In this case the polarising voltage is in quadrature to the faulted phase voltage. Also the positive-sequence voltage is sometimes used for polarisation.

*Polarised MHO characteristic*

The traditional MHO relay with a circle passing through the origin of the R-X diagram uses the voltage of the short-circuit loop (faulted phase(s) voltage) as polarising quantity. It is more precisely called self polarised MHO relay.

The *cross polarised MHO* version adds a certain percentage of healthy phase(s) voltage to the polarising voltage to ensure unlimited direction sensitivity for close-up zero-voltage faults. In consequence, the circle extends in negative X-direction for forward faults depending on the source impedance and draws together excluding the origin in case of reverse faults (see paragraph 3.4.2).

*Reactance characteristic (relay)*

Straight line characteristic parallel to the R-axis with constant X-reach. The reach in R-direction is unlimited. The reactance characteristic must therefore be combined with a starter characteristic (e.g. MHO type)

*Quadrilateral characteristic (relay)*

As the name implies, the characteristic is composed of four straight lines.

*Angle-impedance (OHM) characteristic*

This term designates a straight line characteristic in the R-X plane which is inclined by an angle (often the line angle) against the R-axis. A pair of these straight lines is called blinder characteristic (“blindners”) and is used to limit the zone reach, e.g. of a MHO relay, in positive and negative R-direction against load encroachment (see paragraph 3.1.6).

*Load blocking zone (load cut out)*

A wedge shaped area which is cut out of distance zones to reduce the reach in R-direction and to allow higher loading of the relay (line) (see 6.2.3 and 6.3.2).

*Loadability of distance relays*

As the line load increases, the measured load impedance becomes lower and encroaches the distance zones. The load MVA at which the farthest reaching zone (starting or 3<sup>rd</sup> zone) is on the verge of operation, is called the loadability limit of the relay (see 6.2.3).

*Measuring system (measuring element)*

Module for the measurement of the fault distance and direction, including starting characteristics. The inputs are the short-circuit current and voltage. An active signal appears at the output when the fault lies within the corresponding zone, i.e. when the measuring system picks up.

Conventional relays used an electro-mechanical or static measuring system. With numerical relays the measuring system is a software module for the calculation of the loop impedance and for the value comparison with the set zone characteristic.

### *Full scheme distance protection (non-switched)*

Distance protection generally having separate measuring elements for each type of phase-to-phase fault and for each type of phase-to-earth fault and for each zone measurement [448-14-03].

For numerical protection this implies that all ph-ph and all ph-E loop impedances are simultaneously computed and compared with the zone limits (e.g. 7SA6 or 7SA522).

### *Switched distance protection*

Distance protection generally having only one measurement element for all power system faults and/or for all zones [448-14-04].

In case of numerical protection the term “switched” is not applicable as all measured values are continuously sampled and stored in a buffer. There is no HW-switching in the measuring circuits. Relays which use a fault detector controlled loop selection and only evaluate one fault loop for the distance measurement may be called “single system” distance relays (earlier digital relay versions, e.g. 7SA511).

### *Switched distance protection (multiple measuring system)*

Distance protection with multiple measuring systems need only simplified loop selection. Three measuring systems are normally connected in delta for phase faults and are switched to wye connection in case of single phase to earth faults. (This variant was common in Germany in electromechanical EHV protection, e.g. type R3Z27.)

### *Protection using telecommunication*

Protection requiring telecommunication between the ends of the protected section in a power system [448-15-01]. In US called *pilot protection*.

### *Distance protection with teleprotection channel*

Distance protection requiring telecommunication between the ends of the protected section in a power system [according to 448-15-01].

### *Distance protection in permissive mode*

A distance protection, in which the receipt of a signal permits the local protection to initiate tripping.

### *Distance protection blocking mode*

A distance protection, in which the receipt of a signal blocks the local protection from initiating tripping [448-14-10]

### *Starting time*

The time required from fault incidence until the starting (pick-up) of the measuring system (e.g.  $I > I_{\text{pick-up}}$ , or  $Z < Z_{\text{starting}}$ ). Normally when this time is expired, a further function is released or blocked and an alarm is initiated. A trip command is only generated after evaluation of the tripping logic or following the expiry of a set delay time.

### *Reset ratio*

This is the ratio of the pick-up to drop-off level of a measuring system. This difference is required to prevent intermittent pick-up and drop-off (chattering) of the measuring system. The reset ratio is smaller than 1 for measuring systems that pick up on increasing measured values (e.g. 0.95 for the overcurrent starting) and greater than 1 for measuring systems that pick up on decaying measured values (e.g. 1.05 for the impedance starting).

### *Reset time*

The time during which the output signal is picked up after the measured signal has dropped below the re-set level of the measuring system.<sup>1</sup> The reset time of the starting, after interruption of the short-circuit current, is the most pertinent in the case of distance protection. This time is required to calculate the grading times (refer to paragraph 3.1.14).

### *Tripping time*

The tripping time of the distance protection is the time measured from fault inception until the closing of the trip contacts. The tripping time of the undelayed fast tripping stage or typical tripping time is stated in the technical data sheet. However, this tripping time is not constant. Several factors influence it (short-circuit voltage and current as well as fault location). This dependence is usually shown as a diagram (profile curves). To determine the tripping time of the protection system (scheme), possible delays of signal transmission and channels and external trip relays must be added.

### *Grading times*

Set delay times of the back-up zones.

### *End zone time*

In Germany the starting element of the distance protection is utilised as remote back-up. Following a long time delay the starting element issues a trip. For this function there is a directional end zone time and a non-directional end zone time.

---

<sup>1</sup> For impedance zones the reverse applies: during starting the measured impedance drops below  $Z_A$ . To reset, the measured impedance must exceed the reset level ( $Z_R = 1.05 Z_A$ ).

### *Contour diagram*

Family of isochronic time curves plotted in a diagram of fault location (% of zone reach) versus SIR (the ratio of source to line (zone reach) impedance).

### *Automatic reclosure (ARC)*

On overhead lines most faults are of a transient nature and disappear when the infeed is switched off. After fault clearance the line can be returned to service. This is usually implemented with an ARC after a short time delay (dead time). In some cases a further reclose attempt is made if the first one is not successful – multiple shot ARC.

### *Short-circuit loop (fault loop)*

The short-circuit current path through the system from the infeed to the fault location and back. In the case of distance protection this refers to the short circuit current path from the relay location to the fault location and back.

### *Short-circuit voltage (faulted loop voltage)*

This term refers to the voltage on the short-circuited loop (fault loop). In the case of distance protection this refers to the voltage between the faulted phases (phase to phase short-circuit) or between a faulted phase and earth (phase to earth short-circuit), at the relay location. The short-circuit voltage is required for the distance measurement. When this voltage is used for determining the direction, it is referred to as the faulted loop voltage.

### *Unfaulted loop voltage (healthy phase voltage)*

To determine the fault direction (fault location in front of or behind relay location), the modern distance protection utilises measured voltages that are not affected by the fault, e.g. the voltage  $U_{L2-L3}$  for a short-circuit L1-E. An infinite directional measurement sensitivity is achieved in this manner. This is the case even for close-in faults, where the faulted loop voltage is too small for a reliable measurement (refer to paragraph 3.3.2).

### *Short-circuit impedance*

Impedance in the short-circuit between the faulted phase and earth or between the faulted phases. In terms of the distance measurement, the short-circuit impedance refers to the impedance between the point of connection of the relay measured voltage and the fault location. In connection with short-circuit current calculations this term refers to the impedance of the total short circuit loop from the infeed to the fault location.

### *Apparent impedance*

The impedance to a fault as seen by the a distance relay is determined by the current and voltage applied to the relay. It may be different from the actual impedance because

of current infeed or outfeed at some point between the relay and the fault, or due to remote infeed in case of resistance faults (see 3.5.1 and 3.5.2). In the healthy phase measuring elements impedances appear that depend on fault- and pre-fault load conditions. They approach distance zones and may cause overfunction endangering phase selective tripping. This can be avoided by restricted zone setting or special phase selectors (see 3.1.6). During load the distance relay measures an apparent impedance according to the actual voltage and current at the relay location. During overload and power swing these impedances approach the distance zones and may cause false tripping. This must be prevented by restricted setting of the zone reach in R-direction and the use of power swing blocking features (see 3.1.11).

### *Source impedance*

For a particular fault location, the source impedance is that part of the impedance in the short-circuit loop, which lies between the source voltage (voltage delivering the short-circuit current) and the point of connection of the relay measured voltage.

### *Impedance ratio (SIR)*

At a particular point of measurement this refers to the ratio of the source impedance to the short circuit impedance (impedance of the protected zone) [448-14-14].

This is referred to as the system or source impedance ratio (SIR). It is a measure for the magnitude of the faulted loop voltage seen by the relay.

### *Load impedance*

At a particular point of measurement this refers to the quotient of the phase to neutral voltage (line voltage) over the phase-current while load current is flowing [448-14-15].

### *Fault resistance*

This refers to the resistance between the phase-conductors or between the phase-conductor and earth at the fault location.

### *Phasor*

In this book the phasor notation is used for electrical signals:

$$\underline{A} = A \cdot e^{j\varphi} = A \cdot [\cos \varphi + j \sin \varphi] = B + jC$$

Whereby  $A$  refers to the rms (root mean square) value of the current, voltage or power, and  $\varphi$  to their phase angle at the time  $t = 0$ .

This representation is also extended to include impedances which actually are not time dependant.



---

## 3 Mode of Operation

This chapter will provide a general introduction to distance protection. Based on this, the following chapters will, in detail, deal with the mode of operation and applications of numerical distance protection.

### 3.1 Fundamentals of distance protection

#### 3.1.1 Concept

Distance protection determines the fault impedance from the measured short-circuit voltage and current at the relay location (figure 3.1).

The measured fault impedance is then compared with the known line impedance. If the measured fault impedance is smaller than the set line impedance, an internal fault is detected and a trip command issued to the circuit-breaker.

This implies that the distance protection in its simplest form can reach a protection decision with the measured voltage and current at the relay location. For this basic protection decision no further information is required and the protection therefore does not have to depend on any additional equipment or signal transmission channels.

Due to inaccuracies in the distance measurement, resulting from measuring errors, CT errors and the inaccuracy of the line impedance, which is usually based on a calculation and not a measurement, a protection reach setting of 100% of the line length with a dis-

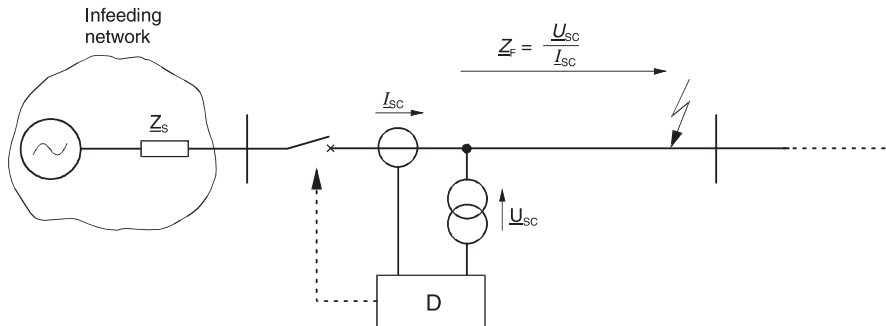


**Figure 3.1** Distance protection principle, measurement of fault impedance

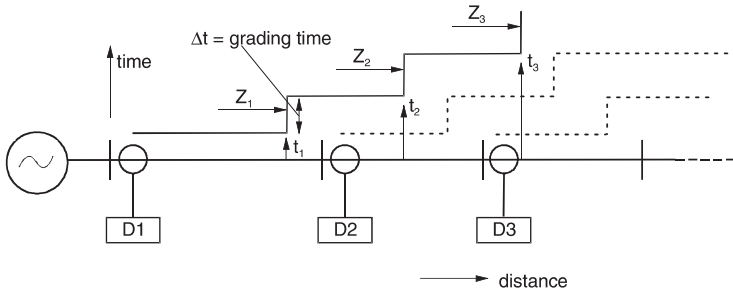


**Figure 3.2** Distance protection principle, graded distance zones

tance zone is not possible in practice. A security margin (10-15%) from the remote end of the line must be selected for the so called under-reaching stage (1<sup>st</sup> zone) to ensure secure protection selection between internal and external faults (figure 3.2).

The remainder of the line is covered by an over-reaching stage (2<sup>nd</sup> zone), which, to ensure selectivity, must be time-delayed (graded) relative to the protection of the adjacent line. In the case of electro-mechanical protection this grading time is 400-500 ms and 250-300 ms in the case of analogue static and numerical protection. Considered in this grading time are the operating time (switching time) of the downstream circuit-breaker, the over-shoot of the distance measuring elements and a security margin (refer to paragraph 3.1.14: grading plan).

Contrary to differential protection, which exhibits absolute selectivity (its protected zone is exactly defined by the location of the current-transformers at both line ends), the distance protection (in its simplest form without a teleprotection supplement) does not exhibit absolute selectivity. Selective tripping must be ensured by time grading with adjacent protection.

However, distance protection additionally provides the option of back-up protection for the adjacent lines. The second stage (over-reaching zone) is used for this purpose. It reaches through the adjacent busbar and into the neighbouring lines. A further third stage is usually applied to protect the entire length of the neighbouring lines, if practicable (figure 3.2).

The co-ordination of the zone reach and time settings is achieved with a so-called grading plan (refer to paragraph 3.1.14).

### 3.1.2 Relay impedance (secondary impedance)

Distance protection relays are implemented as so-called secondary relays, i.e. they are fed with current and voltage measured signals from the primary system (overhead line) via instrument transformers (CT and VT). The relay therefore measures a secondary impedance which results from the transformation ratios of the CT and VT:

$$Z_{\text{sec}} = \frac{I_{\text{prim}}/I_{\text{sec}}}{U_{\text{prim}}/U_{\text{sec}}} \cdot Z_{\text{prim}} \quad (3-1)$$

*Example:*

Rated system voltage:  $U_{\text{prim}} = 110 \text{ kV}$

CT ratio:  $I_{\text{prim}} / I_{\text{sec}} = 600 / 1 \text{ A}$

VT ratio:  $U_{\text{prim}} / U_{\text{sec}} = 110 \text{ kV} / 100 \text{ Volt}$

$$Z_{\text{sec}} = \frac{600/1}{110/0.1} = 0.545 \cdot Z_{\text{prim}}$$

The grading plans are normally done with primary impedances.

The relay settings are done with secondary impedances as the testing of the relay is done with secondary signals. Therefore the relay impedance values must always be converted using equation (3-1).

### 3.1.3 Impedance diagram

To the protection engineer the impedance diagram is an essential tool for the evaluation of the behaviour of distance protection. In this diagram the relay characteristic and the measured load and short-circuit impedance are represented in the complex R-X plane (figure 3.3). In this diagram, the relation of these three impedance components are a clear indicator of the relay performance in the system.

During normal system operation the measured impedance corresponds to the load impedance. Its magnitude is inversely proportional to the amount of transferred load ( $Z_{\text{load}} = U_{\text{line}}^2 / P_{\text{load}}$ ). The angle between current and voltage during this condition corresponds to the load angle  $\varphi_L$  (figure 3.3). It is dependent on the ratio between the real and reactive power ( $\varphi_{\text{load}} = \text{atan}[P_{\text{reactive}} / P_{\text{real}}]$ ).

After fault inception the measured impedance jumps to the short-circuit impedance, which is usually smaller than the load impedance. Its value corresponds to the line impedance between the relay location and the fault location (close-in fault  $Z_{\text{LF1}}$  or remote fault  $Z_{\text{LF2}}$ ). When arc resistance or fault resistance at the fault location is present, an additional resistive component ( $R_F$ ) is added to the line impedance. The angle that is now measured between short-circuit current and short-circuit voltage is the short circuit angle  $\varphi_{\text{SC}}$ .

The operating characteristic of distance protection is defined by a fixed shape in the impedance diagram.<sup>1</sup>

Herewith the fault area is isolated from the load area, and the reach of the distance zones is determined. Over and above this it becomes apparent whether the set reach in R-direction (also referred to as arc resistance tolerance) is adequate for the expected fault resistance. Finally a directional characteristic defines two impedance areas, by means of which the relay establishes whether a short-circuit is in the forward or reverse direction.

---

<sup>1</sup> When healthy phase voltages are used, the shape of the zone characteristic is changed in accordance with the source impedance. This is elaborately elucidated in paragraph 3.3.2.

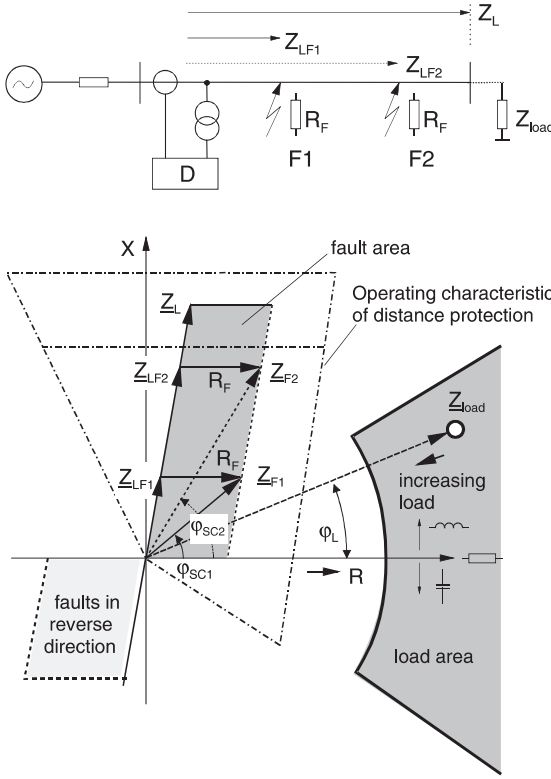


**Figure 3.3**  
Load and short-circuit  
impedance

The traditional relay impedance characteristics were geometric figures made up of straight lines and circles or sectors of circles. This restriction was due to the limitations of analogue measuring techniques.

The increase in processing power of numerical protection relays liberated the choice of operating characteristics and allowed for their optimisation. This will be discussed further below.

#### 3.1.4 Distance measurement

Conventional relays compared the short circuit impedance with the line replica impedance to determine if the fault is in- or outside the protected zone. Electro-mechanical relays manufactured in Germany used a rectifier bridge circuit as an impedance balance. Figure 3.4a shows the principle of this measuring system. The shown equation corresponds to a circle in the impedance plane (figure 3.4b). With appropriate modification of the measuring circuit the circle can be moved in the impedance plane (figure 3.5). A better fault resistance coverage (arc compensation) is achieved in this manner [3.1].

The English and American manufacturers utilised a measuring technique based on the Ferraris principle, with induction relays (figure 3.6a). In this case the moving cup (mobile drum) is equivalent to the rotor of the induction motor. The cup carries the

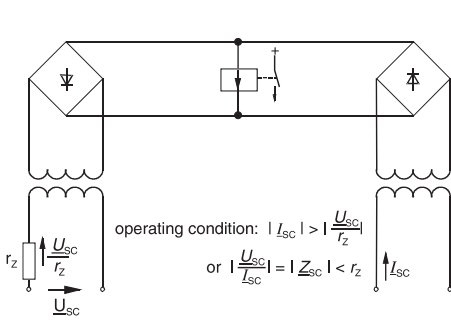


**Figure 3.4a** Rectified bridge comparator

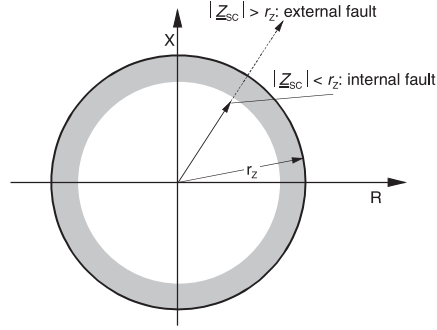


**Figure 3.4b** Impedance circle

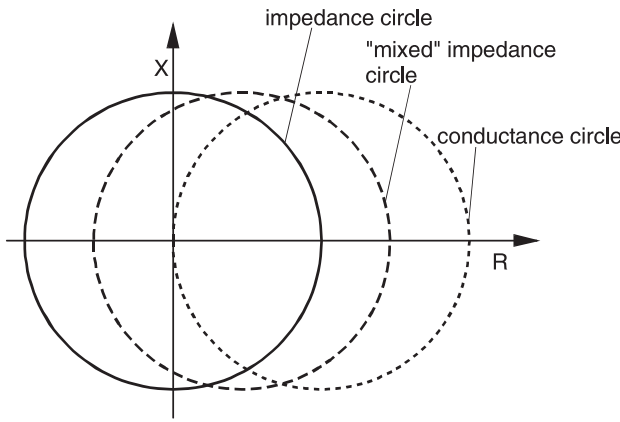


**Figure 3.5**  
Tripping characteristic  
of the electro-mechanical  
protection  
(German manufacturers)

rotor currents while the magnetic circuit is completed through the stationary magnetic yokes and a fixed core. With variations of the measuring circuit, the circular and other characteristics (straight lines, lenses) can also be generated in the impedance plane.

The best known characteristic is the MHO-circle (admittance circle) (figure 3.6b) [3.2]. The circumference of this circle passes through the origin of X-R diagram and therefore inherently combines directional and distance measurement (self-polarised MHO circle). This provided an economical advantage at the times of electro-mechanical and analogue static relaying technologies. But, still today, with digital technology, this type of characteristic is preferred in the US, with the exception of ground fault distance protection of short lines where quadrilateral characteristics have been introduced to extend fault resistance coverage (see further below).

The set relay impedance  $Z_R$  defines the reach of the zone. The angle  $\theta$  is known as the Relay Characteristic Angle (RCA).

The impedance reach, dependent on the short circuit angle, is given by the formula:

$$Z = Z_R \cdot [\cos(\theta - \varphi)] \quad (3-2)$$

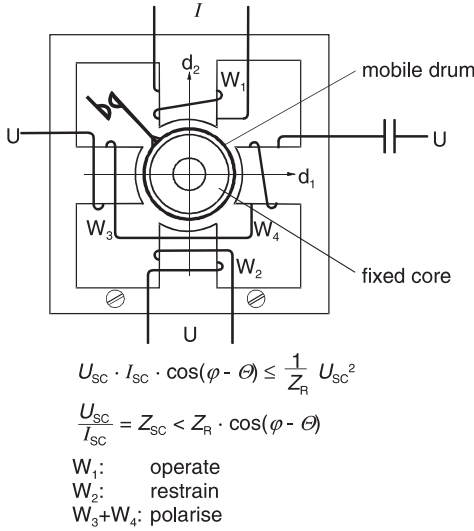


**Figure 3.6a** Induction cup relay

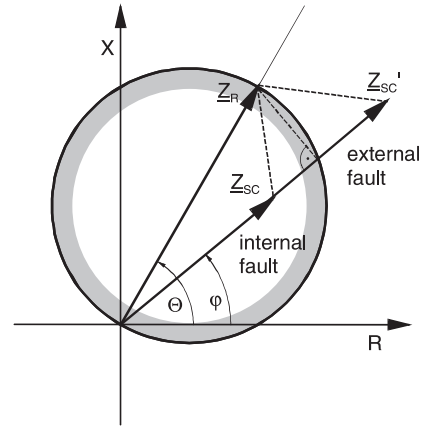


**Figure 3.6b** MHO characteristic

The setting of  $\theta$  is normally adapted to the impedance angle of the protected line so that  $Z_R$  corresponds to a replica of the line. This was important with high speed electro-mechanical and static relays, because they used a transactor (line replica impedance) to eliminate the impact of the DC component of the fault current on the distance measurement (tendency to overreach). In case of short lines, it was general practice to set the RCA lower than the line impedance angle to improve the arc compensation. The transient error caused by the not ideal compensation of the current offset was in general tolerable, in particular with slower relays. In the extreme case, with  $\theta = 0^\circ$ , we arrive at the so-called conductance circle, shown in figure 3.5. This relay characteristic was used in Germany with the electro-mechanical relays for the distribution network, in particular on cables where the short circuit angle is below 30 degrees. For the distance protection measurement only the reactance component  $X_F$  of the fault impedance can be used to effectively determine the distance to fault. The resistive component may vary due to the indeterminate arc resistance (fault resistance) at the fault location. The reach limit in X-direction should therefore be as flat as possible, running parallel to the R-axis (ideally a straight reactance line). The reach in R-direction must be limited to prevent encroachment of load impedances. Electro-mechanical relays attempted to achieve this with a combination of circles and straight lines (figure 3.7).

There is a MHO-circle with healthy phase voltage polarisation<sup>1</sup> (called polarised MHO or cross polarised MHO) which provides an improved arc resistance reserve (figure 3.8). In this case the diameter of the circle changes to include the source impedance (for faults in forward (line) direction). A satisfactory resistance coverage is however only achieved with relatively weak in-feeds, i.e. large source impedances [3.3].

<sup>1</sup> The implementation of healthy phase voltages by the distance protection is referred to in paragraph 3.3.2.

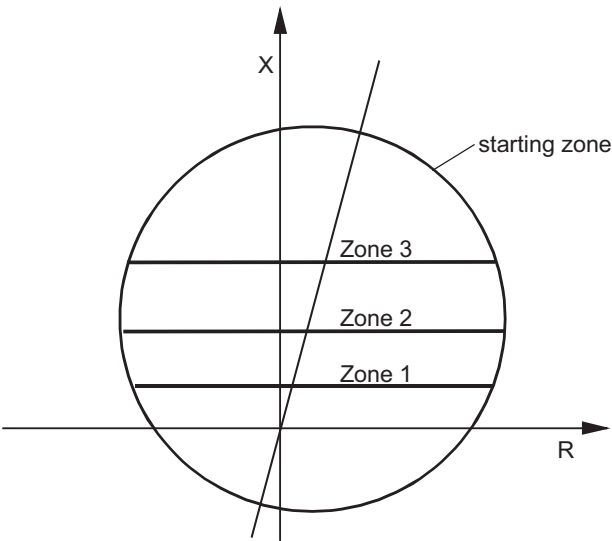


**Figure 3.7**  
Combined circle- and  
straight line characteristic

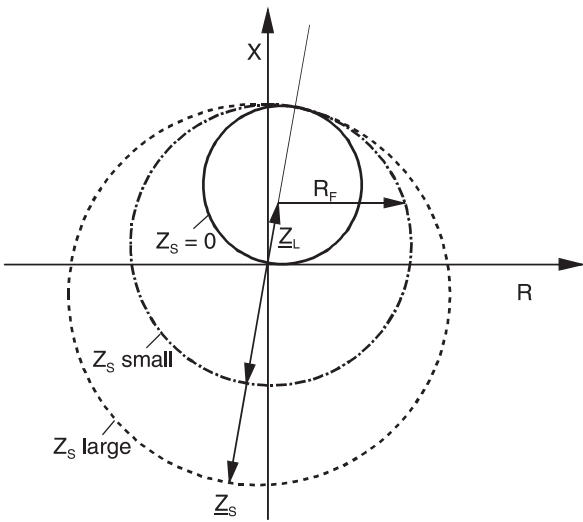


**Figure 3.8**  
Cross polarised MHO  
circle (for faults in for-  
ward (line) direction)

In this regard the quadrilateral characteristics introduced by static relays are ideal (figure 3.9) [3.4]. The resistive reach can in this case be set independent of the zone reach in X-direction. Acceptable arc compensation can therefore be reached even with very short lines or cables.

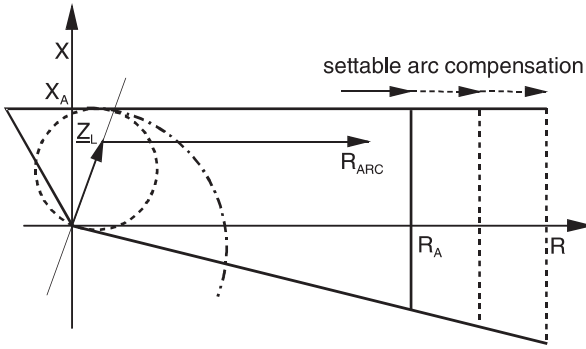


**Figure 3.9**  
Quadrilateral tripping  
characteristic

### Phase comparator

In analogue static technology, distance measurement is based on phase comparison. The sinusoidal signals of the phasors  $\Delta U$  and  $\underline{U}_{\text{ref}}$  are changed to square waves. By means of a comparator, the co-incidence (overlapping) of the squared signals is monitored. Figure 3.10 shows this for the examples of a MHO-circle and a quadrilateral.  $\underline{Z}_R$  is in both cases the set zone reach (relay impedance).

The MHO-circle is produced by measuring the angle  $\varphi$  between  $\Delta U$  and the short-circuit voltage  $\underline{U}_{\text{SC}}$ . At the circumference this angle is 90 degrees corresponding to the pick-up value (coincidence limit angle  $\varphi_{\text{lim}}$ ). Short circuit impedances inside the circle result in larger angles, i.e. longer coincidence, and consequently tripping.

The quadrilateral requires two measurements because the closed operating area is composed of a distance angle and a directional angle. The shown distance angle results from an angle measurement between a reference phasor  $\underline{U}_{\text{ref}}$  and the difference phasor  $\Delta U$ .

Numerical relays utilise a particular algorithm to compute the fault impedance (X- and R-value) from the measured current and voltage. The result is then mathematically compared with the borders of the parameterised pick-up characteristic. Thereby it is possible to implement almost any shape and optimised characteristics, as referred to hereunder.

For circle characteristics the angle measurement between phasors is further used as criterion, but the phasors are now calculated numerically by orthogonal filters (e.g. Fourier-filter). The angle is determined by calculation of the phase shift.

### 3.1.5 Directional fault discrimination

On feeders with in-feed at both sides (e.g. ring network), the protection must be able to identify whether a fault is in the forward or reverse direction, to prevent reverse faults that are not on the protected feeder, from causing incorrect tripping.

The determination of direction can be shown in the current-voltage diagram as well as in the impedance plane (figure 3.11).



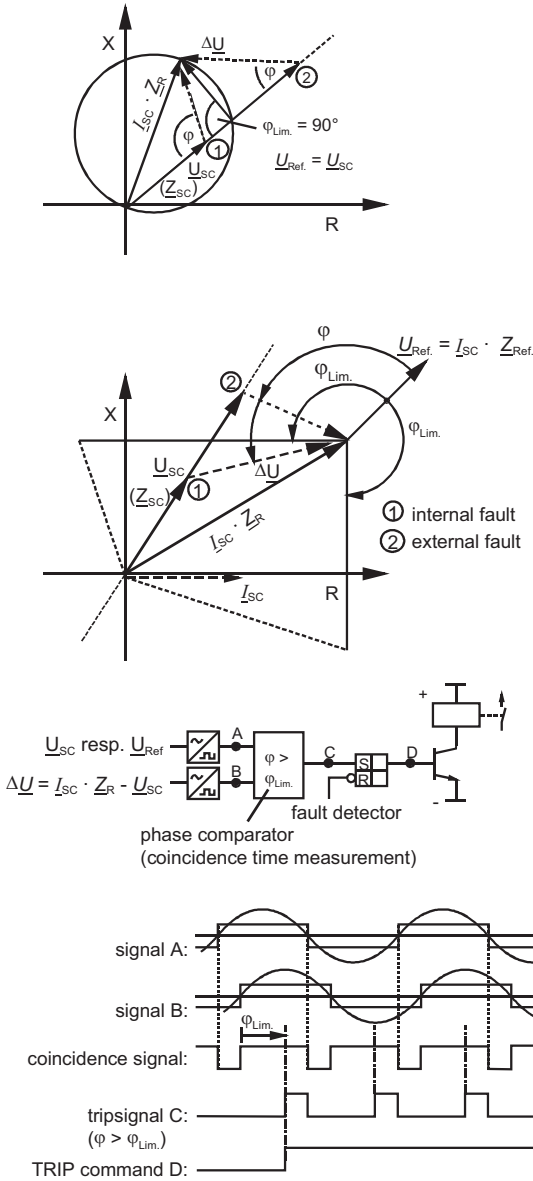


**Figure 3.10**  
Phase comparison  
distance measurement  
(coincidence logic)

In the case of faults in the forward direction, the current flows forward into a short circuit loop made up of inductance and resistance, i.e. with the chosen phase rotation notation the current is lagging the voltage as shown in figure 3.11a, provided that the definition and connection of the measured signals to the relay are the same. The angle  $\varphi_{SC}$  is above  $80^\circ$  on EHV overhead lines, and may be below  $20^\circ$  on cables. The angle may even be  $0^\circ$  in the extreme case of a close-in short-circuit with arc resistance.<sup>1</sup>

<sup>1</sup> The special conditions existing on series compensated lines will be discussed in paragraph 3.5.7.

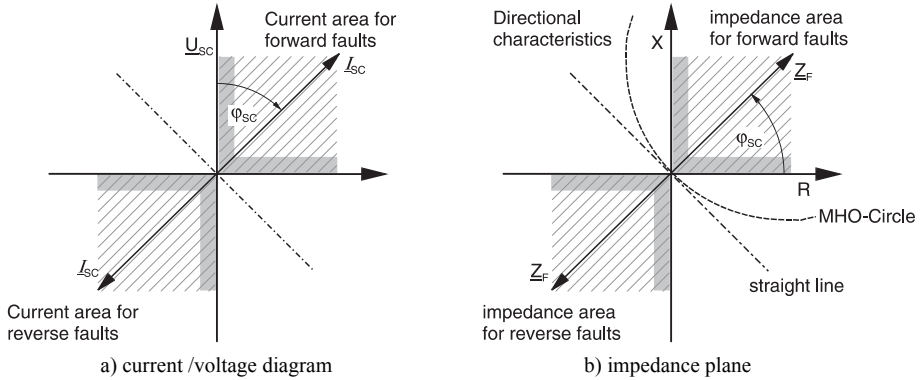


**Figure 3.11** Directional fault discrimination

If the fault is in the reverse direction, the current is reversed i.e. it appears to be rotated by approximately  $180^\circ$  in comparison to the current which flows during a fault in the forward direction.

This current reversal also results in an impedance reversal i.e. the fault impedance lies in the 3<sup>rd</sup> quadrant for the fault in reverse direction. Using this phenomenon, a direction decision can be based on the measurement of the angle between the current and voltage. The measuring circuit of conventional relays was constructed in such a manner that the directional characteristic was a straight line in the voltage or impedance plane.

With numerical relays a similar determination of the fault direction is possible, by analysing the sign of the computed fault impedances.

It has further to be considered that the conductance circle (figure 3.5) and the MHO-circle (figure 3.6b) are inherently directional, i.e. a separate directional measurement is not necessary in these cases.

The directional determination method referred to, utilises the voltage in the short-circuited loop. This method has the disadvantage that for close-in faults directly in front of or behind the relay location, no direction measurement is possible, because the voltage may in theory be equal to zero. Conventional relays of this type therefore have a so-called “dead zone” for short circuit voltages below approximately 0.1 V.

The utilisation of measured voltages from the unfaulted phases was already introduced with mechanical and analogue static relays for HV and EHV applications. In this case a voltage that is not affected by the fault is used as a substitute (cross-polarisation).

For example, the phase to phase voltage L2-L3 is used for a phase L1 to ground fault. Naturally a corresponding angle compensation must be implemented by the relay in this case. For the three-phase fault, where all voltages are affected by the fault, the voltage prior to the fault, which is stored in a voltage memory, is used. To achieve this, analogue relays had to utilise a complex voltage memory (resonant circuit), and this was therefore only used for the protection of EHV circuits.

Numerical relays store the measured sample values in cyclic buffers. The relay can determine the direction of the fault with pre-fault memorised voltage, subject to the fixed size of the cyclic buffer (in the case of the 7SA522 up to 2s).

The directional determination with voltages not affected by the short-circuit (cross-polarisation), and memorised voltages is of particular importance for series compensated lines. This is comprehensively referred to in paragraph 3.5.7.

#### 3.1.6 Starting (fault detection)

The initial task of the starting function is to detect and classify short-circuits in the power system. It must be phase-selective i.e. it must recognise the faulted phases correctly, without incorrect starting in any of the healthy phases.

This is of particular importance during single phase faults to ensure selective single-phase tripping, where single-phase auto-reclosure is implemented.

In the case of switched distance relays with only one distance measuring element, the starting function controls the selection of the measured values processed.

Furthermore, the pick-up and drop-off of the starting function is used to determine the beginning and end of a fault. The starting function may for instance trigger the zone timers (fault detector controlled timing, see figure 3.26) and the fault recorder.

Comment: With the classic American distance protection technology, a separate measuring system was provided for each zone and for each fault type (L1-E, L2-E, L3-E and L1-L2, L2-L3, L3-L1). All measuring systems were independently rooted to the trip output. Three Ph-Ph or three Ph-E measuring systems were combined in one device (zone-package).<sup>1</sup> The delay times of the back-up zones were initiated by the relevant zone measuring system directly. This implies that the time delays were directly zone-dependent. Additional measures to ensure phase-selective tripping during single-phase earth-faults were also not required, as three-phase ARC was implemented almost exclusively. For those few cases of single-phase ARC, an external phase-selector, mostly based on symmetrical components, was provided. Due to the reasons stated above, a fault detection was not required. This philosophy was also transferred to the numerical relays. The resulting structure is shown in paragraph 3.1.8. The supplements for phase-selection and elimination of load impedances are now-a-days included in the relay firmware. The 7SA522 relay is an example for this.

Current increment, voltage decay and impedance change may be used as criteria for the starting function.

---

<sup>1</sup> In the USA, the distance protection in sub-transmission systems is often only implemented for phase-faults. Protection for earth-faults is then either provided by an earth-current directional comparison scheme, or only with an inverse time delayed earth over-current protection. This is the reason for the separate packaging into Ph-Ph and Ph-E units.

### Over-current starting

This is the simplest and fastest method of fault detection.

It can be used in networks with small line impedances and strong in-feeds i.e. everywhere where sufficient large short-circuit currents flow. Thereby the smallest short-circuit current should not be less than approximately twice the maximum load current. The applied setting should be approximately 1.3 times the maximum load current in the phases, and 0.5 times  $I_N$  (rated CT current) for the earth-current.

For parallel lines it must be considered, that when one line is out of service, the other line, at least for a short time, may carry twice the current. In such an event, the setting for the phases must be doubled.

Furthermore it must be noted that in earthed systems, an earth-current starting on it's own is not sufficient. For correct loop selection, the short-circuit current must be large enough to cause pick-up of the corresponding phase as well.

To check the dependability of the fault detection, a two-phase fault must be used, because in this case the fault current is smaller than the three-phase fault current by a factor  $\sqrt{3}/2$ . Figure 3.12 shows as an example.

In the earthed network, the single-phase short circuit current must also be checked.

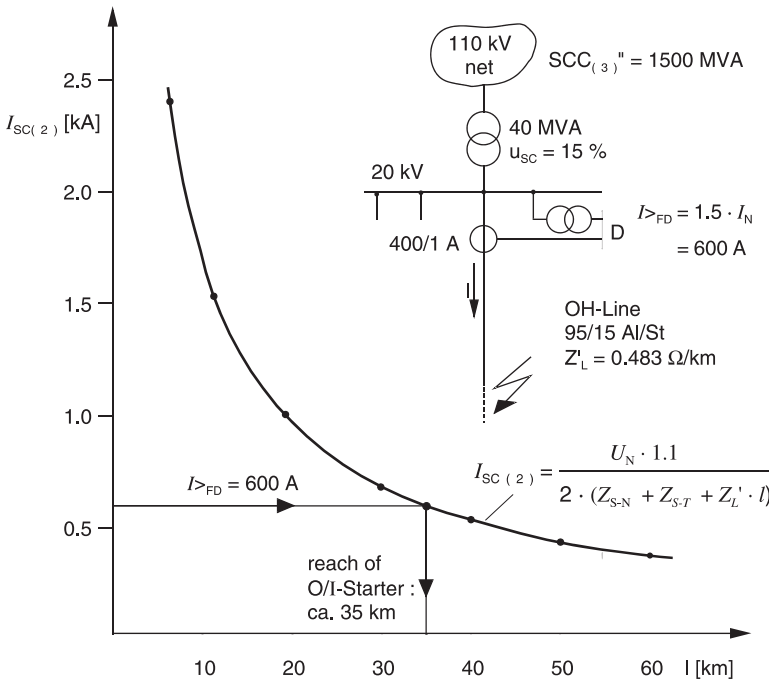


**Figure 3.12** Reach of the overcurrent starter (for phase to phase faults)

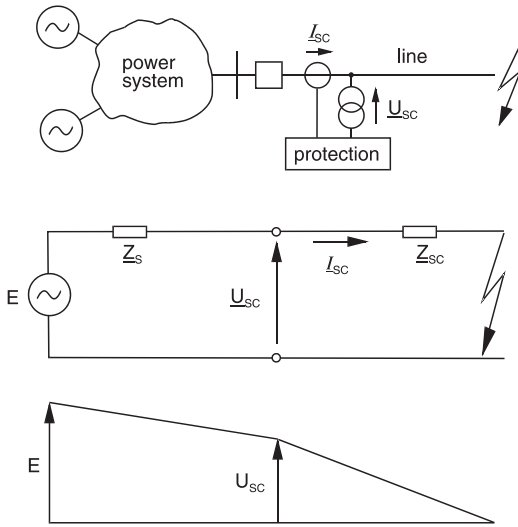


**Figure 3.13**  
Voltage at the relay location during short-circuit

#### Under-impedance starting ( $U <$ and $I >$ )

For the following reasons, the short-circuit current in the feeder bay may be too small for overcurrent starting:

- weak source (high source impedance)
- current splitting in parallel paths of a meshed system
- earth-current limiting by resistance or reactance in the transformer star-point

The monitoring of the voltage presents itself as an useful additional starting criteria in these cases.

The voltage appearing at the relay location is dependant on the source impedance and the fault impedance (distance to fault) (figure 3.13).

To prevent incorrect starting when the feeder is isolated (no voltage), the under-impedance criteria is combined with a low-set ( $0.2$  to  $0.5 I_N$ ) current threshold i.e. the under-voltage starting is only released, when this minimum current flows.

With the starting configuration known as under-impedance starting, the voltage threshold is controlled by the current, so that the pick-up sensitivity of the voltage is increased as the current increases. Figure 3.14 shows the resultant starting characteristic.

In this case  $I >>$  corresponds to an overcurrent starter stage. Typical settings are:  $I > = 0.25 \cdot I_N$  and  $I >> = 2.5 \cdot I_N$ , as well as  $U(I >) = 70\% \cdot U_N$  and  $U(I >>) = 90\% \cdot U_N$ .

#### Effectively earthed system

The under-impedance starting (or the impedance starting described below) is definitely required in the effectively earthed system to achieve phase-selective fault detection. Simple overcurrent starting is in general not sufficient. In an earthed system, it is pos-

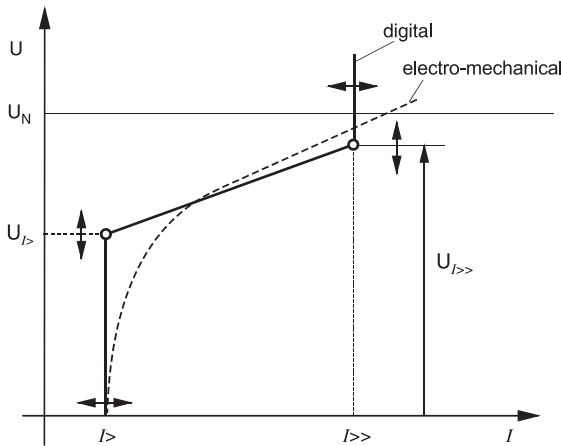


**Figure 3.14**  
Under-impedance  
starting

sible for short-circuit currents to also flow on the healthy phases during earth-faults. The overcurrent starting must be set above these healthy phase-currents. These currents arise due to the difference between the zero-sequence and the positive-sequence system at the two line ends.

Figure 3.15 shows the extreme case where at one line end there is an earthed transformer with no in-feed. At this end, the currents in the three phases are equal, although the fault is only single-phase to ground (Bauch's paradox).

Selective single-phase fault detection is only possible by means of the phase-to-ground voltage (or the corresponding impedance).

Normally the phase-to-phase under-impedance starting units are active using phase-to-phase voltages. During earth-faults, i.e. when earth-current flows or when a displacement voltage is detected, the phase-to-phase units are blocked and the phase-to-ground units are released using phase-to-ground voltages. In this way phase selective fault detection is ensured.

#### *Isolated or Peterson coil earthed systems*

In these systems single-phase earth-faults are detected by a special earth-fault protection and only alarmed. The line must not be tripped, as no short-circuit is present, and the feeder may remain in service without disruption to consumers until appropriate switching in the network can take place.

Incorrect fault detection by the distance protection must therefore be prevented at all cost, as the voltage in the faulted phase is zero in the entire network and the released distance measurement would lead to incorrect tripping.

For this reason the phase-ground measuring loops may only be released during double earth-faults in the isolated or Peterson coil earthed systems. This may be achieved with an earth-current detector set above the earth-current flowing during single-phase earth-fault conditions, while the fault arc was not quenched by the Peterson coil.

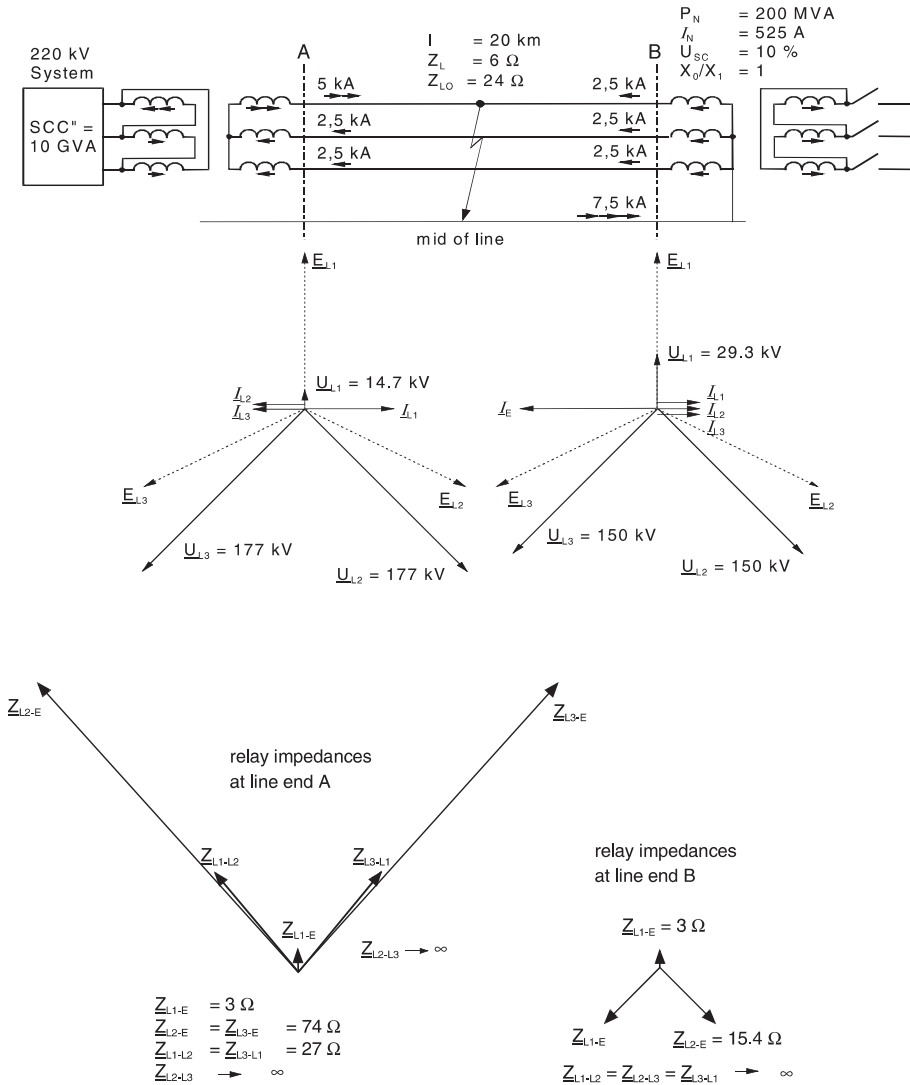


**Figure 3.15**

Short circuit in an effectively earthed system with unequal source and earthing conditions

In large networks this earth-fault current (arc not quenched) may assume the magnitude of the earth-current during double earth-faults (cross country faults). A differentiation between earth-fault and double earth-fault is in this case not simply possible by means of earth-current. In this case a measurement only with positive-sequence or phase-phase voltages is permissible (see also paragraph 5.2.2).

A definite detection of the double earth-fault with earth-current is only possible on the section between the two earth-faults (figure 3.16). A detection by means of displacement voltage  $\underline{U}_E = \underline{U}_{L1} + \underline{U}_{L2} + \underline{U}_{L3}$  would be possible beyond this zone, but is not

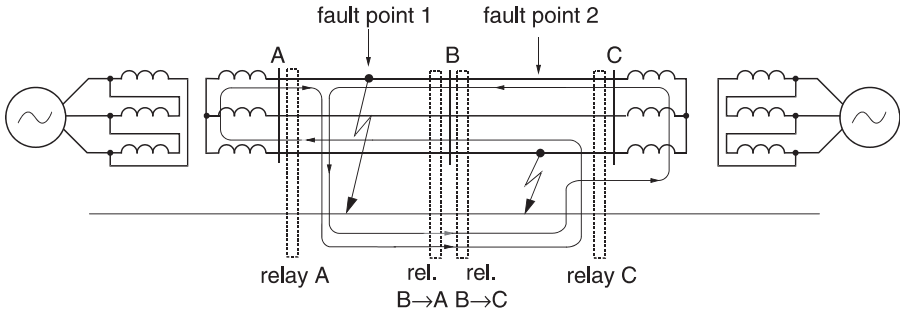


**Figure 3.16** Cross country fault current distribution

implemented at present. Therefore a two-phase fault is detected and measured at the in-feeds. The measured impedance is naturally not accurate and corresponds to an average value of the distances to the two earth-faults. (The distance measurement during double earth-faults in isolated or Peterson coil earthed systems is more closely referred to in paragraph 5.2.2)

#### *U/I/φ-starting (angle dependant under-impedance starting)*

In overhead line networks the short-circuit angle is substantially larger than the load angle. For instance on transmission lines the load angle lies in the range  $\pm 30^\circ$  and the short-circuit angle  $> 70^\circ$ . The angle between current and voltage may therefore be used as an additional starting criterion by the under-impedance starter.

The angle criterion is used to achieve greater sensitivity of the under-impedance starter ( $I_\phi > U_{(I_\phi)}$ ), when the measured short-circuit angle is within a settable range above the load angle (figure 3.17).

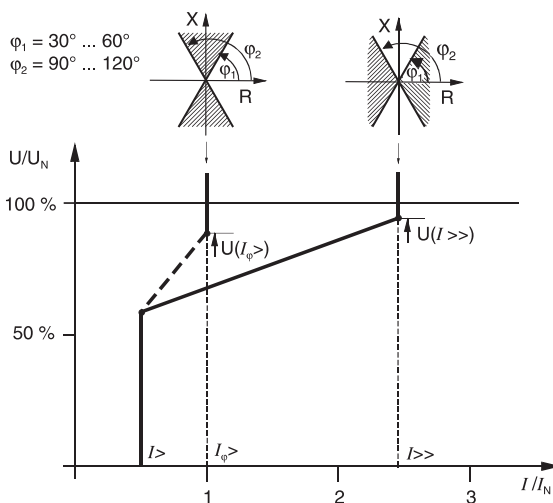


**Figure 3.17**  
*U/I/φ-starting*



The angle criterion extends the reach for the detection of faults at the end of long lines or for the detection on adjacent lines, where remote in-feeds cause an increment of the measured impedance (refer to paragraph 3.5.2).

### *Impedance starting*

As shown in figure 3.3, an impedance characteristic is also well suited to discriminate between fault and load conditions.

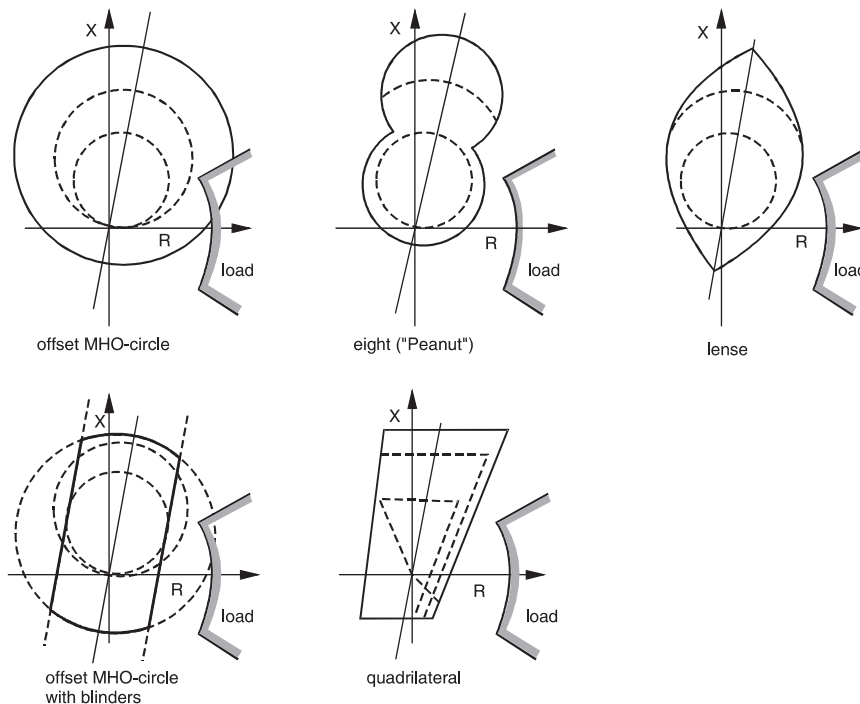
In this case, all six possible fault loops (L1-E, L2-E, L3-E, L1-L2, L2-L3, L3-L1) are continuously measured or computed and monitored with numerical technology.

With conventional relays the starting characteristic was already optimised by implementing variations of the circle and straight line elements (figure 3.18).

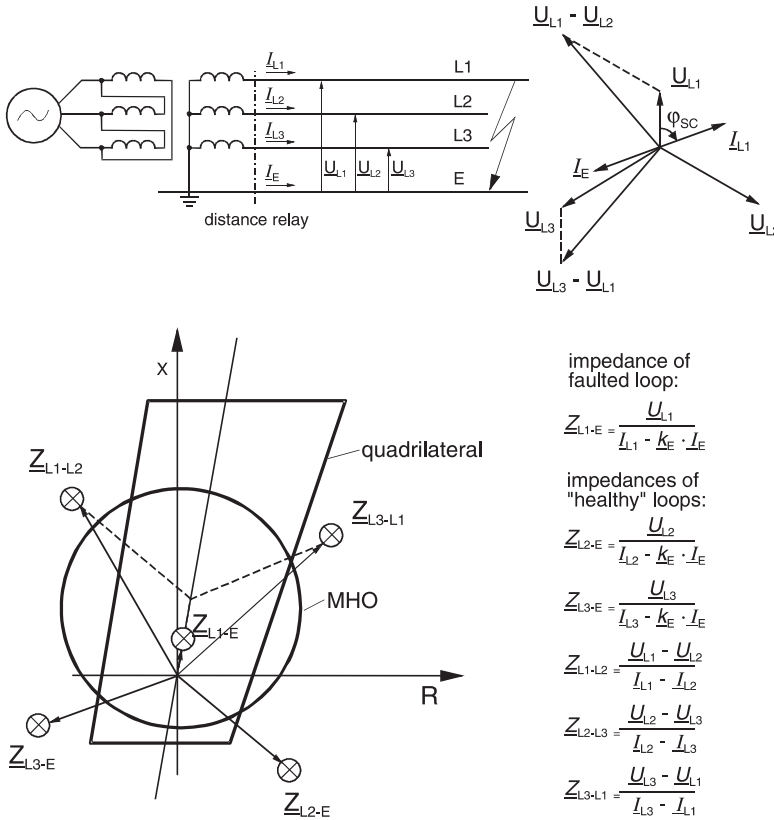
In this case the objectives are:

- large reach in X-direction for the detection of remote faults
- sufficient arc-compensation in R-direction while maintaining secure margin against load encroachment

The larger area of the starting impedance characteristic however also introduces a problem: the so-called “healthy” impedances on the phases not affected by the fault (“apparent impedances”) measured during the short-circuit can fall within the starting



**Figure 3.18** Impedance starting with conventional technology

**Figure 3.19**

Conventional protection: limiting of the area of the starting characteristic for phase-selective fault detection

characteristic, causing incorrect fault detection. Thereby the protection would trip three-phase for a single-phase fault and block the ARC (figure 3.19).

Therefore, on conventional relays, the magnitude of the setting must be correspondingly limited.

In this regard the numerical technology introduced important developments: the shape of the starting characteristic can now be extensively optimised (figure 3.20).

Limiting the area of the starting characteristic to exclude "healthy" impedances is no longer required, as the phase selectivity is ensured by additional measures.

The subject is too extensive to treat it here in all its aspects. The basic principles however shall show the improvements achieved in this field with numerical technology.

The new technique is comparable to the earlier used phase selectors for single-pole tripping and auto-reclosing, it however uses much more sophisticated and effective methods:

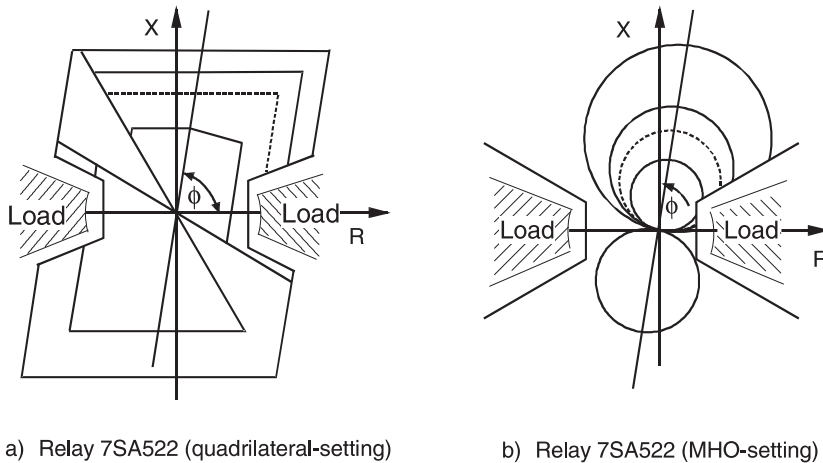


**Figure 3.20** Optimised starting characteristics of numerical relays (7SA522)

- Numerical comparison of the fault loop impedances
- Comparison of symmetrical component phasors
- Use of load compensated (delta) quantities
- Selection by recognition of characteristic fault patterns

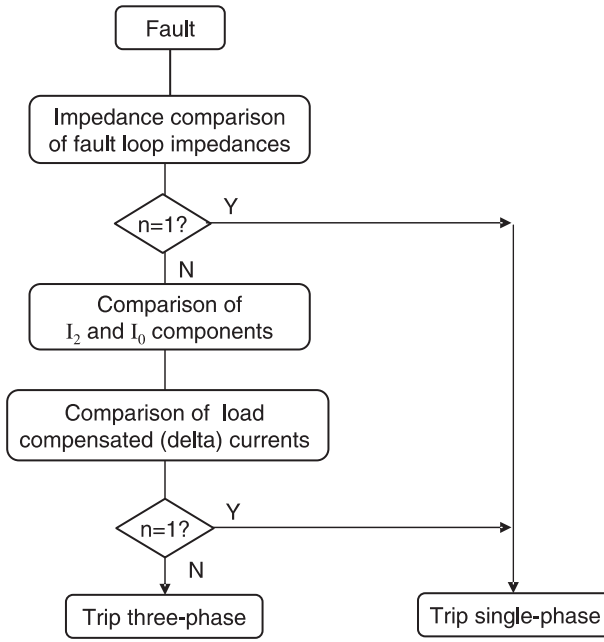
Normally, the smallest loop impedance already indicates the type of fault. A single phase fault, for example, is recognised when one phase-to-earth loop impedance is low and the other loop impedances are much higher (e.g. by a factor 1.5).

If more loop impedances appear close together, the more complex algorithms are called upon to discriminate between faulted loop impedance(s) and load influenced healthy phase impedances (figure 3.21).

The angle comparison of symmetrical component currents is a classical method which has already been used with conventional relays. In case of a single phase to earth fault, the negative and zero sequence currents of the faulted phase are nearly in phase (e.g.  $< 30^\circ$ ) while they are about  $120^\circ$  out of phase in the healthy phases. A double earth fault in the other two phases however may show the same relationship and must be excluded by additional criteria. Phase-to-phase undervoltage or under-impedance criteria have been used in the past.

An advanced method, now possible with numerical technology, uses delta quantities. For this purpose, the pre-fault load currents are stored and subtracted from the present total fault current. This delivers pure (load compensated) fault currents driven by a source voltage at the fault point which allow clear recognition of the fault type by their typical pattern.

In case of a single phase fault, the healthy phase currents are much lower and  $180^\circ$  phase shifted compared to the faulted phase current. In the case of a double phase to



$n$  = number of detected fault loops

**Figure 3.21**  
Phase selection procedure of modern numerical distance relay (principle)

ground fault, the currents in the two faulted phases are larger and nearly in phase opposition (120 to 180° dependent on the earthing conditions).

In this way the faulted phase(s) can also be discriminated with high load and long lines where the load and fault impedances are close together. This is even possible in the extreme case where the fault impedance is higher than the load impedance [5.21].

In reality, the selection process is more complex and also includes adapted selection criteria for faults during the single pole dead time.

#### *Representation of the starting characteristic*

The overcurrent and under-impedance starting is usually depicted in a  $U/I$  diagram (figure 3.17). If one assumes a given fixed source impedance, the  $U/I$  characteristic may be transposed into the impedance plane (figure 3.22). In this case the following relationships apply:

Overcurrent starting:<sup>1</sup>

$$|Z + Z_s| \leq \frac{1.1 \cdot U_N}{I_{>>}} \quad (3-3)$$

<sup>1</sup>  $1.1 \cdot U_N = E$  corresponds to the effective voltage of the in-feed generator which typically is 10% above the system voltage (refer to IEC 60909, guides for short-circuit calculation). In special cases the actual generator effective voltage may be relevant.

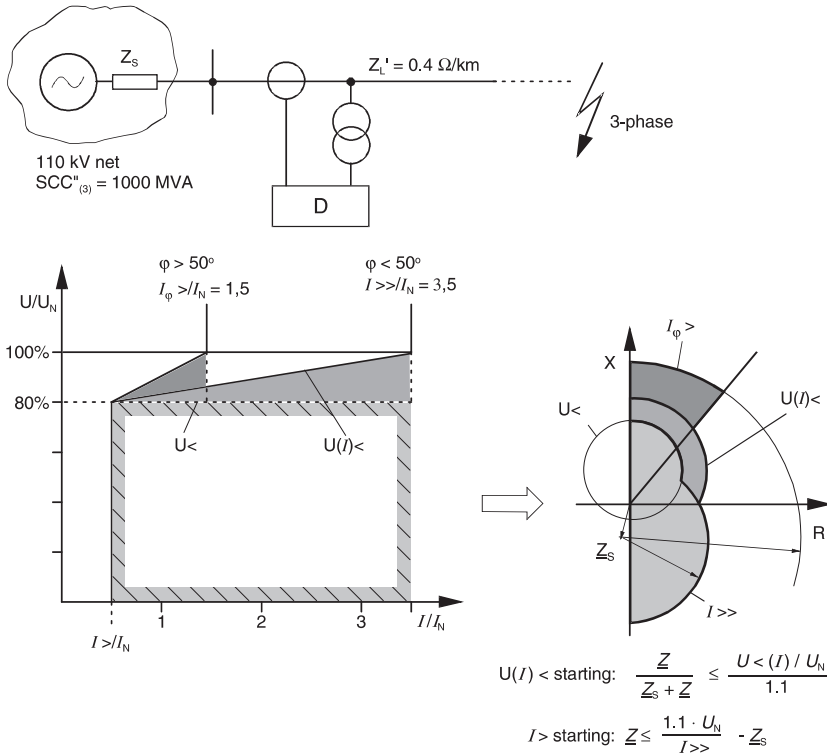


**Figure 3.22** Representation of the  $U/I/\varphi$ -starting in the impedance plane

Undervoltage starting:

$$\left| \frac{Z}{Z_s + Z} \right| \leq \frac{U </U_N}{1.1} \quad (3-4)$$

These always result in circles as shown in figure 3.22.

An approximation of this characteristic can be done by a step-wise approach with the known equation.

This representation in the impedance plane is not common. The advantage of the under-impedance starting particularly lies therein that it's setting is based on current and voltage limits, which depend on the rating of the plant (e.g. permissible over-current of a transformer) or known operating data (e.g. permissible undervoltage in the system) and can therefore be easily derived therefrom.

The reach of the starting characteristic during faults in the system must be determined with a short-circuit current computation.

The impedance starting is naturally always represented in the impedance plane. It has the advantage that the reach on the protected circuit is independent of the source impedance, and that it has a fixed relation to the impedance zones. Furthermore power

swings in the system and their influence on the distance protection are for instance more clearly represented in the impedance diagram, because inter alia the known power swing blocking functions are based on impedance measurement (refer to paragraph 3.1.11).

Conversely it is however not possible to establish in reverse an overloading of the plant from the impedance diagram. This implies that it is for instance not possible to define, for the load despatch centre, a current at which the line protection will trip during an overload condition.

The phase selectivity of the starting plays an important role. It is absolutely imperative for the loop selection in the switched distance protection. With under-impedance starting it is easier to achieve this than with impedance starting, where the elimination of apparent impedances in the healthy phases must be considered (refer to figure 3.19). This was probably, amongst others, a reason for the introduction of under-impedance starting in Germany, where compact switched distance relays have always been implemented in large numbers on meshed medium and high voltage networks.

In other countries the distance protection was practically only used on the transmission system and was always non-switched. A strict phase-selective starting was therefore not necessary, as single-phase auto-reclosure was seldom implemented.

With numerical relays a new situation arose.

With the introduction of intelligent algorithms, for instance an additional impedance comparison, it became possible to achieve absolute phase selectivity with impedance starting without restrictions on the settings.

Ultimately both types of starting characteristic have their advantages and disadvantages.

A preference for the one or the other is largely explained by historical developments.

While the under-impedance (voltage–current dependent) starting is preferred in Germany and in some of its neighbour countries, the rest of the world has always preferred impedance starting.

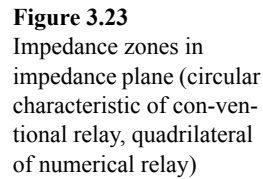
### **3.1.7 Distance zones (steps)**

Figure 3.2 already showed the stepped characteristic of the distance protection.

This corresponds to a set of impedance characteristics in the impedance plane. The origin ( $R = 0$ ;  $X = 0$ ) in the impedance plane corresponds to the relay location, from where the distance is measured.

Figure 3.23 shows the quadrilateral characteristic of a modern numerical protection in comparison to the circular characteristic of a mechanical protection (R1KZ4).

The reach of the protection along the protected feeder always corresponds to the intersection of the relay characteristic with the line that represents the impedance course of the feeder.



Graphical methods were therefore resorted to. At present computer programs are sometimes used. The quadrilateral characteristic (polygonal characteristic) on the other hand has independent settings for  $R$  and  $X$  reach. It is therefore possible to achieve sufficient arc compensation for every line length.

$$x_2 = X_{A-B} + 0.5X_{B-C}$$
$$R_2 = R_{A-B} + 0.5R_{B-C} + R_{ARC2}.$$

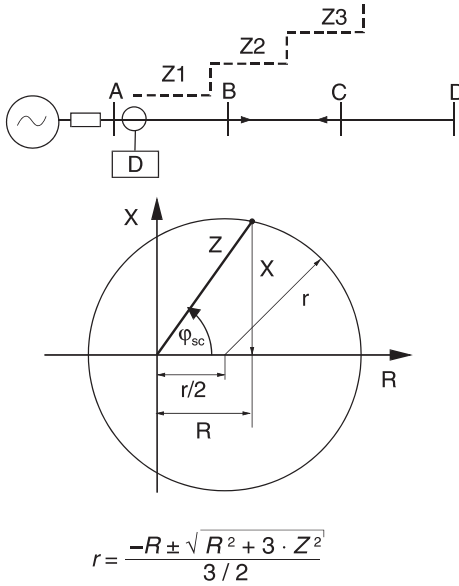


**Figure 3.24**  
Offset impedance circle

Calculations of the settings for numerical protection with quadrilateral characteristics (7SA5 and 7SA6) are therefore substantially simplified. Over and above this, substantially more flexible adaptation to the given system conditions is possible.

A complete distance relay usually contains the following zones (figure 3.25):

- *Starting zone ( $Z_A$ )*  
Only in the case of impedance starting will this starting zone have a fixed characteristic in the impedance plane. The under-impedance starting is represented separately in the  $U/I$ -diagram.  
The starting zone is not required in case of “zone packaged” relay design, i.e. when each zone operates independently (see next paragraph). Instead, a fourth offset zone may then be provided for non direction back-up (7SA522).
- *Staggered distance zones ( $Z_1, Z_2, Z_3$ )*  
Including one under-reaching fast tripping zone (non-delayed) and two over-reaching zones with time-delays. These zones are all directional and usually set in the forward direction.

In many cases only three zones are really used, in particular when breaker failure protection is provided (US practice):

- 1<sup>st</sup> zone: forward under-reaching, undelayed ( $Z_1, t_1 = 0$ )
- 2<sup>nd</sup> zone: forward overreaching, delayed ( $Z_2, t_2$ )
- 3<sup>rd</sup> zone: non directional offset, delayed ( $Z_3, t_3$ )

In Europe, where breaker failure protection was not generally applied in the past, three zones were graded in forward direction and the starting zone together with the directional characteristic were used as far reaching, long time delayed directional



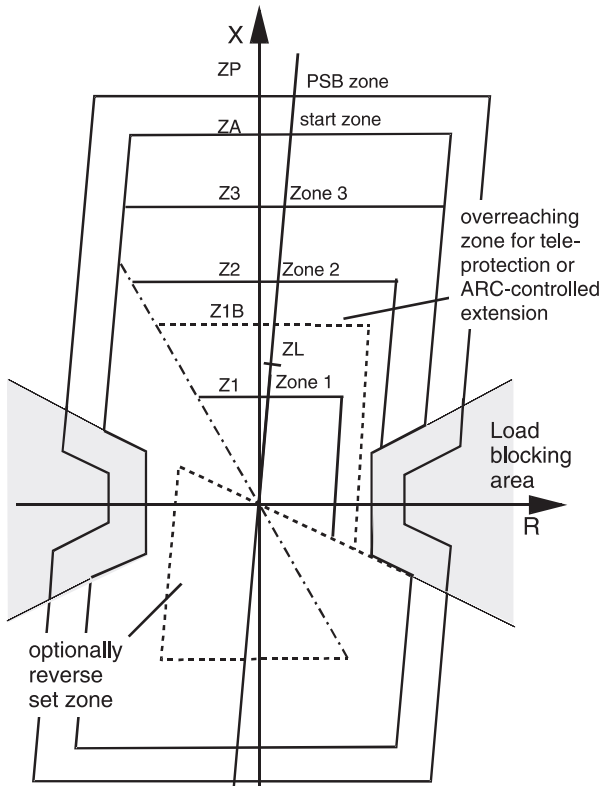


**Figure 3.25**  
Zones of a numerical  
distance protection  
(shaped quadrilateral  
as an example)

and non-directional back-up. This practice has been maintained in most cases, even where the integrated BF protection of numerical relays is used.

Numerical relays allow the selection of each zone in either the forward or reverse direction. This is useful for special applications, e.g. at a bus-coupler or a transformer. With conventional relays this was only possible with the high voltage graded relays (e.g. 7SL24), and then only for one zone.

- *A time-independent over-reaching zone ( $Z_{1B}$ )*  
for a permissive protection scheme (teleprotection) (refer to paragraph 3.1.10), or auto-reclose controlled zone extension (refer to paragraph 3.1.12).
- *A zone for the power-swing blocking ( $Z_P$ )*  
This zone is located around the starting zone in such a manner that a gap equal to  $\Delta Z$  exists between the power-swing zone and the starting zone.

The operating mode of the power-swing blocking function is explained in paragraph 3.1.11.

- *A directional stage with distance relay starting and time setting longer than zone timers*  
The starting combined with the directional characteristic makes up the directional back-up zone in the forward direction. This is utilised as a time-delayed back-up zone following the third distance zone.

In the case of impedance starting this is a true distance zone with a defined reach.

When over-current starting is used, this zone corresponds to a directional time over-current protection, and when under-impedance starting is used, this zone corresponds to a directional voltage-controlled time over-current protection.

- *A non-directional stage with distance relay starting and time setting longer than zone timers*

This non-directional stage is the so-called ultimate back-up, in case none of the prior stages detect the fault. The starting zone corresponds to a non-directional distance zone with associated long time delay or a non-directional time delayed over-current protection, when under-impedance starting is used.

### **3.1.8 Zone- and timer-control**

The functioning of the distance zones must be controlled by the zone-timers and possibly co-ordinated by release or blocking signals from the protection at the opposite line-end. Different device structures result, depending on whether only one measuring system for all zones is available, or whether a separate measuring system is provided for each zone.

In the case of numerical relays, these fundamental structures of the classical technology can be found in the software.

#### *Fault-detection dependent control of the zones and timers*

European manufacturers prefer a fault-detection dependent release and control of the zones and timers. This was necessary with conventional technology, as the relay was only provided with one single or one multiple-phase distance measuring system, the reach of which was switched by timers to the respective higher reaches of the following zones. The fault detection in this case also controls the timers. This implies that the zone timers were simultaneously started and stopped by the fault detection. Furthermore, an external zone-switching by an external ARC-device or a signal from the protection in the opposite station was possible.

Once a trip command was issued by a zone, it was maintained as long as the fault detection took to reset, i.e. until the fault is cleared, even when the impedance had previously left the relevant zone.

This fault detector dependent logic in the static analogue protection had the advantage that the tripping relays could be operated by two independent criteria (fault detection and distance measurement), in a two out of two configuration. This eliminated the possibility of an over-function in the case of component failure.

The additional phase selection task in connection with switched protection is discussed in the next chapter.

The basic philosophy of fault detector dependent logic was still employed in the software of the earlier numerical relays 7SA511 and 7SA513, the difference being, that all zones are available simultaneously and therefore need not be switched by the criteria referred to, but rather only need to be released or blocked. In this way for example, the

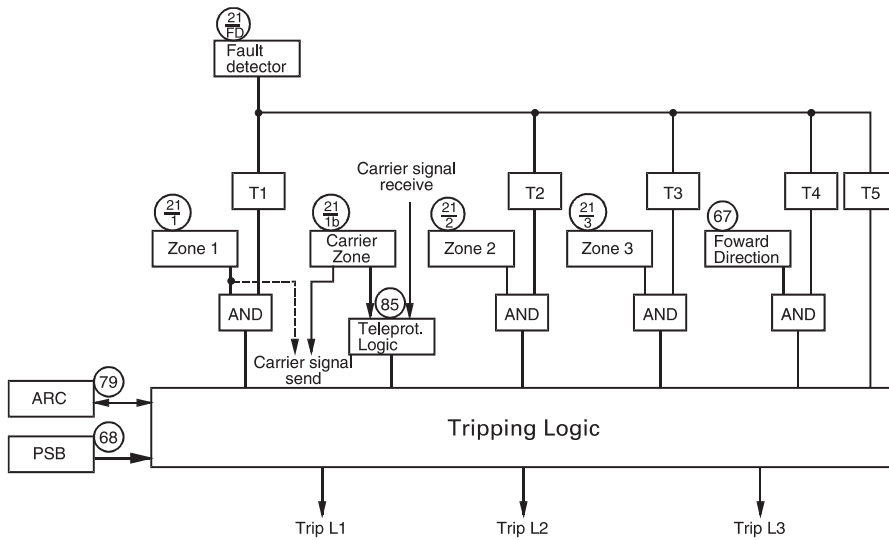


**Figure 3.26** Fault detector controlled timing (7SA511, 7SA513)

under-reaching fast tripping zone and the over-reaching zone for the permissive tripping scheme are simultaneously and independently available and controllable. The resulting structure is shown in figure 3.26.

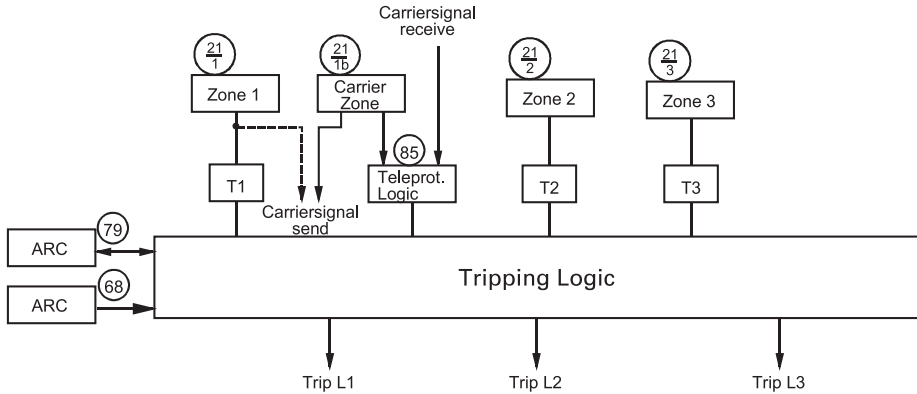
### *Zone-dependent logic*

This technique was already employed by conventional protection in Anglo-Saxon countries (zone-packaged relay). In this case, one multiple-phase measuring system was provided for each zone. A fault detection as described above, did not exist. Each zone controlled its own time delay and the tripping relays.

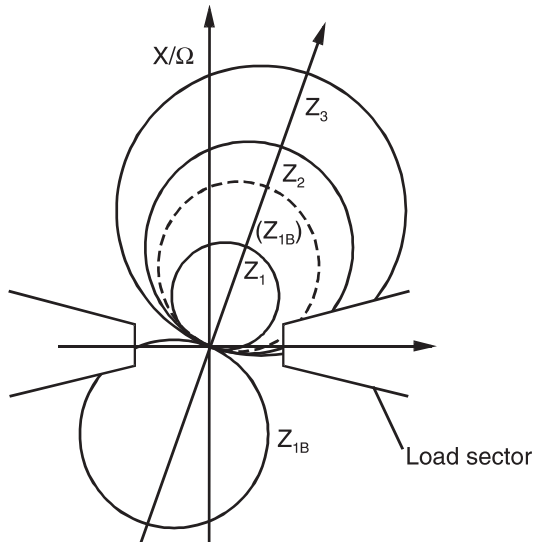
This philosophy had the advantage that in the case of the failure of one zone, the other zones provided independent redundancy. The concept was perfectly suited to the electro-mechanical technology, which tended to under-function. In the case of the analogue static technology, the resulting parallel connections of many independent measuring systems resulted in a tendency to over-function. With numerical technology, this problem is avoided by the integrated self-monitoring.

The structure for this zone-dependent logic is shown in figure 3.27.

The numerical relays 7SA522 and 7SA6 are designed along this structure. The zones function independent of each other, with their own time delays. They only have in common a load-blocking zone which excludes impedances in this range for all zones (figure 3.28) as well as a power-swing zone which automatically positions itself around the largest zone (figure 6.13, paragraph 6.3.6). A fault detection zone as found in the 7SA511 or 7SA513 does not exist in these relays.



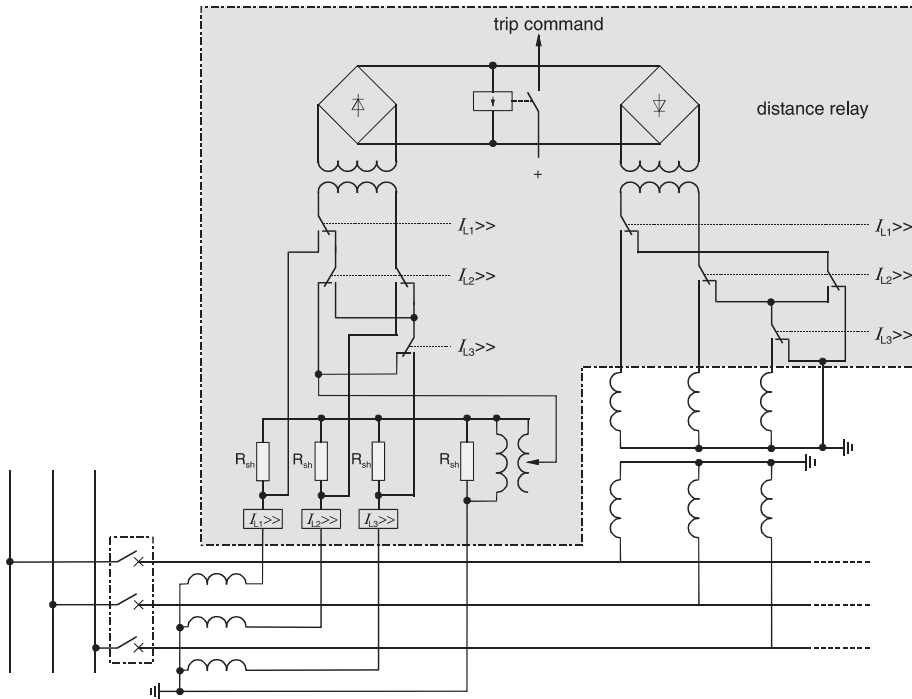
**Figure 3.27** Zone dedicated time control (7SA522 and 7SA6)



**Figure 3.28**  
Zones of a starter independent distance relay

### 3.1.9 Switched and non-switched distance protection

The switched distance protection in conventional technology had only one measuring system for distance or direction. The measuring quantities, voltage and current, had to be selected according to the fault type and switched to the measuring system. Figure 3.29 shows the selection circuit of electro-mechanical distance relays in its simplest form. Only the distance measurement is represented. The selection circuit for the directional determination is similar. The switching relays are in this case controlled by over-current starters dedicated to each phase ( $I >>$ ). High voltage graded relays used under-impedance starters including sensitive earth current detectors and a correspondingly extended selection circuit.

**Figure 3.29**

Electro-mechanical switched distance protection, measured value switching (principle)

The selection relays did not directly switch the CT secondary currents but their proportional shunt voltages. This was to avoid switching of high currents or opening of CT circuits.

The analogue static (solid state) protection devices implemented transistors for the measured value switching without the use of contacts (relays).

By selecting the measuring quantities and switching them to the measuring systems only after pick-up of the starting elements, the begin of the distance measurement is always delayed. In addition, the measurement has to be somewhat delayed (e.g. measurement of two half-cycles), to prevent mal-operations during changing of fault condition. In terms of modern relaying, the operating time of this kind of electro-mechanical distance relays was relatively slow, typically 40 to 60 ms. Static versions however reached already 25 ms as shortest operating times.

Relays with this construction (electro-mechanical: R1KZ4, R1Z23, static: 7SL17, 7SL24) are designated as “distance protection with selection logic” or more commonly, switched distance relays. A large number of these relays are still in service on medium and high-voltage circuits (figures 3.30 and 3.31).

Similarly, for numerical protection the designation “single system” distance protection defines a protection relay that only calculates a single loop-impedance, controlled by the starters (earlier type 7SA511).



**Figure 3.30**  
Electro-mechanical distance relay for  
HV systems (7SL93), without front cover



**Figure 3.31**  
Analogue static (electronic) distance relay  
for HV systems (7SL73), front view

In the case of numerical protection there however is a crucial difference to the analogue protection:

- the measured values of all fault loops are continuously sampled and stored in cyclic buffers. The distance measurement therefore has continuous access to these measured values without the need to first select them by switching (non-switched relay)
- measurement-repetition is no longer linked to the cycle and may be executed in shorter intervals
- the result is that there is only a small difference in tripping-times (7SA511: 25 ms compared to 7SA6: 15 ms)

Electro-mechanical distance relays with three-measuring systems (e.g. Siemens type R3Z27) have been implemented in EHV-systems. The three-measuring systems normally measure the three phase-to-phase loops and revert to the three phase-to-earth loops when the earth-current starter picks up. As a result of the fixed allocation of the measuring systems to the phases, no phase selection is required.

In this manner it was possible to substantially reduce the tripping times compared to a single system switched relay (from 60 to a shortest tripping time of 25 ms).

This three-system measurement has the additional advantage of being able to detect and trip two simultaneous, separately located earth-faults (e.g. a simultaneous earth-fault on a double circuit feeder where on circuit 1 phase L1 to ground and on circuit 2 phase L2 to ground are faulted). With a single-measuring system protection these two faults can only be cleared in sequence.

In systems with isolated/Peterson-coil earthed star-point, this type of behaviour is not desired because only one of the two simultaneous earth-faults must be tripped. The remaining one of the simultaneous earth-faults must self-extinguish or be cleared by manual switching. To this end, in each case, a particular phase is preferred for tripping in the entire system (refer to preference circuits, paragraph 5.2.2). This implies that for systems with isolated/Peterson-coil earthed star-point the elaborate multi-measuring system protection has no advantages in itself. Therefore the single-measuring system (switched) distance protection has traditionally been implemented in these systems. For the sake of completeness, it must be noted that in exceptional cases, a multiple measuring system protection (7SA513, 7SA6) is also implemented on Peterson-coil earthed systems so that during a simultaneous earth-fault, both faults are cleared at the same time.

With analogue electronic (static) technology (7SL31/32) six measuring systems were introduced i.e. in this case a separate measuring system was dedicated to each fault-loop (L1-E, L2-E, L3-E, L1-L2, L2-L3, L3-L1).

In the case of numerical protection (7SA522, 7SA6 and earlier 7SA513) this practically corresponds to the simultaneous computation and evaluation of all six fault-loops. Relays of this design were called “non-switched”.

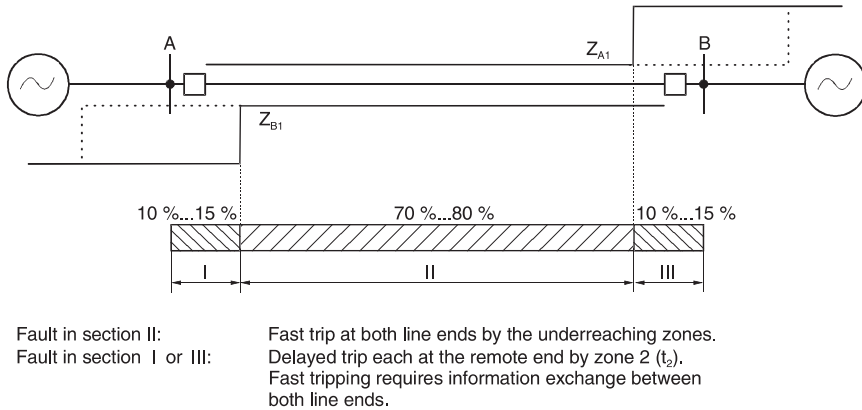
With conventional relay technology the term “full scheme distance protection” existed. It referred to a distance protection which contained for each fault type and distance zone a separate measuring system i.e. in the case of three distance zones eighteen measuring systems.

Thereby under- and over-reaching distance zones are available simultaneously and in parallel. For instance an independent under-reaching zone and an over-reaching zone for teleprotection are available concurrently.

With numerical protection this advantage of concurrent availability of all zones is achieved with significantly reduced effort. With the numerical relays a single fault impedance is computed, valid for all zones, and its position relative to the zones is determined by simple threshold comparison.

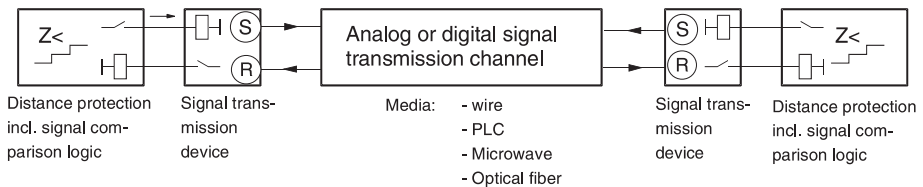
#### **3.1.10 Distance protection with signalling channels**

High speed unit protection is an essential requirement for efficient operation of transmission and sub-transmission lines. Plain distance relays with normal time-stepped zone grading enable fast fault clearing only on 70 to 80% of the line length (figure 3.32) [3-5, 3-6]. By using communication channels for the end-end exchange of information, a teleprotection scheme can be formed capable of selectively clearing all faults on the protected feeder without time-delay (figure 3.33).

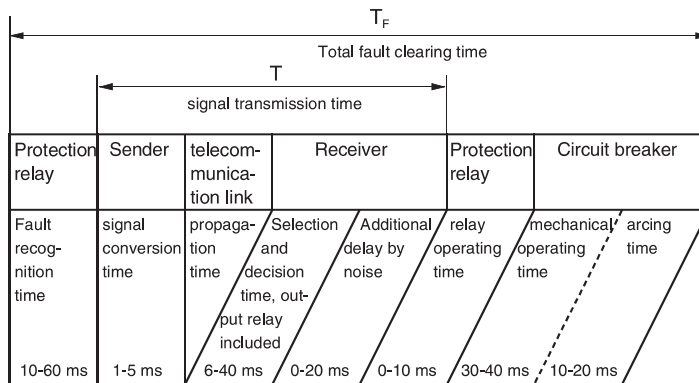
**Figure 3.32**

Plain distance protection with time stepped zone grading: Line sections of fast and delayed tripping

In such a system the protection must transmit either a release (permissive) or blocking signal, depending on whether a permissive or blocking scheme is implemented. In any case only simple YES/NO signals must be transferred.



a) Protection communication system



b) Operating times

**Figure 3.33** Distance protection using communication



Traditional teleprotection schemes have been using analogue signal transmission technique, mostly PLC (power line carrier) channels. State of the art, however, is now digital communication via dedicated optic fibres and data communication networks.

The following communication media apply:

- Pilot wires (special protection signalling cables with screening and isolation against induced voltages) for distances up to approximately 25 km
- PLC channels (power line carrier transmission on high voltage OH lines) for distances up to approximately 400 km
- Directional radio for up to approximately 50 km (line of sight); longer distances via relay stations.
- Dedicated optical fibres up to approximately 150 km; longer distances with repeater amplifiers.
- Digital data transmission networks

The signal transmission time on voice frequency protection data transmission devices (*VF intertrip*) is approx. 15-20 ms. On these channels frequency shift is used as a modulation technique which gives good immunity against interference. Voice frequency channels can be carried by single-sideband PLC (power line carrier), analogue microwave or pilot wires.

In the case of PLC *with direct* (“ON/OFF”) *keying* of the high-frequency carrier (amplitude modulation) the transmission time is reduced to approx. 5 ms. As a result of the lower security against mal-operation (over-function) this method is however only used with blocking systems (especially in the USA).

Data communication via optical fibres with digital transmission has introduced a realm of new possibilities:

- *Dedicated optical fibres* offer ideal conditions in terms of speed, security and dependability. There is practically no interference and by coding the transmitted data, extremely high security is achieved. Signal transmission time is below 5 ms.

Modern numerical relays can be equipped with optic communication modules for direct end-end connection over distances up to about 100 km. External communication devices are in this case not needed.

- Special optic communication devices using laser diodes reach distances of about 150 km without intermediate repeater stations.

Currently, most utilities have *digital communication networks* at their disposal. These may also be used for protection purposes in the TDM<sup>1</sup>-mode. For signal transmission via a number of sub-links in the network, total transmission times to the order of 5ms may arise. Careful planning and checking of dependability and security is necessary in each case. The bit error rate of transmission networks is considerably higher ( $10^{-6}$ ) compared to dedicated optic fibre ( $10^{-9}$ ). Channels may be switched, resulting in change of data transmission time, and the loss of clock or the synchro-

---

<sup>1</sup> Time-Division Multiplexing

nism may cause longer down times in the order of one second. A fixed point to point connection ( $n \times 64$  kbit/s synchronous) with X.21 or G.703 compatibility provides the best solution.

The following methods can be distinguished:

### **Permissive intertrip**

In this case the under-reaching distance zone (usually the first zone) directly trips the circuit-breaker at the local end, and simultaneously sends a signal to the remote end. The received signal from the remote end is used to achieve fast tripping when the fault is close to the remote end, beyond the reach of the under-reaching zone. This permissive system therefore achieves very fast tripping times independent of the signal transmission time on approx. 85% of the protected feeder. On double circuit overhead lines one must however consider that the reach of the first zone may be shortened in case of earth-faults (refer to paragraph 3.5.3).

For the inter-tripping of the circuit-breaker at the remote end, the following possibilities exist:

#### *Direct underreaching transfer trip (DUTT)*

In this case the circuit-breaker is directly tripped by the received signal.

This direct tripping without consideration of any protection criteria at the receiving end, is only used in exceptional cases, as an erroneously received signal would cause an immediate incorrect trip of the circuit-breaker.

An application of this system is therefore only conceivable, when there are no current and voltage transformers available at the remote end, for the connection of a protection relay.

Often two separate transmission channels are used to achieve better security. At the receiving end the signals are logically connected to an AND-gate (e.g. connection of the receive contacts in series).

Alternatively a signal transmission channel with absolute security can be utilised, for example a digital signal transmission via optical fibre with secure transmission protocol (protection communication device SWT 2000 D).

#### *Permissive underreaching transfer trip (PUTT) with starter (fault detector)*

With this method, the received signal only causes tripping of the circuit-breaker when the distance protection relay starters have picked up i.e. a fault has been detected (figure 3.34).

In the case of a single-phase tripping application, the fault detectors also serve the purpose of phase selectors i.e. the received signal in the case of a single-phase fault only causes tripping of the faulted phase. For multiple-phase faults, the tripping of all three breaker poles is initiated.

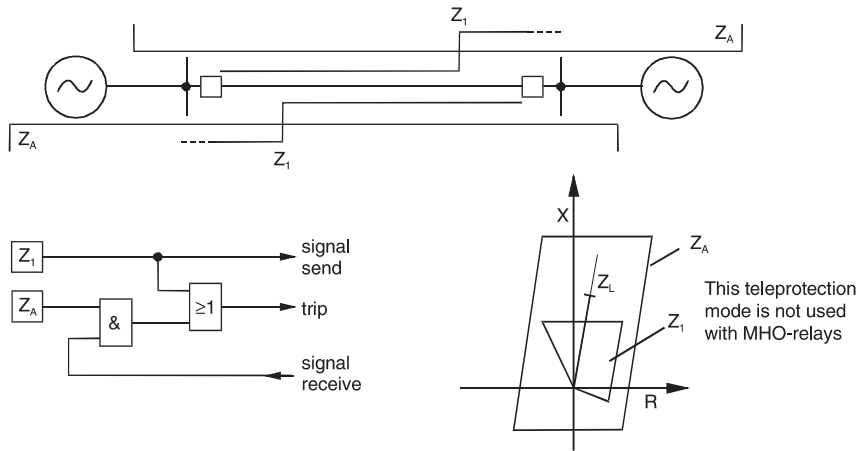


**Figure 3.34** Distance protection with communication, PUTT with starter

### Permissive underreaching transfer trip (PUTT) with zone extension

In this case, the received signal releases an over-reaching distance zone to trip the circuit-breaker (figure 3.35). Conventional relays achieve this by switching over from the first zone to the over-reaching zone. Numerical relays merely release the over-reaching zone in the tripping logic. The remaining time-graded zones are still independently available (also refer to the explanation in paragraph 3.1.9).

PUTT in conjunction with a dedicated over-reaching zone has the advantage of a more selective trip-release in comparison to PUTT with distance relay starters. The trip release is limited to faults in the forward direction within the reach of the over-reaching

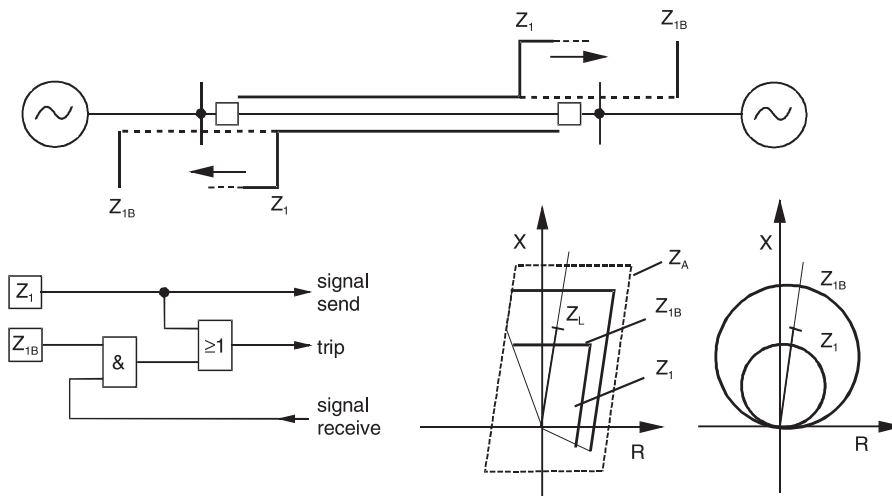


**Figure 3.35** Distance protection with communication, PUTT with overreaching zone

zone i.e. essentially limited to the extent of the protected feeder. Starters however also operate during remote faults in the system. The likelihood of an over-trip when an incorrect signal is received is therefore higher in this case.

With conventional relays the disadvantage was, that following the change-over from the under-reaching to the over-reaching zone, a new measurement had to take place, causing an additional time-delay in the order of tens of milliseconds.

With numerical relays this is however no longer true, as the distance measurement for all zones is simultaneously available. For this reason, the permissive under-reach method with an over-reaching zone is recommended.

### Permissive overreaching transfer trip (POTT)

With this method an over-reaching distance zone is released by the received signal.

In the classical sense, this method only achieves fast tripping when the relays at both ends of the feeder detect a fault in the over-reaching zone and send each other a release signal (figure 3.36). This method is preferred for short feeders, especially when the overhead line or cable is so short that the under-reaching zone can no longer be used because the smallest setting is not sufficient.

In the case of conventional protection with circular characteristic, the additional disadvantage with small distance settings was the poor arc resistance compensation. For this reason the permissive over-reach transfer trip method was already employed on feeders shorter than 20 km, although the under-reaching zone setting would have been possible.

In the case of numerical relays with polygon (quadrilateral) characteristic, this argument is no longer valid, i.e. the permissive over-reach transfer trip method is recommended only for very short overhead lines or cables.

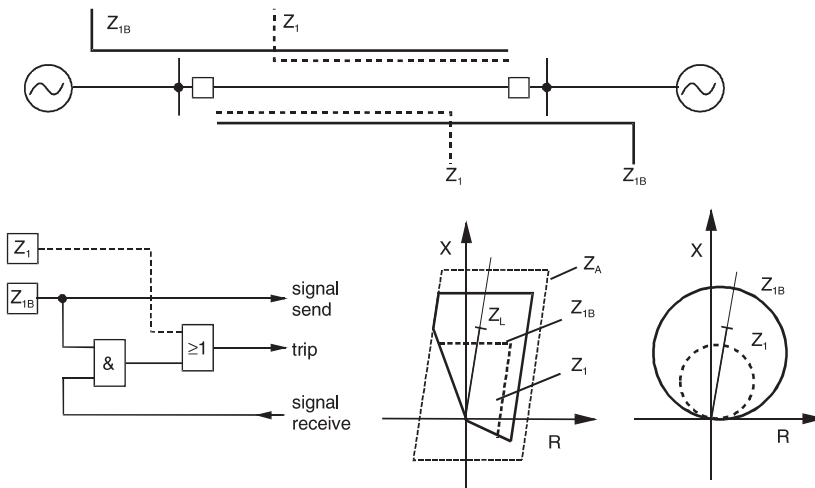


**Figure 3.36** Distance protection with communication, POTT

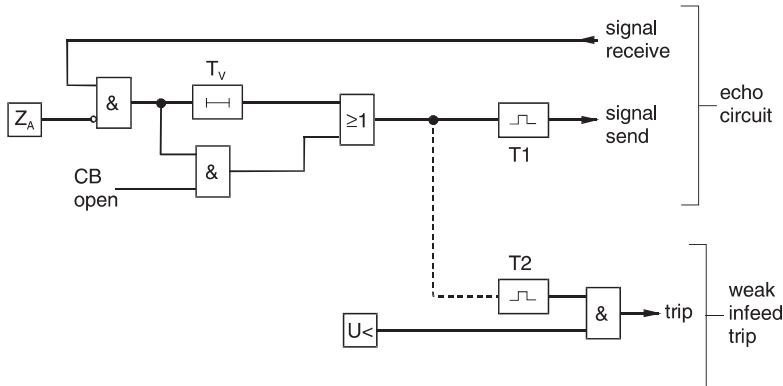


**Figure 3.37** POTT, supplementary functions

A special case for the application of permissive over-reach transfer trip is given when fast tripping must be achieved on a feeder that has a weak in-feed at one end. In this case an additional echo-circuit with tripping supplement must be provided at this end (figure 3.37).

During a fault behind the weak in-feed end, short circuit current flows through the protected feeder to the fault location. The protection at the weak in-feed end will start with this current and recognise the fault in the reverse direction. It will therefore not send a release signal to the strong in-feed end. The permissive over-reach transfer trip protection therefore remains stable.

During an internal fault on the other hand, the protection at the weak in-feed end will not pick up, as insufficient current flows from this side into the feeder. The signal received by the weak in-feed end is returned as an echo and allows the tripping at the strong in-feed.

Simultaneously with the echo, the circuit-breaker at the weak in-feed end may be tripped by the protection. To achieve this, the tripping function shown in figure 3.37 (weak infeed supplement) must be configured. The condition for trip-release and phase selection is an internal voltage drop detector.

The permissive over-reach transfer trip protection requires some co-ordination of the protection and signal transmission channel to prevent signal racing during system switching and changing of fault nature.

Figure 3.38 shows a typical case that may occur during the clearing of an external fault:

During the fault short-circuit current flows on the healthy feeder from A to B, as the fault is located close to B. The signal state shown in figure 3.38a occurs.

If the protection or the circuit breaker on the faulted feeder at B reacts faster than at A, a current reversal on the healthy feeder occurs, resulting in the change of signal state shown in figure 3.38b.

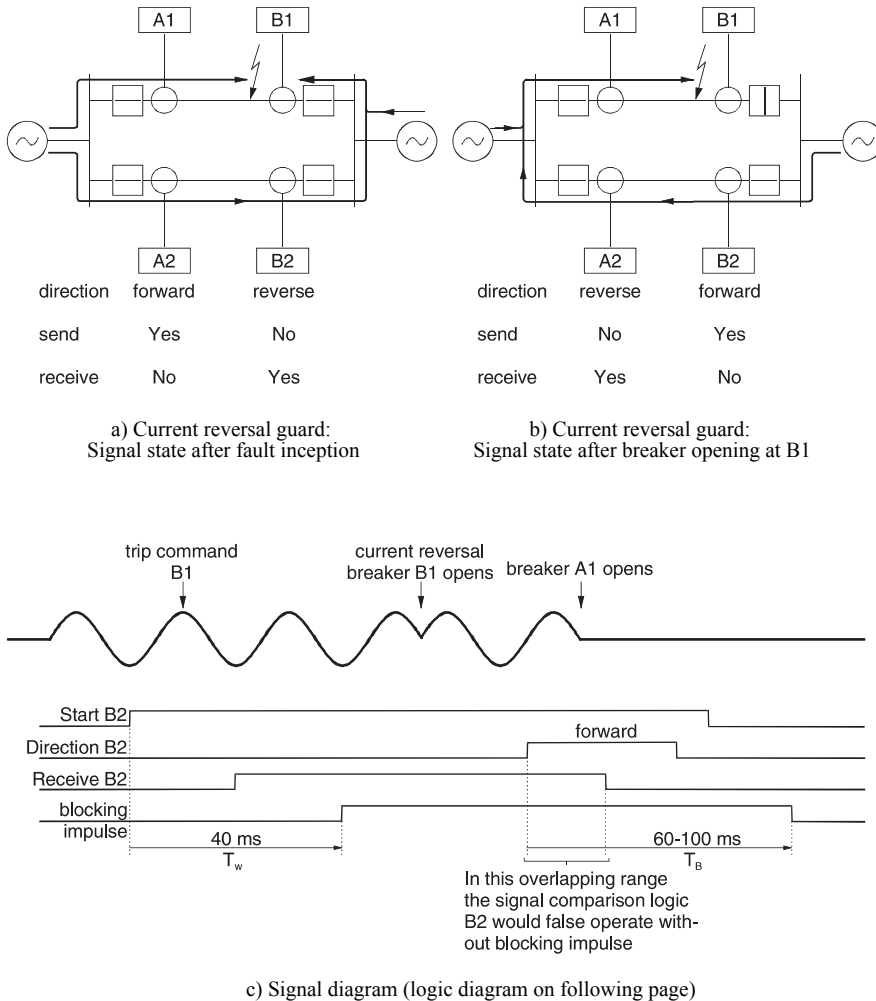


**Figure 3.38** Current reversal guard monitoring for permissive over-reach transfer trip protection

Signal racing occurs. This may lead to an incorrect trip when for example the protection at B has already changed over to the forward direction, while the receive-signal at B is still present. This sequence is to be expected due to the unavoidable drop-off delays of the protection at A and the signalling channels.

For this reason a monitoring supplement is required which detects external faults and then blocks the permissive over-reach transfer trip protection for a short time during which a current reversal could occur (figure 3.38c).

The logic diagram is shown in figure 3.39. The waiting time  $T_w$  (e.g. 40 ms) considers the transmission delay of the remote end signal and makes sure that blocking is not started in case of an internal fault. It should however not be set longer than the breaker time, so that the transient blocking signal has been started before current reversal can

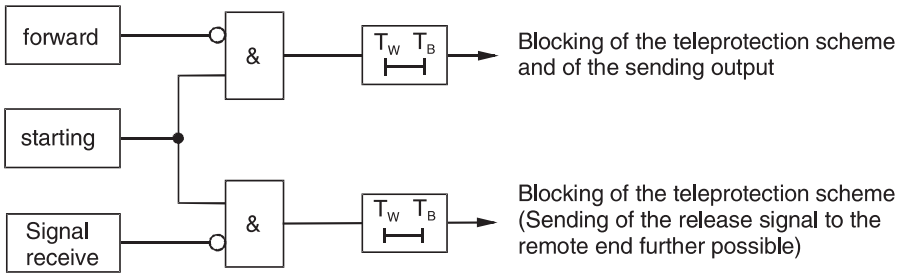


**Figure 3.39** Current reversal guard for POTT, logic diagram

occur. If one of the two criteria for external faults hangs on longer than  $T_W$ , the transient blocking time  $T_B$  is started. It should cover the clearance time of an external fault with certain security margin (e.g. 150 ms)

*Permissive over-reach (POTT) with pilot wire inter-tripping*

On medium-voltage level, e.g. with cables in urban areas, the distance protection is occasionally employed with POTT utilising pilot wire as the signalling channel (figure 3.40). Signal exchange between the two line ends is achieved by looping current from one of the station batteries via the pilot cable through receive relays in both stations.

In the quiescent state the pilot wire is monitored by the DC current flowing through it (relay K2 at both ends picked up).

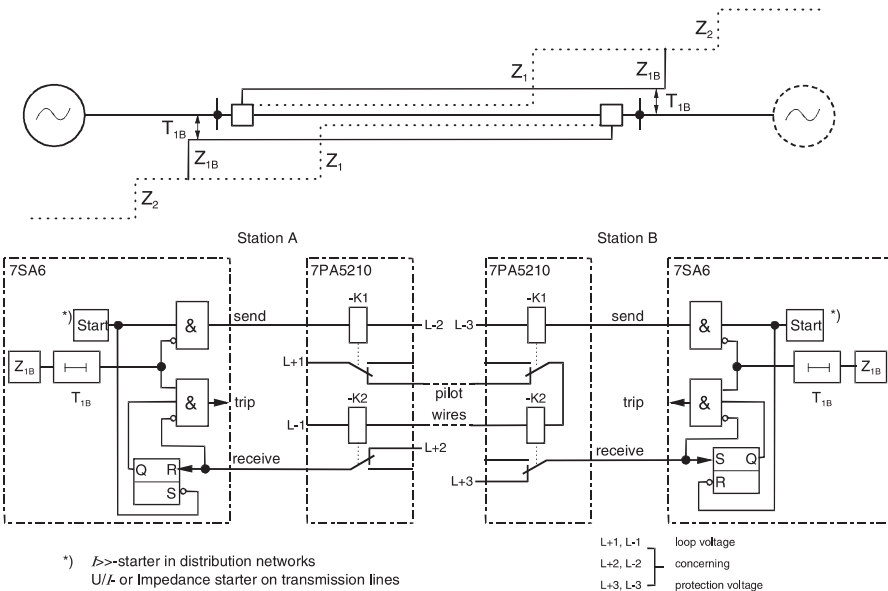


**Figure 3.40** Permissive overreach with pilot wire inter-tripping

Following pick up of a distance relay, the current loop is initially interrupted (relay K1 picks up, K2 drops off). It remains interrupted during external faults. With an internal fault, after the co-ordinating time  $T_{IB}$  the overreaching zone ( $Z_{IB}$ ) will again turn off the relays K1 at both ends. Thereby the current loop is closed again. The K2 relays at both ends pick up again and release the trip signal.

Fast tripping is also achieved for single ended in-feed.

### Blocking techniques

For these systems, the signal transfer is utilised to block the protection during external faults.

#### *Distance protection with blocking (directional comparison blocking)*

This procedure requires two distance zones:

1. A fast starter zone which sends the blocking signal to the remote end when the fault is outside the protected zone, in the reverse direction.
2. A directional over-reaching zone in the forward direction, which inhibits the blocking signal during faults in the forward direction, and initiates tripping of the circuit-breaker if no blocking signal from the remote end is present.

Figure 3.41 shows the classic arrangement of the zones for a MHO relay along with the associated logic of this procedure.

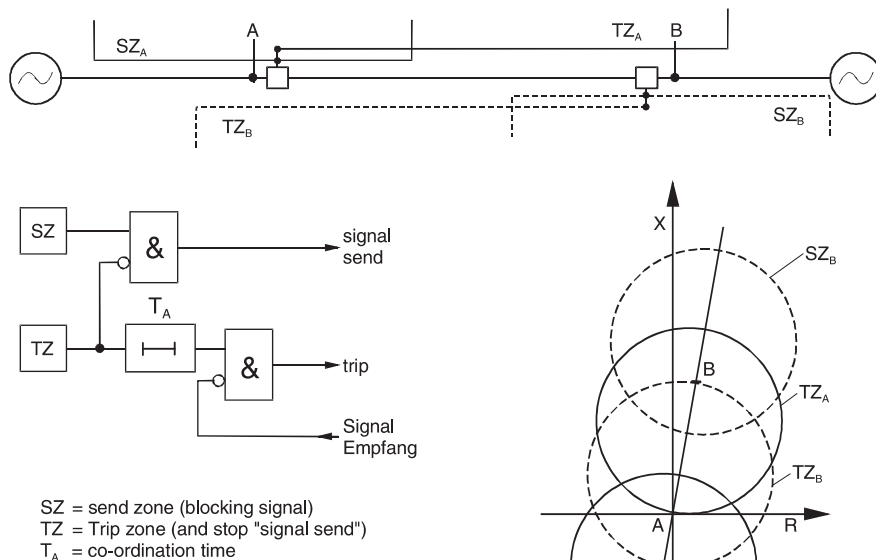


**Figure 3.41**  
 Classic blocking procedure with  
 MHO-characteristic (e.g. 7SA522)



The reverse reach of the blocking signal transmitting zone must be greater than the over-reach of the tripping zone of the relay at the remote end.

Typical settings are:

- tripping zone: 130%  $Z_L$
- reverse reach of the blocking zone 50%  $Z_L$

Ideally, the blocking signal should only be transmitted, when the fault is outside the protected zone, in the reverse direction. With conventional relays the transmitting zone however employed an off-set in the forward direction, to ensure that close in reverse faults are securely detected, and also to increase the speed of this transmitting stage for these close in faults. This was the consequence of directional measurement with voltages in the short circuited loop. The small voltage signal does not allow a secure directional decision. A fast earth-current detector is frequently used as an added signal transmit criterion for the blocking signal during earth-faults.

Consequently close in faults on the protected feeder may initially result in transmission of the blocking signal, which however resets as soon as the forward reaching stage picks up.

The speed of the transmitting stage is a decisive criterion along with the signal transmission time, as these determine the delay of the tripping stage:

$$T_A = T_{\text{send zone}} + T_{\text{channel}} - T_{\text{trip zone}} + \text{security margin (5 ms)}$$

The significant advantage of the blocking procedure is that no signal needs to be transferred during faults on the protected feeder. On power line carrier (PLC) channels therefore, no signal needs to be sent through the fault location.

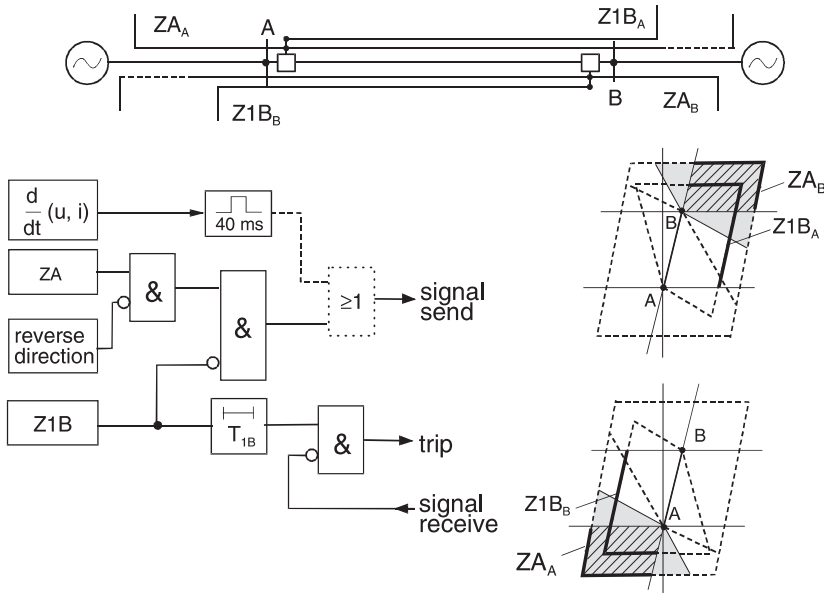
For this reason it is possible to use PLC with single-phase coupling direct to the protected circuit.

The classic application of the blocking principle utilises a simple, but fast PLC channel (< 5 ms) with amplitude modulation. An additional advantage of this method is that the same carrier frequency may be used at each end of the feeder (also on three-ended feeders), as it is immaterial for the blocking technique, from which transmitter the blocking signal is received.

Figure 3.42 illustrates the implementation of this technique with polygonal characteristics of numerical protection. The starter zone for transmission of the blocking signal is defined by the reverse portion of the fault detector, limited by the directional characteristic.

As the directional measurement utilises healthy phase voltages thereby achieving absolute selectivity also for close in faults, the transmission of the blocking signal only occurs for true reverse faults.

The 7SA522 and 7SA6 relays contain an additional jump detector for voltage and current, thereby achieving a fast start of the blocking signal within 5 ms of fault inception. The trip signal delay can therefore be extremely short.

**Figure 3.42**

Distance protection in a blocking scheme with quadrilateral characteristic (7SA522)

The tripping stage is formed by the directional over-reaching zone Z1B.

From figure 3.42 it is evident that the starter zone has a reverse setting, such that it encloses the overreaching tripping zone of the relay at the remote end with a security margin for all faults.

#### *Distance protection with unblocking (directional comparison unblocking)*

The blocking procedure referred to above has the disadvantage that during unfaulted system operation, no signal is transmitted. The communication channel is therefore not monitored.

The unblocking technique was especially developed for voice frequency channels with frequency shift keying, and does not have the disadvantage referred to above.

In addition, this technique is also somewhat faster, as a continuous monitoring signal (pilot) is transmitted. During internal faults, the signal is changed to a permissive signal similar to the POTT method. This implies that no trip delay is required to wait for an eventual block signal.

This procedure is illustrated in figure 3.43. Only a single directional overreaching zone per line-end is required. When the system is not picked up, the channel supervision frequency  $f_{CS}$  is transmitted and tripping is blocked.

Following an internal fault, the overreaching zones Z1B at both line ends pick up, and key their respective frequencies from  $f_{CS}$  to  $f_{UB}$  (unblock).

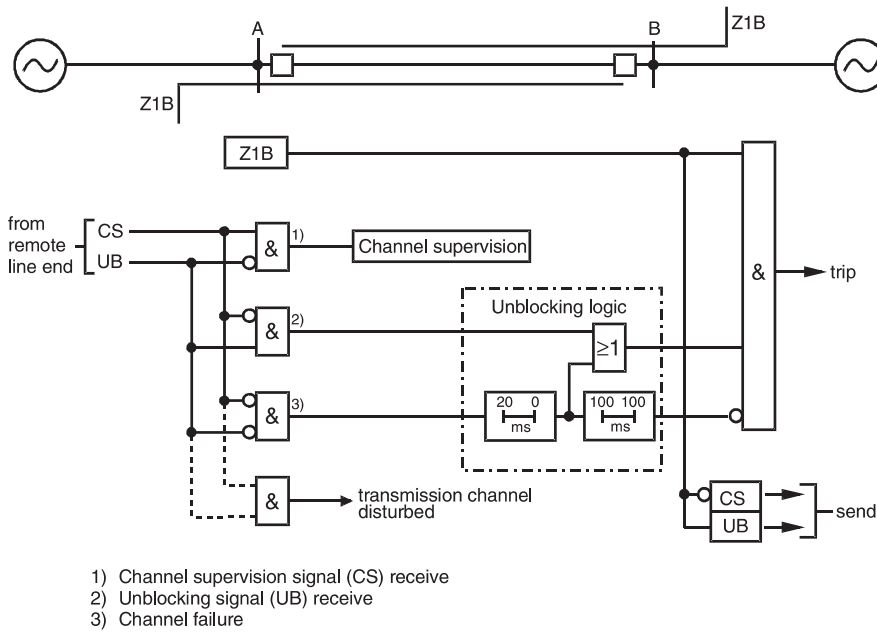


**Figure 3.43** Distance protection in an unblocking scheme

Thereby tripping at both line-ends is achieved (refer to logic diagram in figure 3.43).

During external faults, the Z1B does not pick up (fault in reverse direction), or no unblocking frequency signal is received (fault located behind the remote end).

If Z1B has picked up, and neither  $f_{CS}$  nor  $f_{UB}$  are received (corresponds to channel failure during a system fault), it is clear that the signal could not be transmitted through the fault location i.e. the fault must be on the protected feeder.

The logic is implemented, so that 20 ms after channel failure, it releases the zone Z1B for a period of 100 ms. If this happens during a fault, then tripping will occur. If channel failure occurs during normal system operation, no consequences arise because Z1B is not picked up. 100 ms later, the protection is again blocked for the duration of the channel failure. This blocking is removed (reset time of 100 ms) when a signal is again received.

A simultaneous reception of  $f_{\text{CS}}$  and  $f_{\text{UB}}$  is interpreted as a channel error, and does not cause any further reaction by the protection.

### 3.1.11 Power swing blocking, power swing tripping (out of step protection)

Figure 3.44 illustrates the voltage diagram of an overhead line under load. The connected networks are represented by the two equivalent sources  $E_1$  and  $E_2$ . The source impedances  $Z_{S1}$  and  $Z_{S2}$  correspond to the respective short-circuit power of the two sources. The angle  $\vartheta$  is referred to as the transmission angle. As the transferred real power increases, this angle becomes larger.

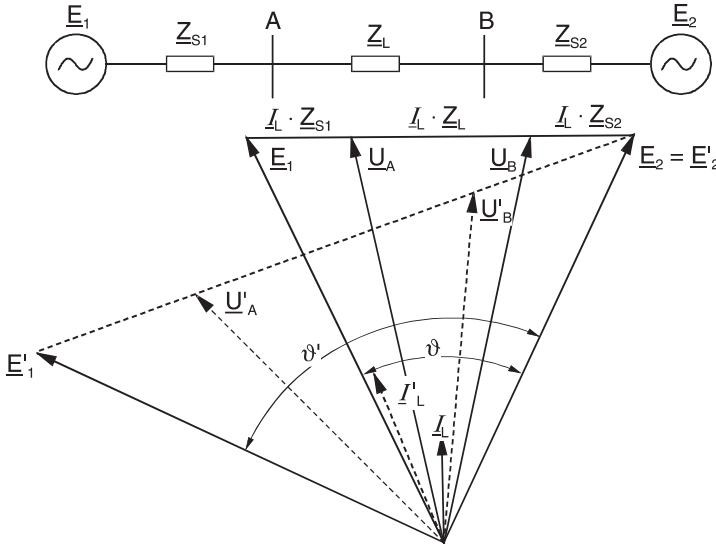


**Figure 3.44** Power swing condition in a transmission system: voltage diagram

The transferred power is defined by the equation below (loss-free line):

$$P_{TP} = \frac{E_1 \cdot E_2}{X_T} \cdot \sin \vartheta \quad (3-5)$$

$$\underline{X}_T = \underline{X}_{S1} + \underline{X}_L + \underline{X}_{S2} \quad (3-6)$$

### Static stability

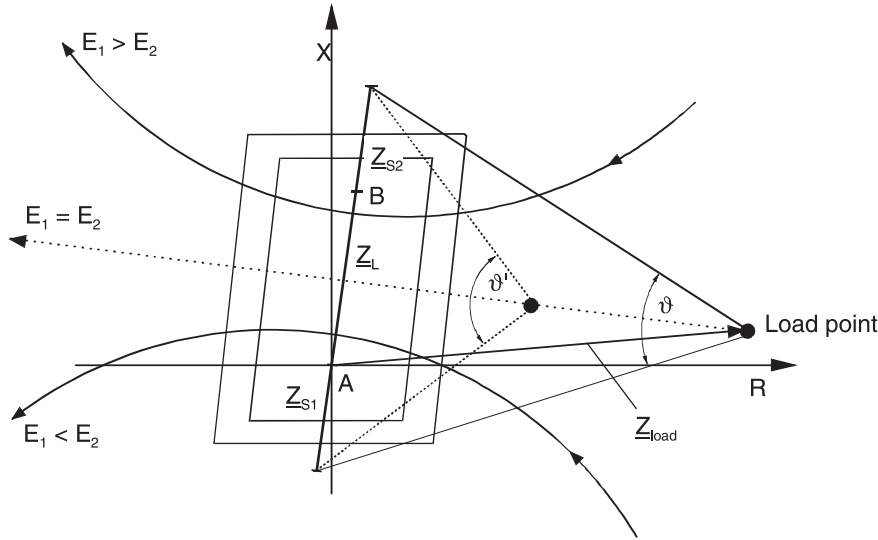
The maximum power transfer is therefore achieved with the angle  $\vartheta = 90^\circ$ . At the same time this corresponds to the static stability limit. No stable operation can be maintained beyond this point.

In practice however one will hardly ever find operation above  $60^\circ$ , as a security margin to the stability threshold must be maintained.

If all the voltages are divided by the load current  $I_L$ , an equivalent impedance diagram of the line under load is obtained. The representation in the impedance plane is done such, that the distance relay under consideration is located in the origin of the co-ordinate system (figure 3.45).

With this representation, the load impedance measured by the relay is evident and it's distance to the relay starting characteristic can be determined.

When the load changes, the load impedance moves along the shown trajectories (circular path) [3-7]. If  $E_1 = E_2$ , which may be used as a first approximation for normal system conditions, the impedance follows a straight line which is perpendicular to the summated impedance  $Z_\Sigma$ . At the permitted maximum steady state power transfer, i.e.

**Figure 3.45**

Power swing process in a transmission system: Measured impedance in the relay R-X diagram

$\vartheta = 90^\circ$ , the load impedance should still maintain a security margin to the largest relay characteristic of approximately 20% ( $Z_{\text{load}} \cdot \cos \varphi_{\text{load}} \geq 1.2 R_p$ ), to prevent starting of the relay during load variations occurring during normal operations.

On double circuit feeders it must be noted that the value of the load impedance may be halved when one circuit is switched off.

The impedance settings in R-direction must correspondingly also be halved.

### *Dynamic stability*

Dynamic angle changes above  $90^\circ$  are permissible without resulting in network instability. This is based on the “equal area” criterion, which is referred to in figure 3.46. The transferred power is defined by the given equation and follows a sinusoidal curve depending on the transmission angle  $\vartheta$ . The rated operating point corresponds to the connected turbine power  $P_T$ .

The generators are accelerated when the transferred power is smaller than the mechanical power from the turbines. This is the case during a short-circuit, when the voltages collapse (Area A). Conversely, the generators will be retarded during the dead time of the auto-reclose cycle (Area B), and following successful auto-reclosure of the feeder (Area C), because the transferred power in this case is greater than the connected turbine power. The generators return to their stable initial operating point as long as the retarding (braking) area (B + C) remains larger than the accelerating area (A).

Clearly, this will only be the case if the fault in a power system is rapidly cleared (critical fault clearance time).

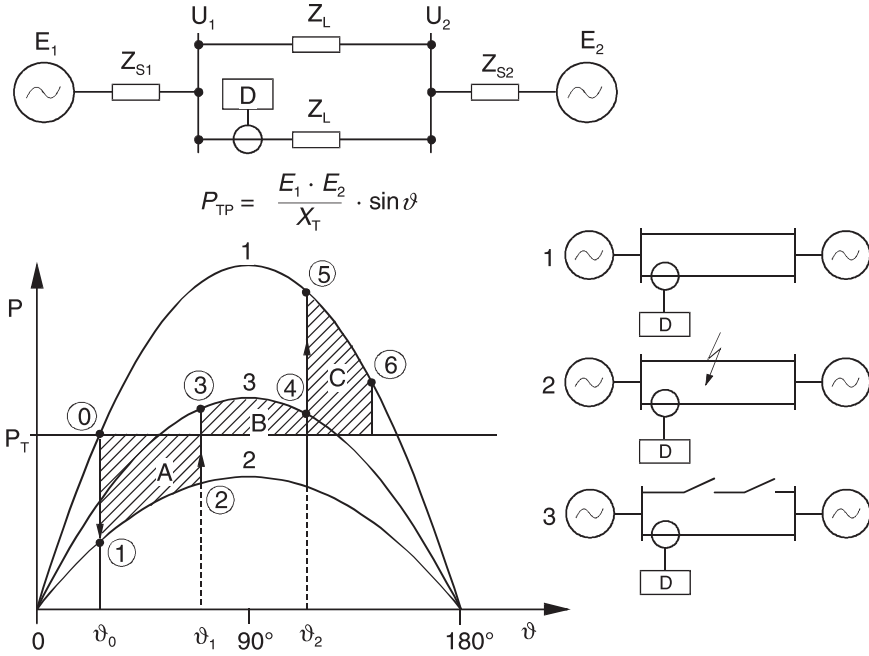


**Figure 3.46** Dynamic system stability, Equal area criterion

### Power swing blocking

The power swing process described above, is shown as an impedance curve in figure 3.47.

During steady state operation, the relay measures the load impedance at the power transfer angle  $\vartheta_0$ .

At fault inception, the impedance initially jumps to the fault impedance, which is recognised as an external fault by the relay (1). After the circuit-breakers on the faulted feeder have been tripped (2) by their protection, the impedance seen by the protection jumps back to a load impedance (3), which now corresponds to the larger power transfer angle  $\vartheta_1$ , and the larger transfer impedance (previously:  $Z_T = Z_{S1} + Z_L/2 + Z_{S2}$ , subsequently:  $Z_T = Z_{S1} + Z_L + Z_{S2}$ ). The transmission angle now moves on to  $\vartheta_2$  (4) as a consequence of the further in leading direction advancing generator rotors.

Following ARC of the feeder, the load impedance vector jumps to the new position (5), and moves further from there into the starting characteristic of the distance protection (6).

If no tripping ensues, the load impedance vector returns to its initial stable position.

If the load impedance vector enters and remains within the corresponding distance protection zones for a sufficient period of time, protection tripping may occur.

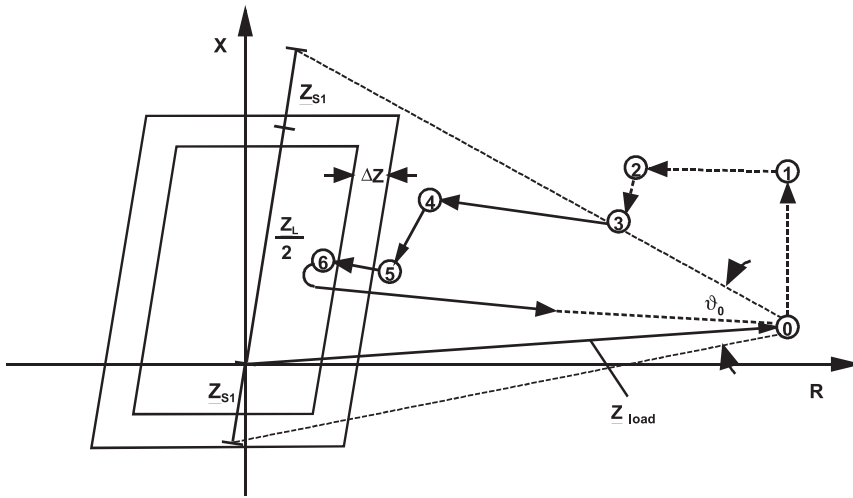


**Figure 3.47** Course of the power swing vector in the impedance plane

Tripping during the power swing may be inhibited by the so-called power swing blocking function. It's mode of operation is based on the fact that after fault inception, the impedance immediately jumps from the operating point to the short-circuit impedance inside the distance protection characteristic. Conversely, during a power swing, the impedance vector exhibits a steady progression. It's rate of change corresponds to the power swing frequency of the system.

By measurement of  $dZ/dt$  or  $\Delta Z/\Delta t$  and comparison with a threshold, it is possible to distinguish between short-circuits and power swings.

The simplest method for this measurement is to determine the elapsed time required by the impedance vector to pass through a zone limited by two impedance characteristics. For this purpose a power swing characteristic is provided. This power swing characteristic encloses the starting characteristic with a fixed distance of  $\Delta Z$ . The time difference  $\Delta t$  is measured (figure 3.47).

The time will be shorter, if the power swing is faster.

To detect large power swing frequencies, the setting of  $\Delta Z$  should be as high, and the setting of  $\Delta t$  as short as possible.

Typical settings are  $\Delta Z = 10\text{-}20\% Z_A$  and  $\Delta t = 20\text{-}40\text{ ms}$ . With these settings, power swings from 2-3 Hz can be detected.<sup>1</sup>

With special measuring techniques, faster power swings up to approx. 7 Hz may be detected (7SA513 and 7SA522). In this case a continuous measurement of  $\Delta Z/\Delta t$  in short intervals (5 ms) is required.

<sup>1</sup> In the case of 7SA511  $\Delta t = 35\text{ ms}$  is fixed.  $\Delta Z$  and the largest  $\Delta Z/\Delta t$  must be set (refer to example in chapter 6.3.6).

Once a power swing is detected, the blocking signal must be maintained until the load impedance vector (in this case power swing vector) exits the starting characteristic. Alternatively it is also possible to remove the blocking signal after a fixed time delay.

The power swing blocking naturally entails the risk, that a genuine short-circuit during the blocking time will not result in tripping. The power swing blocking condition is only generated by balanced symmetrical three-phase system conditions to avoid this. Unbalances ( $> 25\%$ ), or occurrence of earth-fault current remove the power swing blocking condition immediately.

Furthermore, the continuity of the power swing condition may be monitored (7SA6 and 7SA522). If a jump occurs, the blocking condition is removed immediately. Thereby even the unlikely event of a three-phase short circuit occurring, while the power swing vector is inside the starting characteristic of the protection is detected.

Ultimately, it is possible to select which zones of the distance protection will be blocked by the power swing blocking function, i.e. all zones, only the first zone or all zones except the first zone. Sometimes the first zone is not blocked when the transmission angle needs to achieve a very high value (close to  $180^\circ$ ) to initiate tripping (small reach of the first zone in R-direction). In this case it is assumed that the system will no longer remain stable, and therefore tripping is desired.

Blocking of the higher zones is not required when no slow power swings are expected in the system, i.e. the power swing vector exits the relevant zone before the set zone time has expired.

In principle, these limitations originated from conventional methods, where unbalance and discontinuity monitoring were not yet implemented. It was therefore not possible to exclude the eventuality of blocking the tripping of a system fault during the power swing. When the system conditions demand a power swing blocking function, it is recommended to select the blocking of all zones with the digital relays, as the course and frequency of power swings depend on the system constellation and can therefore never accurately be predicted in advance.

In stable systems with strong in-feeds and without long transmission paths, power swing blocking is not required. In Germany such power swing blocking systems are no longer in service.

### **3.1.12 Distance protection with automatic reclosure**

Distance protection is mostly implemented on overhead line systems with automatic re-closure systems (ARC). With conventional relays a separate ARC device was required. In digital relays, this function is integrated.

#### *Three-phase ARC*

In medium and high-voltage systems, without effective earthing, the three-phase ARC modus is implemented in Germany. This technique is also implemented on earthed systems in some other countries, especially in the USA.



With this technique, all short-circuits are tripped three-phase, and automatically re-closed after a dead time between 0.3 and 0.5 seconds. The de-ionising time of the arc at the fault location is approx. [3-8]:

$$t_{3\text{-pole}} = 210 + 0.6 \cdot \text{kV} [\text{ms}] \quad (3-7)$$

To isolate the fault location, and to prevent energy from flowing into the arc, so that the arc can extinguish, both line ends must be tripped without delay.

This is for example possible with one of the described permissive tripping schemes, if a suitable signal transmission channel is available.

At the lower voltage levels, this option is mostly excluded due to cost considerations. In this case distance protection is operated in the zone extension mode. With this method line faults ( $F_1$ ,  $F_2$ ) are tripped by an over-reaching distance zone  $Z_{\text{OVER}}$  (approx. 120%) without time delay at both ends of the line (figure 3.48). During the dead time the reach of the undelayed tripping is restricted to the usual under-reaching zone  $Z_{\text{UND}}$  (80-90%). The protection therefore is selectively graded at re-closure: If the short-circuit is still present after reclosure (unsuccessful ARC) the protection will trip according to the usual time grading.

Following the initial fault inception, a certain risk of also tripping system faults beyond the next station ( $F_3$ ) with the over-reaching zone, exists. This would lead to an unwanted ARC on the corresponding in-feed.

Apart from the short supply interruption at this station, there are no other detrimental consequences. The likelihood of these unnecessary ARC's is in any event very limited in meshed systems, as the over-reaching area is very small due to the effect of additional in-feeds (refer to paragraph 3.5.2).

With conventional relays, the technique of extending or reducing the fast tripping zone exists. This depends on whether the undelayed trip zone was activated by the starter following fault inception or whether it was already active during the quiescent state.

With numerical relays, no zone switching is required. It is merely necessary to release or block the extended reach.

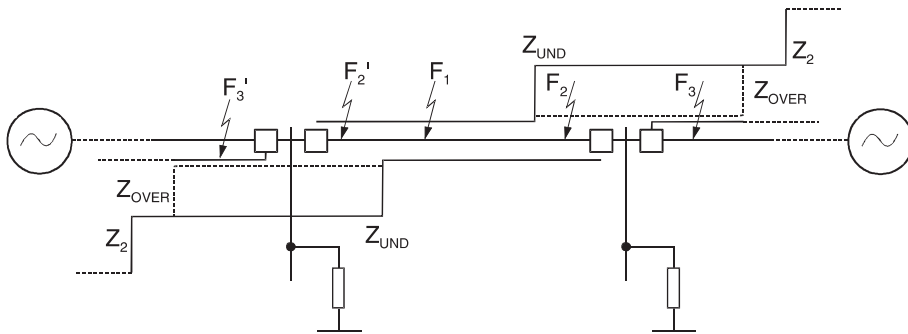


**Figure 3.48** ARC controlled over-reaching zone

*Delayed auto-reclosure*

In medium voltage systems it is common to implement a further delayed auto-reclose cycle, following a failed initial rapid auto-reclosure. To this end, the digital relays provide a separate settable stage.

*ARC on overhead lines with cable sections*

Auto-reclosure only makes sense following transient faults on overhead lines (especially for short-circuits following lightning strikes or flashovers to trees).

In principle there is no ARC for faults on cables.

Generally in the past, no ARC was implemented on overhead lines with cable sections, as the fault location is not known when the protection picks up.

With appropriate zone settings, the numerical protection 7SA is able to distinguish between the overhead line and cable section of the feeder. This allows ARC only for faults on the line section (refer to paragraph 5.2.1).

*Single-phase ARC*

In earthed, high-voltage networks and particularly in extra high-voltage networks single-phase ARC is generally implemented.

In this case, only the faulted phase is isolated, following a single-phase earth-fault. The dead time must in this case be longer than with three-phase ARC, because currents are induced via the healthy phase-conductors, which remain energised, and feed the arc (figure 3.49).

With increasing line length, this induction of currents is exacerbated, necessitating longer dead times. According to [3-9] the single-phase ARC results in successful fault clearance, when the following conditions are met:

$$I_{\text{ARC}}[\text{A}] \leq 43 \cdot (t_{\text{DT}}[\text{s}] - 0.2) \quad (3-8)$$

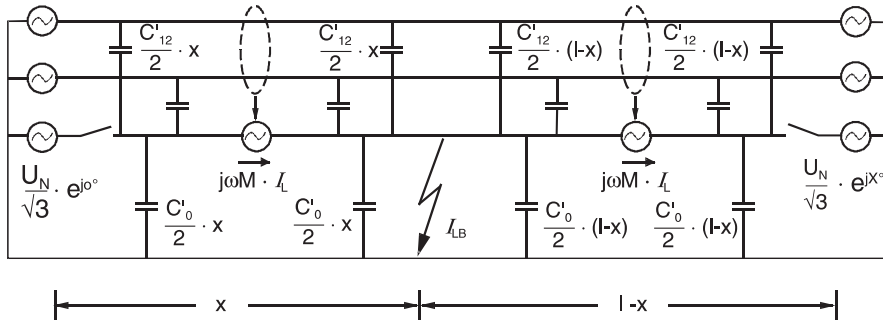
In this formula  $t_{\text{DT}}$  is the ARC dead time.

On long lines where, in addition, stability requirements necessitate short dead times, compensating reactors are required to reduce the arc current.

In Germany the system conditions obviate the need for compensation. The dead time is set to approx. 1 second.

Table 3.1 shows the line lengths up to which single pole ARC is possible dependent on the voltage level, without and with compensation reactors [3-10].

In particular cases, single-phase ARC is also implemented for two-phase faults without earth to for instance prevent three-phase tripping during conductor swinging (galloping). The distance protection relays 7SA facilitate this, whereby it can be selected, whether the leading or lagging phase is tripped.



induced capacitive arc current:

$$I_{LB,C} \approx \frac{U_N}{\sqrt{3}} \cdot \omega \cdot C_{12} \cdot l$$

induced reactive arc current:

$$I_{LB,L} \approx I_L \cdot j\omega M' \left( \frac{l}{2} - x \right) \cdot \omega \cdot (C_0 + 2 \cdot C_{12}) \cdot l$$

**Figure 3.49** Single-phase ARC, induced capacitive and reactive currents

**Table 3.1** Single-pole ARC, admissible line lengths

Rated voltage kV	Range of line lengths that do not require compensating reactors km	Range of line length where arc extinction without compensating reactors is not ensured km
765	0- 80	80-130
500	0-100	100-160
345	0-230	230-420
230	0-430	480-800

Single-phase ARC requires a strictly phase selective distance protection with the facility to trip each phase separately as already discussed in paragraph 3.1.9.

Furthermore the distance protection may not have a false pick up on the other phases during the single-phase dead time, as this would block the ARC in progress.

This is especially a problem on long, heavily loaded feeders.

For this reason conventional relays demanded a severe limitation of the reach in R-direction.

The numerical distance relays 7SA6 and 7SA522 automatically adapt to this situation: During the ARC dead time the residual current (earth-current) is eliminated from the impedance computation for the fault detection. Encroachment of the load impedance on the healthy phases into the starting polygon is thereby prevented.

Comment: If a directional earth-fault comparison protection is utilised (10-20%  $I_N$ ) it must always be blocked during the single-phase dead time to prevent incorrect tripping by this protection due to the load current flowing via earth. (In the 7SA6 and 7SA522 relays, the directional earth-fault comparison protection is integrated. The automatic blocking can be selected via setting parameter.)

With a single-system distance relay (7SA511) the phase selective tripping is always controlled by the fault detection (starters). In this case the ARC must be controlled by the fault detection.

With a full scheme distance relay fast tripping of a faulted phase is only possible when in addition to fault detection the fault is detected inside the relevant distance zone for this phase. The three-phase coupling during multiple phase faults is not done via the fault detection, but via the distance zones. This implies that the phase selection for tripping is improved in this case (figure 3.50a). It is possible to achieve correct single-phase tripping, even with fault detection in several loops.

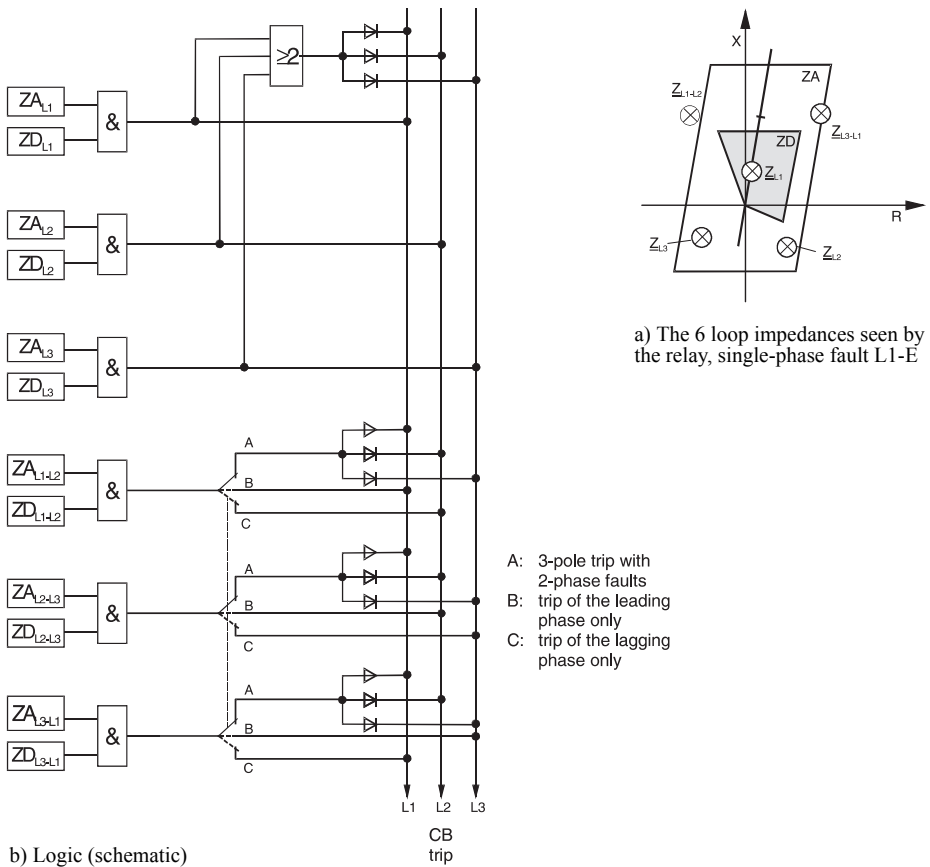


**Figure 3.50** Full scheme distance protection (starter controlled): tripping logic

### *Single-phase ARC during cross-country faults*

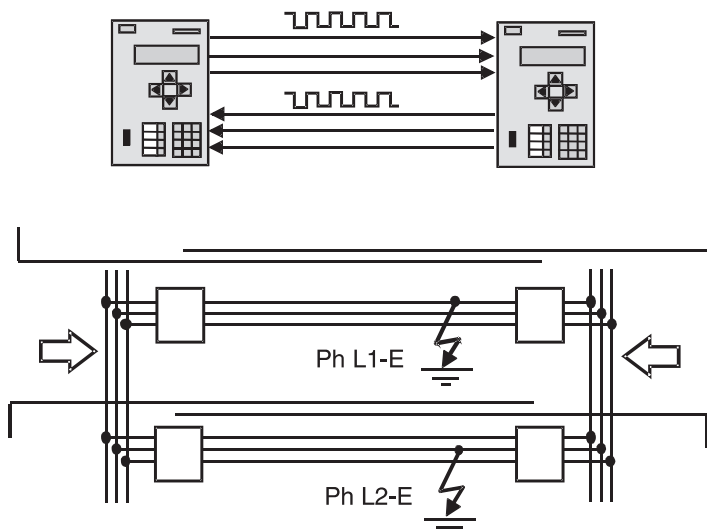
In earthed systems, double earth-faults at physically separated fault locations are rare. However, on multiple-circuit feeders they may be caused by backflash when the tower potential is raised, following a lightning strike. The likelihood of such an event is high when the tower footing resistance is high, e.g. in a rocky area.

In this case the control of the ARC function by the trip decision has an advantage because with these faults, multiple phase fault detection (e.g. L1-L2-E) is almost always present, while the tripping zone of the distance relay, despite over-reach setting (120%), will mostly not “see” this fault. A positive influence is the additional infeed effect in this case (see paragraph 3.5.2).

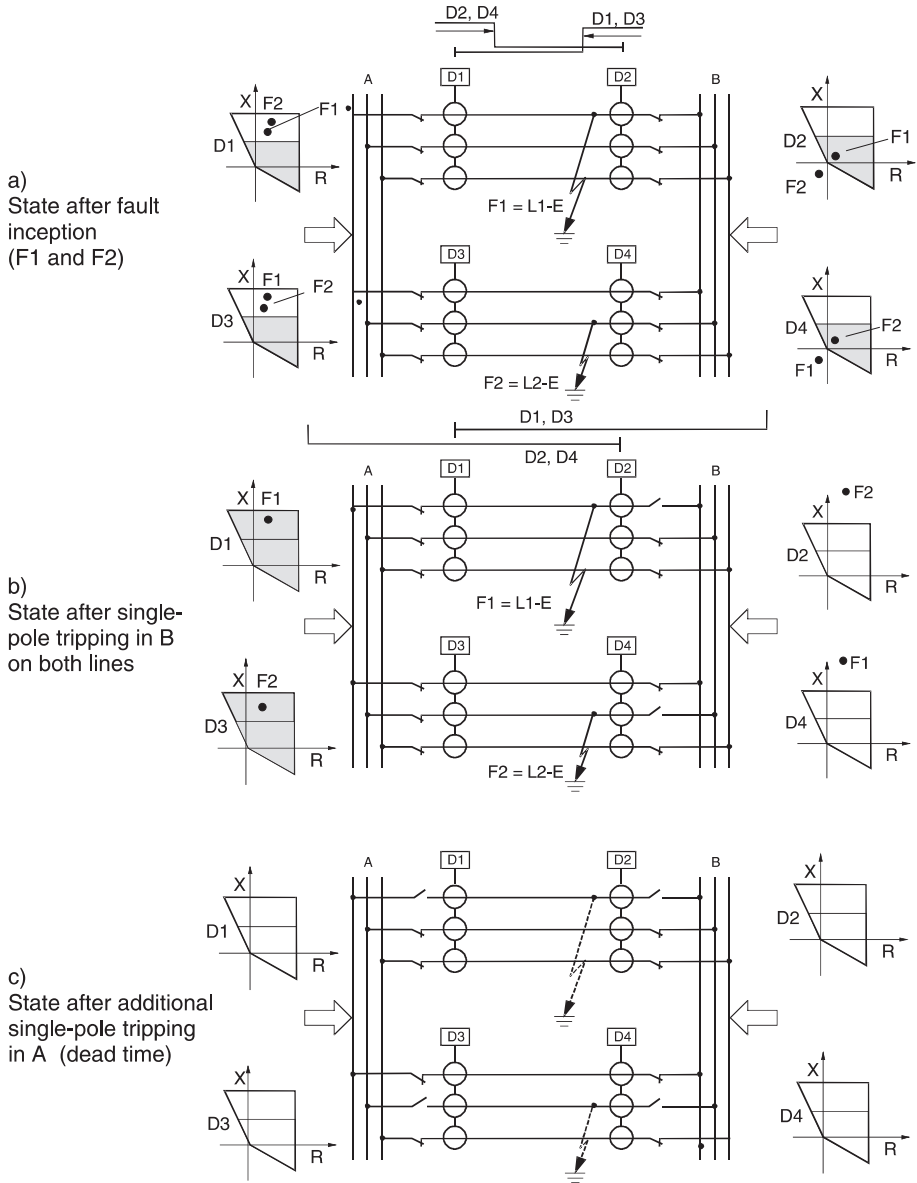
Protection in transmission systems usually employs signal transmission to achieve fast tripping on 100% of the feeder. Due to the utilised over-reaching zones, the described risk of non-selective tripping on cross-country earth-faults however remains. Using the zone extension in the PUTT scheme has an advantage over utilising the fault detection as tripping criteria. The extended distance zone is restricted (120%), while the fault detector reaches far into the network and picks up on remote faults.

Modern numerical relays (7SA6, 7SA522) now allow to set up teleprotection per phase with digital signal transmission. This ensures absolute phase selective tripping in case of cross-country faults independent of the location of the footing points. Figure 3.51 shows a phase segregated directional comparison scheme (POTT).

Selectivity during simultaneous faults on parallel feeders can also be achieved by using plain distance relays with zone extension technique. Figure 3.52 shows the tripping sequence for the crucial case of a close-in cross-country fault. The reach of distance zones along the lines is each shown on top of the line diagram. Additionally, the



**Figure 3.51** Phase segregated teleprotection with digital communication

**Figure 3.52**

Fault clearing sequence of a cross-country fault by distance protection with single phase ARC and recloser controlled zone extension

appearing fault impedances in each step of the fault clearing sequence are shown in the relay diagrams at both sides. The shaded areas each mark the effective zone reach.

In the operating mode “single-phase ARC”, the zone extension is only effective for single-phase faults. When a multiple-phase fault is detected (fault L1-L2-E in the example), the over-reaching zone is reduced to an underreaching zone, prior to release of the

measured signal, thereby reverting to normal underreach grading (figure 3.52a). The external fault is therefore no longer detected within the fast tripping zone, and selective single-phase tripping occurs at side B on each line (figure 3.52b). After that, the fault picture changes and the relays in A detect a single phase fault. They therefore extend the zone reach again and trip the faulted phases also phase selectively. The cross country fault is then selectively cleared leaving a complete three-phase system in operation (figure 3.52c). Finally, ARC ensues on both circuits.

The only disadvantage of this technique is that the remote fault is detected and tripped only after the circuit-breaker at the opposite end has opened (cascaded tripping).

The numerical distance relays have the advantage that both under- and over-reaching zones are available simultaneously. The starter function is therefore not needed for zone “switching” (release of under- or overreaching zone), it can be controlled by the zones themselves. The impedance reach of fault detection is therefore considerably reduced. External footing points in the middle part of the parallel line will then no more be detected. Delayed sequential tripping will then only occur for extremely close-in faults, and then only for the protection at the remote end.

On permissive tripping schemes, absolute selectivity during cross-country faults can be achieved in a similar manner. When two phase to ground fault detections take place simultaneously, while only a single-phase fault is situated in the forward-reaching tripping zone, transmission of the permissive signal is delayed.

### *Single-and three-phase ARC*

General practice in Germany is to employ single-phase ARC in earthed systems only for single-phase faults (in exceptional cases also for two-phase faults). In other countries (e.g. USA) three-phase ARC is always implemented for all fault types or only with single-phase faults.

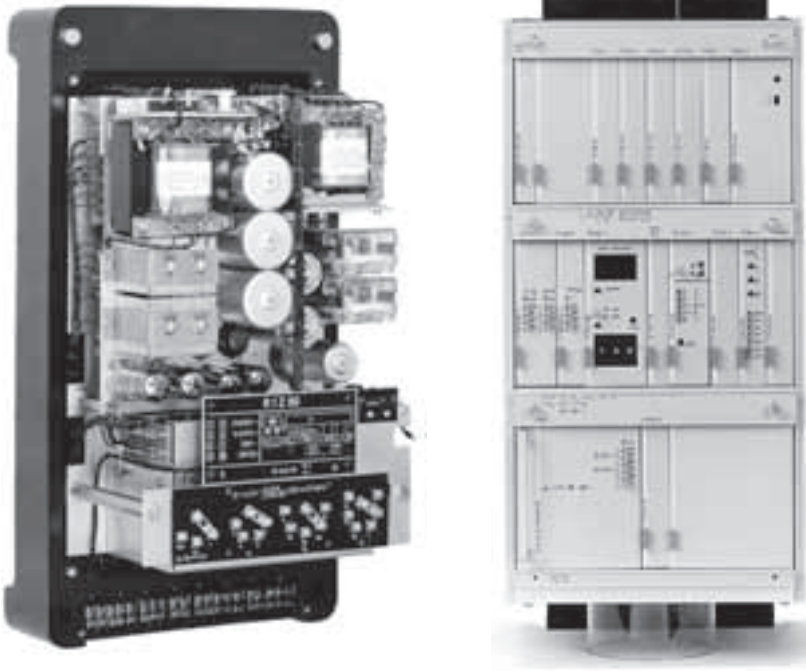
Often, both variants are employed together, i.e. single-phase ARC for single-phase faults and three-phase ARC for multiple-phase faults. For faults arising during the single-phase dead time, the ARC-mode must be switched to three-phase, if the sequential fault starts shortly (inside the set discrimination time) after the first fault. Otherwise a final three-phase trip and ARC block is generated. Alternatively the ARC may be configured to always initiate final trip and ARC-block for sequential faults.

#### **3.1.13 Distance to fault locator**

The distance to fault on simple feeders is proportional to the fault reactance, and can therefore be determined with the measured short circuit current-and voltage:

$$I_{(km)} = \frac{X_{F(Ohm)}}{X'_{(Ohm/km)}} \quad (3-9)$$

$$\text{with } X_F = \frac{U_{SC}}{I_{SC}} \cdot \sin \varphi_{SC} \quad (3-10)$$



7SE90 (R1Z80) measuring technique:  
electro-mechanical

$$Z_F = \frac{|\hat{U}_{sc}|}{|\hat{I}_{sc}|}$$

7SE72 measuring technique:  
static with arithmetic processor

$$X_F = \frac{|\hat{U}_{sc}|}{|\hat{I}_{sc}|} \cdot \sin \varphi_{sc}$$

**Figure 3.53** Conventional distance to fault locators

With conventional relays, dedicated devices were employed for this function. Initially analogue measuring techniques were used; later numerical components were employed (figure 3.53) [3-11 to 3-14].

These devices were relatively expensive (price in the order of a high voltage distance protection). Therefore they were only implemented rarely, and then only in EHV-systems.

The distance to fault information is more or less a by-product of the numerical distance relay measuring technique. This information is used successfully to aid faster fault locating, and rapid re-energisation of the consumer.

The computation of the distance to fault is done with the stored short-circuit current and voltage values. The measuring window is automatically placed so that it starts after fault inception, and ends prior to opening of the circuit-breaker. In this manner it is ensured that pure short circuit quantities are used for the calculation (figure 3.54)

In comparison to the distance relay protection function (minimum measuring time below one half cycle), the distance to fault locator may have a substantially longer data



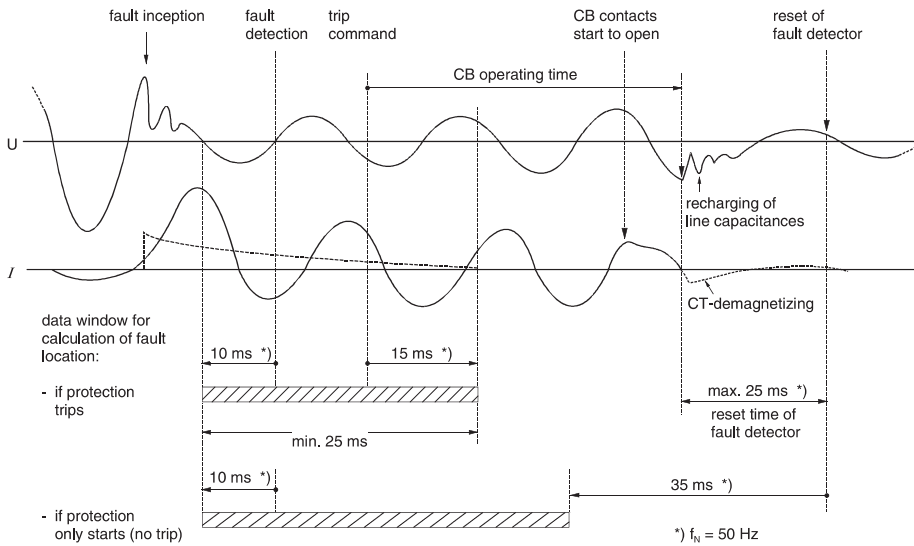


**Figure 3.54** Placing of the data window for the distance to fault computation

window, which corresponds to the operating time of the protection plus the operating time of the circuit-breaker (minimum approx. 2.5 cycles, i.e. 50 ms at 50 Hz).

Therefore it is possible to achieve improved accuracy by digital filtering and compensation of the fault transient.

The stated accuracy for the distance to fault location in relation to the set total line length is better than 2.5% (7SA5 and 7SA6 relays).

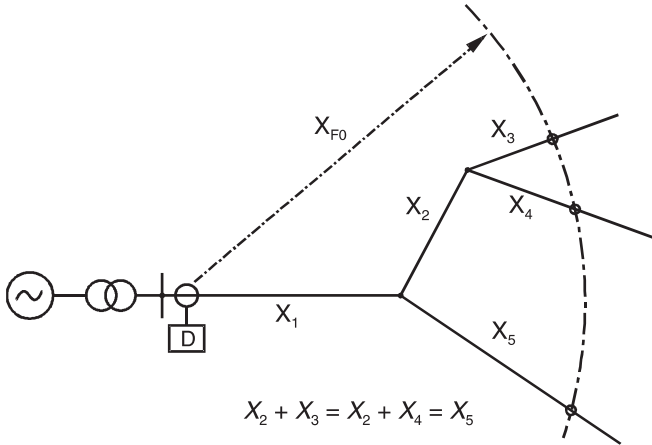
The distance to fault calculation can present it's result in either km, spans or impedance (X, R). Furthermore one may select whether the fault location is calculated every time the protection fault detector picks up, or only following the output of a trip command.

Generally, in meshed systems the distance to fault locator output is accurate and desired only on the faulted feeder (setting: fault locator output with trip command). With feeders connected in series, the upstream devices also provide useful distance to fault data (setting: fault locator output with relay starting).

In distribution systems with outgoing radial feeders a single measured distance to fault may correspond to several fault locations (figure 3.55). The affected feeder may have to be identified by means of additional information (e.g. short circuit targets), or the various fault locations must be patrolled one after the other.

There are two major influencing factors which need to be compensated:

1. On *parallel overhead lines* the distance to fault calculation of earth-faults is influenced by coupling of the zero-sequence systems. By introduction of the earth-current of the parallel feeder, the measurement may be compensated. This is more closely examined in paragraph 3.5.3.

**Figure 3.55**

Distance to fault location in distribution systems, possible fault locations

2. On *loaded lines*, a phase shift of the fault resistance occurs caused by the remote infeed. The appearing false reactance component causes a positive or negative distance measuring error dependent on the direction of load flow [3-13 to 3-17]. This phenomenon and compensation methods are discussed in detail in paragraph 3.5.1.

Accurate distance to fault location through T-points or intermediate in-feeds is practically not possible if merely the measured values at one of the line-ends is utilised. The same factors as for the distance measurement apply here (refer to paragraph 3.5.2).

#### *Two-terminal fault locator*

Distance to fault measurement can be considerably improved by using the synchronised voltage and current phasors of both line ends. This allows in particular to eliminate the impact of pre-fault loading. A number of earlier papers have been published on this subject [3-15 to 3-17].

For this purpose, the data of digital fault recorders have been centrally collected and evaluated on a central computer or PC. The Siemens program SIGRA for fault analysis offers this possibility [3-18]. By using teleprotection schemes with digital communication, end to end synchronisation and fast exchange of the measured phasor data has now become possible and the two-terminal fault locating method can be integrated in the protection itself.

Figure 3.56 shows the principle of a new method which has recently been implemented in distance and differential protection relays (7SA6, 7SD6).

The measured synchronised phasors of the terminal voltages and currents are  $\underline{U}_1$ ,  $\underline{I}_1$  respectively  $\underline{U}_2$ ,  $\underline{I}_2$ .  $\underline{U}_F = (\underline{I}_1 + \underline{I}_2) \cdot R_F$  designates the voltage drop at the fault resistance in the searched location  $x$ .

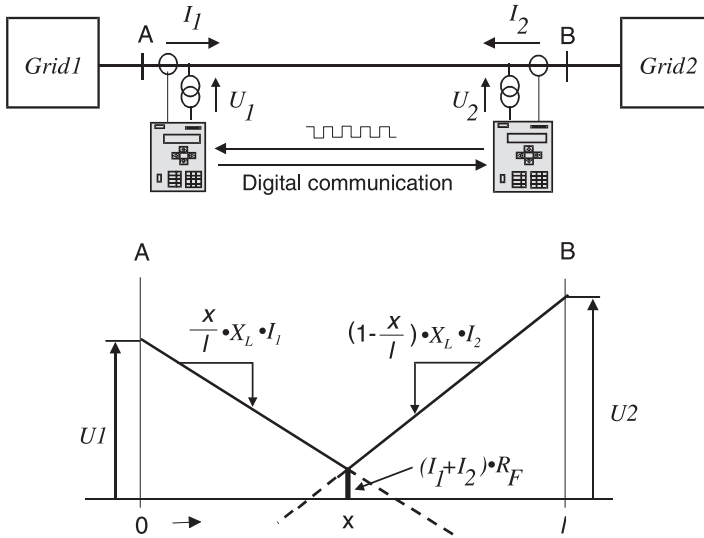


**Figure 3.56** Two-terminal fault locator, implemented in teleprotection scheme (principle)

Neglecting the line capacitances we get the following equations for the two line terminals:

$$\underline{U}_1 = \frac{x}{l} \cdot \underline{Z}_L \cdot \underline{I}_1 + \underline{U}_F \quad (3-11)$$

$$\underline{U}_2 = \left(1 - \frac{x}{l}\right) \cdot \underline{Z}_L \cdot \underline{I}_2 + \underline{U}_F \quad (3-12)$$

By subtracting both equations we can eliminate  $\underline{U}_F$  and get the fault location:

$$\frac{x}{l} = \frac{(\underline{U}_1 - \underline{U}_2) / \underline{Z}_L + \underline{I}_2}{\underline{I}_1 + \underline{I}_2} \quad (3-13)$$

In reality, the measured voltages and currents of both line ends are applied to a distributed model of the line, and the fault location is calculated by an iteration procedure using least squares technique [3-19].

Only the positive sequence component circuit is evaluated, valid for all kind of faults.

In this way, the method has substantial advantages over traditional approaches:

- Inaccurately set earth current compensation factors have no influence.
- Fault resistance has no influence, even not on long heavily loaded lines.
- Mutual coupling of lines has no impact.
- The influence of line unsymmetries is reduced.

Other fault locating techniques have been developed and are partly used in practice (see paper [3.20]).

### 3.1.14 Grading chart

The co-ordination of the zone and time settings for the distance protection is represented in the so-called grading chart [3.21].

The simplest case is given by a single-end fed feeder (figure 3.57).

To ensure selective tripping, with the neighbouring zones, a security margin in the impedance reach, as well as in the tripping time, must be maintained.

The security margin in relation to the impedance setting is expressed as a grading factor (GF). The distance to the neighbouring zone is multiplied by the grading factor to achieve the zone setting. Therefore, to achieve a grading margin of 15%, a grading factor of 0.85 must be used.

This factor takes into account the measuring errors, instrument transformer errors (CT/VT) and the inaccuracies of the line-data.

The following grading factors are typically applied:

- 0.80: for electro-mechanical protection
- 0.85: for static and numerical protection, or for electro-mechanical protection, when the line data is calculated.
- 0.90: for static and numerical protection, when the line data is determined by measurement.

These settings take into account the fact that the zone reach limit is not absolute. Rather, in particular with electro-mechanical protection, the tripping time continuously increases as the end of the zone is approached (figure 3.58).

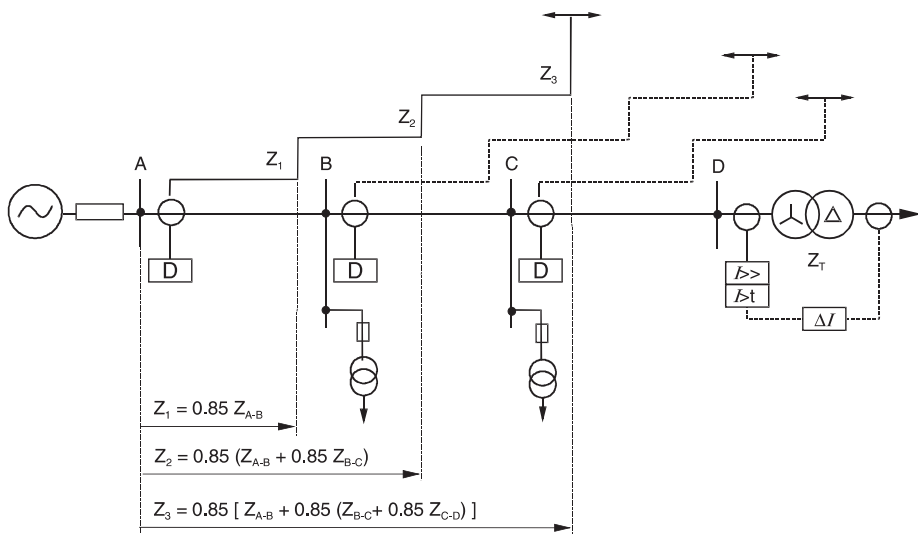


**Figure 3.57** Grading chart of a radial feeder

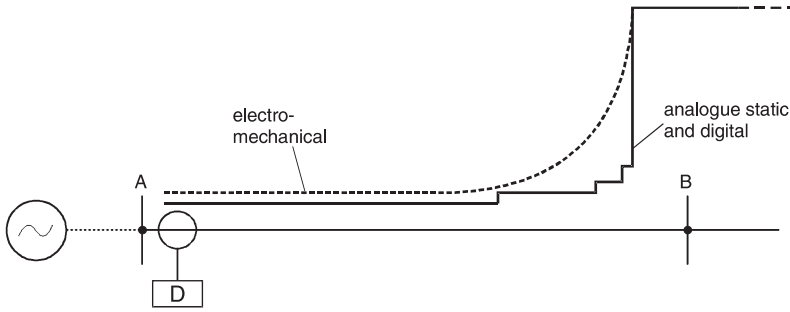


**Figure 3.58** Fading of the tripping time near the zone limit

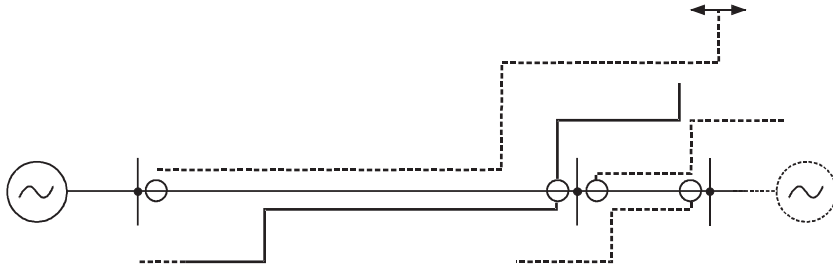


**Figure 3.59** Reverse grading of a distance zone

For the grading calculation, zone 1 is calculated first. This zone is graded with the end of the particular line. The next zone to be determined is zone 2. For zone 2 the reach limit of zone 1 on the neighbouring feeder is used as the reference. Similarly, for zone 3, the end of the zone 2 reach of the neighbouring feeder applies as reference.

To achieve remote back-up protection for busbar faults at the neighbouring substation (especially where no busbar protection is available), the zone 2 setting should, where possible always reach at least 20% beyond the line-end. This is often not achievable, for example where a short cable follows a long overhead line (typical municipal in-feed: figure 3.59). In this case, the slower tripping time of the zone 3 stage must be accepted, unless special measures are employed. For example, a reverse reaching zone in the distance relay at the remote station may be used to securely cover busbar faults in zone 2.

The 3<sup>rd</sup> zone should cover the adjacent feeder as far as possible. When the adjacent feeder is short, similar problems as with zone 2 arise.

The starting zone (fault detector) should be set as sensitive as possible, and should reach beyond the 3<sup>rd</sup> zone. It should be ensured that the longest neighbouring feeder, including the subsequent busbar is completely covered. This ensures that in the event of a protection- or circuit-breaker failure, a remote trip with the last time grading takes place (in meshed systems this is difficult, as intermediate in-feeds reduce the distance relay reach, as will still be referred to).

1 <sup>st</sup> zone:	<p>This zone operates without additional delay, i.e. with the operating time of the protection. A time delay (<math>T_1</math>) is only applied in exceptional cases.</p> <p>The operating time of the protection differs, depending on the relay type:</p> <table><tr><td colspan="2"><u>Mechanical protection:</u></td></tr><tr><td>for medium and high voltage</td><td>(R1KZ4, R1KZ7, R1Z23)</td></tr><tr><td>for EHV</td><td>(R3Z27):</td></tr><tr><td colspan="2"><u>Static protection (analogue electronic):</u></td></tr><tr><td>for medium voltage:</td><td>(7SL17, 7SL70)</td></tr><tr><td>for HV:</td><td>(7SL24, 7SL73)</td></tr><tr><td>for EHV:</td><td>(7SL31, 7SL32)</td></tr><tr><td colspan="2"><u>Numerical protection:</u></td></tr><tr><td>for medium and high voltage:</td><td>(7SA511, 7SA6xx)</td></tr><tr><td>for HV and EHV:</td><td>(7SA6xx, 7SA522)</td></tr></table>			<u>Mechanical protection:</u>		for medium and high voltage	(R1KZ4, R1KZ7, R1Z23)	for EHV	(R3Z27):	<u>Static protection (analogue electronic):</u>		for medium voltage:	(7SL17, 7SL70)	for HV:	(7SL24, 7SL73)	for EHV:	(7SL31, 7SL32)	<u>Numerical protection:</u>		for medium and high voltage:	(7SA511, 7SA6xx)	for HV and EHV:	(7SA6xx, 7SA522)
<u>Mechanical protection:</u>																							
for medium and high voltage	(R1KZ4, R1KZ7, R1Z23)																						
for EHV	(R3Z27):																						
<u>Static protection (analogue electronic):</u>																							
for medium voltage:	(7SL17, 7SL70)																						
for HV:	(7SL24, 7SL73)																						
for EHV:	(7SL31, 7SL32)																						
<u>Numerical protection:</u>																							
for medium and high voltage:	(7SA511, 7SA6xx)																						
for HV and EHV:	(7SA6xx, 7SA522)																						
2 <sup>nd</sup> zone:	<p>It must initially allow the 1<sup>st</sup> zone on the neighbouring feeder(s) to clear the fault.</p> <p>The grading time therefore results from the addition of the following times:</p> <ul style="list-style-type: none"><li>• <i>operating time of the neighbouring feeder 1<sup>st</sup> zone</i></li><li>+ <i>circuit-breaker operating time on the neighbouring feeder</i> (period from output of protection trip command to interruption of the short circuit current)</li><li>+ <i>distance relay reset time</i></li><li>+ <i>errors of the distance relay internal timers</i></li></ul>	<p>(refer above)</p> <p>This ranges from 40 ms (2 cycles) in EHV up to approx. 80 ms in medium voltage.</p> <p>Due to inertia, the relay fault detection does not reset immediately after interruption of the current. It remains picked up for a certain time (resetting time). For mechanical protection this time ranges from 60-100 ms, for static protection it is approx. 30 ms and for numerical protection it is approx. 20 ms.</p> <table><tr><td><i>mechanical:</i></td><td>5% of the set time, minimum 60-100 ms</td></tr><tr><td><i>static:</i></td><td>3% of the set time, minimum 10 ms</td></tr><tr><td><i>numerical:</i></td><td>1% of the set time, minimum 10 ms</td></tr></table>	<i>mechanical:</i>	5% of the set time, minimum 60-100 ms	<i>static:</i>	3% of the set time, minimum 10 ms	<i>numerical:</i>	1% of the set time, minimum 10 ms															
<i>mechanical:</i>	5% of the set time, minimum 60-100 ms																						
<i>static:</i>	3% of the set time, minimum 10 ms																						
<i>numerical:</i>	1% of the set time, minimum 10 ms																						
	<ul style="list-style-type: none"><li>– <i>distance protection starting time</i> this only applies when the internal time delays start after fault detector pick-up. This is the case for all Siemens distance protection relays. (For other manufacturers, the set time delay may be with respect to the fault inception incidence. In this case the starting time must be ignored here.)</li></ul>	<table><tr><td><i>mechanical:</i></td><td>over-current: 10 ms, under-impedance: 25 ms</td></tr><tr><td><i>static:</i></td><td>over-current: 5 ms, under-imp.: 25 ms</td></tr><tr><td><i>numerical:</i></td><td>generally 15 ms</td></tr></table>	<i>mechanical:</i>	over-current: 10 ms, under-impedance: 25 ms	<i>static:</i>	over-current: 5 ms, under-imp.: 25 ms	<i>numerical:</i>	generally 15 ms															
<i>mechanical:</i>	over-current: 10 ms, under-impedance: 25 ms																						
<i>static:</i>	over-current: 5 ms, under-imp.: 25 ms																						
<i>numerical:</i>	generally 15 ms																						

	<div>+ <i>safety margin</i> depends on the type of relay for which the grading is being done</div> <div><ul style="list-style-type: none"><li>• mechanical-mechanical: 100 ms</li><li>• static/numerical-mechanical or vice versa: 75 ms</li><li>• numeric/numeric or static/static: 50 ms</li></ul></div>
3 <sup>rd</sup> zone	Procedure is the same as for the 2 <sup>nd</sup> zone, whereby the operating time of the protection in the neighbouring feeder is given by the zone 2 operating time. It is: starting time + set time delay + time for the trip output (approx. 10 ms)
Delayed trip of directional starter	This stage (marked with → in the grading chart) is made up of the fault detection and the forward directional decision, logically combined with an AND function. It is a directional back-up protection for very remote faults. The time delay is set a grading step longer than zone 3. Calculation is similar to that for zone 3.
Delayed trip of non-directional starter	With this stage the fault detection issues a time delayed trip. Thereby a non-directional zone functions as the final back-up stage. The time delay is usually set one grading step longer than the delayed trip of the directional starter.

Directional Grading

On a feeder, with in-feed from both ends, e.g. a ring feeder, the grading must be done separately for each direction (figure 3.60).

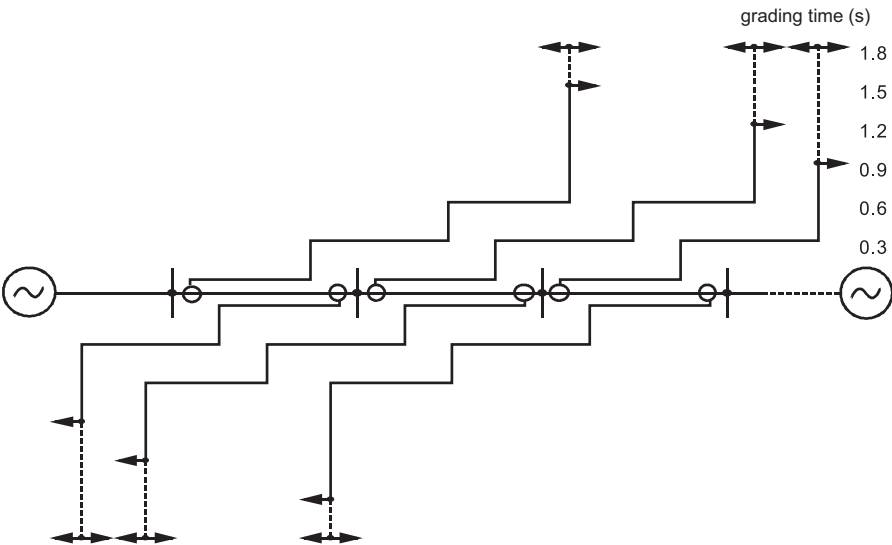


Figure 3.60 Ring feeder with grading against opposite end

This is possible with the directionality of the distance protection zones and the delayed trip of the directional starter. The delayed trip of the non-directional starter reacts to currents flowing in both directions and cannot be selectively integrated into the grading scheme.

It is in fact only possible to implement it as an ultimate back-up, with a time delay that is longer than the slowest directional fault detector trip.

As shown with the radial feeder, the implementation of a zone set with reverse reach may be advantageous.

### Grading in a branched radial system

If several feeders are connected at the remote station, then the 2<sup>nd</sup> zone must be graded with the shortest 1<sup>st</sup> zone of the relays present there (figure 3.61).

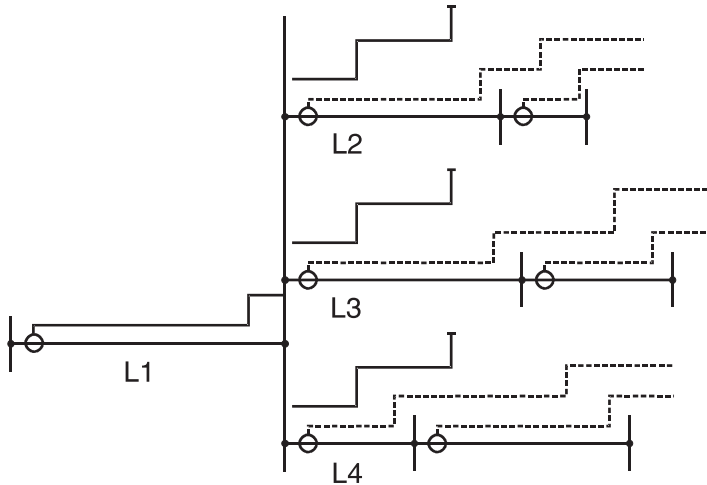


**Figure 3.61** Grading in a branched radial system

In the case at hand, this is zone 1 on feeder 4.

- The 3<sup>rd</sup> zone depends on the shortest 2<sup>nd</sup> zone of the relays at the remote station. In the case at hand this is the 2<sup>nd</sup> zone of the relay in feeder 3.

### Grading for parallel feeders

In the case of parallel feeders, the fault impedance appears to be smaller. This is shown in figure 3.62. For a fault on line 2 at the distance  $x$  from station B, a corresponding impedance on the parabolic curve appears at the relay D1 in station A.

The parabolic trace arises due to the connection in parallel of the impedances  $\frac{x}{l} \cdot Z_2$  and  $Z_3 + \left(1 - \frac{x}{l}\right) \cdot Z_2$ . Strictly speaking, for the zone 2 setting, at D1, the imped-



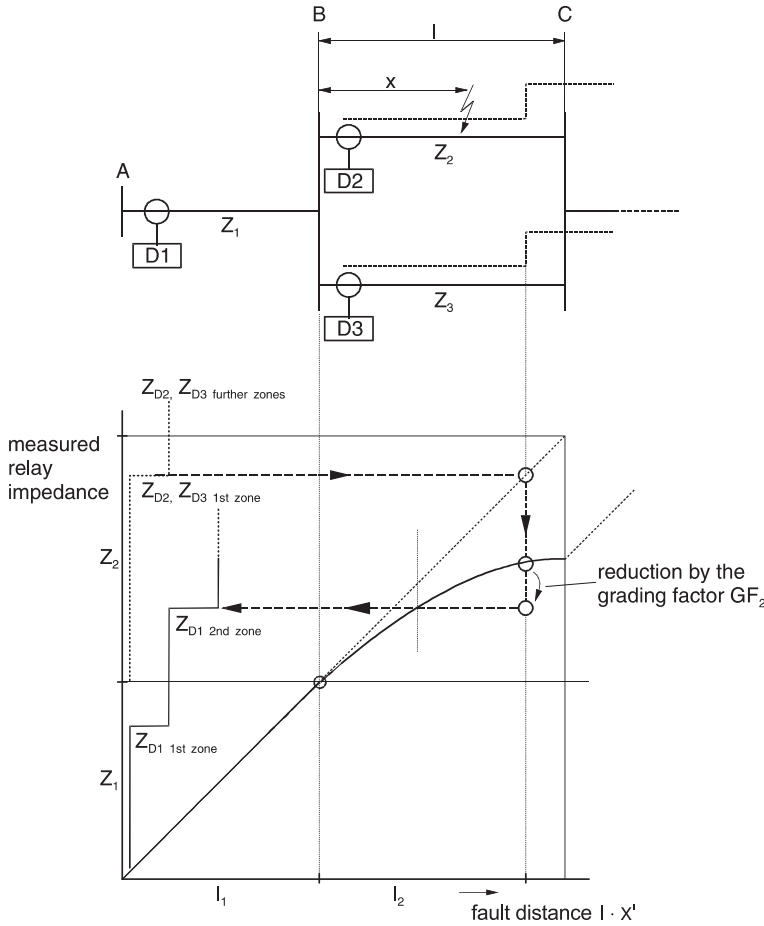


**Figure 3.62** Grading for parallel feeders

ance up to the reach limit of zone 1 on feeder 2 or 3 must be calculated, considering this parallel connection of impedances. The setting is then given by multiplication with the second zone grading factor  $GF_2$ .

$$Z_{D1 \text{ 2nd zone}} = GF_2 \cdot \left\{ \frac{Z_1 + [Z_3 + (1 - GF_2) \cdot Z_2] \cdot GF_1 \cdot Z_2}{Z_2 + Z_3} \right\} \quad (3-14)$$

On parallel feeders, where  $Z_2$  and  $Z_3$  are equal however, half the value of the impedance may be used, as there is hardly any difference due to the parabolic trace. Therefore the setting of zone 2 at D1 is given by:

$$Z_{D1 \text{ 2nd zone}} \approx GF_2 \cdot \left\{ Z_1 + \frac{Z_2}{2} \right\} \quad (3-15)$$

### Effect of intermediate in-feeds

An in-feed between the relay and the fault location influences the measured impedance. The impedance appears to be greater, i.e. the relay “sees” the fault at a greater distance, and may only trip in a higher zone (under-reach). This effect arises because the current from the intermediate in-feed introduces an additional voltage drop in the short-circuit loop. This increases the voltage at the relay location, causing the under-reach (figure 3.63). The magnitude of the measuring error is proportional to the ratio of the current of the intermediate in-feed and the current at the relay location, i.e. the larger the intermediate in-feed, the greater the error.

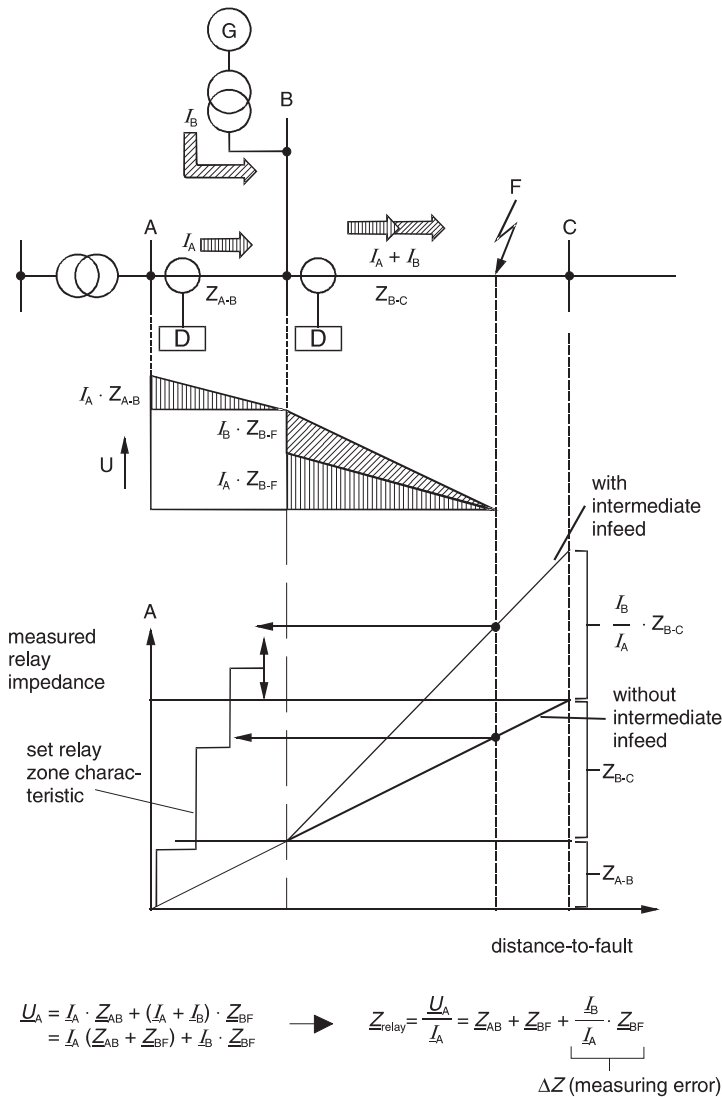


**Figure 3.63** Effect of the intermediate in-feeds on the distance measurement

The selection of the grading index must be determined from case to case, according to the practical system conditions, and it is often a matter of personal opinion. Whereby from one utility to the next the “philosophy” is different.

The following strategies are implemented:

#### *Grading of the 1<sup>st</sup> zones*

In this case intermediate in-feeds only play a role on T-feed feeders or tapped feeders. This is more closely examined in paragraph 3.5.2.

#### *Grading of the 2<sup>nd</sup> zones*

The setting takes place without taking regard of the intermediate in-feed. This ensures selectivity for all system conditions. This appears to be sensible for all applications, as the fault close to the line-end, without permissive tripping, should always be cleared in zone 2 and under no circumstances should an upstream protection trip here. It should always be checked that the 2<sup>nd</sup> zone reaches at least 20% beyond the opposite station, so that it provides back-up protection for the busbar at the remote station. A compromise may be considered here, if several in-feeds are present, which reduce the reach. One may assume that at least a portion of these are always present.

In a meshed system the procedure described here results in relatively short 2<sup>nd</sup> zones and longer protection operating times, following protection or circuit-breaker failure.

#### *Grading of the 3<sup>rd</sup> zones*

Alternative 1:

The intermediate in-feeds are taken into account:

Thereby a large reach is achieved with the 3<sup>rd</sup> zones. If there is no intermediate in-feed, the 3<sup>rd</sup> zones will however not always be selective. Long time delayed tripping in 4<sup>th</sup> or 5<sup>th</sup> grading zone with distance relay starters is however largely avoided. If several intermediate in-feeds are present on one busbar, then it may make sense to compromise here, e.g. only 2 of 3 in-feeds are assumed to be present at all times.

Alternative 2:

The intermediate in-feeds are not taken into account:

Generally very short 3<sup>rd</sup> zones result in meshed systems. This implies that following protection- or circuit-breaker failure, faults are often only cleared by delayed tripping with fault detection. In this case a selective grading of the delayed fault detectors must be present (and also possible), to avoid a more frequent uncontrolled tripping and systems interruptions. Furthermore the longer fault clearing times must be acceptable.

### **Fault detection**

It should reach into the system as far as possible. In meshed systems, the implementation of remote back-up protection is frequently problematic, and only difficult to solve. Due to the intermediate in-feed, the distance to fault appears to be much greater in most cases, and may not even be “seen” by the fault detection stage of the distance protec-

tion relay. When it is not possible to cover the longest neighbouring feeder with the fault detector due to the intermediate in-feed effect, a local back-up protection (breaker-failure protection) must be resorted to. For earth-faults an additional sensitive directional earth-fault protection may be implemented. In Germany a zero-sequence voltage dependant, delayed directional earth-fault protection, which for instance is integrated in the 7SA6, is implemented. In certain cases it may be of benefit if the in-feeds are of different magnitude. It is then possible for the feeder with largest in-feed to still detect the fault and trip. After the disappearance of a large portion of the intermediate in-feed, the remaining relays on the other feeders can also detect the fault and trip. Sequential tripping with a short additional time delay results.

### Grading of distance zones in meshed systems

In meshed systems, the described effects of parallel paths and intermediate in-feeds appear in combination.

Parallel short-circuit paths cause an over-reach, while at nodes the intermediate in-feed effect, with a consequential tendency to introduce an under-reach, arises.

This can be shown with the simple example of a double circuit overhead line (figure 3.64).

For the fault at the 1<sup>st</sup> zone reach limit of the relay D2, which may not be inside the 2<sup>nd</sup> zone of the relay D1, the distance varies depending on the switching state of the parallel line. To avoid an over-reach, a grading factor  $GF_2 = 0.9$  of the shortest impedance is used. This corresponds to the switching state single circuit/double circuit, as was to be expected. This means that the intermediate in-feed effect is not considered, but that all parallel short-circuit impedances are taken account of.

In figure 3.64 one can now see the reach of the 2<sup>nd</sup> zone with the selected setting during the other switching states. The diagram shows on the vertical axis the impedance measured by the relay and the zone setting. On the horizontal axis the distance to the fault is shown, i.e. the line impedances, which at the same time correspond to the physical distance because in this example it is assumed that all lines have the same geometry and earth (same impedance per km).

The impedances for a particular distance to fault depend on the system conditions and appear on a vertical line.

In figure 3.64 this line is shown for a fault at the reach limit of the relay at D2, zone 1. With this, the impedances measured by the relay at D1 can be read off.

Alternatively this diagram may be used to determine the reach of zones by drawing a horizontal line. This is shown for zone 2 in figure 3.64. The variation of the reach, depending on the switching state is thereby readily recognisable.

In a similar manner the measured relay impedances may also be determined for other system constellations. In most cases, on parallel feeders, it is however sufficient to use half the line impedance in the computation. Correspondingly one would use one-third of the impedance in the case of three parallel circuits.

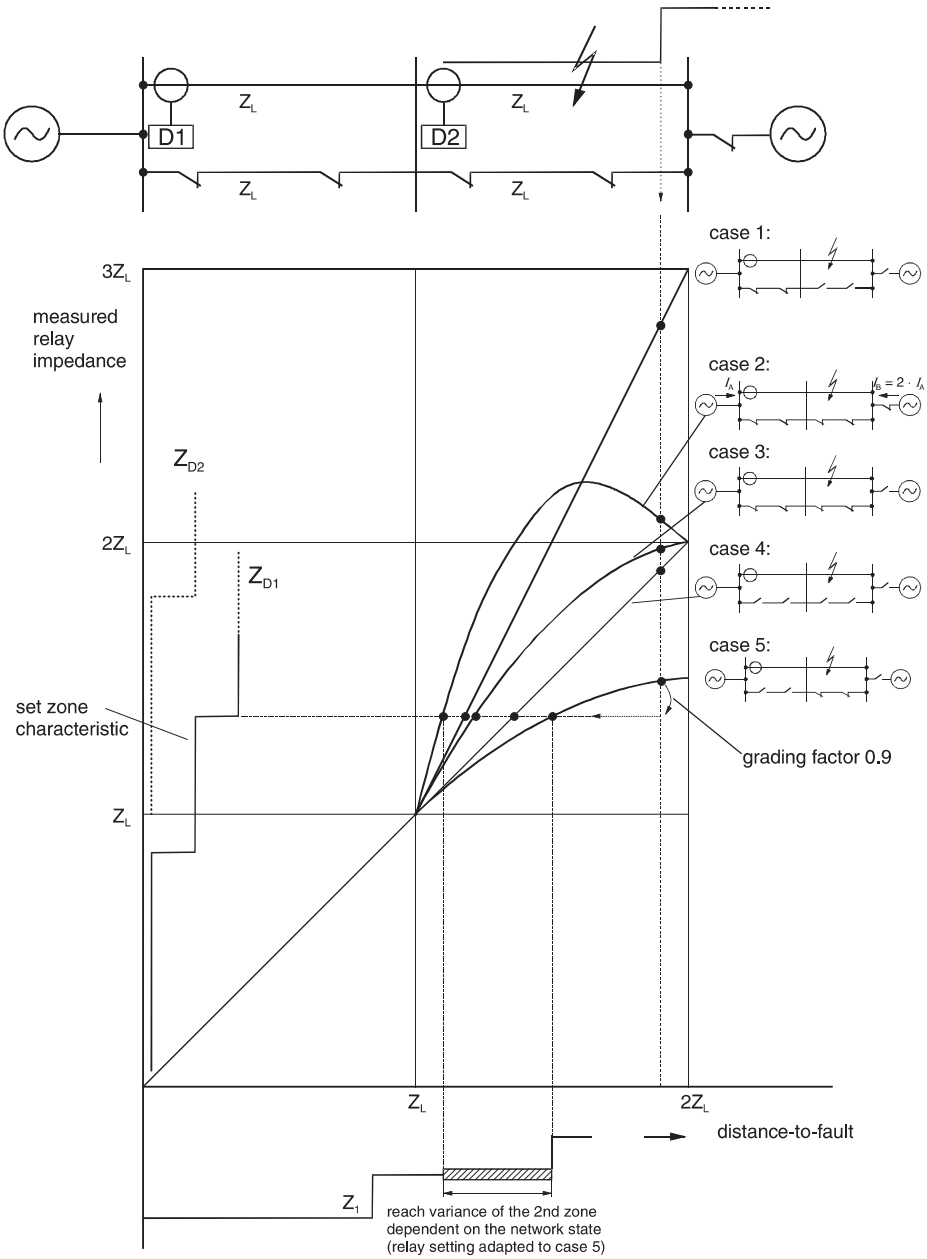


Figure 3.64 System condition dependent zone reach

### Grading of time delayed fault detector stage

The time grading must be done from the consumer towards the in-feed similarly to the grading of over-current protection.

On feeders with in-feed from both ends, and generally in meshed systems, it only makes sense to grade with the directional fault detection stage. Grading with the non-directional stage is not possible in this case. The time delays for the non-directional fault detector stage are usually all set the same at a particular system voltage level, which is one time grading stage longer than the slowest directional fault detector stage [3-22].

### Grading chart programs

To generate the grading chart, a computer program may be used. These programs implement the procedure described here.

For this purpose, Siemens offers the program DISTAL, which is available as part of the short-circuit and load flow software tools SINICAL [3.24].

The program automatically generates the grading chart of the distance zones according to a set algorithm. Individual adaptations and corrections may be applied interactively at the terminal. The grading of the delayed fault detection stages is not included, as cognisance of the system-specific demands (importance of power supply to hospitals, industrial plants etc.) must be taken.

## 3.2 Numerical distance measurement

### 3.2.1 Definition of the fault loop

The equivalent circuit shown in figure 3.65 applies for the fault loop. The relevant signals for the distance measurement can be derived from this circuit.

The diagram shows single-ended in-feed to the fault. For the relay under consideration, it is also valid for two-ended in-feed, if the fault resistance  $R_F$  is negligibly small. This

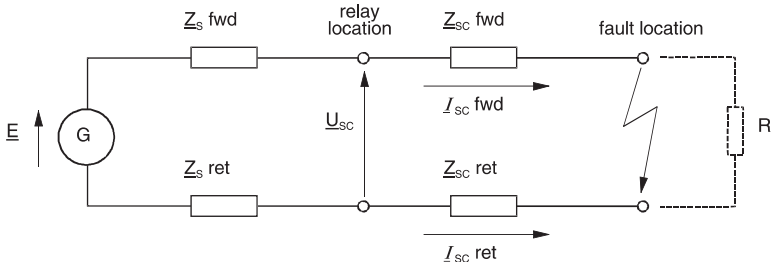


**Figure 3.65** Equivalent circuit of the fault loop

**Table 3.2** Characteristic parameters of the fault loop

short-circuit	$E$	$I_{SC}$ fwd	$I_{SC}$ ret	$Z_S$ fwd	$Z_S$ ret	$Z_{SC}$ fwd	$Z_{SC}$ ret
3-Ph	$1.1 \cdot U_N / \sqrt{3}$	$I_{Ph}$	0	$Z_{S1}$	0	$Z_{SC1}$	0
1-Ph-E	$1.1 \cdot U_N / \sqrt{3}$	$I_{Ph}$	$I_E$	$Z_{S1}$	$Z_{SE}$	$Z_{SC1}$	$Z_{SCE}$
Ph-Ph	$1.1 \cdot U_N$	$I_{Ph1}$	$I_{Ph2}$	$Z_{S1}$	$Z_{S1}$	$Z_{SC1}$	$Z_{SC1}$

is true for almost all cable faults and on overhead lines with steel towers and normal earthing conditions. For larger fault resistances, the distance measurement is influenced by the current from the opposite end, which also flows via the fault. This influencing factor is more extensively analysed in paragraph 3.5.1.

$E$  is the equivalent emf and  $Z_S$  is the source impedance of the system in-feed.  $Z_{SC} = Z'_{SC} \cdot I$  is the short-circuit impedance, with  $Z'_{SC}$  being the impedance per km of the line and  $I$  is the distance to the fault.  $Z_S$  and  $Z_{SC}$  are determined by the summated impedances in the forward and return path.

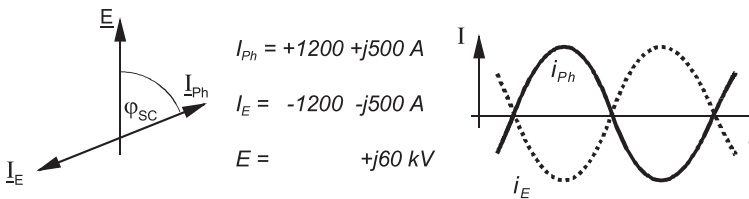
$U_{SC}$  designates the short-circuit voltage and  $I_{SC}$  the short-circuit current at the relay location.

$R_F$  symbolises the resistance at the fault location, which may arise due to the arc or the tower footing resistance with earth-faults.

The overview in table 3.2 shows the significance of  $E$  as well as  $Z_S$  and  $Z_{SC}$  for the classical fault types in a three-phase system. The system rated voltage is designated by  $U_N$ , which is always given as the line voltage (Ph-Ph).

The factor 1.1 takes into account the fact that generators in the system are usually run with over-excitation for better system stability. Therefore, the average internal generator voltage is approx. 10% above the rated system voltage. More information relating to this topic is contained in the guidelines for the calculation of short-circuit currents (IEC 60909 Part 1) [3.25].

For the currents it must be noted that in this representation, the positive sense is towards the line. For the earth-current the following relationship applies:  $I_E = -(I_{L1} + I_{L2} + I_{L3})$ . This must be taken into account in the following equations, when the earth-

**Figure 3.66** Example illustrating the sign convention for the currents (single-phase earth-fault)

current is calculated from the phase-currents. With this convention, the phase and earth-currents have different signs in the computed results. In the vector diagram and fault recording, this sign convention implies that, similar to the phase-currents for a two-phase fault, the phase and earth-currents are always in opposite direction (figure 3.66).

### Source impedance

The source impedance can be derived from the short-circuit power at the relay location, or the given short-circuit currents (figure 3.67).

#### Positive-sequence source impedance

$$Z_{S1} = \frac{1.1 \cdot U_N^2}{SCC''_{(3-pol.)}} \quad \text{or} \quad Z_{S1} = \frac{1.1 \cdot U_N}{\sqrt{3} \cdot I''_{SC(3-pol.)}} \quad (3-16)$$

$SCC''$  is the initial AC short-circuit power of the system, and  $I''_{SC}$  is the initial AC short-circuit current for a three-phase fault on the feeder directly in front of the relay location.

In the case of in-feeds from high voltage and extra high voltage systems, a good approximation is to set  $Z_S = X_S$  as the  $X/R$  ratio of the source impedances is large. For more accurate calculations, the  $R$ -component may be derived from the  $R/X$  values in table 3.3.<sup>1</sup>

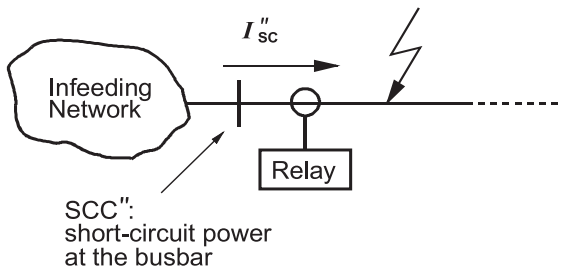


**Figure 3.67**  
Definition of the short-circuit power at the relay location

**Table 3.3**  $X/R$  ratios and system time constants

Voltage level	$X/R$	System time constant $T_N$ [ms]
380 kV	8-10	25-32
220 kV	5-8	16-25
110 kV	3-5	10-16

<sup>1</sup> Typical values for generators, transformers, overhead lines and cables are contained in: Roepfer, Short-circuit currents in three-phase systems, 1985 [10].



Only when the source impedance is mainly determined by medium voltage overhead lines or cables, i.e. when the  $X/R$  is smaller than 5 (for rough estimates smaller than 3) is it recommended to use complex numbers for the computation.

#### *Zero-sequence source impedance*

For system studies with symmetrical components, the zero-sequence system data is usually available.

From this, the corresponding earth impedances can be derived.

The earth impedance of the source  $Z_{SE}$  can be determined as follows, depending on which system data is available (resistive components neglected):

1. The ratio  $X_{S0}/X_{S1}$  at the busbar is given:

$$X_{SE} = \frac{1}{3} \cdot X_{S1} \cdot \left( \frac{X_{S0}}{X_{S1}} - 1 \right) \quad (3-17)$$

2. The single-phase short-circuit power is given:

$$X_{SE} = \frac{1.1 \cdot (U_N / \sqrt{3})^2}{SCC''_{(1\text{-pole})}} - X_{S1} \quad (3-18)$$

3. The single-phase short-circuit current is given:

$$X_{SE} = \frac{1.1 \cdot U_N}{\sqrt{3} \cdot I''_{SC(1\text{-pol})}} - X_{S1} \quad (3-19)$$

#### **Short-circuit impedance**

The short-circuit impedance generally corresponds to the line impedance from the relay location to the fault location, and is calculated using the line impedance per km data:

#### *Positive-sequence system*

$$\underline{Z}_{SC1} = \underline{Z}_{L1} = (R_{L1} + jX_{L1}) \quad (3-20)$$

$$\text{with: } R_{L1} = R'_{L1} [\text{Ohm/km}] \cdot l [\text{km}] \quad (3-21)$$

$$X_{L1} = X'_{L1} [\text{Ohm/km}] \cdot l [\text{km}] \quad (3-22)$$

#### *Zero-sequence system*

$$\underline{Z}_{SCE} = \underline{Z}_{LE} = \frac{1}{3} \cdot (\underline{Z}_{L0} - \underline{Z}_{L1}) \quad (3-23)$$

$$\text{with: } \underline{Z}_{L0} = (R_{L0} + jX_{L0}) \quad (3-24)$$

$$\text{and: } R_{L0} = R'_{L0} [\text{Ohm/km}] \cdot l [\text{km}] \quad (3-25)$$

$$X_{L0} = X'_{L0} [\text{Ohm/km}] \cdot l [\text{km}] \quad (3-26)$$

Typical values for the line impedance per km data are shown in table 3.4:

### Fault loops

In the typical three-phase system there are a number of short-circuit possibilities, depending on which phases are involved, and whether connection to earth is present.

The fault loops applicable to the type of fault must be evaluated (table 3.5).

For single-phase and two-phase faults with-out earth, the allocation is straight forward, as only one useful fault loop exists.

For all other short-circuit types, several possible loops are available.

**Table 3.4** Typical impedance values in overhead lines and cables<sup>1</sup>

	$R'_{L1}$ Ω/km	$X'_{L1}$ Ω/km	$\varphi_{L1}$ ° el.	$R'_{L0}$ Ω/km	$X'_{L0}$ Ω/km	$\varphi_{L0}$ ° el.	$R'_{LE}$ Ω/km	$X'_{LE}$ Ω/km	$R'_{LE}/R'_{L1}$	$X'_{LE}/X'_{L1}$
Overhead line 380 kV Triangular configuration, single-earth-wire, quad-bundle 4×Al/St 435/55	0.018	0.25	86	0.170	0.94	80	0.053	0.230	2.94	0.92
Overhead line 220 kV Triangular configuration, single-earth-wire, twin-bundle 2×Al/St 265/35	0.058	0.30	79	0.220	0.99	77	0.053	0.230	0.91	0.77
Overhead line 110 kV Triangular configuration, single-earth-wire, 1×Al/St 435/35	0.071	0.38	79	0.220	1.10	79	0.050	0.240	0.70	0.63
Overhead line 20 kV, no earth-wire, 95 mm <sup>2</sup> Al	0.310	0.37	50	0.530	1.58	71	0.073	0.400	0.24	1.08
Cable 400 kV, single conductor oil filled cable, 3×1×1200 mm <sup>2</sup> Cu	0.020	0.22	85	0.049	0.11	66	0.010	−0.036	0.50	−0.16
Cable 110 kV, gas cable, 240 mm <sup>2</sup> Cu	0.090	0.14	57	0.390	0.16	22	0.100	0.007	1.11	0.05
Cable 20 kV, shielded cable, 3×120 mm <sup>2</sup> Cu	0.160	0.12	37	1.400	0.25	10	0.410	0.043	3.42	0.36

<sup>1</sup> More extensive tables are contained in Roepert: Short currents in three-phase systems, 1985 [10].

### 3.2.2 Determination of the loop impedance

The measuring circuit of the distance relay is principally laid out such, that for each fault type the line impedance ( $Z_{SC-fwd}$  in figure 3.65) of the fault loop is determined. This impedance corresponds to the positive-sequence impedance if the overhead line is symmetrical and fully transposed.<sup>1</sup>

The advantage of this is, that for each fault type the same measuring results and the line impedance, which is proportional to the distance to fault, is achieved.

**Table 3.5** Short-circuit types and fault loops for the distance measurement

Fault type	phases involved	fault loops for the distance measurement
two-phase short-circuit without earth	L1-L2 L2-L3 L3-L1	L1-L2 L2-L3 L3-L1
three-phase short-circuit without earth	L1-L2-L3	L1-L2 or L2-L3 or L3-L1
single-phase earth-fault	L1-E L2-E L3-E	L1-E L2-E L3-E
two-phase short-circuit with earth	L1-L2-E L2-L3-E L3-L1-E	L1-E or L2-E or L1-L2 L2-E or L3-E or L2-L3 L3-E or L1-E or L3-L1
three-phase short-circuit with earth	L1-L2-L3-E	L1-L2 or L2-L3 or L3-L1 L1-E or L2-E or L3-E

### Conventional distance protection

In this case, the following equations are employed to evaluate the measured values

*Phase-phase loop:*

$$Z_{Ph-Ph} = \frac{U_{Ph-Ph}}{I_{Ph-Ph}} = \frac{U_{Ph1-E} - U_{Ph2-E}}{I_{Ph1} - I_{Ph2}} \quad (3-27)$$

where 1 and 2 designate the faulted phases.

$I_{ph-ph}$  and  $U_{ph-ph}$  are the values for the line current and line voltage.

<sup>1</sup> The influence of the non-symmetry of non-transposed overhead lines is covered in paragraph 3.5.5

For a single-end in-feed and solid short-circuit ( $R_F = 0$ ), the following arises from figure 3.65:

$$\underline{U}_{\text{Ph-Ph}} = \underline{I}_{\text{Ph1}} \cdot \underline{Z}_{\text{SC1}} - \underline{I}_{\text{Ph2}} \cdot \underline{Z}_{\text{SC1}} \quad \text{and} \quad \underline{I}_{\text{Ph1}} = -\underline{I}_{\text{Ph2}}$$

$$\text{From this: } \underline{Z}_{\text{Ph-Ph}} = \underline{Z}_{\text{SC1}}$$

*Calculation example:*

Phase-to-phase short-circuit on a 20 kV OH-line

*Given:*

20 kV OH-line with  $R'_L = 0,31 \text{ Ohm/km}$  and  $X'_L = 0,37 \text{ Ohm/km}$

A fault L2-L3 occurred on the line.

The following data were recorded:

$$\underline{I}_{L1} = 155 \text{ A}, \angle 0,9^\circ = +155 + j2,4 \text{ A}$$

$$\underline{I}_{L2} = 1219 \text{ A}, \angle -151,0^\circ = -1062 - j599 \text{ A}$$

$$\underline{I}_{L3} = 1089 \text{ A}, \angle 33,7^\circ = +907 + j602 \text{ A}$$

$$\underline{U}_{L1} = 11547 \text{ V}, \angle 3,4^\circ = 11483 + j679 \text{ V}$$

$$\underline{U}_{L2} = 9680 \text{ V}, \angle -134,2^\circ = -6738 - j6944 \text{ V}$$

$$\underline{U}_{L3} = 7860 \text{ V}, \angle -52,9^\circ = -4745 + j6265 \text{ V}$$

*Questions:*

Which impedance did the relay measure?

What is the distance to fault?

*Solution:*

With formula (3-27), we can calculate the measured impedance:

$$\begin{aligned} \underline{Z}_{L2-L3} &= \frac{\underline{U}_{L2} - \underline{U}_{L3}}{\underline{I}_{L2} - \underline{I}_{L3}} = \frac{9680 \angle -134,2^\circ - 7860 \angle -52,9^\circ}{1219 \angle -151,0^\circ - 1089 \angle -33,7^\circ} \\ &= \frac{-6738 - j6944 - (-4745 + j6265)}{-1062 - j599 - (907 + j602)} = \frac{-1993 - j13209}{-1964 - j1201} \\ &= \frac{-13359 \angle 81,4^\circ}{-2302 \angle 31,4^\circ} = 5,8 \angle 50^\circ \text{ Ohm} \end{aligned}$$

For the reactance und resistance part, we get

$$X_{L2-L3} = Z_{L2-L3} \cdot \sin \varphi_{\text{SC}} = 5,8 \cdot \sin 50^\circ = 4,44 \text{ Ohm}$$

$$R_{L2-L3} = Z_{L2-L3} \cdot \cos \varphi_{\text{SC}} = 5,8 \cdot \cos 50^\circ = 3,73 \text{ Ohm}$$

From the calculated fault reactance and the given line data, we can determine the fault distance.

$$l = \frac{X_{L2-L3} [\text{Ohm}]}{X'_{L2-L3} [\text{Ohm/km}]} = \frac{4,44}{0,37} = 12 \text{ km}$$

Note: The formula (3-27) can be rearranged so that phasor quantities can be directly entered with magnitude and angle. This will be shown in the following section dealing with numerical impedance calculation (formulas (3-40) bis (3-41)).

### Phase-earth loop

The following equation corresponds to the measurement:

$$\underline{Z}_{\text{Ph-E}} = \frac{\underline{U}_{\text{Ph-E}}}{\underline{I}_{\text{Ph}} - \underline{k}_E \cdot \underline{I}_E} \quad (3-28)$$

The vector  $\underline{k}_E$  is the residual compensation factor. It corresponds to the  $\underline{Z}_E/\underline{Z}_L$  ratio of the overhead line. The value for  $\underline{Z}_E$  must be calculated using equation (3-23).

Using figure 3.65 and table 3.2 the following results:

$$\underline{U}_{\text{Ph-E}} = \underline{I}_{\text{Ph}} \cdot \underline{Z}_{\text{SC1}} - \underline{I}_E \cdot \underline{Z}_{\text{SCE}} = \underline{Z}_{\text{SC1}} \cdot \left( \underline{I}_{\text{Ph}} - \frac{\underline{Z}_{\text{SCE}}}{\underline{Z}_{\text{SC1}}} \cdot \underline{I}_E \right) \quad (3-29)$$

Substituting 3-29 for 3-28 results in:

$$\underline{Z}_{\text{Ph-E}} = \underline{Z}_{\text{SC1}} \cdot \frac{\left( \underline{I}_{\text{Ph}} - \frac{\underline{Z}_{\text{SCE}}}{\underline{Z}_{\text{SC1}}} \cdot \underline{I}_E \right)}{\underline{I}_{\text{Ph}} - \underline{k}_E \cdot \underline{I}_E} \quad (3-30)$$

From this it is apparent that the line impedance  $\underline{Z}_{\text{SC1}}$  is correctly measured, if  $\underline{k}_E = \underline{Z}_{\text{SCE}}/\underline{Z}_{\text{SC1}}$ , i.e. when  $\underline{k}_E$  is set according to the protected feeder.

It must be borne in mind that  $\underline{k}_E$  is a complex number.

With electro-mechanical relays only a magnitude ratio  $k_E = |\underline{k}_E|$  could be set. Correspondingly deviations during earth-faults resulted.

This measuring error can be tolerated on overhead lines, where the angular difference between  $\underline{Z}_E$  and  $\underline{Z}_L$  is relatively small. For cables where  $\underline{Z}_E$  and  $\underline{Z}_L$  may have significant angular differences, the value of  $k_E$  was graphically determined from the intersection of the circular characteristic of the relay with the impedance locus of the earth-fault loop.

Only with the advent of analogue static relays the possibility of also setting an angle-correction became available.

This residual compensation is only accurate for solid earth-faults. For short circuits with fault resistance (arc resistance) the angle compensation  $\underline{k}_E = |\underline{k}_E|e^{j\varphi_E}$  rotates the fault resistance in the impedance diagram, resulting in a corresponding measurement error (see paragraph 3.5.1) [3.26].

This also applies to numerical relays which implement a conventional measuring technique.

*Calculation example:*

*Given:*

110 kV single line with the following data:

Line length:  $l = 50 \text{ km}$

Line characteristics: Positive sequence:  $R'_{L1} = 0.1286 \text{ } \Omega/\text{km}$   
 $X'_{L1} = 0.4023 \text{ } \Omega/\text{km}$   
 Zero sequence:  $R'_{L0} = 0.2409 \text{ } \Omega/\text{km}$   
 $X'_{L0} = 1.0863 \text{ } \Omega/\text{km}$

The following voltages and currents were calculated for a single-phase earth fault L1-E at the end of the line:

$U_{L1} = 53.51 \text{ kV}$  und  $\varphi_{UL1} = -1.4^\circ$   
 $I_{L1} = 1.6415 \text{ kA}$  und  $\varphi_{IL1} = -76.6^\circ$   
 $I_E = 1.6509 \text{ kA}$  und  $\varphi_{IE} = 103.4^\circ$  (sign rule according to figure 3.66)

*Question:*

What fault impedance would a distance relay measure?

*Solution:*

At first we calculate the residual compensation factor  $k_E$  assuming that it shall as usual be adapted to the protected line:

$$\begin{aligned} k_E &= \frac{(Z'_{L0} - Z'_{L1})}{3 \cdot Z'_{L1}} = \frac{0.2409 + j1.0863 - (0.1286 + j0.4023)}{3 \cdot (0.1286 + j0.4023)} \\ &= \frac{0.1123 + j0.684}{3 \cdot (0.1286 + j0.4023)} = \frac{0.693 \angle 80.7^\circ}{3 \cdot 0.4224 \angle 72.3^\circ} = 0.547 \angle 8.4^\circ \end{aligned}$$

We use formula (3-28) to calculate the measured fault impedance:

$$\begin{aligned} \underline{Z}_{L1-E} &= \frac{\underline{U}_{L1}}{I_{L1} - k_E \cdot I_E} = \frac{53.51 \angle -1.4^\circ}{(1.6415 \angle -76.6^\circ) - (0.547 \angle 8.4^\circ) \cdot (1.6509 \angle 103.4^\circ)} \\ &= \frac{53.51 \angle -1.4^\circ}{0.7157 - j2.4352} = \frac{53.51 \angle -1.4^\circ}{2.5382 \angle -73.62^\circ} = 21.08 \angle -72.22^\circ \end{aligned}$$

The reactance and resistance parts are as follows:

$$X_{L1-E} = |Z_{L1-E}| \cdot \sin \varphi_{Z(L1-E)} = 21.08 \cdot \sin 72.22^\circ = 20.07 \text{ Ohm}$$

$$R_{L1-E} = |Z_{L1-E}| \cdot \cos \varphi_{Z(L1-E)} = 21.08 \cdot \cos 72.22^\circ = 6.44 \text{ Ohm}$$

**Note:** In the following we also show the formulas for calculation with polar quantities. The reason is that the conventional measuring method for phase-to-earth faults deviates from the numerical complex calculation method (as used in the 7SA relays) (see section 3.5.1).

For the calculation with polar quantities, we replace the complex number quantities in (3-28) by the corresponding polar quantities with magnitude and angle.

$$Z_{Ph-E} = \frac{U_L \cdot (\cos \varphi_U + j \sin \varphi_U)}{I_L \cdot (\cos \varphi_{IL} + j \sin \varphi_{IL}) + [K_E \cdot (\cos \varphi_{kE} + j \sin \varphi_{kE}) \cdot (\cos \varphi_{IE} + j \sin \varphi_{IE})]} \quad (3-28a)$$

The separation in real and imaginary part results in the following formulas:

$$X_{Ph-E} = \frac{U_{Ph-E}}{I_{Ph}} \cdot \frac{\sin(\varphi_U - \varphi_{Iph}) - k_E \cdot \frac{I_E}{I_{Ph}} \cdot \sin(\varphi_U - \varphi_{IE} - \varphi_{kE})}{1 - 2 \cdot k_E \cdot \frac{I_E}{I_{Ph}} \cdot \cos(\varphi_{Iph} - \varphi_{IE} - \varphi_{kE}) + \left(k_E \cdot \frac{I_E}{I_{Ph}}\right)^2} \quad (3-28b)$$

$$R_{Ph-E} = \frac{U_{Ph-E}}{I_{Ph}} \cdot \frac{\cos(\varphi_U - \varphi_{Iph}) - k_E \cdot \frac{I_E}{I_{Ph}} \cdot \cos(\varphi_U - \varphi_{IE} - \varphi_{kE})}{1 - 2 \cdot k_E \cdot \frac{I_E}{I_{Ph}} \cdot \cos(\varphi_{IL} - \varphi_{IE} - \varphi_{kE}) + \left(k_E \cdot \frac{I_E}{I_{Ph}}\right)^2} \quad (3-28c)$$

*Calculation example:*

For comparison, we calculate the fault reactance of the previous example using formula (3-28b):

$$\begin{aligned} X_{L1-E} &= \frac{53.51}{1.6415} \cdot \frac{\sin(-1.4^\circ + 76.6^\circ) - 0.547 \cdot \frac{1.6509}{1.415} \cdot \sin(-1.4^\circ - 103.4^\circ - 8.4^\circ)}{1 - 2 \cdot 0.547 \cdot \frac{1.6509}{1.415} \cdot \cos(-76.6^\circ - 103.4^\circ - 8.4^\circ) + \left(0.547 \cdot \frac{1.6509}{1.415}\right)^2} \\ &= 20.07 \text{ Ohm} \end{aligned}$$

We get the same result without the need for a complex calculation.

The fault resistance can in the same way be calculated by formula (3-28c).

### 3.2.3 Numerical impedance computation

The numerical computation of the fault-loop impedance, with the sampled current and voltage signals is an initial stage to the distance measurement and fault location. In the case of distance measurement with a quadrilateral characteristic, the R and X-values of the numerically computed fault-loop impedance can simply be compared with the zone-limits in the impedance plane. A magnitude comparison is therefore sufficient to reach a decision on whether the fault is inside or outside a particular zone. In principal, this technique can also be applied to a characteristic with any shape. In the case of MHO-circles, the classic measured angle comparison with current and voltage vectors is however preferred (refer to paragraph 3.4.1).

For the fault location function, the computed X-value provides a measure for the distance to fault (refer to paragraph 3.1.13).

#### *Computational process*

The following differential equation applies to the short-circuit loop in the time domain:

$$u_{SC}(t) = R_{SC} \cdot i_{SC}(t) + L_{SC} \cdot \frac{di_{SC}(t)}{dt} \quad (3-31)$$

In the 7SA relays, the sampled current and voltage signals are integrated with modified Fourier-filters and transformed in the frequency domain. The result is phasor quantities, which are provided in the form of orthogonal components (real and imaginary components). The fundamental component is evaluated, DC component and higher harmonics are suppressed.

From (3-31) the usual equation with vector quantities is derived:

$$\underline{U}_{SC} = R_{SC} \cdot \underline{I}_{SC} + jX_{SC} \underline{I}_{SC} \quad (3-32)$$

By separation of real and imaginary components, two equations for the determination of  $R_{SC}$  and  $X_{SC}$  are obtained (refer to Annexure A.1).

The separate evaluation of the real and imaginary components of the short-circuit loop has the particular advantage that the fault reactance during earth-faults is also measured correctly when the short-circuit angle of the positive and zero-sequence impedances are different (refer to paragraph 3.5.1).

#### *Equations for the impedance calculation*

The theoretical bases for the numerical distance measuring technique is given in Annexure A.1.

The following equations for determining the loop impedance correspond to the measuring technique in all 7SA type distance relays.

The equations may be used in practice to calculate the impedance “seen” by the relevant relay when the short-circuit voltage and short-circuit current at the relay location are known. Hence, the results from short-circuit computations may for example be used in the equations. It must be remembered that the phasor quantities of the currents and voltage must be used.

The magnitude is an rms-value. The angles are differential values, so that any vector may be used as a reference.

The equations are also valid for the unfaulted state, i.e. the result indicates which impedances the distance protection “sees” with load currents. This applies to the impedance starters and the correspondingly released distance measuring systems. By calculating the load impedance measured by the protection and comparing this with the set fault detection characteristic, the security margin against incorrect starting can be



determined (during over-loads, power-swings, etc.). The phase-phase fault detection systems are definitely active when the feeder current is greater than the release-threshold of approx. 20%. The phase-earth loops in the 7SA511 are only released with earth-current or residual voltage and are therefore not active during symmetrical load conditions. In the multi-system versions 7SA513, 7SA522 and 7SA6 they are generally always released, but may be parameterised to only release with earth-current and/or residual voltage.

During injection-testing of the relay, the injected quantities must also be set as magnitude (rms-value) and angle.

#### *Generally applicable loop impedance*

In figure 3.68 the generally applicable short-circuit loop is diagrammatically represented. Initially a solid short-circuit is assumed. The influence of fault resistance will be investigated separately at a later stage.

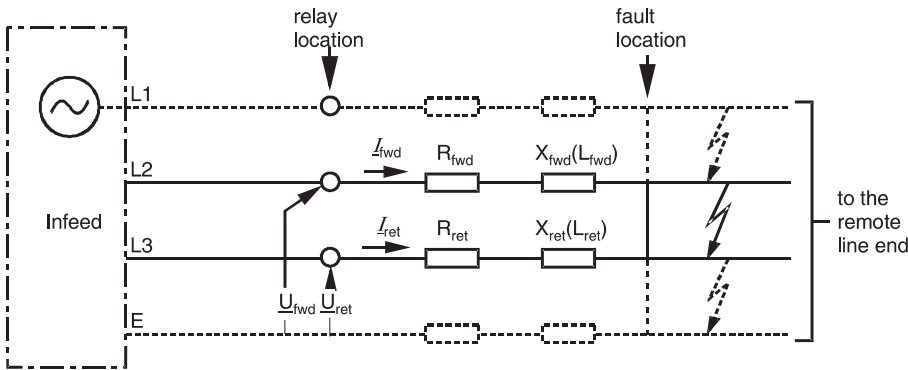


**Figure 3.68** Generally applicable short-circuit loop

It is recognised that in the short-circuit loop the outward-flowing current and the returning current are generally not equal. For a two-phase to ground fault for example, the sum of the currents  $I_{fwd}$  and  $I_{ret}$  flows via ground and returns via a different path to the in-feed(s).

Only for particular fault types and system configurations, such as for example a two-phase short-circuit without earth and single in-feed, the condition that  $I_{ret} = -I_{fwd}$  is given.

In general, the impedance in the forward path ( $R_{fwd}$ ,  $X_{fwd}$ ) is not equal to the impedance in the return path ( $R_{ret}$ ,  $X_{ret}$ ).

In the case of earth-fault loops, the difference between phase impedance and earth impedance must be taken into account. This is done by means of the residual compensation factor  $k_E$ , which is set in the relay.

On non-transposed overhead lines there is a non-symmetry of the phase impedances which in general is not taken into consideration by the measuring systems of the distance protection relay. This implies that for phase to phase loops the same impedance for the forward and return paths (transposed line) is assumed. If large non-symmetries exist the zone settings must be adapted accordingly (refer to paragraph 3.5.5).

### Computational process

We get the following equation for the fault loop

$$\underline{U}_{\text{fwd}} - \underline{U}_{\text{ret}} = R_{\text{fwd}} \cdot \underline{I}_{\text{fwd}} + jX_{\text{fwd}} \cdot \underline{I}_{\text{fwd}} - R_{\text{ret}} \cdot \underline{I}_{\text{ret}} - jX_{\text{ret}} \cdot \underline{I}_{\text{ret}} \quad (3-33)$$

where the phasors are defined as

$$\underline{U} = U \cdot e^{j(\omega t + \varphi U)} = U [\cos(\omega t + \varphi U) + j \sin(\omega t + \varphi U)]$$

$$\underline{I} = I \cdot e^{j(\omega t + \varphi I)} = I [\cos(\omega t + \varphi I) + j \sin(\omega t + \varphi I)]$$

The solution of the equation (refer to Annexure A.1) returns the following results:

#### Phase-phase loops

In this case it is assumed that  $R_{\text{fwd}} = R_{\text{ret}}$ , and  $X_{\text{fwd}} = X_{\text{ret}}$  (symmetrical system).

From this we get (for example loop L2-L3):

$$R_{\text{L2-L3}} = \frac{\text{Re}\{\underline{U}_{\text{L2-L3}}\} \cdot \text{Re}\{\underline{I}_{\text{L2-L3}}\} + \text{Im}\{\underline{U}_{\text{L2-L3}}\} \cdot \text{Im}\{\underline{I}_{\text{L2-L3}}\}}{[\text{Re}\{\underline{I}_{\text{L2-L3}}\}]^2 + [\text{Im}\{\underline{I}_{\text{L2-L3}}\}]^2} \quad (3-34)$$

$$X_{\text{L2-L3}} = \frac{\text{Im}\{\underline{U}_{\text{L2-L3}}\} \cdot \text{Re}\{\underline{I}_{\text{L2-L3}}\} - \text{Re}\{\underline{U}_{\text{L2-L3}}\} \cdot \text{Im}\{\underline{I}_{\text{L2-L3}}\}}{[\text{Re}\{\underline{I}_{\text{L2-L3}}\}]^2 + [\text{Im}\{\underline{I}_{\text{L2-L3}}\}]^2} \quad (3-35)$$

$$\text{with } \underline{U}_{\text{L2-L3}} = \underline{U}_{\text{L2}} - \underline{U}_{\text{L3}} \quad \text{and} \quad \underline{I}_{\text{L2-L3}} = \underline{I}_{\text{L2}} - \underline{I}_{\text{L3}} \quad (3-36)$$

These equations correspond to the following expressions with phasor quantities used in the traditional relaying practice:

$$Z_{\text{L2-L3}} = \frac{\underline{U}_{\text{L2}} - \underline{U}_{\text{L3}}}{\underline{I}_{\text{L2}} - \underline{I}_{\text{L3}}} \quad (3-37)$$

$$R_{\text{L2-L3}} = \text{Re}\left\{ \frac{\underline{U}_{\text{L2}} - \underline{U}_{\text{L3}}}{\underline{I}_{\text{L2}} - \underline{I}_{\text{L3}}} \right\} \quad (3-38)$$

$$X_{\text{L2-L3}} = \text{Im}\left\{ \frac{\underline{U}_{\text{L2}} - \underline{U}_{\text{L3}}}{\underline{I}_{\text{L2}} - \underline{I}_{\text{L3}}} \right\} \quad (3-39)$$

These equations may be used where fault voltage and current are given as complex values, for example with calculation programs.

When the measuring quantities are given as phasor quantities with modulus (rms value) and phase angle, the following formulae may be used

$$R_{L2-L3} = \frac{U_{L2-L3}[I_{L2} \cdot \cos(\varphi_{U_{L2-L3}} - \varphi_{I_{L2}}) - I_{L3} \cdot \cos(\varphi_{U_{L2-L3}} - \varphi_{I_{L3}})]}{I_{L2}^2 - 2 \cdot I_{L2} \cdot I_{L3} \cdot \cos(\varphi_{I_{L2}} - \varphi_{I_{L3}}) + I_{L3}^2} \quad (3-40)$$

$$X_{L2-L3} = \frac{U_{L2-L3}[I_{L2} \cdot \sin(\varphi_{U_{L2-L3}} - \varphi_{I_{L2}}) - I_{L3} \cdot \sin(\varphi_{U_{L2-L3}} - \varphi_{I_{L3}})]}{I_{L2}^2 - 2 \cdot I_{L2} \cdot I_{L3} \cdot \cos(\varphi_{I_{L2}} - \varphi_{I_{L3}}) + I_{L3}^2} \quad (3-41)$$

In case only the phase voltages are known from the short-circuit study, the following equations (3-42) and (3-43) for the phase-phase loops may be applied:

$$R_{L2-L3} = \frac{U_{L2} \cdot I_{L2} \cdot \cos(\varphi_{U_2} - \varphi_{I_2}) + U_{L3} \cdot I_{L3} \cdot \cos(\varphi_{U_3} - \varphi_{I_3})}{I_{L2}^2 - 2 \cdot I_{L2} \cdot I_{L3} \cdot \cos(\varphi_{I_2} - \varphi_{I_3}) + I_{L3}^2} - \frac{U_{L2} \cdot I_{L3} \cdot \cos(\varphi_{U_2} - \varphi_{I_3}) + U_{L3} \cdot I_{L2} \cdot \cos(\varphi_{U_3} - \varphi_{I_2})}{I_{L2}^2 - 2 \cdot I_{L2} \cdot I_{L3} \cdot \cos(\varphi_{I_2} - \varphi_{I_3}) + I_{L3}^2} \quad (3-42)$$

$$X_{L2-L3} = \frac{U_{L2} \cdot I_{L2} \cdot \sin(\varphi_{U_2} - \varphi_{I_2}) + U_{L3} \cdot I_{L3} \cdot \sin(\varphi_{U_3} - \varphi_{I_3})}{I_{L2}^2 - 2 \cdot I_{L2} \cdot I_{L3} \cdot \cos(\varphi_{I_2} - \varphi_{I_3}) + I_{L3}^2} - \frac{U_{L2} \cdot I_{L3} \cdot \sin(\varphi_{U_2} - \varphi_{I_3}) + U_{L3} \cdot I_{L2} \cdot \sin(\varphi_{U_3} - \varphi_{I_2})}{I_{L2}^2 - 2 \cdot I_{L2} \cdot I_{L3} \cdot \cos(\varphi_{I_2} - \varphi_{I_3}) + I_{L3}^2} \quad (3-43)$$

For the case of a two-phase fault with single in-feed, the following additional condition applies (figure 3.69):

$$\bullet \quad I_{L3} = -I_{L2} = I_L \quad \text{and} \quad \varphi_{I(L3)} = \varphi_{I(L2)} + 180^\circ.$$

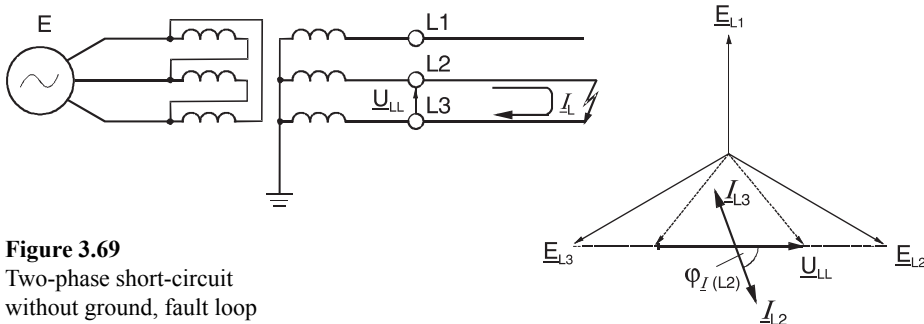


**Figure 3.69**  
Two-phase short-circuit  
without ground, fault loop

This simplifies the equations (3-40) and (3-41) as follows:

$$R_{L2-L3} = \frac{U_{LL} \cdot \cos(\varphi_{U_{LL}} - \varphi_{I_L})}{2 \cdot I_L} = \frac{U_{LL}}{2 \cdot I_L} \cdot \cos \varphi_{SC} \quad (3-44)$$

$$X_{L2-L3} = \frac{U_{LL} \cdot \sin(\varphi_{U_{LL}} - \varphi_{I_L})}{2 \cdot I_L} = \frac{U_{LL}}{2 \cdot I_L} \cdot \sin \varphi_{SC} \quad (3-45)$$

For the three-phase fault the following conditions apply (figure 3.70):

- $I_{L2} = I_{L3} = I_{SC}$
- $\varphi_{U(L2-L3)} - \varphi_{I(L2)} = \varphi_{SC} + 30^\circ$
- $\varphi_{U(L2-L3)} - \varphi_{I(L3)} = \varphi_{SC} + 150^\circ$
- $\varphi_{I(L2)} - \varphi_{I(L3)} = 120^\circ$

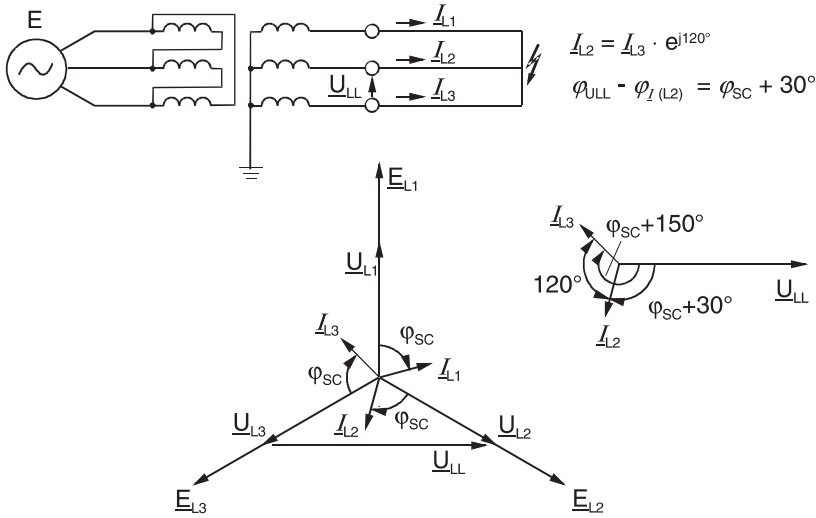


**Figure 3.70** Three-phase short-circuit fault loop

The following simplified equations result:

$$R_{L2-L3} = \frac{U_{LL}}{I_{SC} \sqrt{3}} \cdot \cos \varphi_{SC} \quad (3-46)$$

$$X_{L2-L3} = \frac{U_{LL}}{I_{SC} \sqrt{3}} \cdot \sin \varphi_{SC} \quad (3-47)$$

*Phase-earth loops*

In figure 3.71: the measured fault loop for a phase to earth short-circuit in L1-E is shown.

It must be noted that the loop L1-E is also valid for other short-circuit types, such as for example the two-phase to earth faults L1-L2-E and L3-L1-E or a three-phase short-circuit.

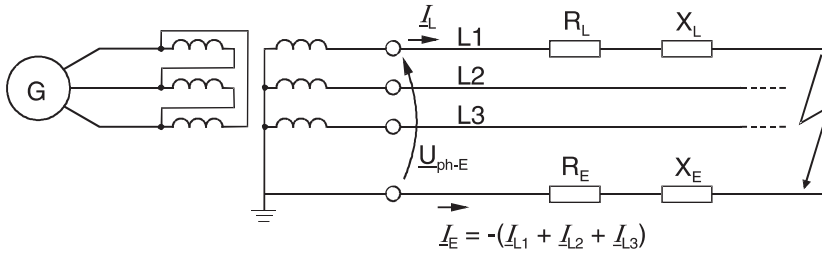


**Figure 3.71** Single-phase earth-fault, fault loop

The following equations generally apply for all earth-fault types (1-, 2- or 3-phase):

$$R_{\text{ph-E}} = \frac{\text{Re}\{U_{\text{ph-E}}\} \cdot \text{Re}\{I_X\} + \text{Im}\{U_{\text{ph-E}}\} \cdot \text{Im}\{I_X\}}{\text{Re}\{I_R\} \cdot \text{Re}\{I_X\} + \text{Im}\{I_R\} \cdot \text{Im}\{I_X\}} \quad \text{and} \quad (3-48)$$

$$X_{\text{ph-E}} = \frac{\text{Im}\{U_{\text{ph-E}}\} \cdot \text{Re}\{I_R\} - (\text{Re}\{U_{\text{ph-E}}\} \cdot \text{Im}\{I_R\})}{\text{Re}\{I_R\} \cdot \text{Re}\{I_X\} + \text{Im}\{I_R\} \cdot \text{Im}\{I_X\}} \quad (3-49)$$

with the composed currents:

$$I_R = I_{\text{ph}} - \frac{R_E}{R_L} \cdot I_E \quad \text{and} \quad I_X = I_{\text{ph}} - \frac{X_E}{X_L} \cdot I_E \quad (3-50)$$

The factors  $R_E/R_L = k_{\text{RE}}$  and  $X_E/X_L = k_{\text{XE}}$  correspond to the residual compensation factors to be set in the relay.

These formulae can again be used with complex calculation.

Where phasor quantities are given, the following formulae are convenient.

$$R_{\text{ph-E}} = \frac{U_{\text{ph-E}}}{I_L} \cdot \frac{\cos(\varphi_U - \varphi_L) - \frac{I_E}{I_L} \cdot \frac{X_E}{X_L} \cdot \cos(\varphi_U - \varphi_E)}{1 - \left(\frac{X_E}{X_L} + \frac{R_E}{R_L}\right) \cdot \frac{I_E}{I_L} \cdot \cos(\varphi_E - \varphi_L) + \frac{R_E}{R_L} \cdot \frac{X_E}{X_L} \cdot \left(\frac{I_E}{I_L}\right)^2} \quad (3-51)$$

$$X_{\text{Ph-E}} = \frac{U_{\text{Ph-E}}}{I_L} \cdot \frac{\sin(\varphi_U - \varphi_L) - \frac{I_E}{I_L} \cdot \frac{R_E}{R_L} \cdot \sin(\varphi_U - \varphi_E)}{1 - \left(\frac{X_E}{X_L} + \frac{R_E}{R_L}\right) \cdot \frac{I_E}{I_L} \cdot \cos(\varphi_E - \varphi_L) + \frac{R_E}{R_L} \cdot \frac{X_E}{X_L} \cdot \left(\frac{I_E}{I_L}\right)^2} \quad (3-52)$$

where:  $U_{\text{Ph-E}}$  = short-circuit voltage (rms)  
 $I_L$  = short-circuit phase-current (rms)  
 $I_E$  = short-circuit earth-current (rms)  
 $\varphi_U$  = phase angle of the short-circuit voltage  
 $\varphi_L$  = phase angle of the short-circuit phase-current  
 $\varphi_E$  = phase angle of the short-circuit earth-current  
 $R_E/R_L$  and  $X_E/X_L$  are the parameters set in the relay for residual compensation.

In the case of single-phase earth-faults, the currents  $I_E$  and  $I_L$  are approximately in phase opposition.

The magnitudes may however be different, depending on the type of earthing. If  $\varphi_E = \varphi_L + 180^\circ$  is assumed, the equations (3-51) and (3-52) are significantly simplified:

$$R_{\text{ph-E}} = \frac{U_{\text{Ph-E}} \cdot \cos(\varphi_U - \varphi_L)}{I_L - \frac{R_E}{R_L} \cdot I_E} = \frac{U_{\text{Ph-E}} \cdot \cos \varphi_{\text{SC}}}{I_L - \frac{R_E}{R_L} \cdot I_E} \quad (3-53)$$

$$X_{\text{Ph-E}} = \frac{U_{\text{Ph-E}} \cdot \sin(\varphi_U - \varphi_L)}{I_L - \frac{X_E}{X_L} \cdot I_E} = \frac{U_{\text{Ph-E}} \cdot \sin \varphi_{\text{SC}}}{I_L - \frac{X_E}{X_L} \cdot I_E} \quad (3-54)$$

in this case:  $\varphi_U$  = phase angle of the short-circuit voltage  
 $\varphi_L$  = phase angle of  $I_L$  and  $I_E$   
 $\varphi_U - \varphi_L = \varphi_{\text{SC}}$  = short-circuit angle of the fault loop (phase-earth loop)

Note: The traditional distance relays and fault locators have been using the following formulae for distance to fault determination:

$$\underline{Z}_{\text{Ph-E}} = \frac{U_{\text{Ph-E}}}{I_L - k_E \cdot I_E} \quad (3-55)$$

$$R_{\text{Ph-E}} = \text{Re}\{\underline{Z}_{\text{Ph-E}}\} \quad (3-56)$$

$$X_{\text{Ph-E}} = \text{Im}\{\underline{Z}_{\text{Ph-E}}\} \quad (3-57)$$

It must be observed that the numerical calculation of the impedances for phase-earth faults, as outlined above, and used with the 7SA type relays, does not always deliver the same results as this traditional calculation.

Formula 3-55 only delivers the true reactance (distance) to the fault point when the set  $k_E$  factor corresponds to the real  $\underline{Z}_E/\underline{Z}_L$  ratio of the fault loop. This is only the case for faults without fault resistance (“dead faults”).

A fault resistance will introduce an error in the X-calculation. This is discussed in paragraph 3.5.1.

#### Calculation example:

The application of the equations on hand is explained by means of the following examples:

A 110 kV single-circuit overhead line with the following data is given:

Line length:  $l = 50 \text{ km}$

Line impedance per km:

Positive-sequence system:  $R'_{L1} = 0.1286 \text{ } \Omega/\text{km}$

$X'_{L1} = 0.4023 \text{ } \Omega/\text{km}$

Zero-sequence system:  $R'_{L0} = 0.2409 \text{ } \Omega/\text{km}$

$X'_{L0} = 1.0863 \text{ } \Omega/\text{km}$

It is a pre-requisite that the setting parameters for the residual compensation in the distance relay 7SA6 are adapted to the feeder:

$$R_E/R_L = (R'_0 - R'_1)/(3 R'_1) = 0.291$$

$$X_E/X_L = (X'_0 - X'_1)/(3 X'_1) = 0.567$$

#### Example 1:

Single-phase earth-fault L1-E at the end of the line.

The following voltages and currents at the relay location were calculated by means of computer program:

$$U_{L1} = 53.51 \text{ kV and } \varphi_{U_{L1}} = -1.4^\circ$$

$$I_{L1} = 1.6415 \text{ kA and } \varphi_{I_{L1}} = -76.6^\circ$$

$$I_E = 1.6509 \text{ kA and } \varphi_{I_E} = 103.4^\circ$$

(sign convention according to figure 3.66)

What is the fault impedance measured by the distance protection relay?

Solution:

With equations (3-53) and (3-54)  $X_{L1-E}$  and  $R_{L1-E}$  can be calculated:

$$X_{L1-E} = \frac{53.51 \cdot \sin(-1.4^\circ + 76.6^\circ)}{1.6415 + 0.567 \cdot 1.6509} = 20.07 \text{ } \Omega$$

$$R_{L1-E} = \frac{53.51 \cdot \cos(-1.4^\circ + 76.6^\circ)}{1.6415 + 0.291 \cdot 1.6509} = 6.44 \text{ } \Omega$$

The values correspond to the line data:

$$X_{L1} = 1 \cdot X'_{L1} = 50 \cdot 0.4023 = 20.12 \, \Omega \text{ and}$$

$$R_{L1} = 1 \cdot R'_{L1} = 50 \cdot 0.1286 = 6.43 \, \Omega$$

The small variances are due to the capacitive charging currents of the line.

*Example 2:*

Two-phase earth-fault L1-L2-E at the end of the line.

The following short-circuit data was derived from the fault recording:

$$U_{L1-E} = 51.939 \text{ kV and } \varphi_{U_{L1}} = -5.21^\circ$$

$$U_{L2-E} = 50.516 \text{ kV and } \varphi_{U_{L2}} = -119.05^\circ$$

$$I_{L1} = 2.098 \text{ and } \varphi_{I_{L1}} = -62.38^\circ$$

$$I_{L2} = 2.153 \text{ and } \varphi_{I_{L2}} = 152.12^\circ$$

$$I_E = 1.291 \text{ and } \varphi_{I_E} = 41.58^\circ$$

What is the impedance measured in the fault loop L1-E?

*Solution:*

With the equations (3-51) and (3-52) the following is obtained:

$$\begin{aligned} X_{L1-E} &= \frac{51.939}{2.098} \cdot \frac{\sin(-5.21^\circ + 62.38^\circ) - \frac{1.291}{2.098} \cdot 0.291 \cdot \sin(-5.21^\circ + 138.42^\circ)}{1 - (0.567 + 0.291) \cdot \frac{1.291}{2.098} \cdot \cos(-138.42^\circ + 62.38^\circ) + 0.291 \cdot 0.567 \cdot \left(\frac{1.291}{2.098}\right)^2} \\ &= 20.02 \, \Omega \end{aligned}$$

$$\begin{aligned} R_{L1-E} &= \frac{51.939}{2.098} \cdot \frac{\cos(-5.21^\circ + 62.38^\circ) - \frac{1.291}{2.098} \cdot 0.567 \cdot \cos(-5.21^\circ - 41.58^\circ)}{1 - (0.567 + 0.291) \cdot \frac{1.291}{2.098} \cdot \cos(41.58^\circ + 62.38^\circ) + 0.291 \cdot 0.567 \cdot \left(\frac{1.291}{2.098}\right)^2} \\ &= 6.32 \, \Omega \end{aligned}$$

The results again closely correlate with the line data.

In a similar manner the fault impedance for the loop L2-E can be calculated.

The impedances measured by the phase-phase loop,  $X_{L1-L2}$  and  $R_{L1-L2}$ , can be derived in a similar manner, using the equations (3-42) and (3-43).

In both cases the same reactance and resistance values as for the loop L1-E should result, because a multiple-phase short-circuit applies, for which all three measurements have a valid short-circuit loop. Checking hereof is left to the reader as an exercise.



### 3.3 Numerical direction determination (polarisation)

In this chapter we will at first have a closer look at the behaviour of direction determination with self polarisation (faulty phase voltage) under different fault and system conditions. After that, we will elaborate in detail upon the direction determination with cross-polarisation (using healthy phase(s)) and memory polarisation which are now generally available with numerical relays.

#### 3.3.1 Direction determination with fault loop voltage (self polarisation)

In paragraph 3.1.5 it was already mentioned that the fault direction can be determined from the relative phase angles of the short-circuit current and short-circuit voltage or from the sign of the measured short-circuit impedance. A pre-requisite for this is that the relay measures an inductive impedance, i.e. that a combination of resistance and inductance is “seen” where the short-circuit voltage always leads the current

This is the normal situation in traditional power systems.

On a line with series compensation the measured fault impedance may however become capacitive (negative) for forward faults behind the capacitor and the voltage will lag the current, as elaborated on in paragraph 3.5.7. Self polarised relays can therefore not be used in this case.

#### *Zero-volt faults*

It must be borne in mind, that during faults directly in front of or behind the voltage transformer, the short-circuit impedance may become so small (theoretically zero), that a secure directional decision is no longer possible. With conventional relays employing moving coil or static technology, the lower limit for directional sensitivity was approx. 0.1 V. For even older induction type relays, the directional sensitivity was in the order of one volt.

This area, where no definite directional decision is possible, is designated as “dead zone”. For these extremely small short-circuit voltages, the only solution lies in the utilisation of pre-selection of fault direction. In Germany, classical relays had a pre-selection of forward, to ensure definite tripping during close-up faults. A risk introduced with this was that when a feeder was switched onto an earthed line (forgotten working earth), all relays on the busbar would trip. Utilities in some other countries therefore preferred a pre-selection of reverse direction.

#### *Impact of line loading*

On long transmission lines, directional discrimination is influenced by the pre-fault load due to the angle shift of the source voltages between both line ends [3-27]. This is critical with reverse faults, where the line fault current is driven by the remote emf and the voltage at the relay location is largely determined by the local emf. A typical example is shown in figure 3.72.

We consider the relay in B for a reverse fault with arc resistance behind the busbar.

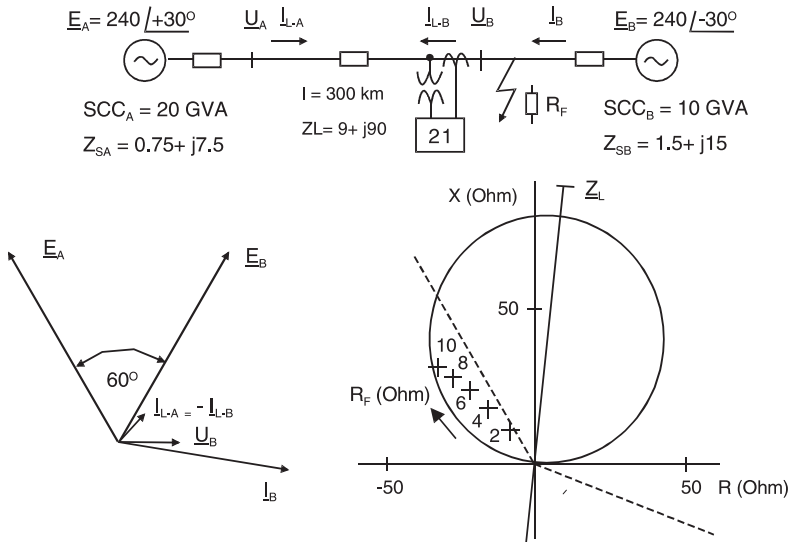


**Figure 3.72**

Influence of line loading on direction discrimination: close up reverse fault with resistance (U-I diagram for  $R_F = 4 \Omega$ )

The fault resistance is assumed to be relatively low so that the currents are mainly determined by the source and line impedances.

The line fault current  $I_{F1}$  is in this situation small compared to the current  $I_{F2}$  from the strong source behind B. The voltage drop at the fault resistance is therefore largely determined by  $I_{F2}$ . The resulting voltage and current diagram is shown in figure 3.72.

The relay in B measures the impedance  $\underline{Z}_R = \underline{U}_B / \underline{I}_{L-B}$ . This impedance appears in the second quadrant of the relay diagram. A self polarised 30° straight line or MHO characteristic would false-operate in this case.

Restricting the forward reach area by a bended directional line, as indicated, mitigates the problem.

Cross polarised directional characteristics are influenced in a similar way as self-polarised types but behave better due to a forward offset in case of reverse faults. This is discussed in detail in the paragraph 3.3.5.

Cross polarised MHO relays show excellent performance due to the shrinking and forward offset of the circle. This will be considered in paragraph 3.4.3.

### *Use of self-polarisation in numerical relays*

Self-polarisation was typically used with distribution system relays for cost reasons. Cross polarisation was originally introduced in transmission and sub-transmission to cover the zero-volt fault. Memory polarisation was only used in transmission. Later, the cross and memory polarisation were also needed for series compensated lines.

Numerical relays can run all three polarisation methods in parallel and auto-select online the most suitable variant. Self-polarisation is the clearest way because it limits the measurement to the faulted loop. This has advantages in case of complex and multiple faults. 7SA relays select the fault loop voltage when the memory is empty and there is no series compensation (see paragraph 3.3.7).

For a similar reason, MHO relays use a low percentage of cross polarisation (15% in the case of 7SA522) for the normal application case without series compensation.

### 3.3.2 Direction determination with healthy phase voltages (cross-polarisation)

The principle of directional decision-making with healthy phase voltages (cross-polarisation) is explained by means of the following example of a single-phase short-circuit (figure 3.73) For simplification the fault is assumed on an unloaded radial feeder, i.e. the influence of load currents is initially neglected. The voltage prior to fault inception is therefore equal to the source emf.

During an earth-fault in phase L1, the current and voltage conditions shown appear.

The short-circuit current is driven by  $\underline{E}_{L1}$  and will lag the voltage  $\underline{E}_{L1}$  by an angle  $\varphi$  if the impedance in the short-circuit loop is resistive and inductive.

The short-circuit voltage  $\underline{U}_{SCL}$  has a magnitude and phase angle dependant on the ratio of  $\underline{Z}_{SC}$  to  $\underline{Z}_S$ . If both impedances have the same phase angle, then  $\underline{U}_{SCL1}$  is in-phase with  $\underline{E}_{L1}$ , and the short-circuit angle  $\varphi_{SC}$  corresponds to the angle  $\varphi$ .

During close-in faults with arc resistance or for cable faults, the angle of the short-circuit impedance is however substantially smaller than the angle of the source impedance. This is especially true when the source impedance mainly consists of generator and transformer reactances. Furthermore it must be considered that for close-in faults  $\underline{Z}_S \gg \underline{Z}_{SC}$ , and therefore the angle  $\varphi$  hardly changes, even for substantially different short-circuit conditions. At the same time,  $\varphi_{SC}$  may assume very small values down to  $0^\circ$  (close-in fault with arc resistance).

An extreme situation arises when the fault is behind a series capacitor. In this case the short-circuit voltage is inverted according to the measured negative reactance  $X_{SC} = -X_C$ .<sup>1</sup> The short-circuit voltage now lags the short-circuit current by about  $90^\circ$  (figure 3.73b), although the fault is in forward direction.

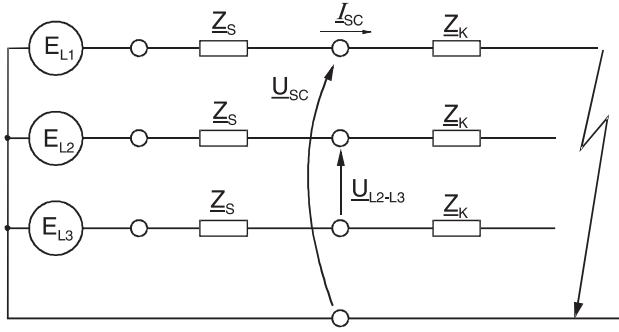
The voltage in the short-circuited phase is therefore also not suitable for a directional decision on series-compensated lines.

For the directional decision, the opposite line voltage  $\underline{U}_{L2-L3}$  is an alternative to the voltage in the short-circuited phase  $\underline{U}_{SCL1}$ .

In figure 3.73b it can be seen that for the described fault cases the relative phase angle  $\underline{I}_{SCL1}$  to  $\underline{U}_{L2-L3}$  is almost unchanged. Only in the case of a true reverse fault will the short-circuit current reverse i.e. rotate by approx.  $180^\circ$ .

---

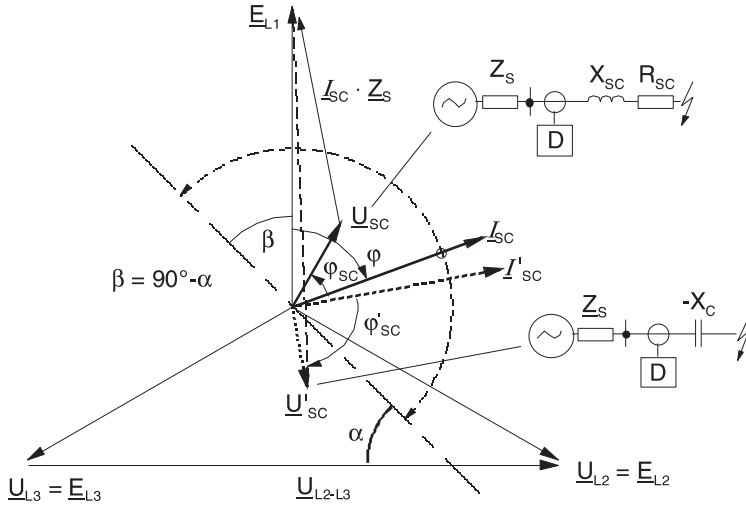
<sup>1</sup>  $|X_C| < |X_S|$ , which is always the case in practice, was assumed (see paragraph 3.5.7)



$$E_{L1} = \underline{U}_{SC} + \underline{Z}_S \cdot \underline{I}_{SC}$$

$$\underline{U}_{L2-L3} = \underline{E}_{L2-L3} = \underline{E}_{L1} \cdot \sqrt{3} \cdot e^{j90^\circ}$$

a) Equivalent circuit



b) Voltage diagram

**Figure 3.73** Directional determination with unfaulted loop voltages (cross-polarisation)

The measurement of the angle between the short-circuit current and the healthy line voltage provides an ideal directional decision.

The phase angle of the healthy line voltage must be adjusted to achieve the same directional characteristic as would be the case for measurement with the faulted loop voltage. To achieve this, the voltage  $\underline{U}_{L2-L3}$  in figure 3.73b must be rotated by  $90^\circ$  in the forward direction to approximately achieve the same phase angle as the voltage in the short-circuited loop ( $\underline{U}_{L1}$ ).

In the case of numerical relays, a polarising impedance is calculated, using the healthy line voltage and the short-circuit current. This impedance is then compared with the directional characteristic in the impedance plane.

The directional characteristic in its simplest form is straight line (e.g. 7SA511) with a slope of  $\alpha = 45^\circ$  relative to the line voltage, as indicated in figure 3.73b.

In this case, a fault in the forward direction is recognised, when  $I_{SC}$  has an angular relationship in the range  $45^\circ$  lagging up to  $135^\circ$  leading relative to the polarising voltage  $\underline{U}_{L2-L3}$ .

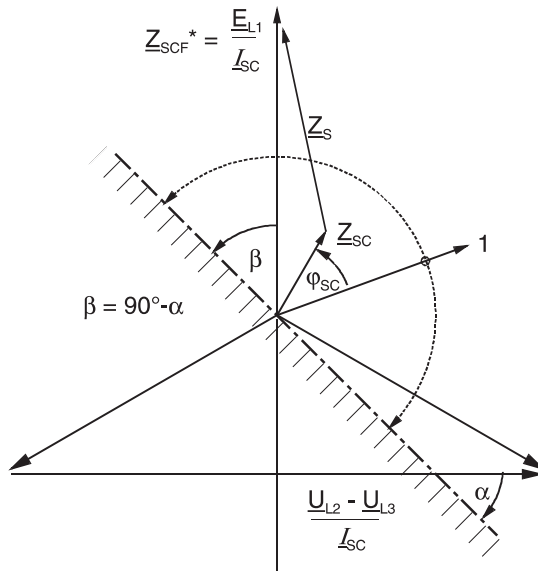
### 3.3.3 Directional characteristic in the impedance plane

To convert the directional characteristic to the impedance plane, the voltages in figure 3.73b are initially divided by the short-circuit current. The diagram shown in figure 3.74 results.

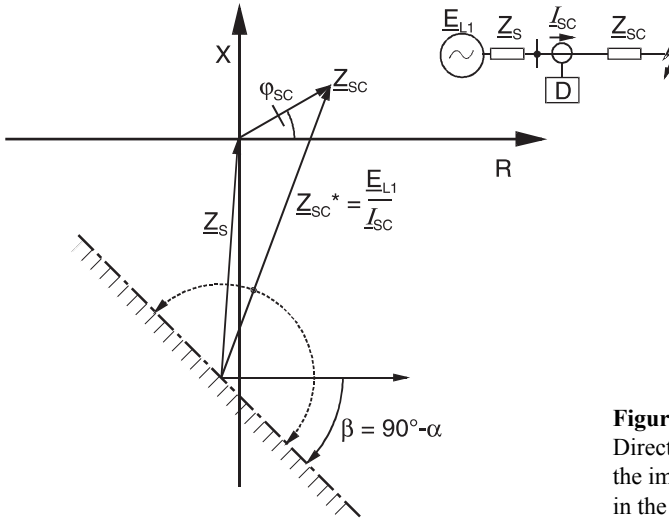
The vector of the polarising impedance  $\underline{Z}_{SCF}^*$  corresponds to the healthy line voltage rotated by  $90^\circ$  in the forward direction. If we fix the unit vector “1” as the real axis of the impedance diagram, and re-arrange the other vectors, we arrive at the representation in the impedance plane (figure 3.75), wherein the short-circuit impedance  $\underline{Z}_{SC}$  and the zone characteristics of the relay in their general form (refer to figure 3.3 in paragraph 3.1.3) are entered.

In the source voltage  $\underline{E}_{L1}$  or the corresponding impedance  $\underline{Z}_{SCF}^*$  are fixed as reference quantities. The relay indicates the forward direction as long as the vector “1”, i.e. the current, is within the angular area represented by the dashed arc.

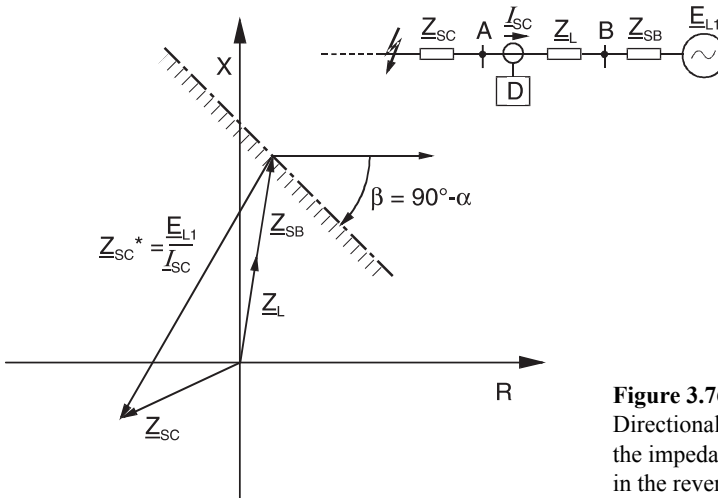
In figure 3.75 the converse condition is shown: the vector “1” is fixed as real axis, and  $\underline{Z}_{SCF}^*$  may correspondingly lie within the angular area represented by the dashed arc to result in a forward decision.



**Figure 3.74**  
Impedance diagram


**Figure 3.75**

Directional characteristic in the impedance plane for faults in the forward direction


**Figure 3.76**

Directional characteristic in the impedance plane for faults in the reverse direction

The shift of the directional characteristic, in proportion to the source impedance, implies that for close-in faults a definite forward directional decision is achieved, even when the short-circuit voltage and hence  $Z_{SC}$  is equal to zero.

Even faults in the forward direction, located behind series-capacitors, resulting in a negative short-circuit impedance are recognised as faults in the forward direction.

Regard is however to be taken that the depiction in figure 3.75 only applies to faults in the forward direction.

In the case of reverse faults, the short-circuit current flows in the opposite direction, through the current-transformers, and therefore also, in the negative sense through the relay. This results in a reversal of the phase relationship between the short circuit cur-

rent  $I_{SC}$  and the polarising voltage  $\underline{U}_{L1-L2}$  or  $\underline{E}_{L1}$ . Faults in the reverse direction must therefore be shown in a separate diagram (figure 3.76).

This again shows that close in faults and faults behind series capacitors in the reverse direction are recognised correctly.

**Note:** In practice it is common to show the directional characteristic as a straight line through the origin (or two straight lines meeting in the origin at angle) of the impedance plane. This is correct for conventional, medium voltage relays (R1KZ4, 7SL70), where the voltage in the faulted loop was utilised. This representation strictly speaking, is also valid for cross polarised relays when the in-feed is assumed to be infinitely strong i.e.  $\underline{Z}_S = 0$ .

In general, this simplification is acceptable as long as no limiting conditions for close-in faults are investigated.

On series-compensated feeders, or long transmission lines with load transfer, the correct representation is required, as is shown below.

### 3.3.4 Selection of the cross polarisation voltage

The principle of direction-determination with healthy (unfaulted) phase voltages was up to now demonstrated at the example of a single-phase-to-earth fault.

This principle similarly applies for all other fault types. Numerical relays always select a polarising voltage, which is rotated by  $90^\circ$  (cross-polarised voltage) (figure 3.77 and table 3.6).

Naturally, in the case of a three-phase fault, no healthy loop voltages are available. For this eventuality, the numerical relays make use of a voltage memory, which stores the polarising voltage available prior to fault inception. This ensures that healthy loop volt-

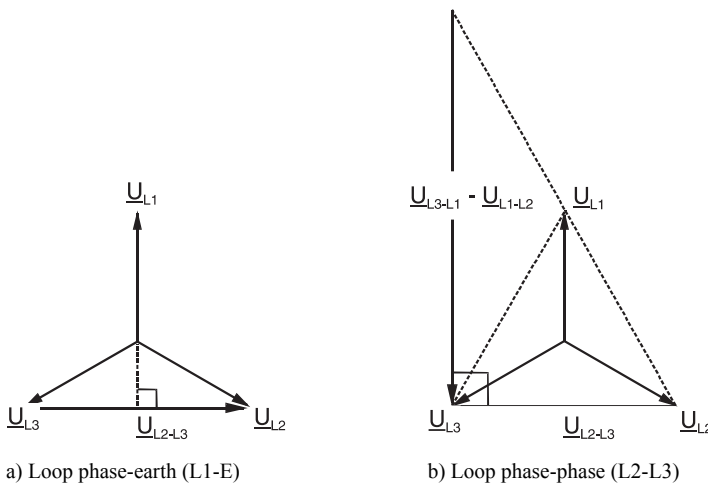


**Figure 3.77** Reference voltage for directional determination

**Table 3.6**Measured values for distance measurement and directional determination  $\underline{k}_E = \underline{Z}_E / \underline{Z}_L$ 

measured loop	measured current (distance)	measured voltage (distance)	measured current (direction)	measured voltage (direction)
L1-E	$\underline{I}_{L1} - \underline{k}_E \cdot \underline{I}_E$	$\underline{U}_{L1-E}$	$\underline{I}_{L1} - (-\underline{k}_E \cdot \underline{I}_E)^1$	$\underline{U}_{L2-L3}$
L2-E	$\underline{I}_{L2} - \underline{k}_E \cdot \underline{I}_E$	$\underline{U}_{L2-E}$	$\underline{I}_{L2} - (-\underline{k}_E \cdot \underline{I}_E)^1$	$\underline{U}_{L3-L1}$
L3-E	$\underline{I}_{L3} - \underline{k}_E \cdot \underline{I}_E$	$\underline{U}_{L3-E}$	$\underline{I}_{L3} - (-\underline{k}_E \cdot \underline{I}_E)^1$	$\underline{U}_{L1-L2}$
L1-L2	$\underline{I}_{L1} - \underline{I}_{L2}$	$\underline{U}_{L1-L2}$	$\underline{I}_{L1} - \underline{I}_{L2}$	$\underline{U}_{L2-L3} - \underline{U}_{L3-L1}$
L2-L3	$\underline{I}_{L2} - \underline{I}_{L3}$	$\underline{U}_{L2-L3}$	$\underline{I}_{L2} - \underline{I}_{L3}$	$\underline{U}_{L3-L1} - \underline{U}_{L1-L2}$
L3-L1	$\underline{I}_{L3} - \underline{I}_{L1}$	$\underline{U}_{L3-L1}$	$\underline{I}_{L3} - \underline{I}_{L1}$	$\underline{U}_{L1-L2} - \underline{U}_{L2-L3}$

<sup>1</sup> with  $\underline{k}_E \cdot \underline{I}_E$  only in case of single phase to earth faults

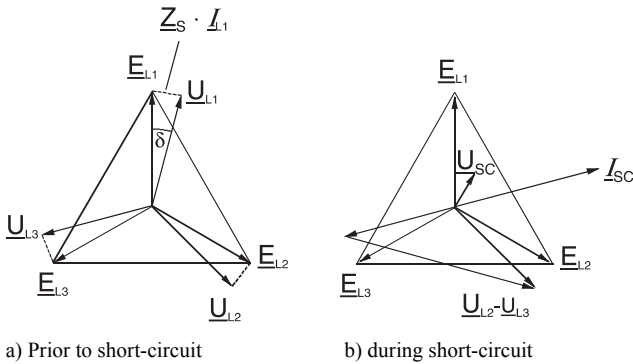
ages for the directional decision are available for a suitable amount of time after fault inception (up to 2 s in the 7SA522 and 7SA6 relays).

### 3.3.5 Influence of load transfer

Until now, the analysis assumed unloaded feeders, so that the healthy loop voltage corresponded to the source emf.

In practice however, the load transfer influences this, because the voltage at the relay location differs from the source voltage corresponding to the voltage drop on the feeder (figure 3.78).

For the directional determination, the decisive influence is the angular rotation  $\delta$ , introduced by the real load current flowing through the line.

**Figure 3.78** Voltage phasor diagram for earth-fault with load flow



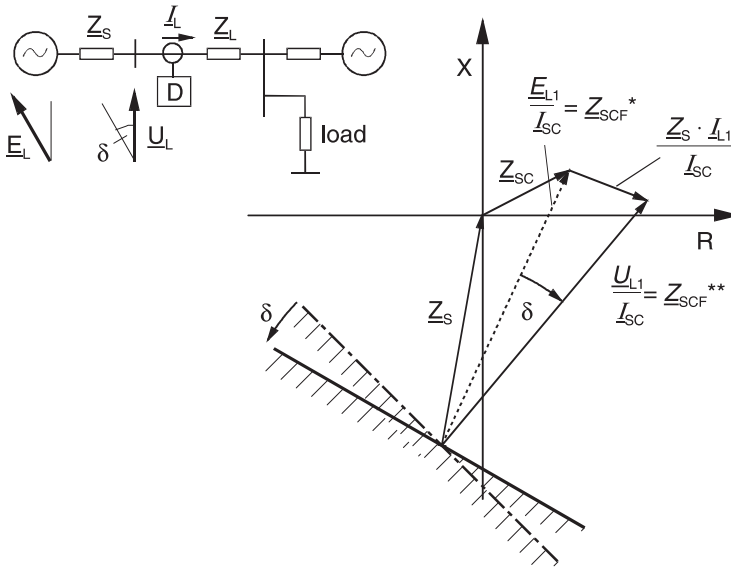


**Figure 3.79** The influence of load transfer on the directional characteristic

The rotation of the unfaulted loop-polarising voltage introduces a corresponding opposite rotation of the directional characteristic (figure 3.79). This can be derived from figures 3.74 and 3.75.

On short lines and strong in-feeds, this effect is relatively small (in Germany, for instance,  $< 10^\circ$ ). On long lines with heavy load, the stationary transmission angle may

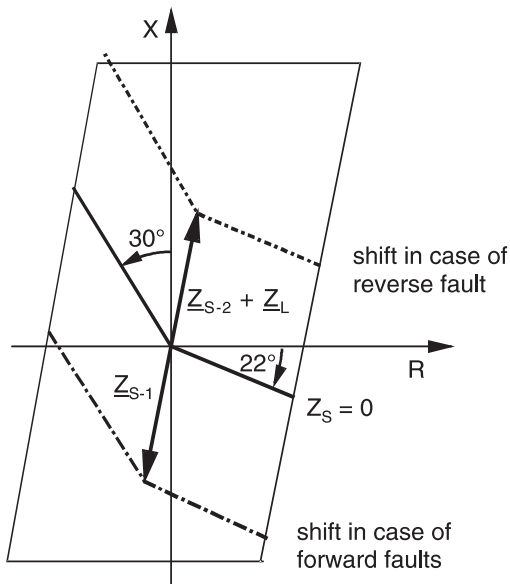


**Figure 3.80**  
Optimised directional  
characteristic for the EHV  
protection (7SA522)

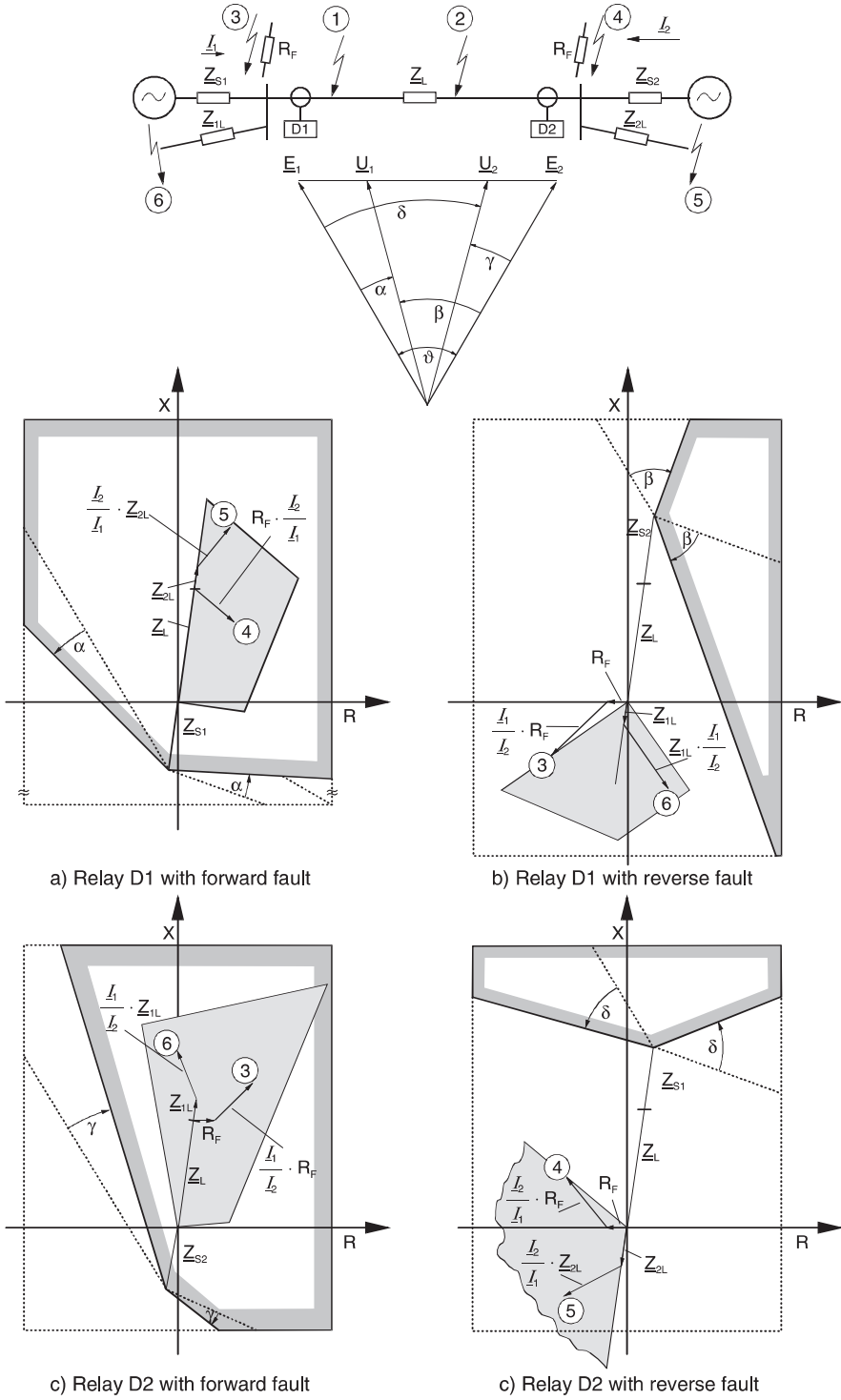


**Figure 3.81** Directional determination with healthy loop voltages on long transmission lines

assume values of approx.  $60^\circ$ , so that an unfaulted loop voltage rotation of this magnitude must be considered.

For this reason the directional characteristic of the EHV distance protection must be optimised. In particular, a larger security margin is necessary for reverse faults where the large angular rotations may occur (figure 3.80). The behaviour on long transmission lines is shown in figure 3.81.

It is apparent that for faults in the reverse direction, there is a large angle difference between the effective source voltage and the voltage at the relay location. The latter corresponds to the healthy phase(s) voltage, or the memory voltage. The difference is especially great for faults in the reverse direction ( $\beta$  and  $\delta$ ), where the emf of the opposite end drives the short-circuit current. In spite of the angle rotation of approx.  $45^\circ$ , the directional decision is correct in each case.

Of special interest is the fault case ④, where as a result of the fault resistance  $R_F$  and the intermediate in-feed  $I_2/I_1$  the short-circuit impedance appears in the second quadrant. This effect arises because the short-circuit current  $I_2$ , driven by  $E_2$  lags the short-circuit current  $I_1$ , driven by  $E_1$  by approx.  $60^\circ$ . A conventional self-polarised MHO-relay, or a relay utilising faulted loop voltage polarisation and a flat characteristic would incorrectly trip for this reverse fault.

### 3.3.6 Implementation of voltage-memory(-ies)

A voltage-memory is of particular importance for close-in three-phase faults and on series compensated overhead lines.

Other than with analogue relays, where the voltage-memory was only available for a few cycles, the numerical technology today in itself allows continuation of the polarising voltage for as long as desired.

A lengthy memorisation of the voltage would however require frequency compensation. Otherwise, any deviation of the system frequency would introduce an angular rotation of the directional characteristic proportional to  $\Delta f \cdot t$ . For example with the distance relays 7SA522 and 7SA6, which provide a memory capacity up to 2 s, this compensation is realised.

In the event that there is no measured voltage present when the voltage memory resets, the last valid directional decision is maintained until the measured voltage recovers. This for example ensures fast tripping, following the three-phase dead time in the event that re-closure onto a close-in fault with  $U = 0$  occurs.

The high directional sensitivity of approx. 100 mV required previously to minimise the “dead zone” is no longer required with numerical relays, because a voltage memory is always available.

The threshold voltage for the release of the directional decision is set at approx. 1 V line voltage in the case of numerical relays. This corresponds to a value which ensures a measured signal with sufficient immunity against interference. If no current or memorised voltage is above this threshold, the forward direction is automatically selected.

The critical case of switching onto a close-in fault with  $U_{SC} = 0$  is therefore immediately tripped. It is furthermore possible to release a non-directional zone or the fault detection for tripping by means of additional switched logic. The other distance relays on the feeders connected to the same busbar “see” the fault correctly as being in the reverse direction, by means of their memorised voltage. In the case of delayed fault clearance, and expiry of the voltage memory, the reverse directional decision is correctly maintained until the measured voltage recovers, following fault clearance.

On series compensated feeders a voltage memory is required to cater for the voltage inversion effect. The duration of the voltage memory must in this case definitely be longer than the fault clearance time. For non-delayed tripping, approx. 100 ms is required. This was the aim with traditional relays. Modern numerical relays (e.g. 7SA522) have a memory capacity up to 2 s and can therefore cover longer fault durations, that may occur when the fault is tripped by back-up zones.

### 3.3.7 Adaptive directional determination

The previous considerations have shown the following:

Directional discrimination with faulted phase voltage (voltage of the fault loop) is limited to the fault loop quantities. Its behaviour is therefore easy to predict even in the case of multiple faults. It may be used as long as the fault voltage is higher than about 10% rated voltage. In any case it has to be used in case of a three-phase fault, when the memory voltage has expired or is not available (switch onto fault).

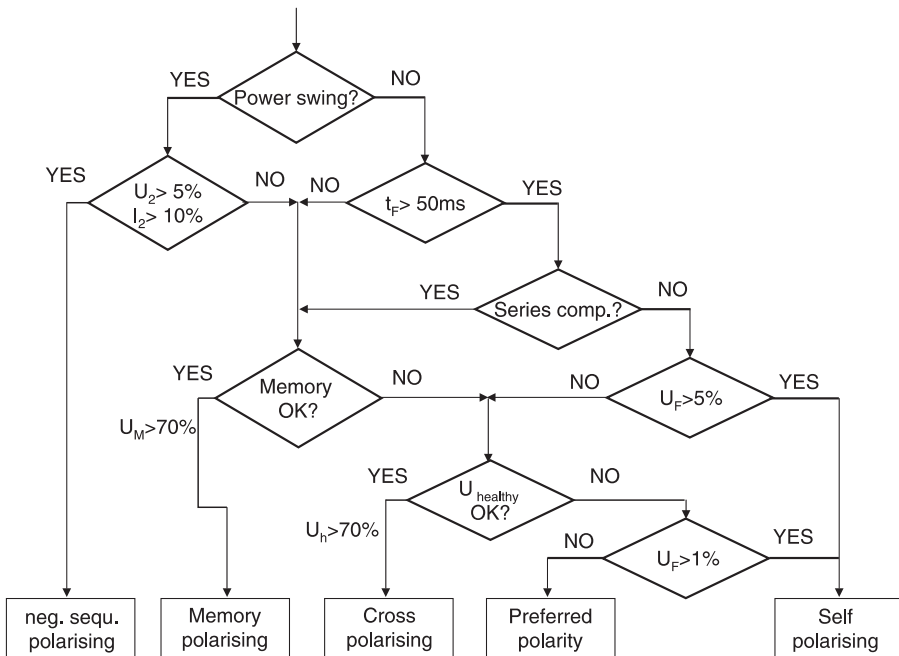


**Figure 3.82** Adaptive polarisation (7SA6 simplified)

Using healthy phase voltages for directional determination (cross polarisation) has the advantage that even zero-voltage forward faults can be absolutely discriminated. It is therefore ideally suited for these kinds of fault.

Memorised voltage ensures directional discrimination also in the case of three-phase zero-volt faults. It has the further advantage that it is not influenced by transients after fault inception. It may therefore be generally used in the first periods after fault inception (2-and-a-half periods in case of 7SA522 and 7SA6). Synchronising with the system frequency is necessary and now state of the art.

In case of long heavily loaded lines, directional discrimination is critical when the transmission angle exceeds 60 degrees. Supervision by a negative sequence directional criterion may then be used always or only in case of a detected power swing.

Series compensated lines, in any case, require full cross- and memory-polarisation.

Modern numerical distance relays use an adaptive polarisation approach and select the most suitable polarisation voltage depending on system conditions (setting parameter), fault case, magnitude of voltages and elapsed time after fault inception.

Figure 3.82 shows the selection logic (simplified) of the relay 7SA6.

## 3.4 Circular characteristics with numerical technology

In the case of quadrilateral characteristics, the R- and X-values of the short-circuit impedance are initially computed, and then their location in the distance zones is determined by a comparison with the zone limits.

With circular characteristics, the classical angle measurement with current and voltage phasors is recommended for the measurement. As an example, the MHO-characteristics are discussed, which are a settable alternative to the quadrilateral at the 7SA522.

### 3.4.1 MHO-circle

The principle for the MHO-circle was already shown in paragraph 3.1.4, figure 3.10.

With numerical technology the sample measured values are available as vector quantities, in the form of a complex number with a real and imaginary part, after processing with orthogonal filters. They can therefore be processed further subject to the complex number calculation rules.

Figure 3.83 shows the representation of the MHO-circle in the impedance diagram and the voltage diagram. The latter results from the multiplication of the impedance values with the short-circuit current.

The illustrated shape corresponds to the classic MHO-circle. It is designated as a self-polarising MHO-circle, as it only utilises the faulted voltage of the short-circuit loop as

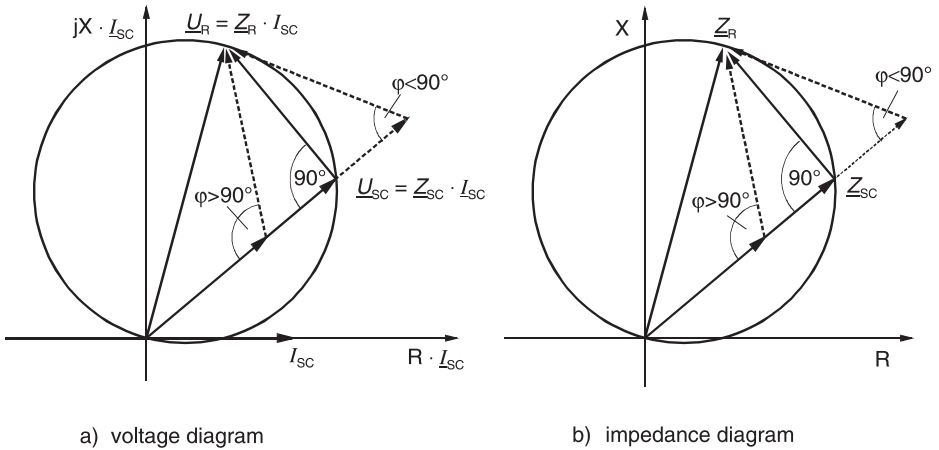


**Figure 3.83** Self-polarised MHO-characteristic

a reference voltage. The implementation of healthy voltages (polarised MHO-circle) will be discussed below.

$\underline{Z}_R$  is the impedance which must be set on the relay. It corresponds to the diameter of the circle and determines the zone reach. Usually,  $\underline{Z}_R$  is matched to the line-impedance of the zone that must be protected. It is therefore also referred to as the replica impedance.<sup>1</sup>

The voltage across the replica impedance results from multiplication with the short-circuit current:  $\underline{U}_R = \underline{I}_{SC} \cdot \underline{Z}_R$  (with conventional relays, the CT-secondary current had to be rooted through an actual replica to achieve this).

$\underline{Z}_{SC}$  is the short-circuit impedance which has to be measured.  $\underline{U}_{SC}$  is the voltage drop across  $\underline{Z}_{SC}$ , i.e. the short circuit voltage at the relay location.

The difference voltage,  $\Delta \underline{U}$  results from the numerical subtraction of the vectors  $\underline{U}_R$  and  $\underline{U}_{SC}$ .

The circular characteristic defines all points for which  $\underline{Z}_{SC}$  has an angle between  $\underline{U}_{SC}$  and  $\Delta \underline{U}$  equal to  $90^\circ$  (Thales-circle above the diameter  $\underline{Z}_R$ ).

Faults inside the zone reach will have an angle  $\varphi$  greater than  $90^\circ$ , and external faults smaller than  $90^\circ$ .

The pick-up criteria  $\varphi \geq 90^\circ$  is satisfied when  $\text{Re}\{\underline{U}_{SC} \cdot \Delta \underline{U}\} \geq 0$ , and can therefore for example be checked with this computational exercise by micro-processor device.

<sup>1</sup> With conventional measuring techniques, the matching to the line angle was important, as this largely allowed the suppression of the DC-component in the current. With numerical technology, the DC-current component is removed with the digital pre-filtering. It is therefore possible to set a flatter angle for  $\underline{Z}_R$  to achieve a somewhat increased arc-reserve.

With the evaluation of the individual fault-loops, the actual values of the respective fault-loops must be implemented for  $\underline{U}_{SC}$  and  $\underline{I}_{SC}$ , as is the case with the direct impedance computation (refer to paragraph 3.2.2).

Ph-Ph fault:

$$\underline{U}_{SC} = \underline{U}_{Ph1} - \underline{U}_{Ph2} \quad \text{and} \quad \underline{I}_{SC} = \underline{I}_{Ph1} - \underline{I}_{Ph2}$$

Ph-E fault:

$$\underline{U}_{SC} = \underline{U}_{Ph-E} - \underline{U}_{Ph-E} \quad \text{and} \quad \underline{I}_{SC} = \underline{I}_{Ph} - \underline{k}_E \cdot \underline{I}_E$$

The complex value  $\underline{k}_E$  is the residual compensation factor. In conventional relays a magnitude and angle-setting is applied.

$$\underline{k}_E = |\underline{k}_E| \cdot e^{j\varphi_E} = \text{Re}\{\underline{k}_E\} + j\text{Im}\{\underline{k}_E\} = \frac{\underline{Z}_E}{\underline{Z}_L} = \frac{\underline{Z}_0 - \underline{Z}_1}{3 \cdot \underline{Z}_1} \quad (3-58)$$

On the other hand, in the Siemens numerical distance relays, the values must be parameterised, as they are required for the R- and X-computation (refer to paragraph 3.2.3). This has the additional advantage that the complex calculation is no longer required.

$$k_{RE} = \frac{R_E}{R_L} = \frac{R_0 - R_1}{3 \cdot R_1} \quad \text{and} \quad k_{XE} = \frac{X_E}{X_L} = \frac{X_0 - X_1}{3 \cdot X_1} \quad (3-59)$$

For the MHO-characteristic, the 7SA522 relay calculates the complex value of  $\underline{k}_E$  internally with the following equation:

$$\underline{k}_E = \frac{(k_{RE} \cdot R_1 + jk_{XE} \cdot X_1) \cdot (R_1 - jX_1)}{R_1^2 + X_1^2}. \quad (3-60)$$

The value of the impedance of the protected section of line must be used in the equation. The residual compensation factor for the first zone and the back-up zones can be set separately in the 7SA522 relay. The first zone is normally set to match the protected line, while the back-up zones may have a differently set value, which takes a neighbouring line or parallel line coupling into account (refer to example in paragraph 7.1).

### 3.4.2 Polarised MHO-characteristic

The self-polarised MHO-circle has a dead-zone during close-in faults ( $\underline{Z}_{SC} \rightarrow 0$  in other words  $\underline{U}_{SC} \rightarrow 0$ ), as the characteristic passes through the co-ordinate origin of the impedance diagram. During close-in faults with a small short-circuit voltage it is therefore not possible to securely determine whether the fault location is in front or behind the relay location. The same problem as exists with directional determination using faulted loop voltages therefore arises. In addition it must be noted that the pick-up time of the relay during close-in faults is longer as the fault impedance appears to be at the border of the tripping characteristic. In electro-mechanical measuring systems, this

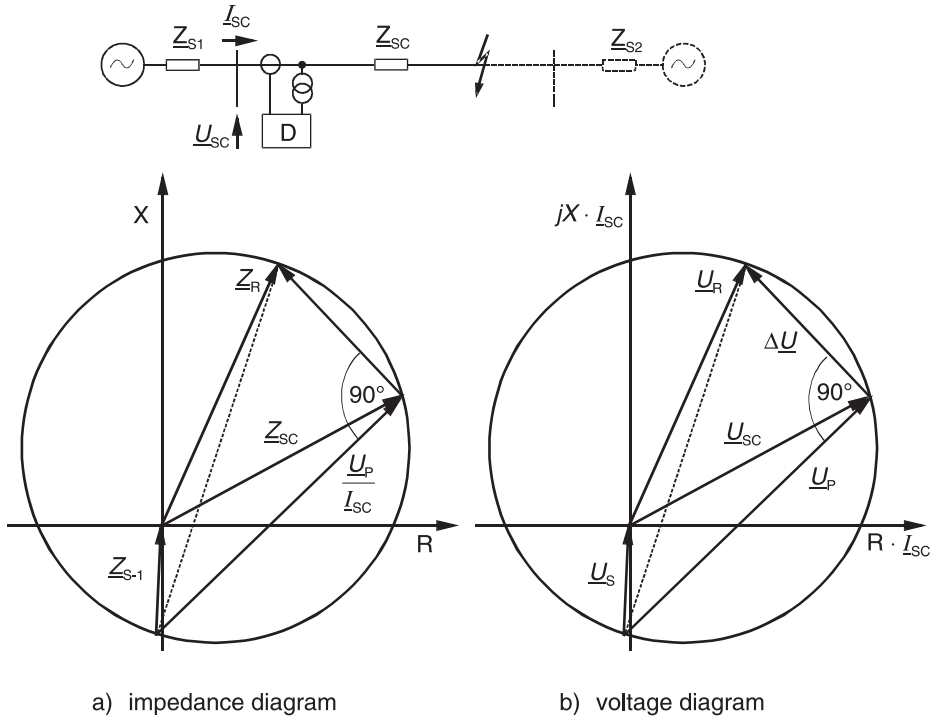


**Figure 3.84** Polarised MHO-circle, fault in the forward direction

materialised due to the small short-circuit voltage which only produced a correspondingly small torque. In numerical relays, measurement repetitions would result, producing a similar effect, particularly when transient interference voltages are superimposed as is expected from capacitive voltage transformers (refer paragraph 5.1.3).

As is the case with direction determination, this problem can also be solved by introduction of a suitable healthy phase or memorised voltage.

The healthy voltage is added to the short-circuit voltage to form a combined polarising voltage  $\underline{U}_P$ . The percentage of the healthy voltage which is added, is determined by the factor  $k_p$ :

$$\underline{U}_P = (1 - k_p) \cdot \underline{U}_{\text{faulty}} + k_p \cdot \underline{U}_{\text{healthy}} \quad (3-61)$$

The magnitude and phase of the healthy voltage is modified prior to addition, so that it equals the voltage across the short-circuit loop prior to fault inception.

As an example, a L1-E fault in the forward direction is assumed. The opposite line voltage (cross-polarised voltage)  $\underline{U}_{L2} - \underline{U}_{L3}$  is the suitable healthy loop voltage in this case, similar to the direction determination with healthy voltages (refer to paragraph 3.3.2).



The line voltage must be rotated by  $90^\circ$  in the positive sense and divided by the factor  $\sqrt{3}$ , so that it corresponds to the phase voltages  $\underline{U}_{L1-E}$  prior to fault inception.

$$\underline{U}_{\text{healthy}} = \frac{1}{\sqrt{3}} \cdot e^{j90^\circ} \cdot (\underline{U}_{L2} - \underline{U}_{L3}) \quad (3-62)$$

In an unfaulted symmetrical three-phase system, the following then applies:

$$\underline{U}_P = \underline{U}_{L1-E}.$$

An unloaded line is initially assumed for the calculation of  $\underline{U}_P$  during the short-circuit. Accordingly figure 3.73 of paragraph 3.3.2 can be reverted to, and the following relationship can be established:

$$\underline{E}_{L1} = \underline{U}_{SC-L1} + \underline{Z}_S \cdot \underline{I}_{SC-L1} \quad (3-63)$$

and

$$\underline{E}_{L2} - \underline{E}_{L3} = \underline{E}_{L1} \cdot \sqrt{3} \cdot e^{-j90^\circ} = (\underline{U}_{SC-L1} + \underline{Z}_S \cdot \underline{I}_{SC-L1}) \cdot \sqrt{3} \cdot e^{-j90^\circ} \quad (3-64)$$

Taking note of the fact that on the unloaded line,  $\underline{U}_{L2} - \underline{U}_{L3} = \underline{E}_{L2} - \underline{E}_{L3}$ , the following is obtained:

$$\underline{U}_{\text{healthy}} = \underline{U}_{SC-L1} + \underline{Z}_S \cdot \underline{I}_{SC-L1} \quad (3-65)$$

$$\underline{U}_{\text{faulty}} = \underline{U}_{SC-L1} = \underline{Z}_{SC} \cdot \underline{I}_{SC-L1} \quad (3-66)$$

The following polarising voltage is therefore obtained:

$$\underline{U}_P = (1 - k_P) \cdot \underline{Z}_{SC} \cdot \underline{I}_{SC-L1} + k_P \cdot (\underline{U}_{SC-L1} + \underline{Z}_S \cdot \underline{I}_{SC-L1}) \quad (3-67)$$

and finally

$$\underline{U}_P = \underline{Z}_{SC} \cdot \underline{I}_{SC-L1} + k_P \cdot \underline{Z}_S \cdot \underline{I}_{SC-L1} \quad (3-68)$$

The influence on the MHO-characteristic is shown in figure 3.84. By measuring the angle between  $\Delta \underline{U}$  and  $\underline{U}_P$  instead of between  $\Delta \underline{U}$  and  $\underline{U}_{SC}$ , the magnitude of the circle is increased, so that the co-ordinate origin is enclosed.

It must be noted that this representation only applies for faults in the forward direction. The negative X-values do not correspond to faults in the reverse direction, but rather to measured negative short-circuit reactances for faults in the forward direction. This condition arises when the short-circuit reactance is capacitive ( $X_{SC} = -X_C$ ), i.e. for faults behind series capacitors. The fault is still correctly “seen” in the forward direction, as long as  $X_C < k_P \cdot X_S$  remains true, because the measured negative short-circuit reactance remains within the circle up to this limit-value (refer to paragraph 3.5.7).

In the case of faults in the reverse direction, the short-circuit current flows through the relay in the opposite direction, and therefore the current in relationship to the voltage is

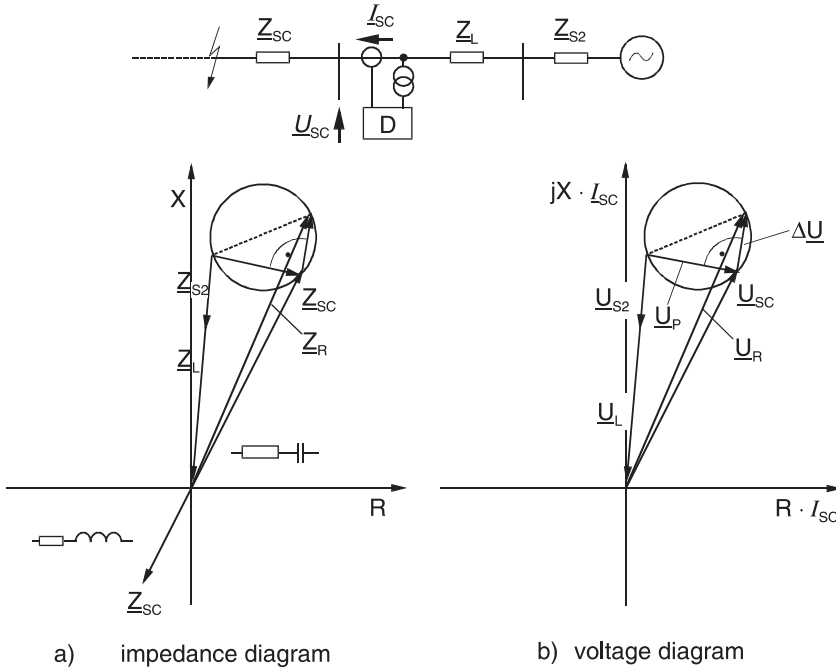


**Figure 3.85** Polarised MHO-circle, fault in the reverse direction

inverted. Accordingly, in the equations above the current must be applied with a negative sign. As will be shown, this changes the relay characteristic. Faults in the reverse direction must therefore be represented in a separate diagram.<sup>1</sup> Note must also be taken that the representation is chosen so that reverse faults appear in the third quadrant as is typical in the illustration of self-polarised characteristics. In relation to the short-circuit impedance, the source impedance now appears in the opposite direction (figure 3.85). The polarised MHO-circle shrinks and is displaced from the origin by  $\underline{Z}_{S2} + \underline{Z}_L$ .

Close-in faults in the reverse direction ( $Z \approx 0$ ) now appear outside the characteristic with a large security margin and are therefore “seen” correctly. Even faults behind series capacitors in the reverse direction, which appear as positive reactances are “seen” correctly, as long as  $X_C < \text{about } k_p \cdot (X_{S2} + X_L)$  again remains true.

The polarised MHO-circle accordingly has a good directional behaviour, similar to the direction determination with healthy phase(s) voltages in the case of quadrilateral characteristics.

An additional advantage in comparison to the self-polarised MHO-circle is the increment of the reach in R-direction (arc-compensation). The increase of the circle is however dependant on the magnitude of the source impedance. As the source impedance

<sup>1</sup> Separate diagrams should actually also be used with self-polarised characteristics for faults in the forward and reverse directions. This is however not done, because in this case the relay characteristic does not change in the case of a current reversal.

increases in relation to the set zone reach (increasing SIR), the arc-compensation increases (refer to figure 3.8 in paragraph 3.1.4).

This is a positive effect, as an increase in the source impedance causes smaller short-circuit currents to flow and the arc resistance to increase.

With strong in-feeds, the effect is however very small and it is recommended to use a quadrilateral characteristic on short lines.

### 3.4.3 Load influence on polarised MHO-circles

The load transfer in this case has a similar influence as is the case with the direction determination. The angle shift of the voltage at the relay location against the source emf is again assumed to be  $\delta^\circ$ . At the end exporting real power, the healthy phase(s) or memorised voltage  $\underline{U}_1$  lags the source emf  $\underline{E}_1$ , as shown in figure 3.86. The single-phase earth-fault, as in the previous example of the unloaded line, is once again looked at (refer to paragraph 3.3.1, figure 3.73).

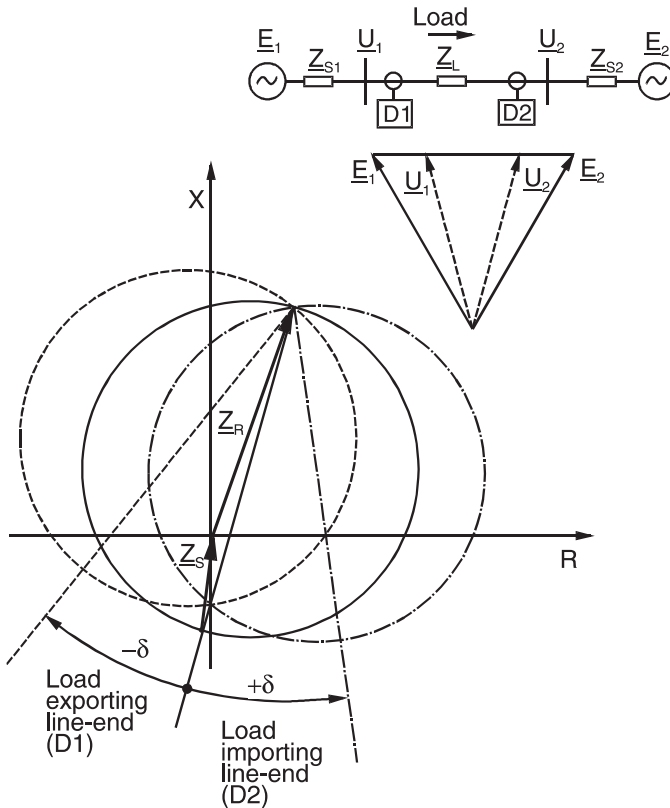


**Figure 3.86**  
Influence of load transfer on the position of the polarised MHO-circle  
(full polarisation with healthy phase(s) voltage)

The following still applies:

$$\underline{E}_{L1} = \underline{U}_{SC-L1} + \underline{Z}_S \cdot \underline{I}_{SC-L1} \quad (3-69)$$

and

$$\underline{E}_{L2} - \underline{E}_{L3} = \underline{E}_{L1} \cdot \sqrt{3} \cdot e^{-j90^\circ} = (\underline{U}_{SC-L1} + \underline{Z}_S \cdot \underline{I}_{SC-L1}) \cdot \sqrt{3} \cdot e^{-j90^\circ} \quad (3-70)$$

Due to the phase angle shift of the healthy (unfaulted) voltage, the following equation results:

$$\underline{U}_{L2} - \underline{U}_{L3} = (\underline{E}_{L2} - \underline{E}_{L3}) \cdot e^{-j\delta} \quad (3-71)$$

The adapted healthy voltage is:

$$\underline{U}_{\text{healthy}} = \frac{1}{\sqrt{3}} \cdot e^{j90^\circ} \cdot (\underline{U}_{L2} - \underline{U}_{L3}) = (\underline{U}_{SC-L1} + \underline{Z}_S \cdot \underline{I}_{SC-L1}) \cdot e^{-j\delta} \quad (3-72)$$

The short-circuit voltage remains unchanged.

$$\underline{U}_{\text{faulty}} = \underline{U}_{SC-L1} = \underline{Z}_{SC} \cdot \underline{I}_{SC-L1} \quad (3-73)$$

The polarising voltage therefore is:

$$\begin{aligned} \underline{U}_P &= (1 - k_P) \cdot \underline{U}_{\text{faulty}} + k_P \cdot \underline{U}_{\text{healthy}} \\ \underline{U}_P &= [(1 - k_P) + k_P \cdot e^{-j\delta}] \cdot \underline{Z}_{SC} \cdot \underline{I}_{SC-L1} + k_P \cdot e^{-j\delta} \cdot \underline{Z}_S \cdot \underline{I}_{SC-L1} \end{aligned} \quad (3-74)$$

In the case of full compensation by healthy phase(s) voltage ( $k_P = 1$ ), the following would result

$$\underline{U}_P = (\underline{Z}_{SC} \cdot \underline{I}_{SC-L1} + \underline{Z}_S \cdot \underline{I}_{SC-L1}) \cdot e^{-j\delta} \quad (3-75)$$

The circle is therefore rotated by the load angle  $\delta$  in the lagging sense, with the terminal point of the relay impedance as the pivot point (figure 3.86). The arc-compensation is correspondingly reduced.

On the power importing end, the circle would be rotated in the leading sense, and the arc compensation would correspondingly be improved.

A particular advantage is that with two ended in-feed and load transfer, the rotation of the polarised MHO-circle is in the same direction as the rotation of the fault resistance. A degree of compensation of the X-measuring error is therefore automatically obtained, and a dedicated load compensation as is sensible for polygonal characteristics, is not required here (refer to paragraph 3.5.1).

The load angle rotation is expected to have the largest influence during faults in the reverse direction, because in this case the largest phase shifts between the in-feed volt-

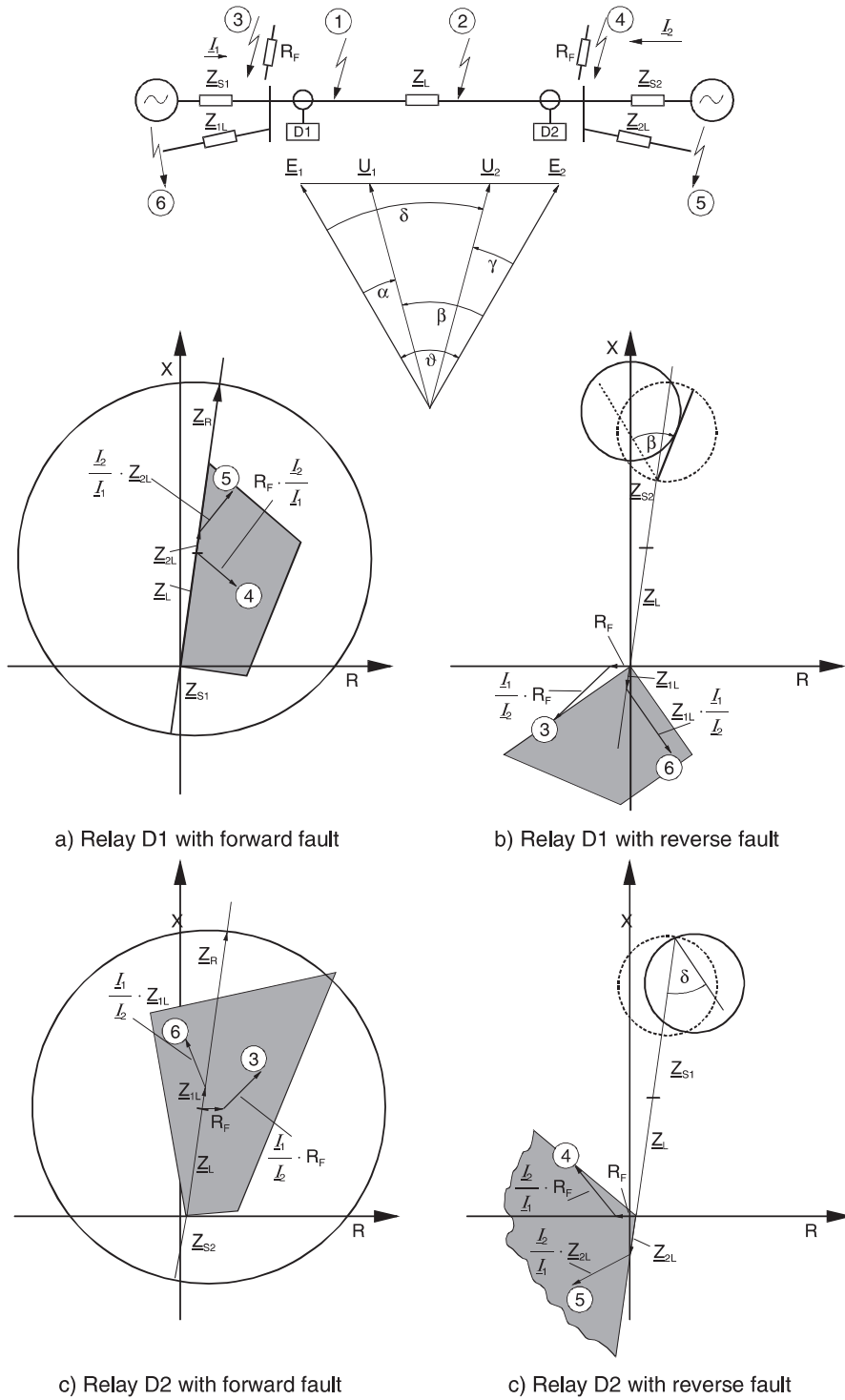


**Figure 3.87** Polarised MHO-circle in the case of long transmission lines.

age, and the voltage at the relay location exist. This was shown for the direction measurement with healthy phase voltages in figure 3.81.

The change of the polarised MHO-characteristic with the same system conditions is shown in figure 3.87. The shrinkage of the MHO-circle results in a definite selectivity during the critical reverse faults.

### 3.4.4 MHO-circle with voltage memory

The voltage memory functions in a manner similar to polarisation with healthy phase voltage, the difference being, that in this case the a percentage of the memorised voltage is added to the short circuit voltage to form the polarisation voltage  $\underline{U}_p$ .

This is true in particular for the relay 7SA522 as it utilises healthy phase voltages which are only slightly modified during single and three phase faults. This implies that the statements regarding the polarised MHO circle in principle also apply here, including the statements regarding the dependence on the source impedance and load influence.

The voltage memory is of particular importance during close in three phase faults where no healthy phase voltage is available. A relatively small portion of 10-20%  $U_N$  ( $k_p = 0.1-0.2$ ) is sufficient in this case.

Full compensation with nominal voltage ( $k_p = 1$ ) is however required in series compensated systems, as the short-circuit voltage may be inverted here, and then be negative in comparison to the memorised voltage. For selective fault detection, the memorised voltage must therefore be larger than the largest expected negative short-circuit voltage. For such applications, 100% of the voltage memory is used in the addition to form  $\underline{U}_p$ . Directionally correct fault detection is then possible up to  $|X_C| \leq |k_p \cdot X_S|$ , as was the case with healthy phase voltage (refer to paragraph 3.4.2).

## 3.5 Distance measurement, Influencing quantities

With the practical implementation of distance protection, consideration must be given to several influencing quantities. They affect the accuracy of the distance measurement, (e.g. coupling of the zero-sequence system on parallel overhead lines), and the setting of the distance zones (e.g. arc compensation).

For a better understanding, the fundamental functioning of these influencing factors will initially be discussed.

The practical application will then be elaborated on in chapter 5.

### 3.5.1 Fault resistance

Initially, a distinction must be made between the simple phase-to-phase fault and the phase-to-earth fault with single-ended in-feed.

*Ph-Ph fault with fault resistance at the fault location*

The corresponding equivalent circuit is shown in figure 3.88.

The short-circuit line voltage at the relay location is given by:

$$\underline{U}_{LL} = \underline{U}_{L2} - \underline{U}_{L3} = 2 \cdot (R_L \cdot \underline{I}_L + jX_L) + R_F \cdot \underline{I}_L \quad (3-76)$$

By substitution of  $\underline{U}_{LL}$  in (3-37) and with  $\underline{I}_{L3} = -\underline{I}_{L2} = \underline{I}_L$ , the following measured impedance is obtained:

$$\underline{Z}_{L2-L3} = \frac{2 \cdot (R_L \cdot \underline{I}_L + jX_L) + R_F \cdot \underline{I}_L}{2 \cdot \underline{I}_L} \quad (3-77)$$

$$\underline{Z}_{L2-L3} = R_L + \frac{R_F}{2} + jX_L \quad (3-78)$$

The solution is as expected, namely that the X-value (distance to fault) is correctly measured. One can imagine the fault resistance to be divided into two halves, one-half onto each phase-impedance. Therefore it is only “seen” by the measurement with half it’s magnitude. This must be borne in mind, when setting the zone reach in the R-direction.

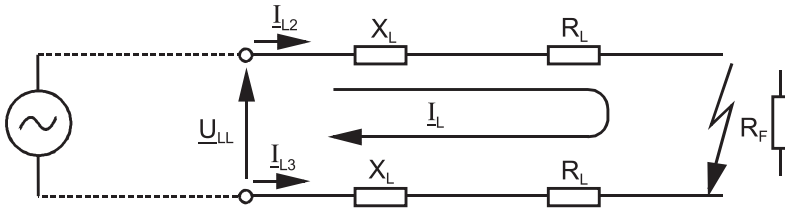


**Figure 3.88** Two-phase short-circuit with fault resistance (single-ended in-feed)

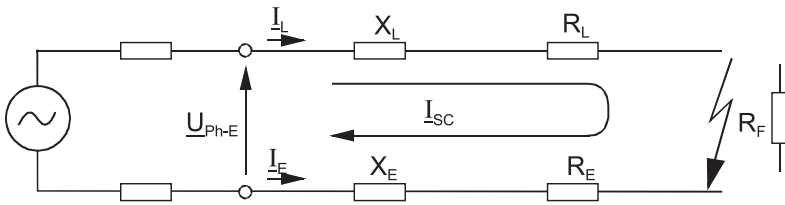


**Figure 3.89** Single-phase earth-fault with fault resistance (single-ended in-feed)

### *Single-phase earth-fault with fault resistance at the fault location*

The corresponding equivalent circuit is shown in figure 3.89.

The short-circuit line voltage at the relay location is given by:

$$\underline{U}_{\text{Ph-E}} = \underline{I}_L \cdot (\underline{I}_L + jX_L) - \underline{I}_E \cdot (R_E + jX_E) + \underline{I}_L \cdot R_F \quad (3-79)$$

Substituted in equations (3-53) and (3-54) we get:

$$X_{\text{Ph-E}} = \frac{X_L \cdot \left( \underline{I}_L - \frac{X_E}{X_L} \cdot \underline{I}_E \right)}{\underline{I}_L - \left( \frac{X_E}{X_L} \right)_{\text{set}} \cdot \underline{I}_E} \quad (3-80)$$

$$R_{\text{Ph-E}} = \frac{R_L \cdot \left( \underline{I}_L - \frac{R_E}{R_L} \cdot \underline{I}_E \right) + R_F \cdot \underline{I}_L}{\underline{I}_L - \left( \frac{R_E}{R_L} \right)_{\text{set}} \cdot \underline{I}_E} \quad (3-81)$$

$(R_E/R_L)_{\text{set}}$  and  $(X_E/X_L)_{\text{set}}$  correspond to the residual compensation factor set in the relay.

By adapting the relay settings to the overhead line, i.e.  $(R_E/R_L)_{\text{set}} = (R_E/R_L)$  and  $(X_E/X_L)_{\text{set}} = (X_E/X_L)$  the following is obtained:

$$X_{\text{Ph-E}} = X_L \quad (3-82)$$

$$R_{\text{Ph-E}} = R_L + \frac{R_F}{1 + \left( \frac{R_E}{R_L} \right)_{\text{set}}} \quad (3-83)$$

The fault reactance is again measured correctly, independent of the magnitude of the fault resistance.

The fault resistance in this case does not appear as 50% of the magnitude in the measured resistance, but rather, depending on the set  $R_E/R_L$  ratio, as  $1/(1 + R_E/R_L)$  of the magnitude.

In general, one would adjust the setting to the overhead line data.

The setting will therefore strongly depend on the type of overhead line or cable (from 0.24 to 3.42 according to the examples in table 3.4).

The reach setting for the distance zones in R-direction for the 7SA relays must take this into consideration.

For the extreme case when 3.42 is set, the fault resistance is reduced by the factor  $1 + 3.42 = 4.42$ , i.e. the reach of the zone is correspondingly extended for earth-faults.



This only applies if the earth-current has approx. the same magnitude as the phase-short-circuit current. In the case of unfavourable distribution of earth-currents in the system (refer to figure 3.15, paragraph 3.1.6), the reduction factor may be substantially smaller.

**Hint:** When setting distance relays, one has to consider that two quantities influence the zone reach in R-direction:

1. the R-setting of the zone itself
2. the  $R_E/R_L$  setting as discussed

The actual R-reach is  $(1 + R_E/R_L) \cdot R_{E-Zone}$  when  $I_E = I_{ph}$  is assumed.

If both settings are high, an extremely high reach may occur.

For example, if the R-reach is set 25 ohm and  $R_E/R_L = 3.0$ , then the actual reach with phase to earth faults may actually be 100 ohm.

This may cause overreach problems with remote external earth faults and superimposed load.

In the 7SA relay manuals, it is therefore recommended to limit the  $R_E/R_L$  setting to 2 even when in seldom cases the actual line or cable value may be higher.

### *Comparison with conventional measuring techniques*

The numerical measurement technique, utilising complex number computation and separate evaluation of the real and imaginary part of the fault loop, has the advantage that faults with fault resistance are always measured correctly (single infeed assumed), even when the short-circuit angle of the positive and zero-sequence system ( $\varphi_L$  and  $\varphi_0$ ) differ.

This is of advantage in cable systems, where this angle difference may be very large.

With the conventional measuring technique, the residual compensation causes a phase rotation of the earth-current. This introduces an inductive component of the fault resistance, which leads to an error in the distance measurement. For comparison, the equation utilised by conventional measuring techniques is derived here:

With  $\underline{Z}_L = R_L + jX_L$  and  $\underline{Z}_E = R_E + jX_E$ , the short-circuit voltage at the relay location is obtained.

$$\underline{U}_{Ph-E} = \underline{I}_L \cdot (\underline{Z}_L + \underline{Z}_E) + R_F \cdot \underline{I}_L \quad (3-84)$$

substituted in equation (3-29) results in:

$$\underline{Z}_{Ph-E} = \underline{Z}_L \cdot \frac{1 + \frac{\underline{Z}_E}{\underline{Z}_L}}{1 + \frac{R_F}{\underline{Z}_L}} + \frac{R_F}{1 + \frac{R_F}{\underline{Z}_L}} \quad (3-85)$$

Adjustment of the relay setting to the line data ( $k_E = \underline{Z}_E / \underline{Z}_L$ ) results in:

$$\underline{Z}_{Ph-E} = \underline{Z}_L + \frac{R_F}{1 + \frac{\underline{Z}_E}{\underline{Z}_L}} \quad (3-86)$$

$$\underline{Z}_{Ph-E} = \underline{Z}_L + \frac{R_F}{1 + \left| \frac{\underline{Z}_E}{\underline{Z}_L} \right| \cdot e^{j(\varphi_E - \varphi_L)}} \quad (3-87)$$

Ultimately the result is:

$$\underline{Z}_{Ph-E} = \underline{Z}_L + \frac{1 + \left| \frac{\underline{Z}_E}{\underline{Z}_L} \right| \cdot \cos(\varphi_E - \varphi_L) - j \left| \frac{\underline{Z}_E}{\underline{Z}_L} \right| \cdot \sin(\varphi_E - \varphi_L)}{1 + 2 \cdot \left| \frac{\underline{Z}_E}{\underline{Z}_L} \right| \cdot \cos(\varphi_E - \varphi_L) + \left| \frac{\underline{Z}_E}{\underline{Z}_L} \right|^2} \cdot R_F \quad (3-88)$$

*Numerical example:*

Cable:  $\underline{Z}_L = 0.387 \cdot e^{j75,8^\circ} \Omega/\text{km}$ ,  $\underline{Z}_0 = 0.332 \cdot e^{j21,3^\circ} \Omega/\text{km}$

The earth-impedance is:  $\underline{Z}_E = \frac{1}{3}(\underline{Z}_0 - \underline{Z}_L) = 0.111 \cdot e^{-j49,9^\circ}$

The result of the fault-impedance is:  $\underline{Z}_{Ph-E} = \underline{Z}_L + (1.11 + j0.31) \cdot R_F$

Due to the inductive component, the measured value of  $X$  is too large. This results in an under-reach of the relay (figure 3.90).

As concerns circle characteristics, the fault resistance has an influence on the  $X$ -reach (measured fault distance) and the coverage of fault resistance. This is shown for the self-polarised MHO relay in figure 3.91.

The impedance  $\underline{Z}_{Ph-E}$ , measured by the relay according to (3-86), corresponds to a point at the MHO circle. The actual fault impedance  $\underline{Z}_F$ , however lies on the angle-shifted ellipse.

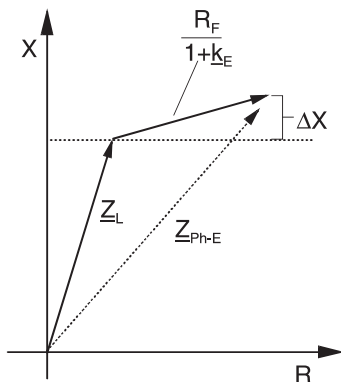


**Figure 3.90**  
Conventional distance measurement,  
measuring errors in cable systems  
for faults with fault resistance

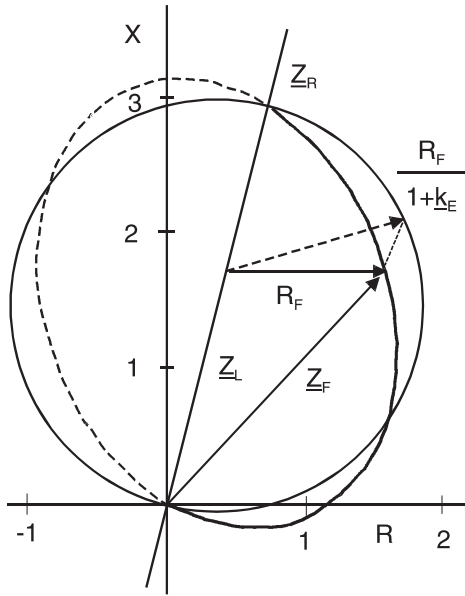


**Figure 3.91**  
Reach and resistance coverage of an MHO relay during phase-earth cable fault.

This is illustrated by the following example:

Relay impedance setting:  $Z_R = 3 \text{ Ohm}$ ,  $\varphi_R = \varphi_L = 76^\circ$

From cable data:  $\underline{k}_E = \underline{Z}_E / \underline{Z}_L = 0.303 \cdot e^{-j118.2^\circ}$ , i.e.  $1/(1 + \underline{k}_E) = 1.11 \cdot e^{-j17.3^\circ}$

The arc compensation for a given point on the cable can be found by drawing a straight line from the corresponding  $\underline{Z}_L$  vector in direction of the MHO circle with the inclination  $\alpha = \arctg[1/(1 + \underline{k}_E)]$ , i.e.  $17.3^\circ$  in the example. The distance from the  $\underline{Z}_L$  point to the MHO-circle must then be multiplied by  $1 + \underline{k}_E$  to get  $R_F$ .

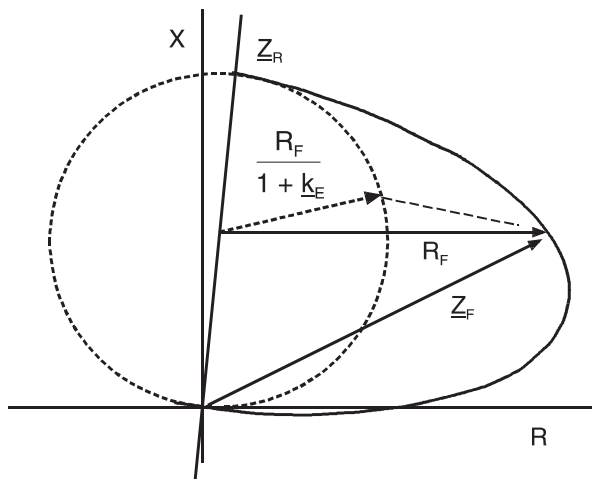


**Figure 3.92**  
Arc compensation of an MHO relay for earth faults on OH-lines

In this example, we also get a reduced arc compensation in addition to the expected underreach in X-direction. This result is typical for cables with small and mainly resistive zero-sequence impedance (figure 3.91).

OH-lines have a higher zero-sequence impedance ( $Z_{L0} \approx 3 \text{ to } 5 \cdot Z_{L1}$ ) at an angle slightly less than that of the positive sequence impedance. In this case higher  $k_E$  values result.

This will be shown in the next example (figure 3.92).

OH-line data:  $Z_{L1} = 25 \cdot e^{j86^\circ} \text{ Ohm}$ ,  $Z_{0L} = 100 \cdot e^{j76^\circ} \text{ Ohm}$ ,

$$k_E = \underline{Z}_E / \underline{Z}_L = 1.0 \cdot e^{-j13.3^\circ}, \quad 1/(1 + k_E) = 0.5 \cdot e^{j6.7^\circ}$$

Relay impedance Setting:  $Z_R = 20 \text{ Ohm}$ ,  $\varphi_R = \varphi_L = 86^\circ$

In this case the  $k_E$  value of about 1 results in a doubling of the arc reserve of the MHO relay.

#### *Influence of in-feed from both sides on the fault resistance*

The short-circuit current flowing from the opposite end through the fault resistance introduces an additional voltage drop. This has a similar effect as an additional in-feed, and thereby increases the measured fault resistance (figures 3.93 and 3.94).

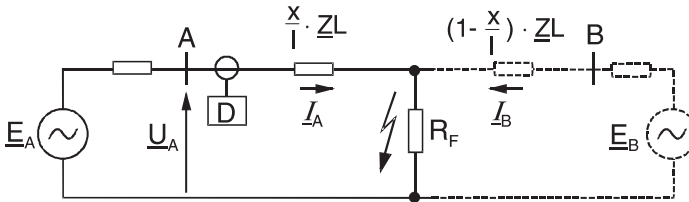


**Figure 3.93** Short-circuit with fault resistance and in-feed from both sides: equivalent circuit

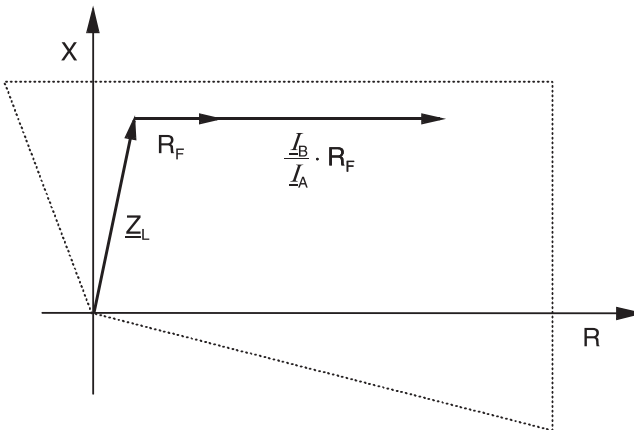


**Figure 3.94** Short-circuit with fault resistance and in-feed from both ends Impedance diagram

We can calculate the appearing impedance at the relay in A as follows:

$$\underline{U}_A = \underline{I}_A \cdot \left(\frac{x}{l}\right) \cdot \underline{Z}_L + (\underline{I}_A + \underline{I}_B) \cdot R_F \quad (3-89)$$

$$\underline{U}_A = \underline{I}_A \cdot \left(\left(\frac{x}{l}\right) \cdot \underline{Z}_L + R_F\right) + \underline{I}_B \cdot R_F \quad (3-90)$$

$$\underline{Z}_D = \frac{\underline{U}_A}{\underline{I}_A} = \left(\frac{x}{l}\right) \cdot \underline{Z}_L + R_F + \frac{\underline{I}_B}{\underline{I}_A} \cdot R_F \quad (3-91)$$

Initially it is assumed that the infeeds  $\underline{E}_A$  and  $\underline{E}_B$  are approx. in phase (no load transfer across the line) and that the source and line impedances have the same short-circuit angle. The short-circuit currents  $\underline{I}_A$  and  $\underline{I}_B$  then have the same phase angle and the current ratio is a real figure. In this case, the fault resistance is simply extended by the value  $\underline{I}_B/\underline{I}_A \cdot R_F$ . This is shown in the corresponding impedance diagram of figure 3.94.

The current ratio  $\underline{I}_B/\underline{I}_A$  increases as the fault location  $x$  moves in direction of the line end (B).

$$\frac{\underline{I}_B}{\underline{I}_A} = \frac{\underline{Z}_{SA} + \frac{x}{l} \cdot \underline{Z}_L}{\underline{Z}_{SB} + \left(1 - \frac{x}{l}\right) \cdot \underline{Z}_L} \quad (3-92)$$

This implies that the influence of the remote infeed increases over-proportional, as the fault location approaches the opposite line-end.

This is illustrated with a practical example in figure 3.95.

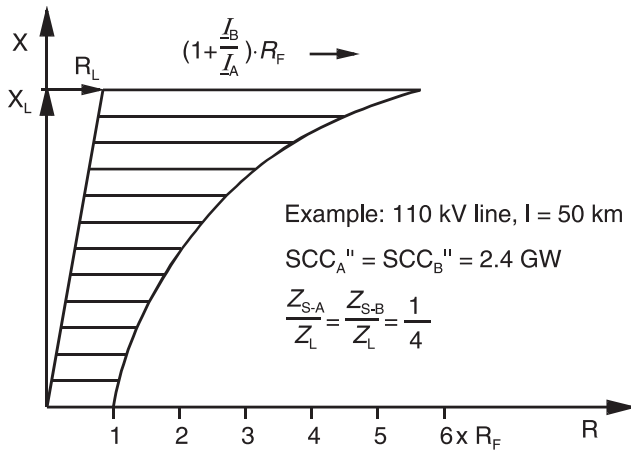


**Figure 3.95**

Apparent fault resistance dependent on fault location (influence of the resistance  $R_F$  on the short-circuit current neglected)

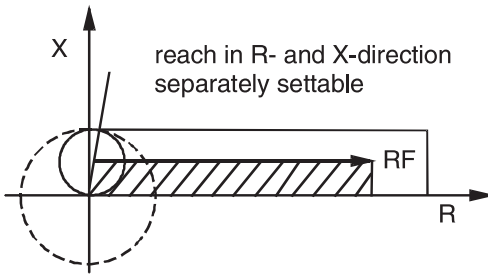


**Figure 3.96**  
High fault resistance coverage  
of the polygonal (quadrilateral)  
characteristic

The remote infeed impact is particularly evident on long lines and strong infeed at the remote end ( $Z_{SB} \ll Z_{SA} + Z_L$ ).

The impedance characteristic of the distance protection must therefore have sufficient reserve in the R-direction.

The quadrilateral characteristic is particularly suited to short overhead lines and cables, where the fault resistance may be a multiple of the line impedance.

It provides a substantially better resistance coverage and arc compensation than the traditional circular characteristics (figure 3.96).

On long transmission lines and for back-up protection, the angle-dependent fault detection and zone characteristics provide an optimal adaptation to the range of possible fault impedance (figure 3.97). In a settable load sector of about  $\pm 30$  degrees, the zone reach in R-direction is reduced to prevent pick-up on overload and power swing. Outside the load sector, the resistance coverage increases with growing fault distance.

Newer relay designs (e.g. 7SA522) also offer a load blocking zone with angular shape, as described, which can also be used with MHO characteristics (refer to figure 3.20).

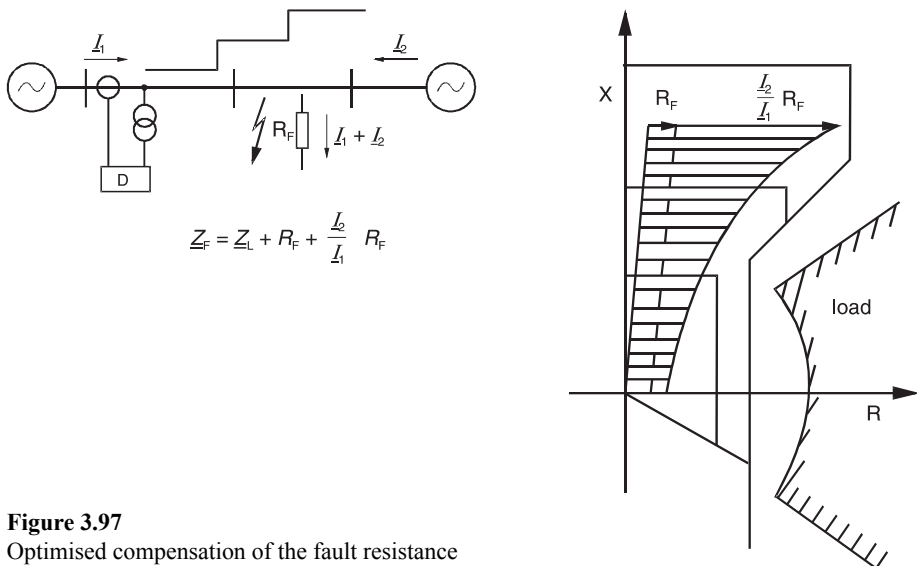


**Figure 3.97**  
Optimised compensation of the fault resistance

### Influence of load-transfer on the line

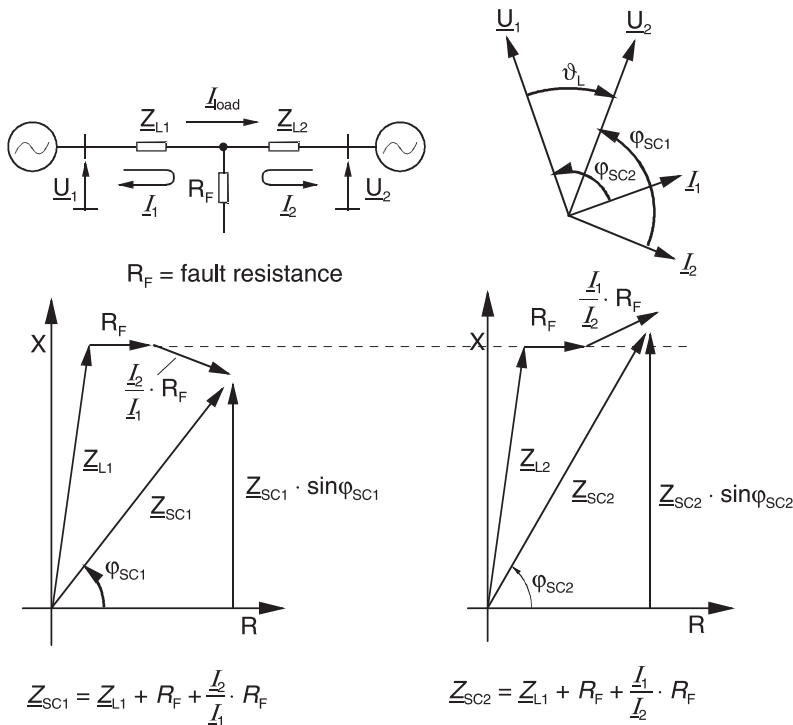
The transfer of real power across long transmission lines requires a phase shift of the system voltage. The equivalent circuit for this system condition is shown in figure 3.98.

In the case of a short circuit, the feeding emfs therefore have different angles. The voltage at the sending end leads the voltage at the receiving end by the transmission angle  $\vartheta_L$ . As a first approximation, the short-circuit currents from both sides are therefore phase shifted by this angle. Correspondingly, the vector  $(I_2/I_1) \cdot R_F$  is tilted down at the power sending end, and is tilted up at the receiving end. A normal distance relay therefore measures a reactance which is too small at the power sending end and tends to over-reach, while at the receiving end an impedance which is too large is “seen”, i.e. a tendency to under-reach exists.

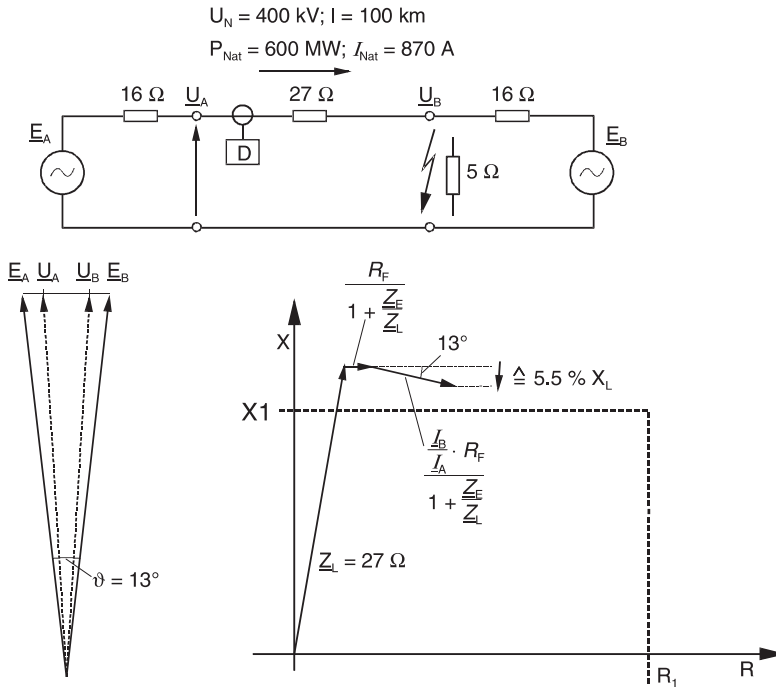
In geographically small industrialised countries with distributed power generation a power transfer over large distances is not required. The transmission angle is therefore small, and in the order of maximally 10-15°.

Figure 3.99 shows a case-example which is typical for Germany, although the line length of 100 km constitutes the upper limit.

In geographically large countries, the power must often be transferred from remote power generating centres (e.g. hydro-electric power stations) to the load centres.



**Figure 3.98** Influence of load flow on the distance measurement for faults with fault resistance



**Figure 3.99** Distance measurement with load flow on a short overhead line

In this case the transmission angle may reach  $60^\circ$ . During overload conditions, or in the event of power swings, even larger transmission angles may occur. In the extreme the protection may have to be configured for transmission angles of  $90^\circ$ .

Figure 3.100 shows the computed measured impedances for a 400 km long, 400 kV overhead line.

In this case the transmission angle  $\vartheta_L$  amounts to approx.  $35^\circ$ . The under-reaching zone must be set such, that it does not over-reach during faults directly behind the remote station. It can be seen that with a normal characteristic (horizontal limit without load compensation), a zone setting of approx.  $65\% Z_L$  would have to be set, when a fault resistance of up to  $20 \Omega$  must be covered.

Modern numerical relays (7SA522, 7SA6) allow to tilt the top line of the quadrilateral of the first zone to avoid overreach in this case (see paragraph 6.3.1, figure 6.7).

In the example at hand, the tilting angle would have to be about 25 degrees at a zone setting of 85 to 90%.

At the load receiving end, with a normal setting of 85% and a fault resistance of 20  $\Omega$ , the 1st stage would only have a reach of approx. 60%.

This is however compensated by the fact that the protection at the sending end has an opposite behaviour. With increasing fault resistance the fault appears nearer and the reach of the non-tilted zone 1, set to 65%, would increase to 85%  $Z_1$  with  $R_F = 20 \Omega$ .



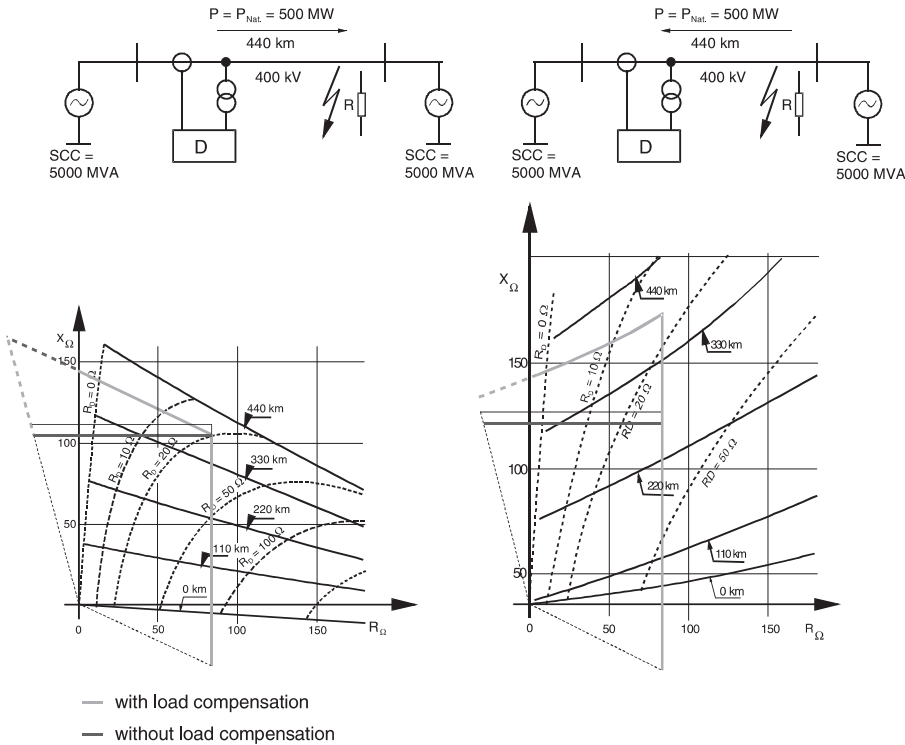


**Figure 3.100**

Distance measuring error for faults with fault resistance in conjunction with load transfer

Tilting of the 1<sup>st</sup> zone characteristic would of course keep the reach constant with the assumed line loading (fixed load direction assumed). Smaller load would however reduce the reach with the same fault resistance, as the curves of the appearing impedances, shown in figure 3.100, would be shifted upward towards the horizontal line.

In any case, the implementation of a permissive under-reach tripping scheme ensures secure fault detection and clearance.

Numerical distance protection provides the possibility of correcting the distance measuring error referred to. Precondition however is that the power system is homogeneous, i.e. the short-circuit angle in the zero sequence system is the same at both sides of the fault location (small but constant angle difference could be compensated by a fixed  $\Delta\varphi$  setting value.)

This so-called load compensation or self-tilting function is effective during single-phase earth-faults and to a certain extend also during double phase to earth faults, where such large fault resistances may occur [3-13, 3-23].

In figure 3.101 the principle of operation is illustrated for the case of a single-phase to earth fault.

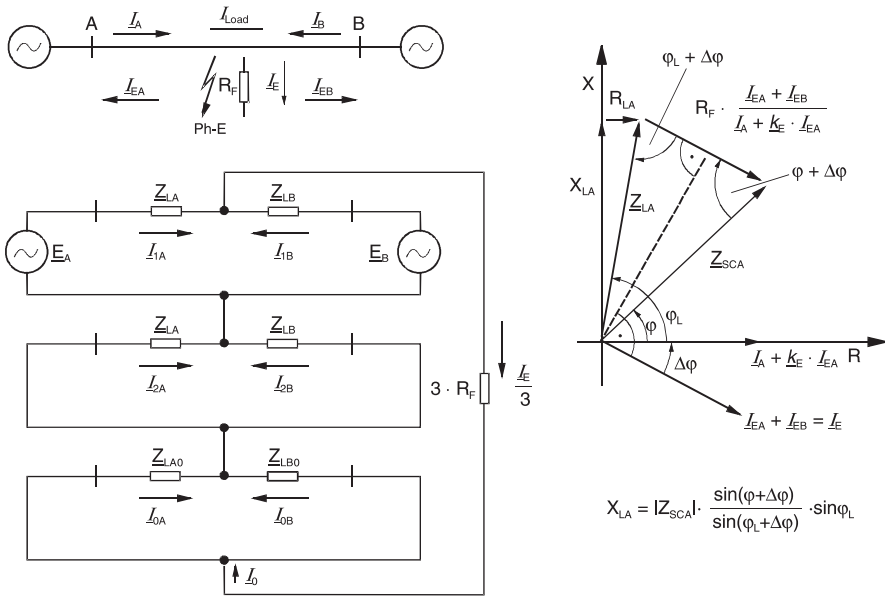


**Figure 3.101** Mode of operation: load compensation during phase-earth-faults

The equivalent circuit with symmetrical components shows the following: The total zero-sequence current  $\underline{I}_0$  which flows via  $3 \cdot R_F$  and equals  $\underline{I}_E/3$ , splits in the zero-sequence system at the fault location and returns to the two sources. The actual earth-currents flowing is three times as large:  $\underline{I}_{EA} = 3 \cdot \underline{I}_{0A}$ , and  $\underline{I}_{EB} = 3 \cdot \underline{I}_{0B}$ . As  $\underline{Z}_{LA0}$  and  $\underline{Z}_{LB0}$  in EHV-systems have approx. the same angle, i.e. the same  $X/R$  ratio, the split currents  $\underline{I}_{EA}$  and  $\underline{I}_{EB}$  have approx. the same phase angle as the total current  $\underline{I}_E = \underline{I}_{EA} + \underline{I}_{EB}$  which flows through the fault resistance.

With this the angle difference  $\Delta\varphi$  can be determined at each line end in the relay. Therefore the measured short-circuit impedance  $\underline{Z}_{SCA}$  can be adjusted to the correct reactance  $X_{LA}$  by reverse calculation.

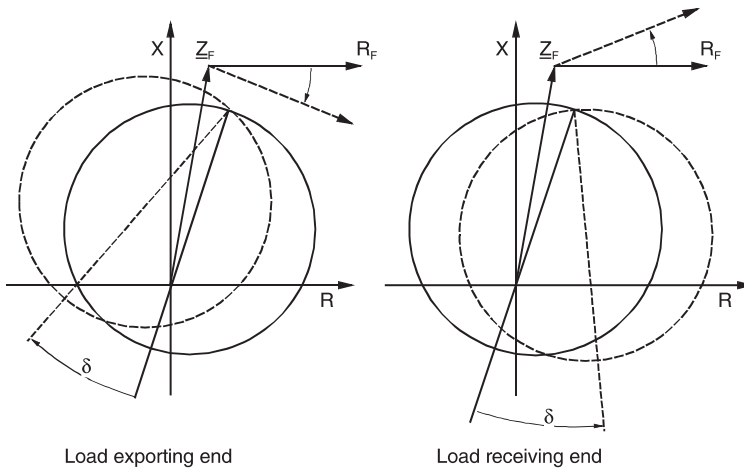
In the impedance diagram the relay characteristic automatically adjusts to the changed impedance trace (figure 3.100), i.e. the X-reach of the distance zone remains theoretically constant and independent of the load effect, and the fault resistance influence.

It should be mentioned that the same compensation method can be set up with the negative sequence currents. The same requirements of homogeneity then apply for the negative sequence system.

### Load influence on a polarised MHO-circle

The rotation of the polarised MHO-characteristic, in connection with the transferred load prior to fault inception, is referred to in paragraph 3.4.3.

The rotation in the same direction as the fault resistance has a positive influence on the distance measurement as mentioned. The measuring error in the reactance due to the

**Figure 3.102**

Adaptation of the polarised MHO-circle to the rotation of the fault resistance in the case of faults with pre-fault load

rotation of the fault resistance is partially compensated (figure 3.102). The full effect is however only achieved with a high degree of polarisation with unfaulted voltage ( $k_p$  close to 1). This is desired, as the following consideration shows:

In the case of a small source-impedance, the cross-polarised MHO-circle has a severe curvature, and a naturally poor arc-compensation. This implies that an over-reach due to the rotation caused by the fault resistance is in any event unlikely.

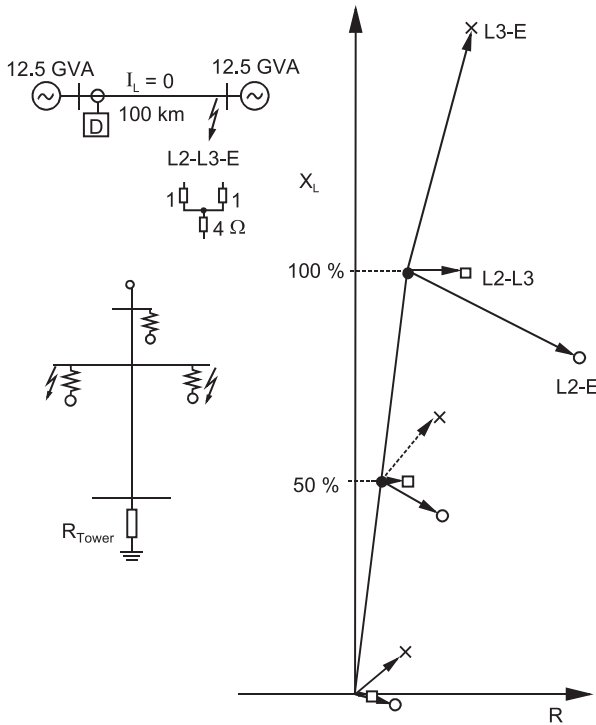
In the event of a large source-impedance and a large percentage of healthy voltage in the polarisation, the circle is enlarged and the border in X-direction is flatter. The tendency to over-reach is therefore increased, similar as with a polygonal characteristic. The more severe rotation of the MHO-circle in this case is therefore a desired effect.

#### *Two-phase earth-fault with fault resistance*

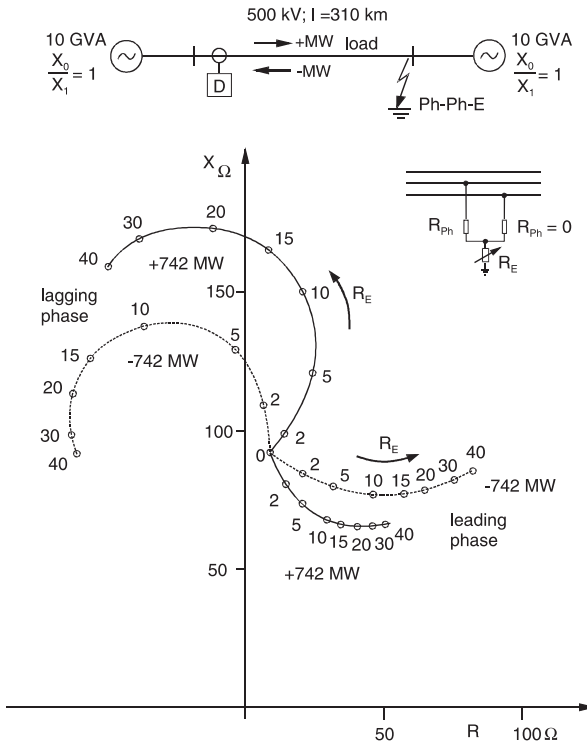
In the case of multiple faults with fault resistances, complex conditions arise for the distance measurement. The fault loops are connected at the fault location. Therefore the voltage drop across the fault resistance introduces a strong mutual coupling.

Figure 3.103 shows the impedances measured during two-phase earth-fault.

There are three fault loops. For this fault example, L2-L3-E they are the loops L2-E (leading phase), L3-E (lagging phase) and L2-L3 (phase-phase loop). The resistance between phases is typically relatively small (arc), while the mutual resistance to earth may assume larger values (during flash-over onto a tree or with high tower footing resistance). The values shown in figure 3.103 correspond to the conditions during a two-phase to earth fault across the isolators of a metal tower. Initially a single sided in-feed was assumed to allow a better understanding.



**Figure 3.103**  
Ph-Ph-E short-circuit with fault resistances at the fault location. Measured loop impedances depending on the fault location.



**Figure 3.104**  
Loop impedances during Ph-Ph-E short-circuit, depending on the fault resistance in the earth path and different load conditions.

From the vector diagram of the measured impedances it is apparent that under the given circumstances (normal conditions), the loop impedance in the leading phase L1-E is “seen” to be too short, while the lagging phase L2-E is “seen” to be too far.

The phase-phase loop L2-L3 is nearly measured correctly (small X-error). The effect of the fault resistances is further amplified by the load influence described earlier.

The results of a computer analysis with a given transmitted power and variable resistances to earth, is shown in figure 3.104.

For the fault-loop selection during two-phase-earth-faults in earthed systems, the following may be derived:

#### *Single-circuit overhead line*

Single-system distance protection:

- selection of the corresponding ph-ph loop

Full scheme distance protection

- general release of all six fault loops
- blocking of the leading Ph-E loop during two-phase-earth-faults to prevent an over-reach of the distance zones.

#### *Double-circuit overhead line*

Because of the possibility of a double earth-fault, at separate fault locations (cross-country fault) on neighbouring systems, the phase-earth measurement must be released in this case. The two single-phase earth-faults in each system can be measured separately in this manner.

Single-system distance protection:

- Selection of the leading phase-earth loop:
- If large ph-E resistances are expected (poor tower earthing), the setting may be reduced correspondingly.
- In the case of parallel line operation, the coupling of zero-sequence systems however causes reduction of the zone reach. An over-reach is therefore unlikely (see paragraph 3.5.3).
- The probability of an over-reach is further reduced by the intermediate in-feed effect (see paragraph 3.5.2).
- The selection of the lagging phase is not recommended as the zone reach may be too small.

Full scheme distance protection:

- Release of all measuring systems.
- Reduction of the under-reaching zone setting for phase-E loops when large fault resistances are expected.

### Short-circuit with arc

In the arc, voltage and current are in-phase (figure 3.105). The arc therefore appears as a resistance in the fault loop. The trapezoidal voltage is thereby added to the sinusoidal voltage drop in the overhead line.

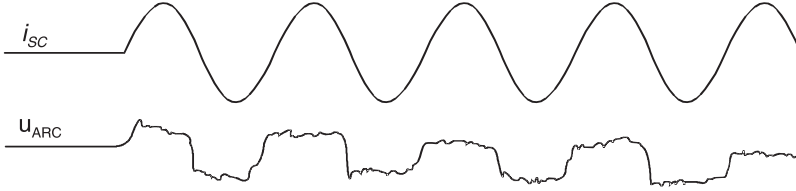


**Figure 3.105** Short-circuit current and arc voltage

The voltage deformation is more pronounced during arc-faults close to relays. An influence on the measuring accuracy only occurs on extremely short lines, where the arc component is still substantial for faults close to the zone limit.

In numerical relays, the influence can be neglected due to the applied digital filtering techniques.

#### *Arc-resistance*

Years ago, the size of the arc-resistance was estimated with measurement on various arc lengths and with system tests [3.28, 3.29].

As a first approximation, it may be assumed that the arc voltage is independent of the current magnitude, and equals approx. 2000-2500 V/m arc [3.28].

The following may apply as standard:

$$U_{ARC} = 2500 \text{ V/m}$$

From this the arc-resistance is:

$$R_{ARC} = \frac{2500 \cdot l_{ARC}}{I_{ARC}} [\Omega] \quad (3-93)$$

$$l_{ARC} = \text{arc length in m, } I_{ARC} = \text{arc current in A}$$

For more accurate studies, the “Warrington” formula is often applied [3.28].

It allows for the current-dependence of the arc-voltage:

$$R_{ARC} = \frac{28700 \cdot l_{ARC}}{I_{ARC}^{1.4}} [\Omega] \quad (3-94)$$

$$l_{ARC} = \text{arc length in m, } I_{ARC} = \text{arc current in A}$$

The arc expands due to wind and the dynamics of the arc.

The following equation represents an approximation of this [3.29]:

$$R_{ARC}^* = \left( 1 + \frac{5 \cdot v \cdot t_B}{l_{ARC}} \right) \cdot R_{ARC} \quad (3-95)$$

$l_{ARC}$  = original arc length in m,  $v$  = wind velocity in m/s,  $t_B$  = arc duration in s

*Numerical example:*

400 kV overhead line, flash-over on isolator (3 long rod isolators, 127.5 cm in series), minimum short-circuit current: 4.0 kA

How large is the arc-resistance at fault inception and after 1 second?

Solution:

For the arc length, the length of the isolators, with an additional 50% margin is utilised:  
 $l_{ARC} = 1.5 \cdot (3 \cdot 127.5) = 573.75$  cm, i.e. approx. 6 m.

Arc-resistance at fault inception (to check the 1<sup>st</sup> distance zone):

$$\text{from (3-93): } R_{ARC} = \frac{2500 \cdot 6.0}{4000} = 3.75 \, \Omega$$

$$\text{from (3-94): } R_{ARC} = \frac{28700 \cdot 6.0}{4000^{1.4}} = 1.56 \, \Omega$$

and after 1 second (to check the 3<sup>rd</sup> zone):

from (3-95):

$$R_{ARC(1s)}^* = \left( 1 + \frac{5 \cdot 3 \cdot 1}{6} \right) \cdot R_{LB} = 3.5 \cdot R_{ARC} = 13.1 \, \Omega \text{ respectively } 5.46 \, \Omega$$

*Arc-influence with double-sided in-feed*

The voltage across the arc, as a first approximation, is always constant, or decays according to the “Warrington”-equation with the factor  $I_{ARC}^{0.4}$ .

The arc-resistance defined above is therefore not constant, but rather decays with the factor  $1/I_{ARC}$  or  $1/I_{ARC}^{1.4}$ .

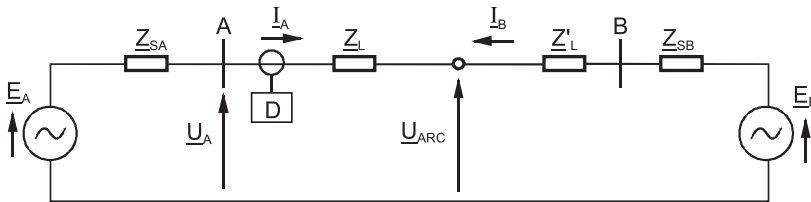


**Figure 3.106** Arc-resistance with double-sided in-feed, equivalent circuit

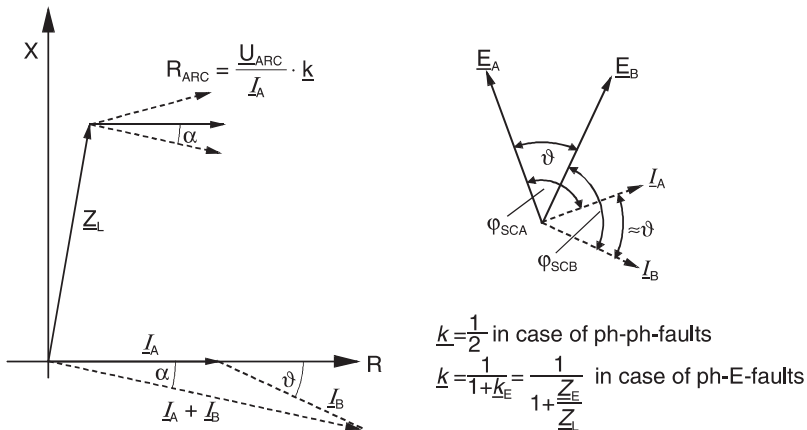


**Figure 3.107**

Short-circuit with arc-resistance and double-sided in-feed, influence on the distance measurement ( $I_{ph} = I_E$ , i.e.  $Z_0/Z_1=1$  at both sides of fault)

An arc therefore behaves differently to a fixed fault resistance (e.g. a tower footing resistance) in the case of double-sided in-feed.

The equivalent circuit shown in figure 3.93, for a short-circuit with double-sided in-feed in principle also applies here. The fixed fault resistance at the fault location however must be replaced by a constant voltage ( $\underline{U}_{\text{ARC}}$ ) (figure 3.106).

The current-dependence is initially neglected.

The voltage at the relay location then is:

$$\underline{U}_A = \underline{I}_A \cdot \underline{Z}_A + \underline{U}_{ARC} \quad (3-96)$$

From this the impedance measured by the relay results:

$$\underline{Z}_A = \frac{U_A}{I_A} = \underline{Z}_L + \frac{U_{ARC}}{I_A} \quad (3-97)$$

From this it can be seen that the arc-resistance apparent to the relay is independent of the current from the opposite side. This leads to the important setting rule:

Rule: The increase of the resistance at the fault location, due to the additional current from the opposite end:  $R_F^* = (1 + \underline{I}_B / \underline{I}_A) \cdot R_F$  only applies to fixed resistances.

For the arc-resistance effective at the relay location, calculated by means of equation (3-93) with constant arc-voltage, the current from the opposite end does not have to be taken into account.

According to the computation in equation (3-94) there even is a reduction of the effective resistance, as the rate of resistance reduction is greater than the rate of current increase (figure 3.108).



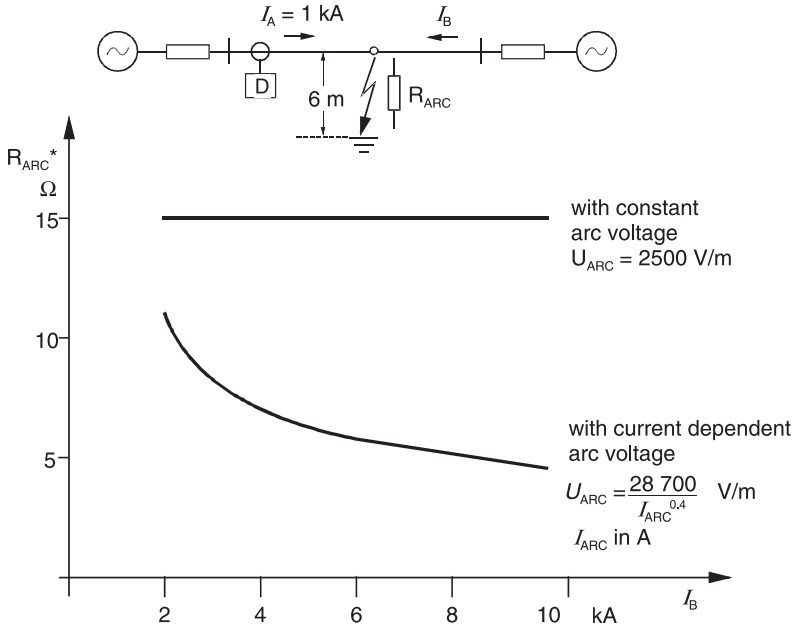


**Figure 3.108**

Effective arc-resistance “seen” by the distance relay with double-sided in-feed (Example)

### Tower footing resistance

Most of the faults on high-voltage overhead lines result from isolator flash-overs.

The short-circuit current in this case flows from the phase-conductor via the arc across the isolator, and into the steel armouring of the tower, and from there further to earth. This implies that at the fault location the arc resistance and the tower footing resistance are connected in series.

On lines with earth-wires (shield conductors) the current flows via several parallel tower footing resistances to earth. The resultant phase-earth resistance which is actually effective, is substantially reduced (figure 3.109) [3.30, 3.31].

The tower footing resistances and the earth-wire on the overhead line can be represented as a large number of T-sections connected in series (ladder network). For faults that are not too close to the substation, the tower footing resistances act like two parallel “ladder networks” ( at the end of the line it appears as one “ladder network” in parallel with the station earth).

From this, the effective tower footing impedance is derived:

$$\underline{Z}_{ETF} = \frac{R_{TF} \cdot \frac{1}{2} \cdot \underline{Z}_{LNW}}{R_{TF} + \frac{1}{2} \cdot \underline{Z}_{LNW}} \quad (3-98)$$

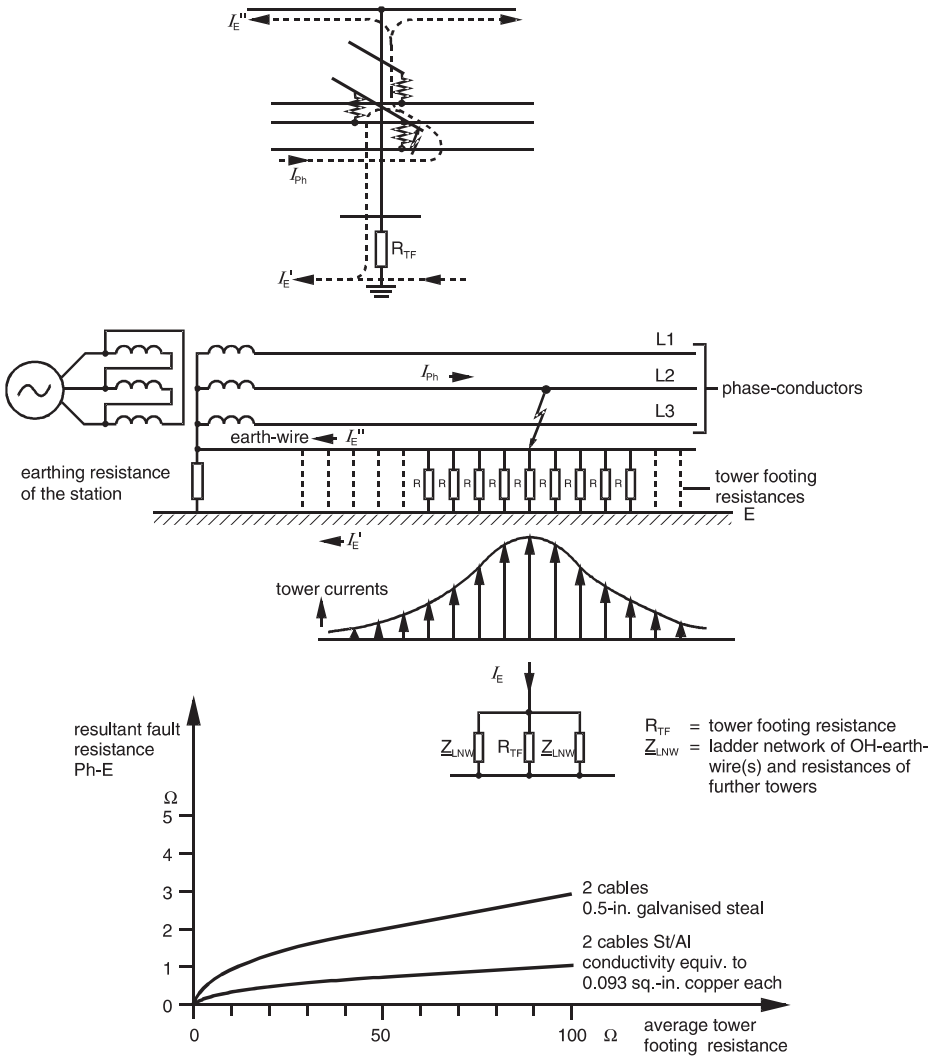


**Figure 3.109** Resultant fault resistance on overhead lines with earth-wire

Where  $Z_{LNW}$  is the impedance of one ladder network:

$$Z_{LNW} = \frac{1}{2} \cdot Z'_{EW} \cdot l_{AS} + \sqrt{\frac{(Z'_{EW} \cdot I_{AS})^2}{4} + R_{TF} \cdot Z'_{EW} \cdot l_{AS}} \quad (3-99)$$

with  $Z'_{EW} = R'_{EW} + jX'_{EW}$

The following definition of terms apply:

$Z_{ETF}$  = Effective tower footing impedance

$R_{TF}$  = Average tower footing resistance

$Z_{LNW}$  = Impedance of one ladder network (OH-earthwire(s) and tower footing resistances connected series-shunt)

$R'_{EW}$  = Resistance of the earth-wire in Ohm/km

$X'_{EW}$  = Reactance of the earth-wire in Ohm/km

$l_{AS}$  = Average span between towers/km

Assuming that the impedance of the parallel connected ladder networks is small in comparison to the tower footing resistance, the resulting earth-fault impedance can be approximated with the following equation:

$$Z_{ETF} = \frac{1}{2} \cdot \sqrt{R_{TF} \cdot Z'_{EW} \cdot l_{AS}} = \frac{1}{2} \cdot \sqrt{R_{TF} \cdot |Z'_{EW}| \cdot l_{AS}} \cdot e^{j \frac{\varphi_{EW}}{2}} \quad (3-100)$$

*Numerical example:*

*Given:*

Earth-wire 120/42 AlSt;  $l_{AS} = 230$  m;  $R'_{EW} = 0.234 \Omega/\text{km}$ ;

$X'_{ES} = 0.748 \Omega/\text{km}$ ;  $R_{TF} = 10 \Omega$

*Calculation:*

Earth-wire:  $|Z'_{EW}| = \sqrt{0.748^2 + 0.234^2} = 0.784$  and

$$\varphi_{EW} = \arctg(X'_{EW} / R'_{EW}) = \arctg(0.784 / 0.234) = 72.6^\circ$$

Effective tower footing impedance:

$$Z_{ETF} = \sqrt{10 \cdot 0.784 \cdot e^{j 72.6^\circ} \cdot 0.230} = 0.67 \cdot e^{j 36.3^\circ} = 0.54 + j0.40 \Omega$$

From the example it is apparent that the tower footing resistances are negligibly small when earth-wires with good conduction are present, and the tower footing resistances are not excessively large.

Furthermore it can be seen that the effective earthing impedance contains an inductive component, i.e. the fault is “seen” as being somewhat too far away by the distance protection. The 0.40 Ohm would correspond to approx. 1.5-2 km line length on a HV transmission line. With in-feed from the opposite end this reactance value would be correspondingly increased, as would the fault resistance (see figures 3.93 and 3.94). An under-reach results.

### 3.5.2 Intermediate infeeds

The influence of intermediate in-feeds was already discussed in connection with grading charts (paragraph 3.1.14).

The effect of the intermediate in-feed on the distance protection is again shown in figure 3.110. Usually there is an increase of the measured impedance.

The intermediate in-feeds in the downstream stations influence the over-reaching zone, the back-up zones and the fault detection stage.

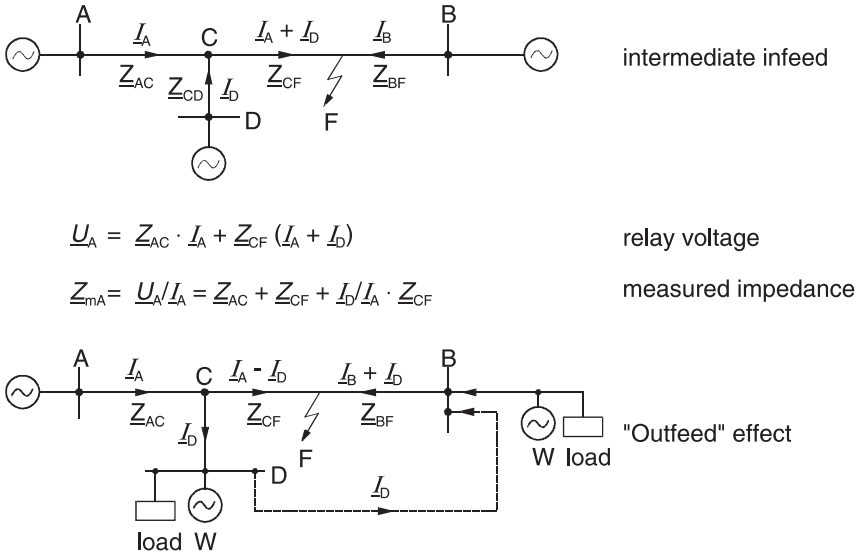


**Figure 3.110** Line with intermediate infeed

The resulting problems relating to the remote back-up protection were referred to in paragraph 3.1.14 (grading chart).

On teed feeders the measured impedance may also decrease due to a “negative in-feed” when the current flows out of the feeder during an internal fault. This is referred to as the out-feed condition. Principally this is a reduction of the fault impedance due to a parallel path in the short-circuit loop. This can only arise when the in-feed at D (figure 3.110) is weak or non-existent.

#### *Influence of earthed transformers*

Earthed transformers function as in-feeds in the zero-sequence system. This also influences the distance measurement.

The earth-current of the transformer generates an additional voltage drop in the zero-sequence system of the short-circuit loop. This leads to an increase of the measured fault impedance (figure 3.111):

The influence naturally increases when the transformer rating increases. In particular on lines with several transformer taps, a reach problem for the fault detection and distance zones results.

$$\underline{U}_{A \text{ Ph-E}} = x[\underline{I}_{\text{Ph-L}} \cdot \underline{Z}'_{1-L} + \underline{I}_{\text{E-L}} \cdot \underline{Z}'_{\text{E-L}}] + y[\underline{I}_{\text{Ph-T}} \cdot \underline{Z}''_{1-L} + \underline{I}_{\text{E-T}} \cdot \underline{Z}''_{\text{E-L}}] \quad (3-101)$$

or

$$\underline{U}_{A \text{ Ph-E}} = x \cdot \underline{Z}'_{1-L} \left[ \underline{I}_{\text{Ph-L}} + \underline{I}_{\text{E-L}} \cdot \frac{\underline{Z}'_{\text{E-L}}}{\underline{Z}'_{1-L}} \right] + y[\underline{I}_{\text{Ph-T}} \cdot \underline{Z}''_{1-L} + \underline{I}_{\text{E-T}} \cdot \underline{Z}''_{\text{E-L}}] \quad (3-102)$$

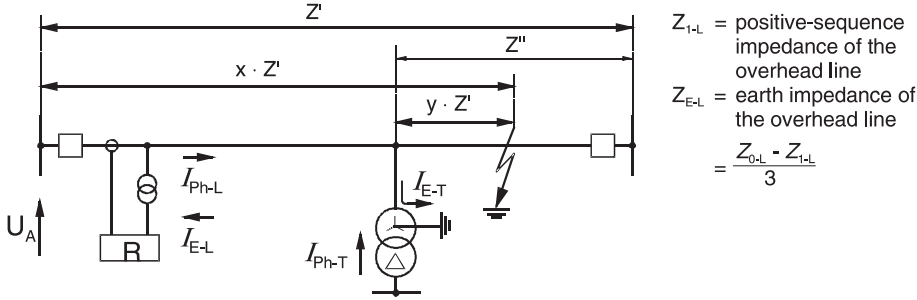


**Figure 3.111** Distance measuring error with intermediate zero-sequence infeed

The measurement of the phase-earth impedance is done with the following equation:

$$\underline{Z}_R = \frac{\underline{U}_{A \text{ Ph-E}}}{\underline{I}_{\text{Ph-L}} + \underline{k}_E \cdot \underline{I}_{E-L}} \quad (3-103)$$

In the event of adaptation of the  $\underline{k}_E$ -setting to the line, i.e.  $\underline{k}_E = \underline{Z}'_{EL} / \underline{Z}'_{1L}$ :

$$\underline{Z}_R = x \cdot \underline{Z}'_1 + y \cdot \underline{Z}'_1 \cdot \underbrace{\frac{\underline{I}_{\text{Ph-T}} \cdot \underline{Z}''_{1-L} + \underline{I}_{E-T} \cdot \underline{Z}''_{E-L}}{\underline{I}_{\text{Ph-L}} \cdot \underline{Z}'_{1-L} + \underline{I}_{E-L} \cdot \underline{Z}'_{E-L}}}_{\text{measuring error}} \quad (3-104)$$

It is simplest to use symmetrical components to determine the impedance measured by the relay. The following example of an overhead line with single in-feed and a transformer tap explains the basic procedure. The equivalent circuit is shown in figure 3.112. It applies for single phase earth short circuits.

To calculate the measured values,  $\underline{U}_A$  and  $\underline{I}_A$ , appearing at the relay location, the following equations are obtained:

$$\underline{U}_{A1} = \underline{U}_{F1} + \underline{Z}_{1AF} \cdot \underline{I}_{A1} \quad (3-105)$$

$$\underline{U}_{A2} = \underline{U}_{F2} + \underline{Z}_{1AF} \cdot \underline{I}_{A2} \quad (3-106)$$

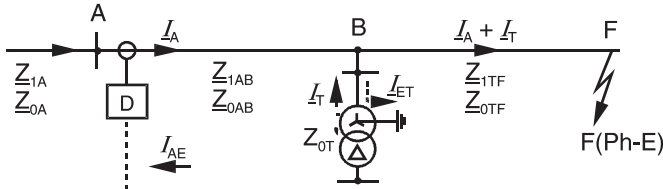
$$\underline{U}_{A0} = \underline{U}_{F0} + \underline{Z}_{0BF} \cdot (\underline{I}_{A0} + \underline{I}_{0T}) + \underline{Z}_{0AB} \cdot \underline{I}_{A0} \quad (3-107)$$

$$\underline{U}_{F1} + \underline{U}_{F2} + \underline{U}_{F0} = 0 \text{ and } \underline{Z}_{0AB} + \underline{Z}_{0BF} = \underline{Z}_{0AF} \quad (3-108)$$

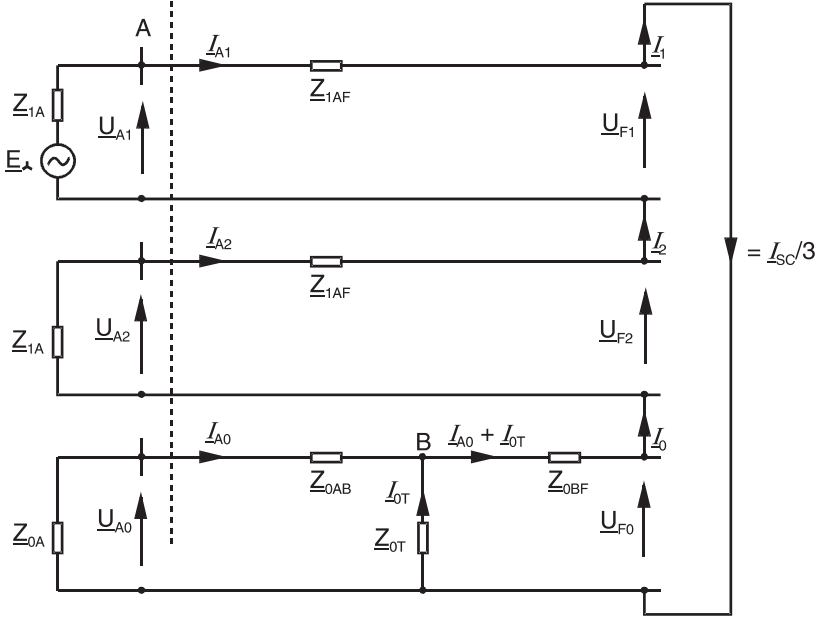
results in:

$$\begin{aligned} \underline{U}_A &= \underline{U}_{A1} + \underline{U}_{A2} + \underline{U}_{A0} = \underline{Z}_{1AF} \cdot (\underline{I}_{A1} + \underline{I}_{A2}) + \underline{Z}_{0AF} \cdot \underline{I}_{A0} + \underline{Z}_{0BF} \cdot \underline{I}_{0T} \\ \underline{I}_{A-\text{Ph}} &= \underline{I}_{A1} + \underline{I}_{A2} + \underline{I}_{A0} \\ \underline{I}_{A-E} &= -3\underline{I}_{A0} \end{aligned} \quad (3-109)$$

a) single-phase equivalent circuit



b) equivalent circuit with symmetrical components


**Figure 3.112** Distance measurement with zero-sequence intermediate infeed (tapped line)

$$\frac{I_{SC}}{3} = \frac{E_{Ph-E}}{Z_1 + Z_2 + Z_0} \quad (3-110)$$

with

$$Z_1 = Z_{1A} + Z_{1AF}, \quad Z_2 = Z_1, \quad Z_0 = \frac{(Z_{0A} + Z_{0AB}) \cdot Z_{0T}}{Z_{0A} + Z_{0AB} + Z_{0T}} + Z_{0BF}$$

$$I_{A0} = \frac{Z_{0T}}{Z_{0A} + Z_{0AB} + Z_{0T}} \cdot I_0 \quad (3-111)$$

and

$$\frac{I_{SC}}{3} = I_1 + I_2 + I_0$$

This can be implemented to calculate the impedance according to equation (3-28):

$$\underline{Z}_A = \frac{\underline{U}_A}{\underline{I}_{A-Ph} - \underline{k}_E \cdot \underline{I}_{AE}}$$

*Numerical example:*

110 kV overhead line with a 40 MVA transformer

Line-data:  $\underline{Z}'_{1L} = 0.4 \Omega/\text{km}$ ,  $\underline{Z}'_{0L} = 1.1 \Omega/\text{km}$ , Sections: A-B = 10 km and B-F = 10 km;

System in-feed:  $\text{SCC}'' = 1000 \text{ MVA}$ ;  $X_0/X_1 = 1$ ;

Transformer:  $P_n = 40 \text{ MVA}$ ,  $U_K = 10\%$ ,  $X_0/X_1 = 1$ ;

results in:

$$U_A = 32.86 \text{ kV}, I_{A-Ph} = 2534 \text{ A and}$$

$$I_{A-E} = -1675 \text{ A}$$

$$\underline{Z}_A = \frac{\underline{U}_A}{\underline{I}_{A-Ph} - \underline{k}_E \cdot \underline{I}_{A-E}} = 9.35 \Omega \quad \text{with} \quad \underline{k}_E = \frac{\underline{Z}'_{EL}}{\underline{Z}'_{1L}} = \frac{(\underline{Z}'_{0L} - \underline{Z}'_{1L})/3}{\underline{Z}'_{1L}} = 0.583$$

The line impedance up to the fault location is  $\underline{Z}_{1AF} = 20 \text{ km} \cdot 0.4 \Omega/\text{km} = 8 \Omega$

Therefore the measuring error is:  $F = \frac{9.35 - 8}{8} \cdot 100 = 16.9\%$ .

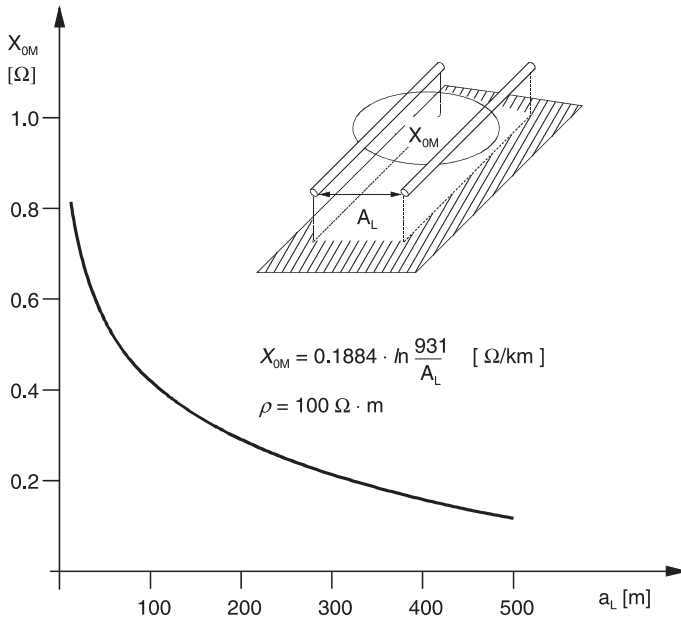
From this it is apparent that especially when several taps with earthed transformers exist, a very large under-reach results. The zone reach can be compensated by a correspondingly larger setting of the  $\underline{k}_E$  factor (in the example to  $\underline{k}'_E = 0.94$ ). The reach of the phase-phase measuring systems where this problem does not arise, remains unaffected.

### 3.5.3 Parallel lines

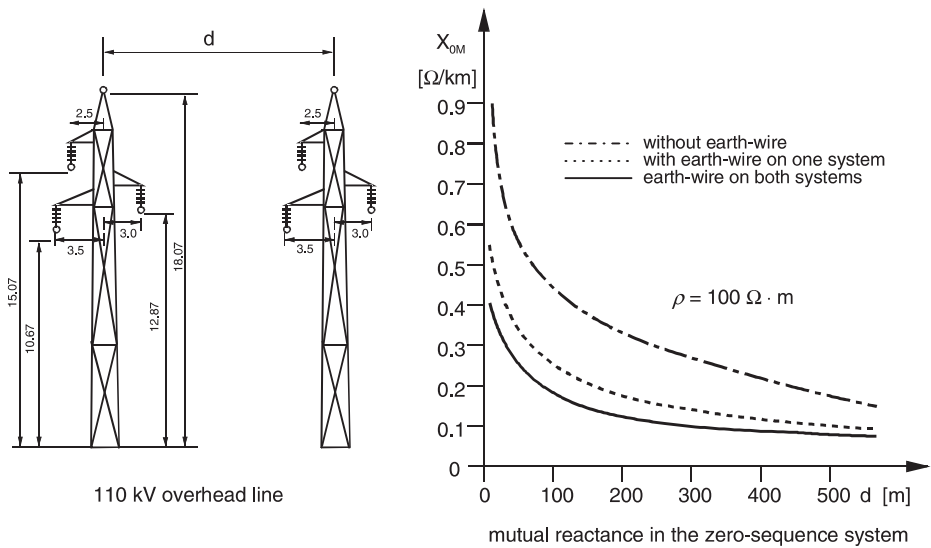
When overhead lines follow parallel paths, a mutual, inductive coupling of the current paths exists. In the case of transposed lines, this effect in the positive and negative sequence system may be neglected for all practical purposes (mutual reactance less than 5% of the self-impedance). This implies that during load conditions, and for all short-circuits with-out earth, the lines may be considered as independent.

During earth-faults, the conductor currents do not add up to zero, but rather a summation current corresponding to the earth current results. For this summated current, a fictitious summation conductor placed at the geometrical centre of the phase-conductors models the three-phase system. Two lines in parallel are modelled by two parallel single conductors with an earth return path, for which the mutual reactance must be calculated. In the case of lines with earth-wires, an additional coupling results, which must be considered in the calculations.

The single-phase substitute conductor-earth loop corresponds to the zero-sequence system of the line, when represented with symmetrical components. According to the definition, the current in the zero-sequence system only equals the portion of the sum-



a) Mutual inductance of two conductor-earth loops



b) Calculated mutual reactance of two 100 kV overhead lines

**Figure 3.113** Zero-sequence system coupling of overhead lines



mated current relating to one phase, i.e. one-third of the earth current ( $I_0 = I_E/3$ ). The zero-sequence impedance therefore corresponds to three times the substitute conductor-earth impedance.

The coupling impedance between the zero-sequence systems of two lines without earth-wire is given by the following equation [3.32, 3.33]:

$$\underline{Z}'_{0M} = \left( 3 \cdot R'_E + j\omega \cdot 6 \cdot \ln \frac{\delta}{A_L} \right) \cdot 10^{-4} \text{ [}\Omega/\text{km]} \quad (3-112)$$

Definition:  $\omega = 2\pi f$  angular frequency in  $\text{s}^{-1}$

of terms

$$\delta = 1650 \sqrt{\frac{\rho}{\omega}} \quad \text{penetration depth in m}$$

$$\rho \quad \text{specific resistance of earth in } \Omega \cdot \text{m}$$

$$R'_E = \frac{\pi}{2} \cdot \omega \cdot 10^{-4} \quad \text{resistance of ground in } \Omega/\text{km}$$

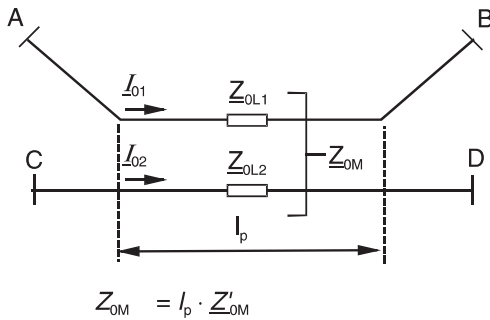
$$A_L \quad \text{geometrical mean distance of the conductors of both three-phase systems (approx. corresponds to the distance between the towers of the two lines).}$$

With a system frequency of 50 Hz and a typical specific earth resistance of  $100 \Omega \cdot \text{m}$ :

$$\underline{Z}_{0M} = 0,15 + j0,1884 \cdot \ln \frac{931}{A_L} \text{ [}\Omega/\text{km]} \quad (3-113)$$

From this it is apparent that the mutual inductance has a logarithmic relationship, and therefore decreases relatively slowly with an increase of line spacing (figure 3.113b). Even with fairly large distance between the lines, mutual coupling is still present.

The zero-sequence current of the one system induces a voltage in the other system, and vice versa (figure 3.114). The lines may follow a parallel path along their full length, or only for a portion thereof. If the systems are connected in parallel on both line ends

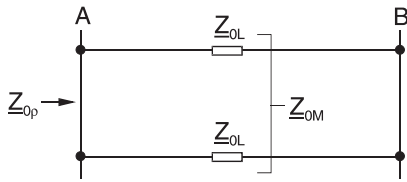


$$\underline{U}_{A-B} = I_{01} \cdot \underline{Z}_{OL1} + I_{02} \cdot \underline{Z}_{0M}$$

$$\underline{U}_{C-D} = I_{02} \cdot \underline{Z}_{OL2} + I_{01} \cdot \underline{Z}_{0M}$$

**Figure 3.114**

Zero-sequence system impedances of a double-circuit line



$$Z_{0p} = \frac{1}{2} \cdot (Z_{0L} + Z_{0M})$$

$$\text{or: } Z_{0M} = 2 \cdot Z_{0p} - Z_{0L}$$

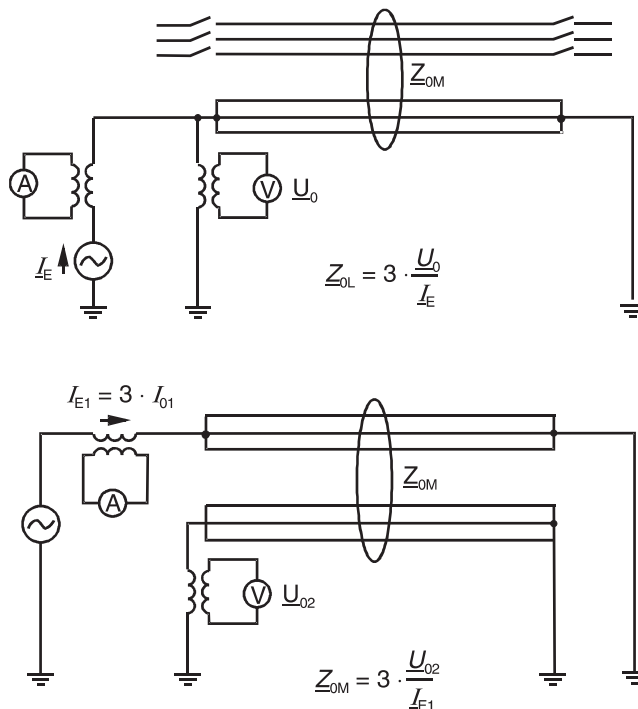
**Figure 3.115**

Parallel overhead lines, zero-sequence system voltages

(true double-circuit line), a fixed relationship between the self-inductance of a single line  $Z_{0L}$ , the self-inductance of a double line  $Z_{0p}$  and the mutual reactance  $Z_{0M}$  exists (figure 3.115).

It may for example be used to calculate the mutual reactance  $Z_{0M}$ , when the zero-sequence impedance of the single and the parallel line are known.

The determination of the self- and mutual inductance is usually done by computation based on the tower construction and spacing. It is however also possible to determine these values by measurement, which should be carried out according to the principle shown in figure 3.116.

**Figure 3.116** Measurement of the  $Z_{0L}$  and  $Z_{0M}$

**Attention!** The measurement is done with low voltage signals. It is however not without risk, as the danger, that other lines nearby, or atmospheric interference, may induce high voltage on the line being measured, exists. Corresponding safety measures must be taken.

### *Influence of the zero-sequence system coupling on the distance measurement*

The summated current (= earth-current) of the parallel line induces a longitudinal voltage in the fault loop of the measured line, and changes the measured short-circuit voltage at the relay location. A measuring error results.

The influence depends on the system configuration, as will be shown later.

The following generally applies:

- the measuring error is positive (measurement of an impedance that is too large, i.e. zone under-reach), when the summated currents in both systems flow in the same direction
- the measuring error is negative (over-reach), when the summated currents flow in opposite directions

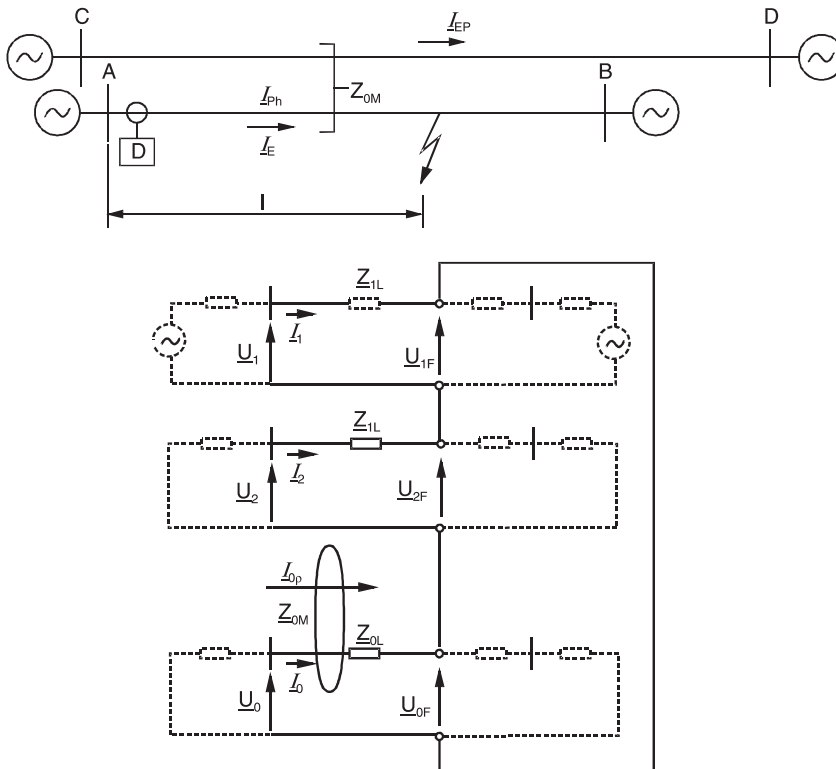


**Figure 3.117** Distance measurement on parallel lines

When the two lines belong to different systems (worst case: different voltage levels), no direct relationship between the summated currents exist. A measuring error in either direction may occur.

On a true parallel line, where the parallel systems at both line ends are coupled via a mutual busbar, a current distribution according to the relative in-feeds and the switching condition of the lines is dictated.

Initially the generally applicable case of a parallel line is looked at (figure 3.117).

The following equations can be derived from the symmetrical component equivalent circuit:

$$\underline{U}_1 = \underline{Z}_{1L} \cdot \underline{I}_1 + \underline{U}_{1F} \quad (3-114)$$

$$\underline{U}_2 = \underline{Z}_{1L} \cdot \underline{I}_2 + \underline{U}_{2F} \quad (3-115)$$

$$\underline{U}_0 = \underline{Z}_{0L} \cdot \underline{I}_0 + \underline{Z}_{0M} \cdot \underline{I}_{0P} + \underline{U}_{0F} \quad (3-116)$$

If the equations (3-115, 3-116, 3-117) are added together, and the following relationship is applied:

$$\underline{U}_1 + \underline{U}_2 + \underline{U}_0 = \underline{U}_A \quad \text{and} \quad \underline{U}_{1F} + \underline{U}_{2F} + \underline{U}_{0F} = 0$$

the result is:

$$\underline{U}_A = \underline{Z}_{1L} \cdot (\underline{I}_1 + \underline{I}_2) + \underline{Z}_{0L} \cdot \underline{I}_0 + \underline{Z}_{0M} \cdot \underline{I}_{0P} \quad (3-117)$$

$$\underline{U}_A = \underline{Z}_{1L} \cdot (\underline{I}_1 + \underline{I}_2 + \underline{I}_0) + (\underline{Z}_{0L} - \underline{Z}_{1L}) \cdot \underline{I}_0 + \underline{Z}_{0M} \cdot \underline{I}_{0P} \quad (3-118)$$

$$\underline{U}_A = \underline{I}_{ph} \cdot \underline{Z}_{1L} - \frac{\underline{Z}_{0L} - \underline{Z}_{1L}}{3} \cdot \underline{I}_E - \frac{\underline{Z}_{0M}}{3} \cdot \underline{I}_{Ep} \quad (3-119)$$

with  $\underline{I}_E = -3\underline{I}_0$ ,  $\underline{I}_{Ep} = -3 \cdot \underline{I}_{0P}$  and  $\underline{I}_{pH} = \underline{I}_1 + \underline{I}_2 + \underline{I}_0$ . By applying  $(\underline{Z}_0 - \underline{Z}_1)/3 = \underline{Z}_E$ , the short-circuit voltage at the relay location can be determined:

$$\underline{U}_A = \underline{Z}_{1L} \left( \underline{I}_{ph} - \frac{\underline{Z}_{EL}}{\underline{Z}_L} \cdot \underline{I}_E - \frac{\underline{Z}_{0M}}{3 \cdot \underline{Z}_{1L}} \cdot \underline{I}_{Ep} \right) \quad (3-120)$$

The measured impedance may now be calculated by using equation (3-28):

$$\underline{Z}_A = \frac{\underline{U}_A}{\underline{I}_{ph} - \underline{k}_E \cdot \underline{I}_E} = \frac{\underline{Z}_{1L} \left( \underline{I}_{ph} - \frac{\underline{Z}_{EL}}{\underline{Z}_L} \cdot \underline{I}_E - \frac{\underline{Z}_{0M}}{3 \cdot \underline{Z}_{1L}} \cdot \underline{I}_{Ep} \right)}{\underline{I}_{ph} - \underline{k}_E \cdot \underline{I}_E} \quad (3-121)$$

By adaptation of the residual compensation factor to the overhead line ( $\underline{k}_E = \underline{Z}_{EL}/\underline{Z}_{1L}$ ), the equation finally is:

$$\underline{Z}_A = \underline{Z}_{1L} \left( 1 - \underbrace{\frac{\frac{\underline{Z}_{0M}}{3 \cdot \underline{Z}_{1L}} \cdot \underline{I}_{Ep}}{\underline{I}_{ph} - \frac{\underline{Z}_{EL}}{\underline{Z}_L} \cdot \underline{I}_E}}_{\text{measuring error}} \right) \quad (3-122)$$

It can be seen that the measuring error is dependent on the polarity and magnitude ratio of the earth current in both feeders.

The equations may now be applied to a simple example:

Figure 3.118 shows a double-circuit line with single-ended in-feed. Herein, the behaviour of the distance relays  $Z_1$  and  $Z_2$  during a single-phase earth-fault on line one can be observed.

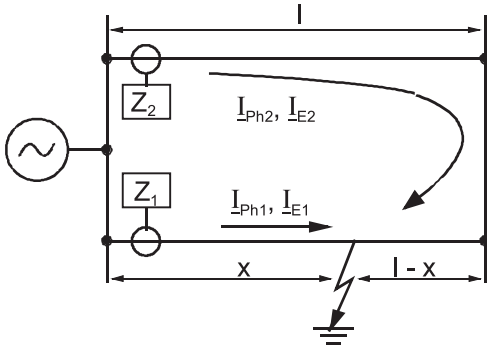


**Figure 3.118**  
Earth-fault on a double-circuit line (single-ended in-feed)

The following relationships apply to the currents in this case:

$$\underline{I}_{E1} = -\underline{I}_{ph1}, \quad \underline{I}_{E2} = -\underline{I}_{ph2} \quad \text{and} \quad \underline{I}_{E2} = \frac{x}{2l-x} \underline{I}_{E1}$$

*Relay Z1 on the faulted line:*

From equation (3-121):

$$\underline{Z}_1 = \frac{x}{l} \cdot \underline{Z}_L + \underbrace{\frac{x}{l} \cdot \underline{Z}_L \cdot \frac{\frac{\underline{Z}_{0M}}{3 \cdot \underline{Z}_{1L}} \cdot \frac{x}{2l-x}}{1 + \frac{\underline{Z}_{EL}}{\underline{Z}_L}}}_{\text{measuring error}} \quad (3-123)$$

Relay Z2 on the unfaulted parallel line:

In figure 3.118 the following voltage for the short-circuit loop may be read off:

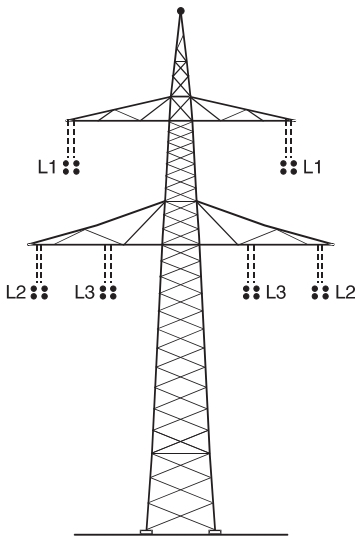
$$\underline{U}_{(\text{Ph-E})2} = (2l-x)(\underline{Z}_L \cdot \underline{I}_{\text{ph}2} - \underline{Z}_E \cdot \underline{I}_{\text{E}2}) - x \cdot \frac{\underline{Z}_{0M}}{3} \cdot \underline{I}_{\text{E}1} + 2(l-x) \frac{\underline{Z}_{0M}}{3} \cdot \underline{I}_{\text{E}2} \quad (3-124)$$

By substitution of  $\underline{U}_{(\text{Ph-E})2}$  in equation (3-28), and taking note of the above current relationships, we get:

$$\underline{Z}_2 = (2l-x) \cdot \underline{Z}_L + \underbrace{\frac{\frac{\underline{Z}_{0M}}{3} \cdot \underline{Z}_{1L}}{1 + \frac{\underline{Z}_{E1}}{\underline{Z}_L}}}_{\text{measuring error}} \cdot \underline{Z}_L \quad (3-125)$$

In figure 3.119 the typical impedance data, as well as the resulting residual compensation factors of a 400 kV double-circuit line are shown (for simplicity, only the magnitudes are used in the calculation).

By substitution of these values in equations (3-123) and (3-125), the measuring errors for this double-circuit line with single-ended in-feed can be calculated. The results are shown in figure 3.120. It is apparent that both relays ( $Z_1$  and  $Z_2$ ) at the in-feeding end return a measured impedance which is too large, as was expected ( $\underline{I}_{\text{E}1}$  and  $\underline{I}_{\text{E}2}$  are in the same direction). The largest measuring error occurs in the case of a fault at the end of the line (35%!)



$$\begin{aligned} R_1 &= 0.032 \, \Omega/\text{km} \\ X_1 &= 0.254 \, \Omega/\text{km} \\ R_0 &= 0.139 \, \Omega/\text{km} \\ X_0 &= 0.906 \, \Omega/\text{km} \\ R_{0M} &= 0.107 \, \Omega/\text{km} \\ X_{0M} &= 0.488 \, \Omega/\text{km} \end{aligned}$$

residual compensation factors

$$\frac{Z_E}{Z_L} = \frac{Z_0 - Z_1}{3 \cdot Z_1} = 0.87$$

$$\frac{Z_M}{Z_L} = \frac{Z_{0M} - Z_1}{3 \cdot Z_1} = 0.65$$

**Figure 3.119** Typical impedance data for a double-circuit line

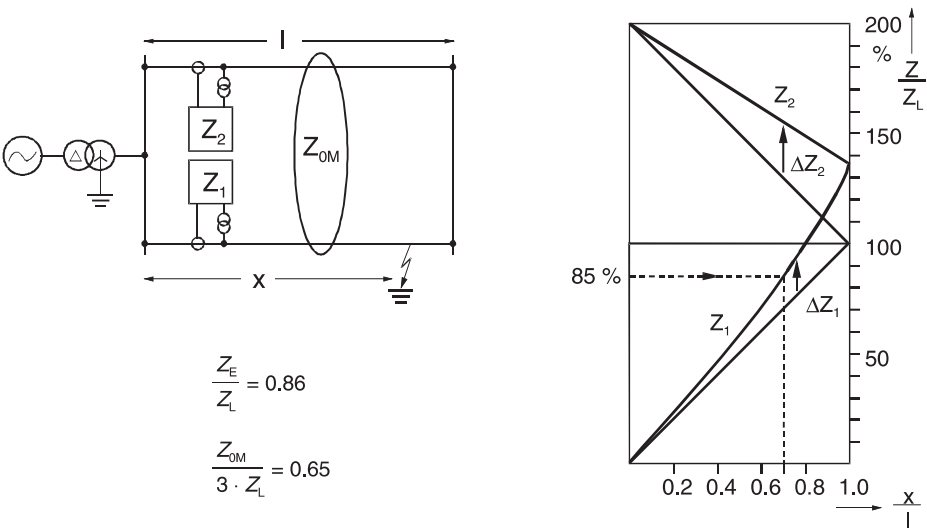


Figure 3.120 Distance measuring error on a double-circuit line with single-ended infeed

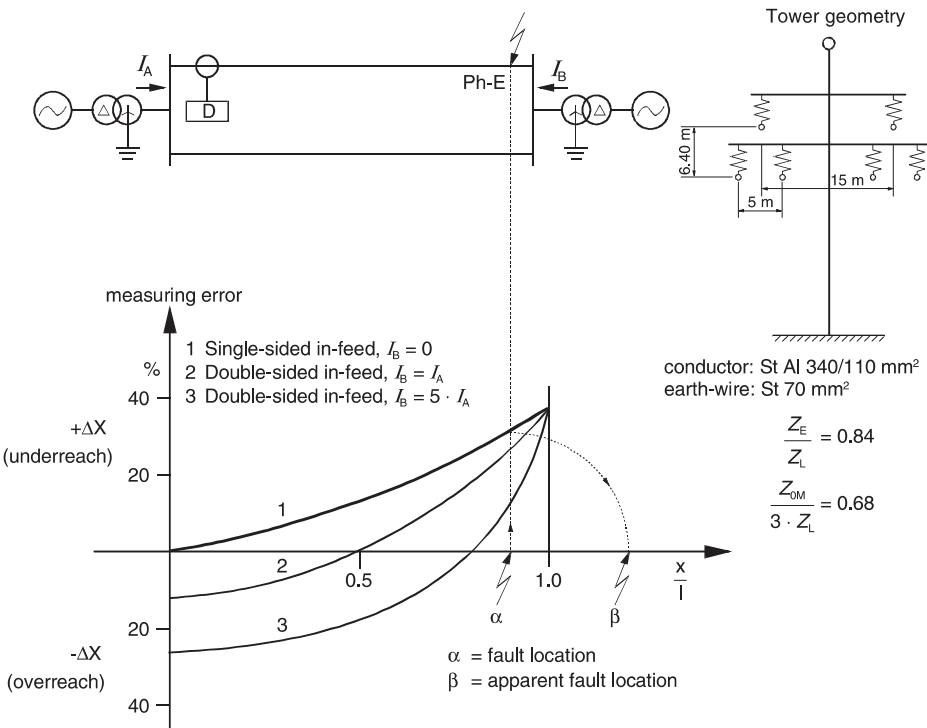


Figure 3.121 Earth-fault on a double-circuit line, distance measuring error with double-sided in-feed

For comparison purposes, figure 3.121 shows the measuring error for the relay on the faulted line in the case of double-ended in-feed. It is apparent that in this case the error is negative for faults on the first fifty/eighty percent of the line. This corresponds exactly to that portion of the line, where the earth current of the parallel line flows in the opposite direction (in comparison to  $\underline{I}_{E1}$ ,  $\underline{I}_{E2}$  has the opposite sign).

This effect assists the distance protection when it is applied in a permissive underreach tripping scheme, as one side always “sees” the fault closer and is therefore able to send a permissive tripping signal, even with small setting of the under-reaching zones.

The influence of the parallel line, in the case of double-circuit lines, is strongly dependent on the switching condition, due to the corresponding difference in the earth-current distribution (figure 3.122).

It is clear that with earth-currents flowing in the same direction ( $\underline{I}_E$  and  $\underline{I}_{EP}$ ), an increase of the measured impedance results, while the measured impedance is reduced, when the earth currents flow in opposite directions.

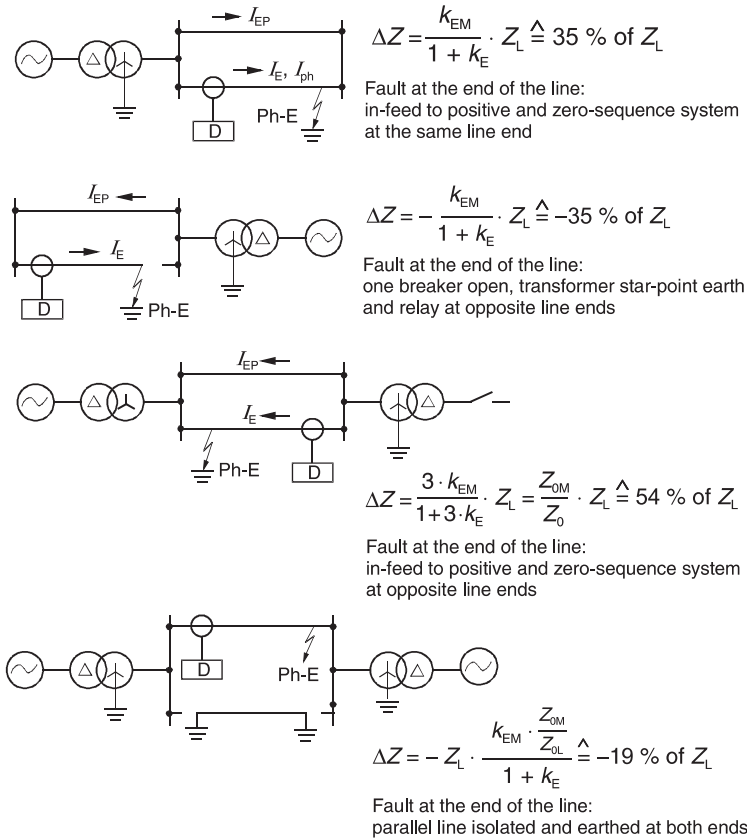


**Figure 3.122**

Distance protection on parallel lines, dependence on switching condition: measuring impedance (values of Fig. 3.119:  $k_E = 0.87$ ,  $k_{EM} = 0.65$ ,  $Z_{OM}/Z_{OL} = 0.54$ )



The setting of the impedance zones on a double-circuit line requires some compromise on the one hand to provide satisfactory reach when both lines are in operation, and on the other hand to avoid a too severe over-reach when the parallel line is switched off, and earthed on both sides (refer to application example in paragraph 7.1) [3-34, 3-35].

### *Parallel line compensation*

From equation (3-121) it is apparent that the fault impedance is measured correctly when the term  $(-Z_{0M}/3 \cdot Z_{1L}) \cdot I_{EP}$  is added to the denominator. With the normal setting ( $k_E = Z_{EL}/Z_{1L}$ ) the denominator is simplified by cancellation with the expression in brackets in the numerator. The measuring result then is  $Z_{1L}$ , i.e. the influence of the parallel line has been cancelled. Accordingly, the earth-current of the parallel line must be introduced to the measurement with a weighting factor.

This procedure is generally known as parallel line compensation.

The equation (3-28), for the impedance calculation of the phase-earth loops is modified as follows:

$$Z_{ph-E} = \frac{U_{ph-E}}{I_{ph-E} - k_E \cdot I_E - k_{EM} \cdot I_{Ep}} \quad \text{with } k_{EM} = \frac{Z_{0M}}{3 \cdot Z_{1L}} \quad (3-126)$$

With electro-mechanical technology, the compensation was simply implemented by adding the earth-current of the parallel line via interposing transformers to the earth-current of the protected line.

Numerical relays provide an additional measuring input, where the earth-current of the parallel line may be connected. The addition is then done numerically. The compensation factor is set by means of the operating software.

### *Earth-current balance*

The parallel line compensation described above naturally not only functions during faults on the protected line, but also for faults on the parallel line.

To illustrate this, the example shown in figure 3.120 is used again.

By substituting equation (3-124) in equation (3-126), the equation for the measurement with parallel line compensation during a single-phase earth-fault on a parallel line is obtained:

$$Z_2^* = Z_L \cdot (2l-x) + \underbrace{\frac{\left(\frac{x}{2l-x} - \frac{2l-x}{x}\right) \frac{Z_{0M}}{3 \cdot Z_L}}{1 + \frac{Z_{EL}}{Z_L} + \frac{Z_{0M}}{3 \cdot Z_L} \cdot \frac{2l-x}{x}}}_{\text{measuring error}} \cdot Z_L \cdot (2l-x) \quad (3-127)$$

The measured impedances with parallel line compensation are shown in figure 3.123. A comparison with figure 3.120 shows that the relay now measures the correct distance

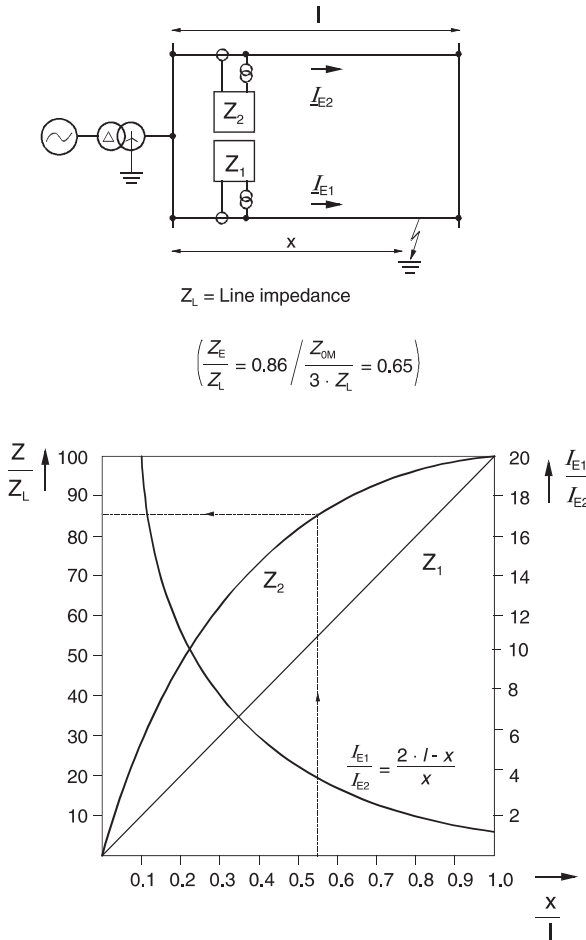


**Figure 3.123**  
Distance measurement on  
double-circuit overhead  
line, operation of parallel  
line compensation

on the faulted line, i.e. the measured impedance has a linear increase with increase of the distance to fault.

The distance to fault measured by the relay on the healthy line is too short due to the coupled earth current of the parallel line.

This is understandable, because a large short-circuit current flows during close-in faults on the faulted line. This current is coupled into the relay on the healthy line and causes this relay to also “see” a small impedance.

For example therefore, with an under-reach zone setting of 85% the protection on the healthy line would also trip for faults on the first 55% of the line length (dashed line).

To prevent this over-functioning, the so-called earth-current balance is implemented. It compares the earth-currents of the two lines and blocks the parallel line compensation (coupled current), when the earth-current of the parallel line exceeds the earth-current on the protected line by a settable percentage margin.

This principle is based on the fact that the earth-current in the faulted line is always at least as large (fault at the end of the line) or greater than the earth-current of the healthy parallel line.

For the double-circuit overhead line the highest coupling effect (highest earth current on the parallel line) occurs with single-ended in-feed. According to figure 3.123, the following relationship between the fault location  $x$  and the earth-current distribution exists in this case:

$$\frac{I_{E1}}{I_{E2}} = \frac{2l-x}{x} = \frac{2-\frac{x}{l}}{\frac{x}{l}} \quad (3-128)$$

In this way it is possible to determine from which distance to fault the compensation shall be active, i.e. the setting on the relay is not the current ratio, but rather the  $x/l$ -ratio directly in percent.

This is explained by way of the following numerical example:

With a setting of  $x/l = 85\%$  (typical setting), the compensation is active for faults on the protected line as well as 15% beyond the remote station into the parallel line for security. This setting then corresponds to  $I_{E1}/I_{E2} = 1.35$ .

This implies that the parallel line compensation is blocked when the earth-current of the parallel line exceeds 135% of the earth-current in the protected line.

It must be noted that in the case of faults on the following lines, the compensation is always active, because in this case the earth-currents on both circuits of the parallel line are equal.

An improved reach of the back-up zones is therefore given in all cases.

#### *Application of parallel line compensation*

The compensation may only be used when both lines end in the same station. This always applies for double-circuit overhead lines. For lines that run only partially parallel, the compensation only finds limited application.

The compensation is in any case recommended for the fault locator, as this is the only means to obtain appropriate measuring accuracy on parallel lines.

For distance protection, the compensation is usually only implemented in difficult cases, where sufficient reach of the back-up zones would otherwise not be possible. This would be the case when a short line follows the double-circuit line.

From a statistical point of view, the parallel line compensation of distance protection found application only relatively seldom in the past [3.42]. The reasoning behind this is that the testing of the protection becomes more complex, due to a dependence on a different feeder-bay.

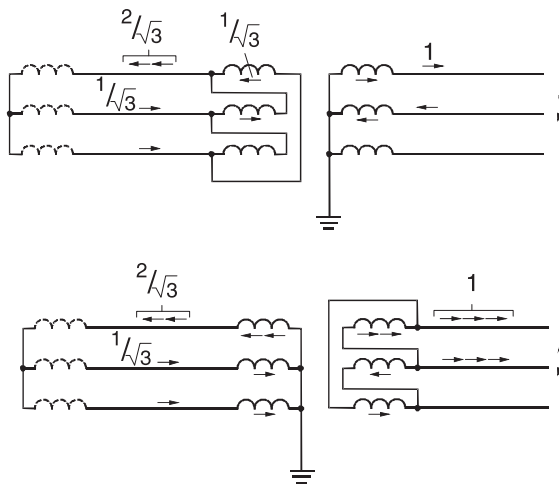
With numerical relays, the compensation is more frequently available, due to the integrated fault locator function.

A selection whether the compensation is active for the fault locator only, or for the distance protection as well may be made via parameter in the relay. An optional selection for the distance protection is therefore available at any time.

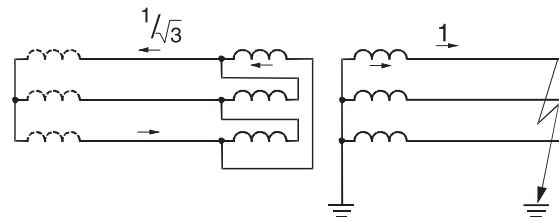
### 3.5.4 Distance protection for transformers

For distance measurement into transformers or through transformers, some peculiarities must be noted:

- Impedance is transformed with the square of the turns-ratio of the windings. This corresponds to the square of the voltage transformation ratio.
- On transformers with tap changer the transformation ratio changes according to the step of the tap changer.
- On star delta transformers a phase rotation in opposite directions, corresponding to the vector group, results for the positive and negative sequence system. The fault current distribution therefore changes from one side of the transformer to the other. A two-phase short-circuit appears as a three-phase fault with unsymmetrical current distribution (figure 3.124a).



a) Conversion of a two-phase fault current



b) Conversion of a single-phase fault current

**Figure 3.124**  
Conversion of fault currents  
by a star/delta transformer

- The zero-sequence system cannot be converted by a star/delta transformer. Earth-faults can therefore not be measured correctly by the distance relay through star/delta transformers.
- A single-phase earth-fault on the star side in this case appears as a two-phase short-circuit on the delta side (figure 3.124b).
- On auto transformers and star-star transformers with an earth on both windings, a measurement through the transformer is possible.

#### *Distribution of the current and voltage transformers*

There are four optional configurations for the connection of the instrument transformers to the distance protection (figure 3.125). Generally the current and voltage transformers are on the same side of the power transformer. All other configurations must be treated as peculiarities.

#### **Instrument transformers on the low voltage side, forward grading (figure 3.125a)**

This configuration is of interest when there are no instrument transformers available on the high voltage side, and the downstream feeder must be protected as for example when the transformer and the downstream feeder are a unit. In this case the transformer and the largest possible portion of the downstream feeder must be covered by undelayed tripping zone.

A similar configuration is also employed for back-up protection of generator-unit transformer combinations. In this case the distance protection is connected to the current-transformers in the generator star point, and to the voltage transformers on the generator terminals.

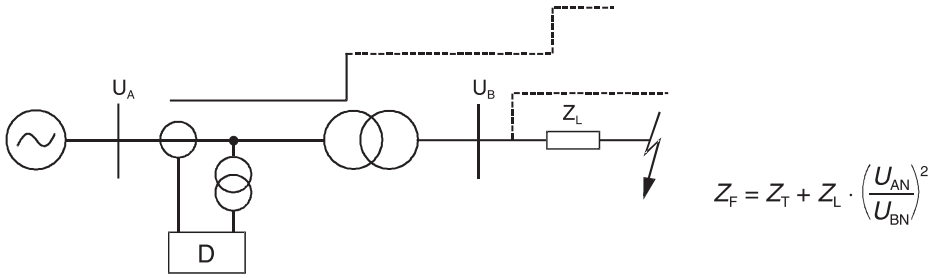
As in general there is a busbar with circuit-breaker and instrument transformers available on the high voltage side, the under-reaching zone is set to cover 80-90% of the transformer and only the back-up zones reach through the transformer.

#### *Reach of the impedance zones on downstream feeders*

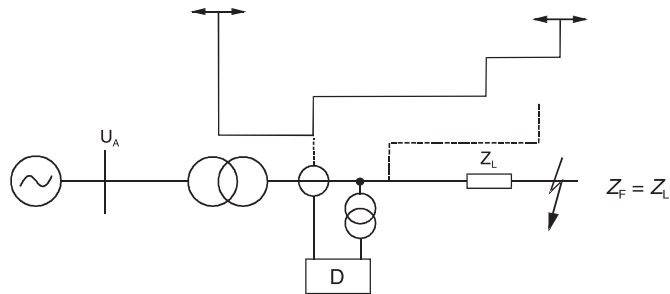
When the distance protection is set to reach through transformers it must be noted that the short-circuit impedance of the transformer can be large in comparison to the impedance of the downstream line. This is especially true when the transformer rating is not very large and the downstream line is short. In this case a normal under-reach setting of 90% will only cover a very small portion of the downstream line. Figure 3.126 provides a numerical example of this.

The variation of the transformation ratio must be observed in transformers that incorporate tap changers. A more or less exact distance measurement is not possible in this case, as the fault impedance varies with the square of  $w_A/w_B$ .

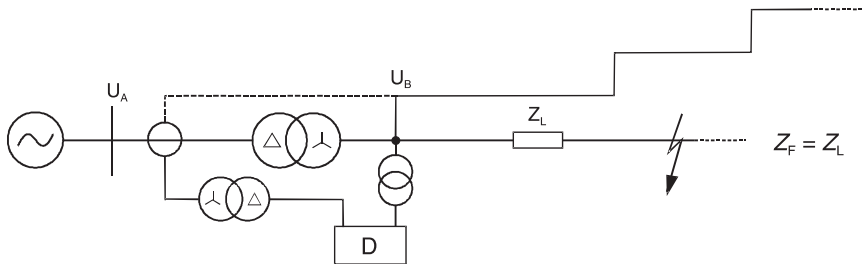
An adaptation of the instrument transformer ratio is too complex, and an adaptation by changing over parameter sets in numerical relays should also only be regarded as a theoretical solution.



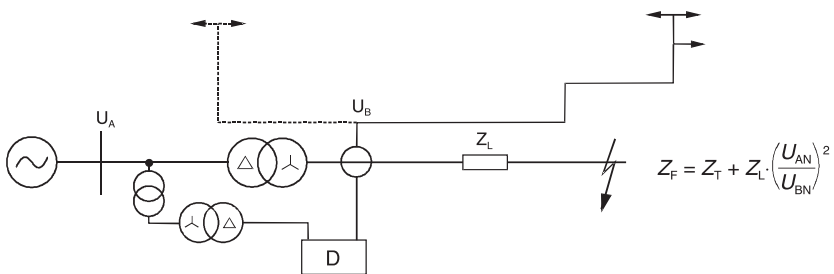
a) CT and VT on the LV-winding



b) CT and VT on the HV-winding

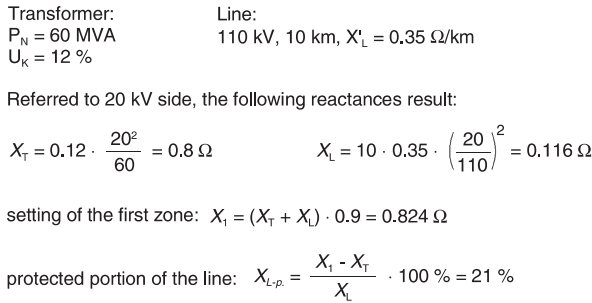


c) CT on the LV-winding, VT on the HV-winding



d) CT on the HV-winding, VT on the LV-winding

**Figure 3.125** Distance protection on transformers, possible termination



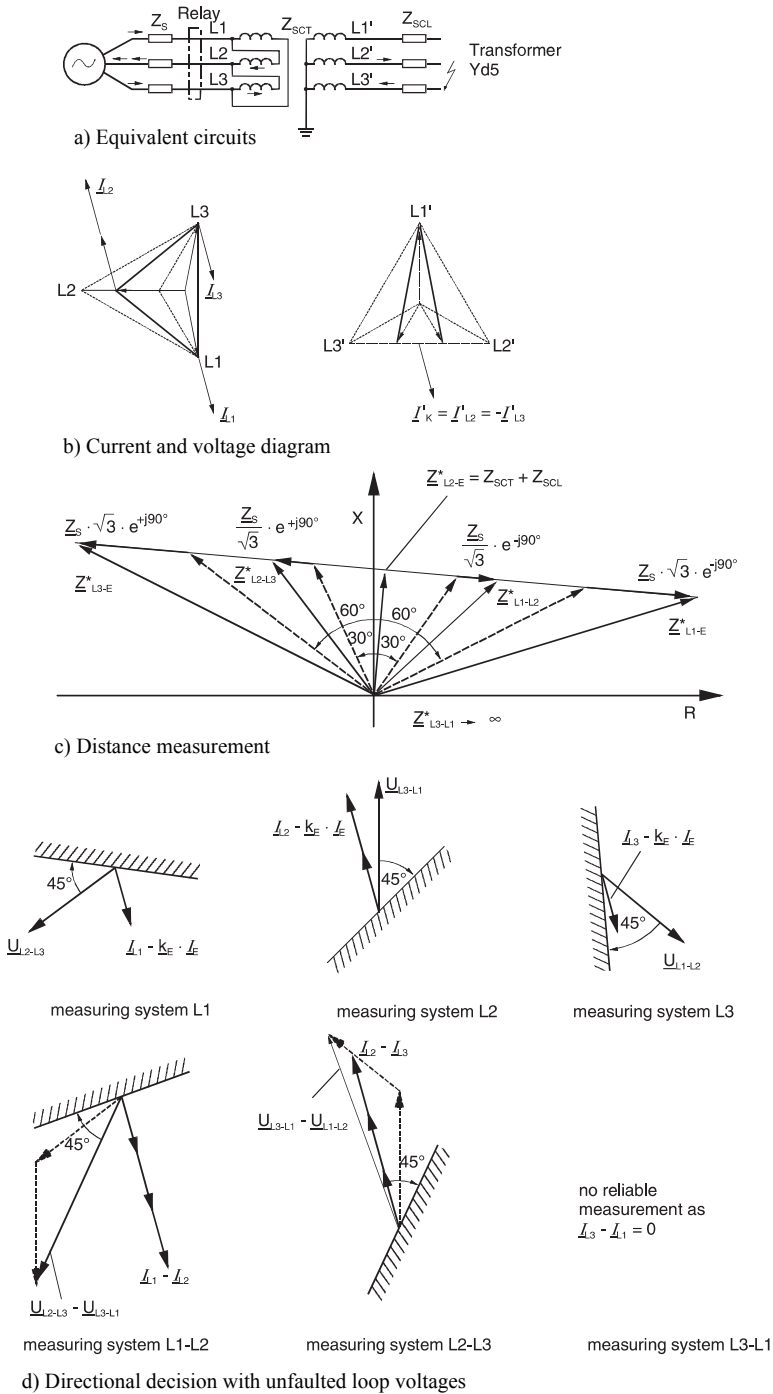


Figure 3.127

Distance measurement through star/delta transformers: two-phase fault, fault on the star side, relay on the delta side



Two phase-phase distance measuring loops (in this case L1-L2 and L2-L3) will in any event detect the fault if the zone reach in R-direction is set greater than  $Z_{SC}/2 + Z_S/\sqrt{3}$ <sup>1</sup>.

In the 7SA6 and 7SA522 relays, the phase-earth loop with correct impedance data will be selected when impedance starting is configured. The reason for this is the integrated impedance comparison, which in any event recognises the smallest fault impedance.

In the case of voltage controlled overcurrent starting ( $U<$ ,  $I>$ ) only the phase-phase loops are measured, as no criterion (neither  $I_E>$  nor  $U_E>$ ) for the release of phase-earth loops is satisfied. Only in the special case, where single-phase starting in the phase with double the short-circuit current flowing occurs, the phase-earth loop with correct impedance data may be selected. The parameter 1630A in the 7SA6 must then additionally be set to phase-earth measurement (“ $I_E$ -release” in conventional relays).

In the event of a single-phase short-circuit on the star side, the fault current distribution of a two-phase fault appears on the delta side (figure 3.128).

Correspondingly, the smallest impedance appears in a phase-phase loop. The other loop impedances again appear on a line perpendicular to this, i.e. all loops again measure a reactance of similar magnitude. In this case, the impedance is seen too far away by an amount of  $0.5 \cdot (Z_{OT} + Z_{OL})$ .

This is understandable, as the zero-sequence system is not converted by the star/delta transformer. The reach is therefore drastically reduced in this case.

If a complete network is connected to the high voltage side, the zero-sequence impedance of this network must be considered. Not only the own transformer zero-sequence impedance is decisive for the measured fault impedance, but rather the zero-sequence impedance of the entire network constellation.

In practice the reduced reach on earth-faults must be accepted.

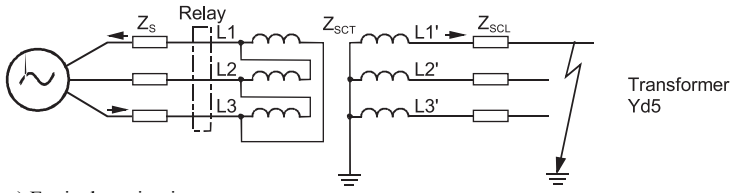
### *Directional decision*

The directional decision with faulted loop voltages, in any event returns a correct result for the loop with the accurate impedance. In the extreme, other loops may return the opposite direction. As shown in figures 3.127c and 3.128c, the fault loop in the outside left portion of the second quadrant does not fall within the forward direction with a 45° characteristic. When unfaulted loop voltages are used, the conditions shown in figures 3.127d and 3.128d result. The measuring principle and selection of unfaulted loop voltages are described in paragraph 3.3.

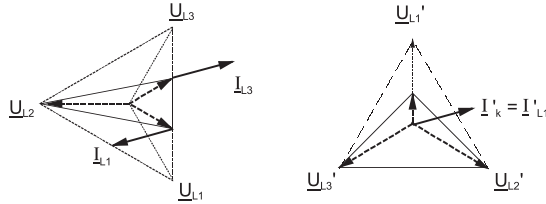
For the examples, a 45° characteristic was assumed. Therefore, the simple rule, stating that the directional characteristic lags the applicable selected unfaulted loop voltage by 45°, may be used to construct the drawing. The composed measuring current (e.g.  $I_{L1} - I_{L2}$ ) must then appear in the non-shaded forward range.

---

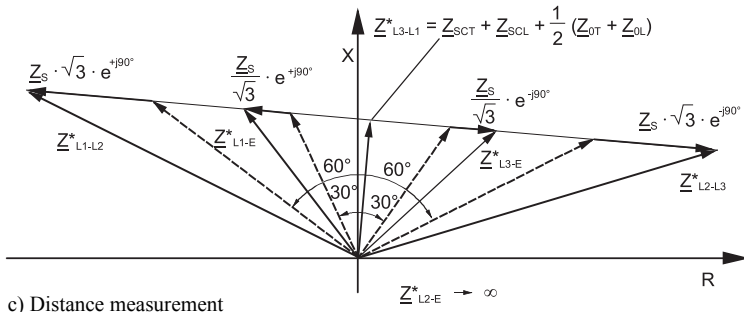
<sup>1</sup> Strictly speaking the source impedance of the negative sequence system  $Z_{S2}$  should be implemented in the drawings. In the system (sufficiently remote from the generators) it suffices to set  $Z_{S2}$  approx. equal to  $Z_S$  (positive sequence source impedance).



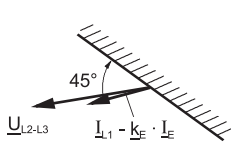
a) Equivalent circuits



b) Current and voltage diagram

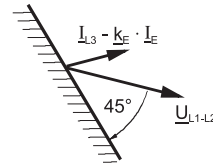


c) Distance measurement

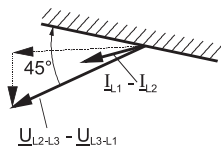


measuring system L1-E

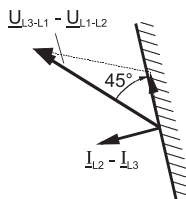
no reliable  
measurement as  
 $\underline{I}_{L3} = 0$



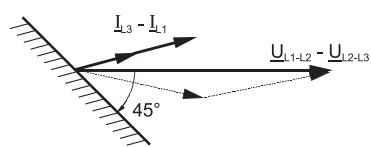
measuring system L3-E



measuring system L1-L2



measuring system L2-L3



measuring system L3-L1

d) Directional decision with unfaulted loop voltages

**Figure 3.128** Distance measurement through star/delta transformers: single-phase fault

With the shown current and voltage distribution all measuring systems return the correct direction. In the worst case condition, when the voltage does not collapse (remote fault), and the current is almost purely inductive (large short-circuit angle) some measuring systems may return incorrect directions. This applies to those measuring systems where the current in the shown examples is already close to the directional characteristic threshold. The fault detection logic therefore should only release the measuring elements which deliver clear directional results.

Using impedance fault detection, the phase selector based on impedance comparison would only release the elements that measure a low fault impedance as stated above.

For the phase to phase fault (figure 3.127) this would be the loop L2-E and for the phase to earth fault (figure 3.128) the loop L3-L1. In both cases a definite directional decision is given.

Using the voltage controlled overcurrent starter ( $I >>$  and  $U <, I >$ ), normally phase to phase loops would be measured. The starters L1-L2 and L2-L3 would pick up in the fault case of figure 3.127. There is a certain probability that the best loop L2-E is selected, but only when starter L2-E picks up alone under the conditions stated above for the distance measurement.

In the fault case of figure 3.128 the phase to phase starter would pick correctly similar to the impedance fault detector.

In any case, the impedance fault detection method should be chosen, because it prefers the true fault loop (lowest impedance) which always guarantees the correct directional decision.

Finally it should be mentioned that the actual characteristic of modern numerical relays is bended and defines each restricted forward and reverse ranges (figure 3.129). This provides addition security for directional discrimination.

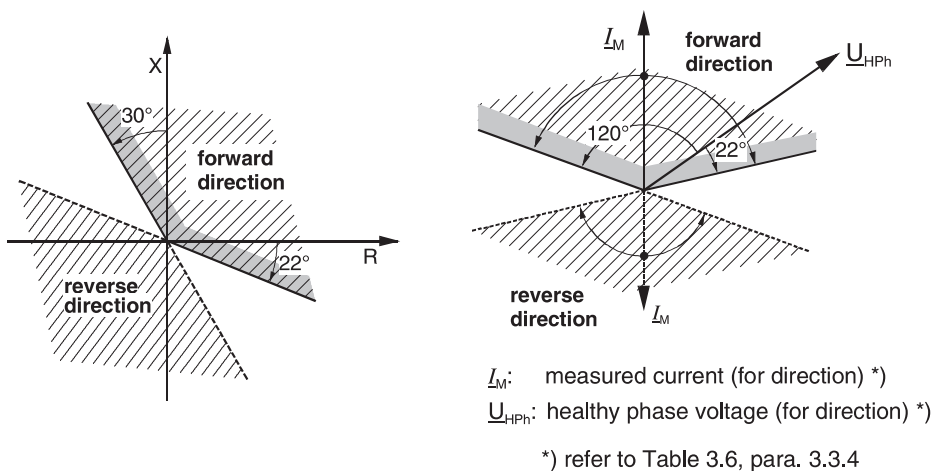


**Figure 3.129** Directional characteristic of modern distance relay (7SA6)

*Grading through star/delta transformers: Summary*

The grading of distance zones through star/delta transformers can only be recommended with the numerical relays 7SA6 and 7SA522, which encompass multiple loop measurement and intelligent loop selection. The directional decision is always correct. With the distance measurement however an under-reach during earth-faults arises which must be tolerated.

The single-system distance protection (earlier relay 7SA511) only has limited suitability, due to the set selection of one measured loop. During two-phase faults, a three phase over-current starting may cause by chance unfavourable loop selection, leading to an under-function of the distance zones, or an incorrect trip decision with the directional time delayed fault detection may result.

**Instrument transformers on the high voltage side (figure 3.125b)**

All fault types on the line return in this case correct impedance measurements.

The zone reaches in a station with outgoing lines must be graded against the zones of the relays on these outgoing lines. This provides a back-up protection for the busbar and the outgoing lines. Additionally, one undelayed zone can be set in reverse, reaching into the transformer.

**Current-transformer on the low voltage side, voltage transformer on the high voltage side (figure 3.125c).**

The advantage of this configuration compared to that shown in figure 3.125a is that during faults on the line, only the line impedance is measured, the transformer impedance is excluded. This is especially an advantage on short lines or cables. For the protection settings, the transformation ratio of the transformer must be allowed for. In the case of star/delta transformers, the current must be adapted according to the vector group of the transformer by means of interposing CTs. Alternatively, the main CTs in the example shown in figure 3.125c may be connected in delta.

The lay-out for the connection of the interposing CTs for vector group correction is shown in figure 3.130.

The vector group of the interposing CT must be selected such that the phase rotation introduced by the transformer is reversed. To check the compensation of the circuit, it is simplest to use the “arrow-method”, as typically used for example with transformer differential protection.

For the conversion of the arrows, it must be noted that the currents on the delta side are weighted by a factor  $1/\sqrt{3}$  in relation to a voltage transformation of 1 : 1. This is due to the induction law ( $U_1/w_1 = U_2/w_2$ ) and the flux law ( $I_1 \cdot w_1 = I_2 \cdot w_2$ ).

The earth-current on the star side cannot be realised with this method, as the zero-sequence system is missing on the delta side of the transformer. It could however be measured by a current-transformer in the transformer neutral and connected to the relay.

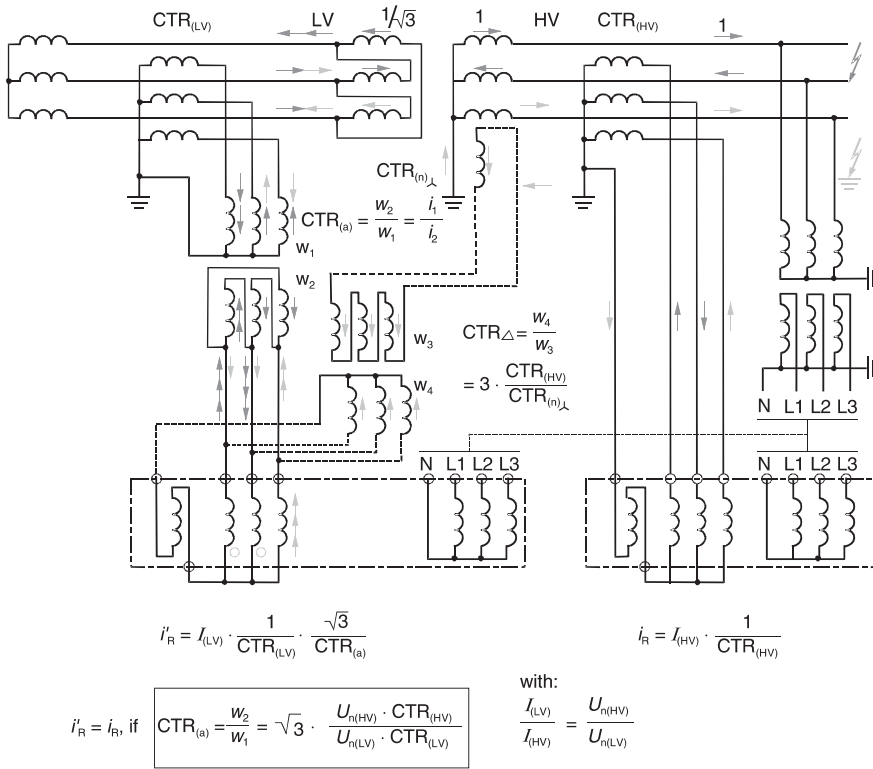


**Figure 3.130**

Lay-out of the interposing current and voltage transformers for accurate impedance measurement

In this way, earth-faults in earthed systems can also be “seen” correctly by the distance relay.

The transformer itself lies within the first zone, although with limitations. During a fault in the transformer, the relay measures the current from the left-hand in-feed, while the voltage on the relay is determined by the current from the right-hand side, producing a voltage drop on the high voltage side short-circuit reactance of the transformer.

The voltage-drop is relatively large in the case of a transformer fault close to the low voltage terminals, when a large short-circuit current flows from the high voltage side ( $U_{SC} = I_{SCB} \cdot Z_T$ ). Thereby the measured impedance ( $Z_{SC} = U_{SC} / I_{SCA}$ ) becomes larger than the transformer short-circuit impedance when  $I_{SCA} < I_{SCB}$ .

If the first distance zone only has a short reach beyond the transformer because the adjacent line is short, it may happen that the measured impedance is outside the zone reach.

This configuration therefore does not provide a 100% reliable protection for the transformer.

### **Voltage-transformers on the low voltage side, current transformers on the high voltage side (figure 3.125d)**

To clarify this configuration, the following basic rule for distance protection must be noted:

Rule:

- The location of the CT determines the origin of the directional decision.
- For the distance measurement, the location of the voltage transformer is always decisive.

In this case, transformer faults are always recognised as being reverse, while the measured impedance must be considered in a similar manner as in the previous case. During a fault on the line, the transformer short-circuit impedance is measured. With star/delta transformers, an additional interposing voltage transformer for compensation of the vector group is required. Nevertheless, it is not possible to measure the distance during earth-faults correctly, because the voltage of the zero-sequence system is not transformed.

### **Grading through auto-transformers**

Large auto-transformers are applied as grid coupling transformers.

In many cases distance relays are used at these big units as main and back-up protection. Generally a non-delayed underreaching zone is graded into the transformer. An additional overreaching zone is graded through the transformer with time delay to ensure selectivity with the grid protection on the other side of the transformer.

The grading of these distance zones has to consider that the zero-sequence impedance of an auto-transformer with grounded neutral can be very low and that setting of a negative residual compensation factor may be necessary to avoid zone overreach in case of earth faults in the grid behind the transformer.

The same is valid for large star-delta-star transformers with neutral grounding at both sides as their short-circuit behavior is similar to that of auto-transformers.

Also the distance back-up zones of relays on the in-feeding lines must be considered as they must also not reach through the transformers to avoid false tripping and system split-up.

The equivalent sequence networks of the considered fault case are shown in figure 3.131 [1-9]

The shown transformer impedances have the following meaning:

- $Z_{T-p-s}$  is the positive sequence short-circuit impedance primary to secondary.
- $Z_{0T-p}$ ,  $Z_{0T-s}$  and  $Z_{0T-t}$  are the star impedances obtained by delta-star transformation from the triangular zero-sequence short-circuit impedances (refer to the below calculation example).

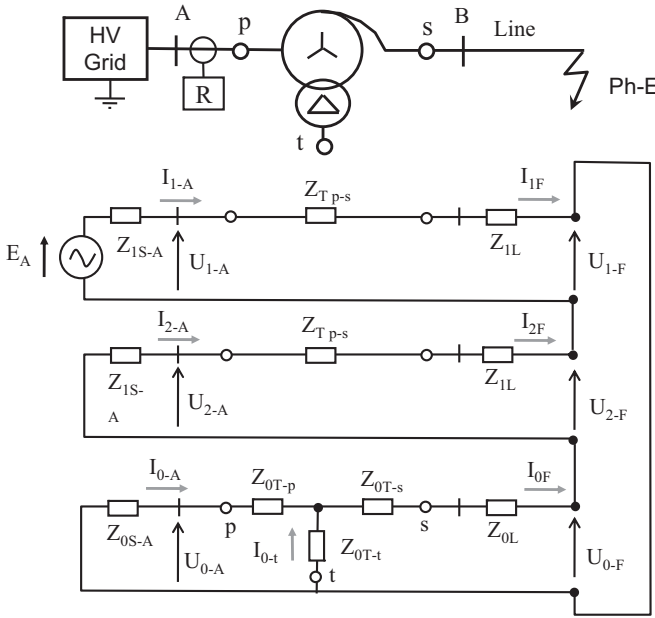


**Figure 3.131** Distance measurement through auto-transformer, equivalent sequence networks

Considering the equivalent sequence networks of figure 3.131, we can develop the following set of equations:

$$\underline{U}_{1A} = \underline{I}_{1A} \cdot (\underline{Z}_{T-p-s} + \underline{Z}_{1L}) + \underline{U}_{1F} \quad (3-129)$$

$$\underline{U}_{2A} = \underline{I}_{2A} \cdot (\underline{Z}_{T-p-s} + \underline{Z}_{1L}) + \underline{U}_{21F} \quad (3-130)$$

$$\underline{U}_{0A} = \underline{I}_{0A} \cdot \underline{Z}_{T-p} + \underline{I}_{0F} \cdot (\underline{Z}_{0T-s} + \underline{Z}_{0L}) + \underline{U}_{0F} \quad (3-131)$$

$$\underline{I}_{0A} \cdot (\underline{Z}_{0S-A} + \underline{Z}_{0T-p}) - \underline{I}_{0-t} \cdot \underline{Z}_{0T-t} = 0 \quad (3-132)$$

$$\underline{I}_{0F} = \underline{I}_{0-A} + \underline{I}_{0-t} \quad (3-133)$$

$$\underline{U}_{L1-A} = \underline{U}_{1A} + \underline{U}_{2A} + \underline{U}_{0A} \quad (3-134)$$

$$\underline{I}_{L1-A} = \underline{I}_{1A} + \underline{I}_{2A} + \underline{I}_{0A} \quad (3-135)$$

$$-\underline{I}_{E-A}/3 = \underline{I}_{0A} \quad (3-136)$$

We further define the apparent zero-sequence impedance (source in A + transformer + line) as:

$$\underline{Z}_{0TL} = \underline{Z}_{T-p-s} \cdot \left[ \underline{I}_{L1-A} - \underline{I}_{E-A} \cdot \frac{(\underline{Z}_{0TL} - (\underline{Z}_{T-p-s} + \underline{Z}_{1L}))}{3 \cdot \underline{Z}_{T-p-s}} \right] \quad (3-137)$$

The solution of the equation system (3-129) to (3-137) delivers the voltage at the relay location in A:

$$\underline{U}_{L1-A} = \underline{Z}_{0T-p} + \frac{(\underline{Z}_{0T-s} + \underline{Z}_{0L}) \cdot (\underline{Z}_{0S-A} + \underline{Z}_{0T-p} + \underline{Z}_{0T-t})}{\underline{Z}_{0T-t}} \quad (3-138)$$

The relay measures the phase-to-earth fault loop according to the following formula:

$$\underline{Z}_{L1-A} = \frac{\underline{U}_{L1-A}}{\underline{I}_{L1-A} - \underline{k}_E \cdot \underline{I}_{E-A}} \quad (3-139)$$

We finally get the measured impedance for single phase to earth through faults:

$$\underline{Z}_{L1-A} = \underline{Z}_{T-p-s} \cdot \frac{\left[ \underline{I}_{L1-A} - \underline{I}_{E-A} \cdot \frac{(\underline{Z}_{0TL} - (\underline{Z}_{T-p-s} + \underline{Z}_{1L}))}{3 \cdot \underline{Z}_{T-p-s}} \right]}{\underline{I}_{L1-A} - \underline{k}_E \cdot \underline{I}_{E-A}} \quad (3-140)$$

We now set the  $\underline{k}_E$  factor so that the distance protection measures the transformer positive sequence impedance  $\underline{Z}_{T-p-s}$  for a phase to earth fault at the terminals of the transformer secondary side:

$$\underline{k}_E = \frac{(\underline{Z}_{0TL} - (\underline{Z}_{T-p-s} + \underline{Z}_{1L}))}{3 \cdot \underline{Z}_{T-p-s}} \quad (3-141)$$

In this way we ensure that the distance protection measures the same impedance for phase-to-phase and phase-to-ground faults through the auto-transformer to the end of the line.

Please note that  $\underline{Z}_{0TL}$  depends on the source impedance. This means that the setting must be checked for the possible range of the infeeding short-circuit power.

#### Calculation example

Given:

Auto-transformer: 400/230/63 kV

	p-s	s-t	t-p
Rated apparent power $S_n$	500 MVA	75 MVA	75 MVA
Short-circuit voltage $u_T$	13.43%	15%	6.54%
$Z_0/Z_1$	0.90	0.95	0.90

Infeeding Grid:  $SCC'' = 20$  GVA,  $Z_0/Z_1 = 1$

Task:

Determine the residual compensation factor for the distance relay on the 400 kV side so that the underreaching distance zone does not overreach the transformer.



Solution:

At first we calculate the equivalent impedances [1-9].

The resistive part of the grid and transformer impedances is very small and can be neglected in this example.

Source impedance:

$$Z_{IS-A} = \frac{1.1 \cdot U_n^2}{SCC''} = \frac{1.1 \cdot 400^2}{20,000} = 8.8 \, \Omega \quad \text{and}$$

Impedances of the auto-transformer:

$$Z_{p-s} = \frac{u_{p-s}}{100\%} \cdot \frac{U_n^2}{S_{p-s}} = \frac{13.43}{100} \cdot \frac{400^2}{500} = 43 \, \Omega \quad \text{and} \quad Z_{0-p-s} = Z_{p-s} \cdot \left( \frac{Z_0}{Z_1} \right)_{p-s} = 38.7 \, \Omega$$

$$Z_{s-t} = \frac{u_{s-t}}{100\%} \cdot \frac{U_n^2}{S_{s-t}} = \frac{15.0}{100} \cdot \frac{400^2}{75} = 320 \, \Omega \quad \text{and} \quad Z_{0-s-t} = Z_{s-t} \cdot \left( \frac{Z_0}{Z_1} \right)_{s-t} = 304 \, \Omega$$

$$Z_{t-p} = \frac{u_{t-p}}{100\%} \cdot \frac{U_n^2}{S_{t-p}} = \frac{6.54}{100} \cdot \frac{400^2}{75} = 140 \, \Omega \quad \text{and} \quad Z_{0-t-p} = Z_{t-p} \cdot \left( \frac{Z_0}{Z_1} \right)_{t-p} = 133 \, \Omega$$

The delta -star transformation delivers the corresponding star impedances:

$$Z_{0-p} = \frac{1}{2} \cdot (Z_{0-p-s} + Z_{0-t-p} - Z_{0-s-t}) = \frac{1}{2} \cdot (38.7 + 133 - 304) = -66.15 \, \Omega$$

$$Z_{0-s} = \frac{1}{2} \cdot (Z_{0-s-t} + Z_{0-p-s} - Z_{0-t-p}) = \frac{1}{2} \cdot (304 + 38.7 - 133) = 104.85 \, \Omega$$

$$Z_{0-t} = \frac{1}{2} \cdot (Z_{0-t-p} + Z_{0-s-t} - Z_{0-p-s}) = \frac{1}{2} \cdot (133 + 304 - 38.7) = 199.15 \, \Omega$$

The apparent zero-sequence impedance (source in A + transformer + line) results from equation (3-137):

$$Z_{0-TL} = -66.15 + \frac{104.85 \cdot (8.8 - 66.15 + 199.15)}{199.15} = 8.5 \, \Omega$$

According to equation (3-141), the following residual compensation factor must be set:

$$k_E = \frac{8.5 - 38.7}{3 \cdot 38.7} = -0.26 \angle 0^\circ \quad \text{or} \quad \frac{R_E}{R_L} = \frac{X_E}{X_L} = -0.26$$

We see that a negative compensation factor is necessary to avoid zone overreach.

The  $k_E$  factor would become a bit smaller with reduced short-circuit power of the infeed ( $k_E = -0.24$  in case of  $SCC'' = 5$  GVA).

### 3.5.5 Non-symmetry of the line

The line impedances are determined by the material and cross-section of the conductors, as well as the geometry of the towers, i.e. the suspension arrangement.

For the zero-sequence impedances, the soil characteristic has an additional influence. The connection of the conductors at the towers causes a natural non-symmetry.

To avoid large negative sequence and earth-currents, long lines (> approx. 40 km) are usually transposed. On short lines, this is often not done to save costs. Instead, it is attempted to compensate differences by using different conductor allocations on series-connected lines.

In this paragraph the influence of this non-symmetry on the measuring-accuracy of the distance protection is estimated, and setting recommendations are derived.

*Transposed lines:*

For the computation of the impedance values of the line ( $R'_1, X'_1$  and  $R'_0, X'_0$ ) one generally assumes a transposed line. These impedance values then correspond to the positive and zero-sequence per kilometre line impedances of a symmetrical line. This implies that there is no coupling between the symmetrical components of a line.

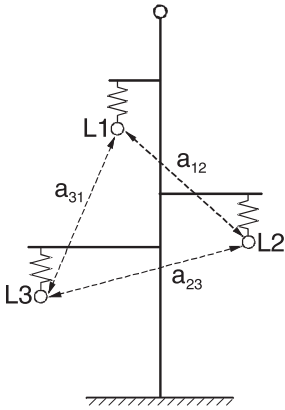


**Figure 3.132**

Tower geometry, single circuit line

For the calculation of the line reactance, the geometrical mean of the conductor spacing is employed in this case (figure 3.132):

$$A = \sqrt[3]{a_{12} \cdot a_{23} \cdot a_{31}} \text{ [m]} \quad (3-142)$$

The impedances are then calculated as follows:

Positive-sequence impedance:

$$Z'_1 = R'_L + j\omega \cdot 10^{-4} \left( 2 \cdot \ln \frac{A}{r} + 0.5\mu_1 \right) \text{ [\Omega/km]} \text{ per conductor} \quad (3-143)$$

Zero-sequence impedance (overhead line without earth-wire)

$$Z'_0 = R'_L + R'_E + j\omega \cdot 10^{-4} \left( 6 \cdot \ln \frac{\delta}{\sqrt[3]{r \cdot A^2}} + 0.5\mu_1 \right) [\Omega/\text{km}] \quad (3-144)$$

Thereby means:

depth of penetration in earth:

$$\delta = 1650 \sqrt{\frac{\rho}{\omega}} [\text{m}] \quad (3-145)$$

earth resistivity:

$$R'_E = \left( \frac{\pi}{2} \cdot \omega \cdot 10^{-4} \right) [\Omega/\text{km}] \quad (3-146)$$

- $a_{12}, a_{23}, a_{31}$  conductor spacing in m
- $A$  geometrical mean of conductor spacing in m
- $r$  conductor radius in m
- $R'_L$  resistance of conductor cable in  $\Omega/\text{km}$
- $R'_E$  resistance of earth in  $\Omega/\text{km}$
- $\delta$  penetration depth in earth (depth of an equivalent return path) in m
- $\rho$  specific earth resistance in  $\Omega \cdot \text{m}$ 
  - 100  $\Omega \cdot \text{m}$  for wet soil
  - 500  $\Omega \cdot \text{m}$  for dry soil
- $\mu_1$  relative permeability (with Cu and Al:  $\mu_1 = 1$ )
- $\omega$  radial frequency  $2\pi f$  in 1/s

For impedance measurement, the loop impedances, which are calculated as follows, are decisive:<sup>1</sup>

Two-phase short-circuit:

$$Z'_{\text{LP(Ph-Ph)}} = 2 \cdot \underline{Z}'_1 = 2 \cdot R'_L + j2 \cdot \omega \cdot 10^{-4} \left( 2 \cdot \ln \frac{A}{r} + 0.5\mu_1 \right) \quad (3-147)$$

Phase-earth short-circuit:

$$\begin{aligned} Z'_{\text{LP(Ph-E)}} &= \underline{Z}'_1 + \underline{Z}'_E = \underline{Z}'_1 + \frac{\underline{Z}'_0 - \underline{Z}'_1}{3} = \\ &= R'_L + R'_E + j\omega \cdot 10^{-4} \left( 2 \cdot \ln \frac{\delta}{r} + 0.5\mu_1 \right) \end{aligned} \quad (3-148)$$

---

<sup>1</sup> With the division of  $Z'_{\text{LP(ph-ph)}}$  by 2 or of  $Z'_{\text{LP(ph-E)}}$  by  $1 + (Z'_E/Z'_L)$ , the result is always the positive sequence impedance  $\underline{Z}'_1$ . Refer to paragraph 3.2.1.

Equation (3-147) indicates that the loop reactance for phase-phase faults is largely determined by the ratio of the conductor spacing to the conductor cable diameter. It can be calculated accurately with the tower geometry.

Equation (3-148) shows that the reactance of the earth loop is influenced by the ratio of the penetration depth in earth  $\delta$  to the conductor cable radius  $r$ . The value of  $\delta$  largely depends on the characteristic of the soil (conductivity  $\rho$ ). This introduces an uncertainty for the calculation of the earth-fault impedance, and may only be determined for a certain region by means of measurement.

### Non-transposed lines

Due to the non-symmetrical geometry of the conductors on the tower, the spacing of the phase-conductors is not equal, and therefore the coupling reactances are not all the same.

Initially the less complicated case of a line without earth-wire is considered.

In figure 3.133, the equivalent circuit for a line section is shown with the per km impedance values.

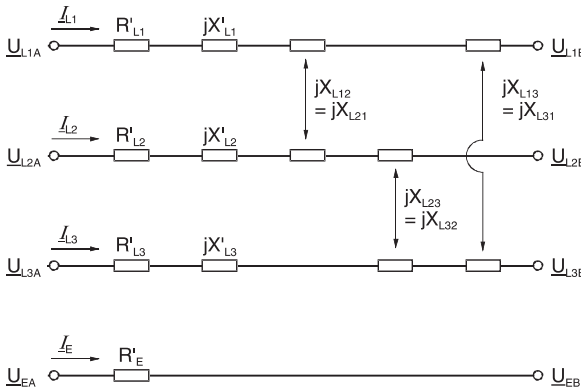


**Figure 3.133**  
Equivalent circuit of  
an overhead line section  
(single circuit  
without earth-wire)

The  $X_L$ -values in this case correspond to the conductor self-impedance with earth return path, so that no reactance is present in the earth path itself.

The coupling reactances  $X_{mn}$  are also defined for the loop with common earth return path.

The following equations can be derived:

$$\Delta U_{L1} = \Delta U_{L1A} - \Delta U_{L1B} = (R'_{L1} + jX'_{L1}) \cdot I_{L1} + jX'_{L12} \cdot I_{L2} + jX'_{L13} \cdot I_{L3} \quad (3-149)$$

$$\Delta U_{L2} = \Delta U_{L2A} - \Delta U_{L2B} = (R'_{L2} + jX'_{L2}) \cdot I_{L2} + jX'_{L21} \cdot I_{L1} + jX'_{L23} \cdot I_{L3} \quad (3-150)$$

$$\Delta U_{L3} = \Delta U_{L3A} - \Delta U_{L3B} = (R'_{L3} + jX'_{L3}) \cdot I_{L3} + jX'_{L32} \cdot I_{L2} + jX'_{L31} \cdot I_{L1} \quad (3-151)$$

$$\Delta U_E = R'_E \cdot I_E \quad (3-152)$$

If similar conductor cables are assumed for the three phases, the following applies:

$$R'_{L1} = R'_{L2} = R'_{L3} = R'_L \text{ and } X'_{L1} = X'_{L2} = X'_{L3} = X'_L$$

this results in:

$$\Delta \underline{U}_{L1} = (R'_L + jX'_L) \cdot \underline{I}_{L1} + jX_{L12} \cdot \underline{I}_{L2} + jX_{L13} \cdot \underline{I}_{L3} + R'_E \cdot \underline{I}_E \quad (3-153)$$

$$\Delta \underline{U}_{L2} = (R'_L + jX'_L) \cdot \underline{I}_{L2} + jX_{L12} \cdot \underline{I}_{L1} + jX_{L23} \cdot \underline{I}_{L3} + R'_E \cdot \underline{I}_E \quad (3-154)$$

$$\Delta \underline{U}_{L3} = (R'_L + jX'_L) \cdot \underline{I}_{L3} + jX_{L23} \cdot \underline{I}_{L2} + jX_{L13} \cdot \underline{I}_{L1} + R'_E \cdot \underline{I}_E \quad (3-155)$$

$$\Delta \underline{U}_E = R'_E \cdot \underline{I}_E \quad (3-156)$$

With this, the reactances are calculated as follows:

$$X'_L = j\omega \cdot 10^{-4} \left( 2 \cdot \ln \frac{\delta}{r} + 0.5\mu_1 \right) \quad (3-157)$$

[Self-reactance of a conductor with earth return path]

$$X'_{L12} = j\omega \cdot 10^{-4} \left( 2 \cdot \ln \frac{\delta}{a_{12}} \right) \quad (3-158)$$

[Coupling reactance of two conductors with joint earth return path (for example  $L_1$ - $L_2$ )]

The individual fault loop impedances can now be calculated. An unloaded line with single-sided in-feed is assumed, i.e. there is no current flowing in the unfaulted phases. This is also true for the case where the fault-current is substantially larger than the load-current.

*Short-circuit L1-L2:*

In this case the following applies:  $\underline{I}_{L1} = -\underline{I}_{L2} = \underline{I}_{SC}$ ,  $\underline{I}_{L3} = 0$  and  $\underline{I}_E = 0$ .

From this we get:

$$\underline{Z}'_{L1-L2} = \frac{\Delta \underline{U}_{L1} - \Delta \underline{U}_{L2}}{\underline{I}_{SC}} = 2 \cdot R'_L + j2 \cdot (X'_L - X'_{L12}) \quad (3-159)$$

Substituting equations (3-157) and (3-158), results in:

$$\underline{Z}'_{L1-L2} = 2 \cdot R'_L + j2\omega \cdot 10^{-4} \left( 2 \cdot \ln \frac{a_{12}}{r} + 0.5\mu_1 \right) \quad (3-160)$$

For the other phase-phase faults,  $a_{23}$  and  $a_{31}$  must correspondingly be used.

*Earth-fault L1-E*

in this case:  $\underline{I}_{L1} = -\underline{I}_E = \underline{I}_{SC}$  und  $\underline{I}_{L2} = \underline{I}_{L3} = 0$ .

From this we get:

$$\underline{Z}'_{L1-E} = \frac{\Delta U_{L1} - \Delta U_E}{I_{SC}} = R'_L + R'_E + jX'_L \quad (3-161)$$

Substituting equation (3-157) results in:

$$\underline{Z}'_{L1-E} = R'_L + R'_E + j10^{-4} \left( 2 \cdot \ln \frac{\delta}{r} + 0.5 \mu_1 \right) \quad (3-162)$$

From (3-160) it is apparent that the spacing of the phase-conductors in the faulted line determines the loop reactance. The smallest conductor spacing results in the smallest reactance and is therefore decisive for the amount of over-reach. The under-reaching zone should be set in accordance with this loop. The amount of under-reach is determined by the loop with the largest conductor spacing. The setting of the over-reaching zone should therefore use this loop as a reference.

On lines without earth-wires all three phase-earth fault systems measure the same impedance, as can be seen in equation (3-162). The conductor arrangement on the tower has no influence! Differences in the height of the conductors above the ground can be neglected, as the equivalent return conductor in earth is at a depth  $\delta$  equal to approx. one kilometre (931 m for  $\rho = 100 \Omega \cdot \text{m}$ ).

The influence of the non-symmetry becomes apparent in the following example:

#### Example

Single-circuit overhead line 110 kV  
 Tower geometry according to figure 3.134  
 Conductor cables: 185/32 mm<sup>2</sup> Al/St.  
 Conductor radius: 0.95 cm =  $9.5 \cdot 10^{-3}$  m  
 $R_L = 0.157 \Omega/\text{km}$   
 Specific earth-resistance  $\rho = 100 \Omega \cdot \text{m}$

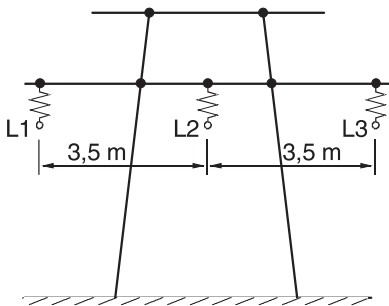


**Figure 3.134**  
 Single-circuit overhead line 110 kV,  
 tower geometry, horizontal conductor arrangement

With these characteristic values, the loop impedances can be calculated:

Transposed line:

From Equation (3-147):

$$\underline{Z}'_{LP(Ph-Ph)} = 2 \cdot \underline{Z}'_1 = 0.314 + j0.803 \, \Omega/\text{km}$$

Non-transposed line:

From equation (3-160):

$$\underline{Z}'_{LP(L1-L2)} = 0.314 + j0.774 \, \Omega/\text{km}$$

$$(\Delta X = -3.6\%)$$

$$\underline{Z}'_{LP(L3-L1)} = 0.314 + j0.861 \, \Omega/\text{km}$$

$$(\Delta X = +7.2\%)$$

In each case  $\Delta X$  is the difference to the calculated transposed value  $\underline{Z}'_{LP(Ph-Ph)}$ , (with the geometrical mean spacing).

#### *Multiple-circuit overhead line without earth-wire*

The set of equations (3-149) to (3-152) may in general be extended to  $n$  conductors and can therefore also be used for multiple-circuit lines without earth-wire. This will be illustrated with the following simple example:

*Example:*

Double-circuit overhead line, 110 kV

Tower geometry according to figure 3.135

Other data as in previous example

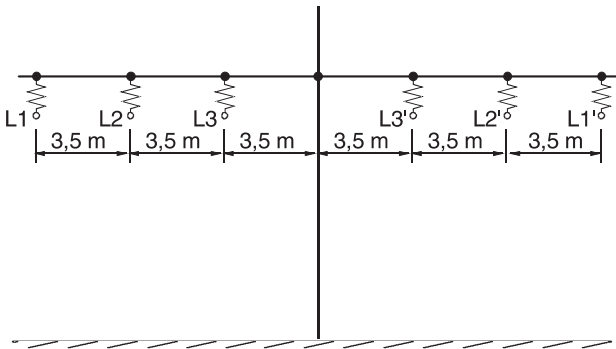


**Figure 3.135**  
Double-circuit line,  
tower geometry

The loop impedance for a L3-L1 fault at the end of the double-circuit overhead line must be determined, and the influence of the parallel line on the distance measurement must be estimated.

Solution:

Only the conductors L1, L3, L1' and L3' carry current.

This can be used to derive the following equations:

$$\Delta \underline{U}_{L1} = (R'_L + jX'_L) \cdot \underline{I}_{L1} + jX'_{L13} \cdot \underline{I}_{L3} + jX'_{L11'} \cdot \underline{I}_{L1'} + jX'_{L13'} \cdot \underline{I}_{L3'} \quad (3-163)$$

$$\Delta \underline{U}_{L3} = (R'_L + jX'_L) \cdot \underline{I}_{L3} + jX'_{L31} \cdot \underline{I}_{L1} + jX'_{L31'} \cdot \underline{I}_{L1'} + jX'_{L33'} \cdot \underline{I}_{L3'} \quad (3-164)$$

Due to the symmetrical arrangement of the conductors in relation to the tower, the currents in the conductors of both lines must be the same. Thereby the following conditions for a two-phase short-circuit apply:

$$\underline{I}_{L3} = \underline{I}_{L3'} = -\underline{I}_{L1} = -\underline{I}_{L1'} = \underline{I}_{SC}$$

Equation (3-163) and (3-164) are therefore simplified as follows:

$$\Delta \underline{U}_{L3} = \underline{I}_{SC}(R'_L + jX'_L - jX'_{L31} + jX'_{L33'} - jX'_{L31'}) \quad (3-165)$$

$$\Delta \underline{U}_{L1} = \underline{I}_{SC}(-R'_L - jX'_L + jX'_{L13} + jX'_{L13'} - jX'_{L11'}) \quad (3-166)$$

$$\underline{Z}'_{L(L3-L1)P} = 2 \cdot R'_L + j(2X'_L - X'_{L31} - X'_{L13} + \underbrace{X'_{L33'} + X'_{L11'} - X'_{L31'} - X'_{L13'}}_{\text{Influence of the parallel line}}) \quad (3-167)$$

By substitution of (3-157) and (3-158) in (3-167) the following is obtained:

$$\underline{Z}'_{L(L3-L1)P} = 2 \cdot R'_L + j2\omega 10^{-4} \left[ 2 \cdot \ln \left( \frac{a_{31}}{r} \cdot \sqrt{\frac{a_{13'} \cdot a_{31'}}{a_{11'} \cdot a_{33'}}} \right) + 0.5 \right] \quad (3-168)$$

Influence of the parallel line

The impedance of the circuit 1 conductor loop is as follows:

$$\underline{Z}'_{LP(L3-L1)P} = \frac{\Delta \underline{U}_{L3} - \Delta \underline{U}_{L1}}{\underline{I}_{SC}} \quad (3-169)$$

and in numbers:

$$\underline{Z}'_{LP(L3-L1)P} = 0.314 + j0.879 \, \Omega/\text{km}$$

In comparison to the single-circuit line ( $j0.861 \, \Omega/\text{km}$ ), the reactance has increased by 2.1%. In comparison to the reactance calculated for the transposed line ( $j0.806 \, \Omega/\text{km}$ ), there is now a total difference of +9.9%.

On the two other loops, the influence of the parallel line is substantially smaller (< 0.5%).

The corresponding worst case two-phase short-circuit without earth may be determined with equation (3-168).

A similar procedure can be used for the phase-earth faults.



*Conductors with earth-wire*

In this case an additional magnetic coupling of the conductors with the earth-wire exists (figure 3.136).

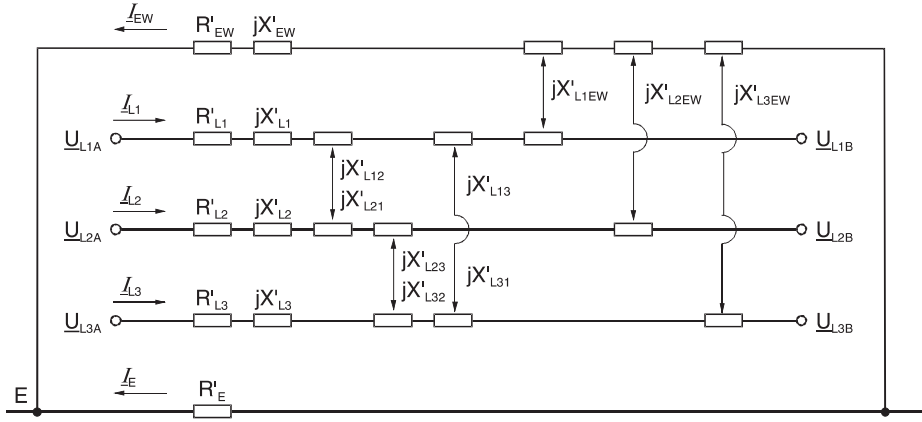


**Figure 3.136** Equivalent circuit of an overhead line section (single-circuit with earth wire)

The set of equations (3-149) to (3-152) must be extended correspondingly. We get as result (3-170) to (3-172):

$$\begin{aligned} \Delta U_{L1} = U_{L1A} - U_{L1B} = & (R'_{L1} + jX'_{L1}) \cdot I_{L1} + \\ & + jX'_{L12} \cdot I_{L2} + jX'_{L13} \cdot I_{L3} - jX'_{L1EW} \cdot I_{EW} + R'_E \cdot I_E \end{aligned} \quad (3-170)$$

$$\begin{aligned} \Delta U_{L2} = U_{L2A} - U_{L2B} = & (R'_{L2} + jX'_{L2}) \cdot I_{L2} + \\ & + jX'_{L23} \cdot I_{L3} + jX'_{L21} \cdot I_{L1} - jX'_{L2EW} \cdot I_{EW} + R'_E \cdot I_E \end{aligned} \quad (3-171)$$

$$\begin{aligned} \Delta U_{L3} = U_{L3A} - U_{L3B} = & (R'_{L3} + jX'_{L3}) \cdot I_{L3} + \\ & + jX'_{L31} \cdot I_{L1} + jX'_{L32} \cdot I_{L2} - jX'_{L3EW} \cdot I_{EW} + R'_E \cdot I_E \end{aligned} \quad (3-172)$$

with the relationships:

$$I_E + I_{EW} = I_{L1} + I_{L2} + I_{L3} \quad (3-173)$$

and

$$\begin{aligned} I_{EW} = & \frac{R'_E + jX'_{L1EW}}{R'_E + R'_{EW} + jX'_{EW}} \cdot I_{L1} + \frac{R'_E + jX'_{L2EW}}{R'_E + R'_{EW} + jX'_{EW}} \cdot I_{L2} + \\ & + \frac{R'_E + jX'_{L3EW}}{R'_E + R'_{EW} + jX'_{EW}} \cdot I_{L3} \end{aligned} \quad (3-174)$$

the equations (3-170) to (3-172) can be changed to:

$$\Delta \underline{U}_{L1} = \underline{Z}'_{L11} \cdot \underline{I}_{L1} + \underline{Z}'_{L12} \cdot \underline{I}_{L2} + \underline{Z}'_{L13} \cdot \underline{I}_{L3} \quad (3-175)$$

$$\Delta \underline{U}_{L2} = \underline{Z}'_{L21} \cdot \underline{I}_{L1} + \underline{Z}'_{L22} \cdot \underline{I}_{L2} + \underline{Z}'_{L23} \cdot \underline{I}_{L3} \quad (3-176)$$

$$\Delta \underline{U}_{L3} = \underline{Z}'_{L31} \cdot \underline{I}_{L1} + \underline{Z}'_{L32} \cdot \underline{I}_{L2} + \underline{Z}'_{L33} \cdot \underline{I}_{L3} \quad (3-177)$$

Impedances are defined as follows:

$$\underline{Z}'_{L11} = R'_E + R'_{L1} + jX'_{L1} - \frac{(R'_E + jX'_{L1EW})^2}{R'_E + R'_{EW} + jX'_{EW}} \quad (3-178)$$

$$\underline{Z}'_{L12} = \underline{Z}'_{L21} = R'_E + jX'_{L12} - \frac{(R'_E + jX'_{L1EW})(R'_E + jX'_{L2EW})}{R'_E + R'_{EW} + jX'_{EW}} \quad (3-179)$$

The simplified equivalent circuit corresponding to this is shown in figure 3.137.

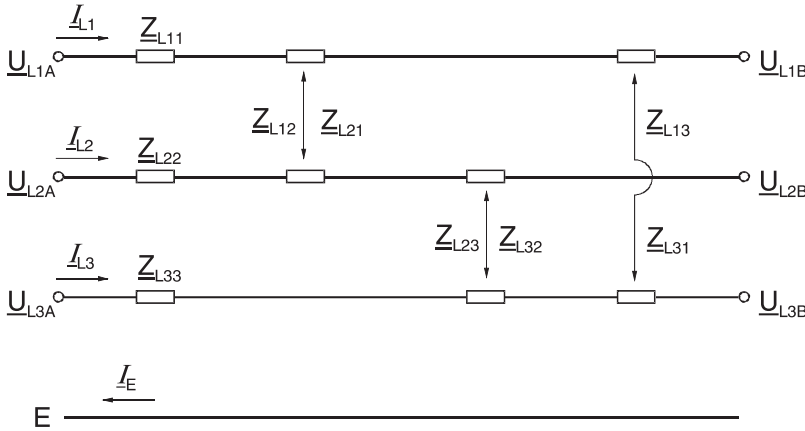


**Figure 3.137** Overhead line, simplified equivalent circuit

The self-reactance of the earth-wire ( $X'_{EW}$ ) is calculated with equation (3-157) in exactly the same way as the conductor cable self-reactance. In un-earthed systems, it is common practice to use steel earth-wires. In this case a relative permeability of  $\mu_1 = 50$  to 100 must be used in equations (3-143), (3-144) and (3-157).

The resistance must also be calculated according to the properties of the material.

For the coupling impedance between the conductor cable and the earth-wire,  $X'_{L1EW}$ ,  $X'_{L2EW}$  and  $X'_{L3EW}$  the equation (3-158) applies, whereby the applicable spacing between each phase-conductor and the earth wire must be used.

The set of equations (3-175) to (3-177) may also be represented in the form of a matrix:

$$\Delta \underline{U} = \begin{bmatrix} \Delta U_{L1} \\ \Delta U_{L2} \\ \Delta U_{L3} \end{bmatrix} = \begin{bmatrix} \underline{Z}'_{L11} & \underline{Z}'_{L12} & \underline{Z}'_{L13} \\ \underline{Z}'_{L21} & \underline{Z}'_{L22} & \underline{Z}'_{L23} \\ \underline{Z}'_{L31} & \underline{Z}'_{L32} & \underline{Z}'_{L33} \end{bmatrix} \cdot \begin{bmatrix} I_{L1} \\ I_{L2} \\ I_{L3} \end{bmatrix} = \underline{Z}'_L \cdot \underline{I} \quad (3-180)$$

$\underline{Z}_L$  in this case represents the longitudinal impedance matrix of the line.

This matrix is often used for computer calculations in this form (figure 3.138). The loop impedances can also be read off directly from the matrix.

*Examples:*

Single-phase earth fault L1-E

For this example, point  $U_{L1B}$  in figure 3.137 must be connected with earth. Therefore only the currents  $I_{L1}$  and  $I_E = -I_{L1}$  flow. The resultant loop impedance is  $\underline{Z}'_{L11} = 0.066 + j0.461$ .

The reactance measured by the distance protection is obtained by division of the imaginary part of  $\underline{Z}'_{L11}$  by  $1 + X_E/X_L$ , where  $X_E/X_L$  corresponds to the residual compensation factor set in the relay.

The impedances of the transposed lines, calculated with equations (3-143) and (3-144) in this case are:

positive-sequence impedance:  $\underline{Z}'_1 = 0.0301 + j0.2537 \Omega/\text{km}$

zero-sequence impedance:  $\underline{Z}'_0 = 0.1360 + j0.9055 \Omega/\text{km}$

This results in:  $X_E/X_L = 0.8564$  and the reactance measured by the relay:

$X'_{L1-E} = 0.461/(1 + 0.8564) = 0.2483 \Omega/\text{km}$ . The difference to the positive sequence reactance  $X'_1$  of the transposed line (0.2537) corresponds to:  $\Delta X' = -2.2\%$ .

Two-phase short-circuit without earth L2-L3

In this case the following applies:

$$I_{L3} = -I_{L2} \text{ and } I_{L1} = 0; U_{L2B} = U_{L3B}.$$

The resulting loop impedance is:

$$\underline{Z}'_{LP(L2-L3)} = \underline{Z}'_{L22} + \underline{Z}'_{L33} - \underline{Z}'_{L23} - \underline{Z}'_{L32} = 0.060 + j0.470 \Omega/\text{km}$$

The reactance measured by the relay in this case corresponds to one-half of the loop impedance:  $X'_{L2-L3} = 0.470/2 = 0.235 \Omega/\text{km}$ .

The difference in relation to  $X'_1$  in this case is:  $\Delta X' = -7.4\%$ .

*Parallel lines with earth-wire(s)*

The loop impedance can be calculated in a similar manner, whereby the coupling impedances between all other conductors and the earth-wire(s) must be taken into account.

**Table 3.7** Measuring error due to non-symmetry of the line (double-circuit line)

Fault type	measured loop	$\Delta X\%$ single-circuit line			$\Delta X\%$ double-circuit line		
single-phase short-circuit:							
L1-E	L1-E	-3.5	...	0.6	-3.5	...	0.6
L2-E	L2-E	1.2	...	-1.5	-1.6	...	-2.1
L3-E	L3-E	1.8	...	-0.5	3.8	...	-0.5
single-phase short-circuit:							
L1-L2	L1-L2	3.4			3.1		
L2-L3	L2-L3	-7.5			-7.7		
L3-L1	L3-L1	3.3			3.3		
three-phase short-circuit							
L1-L2-L3	L1-L2	3.4			2.6		
	L2-L3	-7.5			-7.7		
	L3-L1	3.3			2.8		

For this relatively complex computation, computer programmes are available now.

Table 3.7 shows the calculated measuring error due to the non-symmetry of the line, in relation to the positive sequence impedance of a transposed line [3.36]. The values apply to the 380 kV line shown in figure 3.138.

The loop reactances are determined with equations (3-27) and (3-28).

For the calculation of the phase-earth loops, on the double-circuit line, it is in addition assumed that the parallel line compensation according to equation (3-126) is used, i.e. the measuring errors for the phase-E loops shown in the table are solely due to the non-symmetry of the conductor spacing.

The spread in the phase-earth loop values is caused by varying earthing and in-feed ratios at the two line-ends.

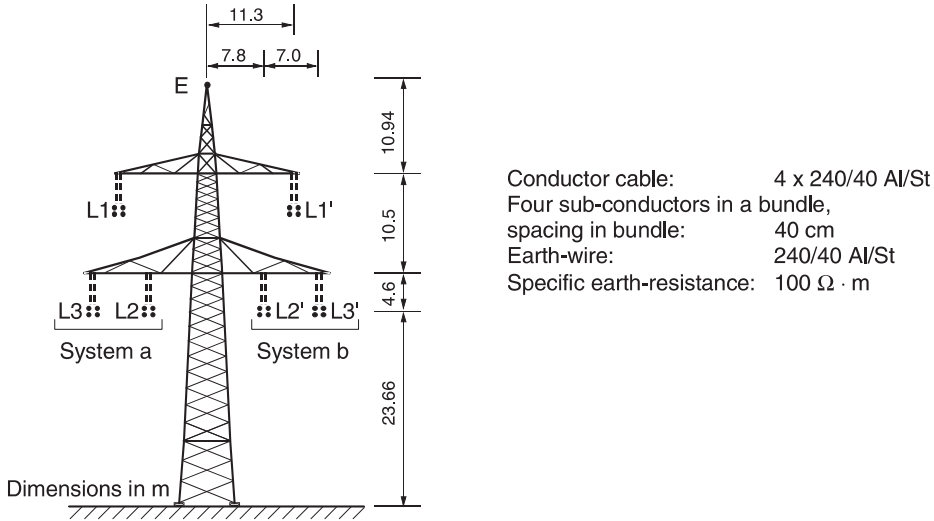
The smallest reactances correspond to the smallest conductor spacing, i.e.

- for the ph-ph loop with the smallest phase-conductor to phase-conductor spacing and
- the ph-E loop with the smallest phase-conductor to earth-wire spacing.

These two loops therefore determine the largest over-reach.

In addition it may be noted that the largest measuring error occurs in the case of faults between phases. The sum of the load-currents in the healthy phases, in the case of non-symmetry of the line, induces an additional voltage in the fault loop. Generally this influence is negligible (< 1%).

On long lines with large power-transfer, or small in-feed capacity (large source-impedance), the load-current may assume a similar magnitude as the fault current. Hereby the influence increases.



$$\underline{Z}'_L = \begin{bmatrix} (0.066 + j0.461) & (0.035 + j0.204) & (0.035 + j0.206) \\ (0.035 + j0.204) & (0.065 + j0.474) & (0.035 + j0.241) \\ (0.035 + j0.206) & (0.035 + j0.241) & (0.065 + j0.478) \end{bmatrix} \frac{\Omega}{\text{km}}$$

**Figure 3.138**

380 kV double-circuit line, tower geometry and longitudinal impedance matrix for the single-circuit line (system b isolated and open circuit)

Additional errors of several percent may occur in the extreme [3.37, 3.38].

#### Phase-current compensation

In theory, the errors introduced by non-symmetry of the line can be completely eliminated. For this, settings must be done on a per-phase basis, as well as a compensation with the phase-currents according to the set of equations (3-175) to (3-177) (healthy phase compensation) [3.37].

In the case of a double-circuit line, the set of equations must be extended by the phase-currents of the parallel line [3.39, 3.40].

Furthermore, the loop measurements on the healthy phases should be blocked, as the risk of an over-function exists here. This phenomenon is similar to the parallel line compensation in the zero-sequence system (refer to paragraph 3.5.3).

As a whole, this would make the distance protection far more complex. The setting and testing would be more unclear.

Compensation with phase-currents is therefore not common in practice. An application for fault location calculation, using stored disturbance record data, is however in the realm of the possible.

*Protection settings on non-transposed lines*

On single-circuit lines, the influence of the non-symmetry is, in comparison to a symmetrical line (triangular conductor spacing), or a transposed line, substantially less than 10%.

With a first zone setting of 85%, the possible amount of over-reach of 7.5% is contained in the security margin of 15%.

With a setting of 90%, the loop with the largest negative error should be used as a reference.

For the over-reach zones, the non-symmetry can be accommodated by a 5% increase of the setting.

In the case of multiple-circuits, the influence must be separately evaluated by means of tower geometry [3.41].

**3.5.6 Distance protection of HV cables**

The characteristic data of cable and overhead lines are significantly different (Refer to Table 3.4 in section 3 and to appendix A.4.4.).

The positive sequence reactance of cables is much smaller due to the small spacing between phase conductors. Therefore the characteristic impedance angle is also much smaller.

For distance relaying, this results in short X-setting and comparatively large R-setting of quadrilateral distance zones to ensure reasonable arc compensation (R/X setting ratios 3 to 5, see section 6.3.2).

In the case of very small characteristic angles below 20 degrees, the X-measurement becomes sensitive to false angles of CTs and VTs and the impedance circle may then be preferred to quadrilateral zone characteristics.

The zero-sequence impedance of cables depends on the material and cross-section of the sheaths and in particular on the sheath bonding and earthing. It is also influenced by parallel running metallic conductors such as parallel cable shields, gas and water pipes or rails.

In case of pipe-type cables, the zero-sequence impedance becomes current dependent due to the non-linear permeability and electromagnetic effects of the steel pipe.

The exact calculation of the cable zero-sequence impedance is therefore difficult and the results are questionable in most cases.

The usual practice is to measure the impedances at the installed cable on site.

*Earth fault relaying*

For cable protection the same protection principles apply as earlier discussed for overhead lines.

The distance relay performance in case of earth faults however requires a basic understanding of the impact of the current return conditions (sheath properties, kind of bonding and earthing).

For detailed studies we would have to consider the phase un-symmetries and calculate with three phase-conductors, three sheaths, optional ground wires and all mutual inductive couplings. This would result in a complex impedance matrix.

For EHV cables with sectionalized and cross-bonded sheaths detailed studies are necessary to determine the apparent zero-sequence impedances [1-9, 3-42].

Nowadays computer programs are used to calculate the impedances from the geometry of the cables.

In the following we neglect the cable un-symmetries and use the positive and zero sequence impedances based on geometric mean values as generally applied for overhead lines (Refer to Appendix A.4.1.).

For short circuit calculations, the cable can then be replaced by two phase-to-earth loop impedances:

- Conductor with earth return  $Z_{0C}$
- Sheath with earth return  $Z_{0S}$

These two loops are coupled by the mutual impedance  $Z_{0M}$ .

Dependent on the return paths we get the following cable zero-sequence impedances:

a) Current return in the sheath only:

$$\underline{Z}_0 = \underline{Z}_{0C} + \underline{Z}_{0S} - 2 \cdot \underline{Z}_{0M} \quad (3-181)$$

b) Current return in the ground only:

$$\underline{Z}_0 = \underline{Z}_{0C} \quad (3-182)$$

c) Current return in the sheath and ground in parallel:

$$\underline{Z}_0 = \underline{Z}_{0C} - \frac{\underline{Z}_{0M}^2}{\underline{Z}_{0S}} \quad (3-183)$$

We take a typical HV- cable to show the calculated zero-sequence impedances for different cable arrangements and sheath earthing.

The structure and data of the chosen cable are shown in figure 3.139.

The cable arrangement itself has only little influence. The zero-sequence impedance however varies significantly dependent on the earthing of the cable sheaths (Table 3.8).

The cases a) and b) correspond to a short-circuit phase to sheath and ground. This kind of fault happens when the cable is damaged by a dig-up or when the fault has burned through the sheath due to slow fault clearance. With the given cable type, the major part of the fault current flows back through the sheath because of the low reduction factor ( $k = 0.2$ ) of the cable. For this reason, the zero-sequence reactance is low.

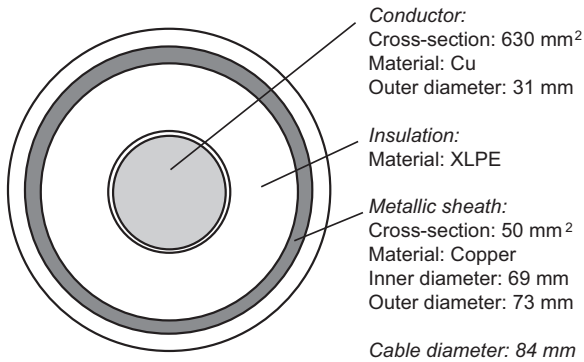


**Figure 3.139** 110 kV XLPE cable

In case c), the cable sheath is earthed only at the local end. The fault occurs directly behind the cable end (fault at the remote busbar) and does not involve the sheath. Therefore the fault current can only flow back through ground. Consequently the effective zero-sequence reactance is much higher similar to values known from overhead lines.

This discontinuity of the zero-sequence impedance is helpful for the distance protection to discriminate between internal and external cable faults.

Please note that a fault at the end of the cable involving the sheath would result in a low zero-sequence reactance as in cases a) and b).

In case d), additional ground continuity conductors (earthed at both sides) are laid between the cables. They care for a low impedance return path of the fault current and result in a low zero-sequence impedance.

#### *Setting of the residual compensation factor*

In the last column of table 3.8 the residual compensation factor  $k_E$  is shown in each case calculated from the corresponding positive and zero-sequence impedance values.

These  $k_E$ -values have to be set at the distance relay to adapt the reach for phase-to-earth faults to the zone setting (based on positive sequence impedances).

The  $k_E$ -factors are complex numbers. Relay setting can be done in phasor quantities (amplitude and angle) or as  $X_E/X_L$  and  $R_E/R_L$  ratios (Refer to section 3.4.1). For cables, the angle of  $k_E$  is normally negative and very large. Small angles only occur when the sheath is not effective and the fault current returns through ground (case c) of table 3.8.

When the cable sheath is earthed at the relay location, the measured impedance increases continuously towards the cable end and selective zone discrimination is possible. Also in the case of a phase to sheath fault (not involving ground) we get nearly equal impedances as given in the cases a) and b) as the major part of the return current flows in the sheath anyway. This however is not generally valid but changes when the sheath cross section is lower or when separate ground wires exist [1-9, 3-42].



**Table 3.8** Cable impedances (50 Hz, soil resistivity: 50  $\Omega\text{m}$ ) dependent on sheath earthing and corresponding residual compensation factors for distance measurement

Case	Arrangement	Sheath Bonding	$R'_1$ $\Omega/\text{km}$	$X'_1$ $\Omega/\text{km}$	$R'_0$ $\Omega/\text{km}$	$X'_0$ $\Omega/\text{km}$	$k_E$
a)			0.031	0.121	0.359	0.129	0.87 $\angle -70.6^\circ$
b)			0.070	0.175	0.365	0.138	0.53 $\angle -75.4^\circ$
c)			0.031	0.190	0.179	1.673	2.59 $\angle +3.6^\circ$
d)	 With ground continuity conductors		0.035	0.183	0.192	0.349	0.70 $\angle -54.2^\circ$

*Calculation example:*

Given:

110 kV XLPE cable according to figure 3.139

Sheath earthed at both ends according to case a) of table 3.8

Zero-sequence impedances (calculated by program):

$$Z_{1C} = 0.031 + j0.121$$

$$Z_{0C} = 0.178 + j1.811$$

$$Z_{0S} = 0.492 + j1.743$$

Task:

A short-circuit occurs phase to sheath (not involving ground).

Which impedance measures the distance relay dependent on the fault location?

Solution:

The equivalent diagram of symmetrical components is shown in figure 3.140.

We get the following set of equations:

$$\begin{aligned} \underline{U}_1 + \underline{U}_2 + \underline{U}_0 &= (\underline{I}_1 + \underline{I}_2) \cdot \underline{Z}_{1C} \cdot x + \underline{I}_0 \cdot \underline{Z}_{0C} \cdot x - \\ &\quad - \underline{I}_{0S-A} \cdot \underline{Z}_{0M} \cdot x + \underline{I}_{0S-B} \cdot \underline{Z}_{0S} \cdot (1-x) \end{aligned} \quad (3-184)$$

$$\underline{I}_{0S-A} + \underline{I}_{0S-B} = \underline{I}_0 \quad (3-185)$$

$$\underline{I}_{0S-A} \cdot \underline{Z}_{0C} \cdot x - \underline{I}_0 \cdot \underline{Z}_{0M} - \underline{I}_{0S-B} \cdot \underline{Z}_{0S} \cdot (1-x) = 0 \quad (3-186)$$

$$\underline{U}_1 + \underline{U}_2 + \underline{U}_0 = \underline{U}_{L1'} \quad (3-187)$$

$$\underline{I}_1 + \underline{I}_2 + \underline{I}_0 = \underline{I}_{L1} \quad (3-188)$$

$$\underline{I}_0 = -\frac{\underline{I}_E}{3} \quad (3-189)$$

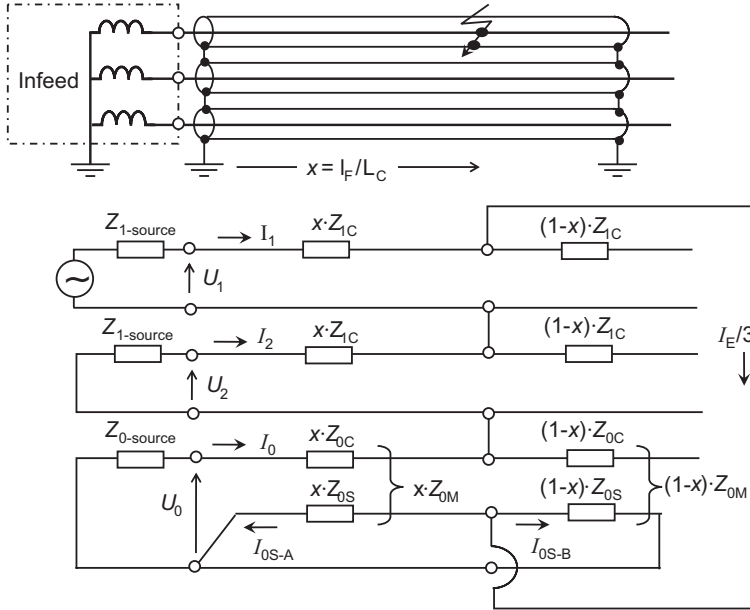


**Figure 3.140** Phase to sheath fault at a cable (sheath grounded at both ends)

Solving the system of equations (3-184) to (3-189) we get the phase to earth voltage at the relay location:

$$\underline{U}_{L1} = \underline{I}_{L1} \cdot \underline{Z}_{1C} \cdot x - \frac{\underline{I}_E}{3} \cdot \left[ \begin{array}{l} \underline{Z}_{0C} \cdot x + \underline{Z}_{0S} \cdot x \cdot (1-x) \\ -2 \cdot \underline{Z}_{0M} \cdot x \cdot (1-x) - \frac{\underline{Z}_{0M}^2}{\underline{Z}_{0S}} \cdot x^2 - \underline{Z}_{1S} \cdot x \end{array} \right] \quad (3-190)$$

The following formula applies to the measurement of the phase L1 to earth loop:

$$\underline{Z}_{L1-E} = \frac{\underline{U}_{L1}}{\underline{I}_{L1} - k_E \cdot \underline{I}_E} \quad (3-191)$$

Inserting the voltage and currents at the relay location, we get

$$\underline{Z}_{L1-E} = \frac{\underline{I}_{L1} \cdot \underline{Z}_{1C} \cdot x - \frac{\underline{I}_E}{3} \cdot \left[ \begin{array}{l} \underline{Z}_{0C} \cdot x + \underline{Z}_{0S} \cdot x \cdot (1-x) \\ -2 \cdot \underline{Z}_{0M} \cdot x \cdot (1-x) - \frac{\underline{Z}_{0M}^2}{\underline{Z}_{0S}} \cdot x^2 - \underline{Z}_{1S} \cdot x \end{array} \right]}{\underline{I}_{L1} - k_E \cdot \underline{I}_E} \quad (3-192)$$

In the case of single infeed, the phase and earth currents have equal magnitude but flow in opposite direction:  $I_{L1} = -I_E$

With this relation we get the following formula for the measured fault impedance:

$$\underline{Z}_{L1-E} = x \cdot \underline{Z}_{1C} \cdot \frac{1 + \frac{1}{3} \cdot \left[ \frac{\underline{Z}_{0C}}{\underline{Z}_{1C}} + \frac{\underline{Z}_{0S}}{\underline{Z}_{1C}} \cdot (1-x) - 2 \cdot \frac{\underline{Z}_{0M}}{\underline{Z}_{1C}} \cdot (1-x) - \frac{\underline{Z}_{0M}^2}{\underline{Z}_{0S} \cdot \underline{Z}_{1C}} \cdot x - 1 \right]}{1 + k_E} \quad (3-193)$$

For a fault at the end of the cable ( $x = 1$ ) the relay must measure  $\underline{Z}_{1C}$ . The  $k_E$  factor must therefore be adapted to

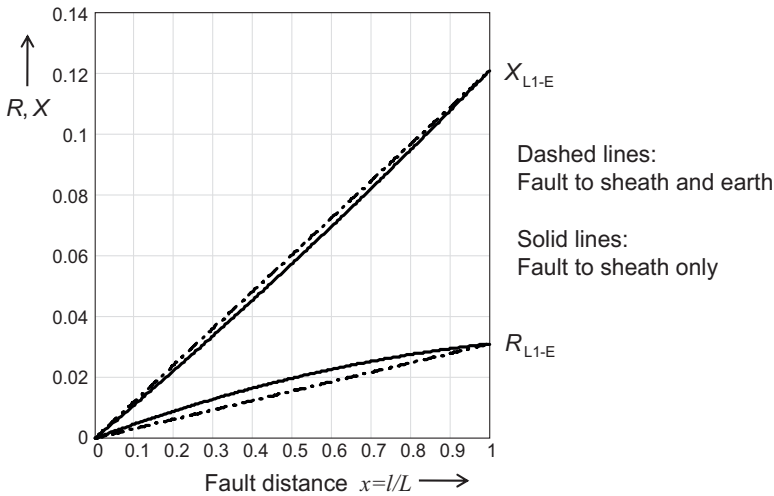
$$k_E = \frac{\left( \underline{Z}_{0C} - \frac{\underline{Z}_{0M}^2}{\underline{Z}_{0S}} - \underline{Z}_{1C} \right)}{3 \cdot \underline{Z}_{1C}} = 0.81 \angle -70.6^\circ \quad (3-194)$$

Figure 3.141 shows the measured fault impedances dependent on the fault location.

For short-circuits to the shield not involving ground, the course of the impedance is not linear but has parabolic shape according to the above formula (3-193). The non-linear course of the measured impedance is of advantage as it improves the zone selectivity of distance measurement.

The impedance course for short-circuits to sheath and ground are added for comparison. It shows a linear course.

The course of the measured impedance is quite different when the cable sheath is not grounded at the local end but only at the remote cable end.



**Figure 3.141** Earth fault on XLPE cable (sheath earthed at both ends), measured impedances dependent on fault location

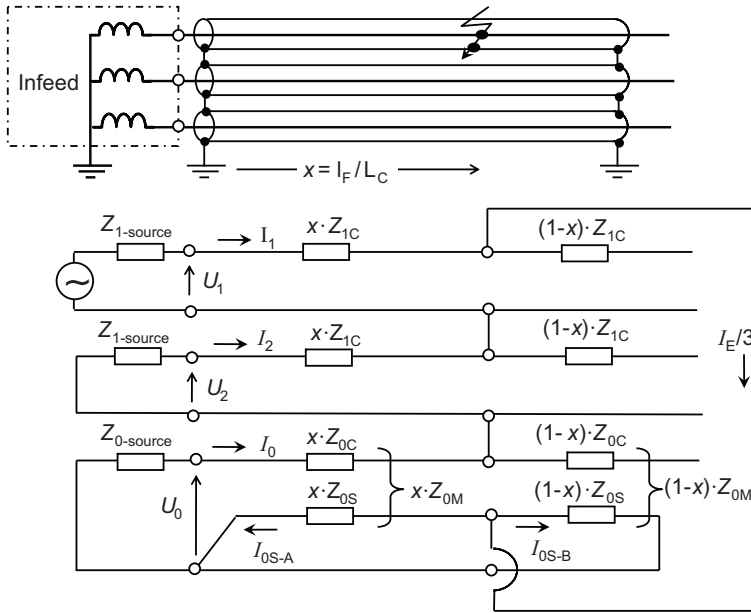


**Figure 3.142** Phase to sheath fault at a cable (sheath grounded at remote end only)

The equivalent diagram of symmetrical components is shown in figure 3.142.

The return path is in this case longer: The current flows from the fault point through the cable sheath to the remote line end and from there back through ground to the infeeding end.

Here we get the following formula for the measured relay impedance:

$$\underline{Z}_{L1-E} = x \cdot \underline{Z}_{1C} \cdot \frac{1 + \frac{1}{3} \cdot \left[ \frac{\underline{Z}_{0C}}{\underline{Z}_{1C}} + \frac{\underline{Z}_{0S}}{\underline{Z}_{1C}} \cdot (1-x) \right]}{1 + \underline{k}_E} \quad (3-195)$$

The following residual compensation factor must be set in this case:

$$\underline{k}_E = \frac{(\underline{Z}_{0C} - \underline{Z}_{1C})}{3 \cdot \underline{Z}_{1C}} = 2.58 \angle +3.6^\circ \quad (3-196)$$

This value corresponds to the data of an overhead transmission line.

The relay measures a high loop impedance (83%  $\underline{Z}_L$ ) already for close-up faults. The course of the measured impedance is then linear from the beginning to the end of the line (figure 3.143). The slope of the reactance course is however very flat and the slope of the resistance course is even negative. Selective fault discrimination by reactance or impedance measurement is in this case not reliable. Underreaching distance zones can therefore not be applied when the sheath is not earthed at the end of the relay location.

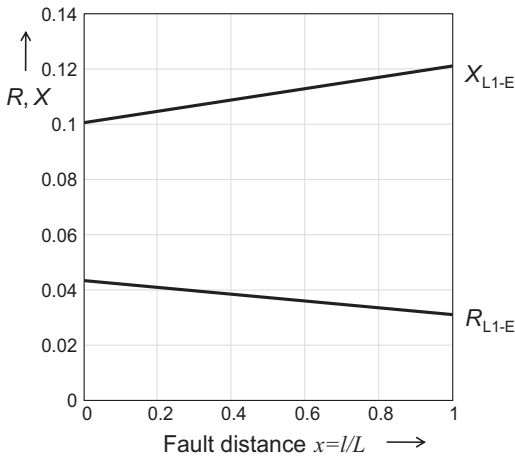


**Figure 3.143** Earth fault on XLPE cable (sheath earthed at remote end only), measured impedances dependent on fault location

### 3.5.7 Series-compensation

The power transfer capacity of long EHV-lines can be increased by means of series capacitor banks. The negative reactance of the capacitors ( $X_C = -1/\omega C$ ) thereby compensates a portion of the longitudinal reactance of the line ( $X_L = 1 \cdot \omega L'$ ), thereby reducing the transmission angle of the line. The capacitor bank can thereby be placed along the line, for example at the mid-point of the line, at one end of the line or split into two halves at each end of the line.

A compensation degree ( $k_C = X_C/X_L$ ) up to approx. 70% is typical.

The series capacitor is protected by a parallel arc-gap against over-voltages (on newer plants, an additional varistor is implemented, which is not considered initially). As

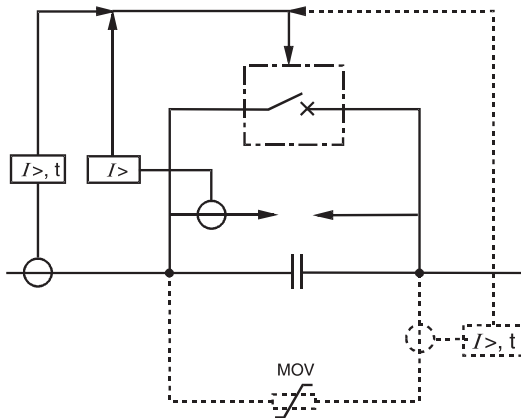


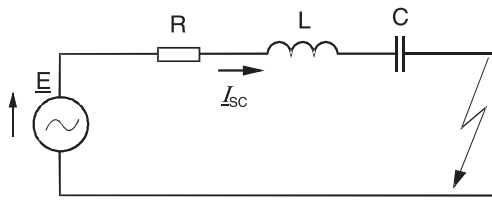
**Figure 3.144** Series-capacitor with protection circuitry (only basic functions shown)

soon as the arc-gap ignites, the capacitor is initially short-circuited by the arc-gap itself, and subsequently by a circuit-breaker (figure 3.144). When current of approx.  $2\text{--}3 \cdot I_N$  flows, the arc-gap ignites, whereby  $I_N$  is the current corresponding to the natural load of the line.

In the case of large short-circuit currents the arc-gap flashes over and short-circuit takes place within half a cycle ( $< 10\text{ ms}$ ).

Following reset of the short-circuit currents, the circuit-breaker is automatically opened after a set time delay (e.g.  $200\text{ ms}$ ), and the capacitor returns to service.

In the case with large short-circuit currents as referred to, the distance protection reacts the same as on a normal, non-compensated line.

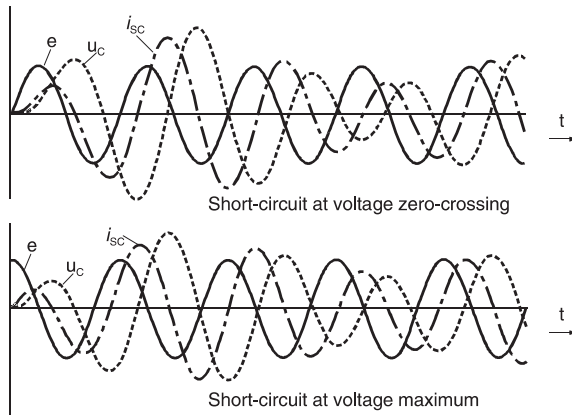


a) Equivalent circuit

$$\hat{E} \cdot \sin(\omega t + \lambda) = L \frac{di_{sc}}{dt} + R \cdot i_{sc} + \frac{1}{C} \int i_{sc} dt$$

$$i_{sc} = \hat{E} \cdot \sin(\omega t + \lambda - \Theta) + e^{-\alpha t} (K_1 \cos \beta t + K_2 \sin \beta t)$$

b) Differential equation and solution ( $i_{sc}$ )



c) Fault transient

**Figure 3.145**

Short-circuit on a series-compensated line, transient of the short-circuit current (degree of compensation  $K_C = K_C/K_L = 50\%$ )

More complex conditions exist, when the arc-gap does not ignite during the short-circuit [3.43 to 3.45].

A transient oscillation of the L-C-R-circuit with a super-imposed sub-synchronous frequency results (figure 3.145). The usual DC-current component in the short-circuit current of L-R circuits is in this case replaced by a slowly increasing resonant oscillation in the range of 10-40 Hz, depending on the network constellation.

The short-circuit current and voltage at the relay depends on the location of the series-capacitor in relation to the relay location.

The following fundamental phenomena arise:

- reduced fault reactance
- voltage inversion
- current inversion

#### *Reduced fault reactance*

Initially the case where the fault reactance remains positive from the fault location to the relay and in-feed is examined (figure 3.146). In this “typical” short-circuit case, the

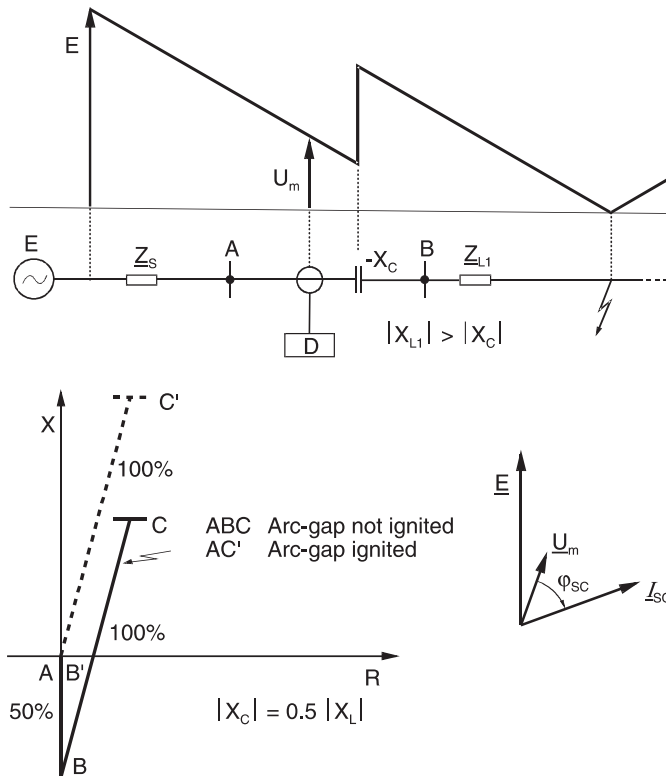


**Figure 3.146** Short-circuit on a series-compensated line, voltage measured positive by the relay

current lags the voltage in the entire short-circuit loop. At the capacitor, a positive voltage increment results. The distance protection measures a positive reactance, as in a non-compensated system. The value of the line-reactance however appears to be reduced by the capacitor reactance. The under-reaching zone of the distance protection must therefore be adapted to the compensated line:  $X_1 = k_{GF1} \cdot (X_L - X_C)$ .

The superimposed sub-synchronous oscillation causes a spiral-shaped homing-in onto the steady-state fault impedance with alternating periods of over-reach and under-reach (figure 3.147).

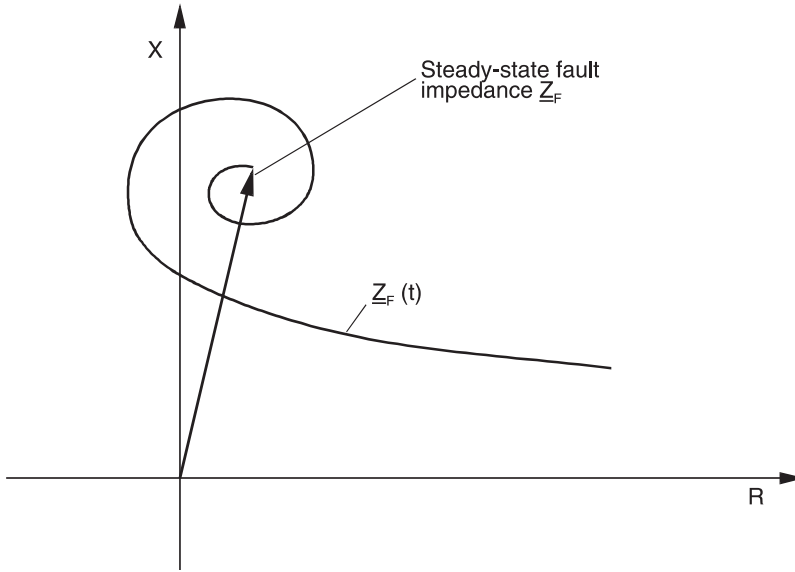


**Figure 3.147** Fault on a series-compensated line, transient of the fault impedance

As the sub-synchronous resonance cannot be completely filtered in the relay, especially when its frequency is close to the system frequency, the under-reaching zone must be reduced by an additional security margin  $k_{Trans}$  to avoid a transient over-reach:  $X_1^* = X_1 \cdot k_{Trans}$ .

If one assumes a linear frequency response in the low frequency range of the filter function in the distance relay (approx. true for the 7SA522), the sub-synchronous oscillation is damped with a factor  $f_{sub}/f_{net}$ . In this case the following equation can be derived by assuming a “worst-case condition”:

$$k_{Trans} = \frac{1}{1 + \frac{\hat{U}_{Gap}}{\sqrt{2} \cdot E}} \quad (3-197)$$

$\hat{U}_{Gap}$  = arc-gap ignition voltage,  $E$  = voltage of the in-feed emf



The following example illustrates the order of magnitude of the transient grading factor  $k_{\text{Trans}}$ :

For  $E = 1.1 \cdot 400 \text{ kV}$  and  $\hat{U}_{\text{Gap}} = 200 \text{ kV}$  we e.g. obtain  $k_{\text{Trans}} = 0.76$ .

With a typical grading factor of  $k_{\text{GF1}} = 0.85$  and a degree of compensation  $k_C = 70\%$ , the reach of the first zone is computed to be:  $X_1 = 0.85 \cdot 0.76 \cdot (1 - 0.7) \cdot X_L = 0.2 \cdot X_L$

From this it is apparent that on series-compensated lines, an un-delayed under-reaching zone can only be effective for very close-in faults.

### Voltage inversion

This occurs when the negative capacitor reactance is greater than the positive line reactance (figure 3.148). The loop reactance from the relay to the fault location is negative in this case. The current how-ever remains inductive, as the total short-circuit reactance up to the feeding emf is positive.

In this case, the voltage at the relay location has a phase inversion, i.e. at the point of measurement, the voltage lags the current by approx.  $90^\circ$ .

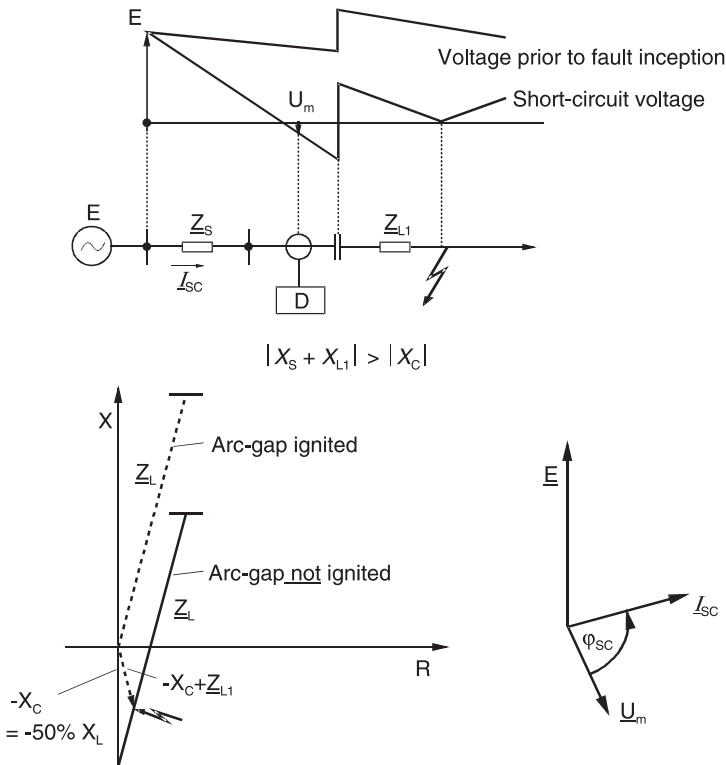


**Figure 3.148**

Short-circuit on a series-compensated line: inversion of the measured voltage ( $U_m$ ) at the relay

The measured fault impedance is therefore negative. This implies that a direction decision, based on faulted loop voltages would indicate the reverse direction, although the fault is on the line in the forward direction.

The direction decision using healthy phase or memorised voltages conversely provides the correct results, as indicated in paragraph 3.3.2.

In figure 3.149, the adapted relay characteristic (over-reaching zone) on a series-compensated line is shown. The quadrilateral distance zone uses faulted loop voltages and is therefore fixed in the impedance plane. The directional characteristic uses memorised or healthy phase voltages, and is therefore shifted with the source impedance, as shown. The MHO-circle must be polarised with a high degree of healthy phase, respectively memorised voltage ( $K_p = 1$ , see paragraph 3.4.2) in order to extend the circle reach far in the negative X-reach.

In spite of the negative capacitor reactance, the entire line length lies within the forward range of the over-reaching zone.

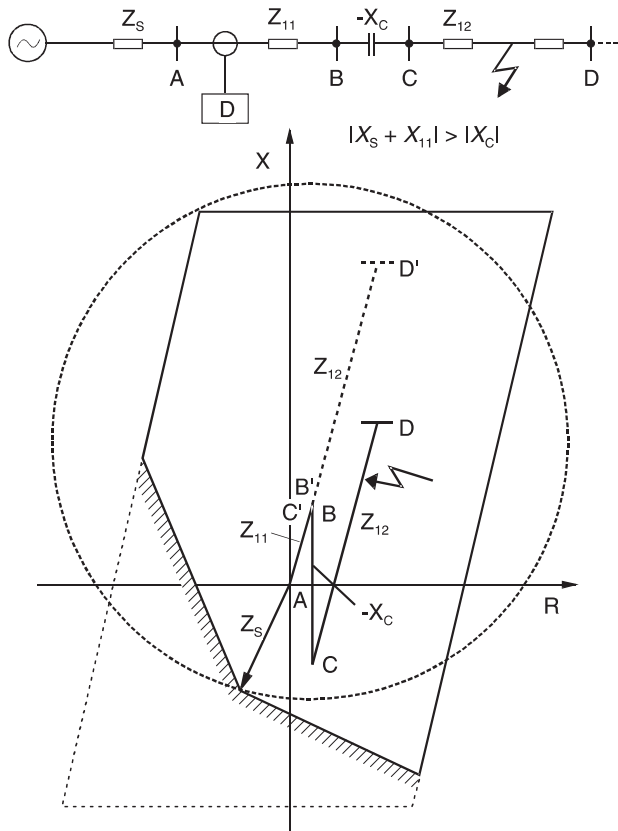


**Figure 3.149**

Series compensated line, distance protection with quadrilateral and memory/cross polarised directional decision memory/cross polarised MHO circle as an alternative

A directional comparison protection with over-reaching distance zones therefore provides a suitable protection arrangement for lines with series-compensation. In this case the over-reaching zone must be set greater than the non-compensated line reactance. The setting requires an additional extension of  $1/k_{\text{Trans}}$  to compensate the effect of the sub-synchronous resonance:  $Z_{\text{OVER}} = 1.2 \dots 1.3 \cdot (1/k_{\text{Trans}}) Z_L$ .

Both the blocking and release techniques can be used in the directional comparison scheme.

### Current inversion

This occurs when the short-circuit impedance from the fault location to the source emf is negative (figure 3.150).

The impedance at the relay location is then also negative, as a current inversion is most likely when the fault is directly behind the series capacitor. There are however some system constellations where the relay impedance will remain positive.

The short-circuit current in any event leads the unfaulted loop or memorised voltages by approx.  $90^\circ$ . The distance protection would therefore reach the incorrect direction decision and block during internal faults or trip for external faults.

Current inversion however only occurs with special system constellations. In general a very large short-circuit current will flow, causing the arc-gap to ignite, thereby by-passing the series capacitor for the duration of the short-circuit. Apart from some exceptions, the protection need therefore not be configured for these special cases.

The current inversion problem can only be dealt with by a directional comparison protection based on delta quantities ( $\Delta U/\Delta I$ -measurement). Even the phase comparison,

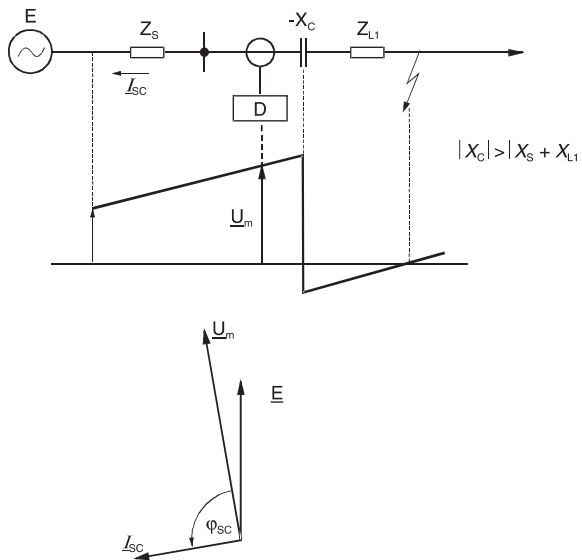
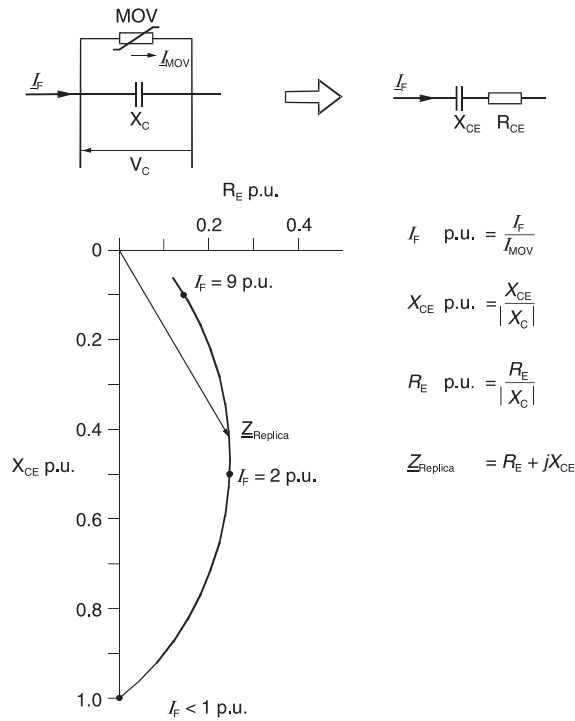


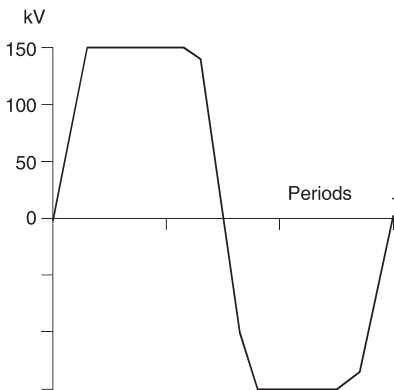
**Figure 3.150**  
Short-circuit on a series-compensated line, phase inversion of the short-circuit current

and in most cases also the differential protection, would block in the case of current inversion, as the protection system recognises a through-fault.

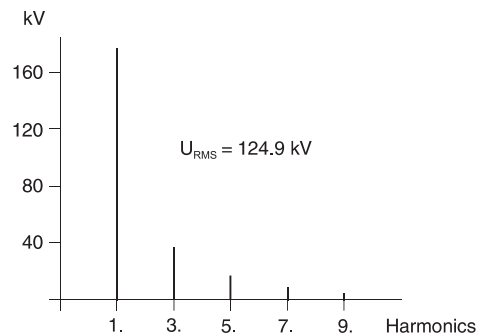
The source for the delta quantities can be assumed at the fault location according to the Thevenin's theorem. The relay therefore measures the current flowing into the source



a) Equivalent series impedance of the capacitor-varistor combination



b) Voltage across the capacitor



c) Spectrum of the capacitor voltage

**Figure 3.151** Series capacitor with MOV (metal oxide varistor)

impedance ( $\Delta I$ ) and the voltage drop at the source impedance ( $\Delta U$ ). The directional decision is correct as long as the source impedance remains inductive independent of the series capacitance on the line side.

The same conditions apply for negative and zero-sequence directional comparison schemes [3-42].

#### *Non-linear resistance (Varistor) in the short-circuit path*

Modern capacitor banks utilise a MOV (metal oxide varistor) to limit the voltage (figure 3.151). The arc-gap is then set so high, that it only ignites when an internal fault with a large current occurs. During external faults only the MOV limits the voltage. The capacitor automatically becomes effective again when the short-circuit current disappears, causing the voltage to drop below the limit voltage of the varistor.

The varistor functions as a variable impedance in the short-circuit path. The equivalent circuit and the current dependant impedance of the capacitor-varistor combination are shown in figure 3.151. The equivalent impedance is applicable to the fundamental component. Due to the non-linear distortion of the varistor voltage, harmonics are also present. In the case of a short-circuit immediately behind the capacitor, these are present in the relay short-circuit voltage. As a result of the Fourier-filters used in modern numerical relays, these signal-disturbances have no significant influence on the measuring accuracy.

The equivalent impedance of the MOV also includes a resistive component ( $R_E$ ), which must be considered in the relay setting (figure 3.151a).

# 4 Device design

The first fully numerical protection relays with integrated communication interfaces were supplied by Siemens in 1985. They were already designed to be integrated in the substation control system (LSA). As a result of the continuing developments in the micro-processor and communication technology, the performance of the devices continuously increased thereafter.

In the following a short summary of the design and functionality of the numerical devices is provided. Detailed information is given in the system and relay manuals provided by the manufacturers [4-1].

## 4.1 Intelligent electronic devices (IEDs)

Modern protection relays are fully digital. This implies that the measured values (currents and voltages) are converted to digital values and processed numerically.

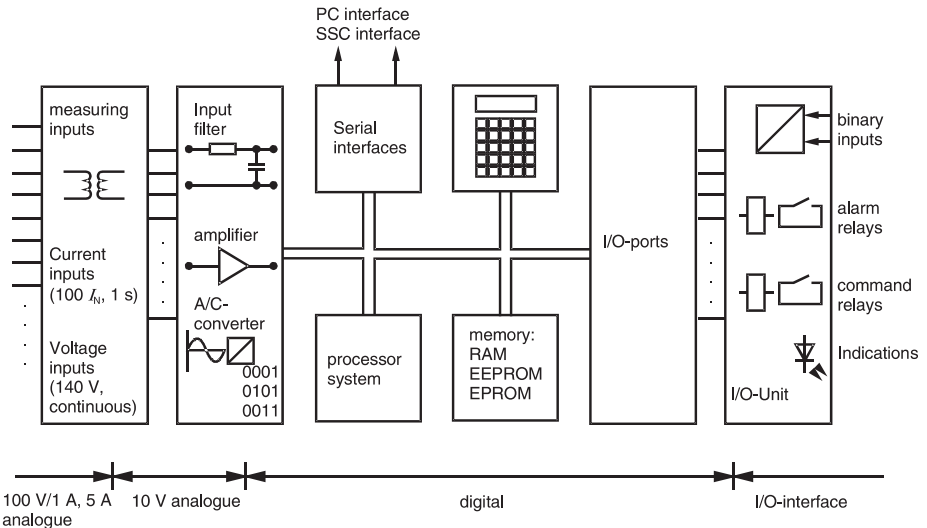


**Figure 4.1** Numerical protection, device structure

The following technical data apply for SIPROTEC 4 relays:

Sampling rate:	1000 Hz (1200 Hz with 60 Hz nominal frequency)
Samples per period:	20
Anti-aliasing filter:	500 Hz (600 Hz) limiting frequency
A/D-conversion:	16 bit, corresponding to 65536 steps
Measuring value storage:	15 s
Program language:	C/C++

Recently, the relays have developed into multi-functional universal devices, generally designated as IEDs (Intelligent Electronic Devices).

The number of functions integrated in relays has been steadily expanded in parallel with the increasing processing power and storage capacity. Table 4.1 shows the relay hardware evolution taking the Siemens SIPROTEC series as an example.

A single powerful processing board is able to handle all integrated functions. Separate small processing modules are dedicated to the communication interfaces to cope with the increased data rates and complex transmission procedures. Exchange of these plug-in modules then allows easy adaptation to present and future communication standards. GPS time synchronisation of microsecond accuracy is optionally offered with the latest device generations.

Distance relays now contain all protection functions necessary for a line. Back-up protection functions must of course be dedicated to a separate IED for the reason of hardware redundancy.

Non-protection tasks, such as metering, monitoring, control and automation, occupy an ever increasing share of the scope of functions. The modular design allows adaptation of the input/output interface to the individual application.

Modern relays are designed for the world market (global relays). They meet the relevant IEC as well as ANSI/IEEE standard requirements and can be adapted to the communication standards used in Europe and USA. The information interface of SIPROTEC 4 relays can for example be delivered to IEC60870-5-103 as well as to DNP3.0 or Modbus. The new IEC 61850 standard for open substation communication has been successfully tested in pilot projects and is now introduced word-wide.

Windows compatible PC programs (DIGSI) allow comfortable local or remote operation of IEDs.

**Table 4.1** Development of digital relay HW performance

Delivery commence	Relay generation	Memory RAM/EPROM	Bus width	Processing power	
1992	SIPROTEC 3	256/512k	16	1.0	MIPS
2000	SIPROTEC 4	512k/4MB + 4 MB D-RAM	32	35	MIPS

## 4.2 Mechanical design

Modern devices are of compact design and in addition to the principle function (in this case distance protection) contain a number of supplementary protection functions (e.g. breaker failure, earth-fault and over-load protection) as well as additional functions for measuring and control (figure 4.2).

Keypad and display are located on the device front. Combined protection and control devices are available with a graphic display for the bay mimic diagram and control keys for local control. These devices are also applied as bay units for the substation control system.

The hardware is scaleable. The device dimension can vary depending on the scope of functions and the number of interfaces. At the medium and high voltage level, devices with a width of 1/3 to 1/2 of a standard 19" rack are usually sufficient. The full 19" rack device versions are intended for the EHV level where a large number of binary inputs and relay contact outputs are required.

The connection is basically the same as with conventional relays.

The current and voltage transformer inputs are isolated via small input transformers from the processing hardware. The burden is very low (below one VA in case of SIPROTEC relays). Status inputs are coupled via binary inputs (opto-couplers), providing a potential barrier. Output relays are provided for alarm signals and trip commands.



**Figure 4.2** Modern numerical relay design (SIPROTEC 4 series)





Parallel wire interface:

Applicable wire cross-sections:  
0.5 to 2.5 mm<sup>2</sup> (AWG 20 to  
AWG13) for voltages and 2.7 to  
6.6 mm<sup>2</sup> (AWG 13 to AWG11)  
for currents.

Ring or fork cable legs recom-  
mended.

Serial interfaces:

Optic fibre (ST connectors)

or

RS232/485 (SUB-D connector)

**Figure 4.3**

Rear side of a SIPROTEC 4 relay, showing the wire connection terminals and the serial interfaces (lower right side)

In the normal version for flush mounting the connection terminals are located on the reverse side of the relay (figure 4.3).

### 4.3 Relay Communications

The serial interfaces for operating and servicing the device, as well as connection to a substation control system, are new to the numerical protection [4-2, 4-3].

In devices with numerical communication between the line ends protection data interfaces are also provided for the transmission of protection data (measured values, commands).

Up to five interfaces may exist:

– *Serial interface for local servicing via PC*

This interface is located on the front of the relay. No standard exists here, the communication for relay operation (setting and up- or download of data and programs) is vendor specific. Siemens relays utilise a V.24/V.28-Interface and the protocol structure IEC 870-5-103 for this purpose.

– *Service interface for remote access*

In this case, a RS 485 daisy chain or an optical interface is used.

The relays of a station may be interfaced via star coupler to a central modem with telephone link for remote operation. The used protocol is the same as that of the front service interface.

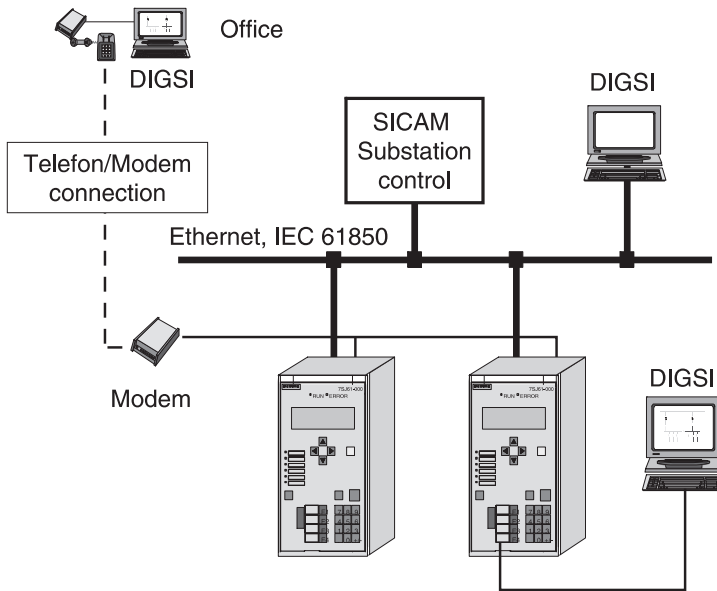


**Figure 4.4** Substation automation system with SIPROTEC 4 devices

- *Time synchronisation interface*

With this interface, a time synchronisation signal (DCF77 of the PTB in Germany or IREG B via GPS satellite system) can be connected for exact time synchronisation.

- *System/Scada interface*

This interface provides the connection of the protection relay to a control system (substation or network control device). The IEC 870-5-103 standard (interface and protocol) are widely used in Europe. LAN interfaces (e.g. Profibus) are also available. Modbus or DNP3.0 are preferred standards in the USA.

Great effort has been taken in the last years to develop a worldwide accepted standard for communication in substations. The new open standard IEC61850 has now been published and first pilot projects are in operation. The major vendors announced 61850 compatible relay series for 2005.

Integration of the SIPROTEC 4 devices in a substation automation system is shown in figure 4.4.

- *Protection data (teleprotection) interface*

It is intended for the communication with the protection at the remote line terminals. No international standard exists for this. A number of optical versions are offered for communication through data networks or direct relay end-to-end- communication via dedicated optic fibres.

In the first case, an optical cable connects the relay with the data terminal device of the communication network within the substation. A 62.5/125  $\mu\text{m}$  multi-mode glass fibre cable is used for this purpose (max. 1.5 km). A signal converter is normally necessary to convert from optical fibre to the standard wired interface of the data terminal device (figure 4.5).

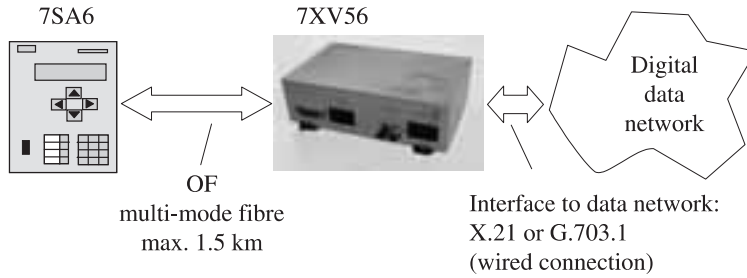


**Figure 4.5** Protection data communication via data network, interfacing

Where dedicated optical fibre cables are available for protection, the relays can also be directly connected using an integrated optic sender/receiver version (1300 or 1550 nm) for distances up to about 100 km. To keep the light attenuation low, mono-mode fibre cables (9/125  $\mu\text{m}$ ) and corresponding interfaces are applied

## 4.4 Integrated functions

Modern numerical distance relays (7SA522 and 7SA6) integrate all functions necessary to protect a line or cable including the supplements for teleprotection schemes which can be set up with traditional signalling (PLC, analogue microwave, pilot wires) or with modern digital communication (figure 4.6).

A complete protection scheme can now be configured using the relay operating program (DIGSI). The functions can be selected from the protection menu. The scope of integrated functions covers a wide application range and corresponds to the main-stream protection practices worldwide.

In general a utility will use the same type of relay for all applications (e.g. lines and cables). The preferred zone characteristics (MHO for long lines and QUADRILATERAL for short OH lines and cables) can be chosen by parameter setting. The supplementary functions (e.g. auto-reclosure for OH-lines and overload protection for cables) can be selected from the function menu.

The state signals of the protection functions (start, trip, etc.) can then be assigned to the relay interfaces (trip and alarm output relays, indications (LEDs, serial interfaces) by mouse click using the marshalling table of DIGSI.

In practice, special functions (logic signal combination, time delay, threshold supervision of currents or voltage, etc.) may be needed to adapt the protection scheme to the given system conditions, for example to co-ordinate tripping and re-closing of a 1-1/2-CB arrangement. External relay combinations and circuits were used for this purpose in the past. The SIPROTEC 4 relays now provide the option to apply additional user-defined logic. Thereby the binary input signals and internal signals (threshold detectors, protection signals) can be linked, logically processed and routed to relay outputs

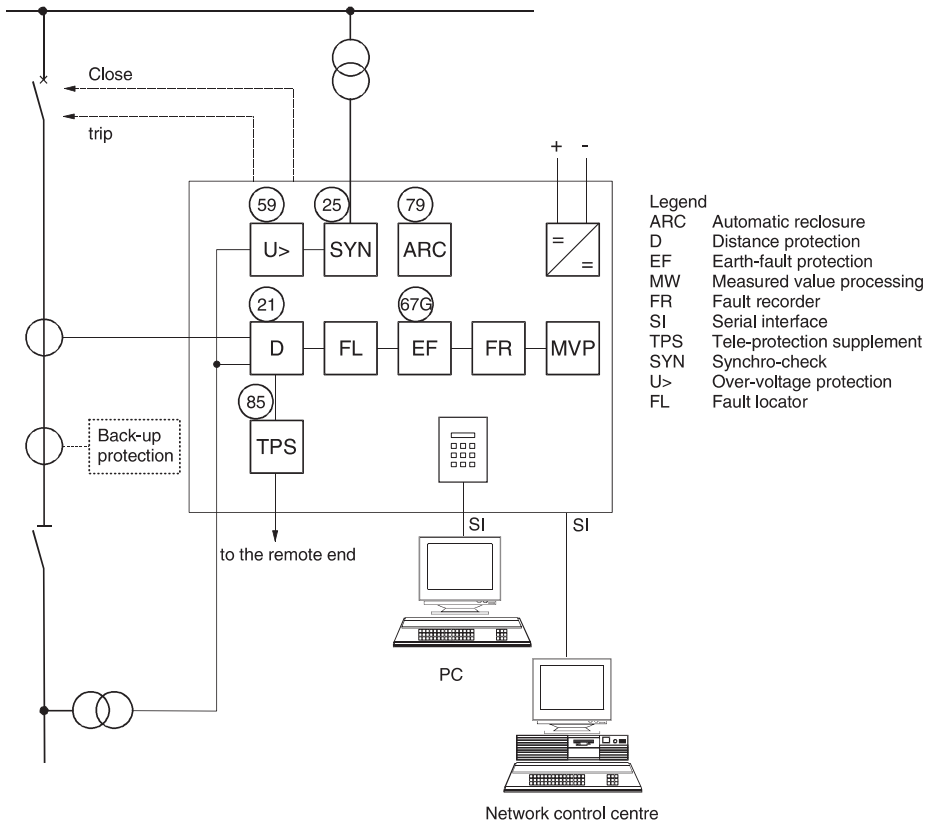


**Figure 4.6** Numerical line protection, integrated functions

and indications. In this way user defined applications without external relay connections can be applied. The logic is implemented with the graphic CFC editor.<sup>1</sup>

In this way the former scheme design and panel wiring has been replaced by configuring and parameterising (parameter setting) at the PC.

This allows to reduce the size of the relay panels/cubicles considerably.

The sum-total of individual devices on a protection panel or a complete protection cubicle is now reduced to the size of a single relay housing (figure 4.7).

In most cases, a single device is sufficient for all the essential protection functions per line end. For the reason of hardware redundancy, the back-up function has to be provided in a separate relay (refer to protection concepts 5.3.2)

<sup>1</sup> CFC means continuous function chart

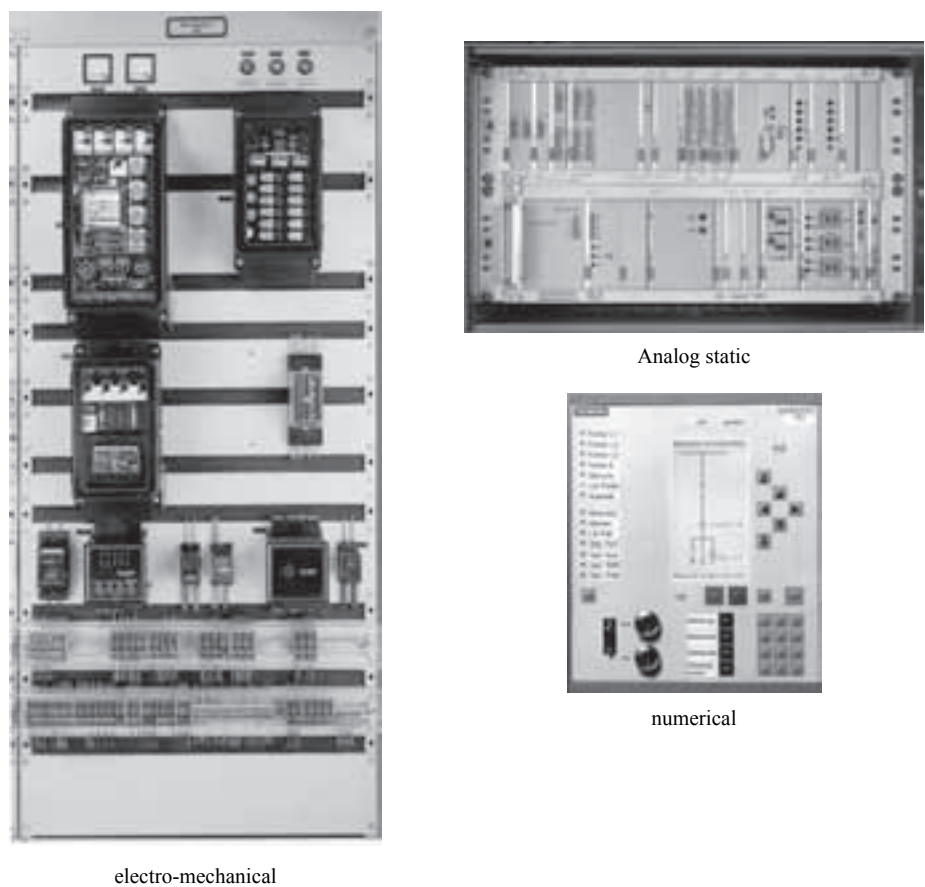


**Figure 4.7** Developments in protection technology (example 110 kV line protection)

The minimisation of space and panel wiring results in considerable saving of cost for panel construction, assembly and testing, and has further reduced the space requirements of relay rooms in substations.

On the other hand, an increased number of relay setting parameters is necessary to adapt the many integrated functions. A standardised basic parameter set should therefore be used and copied to new applications. The actual setting can then be reduced to application specific parameters (e.g. line parameters).

As an example for modern distance relays, the scope of integrated functions is shown for two SIPROTEC 4 relays in Table 4.2.

**Table 4.2** Scope of integrated functions

Functions:	Relay 7SA522	Relay 7SA6xx
<b>Main function:</b>		
Distance protection 21	Full scheme	
Characteristic	Quadrilateral or MHO cross polarised	Quadrilateral or modified impedance
Voltage memory	2 s	
Shortest tripping time	Normal: 17 ms (50 Hz), 15 ms (60Hz) With high speed output relays: 12 ms (50 Hz), 10 ms (60 Hz)	
Distance zones	6 (all gradable forward or reverse)	
Zone setting	0.05 to 600 Ω (1A relay) 0.01 to 120 Ω (5 A relay)	
Load blocking zone (cone) Load impedance	0.1 to 600 Ω (1A relay) 0.02 to 120 Ω (5A relay)	
Load angle	20° to 60°	
Earth current compensation: $R_E/R_L$ and $X_E/X_L$ setting or $K_0$ and $\phi_0$ setting	-0.33 to 7.00  0.00 to 4.00 and -135 to +135°	
Teleprotection modes 85-21	DUTT, PUTT, POTT, Blocking and Unblocking Weak infeed supplement	
Power swing blocking/tripping 68, 68T	Setting free, effective up to 7 Hz	
Multiple setting groups	4 independent setting groups changeable via relay key pad, serial interfaces or binary input	
<b>Add-on protection functions:</b>		
Directional and non-directional earth fault 50N, 51N, 67N	<i>Earthed neutral:</i> $U_0$ , $I_0$ (dual) or $U_2$ polarised DT and IT delay	<i>Isolated neutral:</i> $U \cdot I \cdot \sin \phi$ measurement <i>Compensated networks:</i> $U \cdot I \cdot \cos \phi$ measurement <i>Earthed neutral:</i> $U_0$ , $I_0$ (dual) or $U_2$ polarised DT and IT delay
Directional comparison earth fault 85-67N	tripping, blocking	

**Table 4.2** Scope of integrated functions

Functions:	Relay 7SA522	Relay 7SA6xx
Backup over current 51, 51N	Definite and inverse time	
Overvoltage 59	$U_{ph}>, U_0>, U_1>$ Option: computation of the remote end open line voltage (compensation of the Ferranti effect)	
Undervoltage 27	$U<, U<<$	
Over- and under-frequency 81	4 steps	
Thermal overload 49	–	to IEC60255-8
Breaker failure 50BF	Phase segregated	
Switch onto fault 50HS	Tripping time: 13 ms normally, 8 ms with high speed output relays	
Auto-reclosure 79	1-pole and/or 3-pole, single and multi-shot	
Synchro-check 25	Modes: Synchro-Check $\Delta U, \Delta \varphi, \Delta f$ or Live bus – dead line or Dead bus – live line	
Further add-on functions:		
Event recording	8 records, 600 events	
Fault recording	8 recordings total storage time: 15 s, 1 ms resolution with battery back-up	
Operational measured values	Phase currents IL1, IL2, IL3, IE Symmetrical component currents I1, I2, I0 Phase voltages UL1, UL2, UL3, UL1-2, UL2-3, UL3-1 Symmetrical component voltages U1, U2, U0 Measured load impedances X, R Power (apparent, active, reactive) Energy meters (active, reactive) Long term mean values (I, S, P, Q)	
Programmable logic functions (PLC)	Programmable with graphical CFC editor in DIGSI	
Output relays (trip + alarm)	16, 24 or 32	All in-/outputs and LEDs can be freely assigned to integrated functions by DIGSI with a marshalling table.
Binary inputs	8,16 or 24	
LED's	max. 30	

*Combined protection and control devices (IEDs)*

The increasing power of micro-processing hardware made it possible to integrate measuring, control and automation functions in protection relays.

These so-called combined protection and control devices have control keys and a graphic LCD display on the device front. This allows local control and indication of plant and device information. A bay mimic control indication or measured value indication as well as various annunciation lists can be selected in the display. The control diagram can be configured to suit the users requirements with the software DIGSI 4.

Interlocking and PLC functions can be designed and implemented with the graphical CFC editor. Control of the feeder is done via the cursor and the open/close push-buttons.

In distribution, a single, switchgear integrated device is therefore sufficient for control and protection of one feeder (“One bay, one relay” concept). This is shown in figure 4.8.



**Figure 4.8** Distribution switchgear with combined protection and control relays.



## 4.5 Relay terminal connections

The connection of the instrument transformers, power supply as well as the tripping and alarm circuits is done in the usual manner, as in the case of an electro-mechanical or static distance relay (figure 4.9).

As a result of the integrated additional functions, there is a larger number of terminals, comparable to a classical protection panel when wired parallel interfaces are used.

The serial interfaces for communication are new. The fibre-optic version is usually preferred, as it ensures absolute immunity against interference.

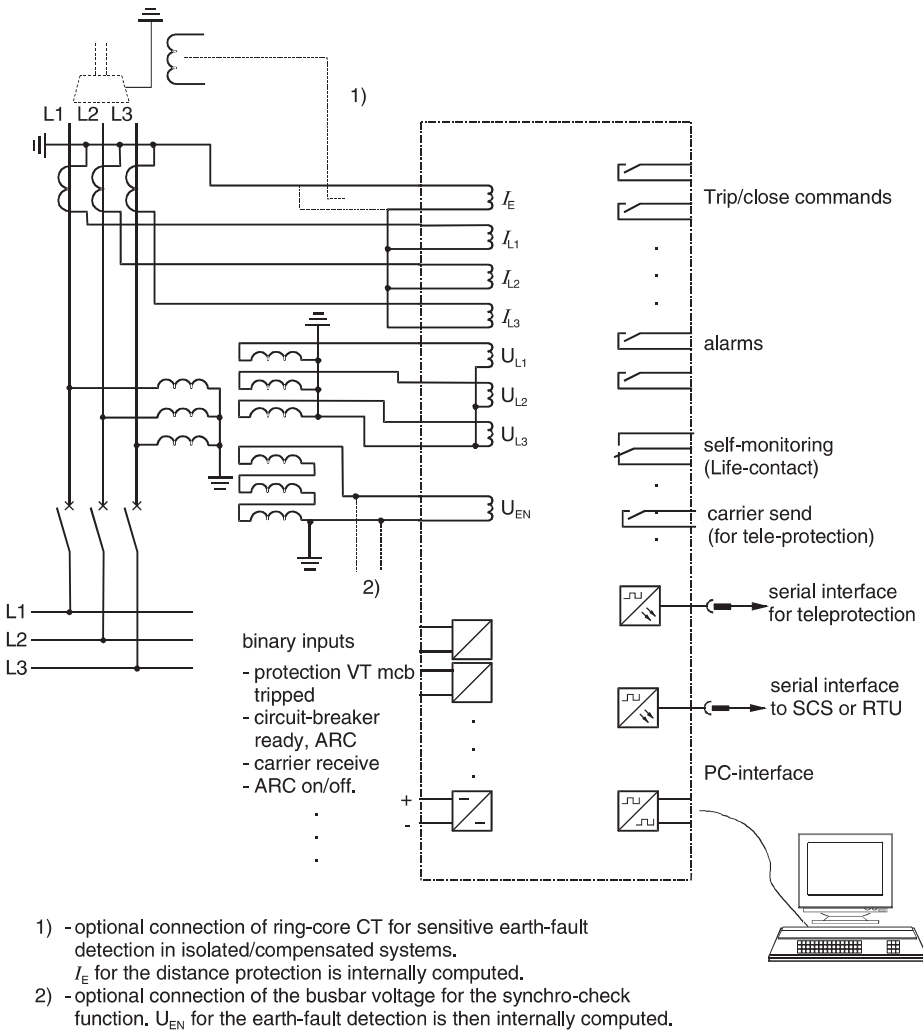


**Figure 4.9** Terminal connections of a numerical relay (7SA610)

The large scope of alarm contacts is actually only required for stand-alone applications of the protection relay. When the relay is implemented as a component of the integrated sub-station control system, these alarm contacts are mostly not used, as events/annunciations/alarm are communicated via the serial interface.

#### *Current-transformer connection*

In earthed systems, a connection to a three phase CT set is made. The earth-current input of the device is connected in the star point of the CT-circuit.

The 7SA6 device provides a version which computes the earth-current for the distance protection from the phase currents. The available  $I_E$  input can then be used for parallel line compensation (connection of the residual current of the parallel line).

In isolated/compensated systems, the 7SA6 is usually implemented with integrated earth-fault direction determination. In this version, the sensitive earth-current input  $I_E$  is provided by a special high-precision input transformer. This input is in general connected to a ring-core (core balance) CT with a small transformation ratio (60/1 in the case of the Siemens type 7XR96). The earth-current for the distance measurement during a double earth-fault is then again computed internally.

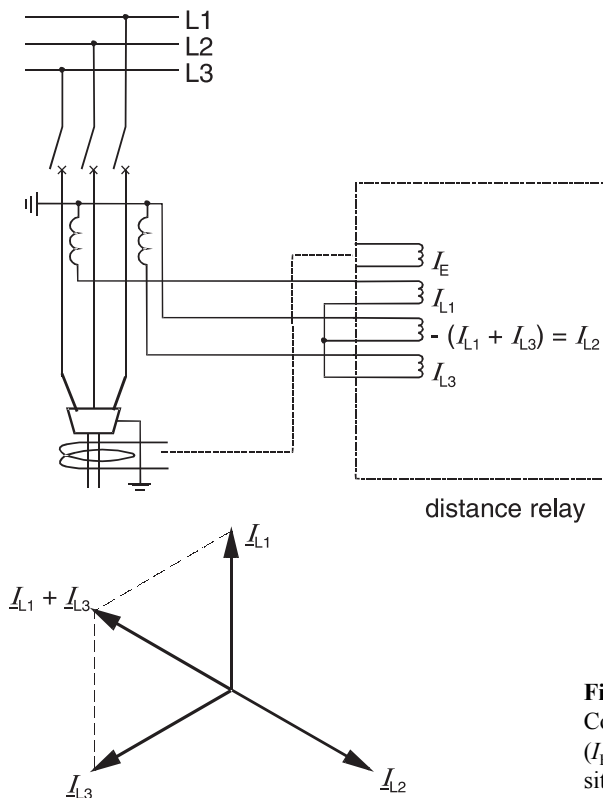


**Figure 4.10**

Connection to only two CTs  
( $I_E$  to core balance CT for sensitive earth fault protection)

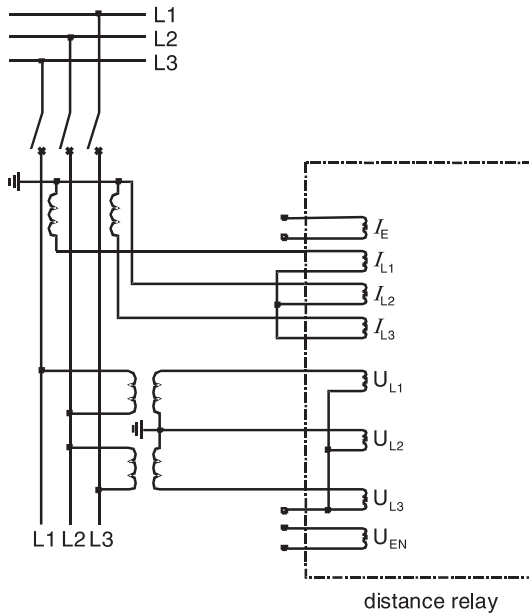


**Figure 4.11**  
Two VTs in V-connection  
combined with connection  
to only two CTs

Sometimes in the past, in small non-earthed systems, where double earth-faults seldom occur, only two current-transformers were used in the phases L1 and L3. The L2-current input of the relay must then be connected in the common return path (see figure 4.10). This was often done in combination with only two voltage transformers in V-connection (figure 4.11).

During phase-to-phase and three-phase faults, the protection measured the correct short-circuit currents with this economical configuration. The double earth-fault is however always “seen” and measured as a two-phase short-circuit. Depending on the location of the relay in relation to the earth-fault locations, different impedances result. It is not possible to set a preference for double earth-faults.

The described device and termination configuration is shown in the 7SA6 manual.

#### *Voltage-transformer connection*

In an earthed system the distance relay must be connected to a three-phase voltage transformer set. An additional open delta-winding in the set of VTs is not required by the distance protection, but is advantageous for the self-monitoring because a total control of the VT-circuits is then possible ( $\underline{U}_{EN} = \underline{U}_{L1} + \underline{U}_{L2} + \underline{U}_{L3}$ ).

In special cases, the displacement voltage  $U_{EN}$  for the self-monitoring, may also be derived from an additional set of auxiliary transformers connected in star/open delta.

In isolated/compensated systems, it is common practice to also use a set of three-phase VTs, so that the distance of the earth loops is measured correctly, according to the double earth-fault preference. Furthermore, this is the only way to derive the displacement voltage for the earth-fault direction determination.

If however it is satisfactory to only measure the correct distance to fault during phase to phase and three-phase faults without earth, it suffices to use two voltage transformers in V-connection. The star point of the voltage input in the relay in this case is not connected, and therefore always lies in the centre of the line voltage delta. In this manner, only the positive and negative sequence components of the voltage are transformed.

During double earth-faults, the measured impedance is too large, as the zero-sequence voltage is not detected by this VT-connection.

The V-connection of the voltage transformers may be combined with the connection requiring only two CTs as described above (figure 4.11)

Such economical configurations are only found in old plants within small networks.

## 4.6 Relay operation

A keypad and alpha-numeric display are located on the front of the device.

The operation is menu-driven. The settings may be entered directly as numbers. The information is given in plain text.

The 4-line display shows operational measured values during the normal load-condition (e.g. selected currents and voltages). In the case of a fault, the display automatically changes to show the selected fault data (e.g. fault type and fault location).

The serial interface (RS232) for connection of a service-PC is located on the front of the device. With the relay operating program DIGSI, the protection may be configured and parameterised comfortably with WINDOWS look and feel (figure 4.12).

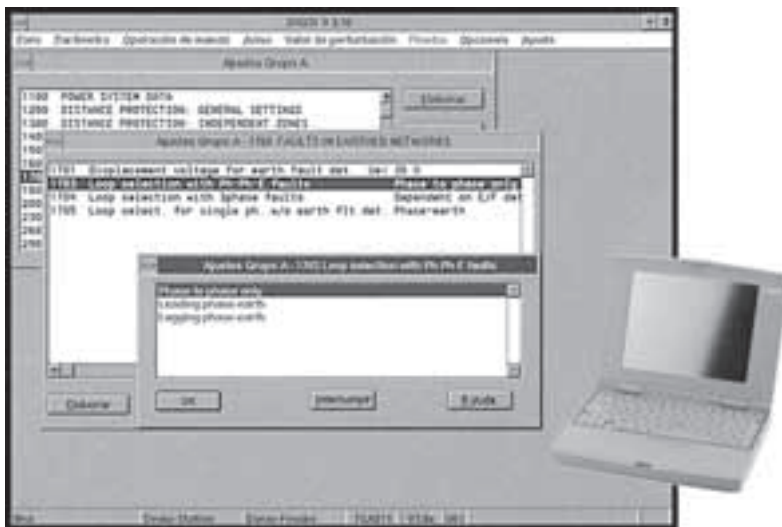


**Figure 4.12** PC-Relay dialogue with the DIGSI operating program

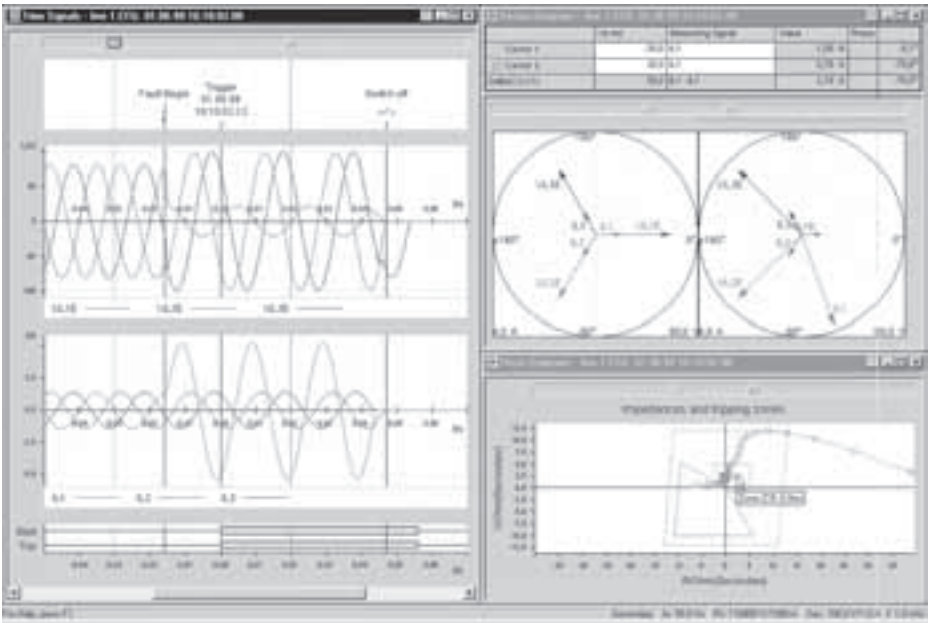


**Figure 4.13** Analysis of a fault record using the SIGRA program tool

Alternatively, the retrieval of settings and stored fault data is possible.

The settings are normally prepared off-line in the protection office. At site they can then be down loaded from a laptop to the relays during commissioning.

Also remote setting and retrieval of fault data is possible via modem links.

DIGSI offers as an option the fault analysis program SIGRA. It allows to display and analyse fault records stored in the relays. This includes time and phasor diagrams of all recorded voltages and currents. In addition, the corresponding symmetrical components can be calculated and presented as phasors. Also fault records of remote line ends can be imported and synchronised to the local record. In this way, the behaviour of tele-protection schemes can be checked.

In the particular case of distance protection, the impedances of the six fault loops (L1-E, L2-E, L3-E and L1-L2, L2-L3, L3-L1) are calculated using the Fourier- transform over a data window of one cycle. The data window can be placed at any instant of the oscillographic fault record by a cursor. Alternatively, the locus of the six fault impedances can be calculated in one milli-second time intervals, again using the one cycle data window. Start and end can be fixed by cursors at the fault record. The displayed course of fault impedances in the R-X diagram provides a powerful tool for analysis of the distance relay performance during the full fault history (figure 4.13).

---

## 5 Application

Initially general aspects for the practical implementation are discussed. Then typical areas of application will be considered in detail.

### 5.1 General aspects

#### 5.1.1 Application criteria

The classic distance protection without teleprotection can be used on all types of plant where a minimum impedance is available for grading of the zones.

In the first place these are overhead lines and cables with a minimum length.

As generators, transformers and compensating reactors have relatively high short-circuit reactances, selective impedance grading can also be achieved here.

A further basic requirement is that suitable current and voltage transformers are available at the relay location.

The current-transformers must be allocated to the protected feeder, and be located between it and the source.

They may be located in front of or behind the circuit-breaker.

The preferred location is on the line side when only one CT-set is provided. In this case the circuit-breaker is not in the forward protected zone.

American practice is to have CT's on both sides of the circuit breaker to get overlapping protection zones. In this case the feeder distance relay is connected to CT's on the bus-side including the circuit breaker in the protection zone.

In HV and EHV systems, it is common practice to have a voltage transformer on each line. The measured voltage may however be derived from the busbar or a different feeder that is galvanically connected to the protected circuit. This is often the case in medium voltage systems. In the case of multiple busbars, a special relay selection circuitry is required (VT replica).

On very short lines or cables, the minimum setting of the distance protection may not suffice. In this case, the distance protection can only be used in a direction comparison scheme with over-reaching distance zones (refer paragraph 3.1.10). In special cases the

distance protection with direction comparison mode can also be used as busbar protection. To achieve this, one distance zone in each line protection is set with reverse reach. The direction comparison of all feeders is provided by an additional logic circuit.

### 5.1.2 Shortest line length

The smallest secondary impedance setting in the numerical distance relays 7SA is 0.05  $\Omega$  for 1A Relays and 0.01  $\Omega$  for 5A relays.

The reach of the numerical relays with quadrilateral characteristic is determined by the reactance. For the first zone, the following applies:

$$X_{\text{line min.}} = \frac{\text{ratio}_{\text{VT}}}{\text{ratio}_{\text{CT}}} \cdot X_{\text{relay min.}} \cdot \frac{1}{GF_1} \quad (5-1)$$

With:  $GF_1$  = grading factor of the under-reaching zone (e.g. 0.85)

$$I_{\text{L min.}} = \frac{X_{\text{line min.}}}{X'_L} \quad (5-2)$$

$X'_L$  corresponds to the reactance/km value in  $\Omega/\text{km}$  for the line.

#### *Example 5.1: Minimum cable length*

Given: 10 kV belted cable 240 mm<sup>2</sup> with  $X'_L = 0.09 \Omega/\text{km}$   
 Current transformer: 400/5 A  
 Voltage transformer: 10 000/100 V

Searched: Minimum cable length that can be protected by an underreaching distance zone.

$$\text{Solution: } X_{\text{line min.}} = \frac{10\,000/100}{400/5} \cdot 0.01 \cdot \frac{1}{0.85} = 0.015 \Omega$$

$$I_{\text{L min.}} = \frac{0.015}{0.09} = 0.167 \text{ km} \triangleq 167 \text{ m}$$

The result shows that the numerical distance protection may be adapted to very short feeders.

It must however be noted that the measuring accuracy is reduced in the case of extremely small voltages.

To maintain an accuracy of approx. 10%, the secondary short-circuit voltage at the relay, being the voltage drop across the reactance, should not fall below 1 V.

The minimum short-circuit current therefore corresponds to:

$$I_{\text{SC min.}} = \frac{U_{\text{SC min.}} \cdot \text{ratio}_{\text{VT}}}{X_{\text{line min.}}} \quad (5-3)$$

In the above example we would get:  $I_{SC \min.} = \frac{1 \text{ V} \cdot \frac{10\,000}{100}}{0.015} = 6670 \text{ A}.$

In the case of a network with current limiting during earth-faults, the minimum line length that can be protected with distance protection will correspondingly increase.

By considering the voltage drop across the earth reactance, the following equation results:

$$I_{SC \min.} = \frac{U_{SC \min.} \cdot ratio_{VT}}{X_{line \min.} \cdot \left(1 + \frac{X_E}{X_L}\right)} \quad (5-4)$$

or

$$X_{line \min.} = \frac{U_{SC \min.} \cdot ratio_{VT}}{I_{SC \min.} \cdot \left(1 + \frac{X_E}{X_L}\right)} \quad (5-5)$$

Assuming that  $X_E/X_L = 0.4$ , and that the earth-current is limited to 2000 A, the following is obtained with this check:

$$X_{line \min.} = \frac{1 \text{ V} \cdot \frac{10\,000}{100}}{2000 \cdot (1 + 0.4)} = 0.036 \, \Omega$$

and

$$I_{L \min.} = \frac{0.036}{0.09} = 0.4 \text{ km} \triangleq 400 \text{ m}$$

This implies that in this case the limitation is not the minimum relay setting value, but rather the minimum required short-circuit voltage.

### 5.1.3 Tripping time

In stable networks, as found e.g. in Europe, extremely short tripping times are not required. A total fault clearance time (protection plus circuit-breaker) of approx. 5 cycles (100 ms in 50 Hz systems) is generally sufficient.

The German utility board (VDEW) states the following requirement for the protection tripping time during the critical three-phase close-in fault [5.1]:

EHV-system:	25 ms
HV-system:	30 ms
MV-system:	40 ms



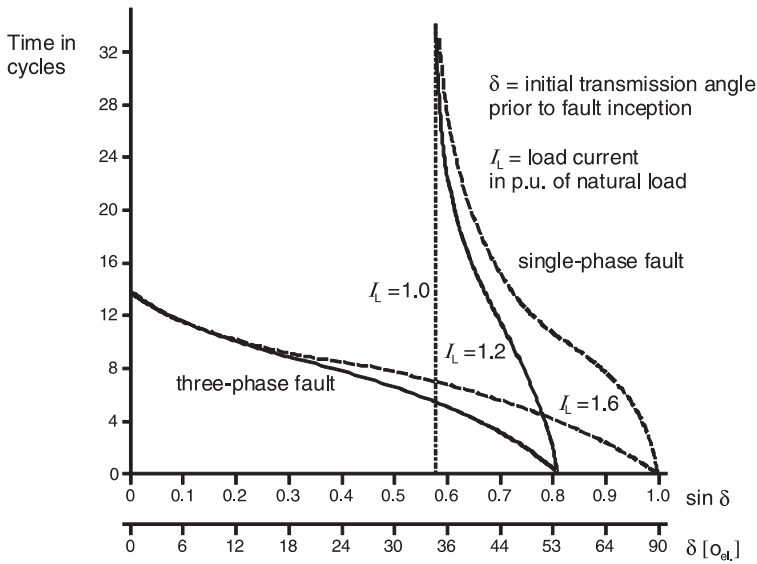


**Figure 5.1** Critical fault clearing time [5.2]

The numerical relay tripping times are substantially less (see table 4.2).

On transmission systems with long, heavily loaded lines a high transmission angle results and the stability is endangered during faults. Therefore, fast tripping is required on 100% of the line length (figure 5.1). A typical requirement is four cycles fault clearance time (80 ms for  $f_N = 50$  Hz), split into two cycles protection tripping time and two cycles circuit-breaker operating time.

As fast tripping on 100% of the line length can only be achieved with a teleprotection supplement, the stated two-cycle trip time includes signal transmission time and relay operating delay for the send and receive signal.

In the case of power line carrier (PLC), and microwave radio links, a maximum delay of 20 ms must be allowed for the signal transmission including I/O-relay reaction times. For the distance protection operating time approx. one cycle (20 ms) remains. Transmission via dedicated fibre-optic links results in shorter signal transmission times of below 10 ms and thus provides better conditions for the protection.

#### *Adaptive measuring techniques*

The numerical distance relays utilise an adaptive algorithm that provides fast operating times for faults that are clearly inside the zone (0 up to approx. 80% of the setting) (figure 5.2). At the same time, by evaluating a longer data window and applying two separate measuring techniques, a high measuring accuracy during faults close to the zone limit is guaranteed.

In the case of the extra high voltage distance protections, e.g. 7SA522, the following tripping times then result:

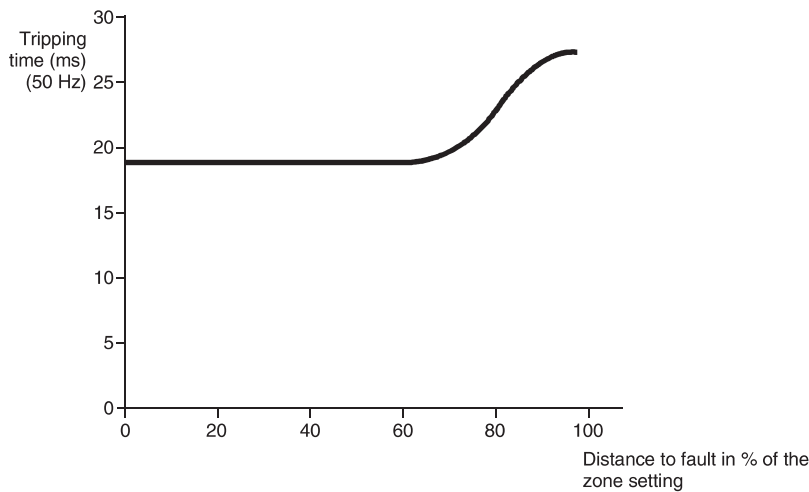


**Figure 5.2** Adaptive distance measuring technique, tripping times

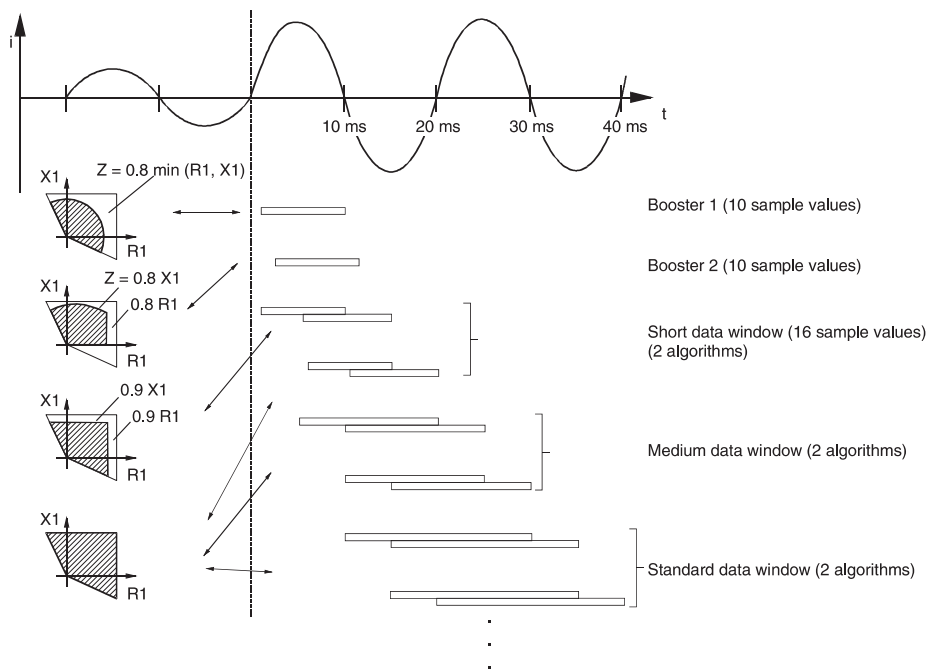


**Figure 5.3** Adaptive distance measuring technique

Due to the overlapping of the fast trip underreaching zones one line end always trips in the very fast time of below 1one cycle (typically 17 ms at 50 Hz) in the event of a permissive under-reach transfer trip scheme. The opposite end issues the trip command inside the required 40 ms, after receiving the transfer trip signal.

When a directional comparison scheme with over-reaching zones is used (permissive over-reach, blocking, un-blocking), the over-reaching zone must be set large enough to include the entire line within the absolutely fast range of the zone, i.e. approx.  $100/0.75 = 130\%$ .

### 5.1.4 Teleprotection, choice of technique

In Europe, under-reach transfer trip and release schemes were historically used and are still mostly used today. In the USA, blocking modes (directional comparison blocking) are almost exclusively used.

The development of these techniques were in the past influenced by the special characteristics of the PLC technology.<sup>1</sup>

The PLC equipment with amplitude modulation and direct keying of the high frequency signal (ON/OFF carrier), widely used in the USA, is fast ( $< 5$  ms), but not very secure against disturbances. The blocking technique is suited to these characteristics.

The voice frequency channels with frequency shift keying which are preferentially used in Europe, in comparison are more secure against electro-magnetic influences (lightning, short-circuits, switching disturbances). They however require a longer transmission and detection time of the signal (15-20 ms). These channels are especially suited for the simple permissive under-reach transfer trip technique, but are also used for permissive over-reach (directional comparison). In any event, the signal path should be separated from the protected line (coupling to a parallel line or coupling between two systems).

The suitability of the release technique is limited when the PLC-signal must be transmitted across the protected line (no parallel path available). During a multiple-phase fault close to the line end, the signal may be so severely damped, that it can no longer be received at the remote station.

Accordingly, the permissive under-reach transfer trip or permissive over-reach techniques can in this case only be used when tripping in the second zone is permitted for faults close to the remote end, with severe signal attenuation.

The blocking technique is better suited for this application, because the protection is released for tripping in the case of a fault on the line, and signal transmission failure.

The unblocking technique combines the permissive over-reach and blocking methods.

Normally, during a fault on the line the over-reach zone at the remote end is released by keying from the monitoring frequency to the release frequency (in this case unblock signal). If a signal channel failure occurs at the same time as fault detection via the protection, this is then interpreted as signal attenuation during a fault on the line, and the over-reach zone is again released for a short time interval.

---

<sup>1</sup> PLC is the abbreviation for the technique of signal transmission with power line carrier frequencies.

**Table 5.1** Distance protection with teleprotection, comparison of various techniques

		Permissive under-reach via zone extension	Permissive over-reach	Blocking	Unblocking
Preferred application	Signal transmission:	Dependable signal transmission channel: <i>PLC with frequency shift keying</i> inter-circuit coupling in case of double circuit lines or to transmit via separate line to avoid transmission through the fault location. <i>Microwave radio</i> , especially digital (PCM) <i>Fibre-optic channel</i>		Channel with high availability (only required during external faults) <i>Amplitude modulated PLC</i> , single-phase coupling to the protected circuit is acceptable (the same frequency for all line ends is allowed)	Only with <i>voice frequency channels and frequency shift keying</i>
	Line configuration	Typical for <i>medium and long lines</i> (on short lines only with quadrilateral characteristics and when fault resistances low)	<i>Short lines</i> specially when high fault resistances can be expected. Teed and tapped lines.	<i>All line types</i> (US practice)	<i>Only EHV lines</i>
Advantages		Simple technique. Under-reach zone is independent of the signal transmission. No co-ordination of zones and times with the opposite end required. (No restrictions regarding the combination with other manufacturers)	No zone over-reach difficulties due to CVTs or high resistance faults with high line loading (see 3.5.1) May be used on extremely short lines, below the minimum setting value. No problems with regard to parallel line coupling.	←	←
Disadvantages		Reach problems on double-circuit lines, teed lines, tapped lines. Parallel line coupling and intermediate in-feed effects must be observed. Low fault resistance coverage with circle zone characteristics. Cannot be used on lines with weak in-feed.	Zone and time-co-ordination with the opposite end is required. Fault clearance is dependent on the signal transmission channel (Can be avoided by using an additional independent under-reaching zone.) Supplement for weak in-feeds required (echo).	← except that no supplement for weak in-feed is required. Channel supervision is not possible!	Same aspects as with permissive over-reach. During faults in the protected zone and transmission failure due to attenuation at the fault location, tripping however ensured (unblock logic)

The unblocking technique is therefore also suited for applications, where the signal must be transmitted across the protected line. It also has an advantage over the blocking technique, as it provides continuous monitoring of the signal channel by means of a quiescent signal. A power line carrier with voice frequency channel and frequency shift keying is required.

Microwave radio is suitable for both permissive under-reach transfer trip and blocking systems.

In the case of fibre-optic communication, it is common practice to select a release method, as the transmission channel is fast and dependable.

In urban cable systems, pilot wire connections are often available (control channels and telephone channels). In this case, a pilot wire mode comparison protection can be used as a special variant.

In table 5.1 an overview of the selection criteria is listed.

### *Digital signal transmission*

Classical teleprotection signal transfer (PLC, analogue microwave radio, pilot wires) are point to point connections with constant signal transmission times. The co-ordination times for the signal comparison logic in the protection can in this case be matched accurately down to milliseconds.

With digital signal transmission, dedicated optical fibres or a separate microwave radio channel can be allocated to the protection, resulting in similar defined signal transmission times. Increasingly however, the available digital communication network must be used for the protection signal transmission and time variations due to channel switching must be expected.

In this case, the permissive under-reach transfer trip, where no co-ordination of the release, delay or blocking times of both line ends is required, is best suited. At worst a delayed trip will ensue.

Blocking techniques cannot be applied here.

With directional comparison protection, a co-ordination of the echo circuit and the transient blocking must be taken into account.

In all cases the transfer via the data network must be carefully checked with regard to the availability and security of the channels.

### **5.1.5 Instrument transformer requirements**

Current and voltage transformers must comply with a defined minimum accuracy and transient behaviour to enable the distance protection to measure selectively and fast.

In particular, the distortion of the measured signals due to CT-saturation and superimposed discharge oscillations of CVT's must remain within defined limits [5.3].

### Current-transformers

For the steady state transformation behaviour of current-transformers, with pure AC-current and no DC-component, the Standard IEC 60044-1<sup>1</sup> applies [5.4].

With this standard, the designation of the CT's for protection purposes starts with the maximum combined error (5 or 10%) at the short-circuit limit current, then the letter P (for protection) and finally the accuracy limit factor (*ALF*).

Two accuracy classes are defined:

**Table 5.2** CT-classes according to IEC 60044-1

Accuracy class	Current error at rated current $I_N$	Phase displacement $\delta$ at rated current $I_N$	Combined error at $ALF * I_N^*$
5P	$\pm 1\%$	$\pm 60$ minutes	5%
10P	$\pm 3\%$	-	10%

\* *ALF* designates the accuracy limit factor of the CT

As a whole, a protection current transformer is determined by the following data:

*Rated transformation ratio:*

$I_{Pn}/I_{Sn}$ , e.g. 600/1 A or 600/5 A

Rated power  $P_N$ :

Power provided by the CT on the secondary side at rated current and rated burden, e.g. 30 VA

*Accuracy class:*

5P or 10P

*Accuracy limit factor:*

*ALF* (e.g. 10 or 20)

This multiple of the rated current, without DC-component, can be transformed by the CT with the defined accuracy class, if the connected burden equals the rated burden ( $\cos \varphi = 1$ ).

With larger current the CT will saturate and distort the secondary current.

*Secondary winding resistance:*

$R_{CT}$  in ohm

<sup>1</sup> Formerly IEC 185

*Example 5.2:*

Protection current transformer: 400/1 A; 5P10; 30 VA;  $R_{CT} = 6.2 \Omega$

The accuracy limit factor  $ALF$  of the CT only applies when the rated burden is connected. If a smaller burden is connected, an increased operating accuracy limit factor  $ALF'$  results:

$$ALF' = ALF \cdot \frac{P_i + P_{Bn}}{P_i + P_B} = ALF \cdot \frac{R_{CT} + R_{Bn}}{R_{CT} + R_B} \quad (5-6)$$

Rated CT-burden:  $P_{Bn}$

Internal burden of the CT:  $P_i = R_{CT} \cdot I_{2n}^2$

Actual connected burden:  $P_B = R_B \cdot I_{2n}^2$   $R_B = R_L + R_R =$  burden resistance

$R_L =$  burden resistance of the connecting leads

$R_R =$  burden resistance of the relay

Due to the increased accuracy, the class 5P is in general used for distance protection.

*Class C according to ANSI/IEEE C57.13 [5-5, 5.6]*

In this American standard the CT is dimensioned such that the transformation error does not exceed a value of 10% in the range from 1 to 20 times nominal secondary current ( $I_{2n}$ ). The class definition C states the secondary terminal voltage at 20 times  $I_{2n}$  and the secondary winding resistance  $R_{CT}$ . This however only applies to 5A CTs generally used in the US. For example, C200 with  $R_{Bn} = 2 \text{ Ohm}$  specifies a rated terminal voltage of  $U_{Bn} = 20 \times 5A \times 2 \text{ Ohm} = 200V$ . In accordance with IEC class P this would correspond to:  $P_{Bn} = 5^2 \cdot 2 = 50 \text{ VA}$ ,  $ALF \geq 20$ .

This conversion can however only be approximate, as the definition of the measuring error is not equivalent.

The actual operating accuracy limit factor  $ALF'$  can be calculated with Equation (5-6) in the same way as with the IEC standard specification.

*Transient behaviour of the current transformer*

In figure 5.4 the simplified equivalent circuit of a current-transformer is shown.

The flux-density of the CT is proportional to the integral of the secondary voltage across the CT magnetising inductance  $L_m$ :

$$B \sim \int (u_2(t) \cdot dt) = (R_{CT} + R_B) \cdot \int i_2(t) \cdot dt,$$

and thereby proportional to the area below the short-circuit current. The DC-component in the short-circuit current therefore results in a single-sided transient magnetisation increase of the CT, up to a multiple of the AC-component, corresponding to the time constant defined by the short-circuit loop (network time constant  $T_N$ ) (figure 5.5). To allow for this, the current transformers must have significantly larger dimensions.

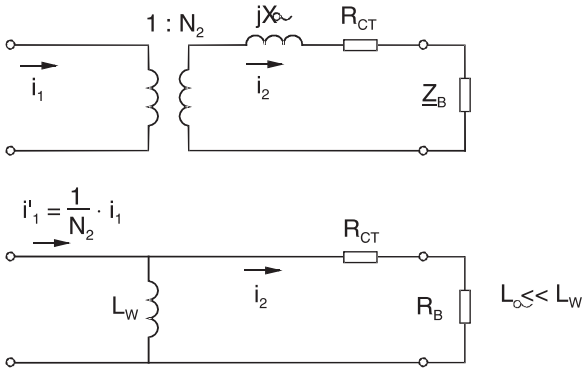


**Figure 5.4**  
Current-transformer  
equivalent circuit

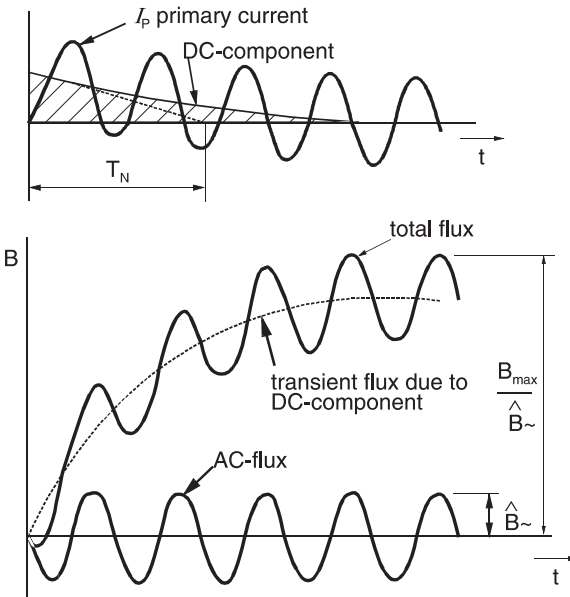


**Figure 5.5**  
Course of the CT-flux  
in the case of off-set  
short-circuit current

The course of the flux-density is defined by the following equation [5.9, 5.10]:

$$\frac{B}{\hat{B}_{\sim}} = 1 + \frac{\omega \cdot T_N \cdot T_S}{T_N - T_S} \left( e^{-\frac{t}{T_N}} - e^{-\frac{t}{T_S}} \right) \quad (5-7)$$

The maximum value:

$$\frac{B_{\text{Max}}}{\hat{B}_{\sim}} = 1 + \omega \cdot T_S \cdot \left( \frac{T_N}{T_S} \right)^{\frac{T_S}{T_S - T_N}} \quad (5-8)$$



is reached at

$$t_{B \max} = \frac{T_N \cdot T_S}{T_S - T_N} \cdot \ln \frac{T_S}{T_N} \quad (5-9)$$

$T_N$  is the network time constant (DC-component time constant) for the applicable short-circuit loop.

$T_S$  is the CT secondary loop time constant. It is determined by the CT magnetising inductance  $L_m$  and the sum of the resistances in the secondary circuit.

$$T_S = \frac{L_W}{R_{CT} + R_B} = \frac{1}{\omega \cdot \tan \delta} \quad (5-10)$$

The secondary CT time constant therefore decreases as the angle error  $\delta$  increases.

This mainly occurs when the CT-core has incorporated air-gaps.

The following equations apply at 50 Hz (60 Hz):

$$T_S = \frac{10900}{\delta_{[\min]}} [\text{ms}] \quad \left( T_S = \frac{9083}{\delta_{[\min]}} [\text{ms}] \right) \quad (5-11)$$

It must be noted that the error angle stated in the CT-data sheet only applies if the connected burden equals the rated burden. If a smaller burden is connected, the error angle reduces and the CT time-constant increases. The increase in flux according to equation (5-7) determines the necessary over-dimensioning of the current transformer, to enable the transformation of the off-set short-circuit current. The ratio  $B_{\max}/\hat{B}$  corresponds to the transient over-dimensioning factor  $K_{TP}$ , that has to be applied.

If the CT has to transform without saturation up to the instant  $t_s$ , then  $t = t_s$  must be set in equation (5-7). If the CT is not allowed to saturate for the duration of the entire short-circuit, then the CT must be dimensioned to allow for the maximum flux, according to equation (5-8).

### De-magnetising

The short-circuit current is switched off by the circuit-breaker at the zero-crossing instant of the current. At this point the flux is at a maximum. Furthermore, following a fast trip, the CT may still be heavily magnetised due to the DC-current component.

The de-magnetisation takes place via a transient relaxing current in the secondary circuit of the CT with the secondary loop time constant  $T_S$ . The flux does not return to zero; a remanent flux  $B_R$  remains (figure 5.6):

$$B = B_R + (B_{\text{Max}} - B_R) \cdot e^{-\frac{t}{T_S}} \quad (5-12)$$

The remanent flux is reached after approx.  $t = 3 \cdot T_S$ . This remanence remains indefinitely in the switched-off state. Under service conditions it is dissipated a little, but the

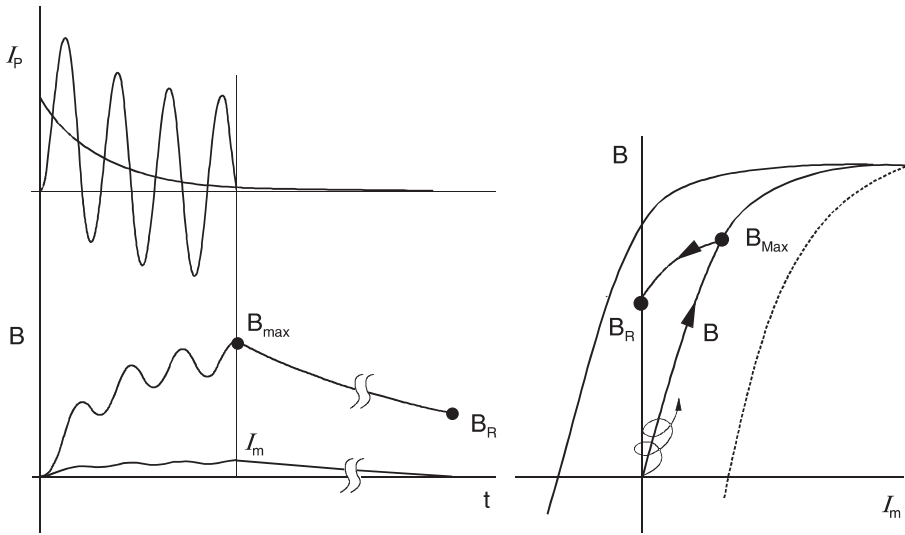


**Figure 5.6** Magnetising and de-magnetising of a current transformer

major part remains in the core until it is demagnetised [5-7]. Only one case of field measurement is known which however confirms substantial remanence at CTs, statistically distributed from 0 to 79% [5-8].

This long term remanence has hardly ever been considered in the CT dimensioning. This may be due to the fact that fully offset currents and high remanence coincide very seldom and practical problems related to this phenomenon have not been reported.

Consideration of this long term remanence would result in very high over-dimensioning of CTs which seems not to be justified for the general case.

The presently practiced dimensioning for the fully offset fault current contains some security margin, statistically seen, because full offset of the fault current is seldom observed.

CTs with air gaps, which have reduced or negligible remanence, may be used in EHV systems. This is discussed further below.

#### *Unsuccessful ARC*

Short term remanence must be considered with auto-reclosure.

In case of non-successful reclosure, the flux starts with a certain remanence when the line is switched on the persisting fault. In case of the most unfavourable switching instant, the flux increases with the same polarity and adds to the remanent flux.

In figure 5.7 the course of the flux for an entire fault cycle (C-O-C-O) is shown.

With a long dead time, the flux had enough time to decrease to the remanence point after clearance of the first fault, and will therefore start again from  $B_R$  (figure 5.7). If

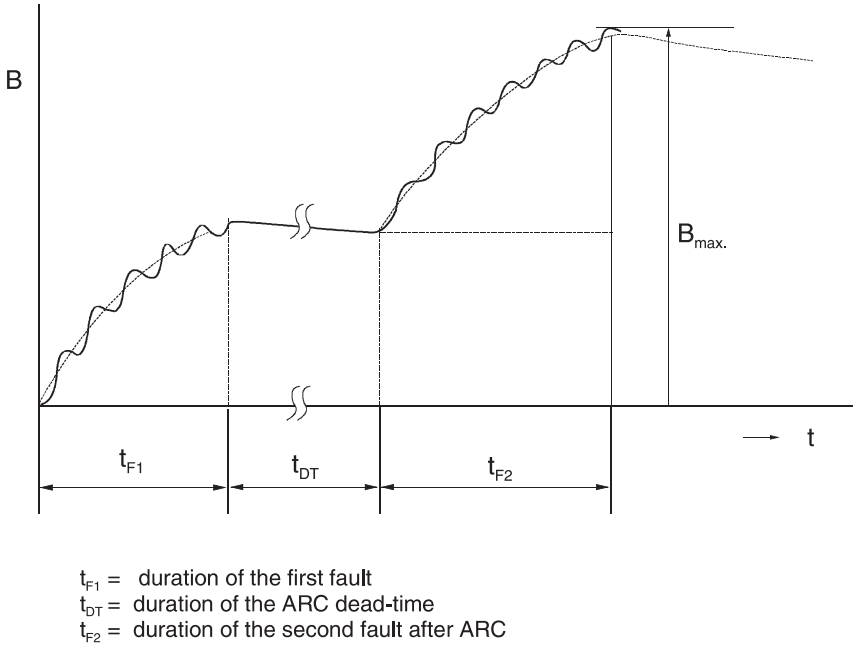


**Figure 5.7** Course of the CT-flux in case of unsuccessful ARC

the line is switched earlier onto the fault (fast auto-reclosure), the flux may not have decayed to  $B_R$  and will then increase from an intermediate value according to Equation (5-13).

For the flux reached at the end of the fault cycle the following equation applies:

$$\frac{B_{\text{Max}}}{\hat{B}_{\sim}} = \left[ 1 + \frac{\omega \cdot T_N \cdot T_S}{T_N - T_S} \left( e^{\frac{t_{F1}}{T_N}} - e^{\frac{t_{F1}}{T_S}} \right) \right] \cdot e^{-\frac{t_{DT} + t_{F2}}{T_S}} + \left[ 1 + \frac{\omega \cdot T_N \cdot T_S}{T_N - T_S} \left( e^{\frac{t_{F2}}{T_N}} - e^{\frac{t_{F2}}{T_S}} \right) \right] \quad (5-13)$$

#### *TP current-transformer classes*

The requirements for transient current-transformer performance with off-set short-circuit currents (Transient Performance Requirements) are defined in IEC 60044-6 [5.11].

This standard distinguishes four classes depending on the lay-out of the CT-core:

##### *Class TPS:*

A closed iron-core CT with small leakage-flux. The transformation behaviour is defined by the CT magnetisation curve (knee-point voltage, magnetising current) and the secondary winding resistance.

This lay-out corresponds to the class X according to British standard 3938 (1973). It is intended for differential protection.

*Class TPX:*

A closed iron-core CT without limitation of the remanence. This construction corresponds to CT's of the class P according to IEC 60044-1. TPX additionally specifies the transient performance.

*Class TPY:*

CTs with anti-remanence air gaps (remanence  $\leq 10\%$ ). Otherwise behaves like TPX.

*Class TPZ:*

CTs with linear core (remanence may be neglected). The stated transformation accuracy only applies to the AC-current component. The DC-current component of the short-circuit current is severely shortened.

The maximum errors for the individual classes are specified as follows:

**Table 5.3** CT transient performance classes acc. to 60044-6

Class	Error at rated current		Maximum error during rated short-circuit limit current
	Transformation	Angle	
TPX	$\pm 0,5\%$	$\pm 30$ Min	$\hat{\epsilon} \leq 10\%$
TPY	$\pm 1,0\%$	$\pm 60$ Min	$\hat{\epsilon} \leq 10\%$
TPZ	$\pm 1,0\%$	$\pm 180 \pm 18$ Min	$\hat{\epsilon} \leq 10\%$ (only AC part)

*Closed iron core CTs*

The closed iron core CTs transform DC- and AC-current components with high accuracy in the defined range. Their remanence is however very large ( $> 80\%$ ) (figure 5.8). The flux reached, following the transformation of a short-circuit current with DC offset, is therefore almost entirely trapped. It will slightly decay when the CT is subjected to load current. A substantial part however remains and can only be removed by demagnetisation.<sup>1</sup>

The consequence of this is, that following an unsuccessful ARC, with circuit-breaker closure at the most inopportune moment, the flux will almost double (figure 5.9). When applied with ARC, the CT must therefore be dimensioned with twice the core cross-section area.<sup>2</sup>

Most protection current transformers in the system are class P to IEC 60044-1 (in older systems the classes 1% and 3%, as the classes 5P and 10P used to be called, may be

<sup>1</sup> An AC voltage of 60% of the kneepoint voltage must be applied to reduce the remanent flux to less than 10% of saturation flux. Reduction of the voltage to zero over a period of about 3 s will demagnetise the core.

<sup>2</sup> The CT dimension reduction in relation to the permitted CT-saturation is not considered here.

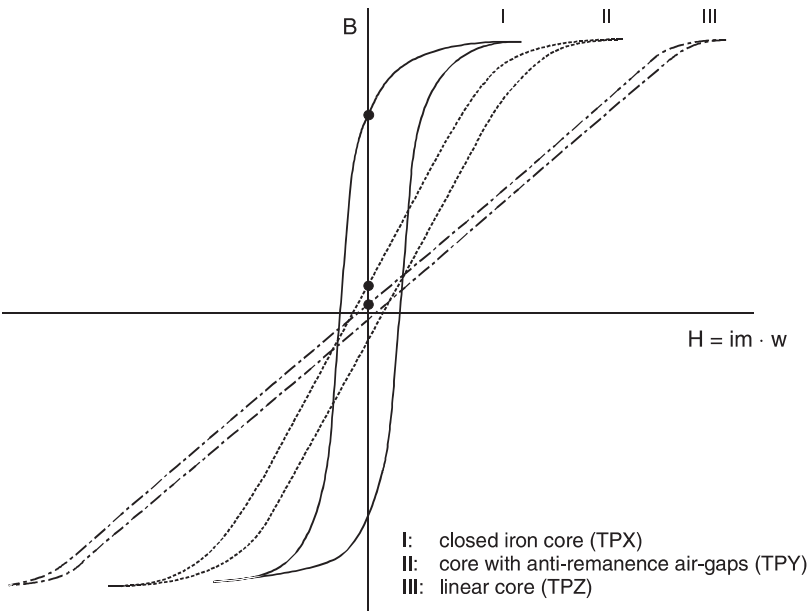


Figure 5.8 CT, magnetisation curve and point of remanence

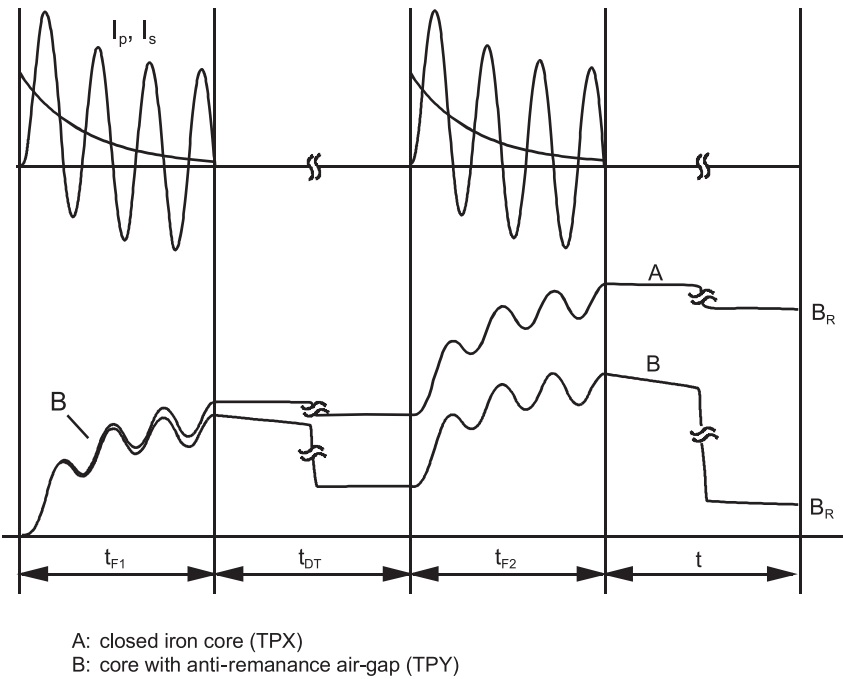


Figure 5.9 Course of the CT flux during unsuccessful ARC

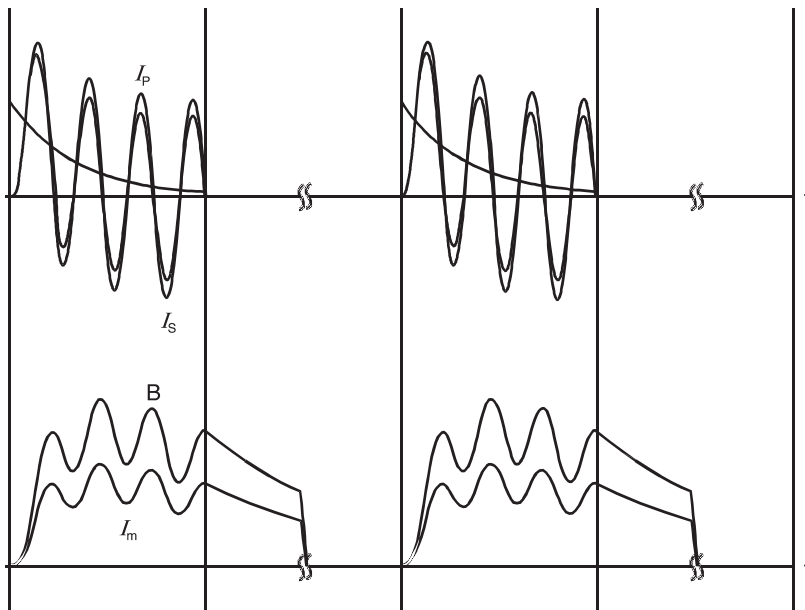
found). The lay-out with consideration of the DC-current component has only been done in the last thirty years, since the transient behaviour of the CT has been analysed more closely [5.5, 5.12, 5.13].

### *Current-transformers with air gaps*

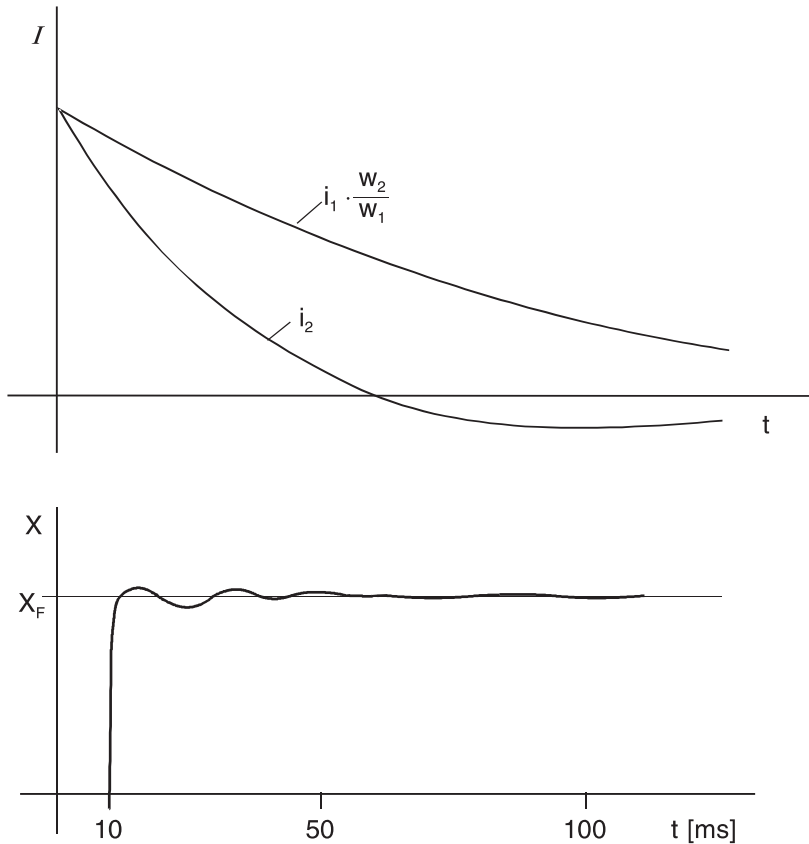
The air-gap in the CT-core dramatically reduces the magnitude of the remanent flux. At the same time, the time required for de-magnetisation is reduced to the order of seconds and less.

The secondary CT time-constant may however not be reduced too far, as otherwise the DC-component of the current will no longer be transformed correctly (refer to equation 5-28 below). Magnitudes of 200 to 300 ms are therefore the lower limit. The TPY CT accordingly only partially de-magnetises during the ARC dead-time (figure 5.9).

With large air-gaps (linear core according to TPZ), the DC-current component is so dramatically shortened during the transformation, that a substantially smaller flux increase results from the start. Furthermore, the core fully de-magnetises in less than 200 ms, as the CT time-constant only equals approx. 60 ms. This implies that even with the shortest ARC dead-time, the flux has decayed to zero, before re-closure takes place (figure 5.10). The core cross-section may therefore have a substantially smaller dimension. The partitioning of the core however requires more complex assembly and fixation. Accordingly a cost-comparison dependent on the required application is necessary (Open-air and GIS-system).



**Figure 5.10** Unsuccessful ARC, course of the flux in a linear CT-core (TPZ)

**Figure 5.11**

Shortening of the DC-component in the short-circuit current by a TPZ-CT and influence on the distance measurement

The TPZ core only transforms the AC-component of the current with the specified accuracy. The DC-component of the current no longer corresponds to the primary system conditions due to the shortened time-constant. As a result thereof, an additional transient error arises in conventional distance relays, that utilise a line replica (figure 5.11).

For this reason, the TPZ-core is not used outside Europe. With the numerical relays 7SA this transient error may be neglected due to the numerical filtering of the measured quantities

In Germany, linear cores are in widespread use, especially in EHV networks.

It must however be noted that in the case of TPZ-cores, a large de-magnetisation current arises, after the short-circuit current has been switched off. The initial value corresponds to the CT magnetisation current at the instant that the primary current is interrupted. The time-constant of the decay equals the CT secondary loop time-constant (figure 5.10).

This de-magnetisation current causes an extension of the re-set time in conventional relays, if the current starting elements have sensitive settings (e.g. with under-impedance starting or with circuit-breaker failure protection). The numerical relays 7SA are hardly influenced by this, as the DC-component of the current is almost entirely filtered out.

### Lay-out of the current transformer

Dimensioning of CTs has to consider the transient performance. In this context, the off-set (DC component) of the fault current has a major influence and requires substantial over-dimensioning. This is now discussed for CTs without and with air gaps.

#### TPX class CT

Initially the typical CT with closed iron core 5P or 10P according to 60044-1 is examined. For these, the class TPX is specified in relation to the transient behaviour. The CT secondary loop time-constant  $T_S = L_W / \sum R_2$  is in this case always large in comparison to the system time-constant  $T_N$ . Usually  $T_S$  is of the order of a few seconds, while  $T_N$  in the system only assumes values over 100 ms in extreme cases.

Equation (5-8) in this case with  $T_S \gg T_N$  simplifies to the following equation:

$$\frac{B_{\text{Max}}}{\hat{B}_{\sim}} = 1 + \omega \cdot T_N \quad (5-14)$$

To ensure saturation-free transformation of the fully off-set short-circuit current for the complete short-circuit duration, the CT would have to be sized with a corresponding transient over-dimensioning factor [5.9 to 5.13].

$$K_{\text{TF}} = \frac{B_{\text{Max}}}{\hat{B}_{\sim}} = 1 + \omega \cdot T_N = 1 + \frac{X_N}{R_N} = 1 + \frac{X_S + X_L}{R_S + R_L} \quad (5-15)$$

$T_N$  is the DC-component time-constant for the applicable short-circuit loop, calculated from the value of the source-impedance ( $X_S$ ,  $R_S$ ) and the line impedance ( $X_L$ ,  $R_L$ ).

From equations (5-6) and (5-15) the required accuracy limit factor of the CT can now be determined:

$$ALF = \frac{I_{\text{SCp}}}{I_{\text{np}}} \cdot \frac{R_{\text{CT}} + R_{\text{B}}}{R_{\text{CT}} + R_{\text{Bn}}} \cdot K_{\text{TF}} \quad (5-16)$$

In this equation,  $I_{\text{SCp}}$  is the maximum primary AC short-circuit current and  $I_{\text{np}}$  the primary rated current of the CT.

Near generators and transformers, and in the EHV-system in general, the X/R-ratio of the short-circuit impedances is generally large. Accordingly, large over-dimensioning factors of  $K_{\text{TF}} = 30$  (with  $T_N = 100$  ms) and more may result.

The implementation of such large CTs is mostly not possible due to cost constraints, especially with enclosed switch-gear, where the CT is situated inside the enclosure.



It is therefore expected of the protection to tolerate a large amount of saturation.

#### *Behaviour of the distance protection with CT-saturation*

During CT-saturation, a portion of the current is missing, so that principally ( $Z = U/I$ ) an impedance which is too large, is measured. This implies that the zone reach is reduced. This is acceptable for close-in faults, because the distance to the zone limit is large.

For faults close to the zone limit, an under-reach is however not permitted, as the protection in this case would only trip in the second zone, i.e. with a time-delay.

The dimension of the CT must accordingly be such, that during faults at the end of the line, there is no saturation during the entire measuring time.

$$K'_{TF} = 1 + \frac{\omega \cdot T_N \cdot T_S}{T_N - T_S} \left( e^{-\frac{T_M}{T_N}} - e^{-\frac{T_M}{T_S}} \right) \quad (5-17)$$

In the case of closed iron core CTs, the condition  $T_S \gg T_N$  applies. Equation 5-17 can be simplified as follows:

$$K'_{TF} = 1 + \omega \cdot T_N \cdot \left( 1 - e^{-\frac{T_M}{T_N}} \right) \quad (5-18)$$

The corresponding diagram is shown in Fig. 5.12.

#### *Lay-out of the TPX-CT in practice*

To reduce the CT size for close-in faults, a limited amount of saturation is permissible.

The CT must however transform sufficient current to ensure tripping without additional delay. The required necessary minimum over-dimensioning factor is known from type-tests.

1) Condition for close-in faults without ARC

$$ALF'_1 \geq a \cdot \frac{I_{SC \text{ max.-close-in-fault}}}{I_N} \quad (5-19)$$

For the over-dimensioning factor  $a$ , the following values apply:

**Table 5.4** CT requirements of numerical distance relays (Siemens)

Relay type	System time-constant		
	$T_N < 30 \text{ ms}$	$T_N < 50 \text{ ms}$	$T_N < 100 \text{ ms}$
7SA511	$a = 2$	$a = 2$	$a = 3$
7SA513	$a = 2$	$a = 2$	$a = 2$
7SA522 and 7SA6xx	$a = 1$	$a = 2$	$a = 2$

## 2) Condition for fault close to the end of the line, without ARC

$$ALF'_2 \geq K'_{TF} \cdot \frac{I_{SC \text{ max.-line end}}}{I_{pn}} \quad (5-20)$$

During faults near the end of the reach of the under-reaching zone CT saturation should not cause a zone reduction as this would lead to delayed zone 2 tripping. It is good relaying practice to design the CT so that it transforms saturation free at least until the end of the measuring time. The necessary over-dimensioning factor  $K'_{TF}$  is calculated with the equation (5-17) or (5-18), using the known system data.

The following values may be used as the minimum necessary measuring time including security margin:

$$\begin{array}{ll} 7SA511: & T_M = 35 \text{ ms} \\ 7SA513, 7SA522, 7SA6: & T_M = 25 \text{ ms} \end{array}$$

The over-dimensioning factors calculated with equation (5-17) are shown in figure 5.12.

It is apparent that due to the limiting of the saturation-free transformation time, a substantial reduction of the required CT dimension is achieved, especially for large system time-constants.

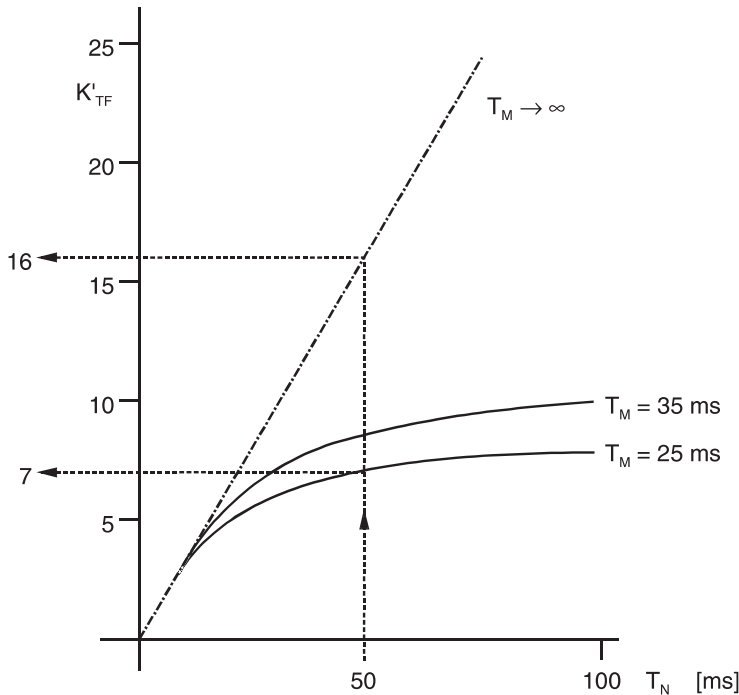


**Figure 5.12** Closed iron-core CT, over-dimensioning factor, saturation-free time limited to  $T_M$

For simple approximations without exact knowledge of the system data a value of 10 may be assumed for  $K'_{TF}$  to be on the safe side (refer to figure 5.12).

Type tests at the latest numerical relay series have shown that lower values are sufficient due to the shorter measuring time and higher tolerance against CT saturation. A value of  $K'_{TF} \geq 5$  may be assumed for the relays 7SA522 and 7SA6.

In any case, relay manuals or application guides of the manufacturers should be consulted for the actually valid dimensioning factors.

*For the simple short-circuit without ARC, the conditions 1) and 2) must be satisfied with regard to the CT-dimension.*

#### *Consideration of remanence*

To cope with remanence, a corresponding factor has to be added to the transient dimensioning factor. The resulting total dimensioning factor then is:

$$K_{\text{Total}} = K_{TF} \cdot K_{\text{Rem}} \quad \text{with} \quad K_{\text{Rem}} = \frac{1}{1 - \frac{\% \text{ remanence}}{100}} \quad (5-21)$$

If a higher CT remanence of 60 to 80% is assumed in addition to full offset of fault current, extremely high CT over-dimensioning would result. Under these circumstances TPY or TPZ cores are often employed. This is the case in some European countries where the CTs in EHV are designed for a non successful auto-reclosure COCO cycle, i.e. two successive faults [5-14]. The detailed design procedure is given in IEC60044-6 [5-11].

#### *Lay-out of the TPX class CT for an ARC-cycle*

As the TPX-CT does not de-magnetise during the ARC dead-time, the following minimum lay-out is required:

#### 3) Condition for close-in fault with ARC

The CT must completely transform the initial short-circuit current until tripping. For the second short-circuit current following reclosure onto the fault, *condition 1)* additionally applies.

For the total C-O-C-O cycle we get:

$$K'_{TF3} = 1 + \frac{\omega \cdot T_N \cdot T_S}{T_N - T_S} \left( e^{\frac{T_{FI}}{T_N}} - e^{\frac{T_{FI}}{T_S}} \right) + a \quad (5-22)$$

Assuming  $T_S \gg T_N$ , the following simplified equation results:

$$K'_{TF3} = 1 + \omega \cdot T_N \cdot T_S \cdot \left( 1 - e^{\frac{T_{FI}}{T_N}} \right) + a, \quad (5-23)$$

whereby the time-constant for close-in faults must be substituted for  $T_N$ .

The operating accuracy limit factor is obtained:

$$ALF'_3 \geq K'_{TF3} \cdot \frac{I_{SC \text{ max.-line end}}}{I_{np}} \quad (5-24)$$

#### 4) Conditions for faults close to the end of the line with ARC

In this case the current transformer must transform the short-circuit current of the initial fault at the zone limit completely, and the subsequent fault current after re-closure up to the end of the relay measuring time.

The following transient dimensioning factor is obtained with this:

$$K'_{TF4} = \left[ 1 + \frac{\omega \cdot T_N \cdot T_S}{T_N - T_S} \left( e^{-\frac{T_{F1}}{T_N}} - e^{-\frac{T_{F1}}{T_S}} \right) \right] + \left[ 1 + \frac{\omega \cdot T_N \cdot T_S}{T_N - T_S} \left( e^{-\frac{T_M}{T_N}} - e^{-\frac{T_M}{T_S}} \right) \right] \quad (5-25)$$

The simplified equation with  $T_S \gg T_N$  is:

$$K'_{TF4} = \left[ 1 + \omega \cdot T_N \cdot \left( 1 - e^{-\frac{T_{F1}}{T_N}} \right) \right] + \left[ 1 + \omega \cdot T_N \cdot \left( 1 - e^{-\frac{T_M}{T_N}} \right) \right] \quad (5-26)$$

The equation for the operational accuracy limit factor therefore is:

$$ALF'_4 \geq K'_{TF4} \cdot \frac{I_{SC \text{ max.-line end}}}{I_{np}} \quad (5-27)$$

*The current transformer lay- out for an ARC-cycle must satisfy the conditions 3) and 4).*

*Example 5.3:*

Given that: 110 kV overhead line and system in-feed according to figure 5.13. For the connection between the relay and the CT an 80 m copper cable, 2,5 mm<sup>2</sup> was used. The CT should have a ratio of 600/1 A. A 5P, 30 VA current transformer is recommended (20% internal burden).

Question 1:

How large must the accuracy limit factor be if a 7SA6 distance relay is used?

Question 2:

How large must the accuracy limit factor be if the CT must be dimensioned for an ARC-cycle C-O-C-O? (The circuit-breaker has an operating time of 60 ms)

Solution:

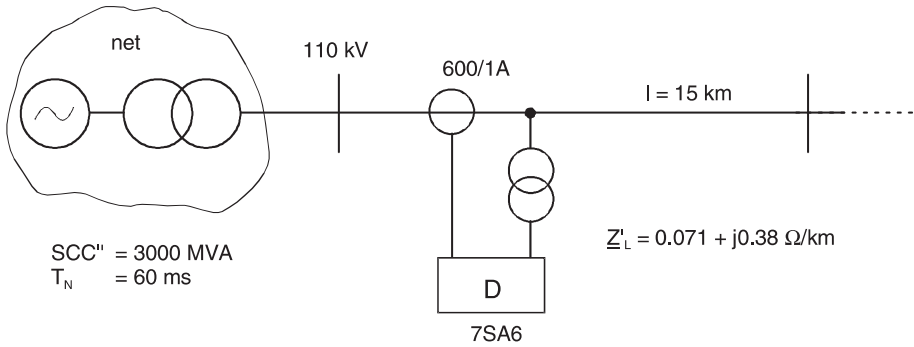


**Figure 5.13** System configuration for the calculation example

Condition 1): close-in fault without ARC

The maximum short-circuit current for the close-in fault is:

$$I_{SC \max.} = \frac{SCC''}{1.1 \cdot \sqrt{3} \cdot U_N} = \frac{3000 \text{ MVA}}{1.1 \cdot \sqrt{3} \cdot 110} = 14.4 \text{ kA}$$

With  $T_N = 60 \text{ ms}$ , in the case of 7SA6:  $a = 2$ .

Thereby the following results from (5-19):

$$ALF'_1 = 2 \cdot \frac{14400}{600} = 48$$

Condition 2): fault at the zone limit with-out ARC

The source impedance is:

$$X_S \approx Z_S = \frac{1.1 \cdot U_N}{\sqrt{3} \cdot I_{SC}} = \frac{1.1 \cdot 110 \text{ kV}}{\sqrt{3} \cdot 14.4 \text{ kA}} = 4.85 \text{ } \Omega$$

$$T_N = \frac{L_S}{R_S} = \frac{X_S / \omega}{R_S}$$

Thus:

$$R_S = \frac{X_S}{\omega \cdot T_N} = \frac{4.85}{314 \cdot 0.06} = 0.26 \text{ } \Omega$$

For a fault at the zone limit (85% of line length), the following line data results:

$$X_L = 0.85 \cdot 15 \cdot 0.38 = 4.8 \text{ } \Omega \text{ and}$$

$$R_L = 0.85 \cdot 15 \cdot 0.071 = 0.91 \text{ } \Omega$$

The corresponding short-circuit current is:

Time-constant of the short-circuit current:

$$I_{SC \text{ balance point}} = \frac{1.1 \cdot U_N / \sqrt{3}}{Z_S + Z_L} \approx \frac{1.1 \cdot U_N / \sqrt{3}}{X_S + X_L} = \frac{1.1 \cdot 110 / \sqrt{3}}{4.85 + 4.8} = 4.85 \text{ kA}$$

$$T_N = \frac{(X_S + X_L) / \omega}{R_S + R_L} = \frac{(4.85 + 4.8) / 314}{0.26 + 0.91} = 26 \text{ ms}$$

With  $T_M = 25 \text{ ms}$ , the following is obtained from (5-18):

$$K'_{TF4} = 6.0 \quad \text{and} \quad ALF'_2 = 6.0 \cdot \frac{7240}{600} = 73$$

The CT must therefore be laid out according to condition 2.

The resistance burden of the connecting cable is:

$$R_L = 2 \cdot \frac{\rho \cdot l}{Q} = \frac{0.0179 \cdot 80}{2.5} = 1.15 \, \Omega$$

The relay burden of the 7SA6 is:

$$R_R < 0.1 \, \Omega$$

The total burden therefore amounts to:

$$R_B = 1.25 \, \Omega$$

The nominal accuracy limit factor is calculated as follows:

$$ALF \geq \frac{6 + 1.25}{6 + 30} \cdot 73 = 14.7$$

In this case, without ARC, the preferential value  $ALF = 20$  may be selected.

Condition 3): close-in fault with ARC

For the initial short-circuit duration, in this case the protection and circuit-breaker operating times must be summated:

$$T_{F1} = 25 + 60 = 85 \text{ ms}$$

Substituting this, and  $T_N = 60 \text{ ms}$  into equation (5-23):  $K'_{TF3} = 15 + 2 = 17$

$$ALF'_3 = 17 \cdot \frac{14400}{600} = 408$$

Condition 4): fault at the zone limit with ARC

With  $T_{F1} = 85 \text{ ms}$ ,  $T_N = 26 \text{ ms}$  and  $T_M = 25 \text{ ms}$  the following is obtained from (5-26):

$$K'_{TF4} = 9 + 6 = 15$$

$$ALF'_4 = 15 \cdot \frac{7240}{600} = 181$$

The lay-out of the CT for the ARC-cycle must in this case be in compliance with the close-in fault, i.e. condition 4):

$$ALF \geq \frac{6 + 1.25}{6 + 30} \cdot 408 = 82$$

In this case, a larger CT should be used, e.g. 60 VA (15 VA internal burden) and double the ratio e.g. 1200/1 A.

For the operating accuracy limit factor, the following would result:

$$ALF'_3 = 17 \cdot \frac{14400}{1200} = 204$$

The rated accuracy limit factor would therefore be:

$$ALF \geq \frac{15 + 1.25}{15 + 60} \cdot 204 = 44$$

A practical value would be  $ALF = 50$ .

The resulting CT 60 VA; 1200/1;  $ALF > 50$  is very large. In this case a linear core is recommended.

#### *Lay-out of the TPY class CT*

The TPY-CT is dimensioned for the entire short-circuit sequence, i.e. in conjunction with ARC for the short-circuit – dead-time – short-circuit – sequence (C-O-C-O).

Due to the lower remanence and the shorter CT time constant, the core is partially demagnetised during the dead-time. The over-dimensioning factor therefore is smaller in comparison to the closed iron core.

The shorter the secondary transformer time constant  $T_s$  is in comparison to the duration of the dead-time ( $T_{DT}$ ), the larger the flux decay is during the dead-time. To maintain the error limit of 10%, the over-dimensioning factor may however not exceed the following limit:

$$K_{TF} \leq 0.1 \cdot \omega T_s \quad (5-28)$$

Equation (5-13) must be applied for the dimensioning, if the total short-circuit cycle must be transformed without saturation. It suffices if the second short-circuit current is only transformed until the end of the relay measuring time.

In this case  $T_{F2} = T_M$  must be used:

$$K'_{TF} = \left[ 1 + \frac{\omega \cdot T_N \cdot T_s}{T_N - T_s} \left( e^{\frac{T_{FI}}{T_N}} - e^{\frac{T_{FI}}{T_s}} \right) \right] \cdot e^{\frac{T_{DT} + T_M}{T_s}} + \left[ 1 + \frac{\omega \cdot T_N \cdot T_s}{T_N - T_s} \left( e^{\frac{T_M}{T_N}} - e^{\frac{T_M}{T_s}} \right) \right] \quad (5-29)$$

*Example 5.4:*

Given that: Data as in the previous example (figure 5.13).

TPY-CT with  $T_S = 0.5$  s

Dead-time:  $T_{DT} = 0.4$  s

Solution:

Condition 1): close-in fault with ARC

From (5-29) and  $T_N = 60$  ms,  $T_{F1} = 85$  ms and  $T_M = 25$  ms:

$$K'_{TF1} = [13.9] \cdot 0.43 + [7.5] = 13.5$$

$$ALF'_1 = 13.5 \cdot \frac{14400}{600} = 324$$

Condition 2): fault at the zone limit

From (5-29) and  $T_N = 26$  ms,  $T_{F1} = 85$  ms and  $T_M = 25$  ms:

$$K'_{TF2} = [7.9] \cdot 0.43 + [5.9] = 9.3$$

$$ALF'_2 = 9.3 \cdot \frac{7240}{600} = 112$$

In this case, as expected, the close-in fault sets the more severe demands with regard to the dimensioning of the CT.

The corresponding nominal accuracy limit factor is:

$$ALF \geq \frac{6 + 1.25}{6 + 30} \cdot 324 = 65.$$

i.e.  $ALF = 80$  would be the next larger preferential value.

A calculation for comparison with a closed iron core CT, i.e. with  $T_S = 5.0$  instead of 0.5 s, returns the following results:

$$K'_{TF1} = [15] \cdot 1 + [7.4] = 22.4$$

With the TPY-CT a reduction of the core cross-section by  $(1 - 13.5/22.4)$  i.e. about 40% results.

*Lay-out of the TPZ class CT*

Linear core CTs are dimensioned to be able to transform the short-circuit current without saturation during the worst case conditions. This implies that the CT's size is determined with equation (5-8):

$$K_{TF}^{**} = 1 + \omega \cdot T_S \cdot \left( \frac{T_N}{T_S} \right)^{\frac{T_S}{T_S - T_N}} \quad (5-30)$$



*Example 5.5:*

Given that: Line and system in-feed according to figure 5.13. How large is the over-dimensioning factor, when a TPZ core is used?

The CT must comply with IEC 60044-6 and have an error angle of  $\delta = 3^\circ$ .

Solution:

Substituting  $\delta = 3^\circ$  into equation (5-11):

$$T_S = 61 \text{ ms.}$$

The system time constant for the close-in fault is:  $T_N = 60 \text{ ms}$ .

From (5-30):  $K'_{TFI} = 8$ .

As the CT is fully de-magnetised during the dead-time, a very small over-dimensioning factor which also applies to the unsuccessful ARC-cycle results.

Comparatively the following reduction in core cross-sections result:

- by  $(1 - 8/22.4)$  i.e. 64% compared to the TPX class CT
- by  $(1 - 8/13.5)$  i.e. 40% compared to TPY class CT.

In the case of large short-circuit currents with long time-constants, especially when ARC is implemented, the TPZ class CTs provide a substantial space saving.

This is especially advantageous in the case of enclosed switch-gear.

The higher costs due to the complex assembly and fixation of the core must be taken into account.

In the following table the technical data of typical linear core CTs used in the German HV and EHV systems is shown.

**Table 5.5** Typical specifications of TPZ current transformers (Germany)

Voltage level	$I''_{SC}$	$T_N$	Ratio	Magnitude error at $I_N$	Angle error	Rated burden
110 kV	24 kA	25 ms	1200/1	$\pm 1\%$	180 min	20 W
380 kV	80 kA	75 ms	2400/1 1200/1	$\pm 1\%$	180 min	20 W 5 W

## Voltage transformers

The voltage transformers convert the primary system voltage to the typical secondary rated voltage 100 or 110 V.

In practice, inductive and capacitive voltage transformers are implemented.

*Inductive VTs* function according to the transformer principle. They provide almost ideal signals with regard to accuracy and transient performance during the fault, for the distance protection. The course of the primary voltage is very accurately replicated, even during severe voltage collapses from 100% to 1% rated voltage. The inductive VT is therefore the preferred type, especially in medium and high voltage applications. In Germany, it is also pre-dominant at the EHV level.

*Capacitive VTs (CVTs)* consist of a capacitive voltage divider from high to medium voltage and an output transformer which further converts to the low voltage. The CVT is more cost-effective at EHV levels and additionally provides the possibility to couple the PLC via the capacitive divider to the line. No separate HF-coupling is therefore required, as is the case with the inductive VT. On the other hand, the discharge of the isolated line is not that simple with CVTs, as the risk of ferro-resonance exists.

CVTs contain a number of stored energy components (capacitors, inductors), which must be charged/discharged during voltage changes. During primary voltage impulse changes, transients arise, which are super-imposed on the secondary voltage [5.15]. During close-in faults with a voltage collapse down to a few percent of nominal voltage, the interference signal may be a multiple of the system frequency short-circuit voltage. This influence is particularly critical when the line is short, and accordingly the zone limit must be measured with small voltage signals. On longer lines the use of CVTs is in general not critical as the voltage collapse is not so severe during faults close to the zone limit. In any event, the ratio of the source impedance to the line impedance is decisive, as this determines the voltage at the relay location during faults close to the end of the line. Usually the interference signals have a frequency of below 25 Hz or above 250 Hz. The numerical relays can therefore filter out these interferences well. Having regard to this, the influence of CVTs may be neglected for short-circuit voltages down to approx. 4% of nominal voltage. This corresponds to a maximum  $Z_S/Z_L$  ratio of 25.

In any event the transient behaviour of the CVT should be controlled. The manufacturers provide type-test reports, which show the transient behaviour during voltage collapse to zero for various fault inception angles (voltage maximum and minimum) and with varied secondary burden. For critical applications, in the past, tests had to be carried out in high voltage laboratories on the CVT with the associated protection [5.16].

Today it is possible to simulate the behaviour of the voltage transformer with a software model in the programs EMTP or NETOMAC. In this way it is possible to test the CVT in conjunction with the distance protection algorithm on a computer [5.17]. The parameters for the linear VT model can be supplied by the manufacturer.

*Inductive voltage transformers*

The special definitions for inductive voltage transformers are supplied by IEC 60044-2.

As a rule, single-phase isolated VTs are used. The second phase is earthed. The rated transformation ratio is then for example:

$$K_R = \frac{110000 \text{ V}}{\sqrt{3}} / \frac{100 \text{ V}}{\sqrt{3}} / \frac{100 \text{ V}}{3}$$

**Table 5.6** VT classes for protection acc. to IEC 60044-2

Class designations	Permissible error at $0.05 \cdot U_N$ and $1.0 \cdot U_N$	
	Voltage error $F_U$	Angle error $\delta$
3P	$\pm 3.0 \%$	120 minutes
5P	$\pm 6.0 \%$	240 minutes

All 3P and 5P protection CTs must additionally comply with one of the below VT measuring classes.

**Table 5.7** VT classes for measurement acc. to IEC 60044-2

Class designations	Permissible voltage error in % at $1.0 \cdot U_N$	Permissible angle error in minutes at $1.0 \cdot U_N$
0.1	0.1	5
0.2	0.2	10
0.5	0.5	20
1	1	30
3	3	Not determined

The second secondary winding with 100/3 V is only used if the displacement voltage must be measured by means of an open delta connection. In the case of full displacement of the star-point in an isolated or compensated system, 100 V will then be measured on the terminals connected to the open delta. Numerical relays are capable of calculating the displacement voltage internally,  $\underline{U}_E = \underline{U}_{L1} + \underline{U}_{L2} + \underline{U}_{L3}$ . This implies that the open delta winding may in this case be omitted for the distance protection and the directional earth-fault protection on the line. It is only of use for the complete monitoring of the voltage measuring circuit.

If two voltage transformers are configured in the V-connection, the two-phase isolated version is required. The nominal ratio then refers to the line voltage, e.g. 20 000/100 V.

A determination of the displacement voltage (the zero-sequence voltage) is principally not possible in this case.

The rating of the voltage transformers ranges from 10 to 300 VA. A large VA-rating is required for the electro-mechanical distance protection (up to 120 VA on short zone settings). In the case of static and numerical distance protection, the VT-burden amounts to less than 1 VA. Accordingly the size of the VT-rating depends on the other connected consumers.

The VT-classes defined in IEC 60044-5 for protection purposes, 3P and 6P, have relatively large accuracy limits. With HV and EHV it is common practice to provide a dedicated secondary winding for the protection. In this case class 3P is sufficient for the distance protection. If the same winding is used for measurement or metering, a class with higher accuracy may be considered.

#### *Capacitive voltage transformers (CVTs)*

Like inductive voltage transformers, they can be specified in relation to their transformation ratio and accuracy class.

**Table 5.8** Error limits of protective CVTs according to IEC 60044-5 (2004)

Class	Percent voltage (ratio) error % $U_N$			Phase displacement $\pm$ in minutes		
	at 2% $U_N$	at 5% $U_N$	at 100% $U_N$	at 2% $U_N$	at 5% $U_N$	at 100% $U_N$
3P	6.0	3.0	3.0	240	120	120
6P	12.0	6.0	6.0	480	240	240

The transient response of CVTs is however critical in particular with large voltage drops after fault inception (high SIR). Additional requirements must therefore be specified.

We will first study the influencing factors of the transient CVT behaviour and then derive a practical specification guide.

Figure 5.14 shows a single line diagram of a capacitive VT. The ferroresonance suppression circuit is designed to prevent sub-synchronous oscillations due to core saturation of the intermediate transformer during overvoltage conditions. It is assumed that the damping resistor in series with a resonant circuit is permanently connected (active suppression circuit). The resonant circuit is tuned to the system frequency and normally blocks current flow but gets conductive and enforces damping during abnormal frequencies. More sophisticated versions using air gaps or static circuits to switch in the damping circuit in case of overvoltage (passive suppression circuit) can improve the CVT transient behaviour, but are not considered here.

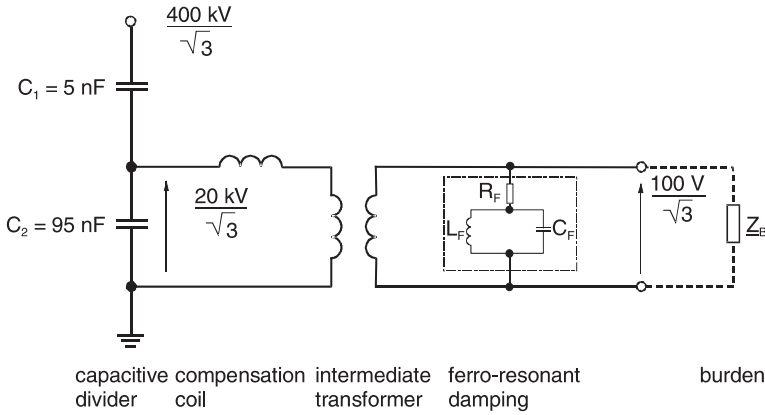
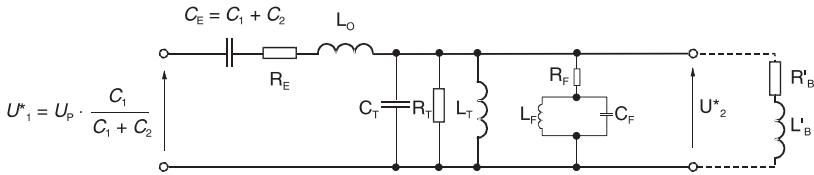


**Figure 5.14** Capacitive voltage transformer, basic circuit



typical values referring to  $\frac{20}{\sqrt{3}}$  kV:

$C_E = 100 \text{ nF}$	$R_F = 135 \text{ k}\Omega$	$U^*_1 = \frac{20}{\sqrt{3}} \text{ kV}$
$R_E = 2 \text{ k}\Omega$	$C_F = 33.7 \text{ nF}$	
$L_0 = 105 \text{ H}$	$L_F = 300 \text{ H}$	
$L_T = 4000 \text{ H}$		
$C_T = 600 \text{ pF}$	$Z_B = \left(\frac{U^*_2}{U_2}\right)^2 \cdot Z_B = \left(\frac{20/\sqrt{3}}{0.1/\sqrt{3}}\right)^2 \cdot Z_B = 40,000 \cdot Z_B$	

**Figure 5.15** Capacitive voltage transformer, equivalent circuit

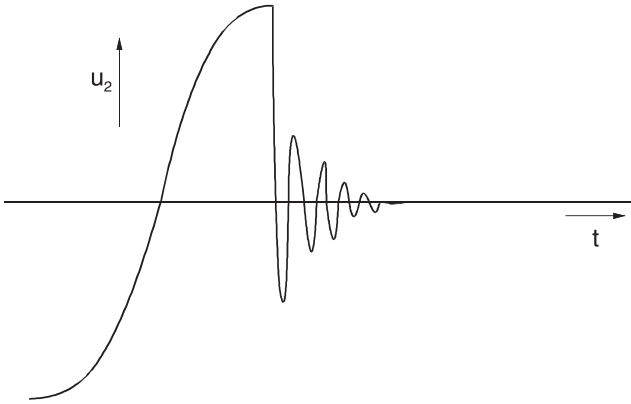
The corresponding replica circuit related to the intermediate voltage is shown in figure 5.15. For a better understanding, technical data of a typical CVT has been added. They refer to an extra high voltage CVT version with an intermediate voltage of  $20/\sqrt{3}$  kV.

Following a collapse of the primary voltage, different phenomena arise, depending on the fault inception angle.

### 1) Fault at the voltage maximum

Faults near the voltage maximum are caused by a insulation failure. They are predominant, in particular in cable networks.

In this case, the earth capacitance  $C_T$  of the intermediate transformer primary winding discharges via the compensation coil  $L_0$  into the short-circuit. A damped oscillation with a frequency of approx. 500-2000 Hz arises (figure 5.16). (A similar oscillation

**Figure 5.16**

Capacitive VT, discharge oscillation following fault-inception at the voltage maximum

also arises in case of the inductive VT, which however is less severe.) If the resistive burden increases, the oscillation is increasingly damped. Due to the relatively high frequency the oscillation can be filtered out effectively. It therefore has no influence on the numerical distance protection

### Fault at the voltage zero-crossing

Faults near voltage zero-crossing only occur with a lightning flash at this particular time instant or with switching onto a fault. The probability is quite low as the experience has shown. For the distance protection, this is the critical case, as we will see.

The main influencing factors are here the burden (magnitude and  $\cos \varphi$ ) and the ferro-resonance circuit.

### Operation without burden

Initially, the case where the VT only has a very small burden is assumed, i.e. it is practically operated without burden. This would be typical in case of static or numerical protection, when no additional burden is connected. In this case the energy stored in the intermediate transformer core dissipates via the capacitance of the capacitive divider  $C_E$  with a slow oscillation of between 5 and 10 Hz. The oscillation reaches its maximum value of between 10 to 20% of the voltage maximum prior to fault inception after approx. 25 to 50 ms.

The following formula applies to this transient behaviour:

$$\frac{U_L}{U_{L0}} = \frac{\omega}{\omega_N} \cdot e^{-\frac{t}{\tau}} \cdot \sin \omega t \quad (5-31)$$

$$\text{with } \omega = \sqrt{\frac{1}{L_T \cdot C_E}} \text{ and } \tau = \frac{2 \cdot L_T}{R_E}$$

*Example 5-6:* with application of the data from figure 5.15:

$$\omega = \sqrt{\frac{1}{4 \cdot 10^3 \text{ H} \cdot 100 \cdot 10^{-9} \text{ F}}} = 50 \frac{1}{\text{s}},$$

$$\text{i.e. } f = \frac{\omega}{2\pi} = \frac{50}{2\pi} = 8 \text{ Hz}$$

$$\tau = \frac{2 \cdot 4 \cdot 10^3 \text{ H}}{2 \cdot 10^3 \Omega} = 4 \text{ s}$$

The initial amplitude is:

$$\left( \frac{U_L}{U_{L0}} \right)_{t=0} = \frac{\omega}{\omega_N} = \frac{50}{314} \hat{=} 16\% \frac{U_N}{\sqrt{3}} \quad (5-32)$$

This low frequency oscillation can now also be largely eliminated by means of numeric fundamental wave filters. Therefore no significant influence results even for very small short-circuit voltage values.

#### *Loaded with resistive burden*

If a resistive burden is connected to the VT, the current in the capacitive divider is increased. In the case of the fault in the voltage zero-crossing, the resultant voltage drop across  $C_E$  is at a maximum. This implies that the stored energy is also at a maximum. Due to the short-circuit (corresponds to short-circuiting the input of the equivalent circuit),  $C_E$  is discharged via the burden resistance with an a-periodic decaying DC-current component.

The following equation applies:

$$\frac{U_L}{U_{L0}} \approx \frac{1}{\omega \cdot C_E \cdot R'_B} \cdot \left( e^{-\frac{t}{\tau_1}} - e^{-\frac{t}{\tau_2}} \right) \quad (5-33)$$

$$\text{with } \tau_1 \approx R_B \cdot C_E \text{ and } \tau_2 \approx \frac{L_0}{R'_B}$$

#### *Example 5.7:*

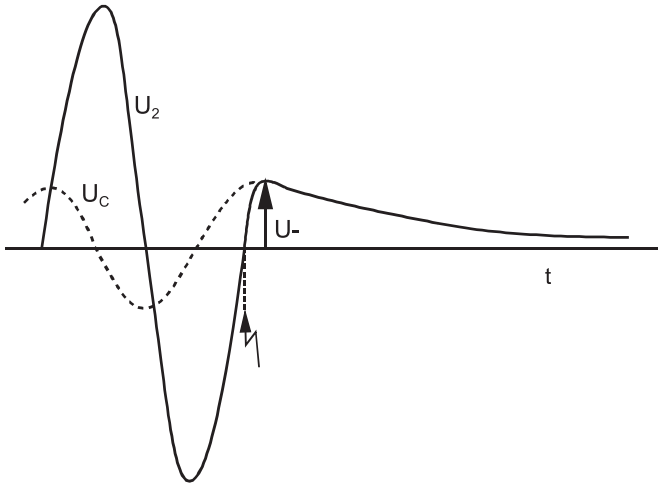
The VT in figure 5.15 applies.

A resistive burden of  $P_B = 100 \text{ W}$  per phase is assumed.

This corresponds to a burden resistance of  $R_B = U_{ph}^2 / P_B = (100/\sqrt{3})^2 / 100 = 33 \Omega$ .

Converted to the intermediate voltage, this is:

$$R'_B = \left( \frac{20000/\sqrt{3} \text{ V}}{100/\sqrt{3} \text{ V}} \right)^2 \cdot 33 \hat{=} 1320 \text{ k}\Omega$$

**Figure 5.17**

Capacitive VT, discharge oscillation after fault inception at the voltage zero-crossing and large resistive burden

The characteristic values of the transient oscillation can be calculated:

$$\tau_1 = 1320 \cdot 10^3 \cdot 100 \cdot 10^{-9} \hat{=} 132 \text{ ms and}$$

$$\tau_2 = \frac{105}{1320 \cdot 10^3} \hat{=} 0.08 \text{ ms}$$

After the rapid increase with  $\tau_2$ , the following amplitude is reached:

$$A = \frac{1}{\omega \cdot C_E \cdot R_B} = \frac{1}{314 \cdot 100 \cdot 10^{-9} \cdot 1320 \cdot 10^3} = 0.024 \hat{=} 2.4\% \frac{U_{n-\max.}}{\sqrt{3}}$$

The decay is with the time-constant  $\tau_1$  (figure 5.17).

The amplitude of this aperiodic damped transient is rather low with the assumed CVT and burden data. It would be much larger with a lower capacitor stack and higher burden, for example 9.6% with  $C_1 + C_2 = 50 \text{ nF}$  and  $P_B = 200 \text{ VA}$ . The time constant of the decay would however be reduced to  $\tau_1 = 33 \text{ ms}$ .

This DC-current component is also filtered out by the numerical distance protection, so that no significant measuring error results.

#### *Resistive/inductive burden*

In this case, a damped periodic oscillation with low frequency may arise, as the inductive burden  $L_B$  and the compensation coil inductance  $L_0$  together with  $C_E$  form a resonant circuit (figure 5.14). Frequency and amplitude are strongly dependent on the burden. Large burdens with small  $\cos \varphi$  must be avoided at all cost, as they cause large amplitude, weakly damped oscillations.



*Ferro-resonance filter*

A resonance filter ( $L_F$ ,  $C_F$ ) with small coupling resistance ( $R_F$ ) may result in severe transient oscillations, similar to those in the case of an inductive-resistive burden [5-18]. The amplitude is often relatively high (about 15 to 20% of the crest value before the fault), but heavily damped about 20 ms after fault inception.

Here, a good compromise must be found between the ferro-resonance damping during energising and de-energising of the line and the reduction of the transient oscillations following fault inception. Generally valid values cannot be given as the transients depend largely on the CVT design. The CVT manufacturer must provide the transient characteristics.

Figure 5.18 shows the subsidence transient measured at a real CVT following a fault at primary voltage maximum and zero-crossing. The technical data of Figure 5.15 apply. The burden was 65 VA,  $\cos \varphi = 0.8$  related to a secondary voltage of  $100/\sqrt{3}$  ( $R'_B = 1660 \text{ k}\Omega$  and  $L'_B = 3950 \text{ H}$  in the replica circuit of figure 5.15).

This curve is typical for EHV applications with a relatively high capacitance of the voltage divider. The transient consists of a DC component, with a superimposed damped AC oscillation, due to the ferro-resonance circuit and the reactive burden component. CVTs used on lower voltage levels may have voltage dividers of lower capacitance and may show subsidence transients with higher initial amplitudes. In general, high resistive burden causes high transients that decay very fast while low burden results in lower amplitudes but longer time constants.

The first approach can be practised with slow electro-mechanical distance relays. The sometimes recommended full burdening of CVTs may however not be the best choice for fast static and numerical relays. A medium resistive burden may ensure the best transient behaviour. In any case the CVT vendor should be consulted.

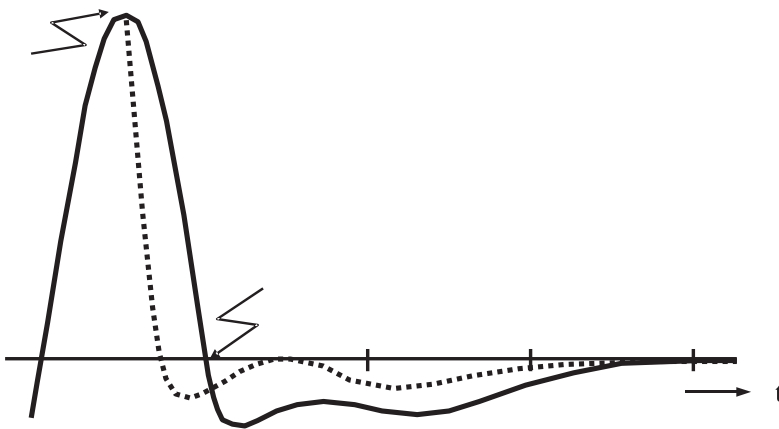


**Figure 5.18**  
CVT subsidence transient, fault at voltage maximum (dotted curve)  
and voltage zero-crossing (full curve)

*Recommendation for the CVT lay-out in conjunction with numerical protection:*

Numerical protection only has a small burden. With this protection alone, the VT would be practically un-burdened. An additional resistive burden (at least half rated burden) will normally be necessary to achieve good damping of the transients. When defining the lay-out it should be observed, that resonance frequencies between approx. 25 and 250 Hz should be avoided, as frequencies close to the nominal frequency (50 or 60 Hz) can in principle not be sufficiently filtered, and may therefore cause measuring errors. Severely inductive burdens must be avoided at all cost.

Specification can be based on the new standard IEC 60044-5. It requires that, the transient oscillation instantaneous value  $U_s(t)$  decays below a certain percentage of the voltage amplitude prior to fault inception at specified times  $T_s$  after fault-inception (figure 5.19).

A number of transient response classes are standardised (table 5.9).

In the case of fast distance relays, with measuring times below one cycle, the specified magnitude of transient alone is not sufficient [5.19]. At high source impedance ratios the transient voltage of the CVT may be much higher than the 50/60 Hz measuring signal and must be filtered out to prevent larger measuring errors. The limitation of the frequency band for interference signals, as stated above, additionally applies. Using a CVT with passive ferro-resonance suppression circuit may also be considered.

In any case, a good balance between speed and zone reach must be found for the under-reaching zone. Fast operation below one cycle would require to reduce the reach considerably to tolerate the impact of the CVT transients with  $Z_s/Z_L$  ratios higher than about 25. Modern digital relays use adaptive algorithms which automatically reduce the reach or extend the operating time in case of faults with extreme voltage drop [5.20, 5.21, 5.22]. Directional determination of numerical relays is not affected by CVT transients as healthy phase voltages (cross and memory polarisation) are used in general. Directional comparison schemes can therefore be applied with CVTs also in cases of short lines and high SIR.

Under the stated conditions, the numerical distance protection 7SA can be implemented with capacitive VTs with a  $Z_s/Z_L$  ratio of up to 25, without encountering any

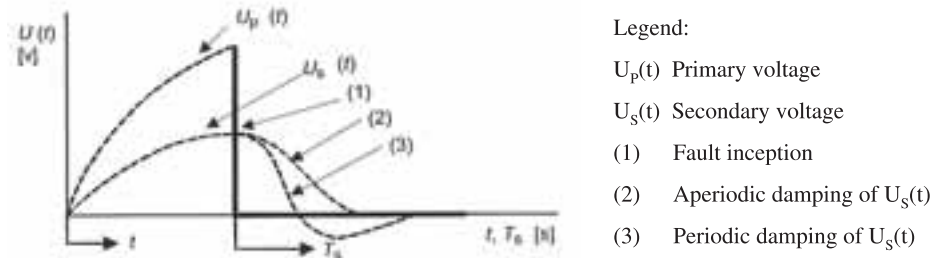


**Figure 5.19** Definition of the CVT relaxation transient acc. to 60044-5

**Table 5.9** Standard transient response classes acc. to IEC 60044-5

Time $T_s$ in ms	Ratio $\frac{U_s(t)}{\sqrt{2} \cdot U_s} \cdot 100\%$		
	Classes		
	3PT1 6PT1	3PT2 6PT2	3PT3 6PT3
10	–	$\leq 25$	$\leq 4$
20	$\leq 10$	$\leq 10$	$\leq 2$
40	$\leq 10$	$\leq 2$	$\leq 2$
60	$\leq 10$	$\leq 0.6$	$\leq 2$
90	$\leq 10$	$\leq 0.2$	$\leq 2$

NOTE 1: For a specified class the transient response of the secondary voltage  $U_s(t)$  can be aperiodic or periodic damped and a reliable damping device can be used.

NOTE 2: CVT for transient response classes 3PT3 and 6PT3 need the use of a damping device.

NOTE 3: other values of the ratio and time  $T_s$  can be agreed between manufacturer and user.

problems [5.20]. Under worse conditions, the influence on measuring accuracy and tripping time should be examined with simulation tests.

## 5.2 Distance protection in the distribution system

### 5.2.1 General

The standard protection on radial distribution feeders is the IDMTL overcurrent relay. Distance protection however is implemented in meshed distribution systems, to maintain selectivity with fast fault clearance times [5.24].

In overhead line networks, the distance protection is in general implemented with ARC-controlled zone extension. The ARC sometimes has an additional long dead-time, DAR (delayed auto-reclosure) over and above the usual three-phase short dead-time, RAR (rapid auto-reclosure). Occasionally (short lines, teed lines), a tele-protection supplement is used.

In cable networks, the distance protection is applied as independent main protection, or as back-up protection for a differential relay. If the distance protection is used as a main protection, this is often done with a permissive tripping arrangement via pilot wires or fibre optic communication.

The majority of short-circuits in the distribution system are accordingly cleared without delay. Only during remote faults, close to the opposite end, and unsuccessful ARC will the tripping take place in the second zone (300-400 ms). Longer protection operat-

ing times only occur following circuit-breaker or protection failure. The distance protection therefore significantly contributes towards the quality of supply in the distribution system.

### *Device technology*

Switched distance protection relays have almost exclusively been used as they are cost effective and may be installed directly into the LV-compartment of the switch-gear. The then introduced single-system numerical feeder protection devices 7SA510/11 contain all the necessary supplementary functions (ARC and earth-fault protection), thereby obviating the need for further relays.<sup>1</sup> In the mean time full scheme relays (7SA6) are state of the art.

The application of distance protection in the distribution system is characterised by the following special features:

### *Non-continuous line-impedances*

Generally, the lines are made up of sections with different technical data: varying conductor-cable cross-sections and tower geometries, diverse cable types, mixed cable/overhead line sections, short-circuit limiting reactors, etc.)

The differences in the short-circuit impedance angle may be substantial (e.g. cable 20° and reactor 87°). In this case it is recommended to represent the entire feeder in the R/X diagram (figure 5.20).

Overhead line impedances may be directly added, because the line angles are mostly in the range of 70° for cross-sections of 95 mm<sup>2</sup> and above.

### *Voltage-transformers on the busbar*

Due to cost constraints, it is common to have one shared voltage-transformer on the busbar in MV sub-stations. If the voltage-transformer protection mcb has tripped, the distance protection on all feeders must be blocked. In the case of the numerical distance relay 7SA6, it is then possible to automatically change over to an emergency over-current protection function.

If the voltage-transformers are protected with fuses, and no failure signal is available, the 7SA6 must be operated with over-current starting for phase-faults. The under-impedance starting may only be used for earth-faults. The under-impedance starting is then only released with earth-currents.

Incorrect starting of the protection, following the blowing of VT-fuses is therefore avoided.

---

<sup>1</sup> The earth-fault protection is integrated in the form of a directional/non-directional earth over-current protection for earthed systems, or as a sensitive watt-metric/var-metric directional protection. In meshed systems with isolated or compensated star-point, the earth-fault direction determination must be done according to the transient wave detection measuring principle. For this purpose, a separate device, 7SN60 must be used.

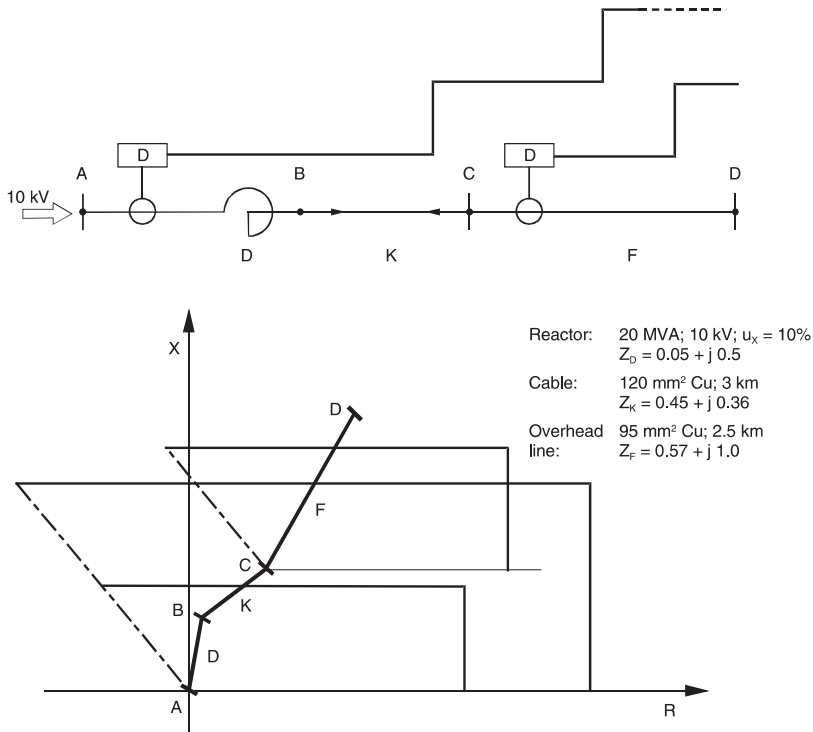


**Figure 5.20** MV-feeder, course of impedance

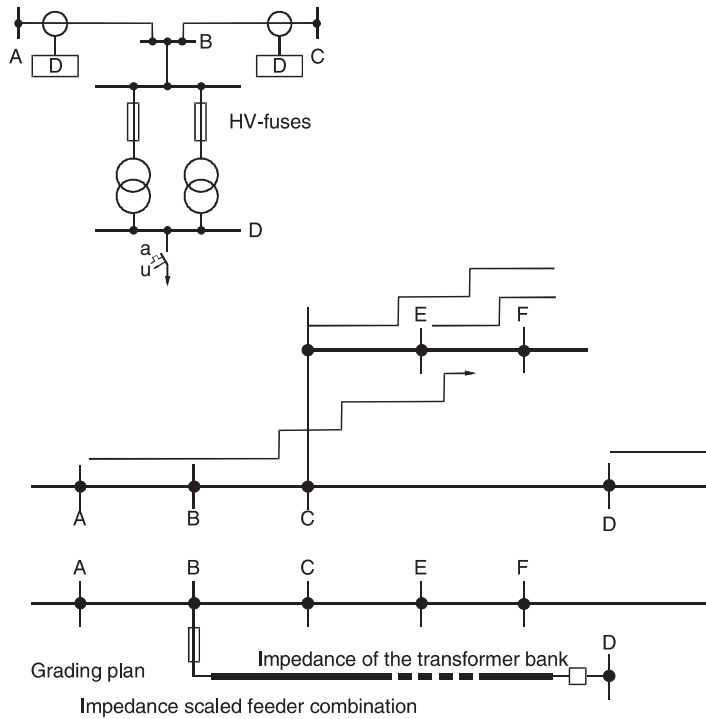
### *Branched feeders*

Especially in rural networks, the feeders are often branched, so that the measured impedance relating to the fault-location is ambiguous, and must therefore be represented on the entire system tree (refer to paragraph 3.1.13, distance to fault locating).

### *Consumer stations along the course of the feeder*

Small consumer transformers are usually connected directly to the line via fuses (figure 5.21). In this case, the first zone can be set to 85-90% of the distance A-C, as the impedance of the small consumer transformers is large in comparison to the line impedance. Accordingly, the first zone only reaches into the winding of the transformers.

Faults in the LV-network are only seen after  $t_2 = 0.3 - 0.4$  s by the second zone. A sufficient grading time for the fault clearance by the LV-fuses and LV-CB's is therefore available. During favourable conditions, short-circuits close to the terminals of the transformer are cleared by the HV-fuses during the initial current rise, before the distance protection operates. With slower clearance by the fuses, i.e. smaller currents, it is accepted that the feeder is tripped in the case of these transformer faults, which only rarely occur.



$$\text{Transformer reactance: } X_{Tr} = (u_k \% / 100) \cdot \frac{U_N^2 [\text{kV}]}{P_N [\text{MVA}]}$$

Example:  $P_N = 630 \text{ kVA} = 0.63 \text{ MVA}$

two parallel transformers correspond to:

$$U_N = 10 \text{ kV}, u_k = 4\%$$

$$120 \text{ mm}^2 \text{ Cu-Cable: } l = \frac{6.35}{2 \cdot 0.2} \approx 16 \text{ km}$$

$$X_{Tr} = \frac{4}{100} \cdot \frac{10^2}{0.63} = 6.35 \Omega$$

$$35 \text{ mm}^2 \text{ Cu-Cable: } l = \frac{6.35}{2 \cdot 0.5} \approx 6 \text{ km}$$

**Figure 5.21** Feeder with consumer transformers, distance protection settings

With larger transformer ratings ( $> 1 \text{ MVA}$ ), and longer lines, it is possible that the transformer impedance may be less than the line impedance B-C. In this case the zone setting must correspondingly be reduced and graded with the end of the transformer reactance.

If the consumer has his own circuit-breaker with over-current protection, the distance protection must be graded to the second zone in front of this circuit-breaker (figure 5.22). This ensures that short-circuits in the consumer network are selectively cleared, while the feeder remains in service.

Even higher grading times may be required, if a small industrial network is direct galvanically coupled to the feeder (figure 5.23). The circuit-breaker E must trip without delay, to split the cable ring into two radial feeders, to ensure that a portion of the in-

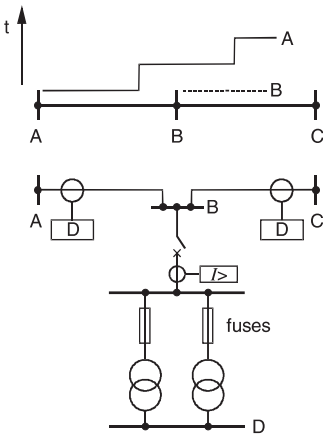


**Figure 5.22**  
Setting of the distance zones in the case of a consumer connected with consumer circuit-breaker

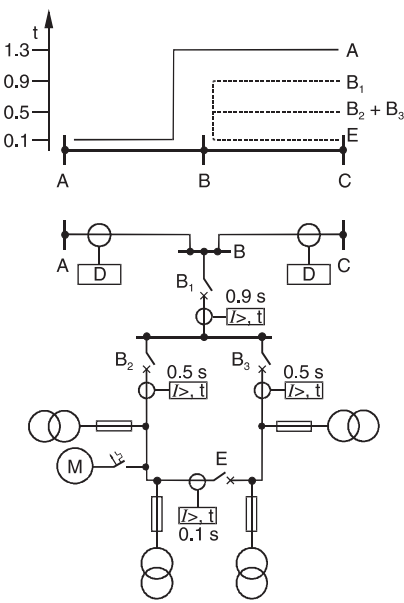


**Figure 5.23**  
Industrial consumer connected to main feeder, setting of the distance zones

feed is maintained in the case of a short-circuit. The time over-current protection at B2 and B3 must correspondingly be delayed by one grading time stage. B1 at the consumer circuit-breaker then is already allocated with the third grading time stage of approx. 0.9 s. Zone 2 of the distance protection must then be delayed by a further grading step to approx. 1.3 s.

### *Intermediate in-feed on the feeder*

At medium voltage levels, de-centralised power generation is ever gaining in importance. The small power stations (hydro, wind, etc.) are mostly connected directly to the feeders. Depending on the contribution of the small generators to the short-circuit

power, it may be necessary to take the resulting intermediate in-feed effect into consideration, when setting the distance protection (refer to paragraph 3.5.2). If ARC is implemented, additional care must be taken to ensure that the de-centralised power generation is de-coupled on time during a fault on the feeder. The in-feed to the main feeder during the ARC dead-time would otherwise prevent the extinguishing of the arc if the current remains above the critical extinguish threshold. The de-centralised power generators must therefore be equipped with under-voltage and frequency relays [5.25, 5.26, 5.27].

#### *Fault detection problems with back-up protection*

The reach determination of the over-current and under-impedance starting was referred to in paragraph 3.1.6.

Problems can be expected here when the protection or circuit-breaker in a feeder fails, causing the time graded protection at the in-feed to take over the back-up protection function (figure 5.24). The over-current starting at the in-feed must be set greater than the permissible transformer over-load current (typical  $1.3 \cdot 2 \cdot I_N$ ), and is therefore relatively un-sensitive. The problematic case is then given when the fault is further away, or on a feeder with a small conductor cross-section. In both cases, the short-circuit current is severely limited and the voltage only shows a small collapse, especially when the transformer has a large rating. This implies that an under-impedance starting will also not solve this problem. The angle dependant under-impedance starting or true impedance starting, which additionally evaluate the short-circuit angle, typically provide a remedy. In the case of copper conductors, the short-circuit angle is greater than  $60^\circ$  for conductor cross-sections of  $95 \text{ mm}^2$  and up (in the case of aluminium conductors, only greater than  $45^\circ$ ). The line angle of the faulted feeder is not exclusively decisive, as the load current of the other feeders are super-imposed on the measured current. This is shown in figure 5.24. In the case at hand, the short-circuit angle is reduced by the real power (half transformer rating) from  $62^\circ$  to  $51^\circ$ . With a setting of approx.  $40^\circ$ , the protection would safely start. If the full transformer rating is applied as real power, the angle is reduced to approx.  $35^\circ$ , which is below the starting threshold.

In summary it can be mentioned that the angle dependent starting or the impedance starting supplies good reach in the case of the large line angles prevalent at HV-levels ( $70^\circ$  and more). At medium voltage levels this does not generally apply, but only for copper conductors or aluminium conductors with large cross-sections. Due to the influence from load-currents the sensitivity is drastically reduced.

In any event, the effectiveness must be checked with a load and short-circuit computation [5.28]. Today, numerical devices intended for distribution systems (7SA6) also provide angle dependent starting or impedance starting, thereby setting up favourable conditions for starting.

What can be done when the angle-dependant starting also does not improve matters? In critical cases the outgoing feeders must be provided with circuit-breaker failure and back-up protection. With numerical relays the circuit-breaker failure protection is integrated, and the separate back-up protection can in general be done without in distribu-



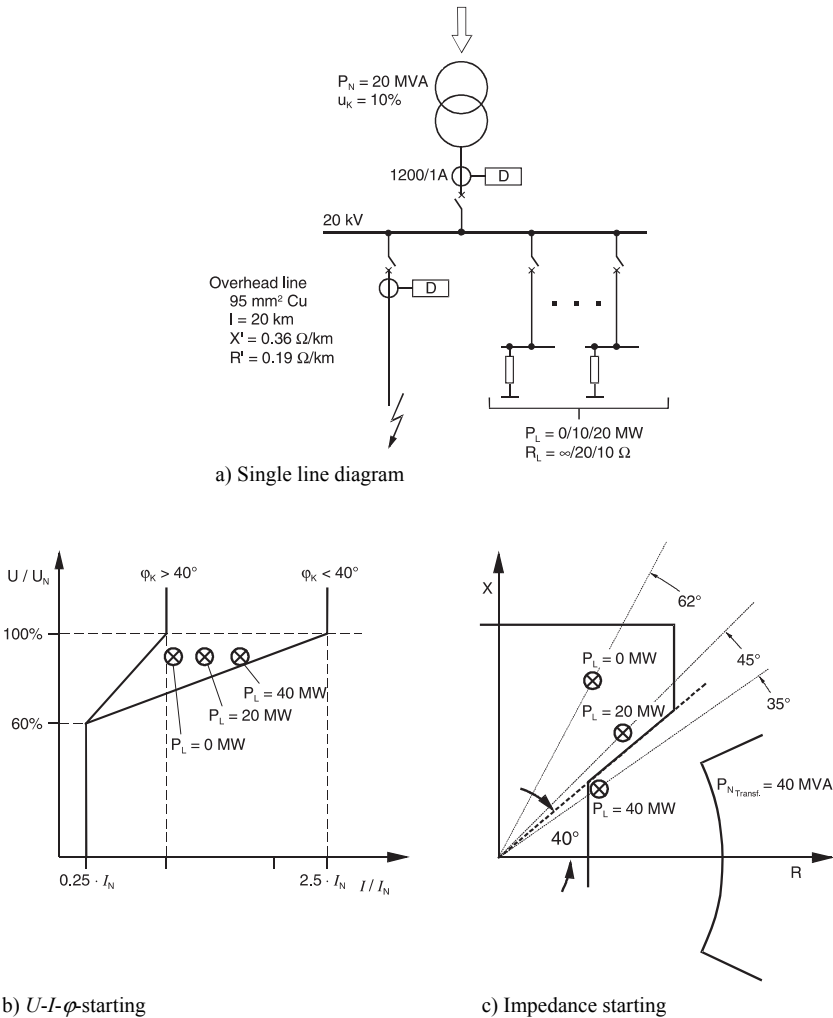


**Figure 5.24** Back-up protection starting

tion systems, due to the continuous self-monitoring of the relays. For non-symmetrical faults, integrated negative sequence and earth-current measurement can be used for final stage tripping at the in-feed. This does not cover the three-phase fault case.

### Multiple-shot ARC

With an ARC dead-time of approx. 0.3 to 0.5 s, about 60-70% of the short-circuits in medium voltage systems are eliminated.

In many cases, a second shot with a long dead-time, DAR (delayed auto-reclose) (in the order of minutes) is implemented, following an unsuccessful initial reclosure, RAR (rapid auto-reclosure) in rural systems. Experience has shown that 40% of the faults with unsuccessful RRC can be cleared in this manner.

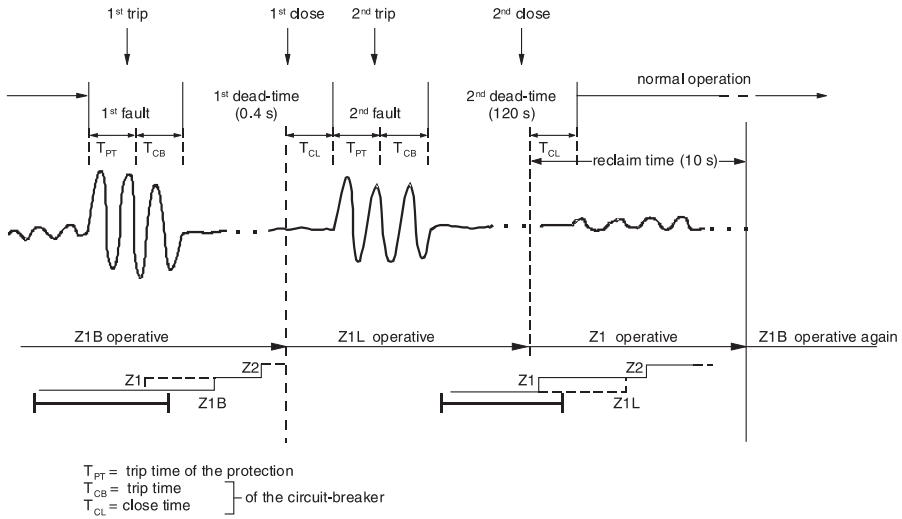


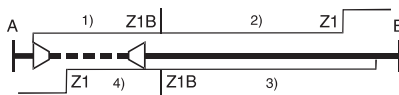
**Figure 5.25** ARC with short and long dead-times (RAR, DAR)

With the numerical distance relays 7SA6, different over-reach characteristics can be set for the RAR and DAR-cycles (figure 5.25). Isolation of the initial fault is usually achieved with the over-reach zone without time delay (Z1B with  $T1B = 0$ ). Settings for the further sequence may then be selected such that prior to the first re-closure, a different reach and time-delay (Z1L with  $T1L$ ), or the usual time graded characteristic is operative. In this way, selectivity for the ultimate tripping is obtained, if the fault is situated on one of the downstream feeders. The slow clearance of the faults on the own feeder, close to the remote end, must then however be accepted.

#### *ARC on sections of the feeder*

On feeders that consist of overhead line and cable sections, the ARC must only be carried out when the fault is on the overhead line section.

This is implemented with the numerical relays 7SA6, by the over-lapping of two zones with the different settings and logical linking of the outputs (figure 5.26).



Station A:

- 1) up to Z1B      ARC blocked
- 2) outside Z1B    ARC released

Station B:

- 3) up to Z1B      ARC released
- 4) outside Z1B    ARC blocked

————— overhead line  
 - - - - - cable

**Figure 5.26**  
Selective ARC on a cable-overhead line section

### 5.2.2 Distance protection in isolated or compensated systems

The high resistance earthing of the star-point requires special treatment by the distance protection during earth-faults.

#### *Single-phase earth fault*

The single-phase earth-fault in this case does not correspond to a short-circuit as only a small capacitive or compensated earth-current flows [5.29]. Due to the limiting or compensation of the earth-current, the earth-fault will in most cases self-extinguish (transient earth-fault). In the remaining cases, the system can be operated with the fixed earth-fault (continuous earth-fault) for several hours, until the earth-fault is located and removed by isolation of the faulted feeder. For indication of the earth-fault, sensitive directional earth-fault relays are implemented. The distance protection must not operate during such single-phase earth faults.

This must be ensured by setting the fault detection correspondingly. A release of the distance measurement would otherwise cause uncontrolled incorrect tripping, as the voltage on the faulted phase during a solid earth-fault may be zero in the entire galvanically connected network; consequently, the impedance measured in conjunction with the load current would also be equal to zero.

#### *Double (cross-country) earth fault*

Due to the rise of the phase-earth voltage by a factor  $\sqrt{3}$ , on the healthy phases in the entire system, double earth-faults may result. The result is similar to a two-phase short-circuit, however, the short-circuit is here from one earth-fault location to the other via earth. The second fault location may be at any other position in the galvanically connected system, depending on where the weakest point in the insulation is.

The probability of a double earth-fault increases, as the size of the network increases [5.29]. In the case that the two fault locations are in close proximity to each other, the short-circuit currents will assume the same order of magnitude as would be the case during a two-phase short-circuit, while the fault current may be below nominal current when the two fault locations are further apart.

The protection strategy usually applied for double-earth faults is aimed at isolating one of the fault locations with the expectation that the second fault location will then extinguish on its own, similar to a single-phase earth-fault, or will be tripped by hand after successful earth-fault searching. To this end, the distance protection relays in isolated/compensated systems must have a so-called double earth-fault phase preference, which selects either the leading or the lagging phase-earth loop for measurement in the entire galvanically connected network. The phase preference functions on those lines that are between the two fault locations, because here earth-current for the double earth-fault detection flows. On the in-feed lines, outside this range, where no, or an earth-current flows that is too small, the fault detection recognises a two-phase fault and therefore selects the corresponding phase-phase loop for the measurement. Usually, in these cases, a trip in a delayed, often the final stage will occur, due to the under-

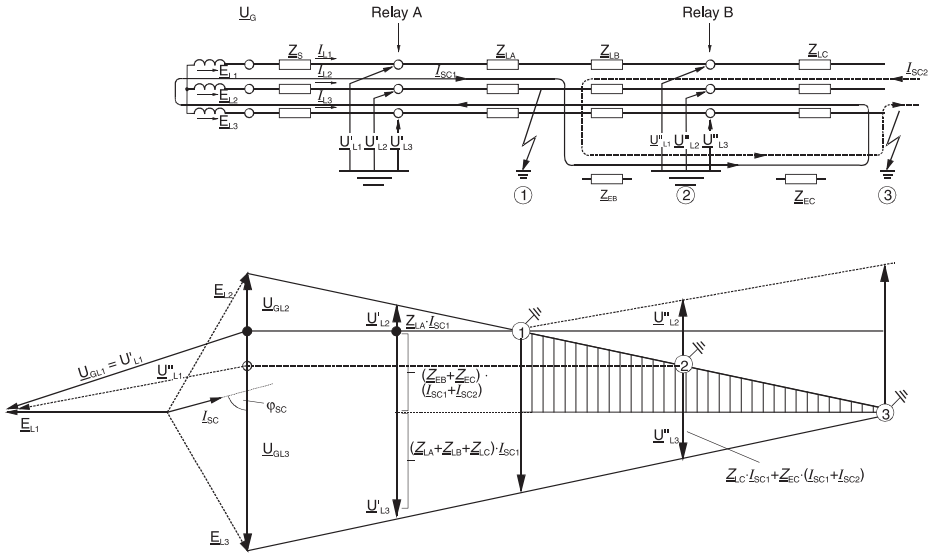


**Figure 5.27** Double earth-fault, current and voltage distribution

reaching of the distance protection (the boundaries of the double earth-fault detection are discussed in detail below).

Intentional isolation of both earth-fault locations with multiple systems distance protection is only done in exceptional cases in compensated high voltage networks.

#### *Distance measuring of double earth-faults*

The short-circuit loop is made up of an inner zone between the two fault locations, and several outer zones, from the in-feeds up to the closest fault-location. This is shown in figure 5.27 for a single-side in-feed.

The short-circuit current is driven by the line emf (in the Figure:  $E_{L2}-E_{L3}$ ), and has a phase relationship similar to that of a two-phase short-circuit. Due to the earth connection, three fault loops can in principle be measured: the ph-ph loop, as well as the leading and lagging ph-E loops.

In the range between the two fault-locations the ph-E loops measure the impedance to the fault locations correctly.

For relay B:

$$\underline{Z''_{L2}} = \frac{\underline{U''_{L2}}}{\underline{I''_{L2}} - \underline{k_E} \cdot \underline{I''_E}} = \underline{Z_{LB}} \quad \text{with} \quad \underline{k_E} = \frac{\underline{Z_{EB}}}{\underline{Z_{LB}}} \quad (5-34)$$

$$\underline{Z''_{L3}} = \frac{\underline{U''_{L3}}}{\underline{I''_{L3}} - \underline{k_E} \cdot \underline{I''_E}} = \underline{Z_{LC}} \quad \text{with} \quad \underline{k_E} = \frac{\underline{Z_{EC}}}{\underline{Z_{LC}}} \quad (5-35)$$

The phase-phase loop in the range between the two fault location does not produce a useful result, as the phase currents belong to different short-circuit loops here.

For the relay at A in the in-feed range the following is obtained:

$$\underline{Z}'_{L2} = \frac{\underline{U}'_{L2}}{\underline{I}'_{L2} - \underline{k}_E \cdot \underline{I}'_E} = \underline{Z}_{LA} \quad (5-36)$$

$$\underline{Z}'_{L3} = \frac{\underline{U}'_{L3}}{\underline{I}'_{L3} - \underline{k}_E \cdot \underline{I}'_E} = \underline{Z}_{LA} + \underline{Z}_{LB} + \underline{Z}_{LC} + (\underline{Z}_{EB} + \underline{Z}_{EC}) \cdot \left(1 + \frac{I_{SC2}}{I_{SC1}}\right) \quad (5-37)$$

$$\underline{Z}'_{L2-L3} = \frac{\underline{U}'_{L2} - \underline{U}'_{L3}}{\underline{I}'_{L2} - \underline{I}'_{L3}} = \underline{Z}_{LA} + \frac{\underline{Z}_{LB} + \underline{Z}_{LC}}{2} + \frac{\underline{Z}_{EB} + \underline{Z}_{EC}}{2} \cdot \left(1 + \frac{I_{SC2}}{I_{SC1}}\right) \quad (5-38)$$

The ph-E measurement in L2 is the only measuring system which returns the correct impedance up to the closest earth-fault location. The corresponding measurement in L3 produces an impedance which is too large, due to the voltage drop across the earth impedances. The under-reaching effect is compounded by the short-circuit current flowing from the remote end.

The ph-ph measurement produces an average impedance relating to the distance to the two fault locations. In the distribution system it can be assumed that the earth and conductor impedances are approximately the same for overhead lines without earth-wires. Due to the in-feed from the opposite end the measured impedance is again increased, so that an under-reach always results in a meshed system.

#### *General practice for the treatment of double earth-faults*

The switched distance relays in service today, measure the ph-ph loop without  $I_E$ -starting, so that outside the two fault-locations an impedance, that is too large, is measured. Therefore relay operation with longer delay times must be expected. This is actually desired, as the ph-ph measurement does not contain an earth-fault phase preference. The relays close to the fault-locations usually have sufficient earth-fault current and select the preferred phase. The relays on the faulted lines largely measure the impedance correctly, and trip without delay or in the second zone.

Both cyclic and a-cyclic phase preference circuit are applied.

In distribution systems, the a-cyclic method is almost exclusively used, as only the fault detection in two phases and earth is required. Mostly, the fault detection  $I_{>L1}$ ,  $I_{>L3}$  and  $I_{E>}$  is used to achieve the phase preference L3-before-L1-before-L2 (in short "L3(L1) a-cyclic"). In this case, the following loops are selected:

Double earth-fault:	Preferred loop:
L1-L2-E	L1-E
L2-L3-E	L3-E
L3-L1-E	L3-E

In high voltage networks, the distance protection has always been provided with a three-phase starting. Therefore, the cyclic phase preference is also found here, e.g. L1-before-L3-before-L2-before-L1 (in short “L1(L3) cyclic”).

In this case, the following loops are selected:

Double earth-fault:	Preferred loop:
L1-L2-E	L2-E
L2-L3-E	L3-E
L3-L1-E	L1-E

The phase preference must be set the same for the entire system.

With conventional switched distance relays, links or plug-settings were provided for the above (in the case of the medium voltage relay R1KZ4 only for the a-cyclic method).

The numerical relays 7SA6 can be parameterised for the various phase preference options. Additionally, tripping of both fault locations is possible with this device (setting of the double earth-fault phase preference to “ALL”).

#### *Boundaries of the double earth-fault detection*

It was already mentioned that on in-feeds, where no earth-fault current flows, a double earth-fault phase preference can not take place. A two-phase fault is always recognised in this case. This results in longer tripping delays. A detection of the double-earth fault by means of the displacement voltage is possible in principle, but is however not implemented in practice.

A further boundary case results when one fault location is on a dead-end feeder (figure 5.28). Earth-current will flow in this case, but the relay always selects the phase on which the dead-end feeder is faulted, as fault detection on the other phases usually is non-existent. Only when the fault on the dead-end feeder is incidentally on the phase that is to be preferred, will the desired selective isolation of the fault locations result. Otherwise, both fault locations are tripped simultaneously.

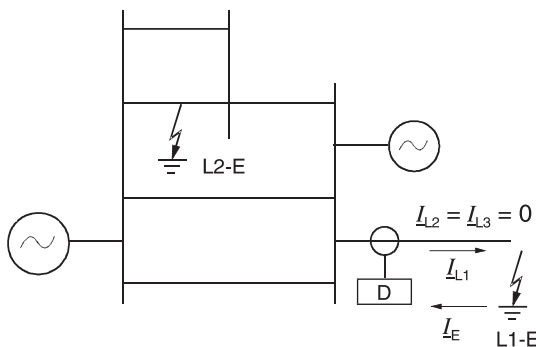


**Figure 5.28**  
Double earth-fault  
with one fault location  
on a dead-end feeder

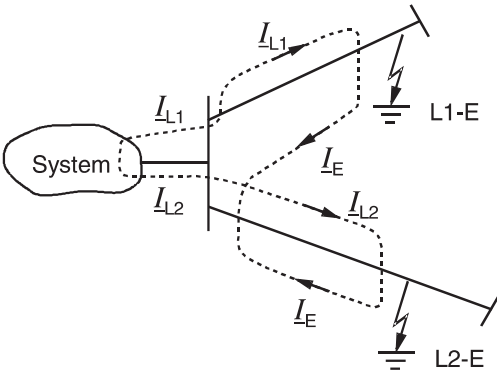


**Figure 5.29**  
Double earth-fault with fault locations on separate spurs in the same distance zone

The simultaneous tripping of both fault locations can also be expected when the fault locations are on separate spurs in the same distance zone (figure 5.29), the reason being that each relay only sees one single-phase earth fault.

Further exceptional cases are possible, depending on the system constellation as well as the relative positions of the fault locations. The under-impedance fault detection improves the selectivity to a degree, because the resulting voltage collapse in the presence of load-currents will still result in fault detection in those cases, where the over-current fault detection fails.

#### *Double earth-faults on parallel lines*

In this case the zero-sequence coupling between the two lines must be considered, as is the case in earthed systems (refer to paragraph 3.5.3). From the example of a single-end fed open double-circuit overhead line this influence's principle of operation becomes clear (figure 5.30).

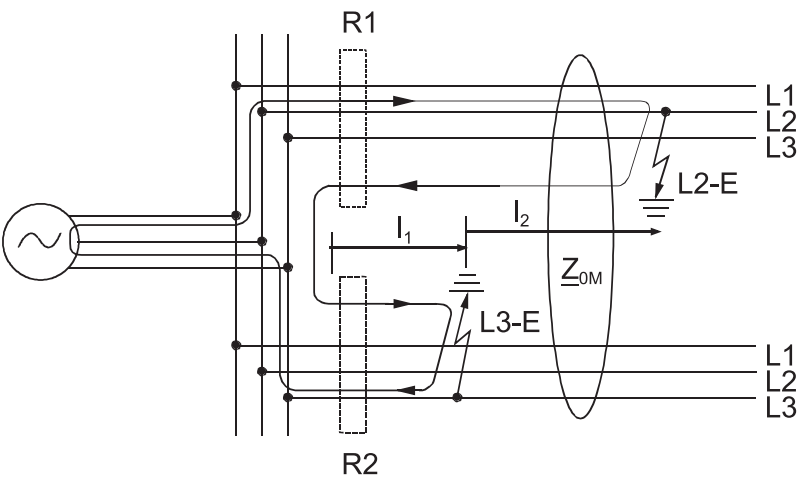


**Figure 5.30** Two-phase earth-fault on a parallel line

For the calculation with the symmetrical component impedances, it must be especially noted that the sum of the currents flowing in the phase conductor always returns as an earth-current below the line, and not directly across to the fault location on the parallel line.<sup>1</sup>

The impedances measured by relay 1 and 2 are calculated as follows:

*Relay 1:*

$$\underline{U}_{L2-E} = l_1 \cdot (\underline{Z}'_L \cdot \underline{I}_{L2} - \underline{Z}'_E \cdot \underline{I}_E) + l_1 \cdot \frac{\underline{Z}'_{0M}}{3} \cdot \underline{I}_{EP} + l_2 \cdot (\underline{Z}'_L \cdot \underline{I}_{L2} - \underline{Z}'_E \cdot \underline{I}_E) \quad (5-39)$$

$\underline{Z}'_{0M}$  = corresponds to the coupling impedance of the zero-sequence systems of both lines.

Hint: Currents in line direction are counted positive (sign rule as per figure 3.66)

With  $\underline{I}_{L2} = -\underline{I}_E = \underline{I}_{EP} = \underline{I}_{SC}$  and  $\underline{k}_E = \frac{\underline{Z}'_E}{\underline{Z}'_L}$  and  $\underline{k}_{EM} = \frac{\underline{Z}'_{0M}}{3 \cdot \underline{Z}'_L}$  the result is:

$$\underline{Z}_{L2-E} = \frac{\underline{U}_{L2-E}}{\underline{I}_{L2} - \underline{k}_E \cdot \underline{I}_E} = \underline{Z}'_L \cdot \left[ (l_1 + l_2) - l_1 \cdot \frac{\underline{k}_{EM}}{1 + \underline{k}_E} \right] \quad (5-40)$$

*Relay 2:* Similarly the following is obtained:

$$\underline{Z}_{L3-E} = \frac{\underline{U}_{L3-E}}{\underline{I}_{L3} - \underline{k}_E \cdot \underline{I}_E} = \underline{Z}'_L \cdot l_1 \left( 1 - \frac{\underline{k}_{EM}}{1 + \underline{k}_E} \right) \quad (5-41)$$

The impedance measured by relay 2 could be rectified to the correct value  $\underline{Z}'_L \cdot l_1$  by utilisation of the parallel line compensation (refer to paragraph 3.5.3). In the case of relay 1 this is not possible, as only a portion of the short-circuit loop is influenced by the earth-current of the parallel line.

Generally, a substantially more complex current distribution results, as the line ends may be a galvanically connected, or even an in-feed from the opposite end also exists. Depending on the system constellation, and the relay location, a corresponding over- or under-reach of the distance zones results (figure 5.31). The distance measurement behaves as in an earthed system: the impedance is measured as being too large (under-reach), if the earth-currents in both lines flow in the same direction (D4, D5), and as being too small (over-reach), if they flow in opposite directions (D1, D6).

<sup>1</sup> In reality, the current appears to flow across from one line to the other, as the assumed earth-current in section 1 cancel each other. If only the out and return currents in the phase-conductors are used for the calculation in this section, then the actual distance between these phase conductors carrying the current of the two systems must be used as the basis to calculate the line reactance. This then results in a different (usually larger) reactance than the positive sequence impedance of the transposed three-phase line (refer to paragraph 3.5.5).



*Example:*

**Task:**

The measuring error of the distance relays D3 and D4 (figure 5.31) must be estimated. The following characteristics of a 100 kV double-circuit overhead line must be used:  $\underline{k}_E = 0.84$  and  $\underline{k}_{EM} = 0.68$

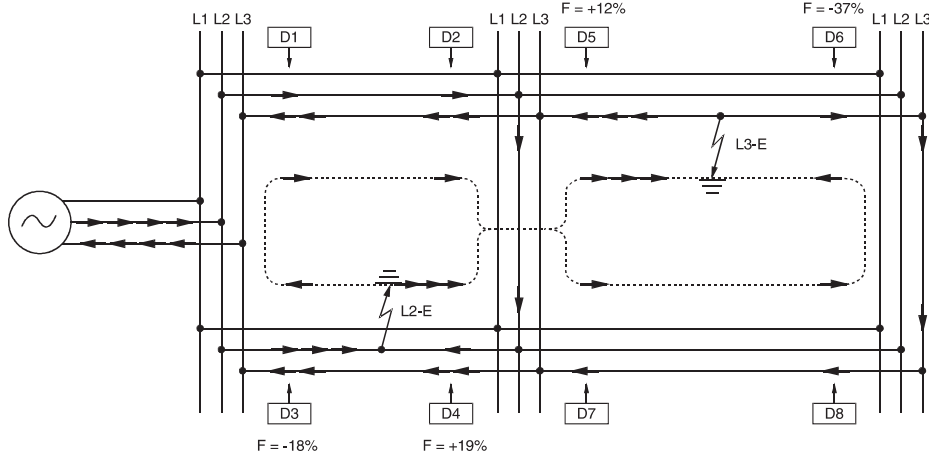


**Figure 5.31** Double-circuit overhead line, current distribution during a double earth-fault

**Solution:**

**Relay D3:**

The short-circuit voltage at the relay location is:

$$\underline{U}_{L2-E} = \left( \frac{3}{4}I_{SC} + \frac{1}{4}I_{SC} \cdot \underline{k}_E - \frac{1}{4}I_{SC} \cdot \underline{k}_{EM} \right) \cdot \underline{Z}_{LF}$$

$\underline{Z}_{LF}$  is the line impedance from the relay to the fault location L2-E.

For the measurement of the ph-E-loop the following results:

$$\underline{Z}_{L2-E} = \frac{\underline{U}_{L2-E}}{I_{L2} - \underline{k}_E \cdot I_E} = \frac{\underline{U}_{L2-E}}{\frac{3}{4}I_{SC} + \frac{1}{4}I_{SC} \cdot \underline{k}_E} = \underline{Z}_{LF} \left( 1 - \frac{\underline{k}_{EM}}{3 + \underline{k}_E} \right)$$

The error therefore is:

$$F_{D3} = -\frac{\underline{k}_{EM}}{3 + \underline{k}_E} = -\frac{0.68}{3 + 0.84} = 0.18 \hat{=} -18\%$$

The same calculation for relay D4 results in:

$$F_{D4} = +\frac{\underline{k}_{EM}}{1 + 3 \cdot \underline{k}_E} = +\frac{0.68}{1 + 3 \cdot 0.84} = +0.19 \hat{=} +19\%$$

The application of the parallel line compensation for distance protection and/or the fault locator would in both cases provide the correct result.

Generally it can be deduced that for double-circuit lines, the relays on the faulted lines measure correctly with parallel line compensation. In the case where both fault locations are on the same line, only the ph-E measurement up to the first fault location is correct (refer to figure 5.30)

#### *Stabilisation of the distance protection during a single-phase earth fault*

As was stated earlier, the distance protection shall not pick up during a single-phase earth-fault in isolated/compensated networks.

This must be especially considered in expansive networks with large capacitive earth-currents. The earth-current amplitude of the arc-ignition oscillation during the initial half-waves may in this case assume values being a multiple of the nominal current, with a frequency close to 50 Hz.

To prevent incorrect fault detection, the numerical distance relay 7SA6 has an intelligent logic, which delays the single-phase fault detection in isolated/compensated networks by a set time (e.g. 40 ms). During a second earth-fault, this function is automatically de-activated. Therefore the fault detection is undelayed if the fault evolves into a double earth-fault.

In some cases, the non-compensated capacitive earth-current in high voltage networks is already greater than 1000 A, which means it is of the same order of magnitude as the minimum short-circuit current during a double earth-fault. It is therefore not possible to differentiate between an earth-fault and an earth short-circuit, using the earth-current criterion. In this extreme case, the phase-earth measuring under-impedance fault detection cannot be selectively controlled. At the relay 7SA6, the option “only phase-phase measurement” must be selected as this only picks up during double earth-faults and not during a single-phase earth-fault because in the latter case the phase-to-phase voltage remains unaffected. The somewhat lower sensitivity of the fault detection during double earth-faults with a large distance between the fault locations, can in general be accepted.

### **5.2.3 Distance protection in distribution networks with low impedance star-point earthing**

In such networks it is common practice to limit the earth-fault current by means of a resistor or reactor in the star-point of the in-feed transformers ( $I_{EK} \leq 2000$  A according to DIN VDE 0141). Alternatively, a special earthing transformer with a zigzag winding may also be used to earth the star-point.

This type of earthing is often used in networks with a large amount of cables (urban networks) to reduce the risk of double earth-faults.

The distance protection may be implemented in the same manner as on solidly earthed networks (setting to “system star solidly earthed”), to also trip single-phase earth-faults.

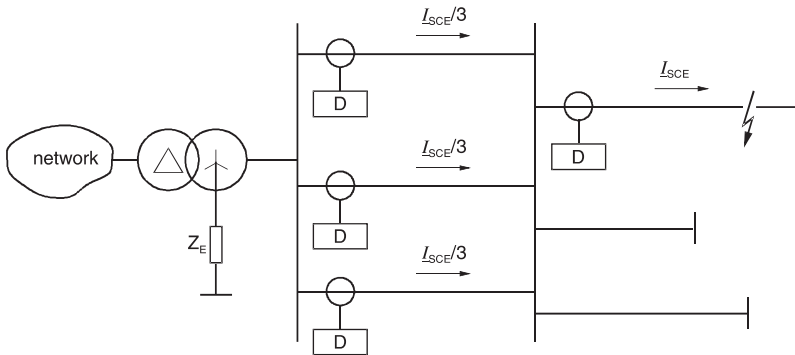


**Figure 5.32** Low resistance earthed network; distribution of earth fault currents

If only radial lines (spurs) emanate from the in-feed sub-station, then generally the magnitude of the short-circuit current is sufficient for the implementation of over-current fault detection. The earth-current however becomes smaller as the distance of the fault point to the earthing point increases. The minimum short-circuit current for the most remote relay must therefore be checked.

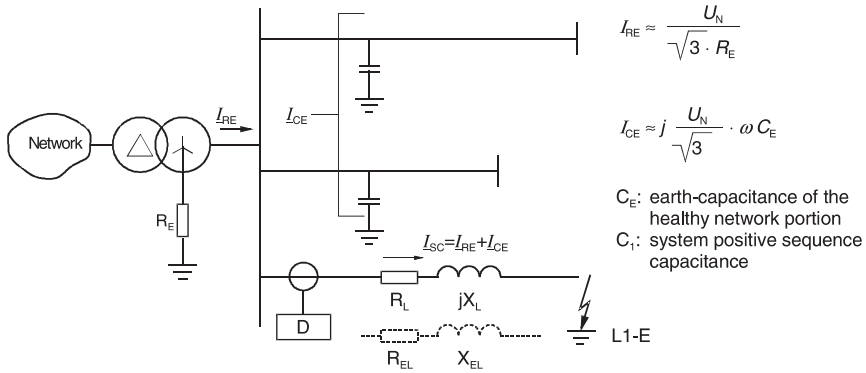
In meshed networks, additional care must be taken because the earth-current is split between several lines, so that only a portion of the already limited short-circuit current is available at the relay location. This largely affects the back-up protection (figure 5.32).

In many cases, the impedance or voltage controlled overcurrent (under-impedance) fault detection must therefore be implemented. It is then possible to detect faults with as little as 20% of nominal current. A corresponding voltage collapse is ensured by the large source impedance, due to the earth-current limiting.

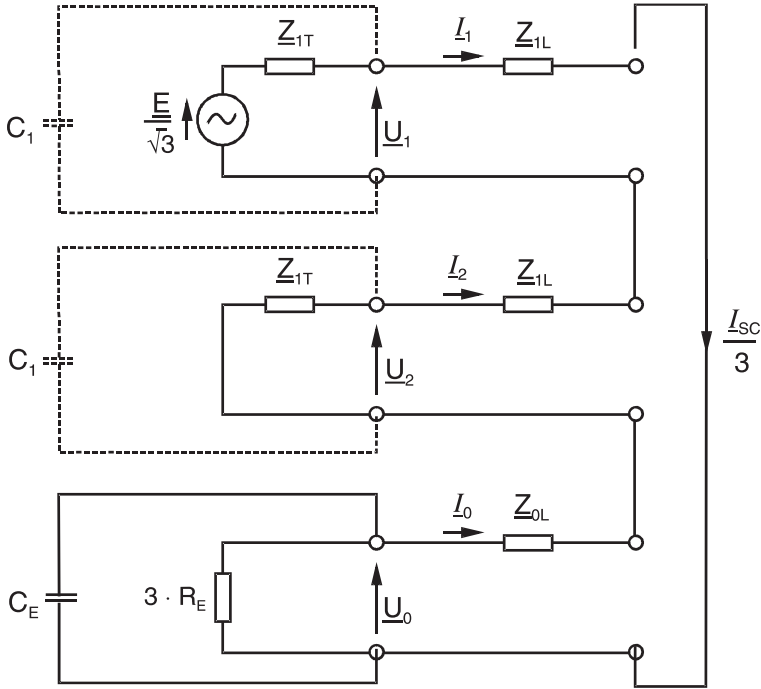
In the case of earth-current limiting by means of a resistor, it must be additionally noted, that the angle between the source-emf and the short-circuit current may be very small. Relative to the unfaulted phase voltage, the current appears to be rotated in the leading sense (figure 5.33). The  $45^\circ$  directional characteristic however provides a sufficient security margin. Problems should only be expected when the capacitive portion of the cable earth-current is of a similar order of magnitude as the resistively limited earth short-circuit current. In this case, the earth short-circuit current in the phase would obtain an additional rotation in the leading sense. This does generally not occur in practice, as with large networks a reactance earthing with larger earth-currents (e.g. 5 kA) must be used.

The following situation is of academic interest:

If, for some reason, the star-point earth in a large cable network should not be present during an earth-fault, the relay would then measure the wrong direction with the capacitive earth (short-circuit) current, and the unfaulted phase voltage. This does not apply to the directional measurement with short-circuit loop voltage and the distance measurement itself, as the measured short-circuit impedance of the protected cable or overhead line is independent of the source.



a) Earth fault in an resistance earthed distribution network

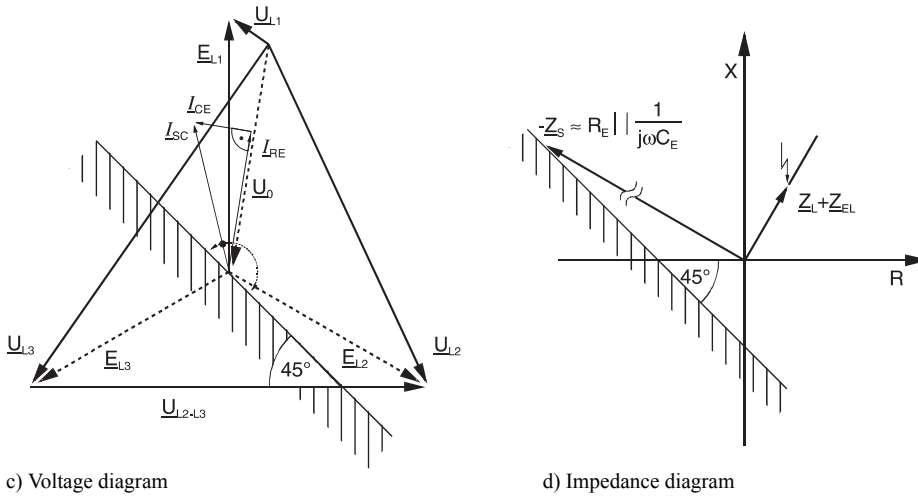


b) Earth fault in an resistance earthed distribution network, symmetrical component representation

**Figure 5.33**

Resistance earthed distribution network; influence of the network earth capacitance on the direction determination ( $R_E \gg Z_T$ ).

For the sake of completeness, it must still be mentioned that on earthed load-transformers, impedance or under-impedance fault detection must always be used, as portions of the short-circuit current flow across the healthy phases, and therefore the over-current

**Figure 5.33** continued

Resistance earthed distribution network; influence of the network earth capacitance on the direction determination ( $R_E \gg Z_T$ ).

fault detection cannot operate selectively (Bauch's paradox, refer to paragraph 3.1.6, figure 3.15).

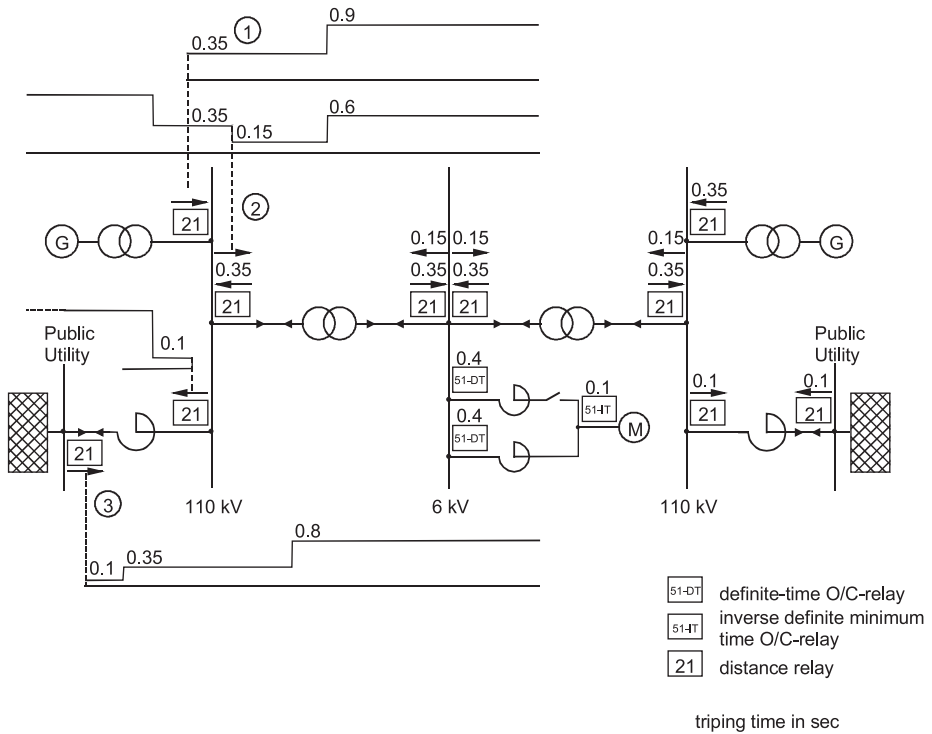
### 5.2.4 Distance protection in industrial networks

Industrial networks exhibit a high plant-density, short cables with small impedances and large short-circuit currents.

Under these conditions the conventional distance protection was often used as back-up protection to the line-differential protection. With numerical technology it is increasingly also used as main protection, as smaller reaches can be set. The independent setting of the quadrilateral zone limits in R- and X-direction is a distinct advantage, as it is always possible to obtain a sufficiently large arc-resistance coverage. Furthermore, the directional determination with unfaulted phase voltage and voltage memory in the case of the numerical 7SA relays also always guarantees absolutely selective trip decisions for close-in faults [5.30].

The smallest setting for the distance zones in the case of the 7SA6 is  $0.05 \Omega$  secondary ( $I_N = 1 \text{ A}$ ). The shortest distances that can be protected without teleprotection are in the range of less than 200 m, depending on the cable cross-section and the instrument transformer ratios. In comparison to the electro-mechanical relay (R1KZ4), this corresponds to a reduction of the minimum settable reach by a factor 5 (refer also to paragraph 5.1.2).

For non-delayed tripping on 100% of the feeder, a permissive over-reach transfer trip with the over-reaching zone has been implemented with pilot wires (transfer trip by

**Figure 5.34**

Industrial network with parallel in-feed; distance protection as back-up protection

pilot wire). In new installations this is generally being done with signal transfer via fibre-optic communication.

The application of distance protection as back-up protection is shown in figure 5.34.

A typical industrial network with parallel in-feeds is referred to.

On the 110 kV level, two independent network segments exist, which are each supplied via utility in-feeds and own generating blocks.

The entire network (cables, transformers, busbars) is protected by differential protection as primary protection. The distance protection acts as a back up protection, and has its first zone delayed by 100 or 150 ms. The grading of the zones is only shown for the left-side in-feed. However, it applies in the same way to the other busbars.

The first distance zone reaches approximately 80% into the impedance of the feeders, which in general are given by the short-circuit impedance of the corresponding transformers. A distinct advantage in this case is the option to freely select the forward or reverse reach of all distance zones in the 7SA6. The relay ② for instance, operates in the reverse direction with stage 3 (0.35 s) as a back up busbar protection, and in the forward direction in stage 1 (0.15 s) and 2 (0.6 s) as back up protection for the cable-transformer range, and the 6 kV network.

## 5.3 Distance protection in transmission networks

### 5.3.1 Generals aspects

Transmission networks are generally meshed, and are almost always solidly earthed. In certain cases, the earth-current is limited by not earthing some of the transformer star-points.

The operating voltages of the networks are in the range between 100 and 800 kV.

In the lower ranges there is an overlap between the transmission and distribution functionality. While for example the German 110 kV network can be seen mainly as a distribution network, 132 kV or even 60 kV lines in developing countries have a transmission character.

In central Europe, the average line length in EHV-networks is smaller 50 km, because power stations and consumers are evenly distributed. Stability is therefore also very high. During close-in faults, a fault clearance time of approximately 100 ms is permitted, while faults close to the line end would not even cause stability problems when they are cleared in the 2<sup>nd</sup> zone (400 ms).

Outside Europe, line-lengths of approximately 400 km occur, as the energy must sometimes be transmitted over large distances, from hydro-electric power stations to consumer centres. Here, system stability is always critical and demands extremely short fault clearance times of below four cycles.

The protection systems must be adapted accordingly.

Distance protection is the most common protection system in the transmission network.

It is mostly supplemented with a teleprotection signalling, to provide a protection system which covers 100% of the line with fast tripping. It furthermore provides a remote back up during protection or circuit-breaker failure.

In German HV-networks, it is often the only protection, with or without a teleprotection signalling supplement. Outside Germany, it is sometimes used in conjunction with a directional over-current protection as back up protection on overhead lines. On cable-feeders it is mainly used without teleprotection signalling, as back up protection to a differential protection.

In EHV-networks, redundant protection systems are typical these days. To achieve this, the distance protection is either duplicated (two different types, usually from different suppliers) or it is combined with a differential or phase comparison protection.

In the case of duplicated distance protection, different modes for the teleprotection signalling are used when possible. Dissimilar principles, like under-reach transfer trip and directional comparison schemes, or release and blocking modes are combined to eliminate the so-called common mode failures.

The following characteristics are common for the distance protection in transmission networks:

*Three phase/single phase ARC*

the following ARC-variants are implemented in transmission networks:

- three-pole ARC with short dead-time for all fault types (preferred in the USA)
- single phase ARC with short dead-time during single phase faults (in seldom cases also during two phase faults without earth) – no ARC during multiple phase faults (common in Germany)
- single phase ARC with short dead-time during single phase faults – three phase ARC with short dead-time during multiple phase faults

In some countries an additional three phase ARC with long dead-time is common.

Beyond this, there are further obscurities such as for example the implementation of three phase ARC only during single phase faults along with the blocking of ARC during three phase faults.

*Common or phase-segregated tripping circuits*

In earthed networks, the single phase earth fault must be detected by the protection, and isolated. In networks without ARC, or with three phase ARC only, the circuit-breaker is tripped three phase. This simplifies the circuit-breaker control and the protection. The latter in this case need not be phase-selective. Each single phase fault would however result in a three phase interruption of the feeder.

This mode of operation is preferred in the USA.

When single phase ARC is implemented, the circuit-breaker poles must have phase-segregated tripping and prior to ARC, the protection may only trip the circuit-breaker pole of the faulted phase during single phase faults. Only the final trip, following unsuccessful ARC is three phase. The control circuit of the circuit-breaker must in this case be phase-segregated, and the distance protection must provide phase-selective tripping logic, with a separate tripping relay for each phase.

This is general practice in Central Europe.

*Distance protection for single phase ARC*

In this case, the distance protection must be specially arranged for the selective detection and isolation of single phase faults. This is the case with the numerical 7SA relays. Phase-selectivity presents problems on long, heavily loaded lines, because the load impedance reaches a similar order of magnitude as the short-circuit impedance (refer to paragraph 3.1.6). For this eventuality, the impedance fault detection of the numerical relays 7SA6 and 7SA522 contain a special supplementary algorithm, which under extreme conditions, securely detects the faulted phase by means of angle comparison and pattern recognition with symmetrical components, as well as by means of evaluation of delta-quantities (total fault current minus memorised pre-fault load-current).

The under voltage controlled overcurrent (under-impedance) fault detection, common in German-speaking countries, is particularly selective during single phase faults,



because the voltage collapse only occurs in the faulted phase. A pre-requisite however is, that the phase-earth voltage is measured for earth faults and the phase-phase measuring systems are blocked.

This can be ensured via the earth fault criteria ( $I_E >$  and  $3 \cdot U_0 >$ ), or only the three phase-earth measuring systems can be used from the onset. The latter was the standard with the electro-mechanical fault detection devices (R3Z2 and R3Z3v). In the case of numerical protection, the first setting method is recommended, because this provides additional fault detection security during two phase faults.

#### *Protection during switching onto faults*

Overhead lines in the transmission system always have a dedicated set of voltage transformers on the line-side of the circuit-breaker, to which the distance protection is connected. When energising the line, the possibility exists that switching onto a short-circuit (working earth not removed) occurs. As in this case no voltage for a direction decision is available, a directional distance zone cannot provide absolutely secure tripping.

In the case of numerical relays, an additional logic is activated, when energising the line. This logic releases, for a set period following the manual close command, the non-directional over-reach or the fault detection zone for un-delayed tripping. In any event, it must be a zone which does not have a boundary crossing the origin of the impedance diagram, but one which encloses the origin with a sufficient security margin (off-set zone).

The reach of the zone should not be too large, to prevent it from picking up with the in-rush current of the line or cable. In the case of long lines in excess of 100 km, or cables with large loading capacitance, the release of the over-reaching zone (non-directional) with only a 20-30% reach beyond  $Z_L$  is preferred over the commonly used starting zone with a long reach (sensitive setting). This problem arose mainly with fast static analogue relays. Numerical relays have effective fundamental frequency filter and are therefore less sensitive.

#### *Parallel-lines*

In industrialised countries, a large portion of the transmission lines are double circuit lines. Often even more than two three-phase systems, which may also belong to different voltage levels, are connected to one tower.

The coupling of the zero-sequence systems demands a corresponding setting of the distance zones, and possibly the implementation of a parallel-line compensation. The latter is in any event essential for an accurate determination of the fault location (refer to paragraph 3.5.3).

#### *High-resistance faults*

Transmission lines are usually suspended from steel towers and provided with one or more earth-wires. Therefore the earth fault resistance during flash-overs on the isolators is only a few ohm. In the case of rare arc-faults, at mid-span (e.g. as a result of a

brush-fire), or during flash-overs to trees, very high impedance faults may result. Depending on the setting of the zones in R-direction, a maximum of some tens of ohms can be detected. Larger resistances are outside the reach of the distance protection, and must be detected by a separate earth fault protection. For this reason, the distance 7SA relays contain a sensitive directional earth fault protection (minimum setting  $I_E \geq 0.1 \cdot I_N$ ). This can be used as a time-delayed back up protection, or in conjunction with a signal transmission device it can be extended to be a fast directional earth fault comparison protection. In this manner, earth fault resistance of several hundred ohm can be detected.

#### *Protection with information transfer*

Important transmission lines are almost always provided with communication channels. Criteria for the selection of the mode of the teleprotection in conjunction with the distance protection are stated in paragraph 5.1.4.

In the past, only narrow band PLC-channels or microwave radio channels, and in some cases aerial co-axial cables were available. Therefore, as a rule, duplicated distance protection or distance protection combined with phase comparison protection was implemented.

With the advent of modern digital communication via optical fibre and microwave radio, fast channels for the transfer of coded information have become available. Here-with, differential protection can now also be implemented on longer feeders. A remaining problem however is the switching of the channel path which may lead to a variance and unsymmetry of the signal transmission times. This can only be compensated by the differential relays with the use of GPS synchronisation. As a result, many utilities still prefer duplicated distance protection systems, when a dedicated communication channel with a defined signal transmission time is not available.

#### *System power-swings*

Loosely meshed networks, with long transmission lines, have a tendency towards power swings. The power swings are in general initiated by short-circuits and switching operations, i.e. when the transfer impedance changes suddenly.

The range of the power swing frequency is wide, depending on the system conditions, and can vary from below one Hertz up to several Hertz. In the case of fast power swings, the system becomes unstable, and loses synchronism (out of step).

The power swing supplement in the distance 7SA relays can be set as a power swing blocking or power swing tripping function (refer to paragraph 3.1.11).

In tightly meshed, high capacity networks, where the feeders are operated with small transmission angles, power swings with large amplitudes do not occur, so that no power swing blocking is necessary (in Germany none are in service at present).

### *Long lines*

In geographically large countries, long transmission lines must be considered.

Due to the following phenomena, these long lines present a special challenge to the distance protection:

- small short-circuit currents, substantially below nominal current, in the range of charging and non-symmetry currents.
- load-impedances which are close to the short-circuit impedance(s).
- rotation of the directional characteristic, due to the large transmission angles (refer to paragraph 3.3.5).
- transient oscillations due to the large charging capacitance and resonance with compensating reactors.
- diverse phenomena relating to series-compensation (refer to paragraph 3.5.7).

Numerical measuring techniques have introduced a decisive improvement of the protection behaviour in relation to all these influencing factors.

- the selective fault detection is achieved with optimised starting characteristics and flexible settings in combination with innovative, intelligent algorithms (impedance comparison, pattern recognition, online computation and evaluation of symmetrical components)
- the influence of higher order harmonics is almost completely suppressed with digital filters.
- the voltage inversion phenomenon in the case of series-compensated lines is largely dealt with by frequency compensated digital voltage memory.

### *Capacitive voltage transformers*

Capacitive voltage transformers are implemented especially in EHV-networks due to cost constraints. At the same time they facilitate the coupling of the power line carrier signals.

The distance protection must be able to deal with these transient oscillations (refer to paragraph 5.1.5).

### *Current transformers with air-gaps in their core*

In the case of large short-circuit ratings, and a lay-out of the current transformer for a complete ARC-cycle C-O-C-O (reclosure onto a fault), the current transformer cores are sometimes provided with anti-remanance air-gaps (class TPY), or linear cores (class TPZ). In the case of linear core CTs, a high de-magnetisation (relaxation) DC-current component arises following tripping of the short-circuit current. The current fault detectors must be provided with suitable filters to avoid reset delays (refer to paragraph 5.1.5).

### 5.3.2 Protection concepts

The protection concepts for typical application examples in transmission networks are referred to below.

#### 5.3.2.1 High-voltage overhead lines

In industrialised countries, this voltage level is characterised by its partial transmission and partial distribution attributes. In Germany, the 110 kV network mostly belongs to the second category. In developing countries however, the high voltage network is often required for power transmission.

For the protection planning, the following criteria are decisive:

- critical fault clearance time (is non-delayed tripping required on 100% of the feeder, or is it permitted to trip faults at the end of the line in the second zone with a delay of 300 to 500 ms?)
- earthing of the star-point (type of earth fault protection)
- Redundancy concept (is a second protection device required, or is remote back up protection sufficient?)

#### *Effectively earthed system*

Typically, distance protection as main protection with directional overcurrent back-up protection is used at this voltage level (figure 5.35)

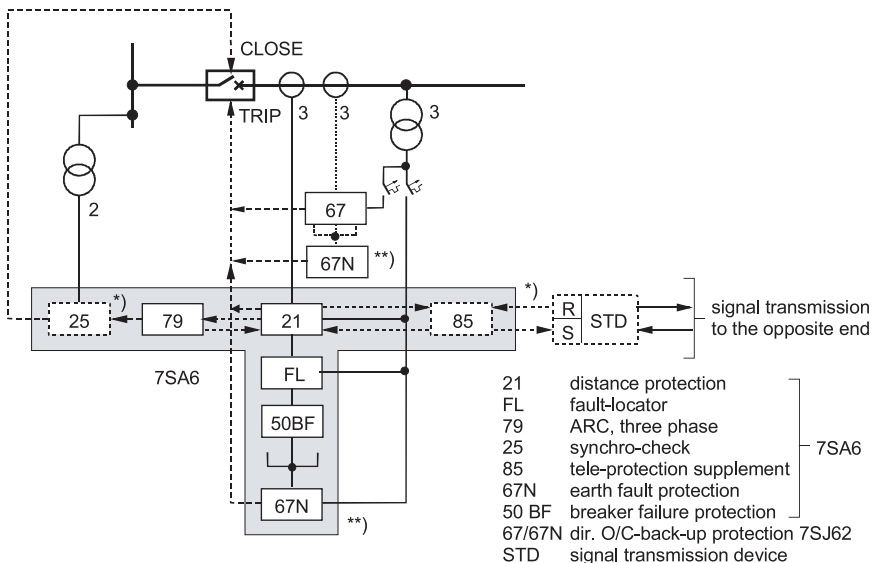


**Figure 5.35** Protection concept for high voltage line

In the case of important lines, or stability problems, fast non-delayed tripping may be required for short-circuits on 100% of the line. In this case, a protection system with signal transfer should be implemented.

The earth faults are usually detected by the distance protection. For high-resistance earth faults, an additional sensitive over-current earth fault protection is required. In the case of conventional protection separate inverse time earth-fault relays were used for this purpose. In the case of the numeric distance protection (7SA6), directional and non directional earth current protection with various modes definite and inverse time-delay (IDMTL) is available. The pick-up sensitivity is in the range of 5 to 20%  $I_N$ .

In special cases, where high-resistance faults with associated small fault-currents must also be cleared with-out time-delay, the directional earth-current element may be used with a signal communication channel to provide an earth-current direction comparison protection.

When the distance protection is implemented as POTT or Blocking scheme, then the same signalling channel may be used for the directional earth current comparison in the permissive or blocking mode.

Three-phase auto-reclosure is normally used at this voltage level.

For single-phase earth faults, the single-phase ARC may also be selected. A pre-requisite for this however is, that phase-segregated operation of the circuit-breaker poles is possible.

With multiple-phase faults, the three phase tripping and ARC is in any event used, in some cases followed by a further longer dead-time ARC-cycle. Single phase rapid ARC is possible for two phase faults without earth with the 7SA6. This is however seldom implemented, as the circuit-breaker is generally not configured for the high stress associated with this.

The ARC practice is different from one utility and country to the next, depending on the individual system conditions and operational experience (refer to paragraph 3.1.12). Modern numerical relays offer a complete range of ARC modes (multiple, fast, delayed, single and/or three-pole) and can be adapted to the current practice by parameter setting.

Should the OH-line include a cable section at an end, then selective ARC for OH-line faults only, could be arranged by special zone setting and an add-on logic.

In the proximity of power stations, a synchro-check function is required to prevent the asynchronous closing of a circuit-breaker and resultant damaging of the generator.

In case of cables, a thermal overload protection may be added.

Breaker failure protection, now offered with numerical relays, is applied with newer installations. Remote back-up protection by time graded distance zones and earth current steps, however, is still wide-spread.

The numerical distance protection 7SA6 includes all the stated protection functions for this application. For lines up to about 100 km, the teleprotection scheme could be oper-

ated with direct communication through optic fibres. Otherwise external communication modems or devices would have to be provided (see paragraph 4.3) corresponding to the available signalling channels.

For the independent directional and non-directional overcurrent back-up protection, the relay 7SJ61 would be appropriate. It would also provide redundant earth fault protection in parallel to the distance relay 7SA6.

#### *Compensated networks (Peterson-coil earthing)*

The implementations for the effectively earthed network also apply in this case, with the exception of the earth fault protection (figure 5.35).

Single phase to earth faults must not be tripped by the short-circuit protection, but shall normally self-extinguish or otherwise be tripped by remote control after appropriate system reconfiguration. The location of the earth fault is indicated by separate directional earth-fault relays. In case of double earth-faults (typically cross country faults), only one preferred phase must be tripped.

The distance relays of German manufacturers can be adapted to this kind of operation by parameter setting (refer to paragraph 5.2.2).

Signalling channels are not required in most cases. For fast fault clearance, the zone extension controlled by the ARC is implemented (refer to paragraph 3.1.12). The fast ARC dead-time is always three phase, with a setting of between 0.3 to 0.5 s.

Plain distance relays without additional back up protection are typically used. This is general practice for example in the German 110 kV network. Following a protection or circuit-breaker failure, the upstream relay has to clear the fault in a higher zone.

The wattmetric directional earth fault relays, used in distribution networks, are only suitable for radial or ring line arrangements and need additionally core balance CTs.

In the meshed HV-networks, special earth fault relays are used which respond to the transient charge oscillation after fault inception (7SN60).

#### **5.3.2.2 EHV-line**

The EHV-networks facilitates power transfer, sometimes over large distances. Due to their importance, lines at this level are provided with redundant protection systems. In general, two different main protection systems are implemented. These are either two full scheme distance protection devices, or one distance protection, and one phase comparison or differential protection. When two distance protection systems are implemented, these are preferably of a different type or from different manufacturers, to avoid common mode failures as far as possible. Distance protection can be implemented on practically any line length. The phase-comparison protection is applied to lines with a length of up to 200 km, mainly using narrow-band PLC-channels (2.5 or 4 kHz). These days, differential protection with digital signal transmission is increasingly used as the second main protection, in conjunction with distance protection. The

signal transmission is implemented with separate dedicated optical fibres, or via channels in a digital communication network, where possible.

The criteria for the selection of the teleprotection operating mode of the distance protection were discussed in paragraph 5.1.4

In Germany, the under-reach transfer trip with zone extension is used almost without exception.

Outside Europe, it is common practice to implement different modes of operation. For example, an under-reach transfer trip in conjunction with a release or blocking mode (see paragraph 5.1.4).

The protection of the EHV-line is characterised by the following features (figure 5.36):

- redundant protection with two main protection systems
- a dedicated signal transmission channel for each protection system, if possible via different media and paths e.g. fibre-optic and PLC or microwave radio
- battery and trip circuits are completely separated for each protection system
- power swing blocking<sup>1</sup> (targeted power swing tripping at selected locations in the network)

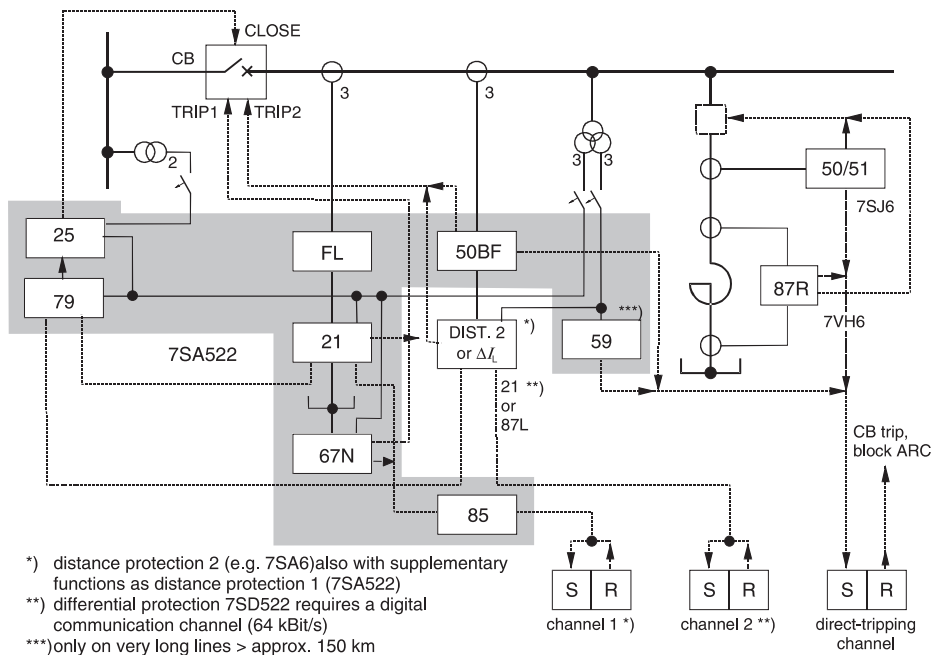


**Figure 5.36** Protection concept for EHV-lines

<sup>1</sup> In Germany, no power swing blocking functions are in service, due to the high system stability. The German utility board however requires that a retro-fit must be possible without undue effort. In the case of numeric distance relays 7SA, this function is always included and can be activated by changing the setting parameters.

- Over-voltage protection on long lines above 100-200 km
- In the case of compensating reactors on the line, additional direct tripping channels are required to trip the circuit-breaker at the remote end and to block auto-reclosure.
- A synchro-check function is recommended when the risk exists, that the system emf at the two line ends may drift apart during the three phase ARC dead-time (during single phase ARC, this function is not required). If one- and three phase ARC are implemented, the synchro-check function is automatically by-passed in the 7SA6 and 7SA522 relays during a single phase ARC cycle).
- In regions, where high-resistance earth faults are expected (rocky ground; flash-overs to earth at the middle of the span due to rapid growth of vegetation or brush fires) an additional directional comparison earth-fault protection scheme must be used. The pick-up sensitivity is in the range from 10-20% of CT nominal current.

This function must be blocked during the single phase dead-time, to prevent it from picking up with the load current flowing via the earth return path, which would result in an incorrect trip. With the 7SA6 and 7SA522 relays the blocking takes place automatically.

- In many cases an earth fault back up protection with a similar sensitivity and definite or current-dependant time-delay is provided instead of, or in addition to the directional comparison earth fault protection.

In Germany, it is common practice to implement a directional earth fault protection with a  $U_0$ -dependent time-delay. This protection detects high resistance faults, for example during flash-overs to trees and in general provides remote back up protection during earth faults, when the distance protection can no longer pick up due to the intermediate in-feeds [5.31].

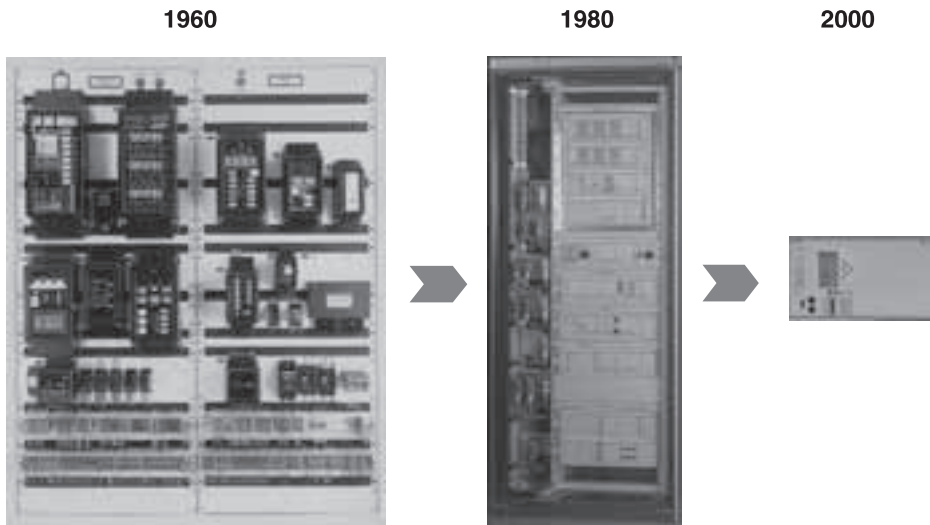


**Figure 5.37**

EHV line protection. One full scheme distance protection scheme with add-on functions in mechanical, static and numerical technology



The  $U_0$ -dependent inverse time-delay provides good selectivity, as the  $U_0$  voltage is largest at the fault location (short trip time-delay), and decreases as the distance to the fault location increases (increasing trip time-delay).

The protection functions required at each line end are provided by the numerical protection in one multi-functional relay (e.g. 7SA6). The second protection is provided by a suitable additional relay (differential relay 7SD522 or distance relay 7SA522). The equivalent scope of protection used to require two full panels or cubicles with conventional technology and individual devices (figure 5.37).

**5.3.2.3 1 1/2 circuit-breaker substations**

The connection of the protection for this type of sub-station is shown in figure 5.38.

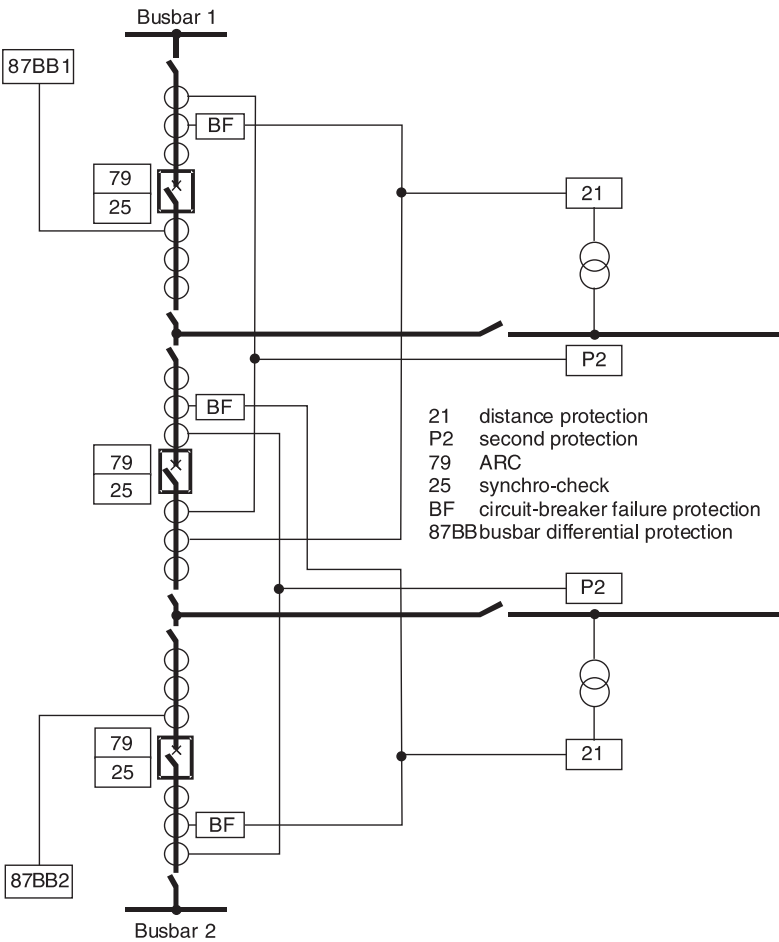


**Figure 5.38** Protection concept for a 1 1/2 circuit-breaker bay

It is characterised by the following special features:

- The current for the feeder-protection must be derived by summation (parallel connection) of the two CT-currents in the diameter (branch between the two busbars).
- The feeder-protection must trip two circuit-breakers. Both circuit-breakers must be tripped simultaneously. Reclosure is done sequentially. The second circuit-breaker will only be closed if the first circuit-breaker remains closed for a set time (no solid fault). Usually a switch is provided to select either the centre or the busbar-side breaker to be closed first.
- The ARC and synchro-check functions are allocated to a separate unit for each circuit-breaker in this case. The numerical protection device 7SK512 is suitable for this application.
- The circuit-breaker failure protection must also be provided for each circuit-breaker separately. For this purpose, the device 7SV512 is best suited. This device is constructed for dual-channel initiation and two-stage operation, to provide high security against over-functions. Its current monitoring and logic is realised on a phase-segregated basis, and is therefore suited to applications in conjunction with single phase ARC.
- The 1 1/2 circuit-breaker configuration requires additional interlocking and selection circuitry, which cannot be referred to in detail here. It must however be noted that the voltage for the synchro-check function must be derived, depending on the circuit-breaker and isolator positions in the diameter and feeder. Programmable logic functions in numeric relays may be used to replace the largest part of the wired circuits.

For the selection of the line protection system, the information provided in relation to HV- and EHV-feeder-protection above, applies.

#### **5.3.2.4 Ring busbar**

For the ring busbar, similar conditions to those of the 1 1/2 circuit-breaker configuration apply. The connection of the protection is represented in figure 5.39.

#### **5.3.2.5 Double circuit line**

In essence, the protection is almost the same as that of a single line. The exceptions result from the zero-sequence system coupling. The possibility of double-faults, which affect neighbouring three phase systems simultaneously, must also be considered. The parallel-line effect and its influence on the distance protection was referred to in paragraph 3.5.3. The parallel-line compensation for the distance protection and/or fault locator function can be optionally selected in the relays and 7SA6 / 7SA522. The connection is shown in figure 5.40 by means of an example.

The calculation and selection of the protection settings for the double circuit line are explained in paragraph 7.1 by means of an example.

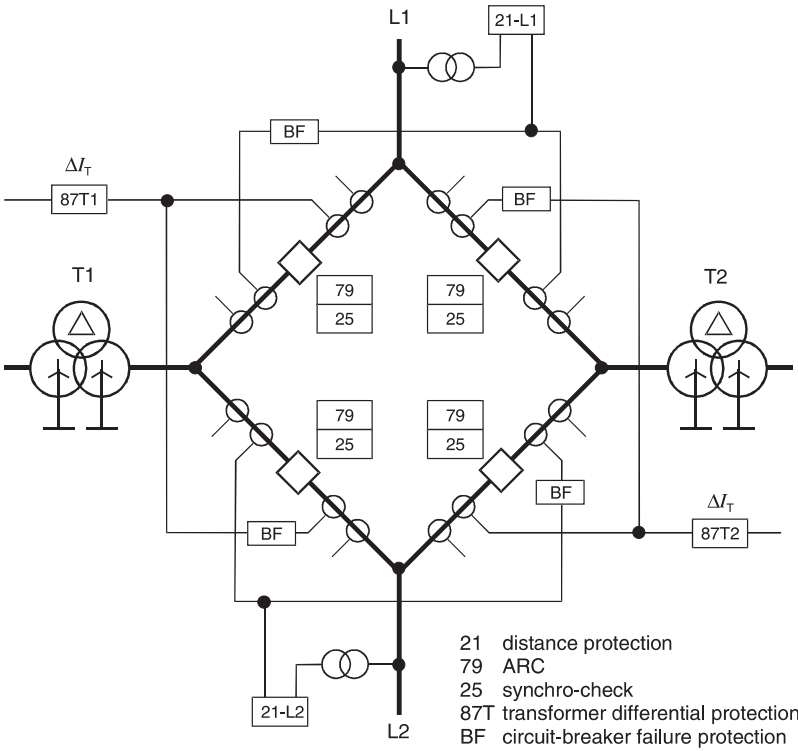


**Figure 5.39** Protection concept for a ring busbar (only one protection system shown)

### 5.3.2.6 Three-terminal line

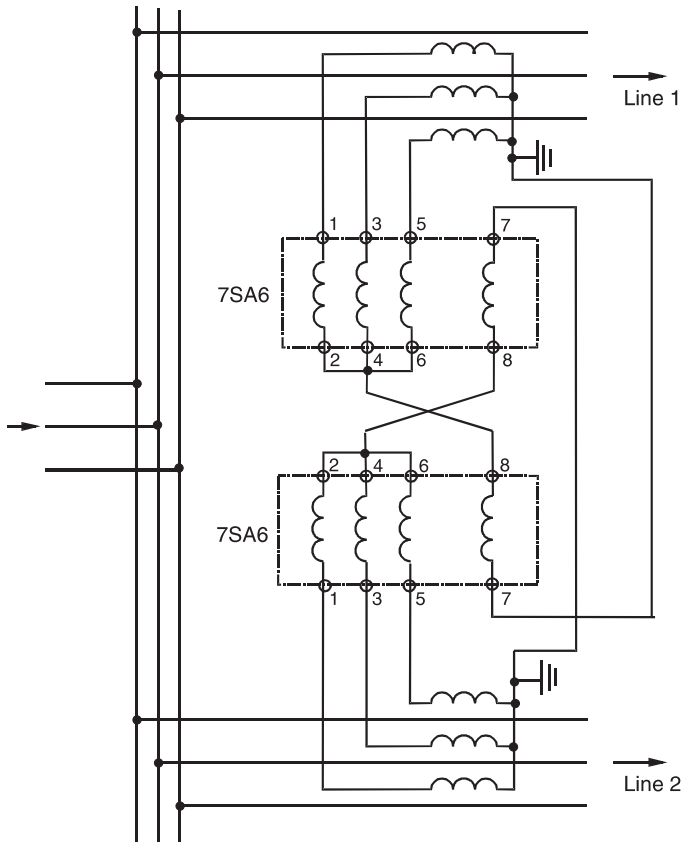
The fundamental problem with this line-configuration is the intermediate in-feed to the fault location from the third terminal [5.32]. This effect was covered in paragraph 3.5.2. The settings are discussed by means of an example in paragraph 7.2.

With selective grading of the back up distance zones, short reaches and slow tripping times must in general be tolerated when there is an in-feed from the third terminal.

If all short-circuits on the three-terminal line must be cleared without time-delay, then a protection system with signal transmission must be applied. For this purpose, communication channels between all three line terminals are required.

The simple under-reach transfer trip can only be implemented under ideal conditions, when all three line-lengths to the node are approximately the same. Only in this special case, can the under-reaching zone of the distance protection be set to reach beyond the node, and thereby ensure that all internal faults are detected by at least one of the under-reaching zones.

Generally, a permissive overreach transfer trip protection with over-reaching zones is implemented. The reach of the zones must be selected such that they reach beyond the most remote opposite end, even during the worst intermediate in-feed conditions. The

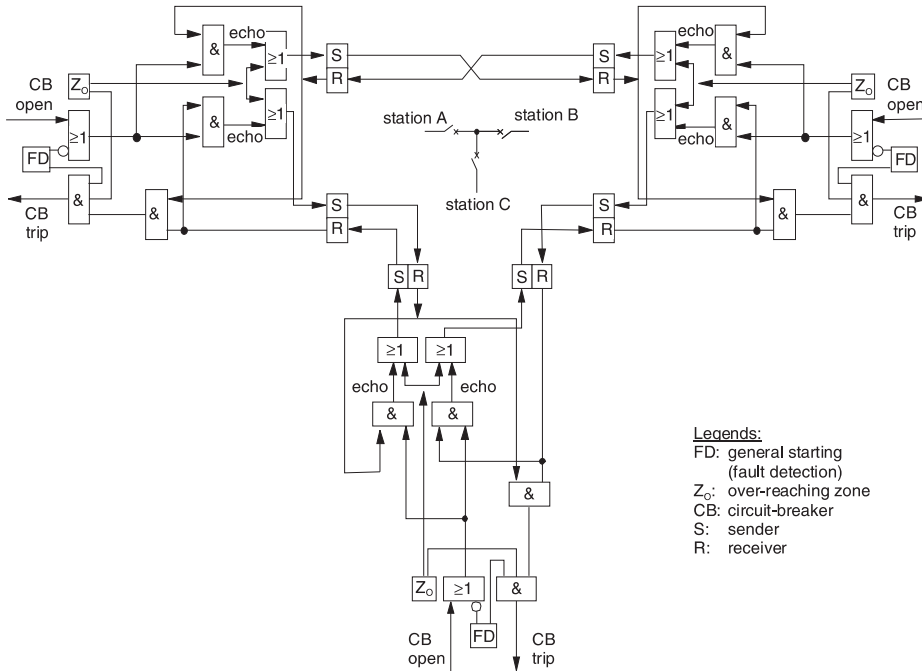


**Figure 5.40** Parallel-line compensation; connection in the case of relay 7SA6

trip-release is activated when the permissive signal from both opposite ends is received (series-connection of the signal-receive contacts). On line ends with weak in-feed or during open circuit-breaker conditions, the received signal is echoed to the corresponding transmitting end. In figure 5.41, the basic circuit-configuration is shown. The details of the weak in-feed supplement are represented in figure 3.37, paragraph 3.1.10.

With the numerical 7SA relays, the under-reaching distance zones are additionally in functional parallel to the signal-comparison protection. This may be beneficial in the case of an “out-feeding” condition (see paragraph 3.5.2). The signal-comparison protection would block in this case. By tripping with the under-reaching zone, at the end closest to the fault, the out-feed condition is terminated, and the remaining two-terminal line can be isolated with the normal or via the echo function.

With three-terminal double circuit lines, relatively complex conditions arise, which may demand additional communication channels [5.33].

**Figure 5.41**

Permissive overreach transfer trip protection for three-terminal line: function diagram

### 5.3.2.7 Series-compensated lines

The following alternatives are possible [5.34]:

- series-capacitor at the centre of the line, with degree of compensation < 50%.
- series-capacitor at a point along the feeder, with degree of compensation > 50%.
- series-capacitor at the line ends.
- current transformers on the line or busbar side of the capacitor.

In the first case, the short-circuit loop is always inductive, similar to that of lines without series-compensation. This implies that a voltage memory for the direction-determination is not required. With the series-capacitor in service, the line-length appears to be reduced. The under-reaching stage can accordingly only be set with a grading factor of below 50%.

For the main protection, only a directional comparison protection based on distance over-reaching zones is suitable. Both blocking and release-modes are acceptable.

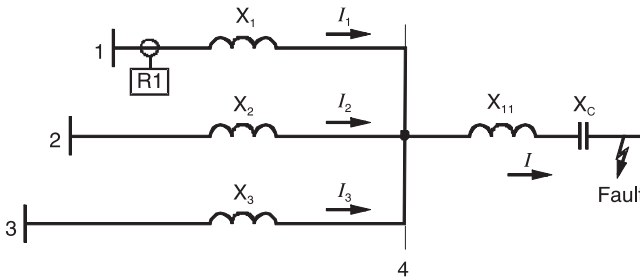
When capacitors are located at the line ends, voltage inversion may occur during short-circuits. A voltage memory is therefore required for the direction determination (refer to paragraph 3.5.7).

In this case, the relays 7SA6 or 7SA522 are to be employed, which are designed and tested for series-compensated overhead lines. They have frequency compensated voltage memories of sufficient length (up to 2 s).

Under certain conditions, a current inversion may occur during short-circuits without ignition of the arc-gap. For such system conditions the distance protection is not suitable as main protection. In such cases a protection utilising  $\Delta U/\Delta I$ -measurement (protection with delta-values or travelling wave protection) must be employed.

The positioning of the voltage transformers also plays a role. When the VT is situated on the line-side, faults on the line are measured with the correct impedance, while with reverse faults, the impedance magnitude may be reduced and voltage inversion may occur. With VTs on the busbar side, the conditions are reversed. When a directional comparison protection is employed with voltage memory, the same protection behaviour results for both cases.

The second main protection may be provided with differential protection when digital signal transmission channels via optical fibre are available. In the past, phase-comparison protection with PLC-communication was often implemented. Due to sub-harmon-



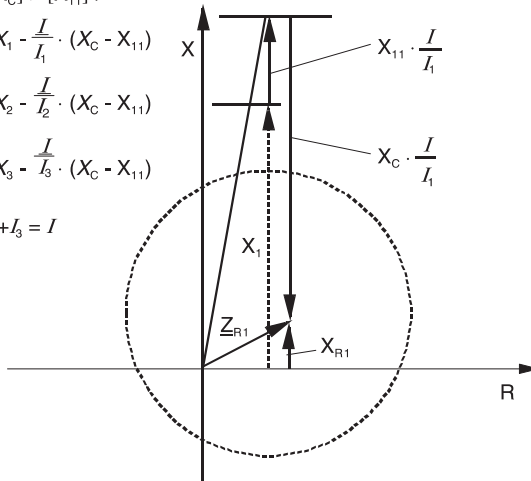
With  $[X_C] > [X_{11}]$ :

$$X_{R1} = X_1 - \frac{I}{I_1} \cdot (X_C - X_{11})$$

$$X_{R2} = X_2 - \frac{I}{I_2} \cdot (X_C - X_{11})$$

$$X_{R3} = X_3 - \frac{I}{I_3} \cdot (X_C - X_{11})$$

$$I_1 + I_2 + I_3 = I$$



$X_{R1}$ : Reactance seen by the relay in station 1

**Figure 5.42** Influence of a series capacitor on neighbouring lines

ics, so-called “creeping” current zero-crossings occur, which the protection must be able to deal with (separate thresholds for positive and negative direction for the current zero-crossing detection).

The earth-current direction comparison protection for high-resistance faults must be set substantially less sensitive on series-compensated lines, as the non-symmetrical ignition of the arc-gaps or varistors causes a relatively large summated current to flow.

### *System analysis*

When series-capacitors are deployed, it is in any event recommended to do a computer-analysis, in which the phenomena and protection influences as described in paragraph 3.5.7 can be examined. Note must be taken, that the voltage inversion may extend to neighbouring feeders without series-compensation (figure 5.42). This implies that the surrounding parts of the network must be included in the analysis.

---

## 6 Protection settings

The protection settings (parameterisation) must achieve the following:

- a) selection and activation of the required protection and supplementary functions;
- b) adaption of the protection to the network and instrument-transformers;
- c) configuration of the interface to the plant (marshalling of the alarms, commands, as well as binary inputs and outputs);
- d) configuration of the serial interfaces;
- e) setting of the pick-up thresholds.

The setting of the numerical protection is done on a PC (figure 6.1). For the Siemens protection relays, the operating programme DIGSI, which runs under Windows, can be used [6.1, 6.2].

The individual setting parameters and the setting procedure are described in detail in the respective relay manuals.

The recommendations for the derivation of the distance protection settings are described below.



**Figure 6.1**  
Protection setting on a PC



## 6.1 General aspects

The following is decisive for the setting:

- *System data*: voltage level, configuration, line impedance per km, line-length
- *Instrument transformer data*: ratio
- *In-feed conditions*: single- and three phase short-circuit rating (maximum and minimum) or corresponding source impedances of the positive and zero-sequence systems
- *Load conditions*: maximum load in terms of real and reactive power, charging currents
- *Fault resistances*: length of isolators, conductor spacing, ground consistency

Depending on the particular application, the following must also be considered:

- *Transient behaviour*: power swings (maximum frequency), in-rush currents (cable, transformer, motor)
- *Series-compensation*, and the phenomena related to this

Numerical distance protection provides optimised characteristics and a high degree of flexibility in regard to the settings. Beyond this, a dynamic adaption of the set values to the system, load or in-feed conditions is possible by means of deliberate switching to a different set of parameters (adaptive protection).

The practical relay settings however in general demand a careful compromise between fault-sensitivity, speed and selectivity.

## 6.2 Fault detection (3<sup>rd</sup> Zone)

The aim is to achieve the largest possible reach and fault sensitivity, without threatening the stability during load and transients. This applies in particular where remote back-up protection is practised.

With single system distance protection (earlier relay 7SA511), the fault detection must be phase-selective to achieve the correct loop selection by the logic and the desired phase-selective tripping with single phase auto-reclosure.

Full scheme numerical distance protection (7SA6, 7SA522) do not need a phase selective fault detection zone for fault loop selection. In this case the fault detection zone takes on the task of a far reaching non-directional back-up (4<sup>th</sup>) zone. In many cases only three zones are used (Anglo-Saxon practice). In this case the following relates to the 3<sup>rd</sup> zone.

Note: Full scheme relay 7SA6 optionally offers  $U/I/\varphi$  fault detectors (starters) to comply with the existing relaying practice in Continental Europe (compensated subtransmission and distribution networks).

### 6.2.1 Fault detection methods and setting philosophies

We have to distinguish between distance relays with common starter (fault detector) control and relays with zone packaged design (see paragraph 3.1.8). In the first case, a separate starting zone exists in addition to the distance zones. It assumes the task of fault detection, phase selection and common timer control. In the second case, each zone is independent, an explicit fault detection zone does not exist.

#### *Distance relays with fault detector (starter)*

In Continental Europe, switched distance relays with overcurrent starters and under-impedance starters (voltage controlled O/C starters) have traditionally been used in distribution and subtransmission networks.

Setting is in this case rather simple and has only to consider the maximum load current of the protected line and the the lowest system operating voltage. The relay setting values are more or less the same in the total network.

Angle dependent under-impedance starters have been used with longer lines, in particular at the transmission level. Their setting had additionally to consider the reactive power flow, i.e. the lowest  $\cos \varphi$ .

For compatibility reasons, the numerical relays of German manufacturers continued this tradition and offered upgraded  $U/I/\varphi$  starters. In addition, impedance starters were implemented to comply with the overseas relaying practice. In the latter case, the setting is in principle based on line and load impedances.

The earlier relays 7SA511 (single system type) and 7SA513 (full scheme) were designed to this concept. The user could now choose between current/voltage and impedance type fault detection by a configuration parameter.

#### *Zone packaged distance relays*

This concept has been used by Anglo-Saxon manufactures also with earlier technologies. In this case each zone is independent. The fault is detected and indicated when the measured impedance enters any zone.

The farthest set zone in X-direction defines the remote back-up reach. The farthest reaching zone in R-direction defines the maximum fault resistance coverage and must be coordinated with the maximum line loading. Normally, zone 3 is the limit in both cases.

With modern relays a cone shaped cutout (see paragraph 3.1.6, figure 3.20) can be set which limits the reach of distance zones in R-direction in a defined angle area and makes the relay less sensitive to load encroachment.

For the setting of the 3<sup>rd</sup> zone and the load blocking area the same rules apply as for the separate fault detector zone.

The relays 7SA522 and 7SA6 are examples for the zone packaged design (At relay 7SA6,  $U/I/\varphi$  starting and common timer control can be chosen as option).

### 6.2.2 Security of the fault detection

The required reach of the fault detection depends on the selected protection concept.

In the case of a concept with remote backup protection, the fault detection must in any event cover the longest of the lines connected to the next station, so that in the case of a protection or circuit-breaker failure on one of the neighbouring lines, the back up protection securely picks up.

In the case of a concept with duplication of the protection, and local back up protection (circuit-breaker failure protection), the fault detection must in principle only cover the protected line with a security margin of approximately 20% to 30%. This concept is typical on transmission networks outside Germany. In this case it is also attempted to achieve the largest possible reach for the fault detection.

The secure fault detection must in any event be checked, assuming a fault at the end of the desired reach, and analysis of the pick-up criteria  $U_{SC}$ ,  $I_{SC}$ ,  $\varphi_{SC}$  and  $Z_{SC}$  at the relay location. The largest possible intermediate in-feeds must be considered.

Additionally, the load-flow can have a negative influence, as it reduces the short-circuit angle (refer to paragraph 5.2, figure 5.24).

Fault resistance at the fault location has a similar effect. This applies to fixed resistances, such as for example the effective tower footing resistance (the reduction due to earth-wires must be considered, refer to paragraph 3.5.1, figure 3.109).

It is correct to consider the arc as a constant voltage and not as a constant resistance. Otherwise the in-feed from the remote end would result in the simulation of an unrealistically large R-value (refer to paragraph 3.5.1).

The consideration of all the influencing parameters, leads to a relatively complex calculation. Accordingly it is recommended to use a calculation programme to check the security of the starting. This programme indicates and, possibly automatically checks the starting criteria at the relay location for a particular fault location in the system.

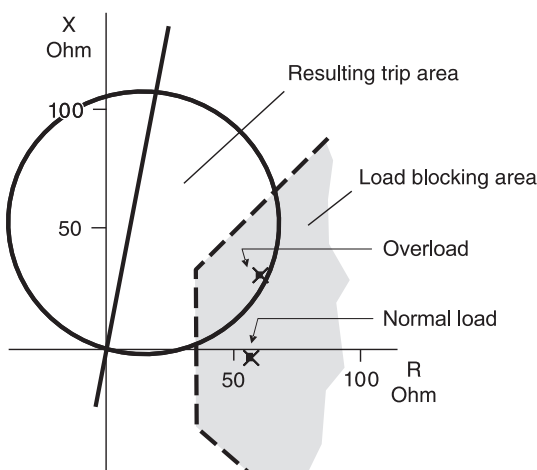


**Figure 6.2**

2003 blackout in the North West of USA and Canada: Overfunction of the 3<sup>rd</sup> zone of a distance relay due to overload and reduced system voltage (NERC report)

### 6.2.3 Relay (Line) loadability

Back-up zones with circle characteristic imply a high reach in R-direction and are therefore prone to overfunction during overload. Figure 6.2 shows a case which occurred during the 2003 blackout in the North West of USA and Canada. Using a shaped characteristic or a load blocking function would have avoided the problem.

It should be mentioned that the problem is increased with Offset MHO characteristics.

This 3<sup>rd</sup> zone problem has several times contributed to blackouts and has caused NERC (North American Electric Reliability Council) to issue recommendations to prevent and mitigate the impacts of future cascading blackouts: [6.3, 6.4] Recommendation 8a.

Evaluate zone 3 settings for the purpose of verifying that zone 3 relay is not set to trip on load under extreme emergency conditions:

- Zone 3 relay should not operate at or below 150% of the emergency ampere rating of a line, assuming 0.85 per unit voltage and a line phase angle of 30 degrees
- Set zone 3 relay to allow 20 min overloading (System operators need 20 min to shed load once a problem has been recognized).
- Distance relays should not be used to provide overload protection
- Relay should be set to ride through all recoverable swings

The relay loadability limit is the value of the load in MVA at which the relay is on the verge of operation. We can estimate it as follows:

Assuming rated voltage condition, the relay pick-up value  $9Z_\phi$  at a given angle  $\phi$  in the impedance diagram corresponds to a MVA line load of

$$S_\phi = \frac{U_{N(ph-ph)}^2 \text{ [kV]}^2}{(r_{VT}/r_{CT}) \cdot Z_{\phi\text{-secondary}} \text{ [Ohm]}} \text{ [MVA]} \quad (6-1)$$

The loadability depends on the relay characteristic and the angle range ( $\cos \phi$ ) of the load. This shows the following example.

#### Example 6.1: Relay (Line) loadability

- Given: Twin bundle 230 kV line: 200 km,  $Z_L = 60 \Omega$ ,  $\phi_L = 79^\circ$   
 Normal loading: 290 MVA, Thermal limit: 542 MVA ( $I_{th} = 1360$  A)  
 Protection: MHO distance relay  
 The relay characteristic angle  $\phi_R$  is adapted to the line angle  $\phi_L$   
 The 3<sup>rd</sup> zone is set to cover a following line of 100 km ( $30 \Omega$ ) by a margin of 25%:  $Z_{R3} = (60 + 30) \cdot 1.25 = 112.5 \Omega$  primary
- Searched: Maximum line loading in an angle range of  $\phi = \pm 30^\circ$
- Solution: In the case of a MHO relay, the pick-up value dependent on the short circuit, respectively load angle  $\phi$  is (see paragraph 3.1.4, equation 3-2):

$$Z_{\phi, MHO} = Z_R \cdot \cos(\phi_R - \phi),$$

where  $Z_R$  is the set zone impedance and  $\varphi_R$  the characteristic relay angle which is normally set equal to the line angle.

$$Z_{\varphi, \text{MHO}} = 112.5 \cdot \cos(79^\circ - 30^\circ) = 112.5 \cdot 0.656 = 73.8 \, \Omega \text{ primary.}$$

We use equation 6-1 to calculate the loading limit. (The VT and CT ratios can be left away as the relay impedance is already available as a primary value.)

$$S_{\varphi} = \frac{230^2 [\text{kV}^2]}{73.8 [\text{Ohm}]} = 717 \text{ MVA}$$

The results are illustrated in figure 6.3.

Comment:

Under rated voltage condition, line can be operated up to its thermal capacity (542 MVA) with a security margin of  $(717 - 542)/717 = 0.24$ , i.e. 24%.

During large system disturbances the voltage often drops due to reactive power control problems. At the same MVA loading, the measured relay impedances are therefore reduced with the square of the voltage.

For the thermal limit current of 1360 A and 85% rated voltage the relay would measure an impedance of

$$Z_{\text{emergency}} = \frac{0.85 \cdot U_N / \sqrt{3}}{I_{\text{th}}} = \frac{0.85 \cdot 230 \text{ kV} / \sqrt{3}}{1360 \text{ kA}} = 83 \, \Omega$$

This would still be outside the MHO limit of  $73.8 \, \Omega$  with a reduced security margin of 12%.

The calculation according to the NERC recommendation with 150%  $I_{\text{th}}$  would however result in  $55.3 \, \Omega$ , i.e. the measured impedance would appear in the MHO circle.

A load blocking cutout as shown in figure 6.2 would then be necessary.

#### 6.2.4 Phase-selectivity

Phase-selectivity of the fault detection is required for the selection of the measured signals in the case of a single system distance protection (early 7SA511 relay), and for the trip signal logic, when single phase ARC is implemented.

When over-current fault detection is used, it must in any event be set high enough to avoid starting of the measuring system in the healthy phases during overload or transient conditions (refer to paragraph 3.1.6).

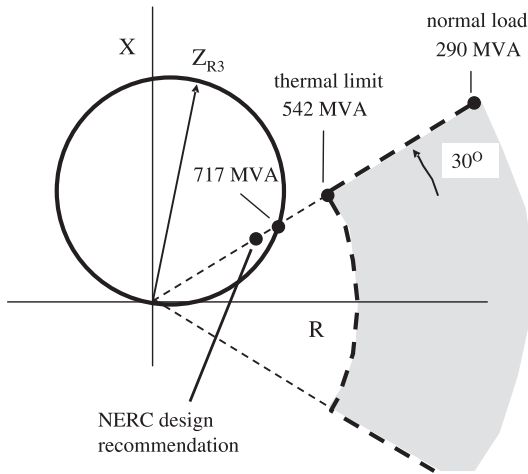


**Figure 6.3**  
Relay loadability in case  
of a MHO characteristic

The setting of impedance fault detection on the numeric 7SA relays is however not critical, as additional plausibility checks (impedance comparison) automatically prevent an over-function of the measuring systems on the healthy phases.

This applies to short and medium length lines of up to approximately 100 km.

On very long lines, substantially longer than 100 km, and with large load-transfer, the load-impedances are in a similar order of magnitude as the short-circuit impedance, so that an impedance comparison alone is no longer sufficient. In this case, additional intelligent algorithms for phase-selection become effective in the relays 7SA6 or 7SA522 as discussed in paragraph 3.1.6.

It is accordingly no longer necessary to severely restrict the tripping area, as was the case with electro-mechanical or static analogue protection (refer to paragraph 3.1.6, figure 3.19).

The detection of the faulted phase during single phase earth faults (important for single phase ARC) is achieved by angle comparison between the zero- and negative-phase sequence system currents, corresponding to the characteristic current distribution of the symmetrical components during a single phase fault.<sup>1</sup> Additionally, the load-currents flowing prior to fault inception are memorised and subtracted from the total current after fault inception, so that the “pure fault-currents” are available for the comparison.<sup>2</sup> The implementation of the super-position principle in electric circuits in this manner produces clear fault images, also in cases where the short-circuit current only amounts to a fraction of the load current.

Special settings are not required for this condition.

<sup>1</sup> This technique has already proven itself with analogue technology. Incidentally, it is also been used for the phase selection of the directional earth fault comparison protection in the 7SA522 and 7SA6 relays, where earth fault currents as small as 10%  $I_N$  can be detected.

<sup>2</sup> These fault-currents flow, if an emf with a voltage as was present prior to fault-inception, and of opposite polarity, is applied at the fault location. The actual source emfs are short-circuited.

### 6.2.5 Setting of the $U$ - $I$ - $\varphi$ fault detection

The pick-up characteristic is shown in paragraph 3.1.6, figure 3.17. Usually, the protection is set in such a manner that without earth-current the Ph-Ph measuring systems are released, and with earth-current detection a switching to Ph-E measurement takes place.

For most applications, the following settings are then suitable:

Setting parameters	Typical setting
$I_{ph>}$	$0.25 \cdot I_N$
$U_{(I>)}$	$70\% U_N$
$I_{ph>>}$	$2.50 \cdot I_N$
$U_{(I>>)}$	$90\% U_N$
$I_{\varphi>>}$	$1.00 \cdot I_N$
$U_{(I_{\varphi>>})}$	$90\% U_N$
$\varphi>$	$45^\circ$ el
$\varphi<$	$110^\circ$ el
$I_{E>}$	$0.25 \cdot I_N$ in the earthed system $0.5 \cdot I_N$ in the isolated/compensated system
$U_{E> (3 \cdot U_{0>})}$	$20 \text{ V}^*$ in the earthed system – not effective in isolated/compensated system

\* 100 V corresponds to the full displacement of the star-point by  $U_N/(\sqrt{3})$

For the Ph-Ph and Ph-E measuring systems, the same % setting is applied. In the case of the Ph-Ph measuring system,  $U_{ph-ph}$  (100 V secondary), and for the Ph-E measuring system,  $U_{ph-E}$  (58 V secondary) applies.

The following adjustments may be useful:

- the relatively high setting of  $I_{ph>>} = 2.5 \cdot I_N$  is for the consideration of the over-current which may arise when the parallel line is switched off. On single lines (radial feeders), the setting may be reduced down to  $1.3 \cdot I_N$ , when no larger than normal over-loads and in-rush currents are possible.  $U_{(I>>)}$  must then be reduced to  $80\% U_N$ .
- On long lines, where no large reactive power can be transferred, and short-circuit currents with a magnitude which is less than nominal current may arise, the setting of  $I_{\varphi>>}$  may be below nominal current (e.g.  $0.5 \cdot I_N$ ).
- The earth-current fault detection  $I_{E>}$  “switches” the  $U$ - $I$ - $\varphi$  fault detection from Ph-Ph to Ph-E measurement. In the numerical relay 7SA6 this pick-up threshold is stabilised with the phase-current to avoid an incorrect pick-up when large phase short-circuit currents and CT-saturation occur.

The value  $0.5 \cdot I_N$  is suitable for isolated and compensated systems with an un-extinguished earth-current of up to approximately  $0.35 \cdot I_N$ . In very large compensated

networks, where a larger earth-current flows during single phase earth faults, the setting threshold must correspondingly be increased ( $I_E \geq 1.3 \cdot I_{CE}$ ). In the extreme, the Ph-E fault-detection must be switched off (setting parameter “ineffective”).

Double earth faults are then detected by means of the Ph-Ph fault detection.

- In the earthed system, the  $U_E$  fault detection should always be activated when not all transformer star-points are earthed. Thereby the correct Ph-E loop is also measured at system locations where no earth-current flows during earth faults (refer to paragraph 3.1.6, figure 3.15).

When the numerical relays 7SA6 are parameterised for isolated/compensated networks, the  $U_E$  fault detection is automatically ineffective. Accordingly, incorrect fault detection during single phase earth fault cannot occur.

### 6.2.6 Setting of the impedance fault detection

In the earlier distance relays 7SA11 and 7SA513 the fault detection zone releases the distance zones and controls the timing (see paragraph 3.1.8).

In case of the relays 7SA6 and 7SA522 there is no common fault detection zone but each zone is independent (zone packaged design). The settings discussed here refer to the largest set zone and to the cone shaped load blocking zone.

The reference for impedance type fault detection is the nominal load impedance derived from the transmitted power at nominal voltage and nominal CT-current:

$$P_N = U_N \cdot I_N \cdot \sqrt{3}$$

*Example 6.2:*

$U_n = 110 \text{ kV}$  and CT 600/1 A

$$P_N = 110 \cdot 10^3 \text{ V} \cdot 600 \text{ A} \cdot \sqrt{3} = 114 \text{ MVA}$$

With this power, the relay measures a secondary load -impedance corresponding to:

$$Z_{Lsec.} = \frac{U_{n(sec.)}/\sqrt{3}}{I_{n(sec.)}} = \frac{(100 \text{ V})/\sqrt{3}}{1 \text{ A}} = 57.7 \Omega$$

Instrument transformers with a transformation to 1 A and 100 V are assumed. The relay rated current always corresponds to the rated secondary current of the CT.

In the case of 5 A rated current, the secondary load-impedance would be reduced by a factor 5.

*Comment:*

In the analyses below, it is assumed that the nominal current of the CT is matched to the natural load (long line  $\geq 100 \text{ km}$ ), or the permitted continuous thermal loading of the line. Moreover it is assumed that the line must be able to transfer approximately twice the nominal CT-current when parallel lines or network portions are switched off.



If the current transformers are dimensioned for larger nominal currents, smaller secondary currents appear at the relay with correspondingly larger secondary impedances (see conversion equation (3-1) in paragraph 3.1.2).

In this case, the current settings must be reduced by the corresponding ratio and impedance settings increased by the same ratio.

With twice the CT nominal current flowing, the measured operational impedance is halved ( $29\ \Omega$ ). If one assumes a 20% security margin, to allow for the reset ratio (1.05), and other influences (refer to grading plan), a maximum pick-up sensitivity is obtained as follows:

$$Z_{FD-(max.)} = \frac{57.7\ \Omega}{2} \cdot 0.8 = 23\ \Omega$$

With modern relays (7SA522, 7SA6) a cone shaped load blocking area is available. The permitted R-reach of this area is derived from the maximum load-angle  $\varphi_L$  with the following equation (figure 6.4):

$$R_{LB(max.)} = Z_{L(min.)} \cdot \cos \varphi_L$$

With a typical range of  $\varphi_L \approx \pm 30^\circ$ , a maximum R-reach of approximately  $20\ \Omega$  results.

The limiting angle for the load cut-out segment must be set greater than  $\varphi_{L(max)}$  with a security margin of at least 5 degrees. This would result in  $\varphi_{LB} = 35^\circ$ . On lines, shorter than 100 km, higher reactive load transfer is possible. In this case the default value of  $45^\circ$  may be appropriate.

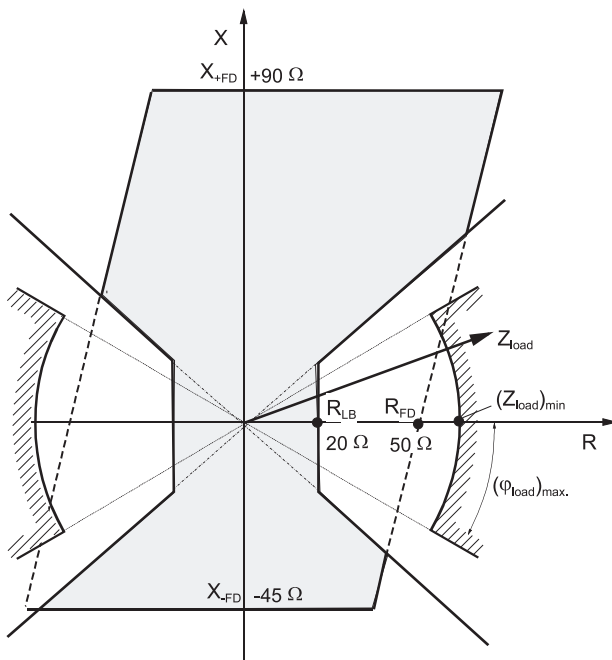


**Figure 6.4**  
Settings of the impedance  
fault detection: maximum  
reach in the R-direction

If one wants to detect fault currents as small as nominal current with a short-circuit angle that is greater than  $35^\circ$ , and with full rated voltage ( $U = U_N$ ), then the impedance reach at this angle must approximately be  $58 \Omega$ . This is achieved with a setting of  $R_{FD} = 50 \Omega$  (figure 6.4).

The reach in X-direction should cover the longest following line with a security margin of about 25%. Intermediate infeeds would have to be considered. Settings up to about  $200 \Omega$  (1 A relays) may be necessary with long lines. We assume here  $90 \Omega$  as an example for medium long lines.

For the reach setting in reverse direction, the same setting as in the forward direction may be used. As a rule however, a smaller setting of about one half of the forward setting should be sufficient. We take  $45 \Omega$ .

A more accurate calculation of the impedance fault detection reach requires an analysis based on the line impedances, all infeeds and the load flow. This basis for the analysis is particularly recommended for the transmission system. The principle is illustrated by the following example.

*Example 6.3:* Calculation of the setting values for the impedance fault detection

*Exercise:*

The network illustrated in figure 6.5 is given. The setting values for the fault detection of relay D must be calculated. The fault detection should cover the adjacent line in the forward direction, and reach with a security margin of 30% beyond the next but one sub-station.

In the reverse direction, the fault detection must reach 30% beyond the most remote station in terms of impedance.

*Solution:*

Initially, a short-circuit calculation must be executed for a Ph-Ph short-circuit in the sub-station E. For the sake of simplicity, pure X-values may be used in the calculation, as the R-components in the EHV-system are small ( $R < 0.1 \cdot X$ ).

The most unfavourable conditions for the reach arise when the three phase parallel line D-E is out of service.

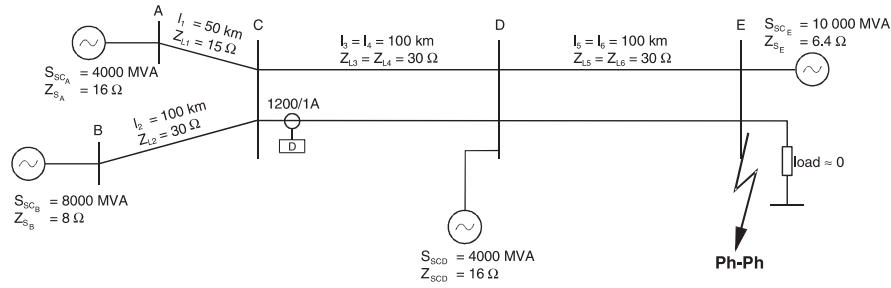
The results are shown in figure 6.5b. The Ph-Ph short-circuit voltage at the relay location amounts to 378 kV, and the short-circuit current to 900 A. The measured reactance according to equation (3-37) is:  $Z_{Ph-Ph} = 378\,000 / (2 \cdot 900) = 210 \Omega$ . Due to the intermediate in-feeds, the pure line impedance of  $2 \cdot 30 = 60 \Omega$  has increased by a factor of 3.5.

With the 30% margin, the following primary setting results:

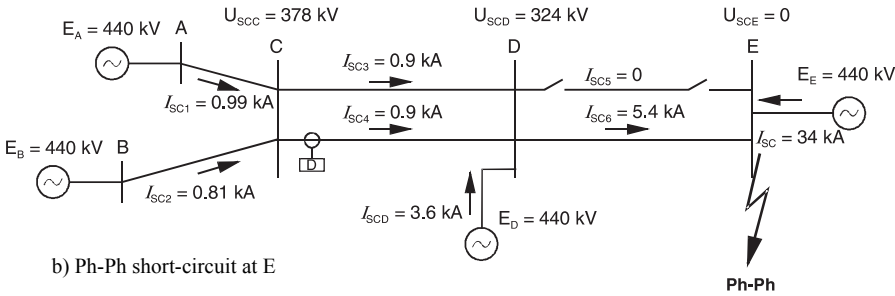
$$X_{+A \text{ primary}} = 1.3 \cdot 210 = 273 \Omega$$

The impedance conversion factor to the secondary side of the instruments transformers is:

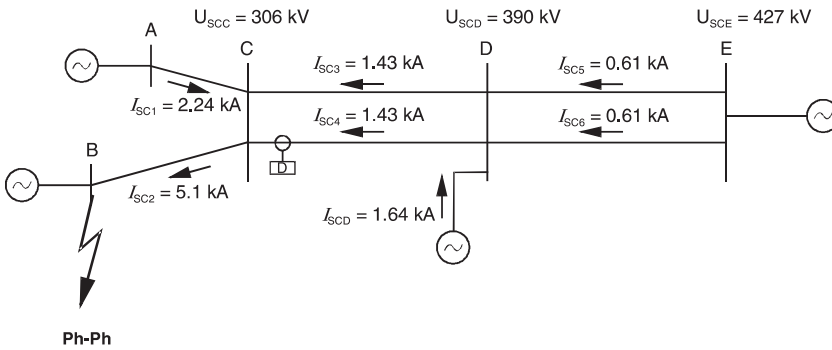
$$ratio_Z = \frac{ratio_{CT}}{ratio_{VT}} = \frac{1200/1 \text{ A}}{400/0.1 \text{ V}} = 0.3$$



a) Calculation example: network configuration and data



b) Ph-Ph short-circuit at E



d) Ph-Ph short-circuit at B

**Figure 6.5** Calculation example: current and voltage distribution

From this, the following setting value is obtained:

$$X_{+FD \text{ secondary}} = 0.3 \cdot 273 = 81.9 \, \Omega, \text{ chosen } 90 \, \Omega$$

In the case of faults at B the most unfavourable conditions arise during fault detection in reverse direction. The results of the short-circuit calculation are shown in figure 6.5b.

The impedance measured in reverse direction is:  $Z_{Ph-Ph} = 306 / (2 \cdot 1.43) = 107 \, \Omega$

In this case, the intermediate in-feeds cause an increase of the line impedance by a factor of 3.6.

The setting of the fault detection in reverse direction therefore results in:

$$X_{\text{FD secondary}} = 1.3 \cdot 0.3 \cdot 107 = 42.0 \, \Omega; \text{ selected } 45 \, \Omega$$

The natural load of each 400 kV single overhead line from C to D amounts to 460 MW. This corresponds to a load current of:

$$I_{\text{Load}} = \frac{P_{\text{Nat}}}{\sqrt{3} \cdot U_N} = \frac{460 \text{ MW}}{\sqrt{3} \cdot 400 \text{ kV}} = 664 \text{ A}$$

The load impedance therefore is:

$$Z_{\text{Load}} = \frac{400000 \text{ V} / \sqrt{3}}{664 \text{ A}} = 348 \, \Omega$$

For the set point  $R_{\text{LB}}$  (limit of the load-blocking section) half the load impedance (maximum over-current  $2 \cdot I_N$ ) reduced by a security margin of 30% is again used:

$$R_{\text{LB-secondary}} = 0.3 \cdot \frac{348}{2} \cdot 0.7 = 36.5 \, \Omega; \text{ selected: } 35 \, \Omega$$

For the angle  $\varphi_{\text{LB}}$  a value of  $40^\circ$  is assumed as a typical value at the EHV-level.

For the set point  $R_{\text{FD}}$  of the fault detection quadrilateral 2 times  $R_{\text{LB}} = 70 \, \Omega$  is chosen. This results in a good compromise between tolerable reactive load and security of fault detection during remote faults.

In practice, the following method for the determination of  $\varphi_{\text{LB}}$  and  $R_{\text{FD}}$  has proven itself:

- the load distributor determines how much reactive power in relation to the real power is transferred. The power value pairs are then converted with the following equations

$$R = \frac{U_N^2 \cdot P_{\text{active}}}{P_{\text{active}}^2 + P_{\text{reactive}}^2} \quad \text{and} \quad X = \frac{U_N^2 \cdot P_{\text{reactive}}}{P_{\text{active}}^2 + P_{\text{reactive}}^2} \quad (6-2)$$

to R- and X-values, which are entered in the impedance diagram. Subsequently, the fault detection characteristic is adapted to maintain a security margin of 20-30%.

In a subsequent step, the security of the fault detection is checked by means of a fault calculation. The load current must be considered, as a superposition of the short-circuit and load current at the relay location arises during remote faults beyond the next station, causing the measured fault impedance to be shifted in the R-direction. For the sake of convenience, the calculation is executed with a load flow/short-circuit programme. From the currents and voltages at the relay location, the relay impedances can be calculated. The equations contained in paragraph 3.2.3 are to be used (see examples in chapter 7).

*Setting of the Ph-E measuring system*

The Ph-E measuring systems in the 7SA relays have separate R-direction settings. A higher sensitivity can be achieved in special cases, where large earth fault resistance are expected (poor tower earthing). The application can only be employed on earthed networks.

The setting inside the load area is possible, when the Ph-E measuring systems are only released during earth faults by means of  $I_E >$  or  $U_E >$ . Sufficiently large settings must be applied to these parameters to avoid incorrect pick-up and tripping due to system unsymmetries, for example during an external single phase ARC.

Additionally it must be noted that the setting of the residual compensation factor  $k_E$  influences the reach of the fault detection.

The factor  $k_{XE} = X_E/X_L$  influences the reach in X-direction. In general it is adapted to the line on which the relay is applied. Accordingly, the same reactance is measured during earth faults as is measured with Ph-Ph measuring system during phase faults on this line (refer to paragraph 3.2.2). If the neighbouring lines have the same  $X_E/X_L$  values, the reach of the fault detection for phase and earth faults remains the same. Otherwise, differences will result. In this case, or with parallel lines it may be of advantage to apply the separate residual compensation factor  $k_{XE-2}$  for the overreaching zones which is offered with modern numerical relays (7SA522, 7SA6). In the calculation example 7.1 this is analysed more closely.

The setting  $R_E/R_L$  influences the reach in R-direction. The principle is discussed in detail in paragraph 3.5.1. In case of a fault loop with single-sided infeed ( $I_{ph} = I_E$ ), the fault resistance is only effective in the measurement with the factor  $1/(1 + R_E/R_L)$  according to the set  $R_E/R_L$ -ratio. The actual  $R_E/R_L$ -value of the line strongly depends on the conductor and earth-wire cross-sections, and may assume a value of up to 3 (refer to paragraph 3.2.1, table 3.4). In this case the fault resistance would be reduced by a factor 4.

For simplicity, the value of  $k_{RE} = R_E/R_L$  on an overhead line may be set to be equal to 1 in the relay, and it may generally be assumed that the fault resistance appears to be reduced by a factor 2 in the resistance measurement. This applies for the normal case with symmetrical  $Z_0/Z_1$  ratios of the infeeds at both line ends. In extreme cases the earth current could be small compared to the phase current and a factor of only 1 would result (see paragraph 3.1.6, figure 3.15).

In any case, settings higher than 2 are not recommended, in particular with large R-reach setting, as this could cause overreach in case of external faults and superimposed load.

The calculation of the fault detection impedances for phase faults referred to above, must also be executed for Ph-E short-circuits. For the impedance calculation, the corresponding equation of the Ph-E loops must then be applied (refer to paragraph 3.2.3). This is shown in the calculation example of paragraph 7.1.

## 6.3 Setting of the distance zones

### 6.3.1 Reach (X-setting) and grading time

The setting is done according to the previously established grading plan. The fundamental rules for this were discussed in paragraph 3.1.14.

#### *First (underreaching zone)*

On single-circuit overhead lines, the first zone is generally set to 85-90% of the line-length, and therefore does not require any further consideration. The exception thereto are long EHV-lines, because in this case, with larger fault resistances, the load influence can cause over-reach (refer to paragraph 3.5.1). Here, a reduction of the reach to 75% or less of the line-length may be necessary.

This can be avoided when the reactance line of the quadrilateral can be negatively tilted by a corresponding angle  $\alpha$  (7SA522, 7SA6).

As a typical example, figure 6.6 shows the influence of pre-fault loading on a 300 km long 400 kV line. We assume the fault at the remote busbar (100% line) and consider the load exporting state because this is the critical situation for which overreach must be avoided.

The measured impedance depends on the fault resistance and the transmission angle (angle between infeed EMFs at both line ends). For a maximum transmission angle of 30 degrees, we would have to tilt the reactance characteristic by about 22 degrees (figure 6.7).

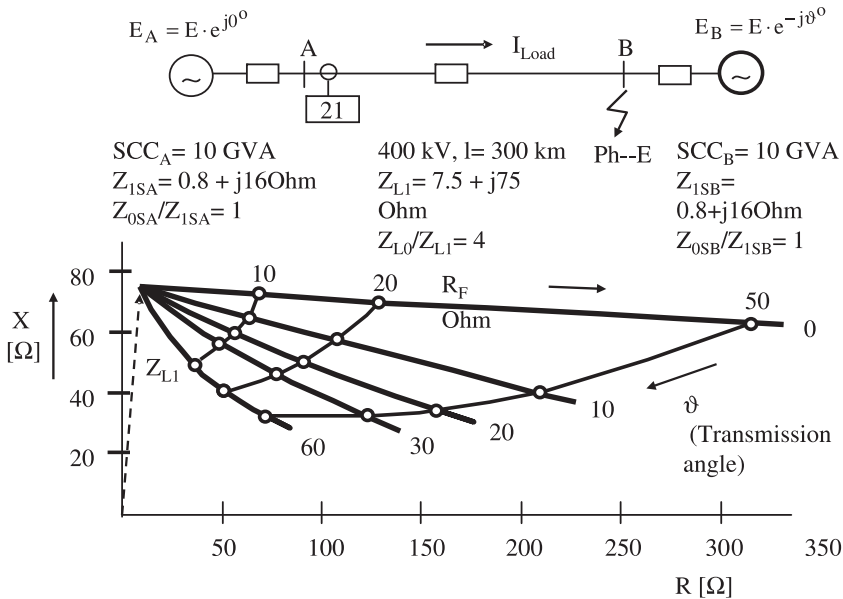


**Figure 6.6** Impact of pre-fault load on distance measurement (example)

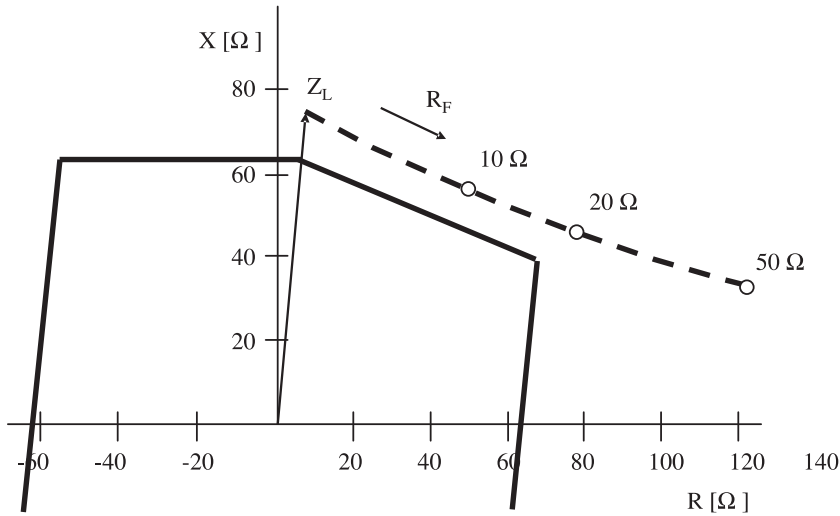


**Figure 6.7**

Tilting of the zone 1 top line to avoid overreach with pre-fault line loading. Setting for the system data of figure 6.6 ( $\vartheta = 30^\circ$ ):  $Z_1 = 85\%Z_{L1}$ ,  $R/X = 1$ , Tilt  $\alpha = 22^\circ$

In general, the system configuration can be reduced to the line connection and two infeeding sources as shown in figure 6.6. This applies in particular for long lines where the tilting effect is large.

For this case the formulae for the estimation of the zone tilt are given in chapter 11, Appendix A.6.

However, computer analysis should be used to study the impact in detail.

Some relays provide automatic tilting of characteristic based on the method outlined in paragraph 3.5.1, figure 3.101 (relay 7SA513 is an example).

It is also noted that the zone reach in R-direction is reduced due to the remote infeed effect and that fault resistances above about 20 ohm can hardly be covered, even with the high R-setting chosen for the example (a setting of  $R/X = 0.5$  is more common for such long lines). Separate earth fault protection must be considered for higher fault resistances.

For the special cases of double circuit overhead lines and three-terminal lines, examples are calculated in the paragraphs 7.1 and 7.2.

In case of series compensated lines, the value  $(X_L - X_C)$  has to be taken as basis for the setting. Also a capacitor at the beginning of a following line may have to be considered. Further, some extra security margin has to be included to compensate the impact of subsynchronous oscillations (refer paragraph 3.5.7, equation 3.168). In total this results in extreme short 1<sup>st</sup> zones which only can cover close-in faults.

*Back-up zones*

The settings for the back up zones 2 and 3 present some difficulties, as the reach is dependant on the switching state of the network and the in-feed conditions. Only in the case of spur or ring-feeders without intermediate in-feed, clear conditions arise, so that the distance zones can be set with fixed grading factors (e.g. 0.9) against the stage of the relay on the neighbouring line. In meshed systems the settings for the back up zones can however only be calculated for a particular system constellation. Following changes in the switching state or in-feed a longer tripping time or loss of selectivity must be accepted.

The following alternative strategies are pursued:

Grading strategy 1: (absolute selectivity ahead of tripping time)

Intermediate in-feeds are not considered. In the case of parallel circuits, the corresponding reduction of the impedance is taken into account.

In this case, a grading which is 100% selective for all switching and in-feed conditions is obtained. The stages however may sometimes become very short, therefore more frequent back up tripping in the form of a final stage trip must be accepted. A selective final stage trip grading is required to restrict uncontrolled shut-downs. This grading philosophy can only be applied when the slow tripping times are tolerable (stable, tightly meshed system, distribution system).

Grading strategy 2: (short tripping times with limited selectivity)

Intermediate in-feeds are considered in the grading plan. Parallel circuits are not taken into account. The second zone is set to reach up to the centre of the shortest neighbouring line. The third zone is set to reach beyond the longest neighbouring line (similar to the impedance fault detection in the example calculated above).

Large zone reaches are obtained in this manner, and all short-circuits are detected at the latest in the third zone. Over-reaches with additional shut-downs must be accepted when system conditions (in-feeds, switching state) change. A special final stage trip grading plan is not required, i.e. all final stage trip times can have the same setting (outside Europe, the distance protection typically only has three zones; back up protection with directional non-directional final stage tripping is not common).

This strategy may be sensible, when it must be assumed that fault durations beyond  $t_2$  are unstable and the system will disintegrate anyway (HV and EHV systems with stability problems).

Grading strategy 3: grading suited to the situation

In most cases, a mixture of strategies 1 and 2 will be employed. In this way, it can be assumed that for a power station with four units, at least two will always be in service, or that in the case of three parallel lines in general only one may be switched off. On the basis of this decision co-ordinated with operations, a setting is calculated.

Suggestions to adapt the settings to a statistical average system condition have not taken hold. The secure supply to important consumers (hospitals, industrial plants), or



the stability of feeding power stations on the other hand are criteria which must be considered as higher-ranking in the grading plan.

### *Back-up zone grading in distribution networks*

The structure of distribution and sub-transmission networks is often simple (radial, parallel feed or ring) with a low degree of interconnection. There is normally only one main protection and signaling for teleprotection is in most cases not available. Busbar protection does often not exist.

System stability is not an issue and delayed tripping of remote faults is therefore acceptable.

Under these conditions selectivity can be achieved by increasing the number of back-up zones.

In Germany and some neighboring countries, which use meshed distribution networks, it is general practice to grade 3 or 4 distance zones and to use the starting (fault detection) zone additionally as final directional and non-directional back-up zones. The grading is made selective and zone overlapping is strictly avoided. The time delay of the last zone may then be in the range of 1.5 to 2 seconds (refer to chapter 3.1.14).

### *Back-up zone grading on transmission grids*

The use of redundant main protection and local back-up protection (breaker failure protection) is now the general practice with EHV grids.

Remote back-up protection by graded distance zones and sensitive earth fault relays are however still necessary as a last resort when telecommunication fails or in the case of a catastrophic event such as fire in a substation [6-4, 6-5].

The zone setting on heavily interconnected systems with multiple infeeds is difficult to achieve: On the one hand the reach should be as far as possible to ensure remote back-up fault clearance, but on the other hand the settings should allow unrestricted use of the primary equipment up to the thermal limit.

In the last years remote back-up distance zones have earned a bad reputation ("Third zone problem") because they have several times contributed to system blackouts [6-3, 6-4].

The classical MHO characteristic which expands in the impedance plane by half its diameter in R-direction overfunctioned and false tripped during overload.

All back-up zone settings in USA and Canada had therefore to be reviewed according to NERC recommendations. A number of third zones on longer lines had even to be put out of service (refer to chapters 6.2.2 and 6.2.3.).

Modern numerical relays provide a solution for this problem. They offer shaped distance zones which can be set to a far reach in X-direction while keeping the reach in R-direction below the critical load impedance (refer to chapter 6.2.6).

In transmission grids only three distance zones (non-delayed underreaching zone 1 and overreaching back-up zones 2 and 3) are generally used.

Zone 2 must take on the protection of the final section of the line beyond zone 1 when the protection communication between the line ends is not in service or fails.

It must also protect the remote busbar when the busbar protection (normally not redundant) is out of service or fails.

The 2<sup>nd</sup> zone should overreach the line end by a margin of at least 20% in case of single lines. For double circuit lines with mutual zero-sequence coupling the margin should at least be 50% as the appearing fault impedance for a line end or remote busbar fault may reach about 135% line impedance ( $Z_L$ ) (refer to chapter 3.5.3.).

These settings can cause selectivity problems when following lines are short and consecutive second zones overlap (refer to chapter 3.1.14). If the concerned following lines have redundant teleprotection, the overlap may be acceptable as fault clearance in second zone time is unlikely. Otherwise it must be checked if an increase of the time delay (half grading step, 150 to 200 ms) is acceptable.

The 3<sup>rd</sup> zone should ideally reach beyond the longest line following at the next substation under the worst case grid conditions. The maximum appearing impedance for a fault at the end of the concerned line (remote breaker open) must be considered dependent on switching state and intermediate infeed conditions. The required long settings are however not feasible in many cases: It must be considered that the 3<sup>rd</sup> zone should not overreach through the step down transformers into the distribution network if fast fault clearance by the distribution protection one grading step below the 3<sup>rd</sup> zone time is not guaranteed. All parallel connected step-down transformers must be taken into account to get the lowest through fault impedance for checking the overreach. Conversely further EHV lines or power plants feeding into the concerned transformer substation act as intermediate infeeds and increase the appearing transformer short-circuit impedance. Computer programs (for example SINICAL of Siemens) can be used to calculate the appearing impedances for faults in the lower level network and to find the appropriate zone settings.

In the case of large coupling transformers (mostly auto-transformers) the appearing short-circuit impedance may be very low and selective zone grading between the coupled networks is hardly possible.

Fault clearance latest in second zone is therefore absolutely necessary in both grids (e.g. 230 kV and 400 kV).

Selectivity between the third zones is normally not considered. The emphasis is placed on the security of fault detection rather than optimum grading.

In the European protection practice a 4<sup>th</sup> zone or fault detection zone is additionally used as final stage of back-up protection. Its purpose is to detect remote faults or high resistance faults and to respond to not cleared faults in the distribution system. The operating time of this final back-up zone must in this case be graded above the longest operating time of the distribution network protection. In the German 230/400 kV transmission grid the typical reach setting of this fault detection zone in X-direction is 150 to 200  $\Omega$  primary but may in countries with long lines be extended to about 400  $\Omega$ .

The policy for application and setting of back-up protection on a national supergrid is discussed in detail in [6-5].

### 6.3.2 Arc compensation (R-setting)

The R-setting of the distance zones must cover the line/cable resistance, and additional fault resistances. In the case of fault resistances, the resistance increases due to the in-feed from the remote end, must be included in the calculation (refer to paragraph 3.5.1). With the back up zones, it must furthermore be considered, that during remote faults, a load current component exists, which reduces the short-circuit angle measured at the relay, as was already determined during the setting of the impedance fault detection.

#### Setting the under-reaching zone (R1 and R1E)

*Ph-Ph measuring system(s):*

Ph-Ph faults on overhead lines result from conductor oscillations or from electrically conducting objects (branches, wires, airborne missile) falling on the line.

During conductor oscillation, two phase-conductors (or one phase- and one earth-wire) approach each other. The flash-over occurs at the instant when the distance is below the 50 (60) Hz flash-over voltage in air:

$$I = \frac{U_{n(Ph-Ph)}}{300 \text{ kV/m}} [\text{m}]$$

For the non-delayed tripping distance zone, this distance is the effective arc-length (approximately 1.3 m at 380 kV). When the flash-over is caused by objects, the total conductor spacing must be used as the arc-length. This less favourable case must be considered for the setting.

The corresponding arc-resistance may be estimated with the following equation (refer to paragraph 3.5.1):

$$R_{\text{ARC}} = \frac{2500 \text{ V} \cdot I_{\text{ARC}} [\text{m}]}{I_{\text{SC-min}} [\text{A}]} \Omega$$

$I_{\text{SC-min}}$  is the minimum fault current flowing from the relay location to the fault location. For the various voltage levels, the following average values are obtained:

**Table 6.1** Typical arc resistances of OH-lines

Voltage level	Average conductor spacing	Arc-resistance	
		at $I_{\text{SC}} = 1000 \text{ A}$	at $I_{\text{SC}} = 10\,000 \text{ A}$
380 kV	11 m	27.5 $\Omega$	2.75 $\Omega$
220 kV	7 m	17.5 $\Omega$	1.75 $\Omega$
110 kV	3.5 m	7.5 $\Omega$	0.75 $\Omega$
20 kV	< 1 m	< 2.5 $\Omega$	< 0.25 $\Omega$

It must still be considered that the fault resistance only appears in the Ph-Ph distance measurement reduced by a factor 2 (refer paragraph 3.5.1).

The security margin therefore is 100% if the calculated arc-resistance is fully considered in the setting. This large security margin for Ph-Ph arc faults is acceptable, as the resulting resistance values can readily be set, even on short lines. The margin to the load impedance is usually large.

*Example 6.4: R-setting of the first zone for Ph-Ph short-circuits*

*Given:*

110 kV overhead line,  $l = 10$  km,  $R'_L = 0.07 \Omega/\text{km}$ ,  $X'_L = 0.38 \Omega/\text{km}$   
 $I_{\text{SCmin (Ph-Ph)}} = 1.2$  kA; maximum load-current:  $I_{L\text{-max}} = 530$  A.

*Solution:*

Arc-resistance:

$$R_{\text{ARC}} = \frac{2500 \cdot 3.5}{1200} = 7.3 \Omega.$$

Setting referring to primary values:

$$R_1 = R'_L \cdot l + R_{\text{LB}} = 0.07 \cdot 10 + 7.3 = 8.0.$$

Corresponding X-setting of the 1<sup>st</sup> zone:

$$X_1 = 0.9 \cdot X_L = 0.9 \cdot 10 \cdot 0.38 = 3.4 \Omega.$$

The R/X ratio of the zone settings is therefore  $8.0/3.4 = 2.35$ .

In the case of the R-setting, the security against incorrect fault detection during load conditions must also be observed:

Minimum load impedance:

$$Z_{L\text{-min.}} = \frac{U_N / \sqrt{3}}{I_{L\text{-max.}}} = \frac{110000 / \sqrt{3}}{530} = 120 \Omega$$

If one considers an occasional overload of up to twice the maximum load current, as well as a security margin of 30%, the maximum permitted setting in the R-direction is:

$$R_{1\text{-max.}} = 0.7 \cdot \frac{1}{2} \cdot 120 = 42 \Omega.$$

A mean setting between the maximal permissible value of  $42 \Omega$  and the required value of at least  $8.0 \Omega$  is to be considered. We take a security margin of 50% and choose a value of  $12 \Omega$ . This corresponds to a R/X-ratio of 3.5.

*Ph-E measuring system(s):*

Earth short-circuits usually result from flash-over across the isolators. In addition to the corresponding arc-resistance, the tower-footing resistance must be considered. The latter is severely reduced by the influence of the earth-wire(s) (refer paragraph 3.5.1).

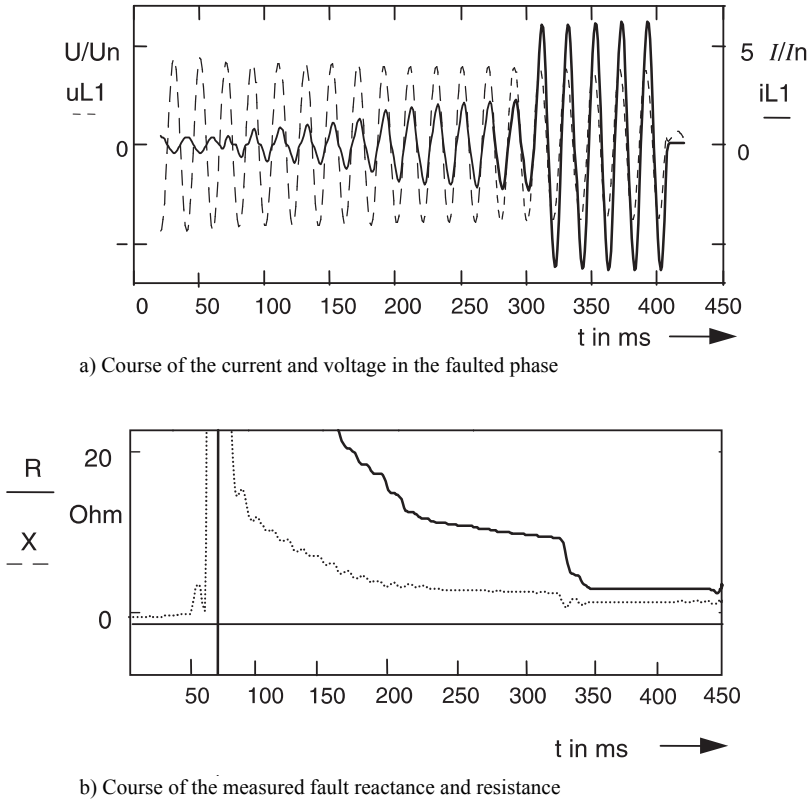


**Figure 6.8** 110 kV line, flash-over to a tree

During flash-overs to trees along the conductor span, an initial large fault resistance of several hundred ohms exists, which however rapidly becomes a small resistance (figure 6.8).

The first zone  $R_E$ -setting must in any event securely detect the normal earth fault occurring due to a flash-over on an isolator. The detection of earth faults with the distance protection is only possible up to some few tens of ohms, under consideration of the  $R$ -reach which is permissible due to load encroachment.

With fixed fault resistances, the situation is aggravated, as the resistance appears to be magnified by the in-feed from the remote end.

For high resistance earth faults in the range of 100  $\Omega$  and above, a separate earth fault protection must definitely be provided.

For the setting, the following equation is derived:

$$R_{I(\text{prim.})} \geq 1.2 \cdot \left( R_L + \frac{R_{LB} + R_F + \frac{I_{Ph2}}{I_{Ph1}} \cdot R_F}{1 + \frac{R_E}{R_L} \cdot \frac{I_{E1}}{I_{Ph1}}} \right) \quad (6-3)$$

with:

$R_L$  line resistance

$R_{LB}$  arc-resistance

$R_F$  earth fault resistance at the fault location

$I_{ph1}$  phase short-circuit current at the relay location during single phase fault

$I_{ph2}$  phase short-circuit current from the opposite end in the case of a single phase fault

$R_E/R_L$  residual compensation set on the relay (resistive component)

$I_{E1}/I_{ph1}$  ratio of earth to phase short-circuit current at the relay location

The factor 1.2 corresponds to a security margin of 20%.

In meshed systems with evenly distributed earthing of star-points, the ratio  $I_{E1}/I_{ph1}$  usually is close to 1. In the extreme, a value of  $I_{E1}/I_{ph1} = 0$  must be counted on, if no earth current source is available on the in-feed side of the relay (refer paragraph 3.1.6, figure 3.15)

*Example 6.5: RE-setting of the first zone for Ph-E faults*

Given that:

110 kV overhead line without earth-wire,  $l = 10$  km,

$R'_L = 0.07 \Omega/\text{km}$ ,  $X'_L = 0.38 \Omega/\text{km}$ ,

$R'_{LE}/R'_{L1} = 0.7$  Isolator length  $l = 1.3$  m

$I_{SC \text{ min (single phase)}} = 0.9$  kA

$I_{ph2}/I_{ph1} = 3$  in the event of a Ph-E fault at the reach threshold

and  $I_E \approx I_{ph}$  at the relay location

tower footing resistance  $R_M = 5 \Omega$

Load conditions are the same as in the previous example.

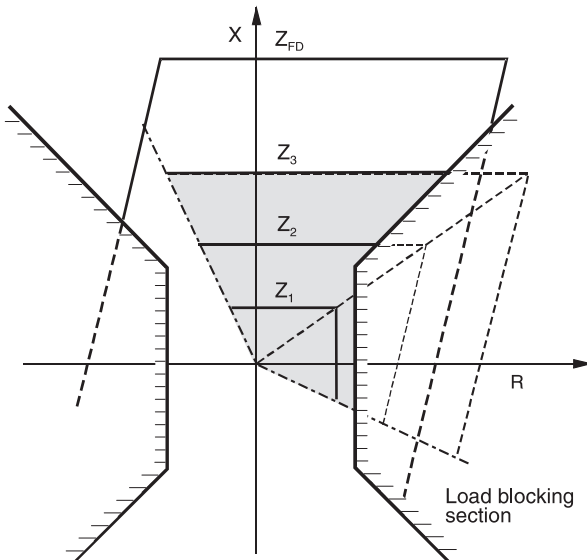


**Figure 6.9**

Limiting of the impedance zones by a load blocking area

Solution:

$$R_{I(\text{prim.})} = 1.2 \cdot \left( 0.07 \cdot 30 + \frac{\frac{2500 \cdot 1.5 \cdot 1.3}{900} + 5 + 3 \cdot 5}{1 + 0.7 \cdot 1} \right) = 17.1 \, \Omega$$

1.5 times the isolator length was assumed for the arc length, to allow for the curved shape of the arc. The R/X ratio in this case would be  $17.1/3.4 = 5.0$ .

We see that the consideration of the remote infeed leads to very high R-settings in the case of solid fault resistances. This results with short lines also in a high R/X-ratio of the zone. To avoid zone overreach as a consequence of CT errors (angle error), the X-setting should be reduced (see paragraph 6.3.4).

### **Setting of the R-reach for the over-reaching zone Z1B (zone extension)**

This must be dealt with in the same manner as the under-reaching zone. The fault for the determination of the required arc reserve taking the in-feed from the remote end into account, must however be placed at the end of the line.

### **Setting of the R-reach for the back up distance zones**

In principle, the statements made for zone 1 also apply here.

The increase of the arc length due to the dynamic behaviour of the arc and wind must be considered when determining the arc resistance. Equation (3-95) in paragraph 3.5.1 applies here.

As a rule it is sensible to increase the reach in R-direction of the under-reaching zone proportional to the X-reach in the higher zone, because the intermediate in-feed effect also acts to correspondingly increase the fault resistance.

If the ratio of the R/X-reach of the first distance zone is already greater than 1, then the calculated proportional R-setting of the second, and especially the third zone may encroach on the load impedance. In conjunction with a shaped fault detection zone or load blocking area, these stages are automatically limited (figure 6.9). Accordingly no further adaption is required. In the event of  $U/I/\phi$  starting, the larger reach is however effective. In this case, the R/X-ratio of the Ph-Ph zones should be correspondingly reduced, as this high sensitivity is not required. For the Ph-E measuring systems, the R-reach should be set to be only large enough to ensure secure fault detection.

### **6.3.3 Specifics for the zone settings in cable networks**

The angle of the positive sequence impedance on cables is substantially less than on overhead lines, at the same voltage level. In particular, medium voltage cables have an R/X-ratio greater than 1. The corresponding short-circuit angle is located in the range of  $30^\circ$  and below.

In cable networks, the phase angle of the positive and zero sequence impedance differ substantially (refer to table 3.4 in paragraph 3.2.1). The residual compensation

factors  $k_{XE} = X_E/X_L$  and  $k_{RE} = R_E/R_L$  in the distance relay must be closely matched to this, to ensure that the distance in the event of earth faults is measure correctly (compare the analysis in paragraph 3.5.1).

In urban networks, the problem exists that metallic rails and pipes parallel to the cable influence the zero sequence impedance. An exact determination of the zero sequence impedance is only possible by measurement of the cable once it is laid.

This is in any event recommended when the system is earthed and Ph-E short-circuits must be detected with a normal grading factor, because the setting of the under-reaching zone to 90% cable length is only meaningful with measured zero sequence impedances. If only calculated values are available, a setting of 80-85% would be appropriate.

#### *Arc compensation on cables*

In the event of insulation failure on cables, an arc results which has a relatively high arc voltage due to the large gas pressure.

The following values were reported:

**Table 6.2** Arc resistances of cables

Rated voltage of the cable	Arc voltage	Arc resistance at 1 kA short-circuit current
6-20 kV	0.4 kV	0.5 $\Omega$
110 kV	1.5 kV	1.5 $\Omega$
380 kV	2.5 kV	2.5 $\Omega$

The compensation of these arc resistance requires a relatively large R/X ratio for the zone settings on short cables.

#### *Example 6.6:*

*Given:*

110 kV atmospheric pressure cable 240 mm<sup>2</sup> Cu,  $l = 3$  km

Cable data according to table 3.4, paragraph 3.2.1

system star-point earthed

The minimum phase short circuit current equals 2.5 kA.

The minimum earth short-circuit current equals 0.5 kA.

The setting for the first zone must be determined.

*Solution:*

It is assumed that the zero sequence impedance of the cable was determined by measurement of the laid cable, and therefore a grading factor of 90% is selected.

$$X_1 = GF_1 \cdot l \cdot X_{L1} = 0.9 \cdot 3.0 \cdot 0.14 = 0.378 \Omega$$



$$R_1 = l \cdot R'_{L1} + \frac{U_{LB}}{I_{SC-min.}} = 3.0 \cdot 0.09 + \frac{1.5 \text{ kV}}{2.5 \text{ kA}} = 0.87 \Omega$$

This corresponds to a R/X ratio of 2.3. A security margin of 100% is again incorporated for the arc resistance as only one half of it appears in the measurement.

Reach of the Ph-E measurement:

From (6-3):

$$R_{E1} = l \cdot R'_{L1} + R_{LB} \cdot \frac{1}{1 + \frac{R_E}{R_L} \cdot \frac{I_{E1}}{I_{Ph1}}} = 1.2 \cdot \left( 3.0 \cdot 0.09 + \frac{1.5 \text{ kV}}{0.5 \text{ kA}} \cdot \frac{1}{1 + 1.11 \cdot 1} \right) = 2.0 \Omega$$

The R/X ratio in this case is 5.4.

In the case of small impedances, no regard has to be taken of the load, and  $R_1 = R_{E1} = 2.0 \Omega$  may be selected.

For the setting of the arc compensation in the back up zones a flash-over on the cable termination or on the busbars must be considered. If there are downstream overhead line feeders, faults in this range must be included. The calculation is done in a similar manner as shown above.

The same rules as exist for overhead lines, apply to the fault detection. Due to the small cable impedances, the fault detection conditions are simple. In most cases, over-current fault detection should be sufficient because the short circuit currents are a multiple of the maximum load current. Under-impedance fault detection for earth faults is only of interest in systems with earth current limiting.

When applying impedance starting, relatively small X-settings result if only the neighbouring cable section is covered by the setting. Larger settings are sensible to achieve better back up protection and larger arc compensation. A secure margin to the load impedance is still possible. In this case, the following secondary settings may typically be selected here:

$X_{+FD} = 40 \Omega$ ,  $X_{-FD} = 20 \Omega$ , and  $R_{FD} = R_{FDE} = 20 \Omega$ , assuming that the current transformers are approximately matched to the maximum continuous current of the cable.

If large motor starting currents in industrial plants are to be expected, it may be necessary to reduce the setting of  $X_{+FD}$  to below

$$X_{+A} \leq \frac{U_N / \sqrt{3}}{\sum I_{mot.-max.}} \cdot \sin \varphi_{mot.} \cdot \frac{CT\text{-ratio}}{VT\text{-ratio}}$$

The motor starting currents are in the range of 5 to 6 times the rated motor current, but in relation to the CT nominal current of the in-feed, a substantially smaller value typically results.

### 6.3.4 Adjusting the zone reach in case of large R/X-setting

The angle errors of the voltage transformers ( $\delta_U$ ) and current transformers ( $\delta_I$ ) cause a turn of the short-circuit impedance towards the R-axis. This causes a negative error (overreach) in the X-measurement. This effect is the stronger the smaller the angle of the short-circuit impedance is. This means that it occurs in particular with cables of low cross-section ( $\varphi_{SC} < 30^\circ$ ) and always if the fault resistance is large compared to the reactance of the line.

With high R/X-setting, the X border line of the quadrilateral should therefore be tilted by the corresponding angle  $\alpha = \delta_U + \delta_I$  as is possible with the relay 7SA6 or 7SA522.

With older relays that do not provide this tilting possibility, it is recommended to slightly reduce the X-reach of the underreaching zone. The grading factor 90% should only be applied, when  $R/X \leq 1$ . With larger R/X-settings, the reduced grading factor can be calculated according to the following formula:

$$GF \leq \left[ 1 - \frac{R}{X} \cdot \operatorname{tg}(\delta_U + \delta_I) \right] \cdot 93.5\% .$$

#### *Typical setting of the arc compensation*

The ratio of the R/X setting is in the following range in practice:

**Table 6.3** Typical R/X setting of quadrilaterals

Overhead line/cable	R/X ratio of the zone settings
Short cables (approx. 0.5-3 km)	3 to 5
Longer cables > 3 km	2 to 3
Short overhead lines < 10 km	2 to 5
Overhead lines < 100 km	1 to 2
Long overhead lines 100-200 km	0.5 to 1
Long EHV lines > 200 km	$\leq 0.5$

The angle error of the voltage and current transformers is not higher than  $1^\circ$  el. each if class 1 voltage transformers and class 5P current transformers are used. This is in particular the case when the VTs and CTs are under-burdened which is normally the case due to the low burden of the numerical relays.

The total angle error therefore remains below  $2^\circ$  el. which would be the setting value for the tilting of the reactance characteristic.

Without tilting we would have to reduce the zone grading factor to

$$GF \leq \left[ 1 - \frac{R}{X} \cdot \operatorname{tg} 2^\circ \right] \cdot 93.5\% = \left[ 1 - \frac{R}{X} \cdot 0.035 \right] \cdot 93.5\% .$$

For  $R/X = 3$  we get  $GF \leq 84\%$  and for  $R/X = 5$  the result is  $GF \leq 77\%$ .

In case of linearised CTs (TPZ) it has to be considered that the false angle may be as high as  $3^\circ$  el. if the CT is fully burdened. In this case  $4^\circ$  instead of  $2^\circ$  has to be inserted in the above formula. Strong under-burdening results also here in much smaller false

angles ( $\delta = \frac{P_i + P_B}{P_i + P_N} \cdot \delta_N$ ).

#### *Very low short-circuit angle*

When the short-circuit angle of a cable is lower than about  $20^\circ$ , the reactance measurement is no more reliable considering the sum of tolerances of cable impedance, instrument transformer and relay.

In this case it may be better to change to an impedance measurement with a circle characteristic. This is justified as only low arc resistances occur in cable systems. Relay 7SA6 offers a plain impedance and modified impedance characteristics for this purpose.

### **6.3.5 Grading of distance zones with different characteristics**

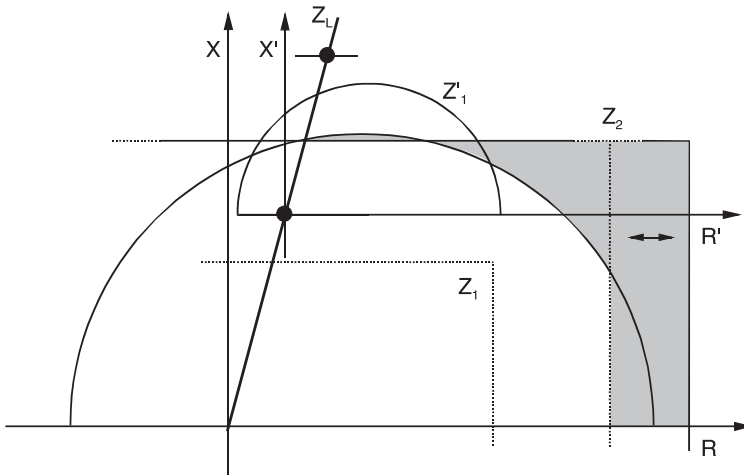
The devices of various manufacturers and relay generations are in service today. Accordingly it is often required to co-ordinate the different characteristics of the distance zones in the grading plan. A typical example is the application of a circular characteristic (mechanical relay) and quadrilateral characteristic (numerical relay) in sequence (figure 6.10).

In this case, the grading must use the X-reach of the zones at the intersection point of the zone reach with the line characteristic as a guideline (refer to paragraph 3.1.7, figure 3.23).

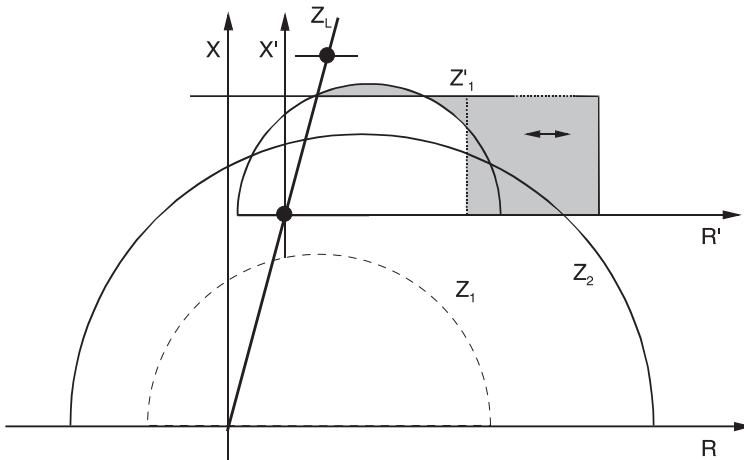
In the respect of the arc compensation, larger deviations naturally occur. The greater R-reach of the numerical relays in any event is a positive effect. The quadrilateral characteristics detect large fault resistances already with short reaches, while the circular characteristics may only have the required R-reach in the back up zones. Unselective tripping cannot occur.

A special situation arises when relays with different characteristics are combined to form a permissive overreach transfer trip scheme.

If the echo function is implemented, the reverse reach of the fault detection stage must be greater than the over-reach of the tripping stage of the relay of the opposite line end, to avoid an incorrect echo signal during external short-circuits. The fault detection characteristic must therefore fully enclose the overreaching zone in the third quadrant, where the external fault impedances appear. The same applies for the blocking technique, while in this case, for Anglo-Saxon relays, the reverse transmitting zone instead of the fault detection must be analysed (figure 6.11).



a) Difference between quadrilateral and circle in the second stage



b) Difference between quadrilateral and circle in the first stage

**Figure 6.10** Grading of circle and quadrilateral Grading of circle and quadrilateral characteristic

If the  $U-I-\phi$  starting is used in conjunction with permissive overreach transfer trip, the co-ordination must be checked with a corresponding short-circuit calculation, taking the maximum expected fault resistance into account. The fault locations must be applied at the reach limit of the overreaching zone in the third quadrant for the short-circuit calculation.

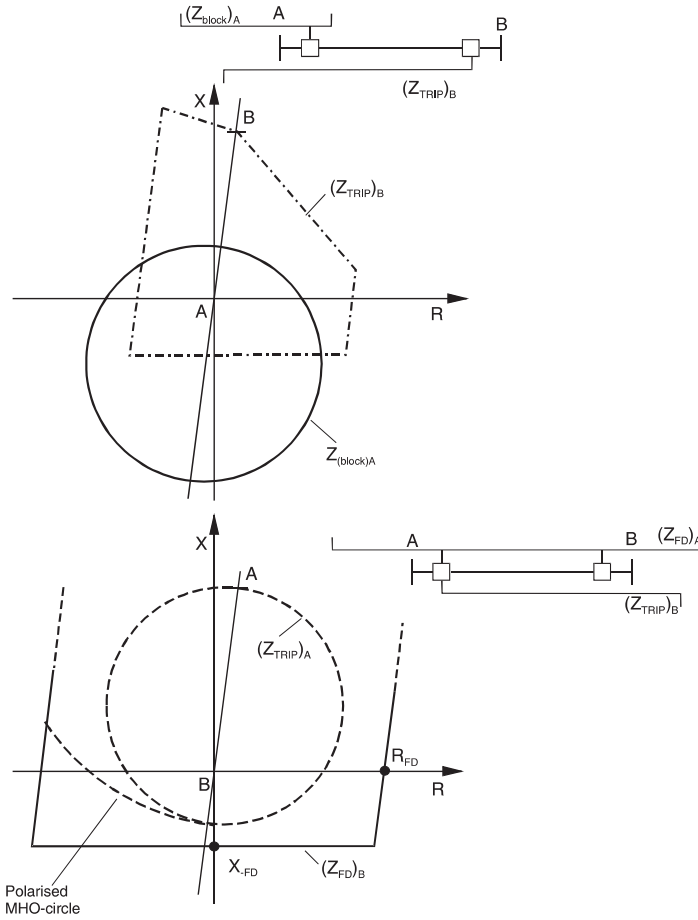


**Figure 6.11** Blocking scheme: co-ordination of a MHO-circle with a quadrilateral

### 6.3.6 Setting of the power swing blocking

The power swing blocking reacts to the rate of change of the power swing vector.

Close to the fault detection zone, this is dominated by the resistive component  $dR/dt$  (refer to paragraph 3.1.11, figure 3.45). This especially applies to the EHV system, where the line angles typically exceed  $85^\circ$ .

For the classical two-machine arrangement, the course of  $dR/dt$  can be approximated as follows:

The impedance measured at the electrical midpoint is:

$$Z_{\text{middle}} = \frac{U_{\text{Ph-E}}}{I_{\text{Ph}}} = E \cdot \frac{\cos \frac{\vartheta}{2}}{\left(2 \cdot E \cdot \sin \frac{\vartheta}{2}\right) / Z_{\Sigma}} = \frac{Z_{\Sigma}}{2} \cdot \cos \left( \frac{\vartheta}{2} \right) \quad (6-4)$$

with  $Z_S = Z_{S1} + Z_L + Z_{S2}$

Equal generator emfs are assumed:

$$E_1 = E_2 = E.$$

During a power swing, source emfs move away from each other. For simplicity, a constant power swing frequency is assumed, so that one emf rotates relative to the other

with a constant angular velocity. The covered angle is then given by  $\vartheta = \omega_p \cdot t$ . The angular velocity  $\omega_p$  determines the speed at which the changing emf rotates in relation to the fixed emf.

From equation (6-4):

$$Z_{\text{middle}} = \frac{Z_\Sigma}{2} \cdot \cot\left(\frac{\omega_p \cdot t}{2}\right) \quad (6-5)$$

In the numerical relays 7SA the change of the power swing vector is separately evaluated for the R and X-direction. Hereunder only the R-component is examined, as in general it represents the decisive criteria in transmission networks.

$$R_p = \frac{X_\Sigma}{2} \cdot \cot\left(\frac{\omega_p \cdot t}{2}\right) \quad (6-6)$$

By differentiation, the velocity at which the power swing vector changes, is obtained.

$$\frac{dR_p}{dt} = \frac{Z_\Sigma}{2} \cdot \frac{\omega_p}{2} \cdot \operatorname{tg}\left(\frac{\vartheta}{2}\right) = \frac{\pi}{2} \cdot Z_\Sigma \cdot f_p \cdot \operatorname{tg}\left(\frac{\vartheta}{2}\right) \left[\frac{\Omega}{s}\right] \quad (6-7)$$

The power swing blocking function utilises this data to reach a decision. This is discussed by means of an example below.

#### *Example 6.7: Traditional setting of PSB*

In conventional technology and with earlier numerical relays (7SA511),  $dR/dt$  was measured as  $\Delta R/\Delta t = (R1 - R2)/\Delta t$  with two concentric characteristics or blinders and a timer (see paragraph 3.1.11). In the following example, setting of this classical PSB arrangement is used to show the basic principle.

Given that:

230 kV transmission system according to figure 3.44, of paragraph 3.1.11

Line length 200 km,  $Z'_L = 0.3 \Omega/\text{km}$

Three-phase short-circuit power at both line ends: 5 GVA

Maximum power swing frequency at which the system remains stable:  $f_p = 2 \text{ Hz}$ .

Current transformers: 800/1 A, voltage transformers: 230/0.1 kV

Task:

Determine the relay settings for the power swing blocking

Solution:

Line impedance:

$$Z_L = 200 \text{ km} \cdot 0.3 \text{ } \Omega/\text{km} = 60 \text{ } \Omega$$

Source impedances:

$$Z_{S1} = Z_{S2} = \frac{230^2 \text{ kV}^2}{8000 \text{ MVA}} = 6.6 \text{ } \Omega$$

The sum of the impedances is therefore:  $Z_\Sigma = 6.6 + 60 + 6.6 = 73.2 \text{ } \Omega$

It is assumed that the transmission angle  $\vartheta$  during normal operation is not greater than  $60^\circ$ . From that, the outer blinder (PPOL) should keep a small security margin. This is to avoid a pick-up of the power swing blocking during steady state load conditions. In this case, the setting of the power swing polygon is selected such that the power swing vector only enters the power swing polygon at  $\vartheta = 70^\circ$  (figure 6.12).

The R-reach of the power swing polygon is obtained with Equation (6-4):

$$R_{\text{PPOL}} = \frac{73.2}{2} \cdot \cot\left(\frac{70}{2}\right) = 53.2 \text{ } \Omega \text{ primary}$$

The velocity at which the vector changes at this point is:

$$\left(\frac{dR_{\text{Relay}}}{dt}\right)_{\text{PPOL}} = \frac{\pi}{2} \cdot 73.2 \text{ } \Omega \cdot 2.0 \frac{1}{\text{s}} \cdot \tan\left(\frac{70^\circ}{2}\right) = 161 \frac{\Omega}{\text{s}}$$

At least 35 ms should be available for measurement while the power swing vector passes from the outside to the inside polygon in the 7SA511.

The fault detection polygon (SPOL) should therefore be set smaller than the power swing polygon (PPOL) by a minimum  $\Delta Z$  value.

The following results:

$$\Delta Z_{\text{primary}} \geq 0.035 \text{ s} \cdot \frac{dR_{\text{Relay}}}{dt} = 0.035 \cdot 161 = 5.6 \text{ } \Omega$$

$$R_{\text{SPOL-Primary}} = 53.2 - 5.6 = 47.6 \text{ } \Omega$$

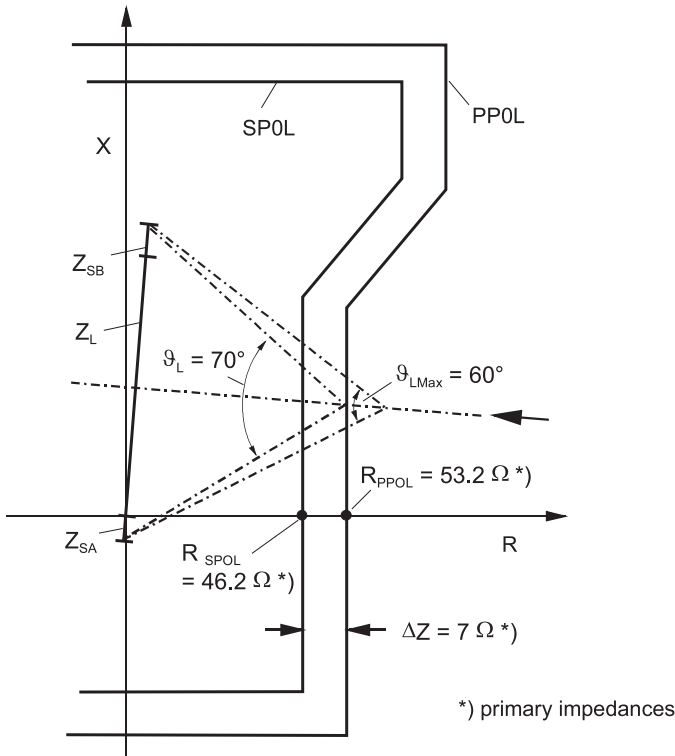
It must still be noted that the power swing vector has been accelerated from entering of the power swing polygon up to reaching the fault detection polygon. The time needed from entering the power swing polygon to reaching the fault detection polygon must therefore be checked again.

The load angle at which the power swing vector enters the fault detection polygon is obtained in reverse with Equation (6-4).

$$\delta = 2 \cdot \operatorname{arccot} \frac{R_{\text{SPOL}}}{Z_\Sigma/2} = 2 \cdot \left( \operatorname{arctg} \frac{Z_\Sigma/2}{R_{\text{SPOL}}} \right) = 2 \cdot \operatorname{arctg} \left( \frac{73.2/2}{47.6} \right) = 75^\circ \quad (6-8)$$

The velocity of change at this point amounts to:

$$\left(\frac{dR_{\text{Relays}}}{dt}\right)_{\text{SPOL}} = \frac{\pi}{2} \cdot 73.2 \text{ } \Omega \cdot 2.0 \frac{1}{\text{s}} \cdot \tan\left(\frac{75^\circ}{2}\right) = 177 \frac{\Omega}{\text{s}}$$

**Figure 6.12**

Setting of the power swing blocking in the 7SA511 (Figure for the calculation example)

This amounts to an increase of approximately 12%, compared to the velocity at which the vector entered the power swing polygon. The transition time of the vector from entering the power swing polygon up to reaching the fault detection polygon is therefore smaller than the required 35 ms. For this reason, the setting of  $\Delta Z$  is increased from approximately 5.6 to 7  $\Omega$  primary. The setting of the fault detection polygon therefore reduces to  $53.2 - 7.0 = 46.2 \Omega$  primary.

To apply the calculated settings to the relay, they must be converted to the secondary side of the instrument transformers:

$$\text{The impedance conversion factor is: } \text{ratio}_Z = \frac{\text{ratio}_{CT}}{\text{ratio}_{VT}} = \frac{800/1}{230/0.1} = 0.348$$

From this the final relay settings are obtained:

$$R_{\text{SPOL-secondary}} = 46.2 \cdot 0.348 = 16.1 \Omega;$$

chosen 16  $\Omega$ .

$$\Delta Z = 7.0 \cdot 0.348 = 2.44 \Omega; \text{ selected } 2.5 \Omega (\Delta T = 35 \text{ ms, as assumed}).$$

$\Delta Z$  and  $\Delta T$  had to be set at traditional power swing blocking relays.

At the relay 7SA511,  $dR/dt$  has to be set instead of  $\Delta T$ .



$$\left(\frac{dR_{\text{Relay}}}{dt}\right)_{\text{secondary}} = 177 \cdot 0.348 = 62 \frac{\Omega}{s}$$

The power swing logic must still be selected (blocking of particular or all zones, and power swing tripping).

In the case at hand the standard setting “block all zones” is selected.

Power swing tripping should be selected as well if the line must be deliberately tripped at the relay location in the event of an out-of-step condition in the system (refer to paragraph 3.1.11).

#### *Setting free power swing blocking*

The 7SA6 and 7SA522 relays do not require settings. The outer PSB characteristic surrounds automatically the largest set zones by a fixed  $\Delta Z$  value of  $5 \Omega$  secondary (1 A relay) as shown in figure 6.13. This advanced method also satisfies additional EHV system requirements:

- The blocking is effective up to higher swing frequencies (about 7 Hz).
- The power swing blocking function is only active during three phase symmetrical conditions (non-symmetry < 25%) and can also be cancelled if an earth current is detected (option).
- The power swing blocking is set up three-phase and functions in conjunction with single-phase ARC, also during the dead time
- The measuring technique also recognises three phase faults during the power swing, and cancels an active power swing block condition.

Note: When implementing the power swing blocking, the impedance fault detection must be selected, as a co-ordination of the power swing polygon with the  $U-I-\phi$  fault detection is not possible. The  $U-I-\phi$  fault detection characteristic changes its size in the impedance plane, depending on the source impedance (refer to paragraph 3.1.6, figure 3.22), while the power swing polygon is fixed.

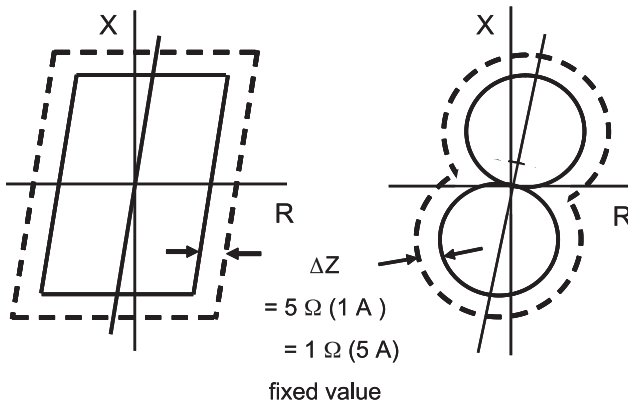


**Figure 6.13**  
Setting free power swing blocking function in the relays 7SA522 and 7SA6.

---

## 7 Calculation examples

The setting procedure for a common single circuit line is explained in the relay manuals by means of an example. At this point additional special applications are discussed.

### 7.1 Double circuit lines in earthed systems

In this case, zone settings for earth faults demand closer inspection due to the coupling of the zero sequence system. The basic discussion in paragraph 3.5.3 may be referred to.

#### *General procedure*

It is recommended to initially do the grading of the phase fault distance zones, without consideration of the parallel line coupling.

In a second stage, the zone reaches for the earth faults are checked, and a suitable earth current compensation factor is selected.

The implementation of the parallel line compensation must be considered, to ensure sufficient remote back up protection coverage of earth faults.

#### *Grading of the distance protection for phase short-circuits*

The zones must be set according to the basic principles for grading plans (refer to paragraph 3.1.14). The parabolic shape of the impedance course depending on the fault location is significant for the back up zones (figure 3.62, paragraph 3.1.14).

Furthermore, when double circuit lines are connected in series, different reaches of the back up zones result, depending on the service condition and the in-feed at the remote end (figure 3.64, paragraph 3.1.14).

Theoretically, the compilation of the grading plan for double circuit lines is therefore complex [3-21, 3-34].

In practice however a simpler procedure is followed.

For the practical grading of the second zone, half the impedance of the following parallel line can be used (double circuit line after single circuit line). The result is:

$$Z_{2A} = GF2 \cdot (Z_{A-B} + 0.5 \cdot Z_{B-C}) \quad (7-1)$$

The third zone must be graded according to the selected back up protection strategy. A grading plan which remains selective for almost all system conditions results in relatively short third zone settings, which are hardly longer than the corresponding Zone 2.

In HV and EHV systems an attempt will be made to cover the downstream double circuit line during normal parallel line operation with the third zone. In this case, the following zone setting results:

$$Z_{3A} = 1.1 \cdot (Z_{A-B} + Z_{B-C}) \quad (7-2)$$

For the fault detection zone (offset 4<sup>th</sup> zone), the downstream lines must, in the least favourable switching condition (single circuit line after parallel line), be inside the protected zone. The following setting must be selected:

$$Z_{+FD-A} = 1.1 \cdot (Z_{A-B} + 2 \cdot Z_{B-C}) \quad (7-3)$$

In general, there will be an in-feed at the intermediate stations of the double circuit line, which must be considered when grading the back up zones. This is illustrated with the following example.

*Example:*

Double circuit line

setting of the distance zones for phase short-circuits

*Given:*

400 kV double circuit line

line data:

configuration according to figure 7.1

$l_1$  and  $l_2 = 150$  km,  $l_3$  and  $l_4 = 80$  km

$Z'_{1L} = 0.0185 + j 0.3559 \Omega/\text{km}$

$Z'_{0L} = 0.2539 + j 1.1108 \Omega/\text{km}$

$Z'_{0M} = 0.2354 + j 0.6759 \Omega/\text{km}$

$P_{\text{nat.}} = 518$  MW per line

current transformer: 2000/1 A

voltage transformer: 400/0.1 kV

In-feed data as stated in figure 7.1.

*Task:*

Calculation of the zone setting for relay D1.

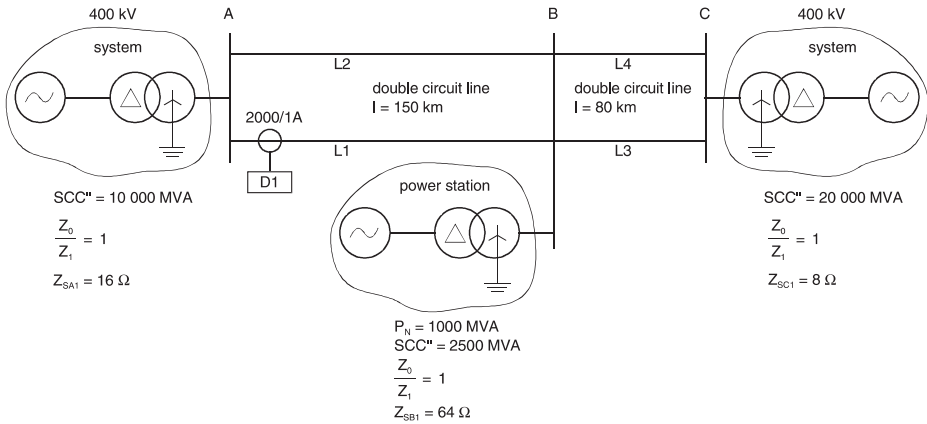
*Solution:*

For the sake of simplicity, the calculation of the short-circuit is only done with X-values:

$$X_{L1} = X_{L2} = 0.3559 \Omega/\text{km} \cdot 150 \text{ km} = 53.4 \Omega$$

$$X_{L3} = X_{L4} = 0.3559 \Omega/\text{km} \cdot 80 \text{ km} = 28.5 \Omega$$

Generally a grading factor of 85% is used.

**Figure 7.1**

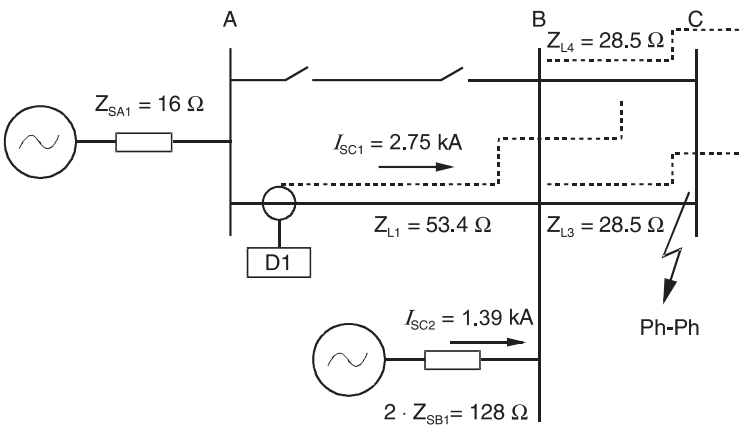
Protection settings on a double circuit line: system data for the calculation example

The zone reaches are calculated as follows:  $X_1 = 0.85 \cdot 53.4 = 45.4 \Omega$

For the selective grading of the second zone, it is assumed that the parallel line L2 is open, but that the intermediate in-feed in B is always at least half its short-circuit rating.

Selective grading up to the end of the first zone of the distance relay on the downstream feeders 3 and 4 is done. This implies that approximately half the line impedance may be used. A simplified equivalent circuit results (figure 7.2).

For a three phase fault at C, the short-circuit currents shown in the drawing are calculated.

**Figure 7.2**

Protection setting in the case of double circuit lines: equivalent circuit for the calculation example

Considering the intermediate in-feed effect, the following is obtained:

$$X_2 = \left[ 53.4 + \frac{28.5}{2} \cdot \left( 1 + \frac{1.39}{2.75} \right) \right] \cdot 0.85 = 63.6 \, \Omega = 119\% X_{L1}, \text{ chosen } 120\%$$

According to the recommendations above, the following is obtained for zone 3:

$$X_3 = (53.4 + 28.5) \cdot 1.1 = 90.1 \, \Omega = 169\% X_{L1}$$

and for the fault detection zone (respectively 4<sup>th</sup> zone, if used):

$$X_{+FD} = (53.4 + 2 \cdot 28.5) \cdot 1.1 = 121 \, \Omega = 226\% X_{L1}$$

We must now check the reach of the distance zones under the actual multiple infeed conditions as shown in figure 7.1.

The parallel connection of lines 3 and 4 result in a parabolic course of the measured impedances (refer to paragraph 3.1.14). This is amplified by the strong remote infeed (figure 7.3).

The calculation procedure is outlined in Appendix 11.A.5.

We see that the reach of the back-up zones is rather short. The second zone covers only 8% of the following lines, the third zone only 28% and the fault detecting zone has a “blind” range where faults are not detected on the following lines.

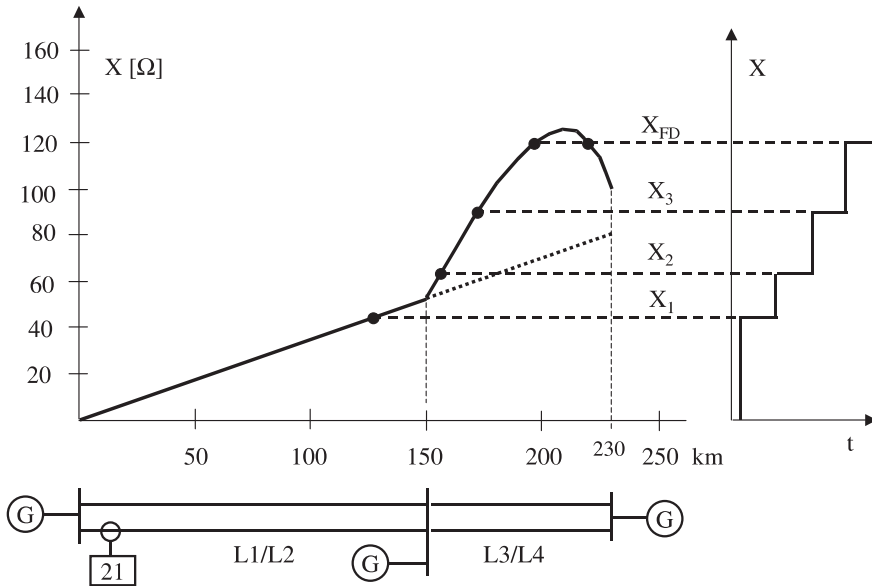


**Figure 7.3** Reach of distance zones for phase to phase faults (example)

### *Zone reach during earth faults*

The residual compensation factor  $\underline{k}_E$  is decisive in the case of the ph-E measuring systems. On single circuit lines, it is set to a corresponding  $\underline{Z}_E/\underline{Z}_L$  value of the line. The protection then measures the same impedance for Ph-Ph and earth faults.

In the case of double circuit lines, a measuring error during earth faults results due to the zero sequence system coupling (see paragraph 3.5.3). The measurement can be corrected with the parallel line compensation. In the 7SA relays this function is optionally available. The parallel line earth current must only be connected to the relay and the mutual impedance must be set. The residual compensation factor  $\underline{k}_E$  in this case must be matched for the single circuit line. The earth current balance, that prevents an over-reach of the distance relay on the healthy parallel line (refer to paragraph 3.5.3), may be left on the standard value  $x/l = 85\%$ .

### *Setting of the $\underline{k}_E$ factor (operation without parallel line compensation)*

In the event that the parallel line compensation is not used, a suitable  $\underline{k}_E$  factor must be found, to ensure sufficient protection coverage for all possible operating states of the double circuit line (table 7.1).

The adaptation of the setting to a particular operating condition results in an over or under-reach for the other operating conditions. GF1 in % is the selected grading factor for the first zone (reach for Ph-Ph faults). The ratio  $x/l$  in % then indicates how far the first zone (Ph-E loop) reaches for earth faults in relation to the line length.

The determination of the relay setting value  $\underline{k}_{ER}$  is shown by means of the double circuit operation example:

For a fault at the distance  $x/l$ , the voltage at the relay location is:

$$U_{Ph-E} = \frac{x}{l} \cdot \underline{Z}_L \cdot \underline{I}_{Ph} - \frac{x}{l} \cdot \underline{Z}_E \cdot \underline{I}_E - \frac{x}{l} \cdot \frac{\underline{Z}_{OM}}{3} \cdot \underline{I}_{EP}$$

The single sided in-feed is initially considered to estimate the zone reach depending on the switching state of the parallel line.

In this case the following current relation is valid:

$$\underline{I}_E = -\underline{I}_{Ph} \text{ and } \underline{I}_{EP} = \frac{x/l}{2-x/l} \cdot \underline{I}_E$$

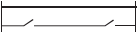
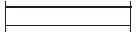
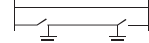
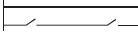
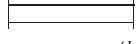
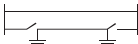
For the measurement of the Ph-E loop, the following is obtained:

$$\underline{Z}_{Ph-E} = \frac{U_{Ph-E}}{\underline{I}_{Ph} - \underline{k}_{ER} \cdot \underline{I}_E} = \frac{x}{l} \cdot \frac{\underline{Z}_L + \underline{Z}_E + \frac{\underline{Z}_{OM}}{3} \cdot \frac{x/l}{2-x/l}}{1 + \underline{k}_{ER}} \quad (7-4)$$

$\underline{k}_{ER}$  is the complex residual current compensation factor set in the relay.

**Table 7.1**

Distance measurement for earth faults: reach (in X-direction) depending on the relay setting  $k_{\text{XER}}$  and the switching condition.

Relay setting	Reach $x/l$ for Ph-E short-circuits		
1 <sup>st</sup> zone grading: $GF1 = 0.85$	 $\frac{x}{l} = GF1 \cdot \frac{1 + k_{\text{XER}}}{1 + k_{\text{XEL}}}$	 $\frac{x}{l} =$ refer to equation 7-7	 $\frac{x}{l} = \frac{(1 + k_{\text{XER}}) \cdot GF1^{(*)}}{1 + k_{\text{XEL}} - k_{\text{XEM}} \cdot \frac{X'_{\text{OM}}}{X'_{\text{OL}}}}$
Residual compensation factor $k_{\text{XER}}$ :			
 $k_{\text{ER}} = \frac{1 + k_{\text{XEL}}}{GF1} \cdot \frac{x}{l} - 1 = 0.71(0.5)$	85% (75%)	70% (63%)	114% (100%)
 $k_{\text{XER}} = \frac{1 + k_{\text{XEL}} + k_{\text{XEM}} \cdot \frac{x/l}{2 - x/l}}{GF1} \cdot \frac{x}{l} - 1 = 1.21$	110%	85%	148%
 $k_{\text{XER}} = \frac{1 + k_{\text{XEL}} - k_{\text{XEM}} \cdot \frac{X'_{\text{OM}}}{X'_{\text{OL}}}}{GF1} \cdot \frac{x}{l} - 1 = 0.27$	65%	55%	85%

Line data:  $X'_{\text{OM}} = 0.72 \Omega/\text{km}$ ,  $X'_{\text{OL}} = 1.11 \Omega/\text{km}$ ,  $X'_{\text{IL}} = 0.356 \Omega/\text{km}$

Earth comp. Factors of the line:  $k_{\text{XEL}} = \left( \frac{X'_{\text{EL}}}{X'_{\text{IL}}} \right)_{\text{line}} = 0.71$   $k_{\text{XEM}} = \left( \frac{X'_{\text{OM}}}{3 \cdot X'_{\text{IL}}} \right)_{\text{line}} = 0.674$

\*) this equation applies for  $\frac{x}{l} \leq 1$ . If  $\frac{x}{l} > 1$  then:  $\frac{GF1(1 + k_{\text{XER}}) + k_{\text{XEM}} \cdot \frac{X'_{\text{OM}}}{X'_{\text{OL}}}}{1 + k_{\text{XEL}}}$

In the case of the numerical relays 7SA, the values of  $X$  and  $R$  are separately calculated.

If the phase and earth currents have the same phase relationship, then the simplified equations (3-53) and (3-54) apply. Accordingly from equation (7-4):

$$X_{\text{Ph-E}} = \frac{U_{\text{Ph-E}} \cdot \sin \varphi_K}{I_{\text{Ph}} - \left( \frac{X_{\text{E}}}{X_{\text{L}}} \right)_{\text{R}} \cdot I_{\text{E}}} = \frac{x}{l} \cdot X_{\text{L}} \frac{1 + \frac{X_{\text{E}}}{X_{\text{L}}} + \frac{X_{\text{OM}}}{3 \cdot X_{\text{L}}} \cdot \frac{x/l}{2 - x/l}}{1 + \left( \frac{X_{\text{E}}}{X_{\text{L}}} \right)_{\text{R}}}$$

$$R_{\text{Ph-E}} = \frac{U_{\text{Ph-E}} \cdot \sin \varphi_K}{I_{\text{Ph}} - \left( \frac{R_{\text{E}}}{R_{\text{L}}} \right)_{\text{R}} \cdot I_{\text{E}}} = \frac{x}{l} \cdot R_{\text{L}} \frac{1 + \frac{R_{\text{E}}}{R_{\text{L}}} + \frac{R_{\text{OM}}}{3 \cdot R_{\text{L}}} \cdot \frac{x/l}{2 - x/l}}{1 + \left( \frac{R_{\text{E}}}{R_{\text{L}}} \right)_{\text{R}}}$$

For the reach, only the measured X-value is relevant.

With the line constants  $k_{XEL} = \frac{X_E}{X_L}$  and  $k_{XEM} = \frac{X_{OM}}{3 \cdot X_L}$  and the relay setting value  $k_{XER} = \left(\frac{X_E}{X_L}\right)_R$  the following results:

$$X_{Ph-E} = \frac{x}{l} \cdot X_L \cdot \frac{1 + k_{XEL} + k_{XEM} \cdot \frac{x/l}{2 - x/l}}{1 + k_{XER}} \quad (7-5)$$

As the Ph-E and Ph-Ph measuring systems have the same impedance pick-up value (common setting value  $Z_1$ ), the following applies:  $Z_{Ph-E} = Z_{Ph-Ph} = Z_1 = GFI \cdot Z_L$ ,

where GFI is the grading factor of the first zone.

The following equation is derived for the residual current compensation factor that has to be set in the relay:

$$k_{XER} = \frac{1 + k_{XEL} + k_{XEM} \cdot \frac{x/l}{2 - x/l}}{GFI} \cdot \frac{x}{l} - 1 \quad (7-6)$$

The reach of the Ph-E measuring systems can be varied by changing the setting of the  $k_{XER}$  factor while maintaining a given zone reach for phase faults (GFI in % of  $Z_1$ ).

Equation (7-6) can be rearranged to provide a solution for  $x/l$ . The reach for a given  $k_{XER}$  setting is then obtained:

$$\begin{aligned} \frac{x}{l} = & \frac{[GFI \cdot (1 + k_{XER}) + 2(1 + k_{XEL})]}{2 \cdot (1 + k_{XEL} - k_{XEM})} - \\ & - \frac{\sqrt{[...]^2 - 8(1 + k_{XEL} - k_{XEM}) \cdot (1 + k_{XER}) \cdot GFI}}{2 \cdot (1 + k_{XEL} - k_{XEM})} \end{aligned} \quad (7-7)$$

The equations given in table 7.1 for the cases of “parallel line open” and “parallel line open and earthed on both sides” can be derived in the same manner.

#### *Setting strategy for the first zone of the parallel lines)*

The selection of the  $k_{XER}$  setting requires a compromise which considers all three operating configurations (table 7.1)<sup>1</sup>.

With a grading factor of  $GFI = 85\%$ , adaptation to a single circuit line normally is an acceptable solution. The isolation of a line at both ends with earthing at both ends is

<sup>1</sup> The numeric values in table 7.1 were calculated with the line data of the previous example. The complex factors  $k_{EL} = 0.71 - j 0.18$  and  $k_{EM} = 0.67 - j 0.18$  for the sake of simplicity were only considered with their real components which as a first approximation correspond to the values  $k_{XEL} = X_E/X_L$  and  $k_{XEM} = X_M/(3 \cdot X_L)$ . For the EHV system this provides sufficient accuracy.



only done during maintenance, so that the small overreach of 14% is only seldom present. In general, the overreach is considerably reduced by intermediate in-feeds (see further below). In conjunction with single phase ARC, the overreach would in any event only cause an unnecessary ARC, and would not cause final tripping, with the presumption that the short-circuit is of a transient nature (approximately 90% of all short-circuits).

Alternatively, the reach during earth faults could be somewhat reduced by setting a smaller  $k_{\text{XER}}$  factor. In the example, a reduction of  $k_{\text{XER}} = 0.71$  to  $k_{\text{XER}} = 0.5$  would only just result in no more overreach. The reach with both lines in service would however only be 63%, whereby it must be noted that the parallel line coupling only reaches its maximum influence during the worst case condition of single ended in-feed. Under normal conditions, with two ended in-feed, the earth current on the parallel line for faults close to the middle of the line is substantially smaller and the zone reach almost corresponds to that of a single circuit line (see figure 7.5 below).

Additionally, the parallel line coupling at the other line end always acts in the opposite direction, i.e. causes an increase of the zone reach. With permissive tripping, secure fast fault clearance is always ensured.

It must however be noted that a reduction of the  $k_{\text{XER}}$  factor would also reduce the reach of the back up zones for earth faults. This could be compensated by using the separately settable residual compensation factor for overreaching zones, now provided by modern numerical relays (7SA6, 7SA522). This is discussed below.

At earlier relay types, where only one common  $k_{\text{XER}}$  factor exists, a small zone reach reduction (e.g.  $GFI = 0.8$ ) should alternatively also be considered to avoid reduction of the back-up zones.

#### *Setting of the overreach zone*

The zone  $Z_{\text{OR}}$  for teleprotection or ARC controlled zone extension, should be set to 120-130% of  $Z_L$ . This reach would also apply for earth faults in conjunction with parallel line compensation.

Without parallel line compensation, the 120% reach must be dimensioned for the operating condition with parallel lines by consideration of the  $k_{\text{XER}}$  factor which was previously determined.

For this purpose, equation (7-6) is solved for  $GFI$  and  $GFI$  is replaced by  $GF$ :

$$GF = \frac{1 + k_{\text{XEL}} + k_{\text{XEM}} \cdot \frac{x/l}{2 - x/l}}{1 + k_{\text{XER}}} \cdot \frac{x}{l} \quad (7-8)$$

To reach to the end of the line ( $x/l = 1$ ), the grading factor must be

$$GF_{x/l=1} = \frac{1 + k_{\text{XEL}} + k_{\text{XEM}}}{1 + k_{\text{XER}}}$$

Including a security margin of 20%, the following equation for the overreaching zone is obtained:

$$X_{OR} = \frac{1 + k_{XEL} + k_{XEM}}{1 + k_{XER}} \cdot X_L \cdot 1.2 \quad (7-9)$$

With the selected  $k_{XER} = 0.71$ ,  $X_{OR} = 165\% X_L$  is obtained.

Accordingly, the overreaching zone must have a very large setting if a parallel line compensation is not used, to ensure the 20% security margin when both lines are in service.

Note: Modern numerical relays offer the option to set a separate residual compensation factor for the overreaching zones.

We could in this case determine the setting for the overreaching zone as follows: For the zone to cover 100% if the line, we would initially assume a grading factor of  $GF = 1$  and calculate the residual compensation factor for  $x/l = 1$  from (7-6):

$$k_{XER-2} = \frac{1 + 0.71 + 0.64}{1} - 1 = 1.35$$

Using a security margin of 20%, we would finally get the setting for the overreaching from (7-9):

$$X_{OR} = \frac{1 + 0.71 + 0.64}{1 + 1.35} \cdot X_{L1} \cdot 1.2 = 1.2 \cdot X_{L1}$$

### Reach of the back up zones during earth faults

The behaviour of the distance protection with and without parallel line compensation is looked at.

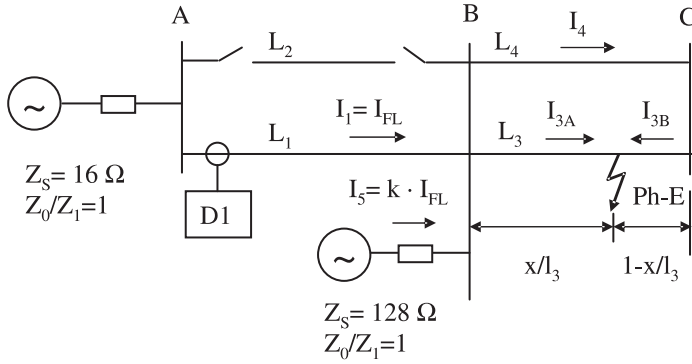
#### *Single side infeed:*

We first consider this easier to study case, which gives a first insight in the calculation method. The system state of a single line (e.g. L1) followed by the parallel connection of L3 and L4 results in the highest reach of the second zone and should be used to check the selectivity between zone 1 on lines 3 and 4 and the second zone of L1.

For the intermediate infeed half the short circuit power is assumed as for the definition of the second zone for phase to phase faults. The relevant circuit diagram is shown in figure 7.4. The intermediate infeed contributes  $k$  times the current of the line to the total fault current. From the given system data the value  $k = 0.84$  can be derived.

For the derivation of a generally valid formula, we define that the fault current of the intermediate infeed from the power plant is  $k$  times the current flowing through line 1 where the considered relay is installed. We then get:

$$I_{Ph} = -I_{E1} = I_{FL} \text{ and } I_{Ph5} = -I_{E5} = k \cdot I_{FL}$$

**Figure 7.4**

Protection setting in case of double circuit lines: equivalent circuit for the calculation example (Ph-E faults)

The total fault current then is  $(1 + k) \cdot I_{FL}$ . It splits up in two loops via lines 3 and 4 to the fault point.

For the voltage at the relay location we get the following equation:

$$\underline{U}_{Ph-E} = \underline{Z}_{L1} \cdot \underline{I}_{Ph1} - \underline{Z}_{E1} \cdot \underline{I}_{E1} + \frac{x}{l_3} \underline{Z}_{L3} \cdot \underline{I}_{Ph3A} - \frac{x}{l_3} \underline{Z}_{E3} \cdot \underline{I}_{E3A} - \frac{x}{l_3} \cdot \frac{\underline{Z}_{0M3-4}}{3} \cdot \underline{I}_{E4} \quad (7-10)$$

$$\underline{I}_{Ph3A} = -\underline{I}_{E3A} = (1 + k) \left( 1 - \frac{1}{2} \cdot \frac{x}{l_3} \right) \cdot \underline{I}_{FL} \quad \text{and} \quad \underline{I}_{E4} = -(1 + k) \cdot \frac{1}{2} \cdot \frac{x}{l_3} \cdot \underline{I}_{FL}$$

Inserting the currents in equation (7-10), we can calculate the measured impedance, by dividing the voltage  $\underline{U}_{Ph-E}$  by the composed current  $\underline{I}_{Ph1} - k_{XER} \cdot \underline{I}_{E1} = (1 + k_{XER}) \cdot \underline{I}_{FL}$ .

$$\begin{aligned} X_{Ph-E} &= \frac{1 + k_{XEL-1}}{1 + k_{XER}} \cdot X_{L1} + \\ &+ (1 + k) \cdot \frac{\left[ \frac{x}{l_3} \left( 1 - \frac{x}{2 \cdot l_3} \right) \cdot (1 + k_{XEL-3}) + \frac{1}{2} \cdot \left( \frac{x}{l_3} \right)^2 \cdot k_{XEM3-4} \right]}{1 + k_{XER}} \cdot X_{L3} \end{aligned} \quad (7-11)$$

Again, by solving for  $x/l_2$ , the equation for the zone reaches is obtained:

$$\frac{x}{l_3} = \frac{(1 + k_{XEL-3}) - \sqrt{(1 + k_{XEL-3})^2 - (1 + k_{XEL-3} - k_{XEM3-4}) \cdot \Delta}}{(1 + k_{XEL-3} - k_{XEM3-4})} \quad (7-12)$$

$$\text{with } \Delta = \frac{2}{1 + k} \cdot \frac{X_{L1}}{X_{L3}} \cdot \left[ (1 + k_{XER}) \cdot \frac{X_{Zone}}{X_{L1}} - (1 + k_{XEL-1}) \right]$$

With the given intermediate infeced condition  $k = 0.84$  the following results:

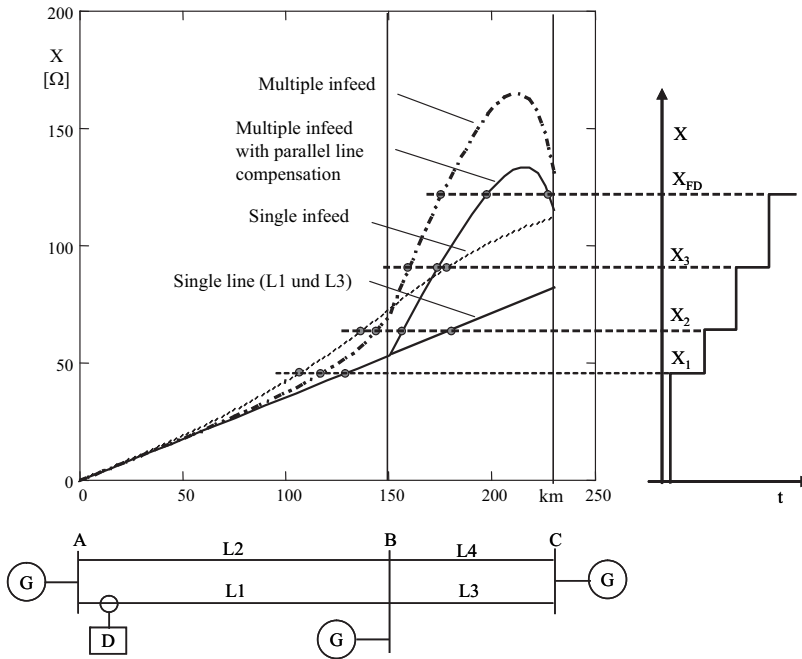


**Figure 7.5** Reach of distance zone in case of Ph-E faults (Calculation example)

For zone 2 (120%  $X_{L1}$  setting), a reach of  $x/l_3 = 22\%$  is obtained. For the third zone (169%  $X_{L1}$  setting) a reach of  $x/l_3 = 104\%$  is calculated. This means, this zone reaches beyond station C. The fault detection zone overreaches C by far.

Zone selectivity is assured for the most unfavourable case.

We must now check the reach of the zones for Ph-E faults for the actual case of multiple infeeds, to see if remote back-up can be sufficiently guaranteed.

The calculations for this study is onerous and suitable computer programs are nowadays used for this purpose. For the calculation by hand, we neglect load and assume equal infeeding EMFs. This is an acceptable approximation for the practical estimation of the zone reaches (larger fault resistances are not considered here). The calculation is outlined in detail in Appendix 11 A.5.

The calculated reach of zones is shown in figure 7.5.

We can observe the following:

- The shortest reach of *zone 1* on the protected line is 70% of the line length. With multiple infeed the reach is a bit higher. With parallel line compensation it extends to about 85%.
- The reach of the *back-up zones* is dramatically reduced with the strong remote infeed in C and the intermediate infeed in B. Without parallel line compensation, the 2<sup>nd</sup> zone does not even reach to the line end  $L_1$ .

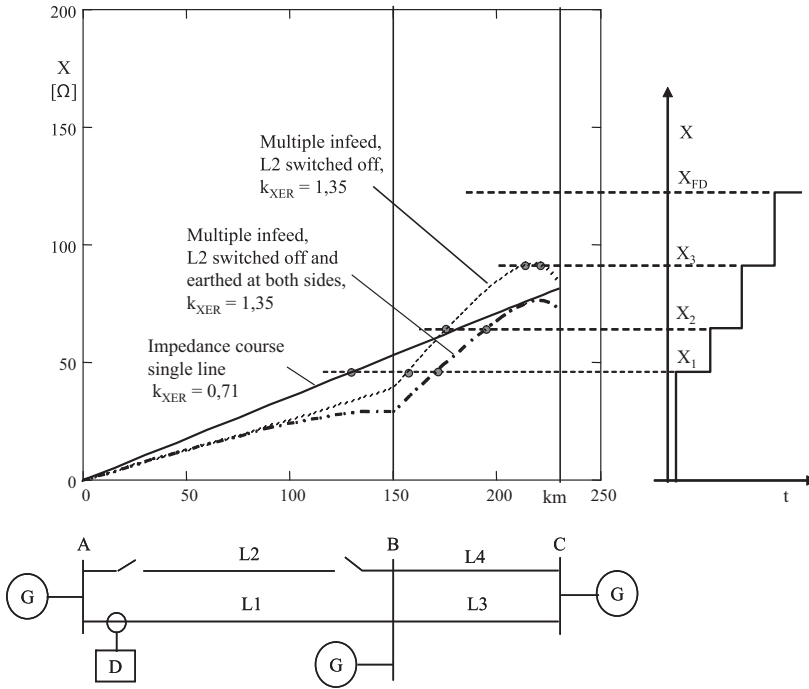


**Figure 7.6** Reach of distance zone in case of Ph-E faults (Calculation example)

- With parallel line compensation, the zone reach is somewhat improved. This is due to the fact that beyond the opposite station B the residual compensation factor  $k_{XER}^* = \frac{1 + k_{XER} + k_{XEMR}}{1 + k_{XER}}$  becomes effective. For example, in equation (7-12) the term  $k_{XER} = 0.71$  must be replaced by the term  $k_{XER} + k_{XEMR} = 0.71 + 0.64 = 1.35$ .
- Modern numerical relays allow to set a separate residual compensation factor  $k_{XER-2}$  which is effective for the overreaching and back-up zones. For these zones, a setting of  $k_{XER-2} = 1.35$  would have the same effect as the parallel line compensation. A much higher setting of  $k_{XER-2}$  however is not reasonable. An overreach of the second zone would occur for faults near C because a reduced impedance is measured behind the maximum of the parabola. This is shown in figure 7.6 for the case that the parallel line L2 is switched off. The critical case occurs when the switched off line is earthed at both ends. In this case a fault in C would appear near the border of the second zone.

### R-Setting

The reach of the zones in R-direction is co-ordinated with the impedance of the natural load of the line:

$$Z_{Nat.} = \frac{U_n^2}{P_{Nat.}} = \frac{400^2}{518} = 309 \, \Omega$$

It is assumed that each line must be capable of carrying twice the rated current for a short time and include an additional security margin of 30%.

From this, the maximum R-reach of the fault detection would be:

$$R_{\max.} = 0.7 \cdot \frac{309}{2} = 108 \, \Omega \text{ primary}$$

A setting of  $R/X = 1$  ( $R = 50$ ) for the 150 km lines and  $R/X = 2$  ( $R = 50 \, \Omega$ ) for the 80 km lines should normally be sufficient for zone 1.

One could then set the load blocking cone (see paragraph 6.2.6) to let say  $R = 50$  and an opening angle  $\varphi_A$  somewhere between 30 and 50° dependent on the reactive load which shall be transported on the lines. The R-reach of the back-up zones could then be increased by keeping the ratio  $R/X=1$  for the 150 km line, and 2 for the 80 km line.

### Conclusions

The example shows that selective remote back-up protection is not feasible in transmission systems with varying switching states and strong multiple infeed conditions.

With normal parallel line operation, the distance back-up zones can only cover a small fraction of the following lines because selective zone grading must be based on the single line condition where the highest reaches occurs. A loss of the remaining single line could be disastrous.

Therefore, double unit protection systems (e.g. PUTT and POTT or PUTT and differential protection) combined with local back-up (breaker failure) protection should be applied.

The additional remote back-up protection of distance zones should be optimised as far as possible:

Setting of a higher residual compensation factor for the overreaching zones, when available, should be used. A value of  $k_{\text{XER-2}} = k_{\text{XEL}} + k_{\text{XEM}}$  is reasonable. It enables the same zone reach as the parallel line compensation.

*Parallel line compensation* is not needed from the protection point of view. The reach of the underreaching zone 1 is not significantly reduced. The critical case would be the single infeed condition which however must not be expected with multiple infeeds.

The sufficient reach of the overreaching carrier zone and the back-up zones can be guaranteed by using the separate residual earth compensation factor as mentioned above.

Parallel line compensation should however be considered for the fault locator, because only with it accurate distance to fault measurement is possible.

The topic of zone grading on double circuit lines in earthed systems is extensively covered in [3.34]. Calculation programs nowadays are available for the relatively complex checking of the back up zones and the fault detection.

## 7.2 Three terminal line (teed feeders)

The in-feed from the respective third end influences the zone reach. This is the deciding criteria when selecting the protection mode and the setting of the distance zones.

### *Protection without signalling channels*

In this case, selective protection grading is hardly possible if internal faults must be cleared inside the zone 2 time at the latest. The zone 2 would have to be set to securely reach beyond the furthest opposite end under consideration of the intermediate in-feed effect.

An enormous overreach into the system results when one in-feed is switched off.

If it is acceptable that during close in faults the circuit breakers at the two opposite ends switch off in succession, i.e. cascaded tripping, a somewhat smaller reach setting is possible. In this case the zone 2 setting must be done according to “Formula 2”.

$$X_2 = X_{L(\text{local line end to node})} + 2 \cdot X_{L(\text{node to farthest remote end})} \quad (7-13)$$

This setting ensures that at least one line end “sees” the remote fault in zone 2, and trips. The other line end will also “see” the fault in zone 2 now and also trip, as the intermediate in-feed is switched off. For earth faults this “Formula 2” is however only valid if the system is homogeneous. This means that lines and infeeds must have the same  $Z_0/Z_1$ -ratios.

### *Protection with signalling channels*

The simplest case applies when the three line sections from the node to the line ends are approximately the same length. In this case it would be possible to set the under-reaching zone at each end to reach beyond the node. All internal faults would then be detected by at least one under-reaching zone, allowing the circuit breakers at the opposite ends to be tripped permissively.

If permissive tripping with zone extension is used, it must be ensured that the over-reaching zone reaches beyond both opposite ends, under consideration of the worst case intermediate in-feed situation (see paragraph 3.5.2).

With unfavourable conditions, it is better to use the permissive tripping with the fault detecting zone, as the maximum reach is then available.

In extreme cases, when it cannot be ensured that the protection at the opposite end picks up during close in faults, a direct inter-tripping function via dedicated communication channel must be implemented.

Single transmission channels from each station to each of the opposite stations is required irrespective of which type of permissive tripping scheme is used.

In general, the line sections have different lengths and the in-feeds differ from each other by a greater or lesser degree. The permissive under-reaching scheme cannot be

used in this case as the zone 1 of at least one line end does not reach beyond the node. In this case a directional comparison or blocking technique must be implemented.

The signalling logic in this case is substantially more complex.

The permissive overreach transfer trip scheme for a three terminal line is shown in figure 5.41, paragraph 5.3.2 The receive signals must be combined with AND-gates (by simply connecting the receive contacts in series). The receive signal must be returned to the sending end when the circuit breaker is open, or during a weak in-feed condition (protection does not pick up) to ensure that tripping can take place there.

With the numeric relays 7SA it is additionally possible to directly trip the local circuit breaker with the simultaneously measuring under-reaching zone. This is important in the case where the relays at the opposite ends do not pick up during close-in faults with high fault resistance, because the resistance appears larger there due to the smaller fault current (refer to paragraph 3.5.1 and the following example). By switching off the end closest to the fault, the measured fault resistance is reduced to the other line ends, allowing the permissive overreaching scheme to then trip the remaining two terminal line as well.

The independent undereaching zone is also useful in the event that during an internal fault, current flows out of the three terminal line due to the system conditions (“outfeed condition”, refer to paragraph 3.5.2). Direct tripping of the end closest to the fault in this case again introduces a new fault scenario (reversal or interruption of the current flowing out of the three terminal line) which is recognised as an internal fault by the permissive overreaching scheme. Tripping again results in cascade.

The blocking schemes often implemented outside Europe, have an advantage on the three terminal application, in that they implement an amplitude modulated PLC (on-off carrier) with a single frequency. Per line end only one transmitter and receiver is therefore required. For the zone settings, similar procedures as for the permissive overreach scheme apply.

*Example:*

Calculation of the zone settings for a three terminal line.

*Given:*

Three terminal line 110 kV according to figure 7.7.

Line data (applicable to all line segments)

$R'_{L1} = 0.071 \text{ } \Omega/\text{km}$  and  $X'_{L1} = 0.380 \text{ } \Omega/\text{km}$

$R'_{L0} = 0.220 \text{ } \Omega/\text{km}$  and  $X'_{L0} = 1.110 \text{ } \Omega/\text{km}$

Effective tower footing resistance: 5  $\Omega$

Maximum short time line current rating:

$I_{L-\text{max.}} = 2 \cdot I_{L-\text{thermal}} = 2 \cdot 630 = 1260 \text{ A}$

Current transformer: 600/1

Voltage transformer: 110/0.1 kV

Transmission channels will be provided

*Task:*

Determine the fault detection and zone settings



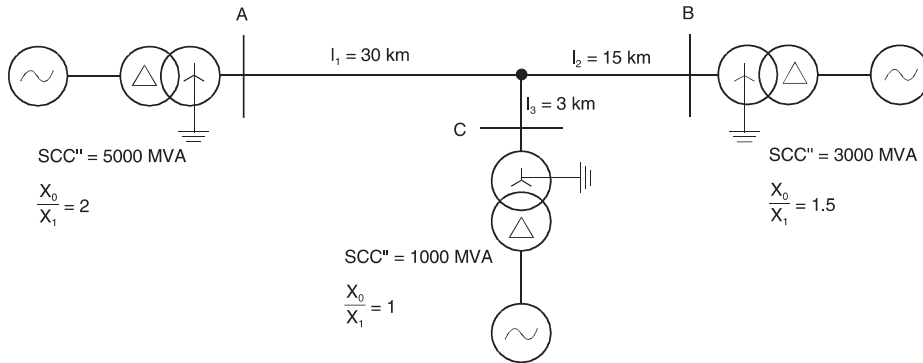


**Figure 7.7** Three terminal line: data for the calculation example

*Solution:*

The phase short-circuits are looked at initially and the reach of the zones in X-direction is determined.

#### *Under-reaching zones*

The reactances of the under-reaching zones are graded relative to the closest opposite end, without considering intermediate in-feeds:

$$(X_{1-U})_A = 0.85 \cdot (11.4 + 1.14) = 10.7 \, \Omega$$

$$(X_{1-U})_B = 0.85 \cdot (5.7 + 1.14) = 5.8 \, \Omega$$

$$(X_{1-U})_C = 0.85 \cdot (1.14 + 5.7) = 5.8 \, \Omega$$

For the  $R_1$  setting, a value equal to twice the reactance is chosen ( $R/X = 2$ ).

Initially it is determined that  $(X_{1-U})_A$  does not reach up to the node, and that  $(X_{1-U})_B$  only marginally reaches beyond the node. Permissive under-reach transfer trip can therefore not be applied. A permissive overreach scheme must instead be chosen.

#### *Overreaching zones for the POR scheme*

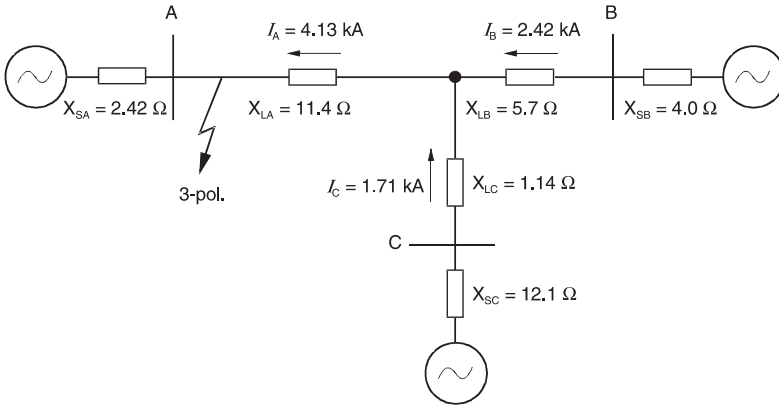
The intermediate in-feeds must be considered when determining the reach of the overreaching zones. In practice the following is to be selected:

- at the own end: the minimum short-circuit rating;
- at the other ends: the maximum short-circuit rating.

In the example, constant short-circuit ratings are given for the sake of simplicity.

In this example, the relay at B is considered:

The short-circuit currents and voltages shown in figure 7.8 were determined by short-circuit calculation of a fault at the line end A.

**Figure 7.8**

Calculation example three terminal line: current distribution during three phase short-circuit at A

Only the reactances of the lines and in-feeds were considered for the approximation calculation.

The overreaching zone is calculated as follows:

$$(X_{1-0})_B = 1.2 \cdot \left( X_{LB} + X_{LA} \frac{I_C + I_B}{I_B} \right) = 1.2 \cdot \left( 5.7 + 11.4 \cdot \frac{1.71 + 2.42}{2.42} \right) = 30.2 \, \Omega$$

The fault in front of C resulted in a smaller reactance 7.6 Ω.

Due to the larger zone length,

$(R_{1-0})_B = (X_{1-0})_B = 30.2 \, \Omega$  is selected.

The minimum load impedance is:

$$Z_{\text{load-min.}} = \frac{U_N / \sqrt{3}}{I_{L-\text{max.}}} = \frac{100 / \sqrt{3} \, \text{kV}}{1,260 \, \text{kA}} = 50 \, \Omega$$

A large security margin against load encroachment is therefore maintained.

### Earth faults

The safe overreach of the POTT zone must be checked for faults at the two opposite line ends each.

In the following, the distance measurement at B is analyzed in detail as an example.

The procedure for the relays at the other line ends is the same.

The calculation with symmetrical components produced the short-circuit results shown in figure 7.9.

The large short-circuit current from the end A produces a very large voltage drop across the fault resistance. The angle between the source emf and the short-circuit cur-

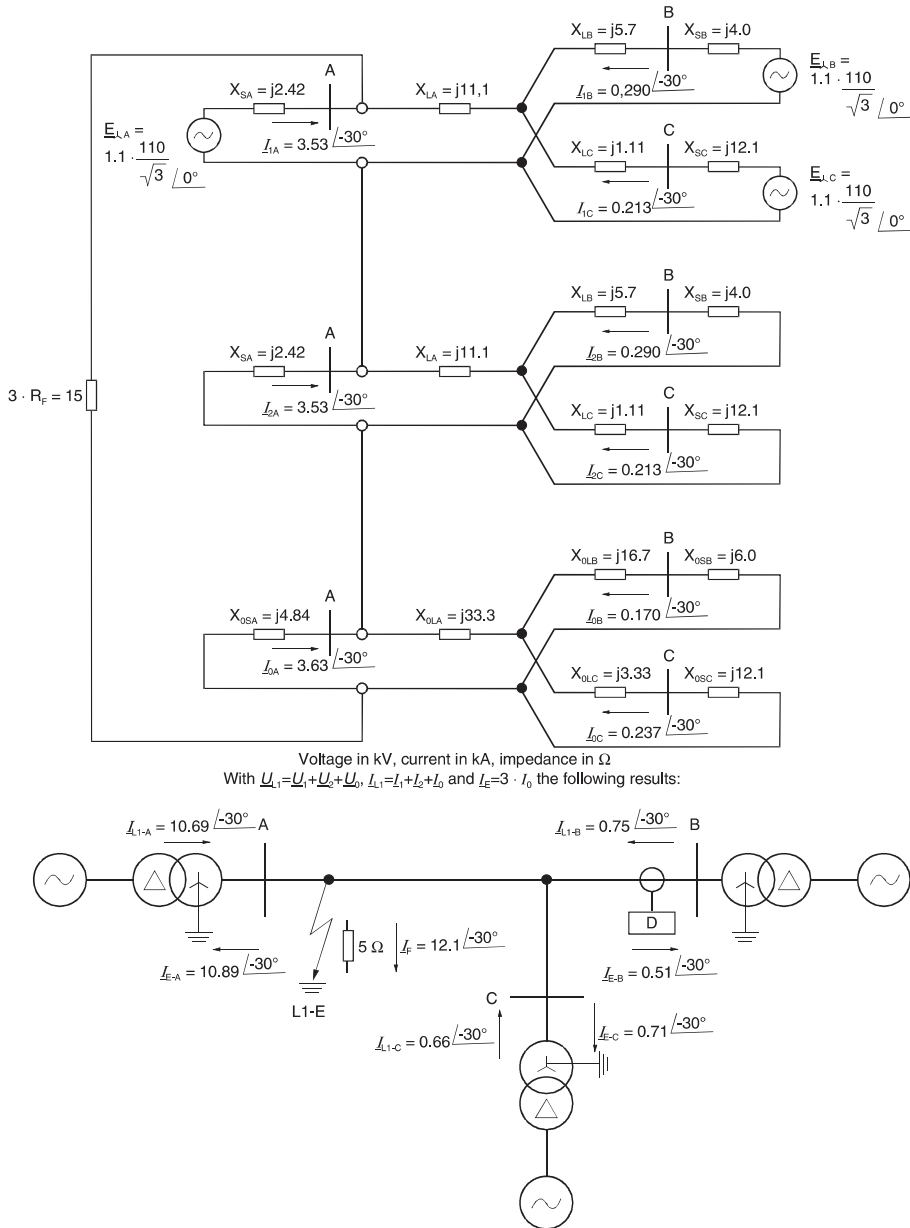


**Figure 7.9**  
Three terminal line: earth fault with fault resistance calculation with symmetrical components

rent is only  $30^\circ$  as a result of the small source impedance at A. The short-circuit angle at the relay location in B is even smaller at  $27.3^\circ$  (figure 7.10).

At the relay location under consideration, B, the short-circuit current is substantially smaller, as was expected.

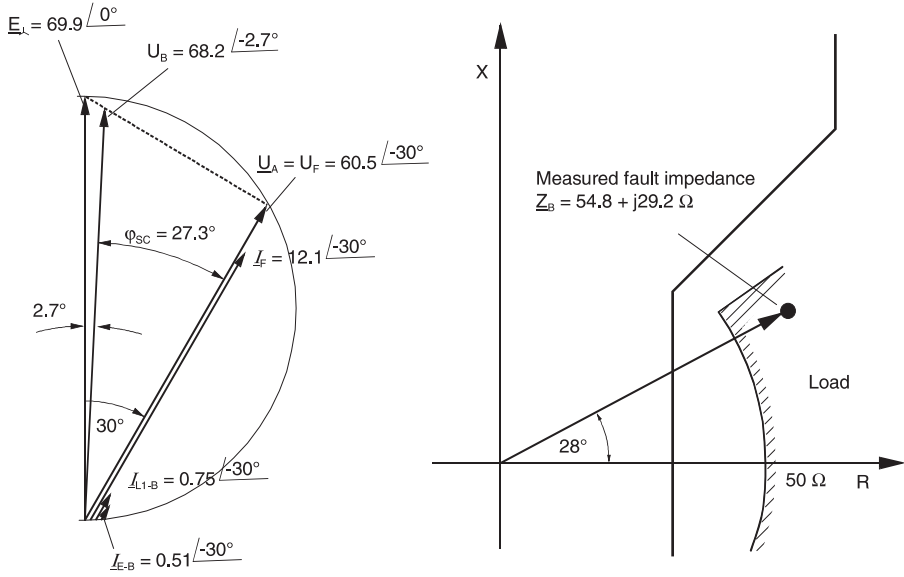


**Figure 7.10** Three terminal line: current/voltage and impedance diagram relating to figure 7.9

As  $I_{Ph}$  and  $I_E$  have the same phase relationship, the simplified equations (3-53) and (3-54) in paragraph 3.2.3 may be used for the computation of the measured  $X$  and  $R$  values:

$$(X_{L1-E})_B = \frac{U_{Ph-E} \cdot \sin \varphi_{SC}}{I_{Ph} - \frac{X_E}{X_L} \cdot I_E} = \frac{68.2 \cdot \sin 27.3^\circ}{0.75 + 0.63 \cdot 0.51} = 29.2 \, \Omega$$

$$(R_{L1-E})_B = \frac{U_{Ph-E} \cdot \cos \varphi_{SC}}{I_{Ph} - \frac{R_E}{R_L} \cdot I_E} = \frac{68.19 \cdot \cos 27.3^\circ}{0.75 + 0.70 \cdot 0.51} = 54.8 \, \Omega$$

For the calculation we have considered that in formulas 3-53 and 3-54 the earth current is counted positive when it flows into the line.

It is noted that the resistance is very close to the minimum load impedance (figure 7.10).

Accordingly the problem exists that this fault cannot even be securely detected by the fault detection. Due to the small short-circuit angle, the angle dependent fault detection will also not pick up because pick up angles below  $30^\circ$  cannot be set to allow for the required reactive power transfer.

The under-reaching zone in A, which is configured to directly trip, provides a solution in this case. It measures a small resistance due to the large short-circuit current and therefore securely trips the circuit breaker at A:

$$(X_{L1-E})_A = 0$$

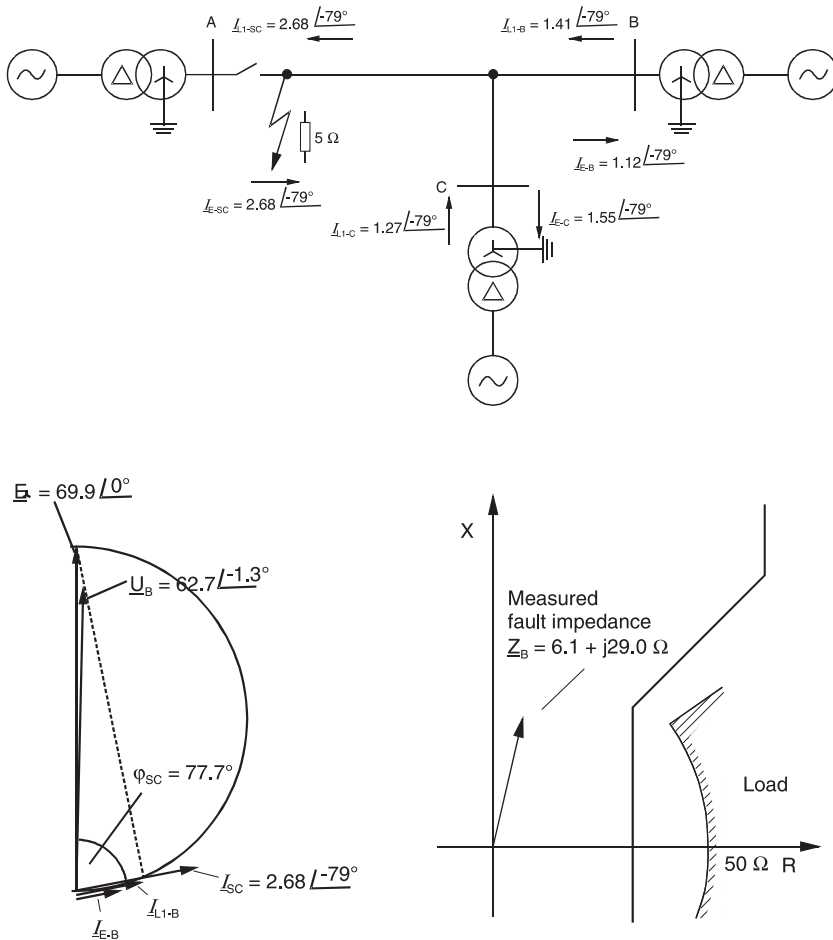


**Figure 7.11**

Three terminal line: earth fault with fault resistance, condition after tripping at end A

$$(R_{L1-E})_A = \frac{U_{Ph-E} \cdot \cos \varphi_{SC}}{I_{Ph} - \frac{R_E}{R_L} \cdot I_E} = \frac{60.5 \cdot \cos 0^\circ}{10.69 + 0.70 \cdot 10.88} = 3.3 \, \Omega$$

After the in-feed at A has been tripped, the fault condition shown in figure 7.11 results. The short-circuit current at the ends B and C is approximately doubled, while the short-circuit angle increases to almost  $79^\circ$  (in actual fact approximately  $10^\circ$  less, because the resistive component of the line was neglected in the calculation).

An angle dependent under-impedance starting, or impedance starting with an angle criterion of  $45^\circ$  would now securely pick up. An overcurrent or under-impedance fault detection alone would however still not be sufficient.

The relay at B measures the following impedance after the end A has tripped:

$$(X_{\text{Ph-E}})_B = \frac{U_{\text{Ph-E}} \cdot \sin \varphi_{\text{SC}}}{I_{\text{Ph}} - \frac{X_E}{X_L} \cdot I_E} = \frac{62.7 \cdot \sin 77.7^\circ}{1.41 + 0.63 \cdot 1.12} = 29.0 \, \Omega$$

$$(R_{\text{Ph-E}})_B = \frac{U_{\text{Ph-E}} \cdot \cos \varphi_{\text{SC}}}{I_{\text{Ph}} - \frac{R_E}{R_L} \cdot I_E} = \frac{62.7 \cdot \cos 77.7^\circ}{1.41 + 0.70 \cdot 1.12} = 6.1 \, \Omega$$

The resistive component is substantially reduced as was expected, and is now substantially less than the set reach of the distance zone.

The measured X-value  $(X_{\text{Ph-E}})_B = 29.0 \, \Omega$  appears just below the set limit of the overreaching zone  $(X_{1-0})_B = 30.2 \, \Omega$ .

For the relay in C the situation is more favorable:

By a calculation similar as for the relay at terminal B we get  $(X_{1-0})_C = 34.4 \, \Omega$  as zone setting and  $(X_{\text{Ph-E}})_C = 23.0 \, \Omega$  as measured X-value.

Consequently the POTT teleprotection scheme would trip in B and C subsequent to fault clearance in A.

Note: We have determined the setting of the overreaching zone based on the three-phase fault condition.

The above calculation however shows that the originally intended overreach security margin of 20% is not achieved in the case of phase-to-earth faults.

It is only  $(30.2 - 29.0)/29 = 4.1\%$  due to the dissimilar  $Z_0/Z_1$ -ratios of lines and infeeds.

In each case it is therefore necessary to check additionally the reach conditions for earth faults.

In the case at hand the setting of overreaching zone would have to be extended to  $1.2 \times 29.0 = 34.8 \, \Omega$ .

Alternatively a separate residual compensation factor for overreaching zones, now available in numerical relays, could be set higher to get a longer reach in the case of earth faults.

With a setting value  $X_E/X_L = 0.91$  (instead of 0.63) we would get an appearing (a measured) impedance of  $(X_{\text{Ph-E}})_B = 25.2 \, \Omega$  (instead of  $29.0 \, \Omega$ ) which is about 20% below the set zone limit ( $30.2 \, \Omega$ ).

### Arc resistance

Up to now the arc resistance at the fault location has been ignored. Its influence is now estimated.

An isolator length of 1.3 m is assumed, and a security margin of 50% is included.

$$U_{LB} = 1.5 \cdot 1.3 \text{ m} \cdot 2.5 \text{ kV/m} = 5 \text{ kV}$$

With the in-feed from A, a voltage of  $U_F = 12.1 \text{ kA} \cdot 5 \Omega = 60.5 \text{ kV}$  appears across the fixed fault resistance. This implies that the influence of the fixed arc resistance is less than 10%.

After A has tripped, the voltage across the resistance drops to:

$$U_F = 2.68 \text{ kA} \cdot 5 \Omega = 13.4 \text{ kV. The arc voltage remains constant, and in comparison is 37\%.$$

As the distance protection zone is set to a large value to allow for the in-feed from A, the arc resistance only has a small influence in comparison to the fixed resistance (tower footing resistance) in the case at hand. It can be allowed for with a reach increase of 10%.

**Note:** The example again clearly shows that the arc resistance may not be considered as a fixed resistance because an unrealistically large resistance would appear at the relay if there is an in-feed from the opposite end. Furthermore is apparent, that fixed fault resistances demand very large R-settings of distance zones, when the in-feed from the opposite end is strong. The limiting influence of the earth wires should therefore be considered when setting problems arise (refer to paragraph 3.5.1).

### *Back up zones*

In the case at hand, the second zone should in any case reach beyond the opposite end to provide back up protection for the busbars. It must be set according to the “Formula 2” method.

This would result in the following for terminal B of the lines:

$$(X_2)_B = X_{LB} + 2 \cdot X_{LA} = 5.7 + 2 \cdot 11.4 = 28.5 \Omega$$

We realize however that the reach of the second zone, calculated by the “Formula 2”, is not far enough in the case of earth faults. It would not even cover the line end (29.0  $\Omega$ ). As in the case of the above calculated POTT zone, we would have to extend the zone to 34.8  $\Omega$  or choose a higher residual compensation factor ( $X_E/X_L = 0.91$ ).

The third zones are not examined in the example. They must be matched to the surrounding network and protection located there.

### *Fault detection*

The setting is as sensitive as possible, to cover as large a portion of the network as possible, with back-up protection despite the intermediate in-feed effect.

*U-I- $\varphi$  fault detection*

$$U(I>) = 0.7 \cdot U_N \text{ and } I> = 0.25 \cdot I_{N-CT} = 150 \text{ A}$$

$$U(I>>) = 1.0 \cdot U_N \text{ and } I>> = 1.2 \cdot 2 \cdot I_{L-\text{thermal}} = 1.2 \cdot 1260 = 1500 \text{ A}$$

$$U(I\varphi>) = 1.0 \cdot U_N \text{ and } I\varphi> = 0.7 \cdot I_{L-\text{thermal}} = 0.8 \cdot 630 \text{ A} = 500 \text{ A}$$

$\varphi_A = 35^\circ$ , i.e. marginally above the maximum permitted load angle

$$I_{E>} = 0.25 \cdot I_{N-CT} = 150 \text{ A}$$

$U_{E>} =$  corresponding to the displacement voltage of 20%  $U_N/\sqrt{3}$ .

*Impedance fault detection*

The same sensitivity as for the angle dependent fault detection is selected, and the point of inflection is converted to an impedance.

We get the following settings (zone shape and meaning of setting parameters according to figure 6.4 in section 6.2.6):

$$X_{+FD} = \frac{U(I\varphi>)}{I\varphi>} = \frac{100/\sqrt{3} \text{ kV}}{0.5 \text{ kA}} = 127 \Omega$$

$$X_{-FD} = X_{+FD} = 127 \Omega$$

$$R_{LB} = 0.8 \cdot Z_{\text{Load-min}} \cdot \cos \varphi_{L-\text{max.}} = 0.8 \cdot 50 \cdot \cos 30^\circ = 34.6 \Omega$$

$$\varphi_{LB} = 35^\circ$$

$$R_{FD} = 2 \cdot R_{LB} = 69.2 \Omega$$

Note: We have seen that setting of the distance zones for a three-terminal line is rather complex.

The reach of the distance zones in the case of phase-to-earth faults may differ from the reach during phase-to-phase faults. This occurs when the system is non-homogeneous, i.e. when the  $Z_0/Z_1$ -ratios of the infeeding sources differ from the line values.

One of the now available computer programs (e.g. SINCAL of Siemens) should be used to calculate and check the zone grading for all kinds of faults.



---

## 8 Commissioning

Commissioning of protection systems may only be carried out by qualified personnel with the corresponding educational background.

The protection system must be fully tested and set prior to energising the line for the first time. After energisation, a subsequent test with load current is done, before the line is released.

### 8.1 Testing of the protection system

The protection system consists of the following components:

- protection equipment  
With analogue technology, this consisted of the combination of protection and auxiliary devices, mounted and wired on a protection panel, in a protection cubicle or in the LV compartment of a medium voltage switch gear bay.  
It is generally supplied to the site pre-tested.  
With numerical technology, this is often reduced to a single factory pre-tested multi-functional protection relay.
- current and voltage transformers
- circuit breaker
- battery
- tripping and closing circuits
- signalling circuits
- serial connection to a SCADA-system
- protection communication channels to the opposite station.

Redundant protection is provided at higher voltage levels, with galvanically separated measuring inputs and control circuits.

Testing of the protection system is comprised of the following steps:

- *Setting of the protection devices*  
The setting programme DIGSI provides a convenient tool for this. It is general practice to have the settings prepared and stored as a DIGSI file by an expert protection engineer in the office. On site, these values can then be down loaded to the protection relay by the commissioning personnel.



**Figure 8.1**  
Testing of distance protection with PC controlled test equipment

- *Checking of the pick up values*

The test signals are generated with a secondary injection test set and injected into the relay. The test equipment is connected via the terminal rail of the protection equipment (panel or cubicle), or via a test switch provided for this purpose. A three phase test set for current and voltage is recommended for testing of numerical distance protection, as these modern relays use unfaulted voltages for direction determination and have continuous symmetry monitoring of the current and voltage inputs.

All current and voltage thresholds must be checked. A check of the pick up value on the R- and X-axis with the corresponding delay times for one, two and three phase faults is sufficient for the respective distance zones.

Electronic PC controlled test equipment which exactly simulates the fault types and allows for substantial automation of the test sequence is available today (figure 8.1) [8.1].

- *Checking of the instrument transformer circuits*

It is preferable to check the current transformer circuits with a primary injection test set. The secondary currents arriving on the relay terminals can be directly displayed with the integrated measuring function integrated in the numerical relays.

The VT circuits are checked from the secondary side terminals of the VT.

- *Circuit breaker trip and close circuits including the signalling circuits* and serial interfaces are checked by proving that the corresponding function in the protection picks up when it is injected with the secondary injection equipment.

- *Circuit breaker*

With open isolators, the protection trip and re-close function is tested by simulation of a fault with the secondary injection test equipment.

- *Testing of the teleprotection system*

In this case, two sets of test equipment must be used to simulate internal and external faults at both line ends. For synchronised switching, additional communication channels are required. By energising the line from one side, and starting the test equipment with the appearing voltage, it is possible to trigger a synchronised start of the test equipment.

A so-called end-to-end check with close to real current and voltage signals is possible with modern digital controlled test sets. The test sets at all line ends are in this case synchronised via GPS with an accuracy of some micro-seconds [8.2].

## 8.2 Test with load

After the protection system has been successfully tested, the line may be energised while observing the relevant safety measures.

It is however strongly recommended to set the times of available back-up zones zero before and during the tests to enable instantaneous tripping in case of a fault.

### *Verification of correct CT and VT connections*

With load currents of approximately  $10\%I_N$  or greater, the complete measuring circuit can be tested by comparing the operational measured values (U, I, P, Q) with the known data from the load dispatch centre or separate power measurement in the substation.

### *Directional check*

This is an important test which proves that the distance protection functions with the correct polarity, i.e. faults in the forward direction on the line are actually correctly recognised as being in the forward direction. By using primary currents and voltages for this test, it is ensured that swapped polarities in the CT and VT circuits are definitely recognised.

The real and reactive power transferred across the line determines the impedance measured by the relay, from which the direction is determined. It can be calculated as follows:

$$Z_{\text{load}} = \frac{P_{\text{active}}}{3 \cdot I_{\text{load}}^2} + j \frac{P_{\text{reactive}}}{3 \cdot I_{\text{load}}^2} = R_{\text{load}} + jX_{\text{load}} \quad (8-1)$$

The real power flowing into the line is designated as being positive. This corresponds to the case where the consumer is located at the end of the line. Reactive power is designated as being positive when inductive power flows into the line, i.e. when the line appears to be inductive.

An overexcited generator supplies inductive power, while an underexcited generator consumes inductive power (figure 8.2).

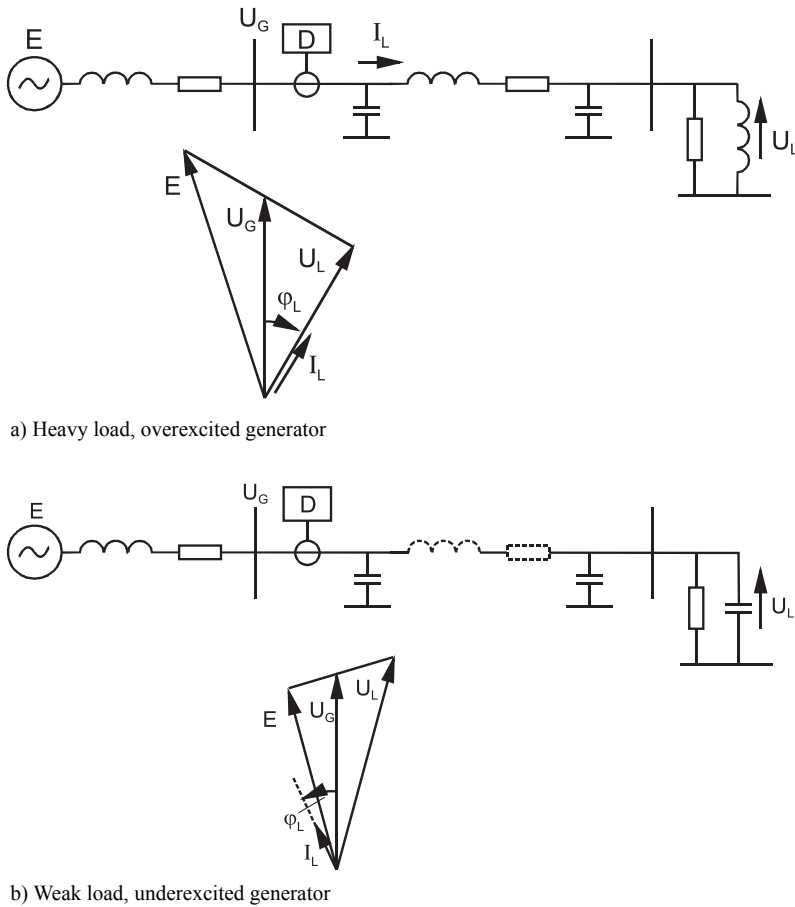


**Figure 8.2** In-feed to a network, load dependent load angle at the relay

In the case of a weakly loaded line or a weakly loaded network, the capacitive loading dominates, i.e. the measured reactive power is negative. With heavy loading, the inductive reactive power demand of the line inductivities dominates, so that the measured reactive power is positive.

Figure 8.3 shows these situations for long transmission lines. With natural loading of the line, the line is at reactive power balance and only real power flows into or out of the line. Accordingly the protection will measure a positive or negative  $R$ .

The  $R$  and  $X$  values calculated with equation (8-1), are entered in the impedance diagram (figure 8.4). By comparing the location of the impedance relative to the directional characteristic, it is immediately evident whether the protection must recognise the forward or reverse direction under the given load conditions.

The direction check initiated in the relay by entering parameters, must return the correct direction decision for all 6 measuring loops.

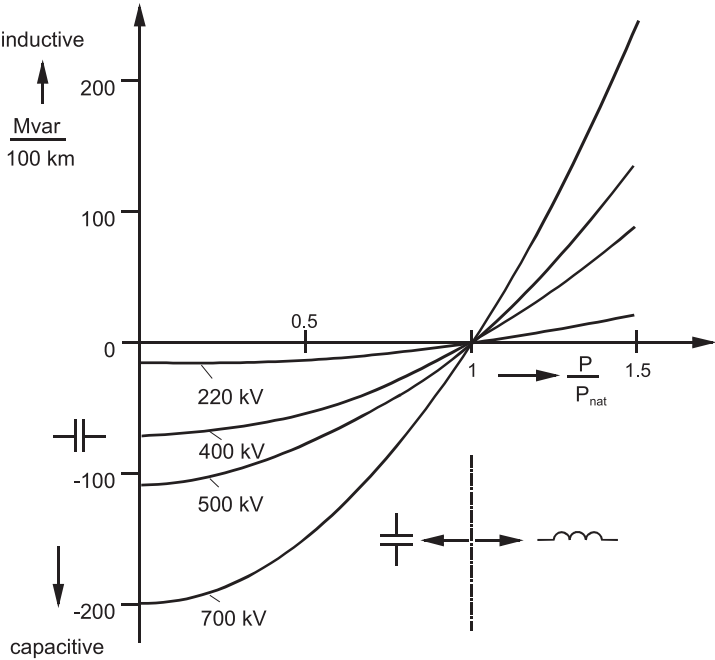


**Figure 8.3** Reactive power demand of a transmission line

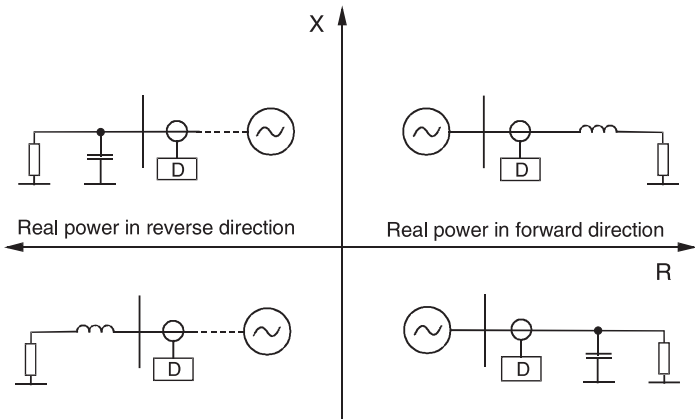


**Figure 8.4** Directional check with load current, sign of the measured impedance,  $Z = R + jX$

After successful direction check and a final update and control of the settings, the line may be commissioned.

---

## 9 Maintenance

Due to the continuous self-monitoring in the numerical protection, a different maintenance strategy has to be employed. In comparison to analogue protection, routine maintenance can be substantially reduced. The trend is toward event based maintenance and repair.

### 9.1 Self monitoring

The numerical protection implements substantial self monitoring from the measuring inputs up to the command relays.

The essential monitoring functions are:

- measuring circuits:
  - current sum
$$|\underline{I}_{L1} + \underline{I}_{L2} + \underline{I}_{L3} - \underline{I}_E| < \Delta \underline{I}_{\max}.$$
  - voltage sum
$$|\underline{U}_{L1} + \underline{U}_{L2} + \underline{U}_{L3} - \underline{U}_E| < \Delta \underline{U}_{\max}.$$
  - non-symmetry of current
$$|I_{\text{Ph-Max.}}|/|I_{\text{Ph-Min.}}| < k_I$$
  - non-symmetry of voltage
$$|U_{\text{Ph-Max.}}|/|U_{\text{Ph-Min.}}| < k_U$$
  - phase sequence:
$$U_{L1} \text{ before } U_{L2} \text{ before } U_{L3}$$
  - voltage failure:
$$U_{\text{Ph-Ph}} < U_{\text{Min.}} \text{ at } I_{\text{Ph}} > I_{\text{Min.}}$$
- Hardware:
  - A/D converter: conversion and checking of a fixed reference value
  - processor: watchdog
  - memory chips: read/write cycles
  - switching of the relay coils: single pole switching and feed back monitoring

The contact of the command relays cannot be self monitored. The trip and ARC test function is provided for this purpose. It can be initiated locally or remotely via a modem and telephone line.

## 9.2 Maintenance strategy

The availability of protection is substantially increased by self monitoring. The order of magnitude can be statistically determined (figure 9.1). The non-availability indicates how many devices in percent of the installed base on average are not functional at a particular point in time. Without self monitoring the number of failed devices naturally increases sharply with increasing service time. With continuous self monitoring, the percentage of failed devices is reduced to a similarly low level as with routine maintenance.

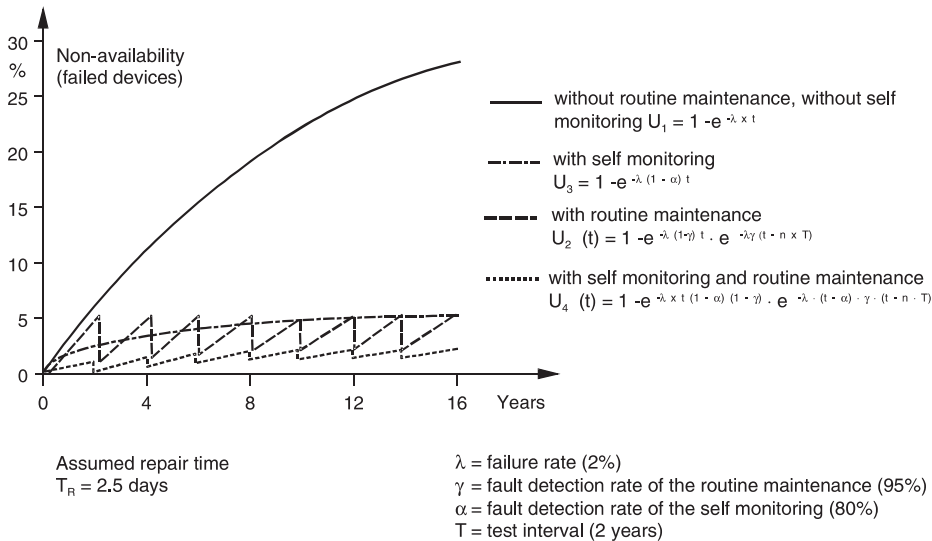


**Figure 9.1** Protection availability, influence of self monitoring  
(values in brackets were assumed as an example)

The combination of continuous self monitoring with routing maintenance at larger intervals has proven itself as a balanced approach in practice.

The VDEW (German utility board) working group “relay and protection technology” published the following recommendations for the maintenance of numerical relays in 1995 [9.1]:

- **Bi-annually:** simple function check (without test equipment)
  - comparison of the operational measured values ( $U$ ,  $I$ ,  $P_W$ ,  $P_Q$ ) indicated by the relay with the data obtained from an independent operational measurement or from the load distributor.
  - trip test (e.g. with a test ARC cycle)
  - read out and evaluation of the event recording
  - check of the protection fault recordings and the tele-protection signalling
- **every four years:** protection test (with test equipment)

- check of one measured value in each of the input channels ( $U$  and  $I$ ) and comparison with the display of the relay or on the operator PC
- check of the utilised inputs and outputs including operation of the circuit breaker.
- read out and evaluation of the event recording and disturbance recording
- Check of the interfaces (PC and SCADA connection)
- Read out of the setting parameters and comparison to the required values
- check of the protection fault recordings and the tele-protection signalling
- **every eight years:** additional dynamic tests of the threshold of the first zone
  - for all fault types (hardware changes in the input filters should be detected with this test).

In this way, the self monitoring results in a considerable cost saving with regard to maintenance in comparison to analogue technology.

Note: Now, after sufficient experience with numerical relays and self-monitoring, it is recommended to perform the test with test equipment every six instead of four years.



---

# 10 Bibliography

## 10.1 Technical papers

- [1-1] Kumar, A.; Mainka, M.; Ziegler G.: 20 years of digital protection; Siemens EV-Report 4/94, September 1994, pp. 10-13
- [1-2] IEEE Tutorial Course: Computer relaying; Course Text 79 EH0148-7-PWR, 1979
- [1-3] Koch, G.; Westerholt, H.: Microprocessors enter the substation; Electrical Review 6/13, 1985
- [1-4] Matla, W.; Ziegler, G.: Numerical EHV feeder protection, concept and realisation; CIGRE Conference, Paris 1994, Report 34-103
- [1-5] Koch, G.; Renz, K.: Fully Microprocessor Based Feeder Protection, Siemens Power Energy & Automation, Vol. VII, (1985), pp. 174-177
- [1-6] Mainka, M.; Koch, G.: Design aspects of a fully microprocessor-based feeder protection system for HV lines; CIGRE Conference, Paris 1986, Report 34-12
- [1-7] Lemmer, S.; Meisberger, F.: Universeller Distanzschutz; etz, Bd. 113 (1992) H. 17, pp. 1076-1080 (in German); (Title: Universal distance protection)
- [1-8] Claus, M.; Lemmer, S.; Ziegler, G.: Proceedings in distance relaying; IEE Conference on Developments in Power System Protection, Nottingham (UK), 1997, IEE Conference publication No. 434, pp. 28-31
- [1-9] CIGRE Technical Brochure No. 359: Modern Distance Protection, Functions and Applications; CIGRE Office, Paris, 2008
  
- [2-1] International Electrotechnical Vocabulary (IEV), Chapter 448: "Power System Protection"
  
- [3-1] Neugebauer, H.: Gleichstrom-Drehspulrelais mit Gleichrichter für die Selektivschutztechnik; ETZ Jg. 71 1950, pp. 389-393 (in German). (Title: Rectifier bridge comparator for relaying)
- [3-2] Warrington, A. R. van C.: Application of the OHM and MHO Principles to Protective Relays; Transactions of the American Institute of Electrical Engineers, Volume 65, 1996 (Paper 46-38)

- [3-3] Wedepohl, L. M.: Polarized MHO Distance Relay; Proc. IEE, Vol. 112, No. 3, 1965, pp. 525-535
- [3-4] Zurowski, E.: Elektronischer Distanzschutz mit polygonaler Auslösecharakteristik Siemens Zeitschrift, Jg. 45, 1971, pp. 266-268 (in German); (Title: Static distance relay with quadrilateral characteristic)
- [3-5] CIGRE Working Group Report: Protection Systems Using Telecommunication; Technical Brochure 13, 1987, CIGRE Central Office, Paris
- [3-6] CIGRE Working Group Report: Protection using telecommunication; Technical Brochure No. 192, CIGRE Central Office, 2001
- [3-7] Clarke, E.: Impedances seen by relays during power swings with and without faults; AIEE Transactions 1945, Volume 64, pp. 373-384
- [3-8] AIEE/PES T&D Committee Working Group Report: Arc deionization times on high speed three pole reclosing; IEEE Transactions on PAS, Vol. 82, 1963, pp. 236-253
- [3-9] Haubrich, H.: Einpolige Kurzunterbrechung in Höchstspannungsnetzen über 500 kV; ETZ-A, Bd. 91 (1970), H.8, pp. 453-458 (in German); (Title: Single-pole ARC in EHV systems above 500 kV)
- [3-10] IEEE Committee Report: Single Phase Tripping and Reclosing of Transmission Lines; IEEE Paper, 91 SM 360-8 PWRD, 1991
- [3-11] Krieser, F.: Ein Meßgerät zur Anzeige der Fehlerentfernung während des Kurzschlusses; Siemens Zeitschrift Jg. 33, 1959, pp. 232-235 (in German); (Title: A measuring instrument for the indication of the fault location during the short-circuit)
- [3-12] Buurman, E. und Schaale, J.: Fehlerorter 7SE1 mit Arithmetikprozessor, Siemens Energietechnik 4/1980; pp. 118-120 (in German) (Title: Fault locator 7SE1 with a numeric processor)
- [3-13] Ziegler, G.: Fault location in H.V. power systems; IFAC Symposium on Automatic Control in Power Generation, Distribution and Protection; Pretoria, 1980, pp. 121-129
- [3-14] Hagenmeyer, E. und Zurowski, E.: Decentralized fault location combined with centralized computer evaluation in a main control centre gives optimized network operation; CIGRE Conference, Paris 1982, Report 34-09
- [3-15] Cook, V.: Fundamental aspects of fault location algorithms used in distance protection; IEE Proc., Vol. 133, Pt. C, No.6, Sept. 1986
- [3-16] Eriksson, L., Saha, M. M., Rockefeller, G. D.: An accurate fault locator with compensation for apparent reactance in the fault resistance resulting from remote-end infeed; IEEE Trans. On Pow. App. and Syst. Vol. PAS-104. No. 2, February 1985
- [3-17] Sachdev, M. S., Agarwal, R.: A technique for estimating transmission line fault locations from impedance relay measurements; IEEE Trans. on Power Delivery, Vol. 3, No. 1, January 1988

- [3-18] G Kiessling & S Schwabe: Software solution for fault record analysis in power transmission and distribution; IEE DPSP Conference, Amsterdam, 2004, Session 6, paper 48
- [3-19] Philippot, L.: Parameter estimation and error estimation for line fault location and distance protection in power transmission systems; Ph. D. Thesis, Université Libre de Bruxelles, February 1996
- [3-20] IEEE Tutorial Course on "Advancements in microprocessor based protection and communication"; 1997, IEEE Catalogue Number: 97TP120-0,
- [3-21] Ulbrich, R. und Kadner, G.: Richtlinien für das Aufstellen von Staffelpänen; Mitteilungen des Instituts für Energetik, 1957, H. 7, pp. 24-68 (in German); (Title: Recommendations for the design of grading charts)
- [3-22] VDEW-Ringbuch Schutztechnik; Teil 9: Empfehlungen zur Endzeitstaffelung; VDEW-Verlag Frankfurt/M., 1988 (in German);
- [3-23] P.J. Moore, R.K Aggarwal, H. Jiang and A.T. Johns: New approach to distance protection for resistive double-phase to earth faults using adaptive techniques; IEE Proc.-Gener. Transm. Distrib. Vol. 141, No. 4, July 1994 (Recommendations of the German Utility Board for the grading of final back-up zones)
- [3-24] Lemmer, S., Linker, K.-W., Stöber, K.-J.: Leistungsfähige Software unterstützt die Koordination des Distanzschutzes in Mittelspannungsnetzen; Siemens EV-Report 1/93, pp. 24-26 (in German); (Title: Powerful program assists distance relay co-ordination)
- [3-25] IEC/TR2 60909-1: Short-circuit current calculation in three-phase a.c. systems, Part 1: Factors for the calculation of short-circuit currents in three phase systems according to IEC 909 (Technical report)
- [3-26] Lienart, P., et al.: La Protection des Réseaux MT par un Relais Numérique à Base d'Algorithme de Distance. Résultats d'Essais en Laboratoire et de Mise en Exploitation sur un Réseau MT en Belgique; CIRED 1989, Conference manual pp. 144 -150
- [3-27] Marttila, R.J.: Directional characteristics of distance relay mho elements (Part I: A new method of analysis; Part II: Results); IEEE Transactions on Pow. App. and Syst., Vol. PAS-100, No. 1, 1981, pp. 96-113
- [3-28] Walter, M.: Der Selektivschutz nach dem Widerstandsprinzip; Verlag Von Oldenbourg, München Berlin, 1933 (in German) (Title: Protection according to the impedance principle)
- [3-29] Warrington, A.R. van C.: Protective Relays, Their Theory and Practice; Volume1; Chapman and Hall, London, 1962
- [3-30] Sebo, S.A.: Zero-sequence current distribution along transmission lines; IEEE Transactions on PAS, Vol. PAS-88, No. 6, June 1969, pp. 910-919
- [3-31] Gammelsaeter, H. und Nordboe, A.: Shield wire conductivity cuts fault effects; Electrical World, April 24, 1961, pp. 50-51

- [3-32] Blackburn, J. L.: Symmetrical Components for Power Systems Engineering; Marcel Dekker, Inc., New York, Basel, Hong Kong, 1993
- [3-33] Roeper, R.: Short-circuit currents in three-phase systems; Siemens AG, 1985
- [3-34] Kadner, G. und Wacarda, G.: Verhalten von Distanzrelais in starr geerdeten Hochspannungsnetzen; Mitteilungen des Instituts für Energetik, Heft 17, 1959, pp. 361-378 (in German); (Title: Behaviour of distance relays in effectively earthed power systems)
- [3-35] Wheeler, S.: Influence of mutual coupling between parallel circuits on the setting of distance protection; PROC. IEE, Vol. 117, No. 2, 1970, pp.439-445
- [3-36] Simon, R.: Netzbedingte Unschärfen des Distanzschutzes; Dissertation D386 der Universität Kaiserslautern (in German); (Title of the thesis: Power system conditioned inaccuracies of distance protection)
- [3-37] Adamson, C., Türeli, A.: Errors of sound-phase-compensation and residual-compensation systems in earth-fault distance relaying; PROC. IEE, Vol, 112, No. 7, 1965
- [3-38] Davison, E. B. and Wright, A.: Some factors affecting the accuracy of distance-type protective equipment under earth-fault conditions; Proc. IEE, Vol. 110, No. 9, 1963, pp. 1678-1688
- [3-39] Phadke, A.G. und LU Jiuang: A computer based integrated distance relay for parallel transmission lines; IEEE Transactions on Pow. App. and Syst., Vol 104, No. 1, 1985. pp. 445-452
- [3-40] Gilany, M.I., Malik O.P., Hope, G.S.: A digital technique for parallel transmission lines using a single relay at each end; Transactions on Power Delivery, Vol. 7, No. 1, 1992, pp. 118-125
- [3-41] Requa, R.: Die Grenzen der Anwendbarkeit des Distanzschutzprinzips; ETG Fachbericht 12: Selektivschutz, pp. 22-28; VDE-Verlag, Berlin, Offenbach, 1983 (in German); (Title: The application limits of distance protection)
- [3-42] Leitloff, V., Bourgeat, X., Duboc, G.: Setting constraints for distance protection on underground lines; 7<sup>th</sup> IEE DPSP Conference, Amsterdam, 2001, Conference Publication pp. 467-470
- [3-43] CIGRE Technical Brochure No. 64: Application Guide on Protection of Complex Transmission Network Configurations; CIGRE Office, Paris, 1992
- [3-44] Newbould, A.: Series compensated lines issues relevant to the application of distance protection; Canadian Electrical Association (CEA) Spring Meeting 1987
- [3-45] Elmore W., Anderson F.: Overview of Series-Compensated Line Protection Philosophies; 20<sup>th</sup> Annual Western Protective Relay Conference, Spokane, Washington, USA, Oct. 1990

- [4-1] System description SIPROTEC 4, Siemens PTD PA, 2003
- [4-2] [www.siprotec.com](http://www.siprotec.com)
- [4-3] Ziegler, G.: Protection and Substation Automation, State of the Art and Development Trends; ELECTRA No. 206, Febr. 2003, pp. 14-23
- [4-4] Brand, K.-P.: „The introduction of IEC 61850 and its impact on protection and automation within substations“, ELECTRA No. 233, Aug. 2007, pp. 21-29 and CIGRE Brochure No. 326, 2007
- [5-1] VDEW-Ringbuch Schutztechnik, Teil 2: Richtlinien für statische Schutzeinrichtungen, VDEW-Verlag, Frankfurt/M., 1987 (in German);  
(Title: Recommendations of the German Utility Board for static protection systems)
- [5-2] Davey, J.: Independent pole tripping: Key to system stability; Electrical Light and Power, T/D Edition, November 1979, pp. 81-83
- [5-3] Freygang, H.-J.: Meßwandler für den Selektivschutz; ETG Fachberichte 12: Selektivschutz, 1983, pp. 156-171 (in German)  
(Title: Instrument transformers for protection)
- [5-4] IEC 60044-1: Instrument transformers – Part 1: Current transformers; First edition 1996-12
- [5-5] IEEE /ANSI C.57.13 (1986): Standard Requirements for Instrument Transformers
- [5-6] IEEE Std C37.110-1996: IEEE Guide for the Application of Current Transformers Used for Protective Relaying Purposes.
- [5-7] Bruce, R.G. and Wright, A.: Remanent flux in current transformer cores; Proc. IEE, Vol. 113, No. 5, May 1966, S. 915 –920
- [5-8] Iwanusi, O.W.: Remanent flux in Current Transformers; Ontario Hydro Research Quarterly, 3<sup>rd</sup> quarter, 1970, pp. 18 to 21
- [5-9] Zahorka, R.: Das Verhalten von Stromwandlern bei Einschwingvorgängen mit Gleichstromgliedern unter Berücksichtigung der Sättigung; AEG-Mitteilungen 57 (1967), pp. 19-27 (in German)  
(Title: Transient CT performance considering asymmetrical currents and saturation)
- [5-10] Fischer, A. und Rosenberger, G.: Behaviour of current transformers with linear characteristics and closed magnetic circuits when subjected to asymmetrical short-circuit currents; Reprint from Elektrizitätswirtschaft (1968), Volume 12, pp. 310-315
- [5-11] IEC-60044-6: Instrument transformers – Part 6: Requirements for protective current transformers for transient performance; First edition 1992-03
- [5-12] Hodgkiss, J.W.: The behaviour of current transformers subjected to transient asymmetrical currents and the effects on associated protective relays; CIGRE Report No. 329, 1960

- [5-13] IEEE Committee Report: Transient Response of Current Transformers; IEEE Paper 76 CH 1130-4-PWR, 1976
- [5-14] G. Duboc et al: Old-time saturating current transformers and new digital distance protections. CIGRE SC34 Colloquium, Sibiu, Romania, 10-14 Sept. 2001, Report 302
- [5-15] Gertsch, G.A., Antolic, F. und Gyax, F.: Capacitor voltage transformers and protective relays; CIGRE Conference, Paris 1968, Report 31-14
- [5-16] Born, E.: Schneller Selektivschutz mit kapazitiven Spannungswandlern; ETZ-A, Bd. 86 (1965), pp 557-560 (in German); (Title: Fast system protection with CVTs)
- [5-17] Kezunovic, M., Frommen, C.W. and Nilsson, S.L.: Digital models of coupling capacitor voltage transformers for protective relay transient studies; IEEE Power System relaying Committee, Paper 92 WM 204-8 PWRD, 1992
- [5-18] Wiszniewski, A. and Izykowski, J.: Influence of ferroresonance suppression circuits upon the transient response of capacitive voltage transformers; IEE Conference, Publication No. 125, pp. 182-188
- [5-19] IEEE Relay Committee Report: Transient response of coupling capacitor voltage transformers; IEEE Transactions on Pow. App. and Syst., Vol. PAS-100, No. 12, 1981, pp. 4811-4814
- [5-20] Holbach, J. und Claus, M.: Zuverlässiger Distanzschutz auch bei gestörten Meßsignalen; Elektrizitätswirtschaft, Jg. 97 (1998), pp. 57-61 (in German); (Title: Reliable distance protection also with disturbed measuring signals)
- [5-21] Steynberg, G. and Kereit, M.: Analysis of numerical distance performance under extreme conditions; South African Conference on Power System Protection 2000
- [5-22] Salle, P.: Influence des régimes transitoires des TCT sur le fonctionnement des protections de distance; RGE (Revue Général d'Electricité), No. 4, April 1990, pp. 14-17
- [5-23] Kasztenny, B. et al: Distance relays and capacitive voltage transformers – Balancing speed and transient overreach, 55<sup>th</sup> Annual Georgia Tech Protective Relaying Conference, Atlanta, May, 2001
- [5-24] Ziegler, G.: Digitaler Schutz für Mittelspannungsnetze; Elektrizitätswirtschaft 95 (1996); pp. 120-124 (in German); (Title: Numerical protection of medium voltage systems)
- [5-25] Ziegler, G.: Protection of distributed generation, current practice; CIGRE Symposium in Neptun, Rumania, September 1997; Report No.
- [5-26] AIEE Committee Report: Protection of multiterminal and tapped lines; AIEE Transactions, Pt. III (Pow. App. and Syst.) Vol. 80, 1961, pp. 55-66
- [5-27] IEEE Relay Committee: Protection Aspects of Multi-Terminal Lines; IEEE Paper 79 TH0056-2-PWR, 1979

- [5-28] VDEW-Ringbuch Schutztechnik, Teil 11: Anregeprobleme beim Reserveschutz, VDEW-Verlag, Frankfurt/M.;, 1998 (in German);  
(Title: Fault detection problems with back-up protection)
- [5-29] Willheim, G. and Waters, M.: Neutral Grounding in High Voltage Transmission; Elsevier Publishing Company, New York, 1956
- [5-30] Ziegler, G.: Digitaler Schutz für Industrieanlagen; etz 1997, H. 18, pp. 30-35  
(in German);  
(Numerical protection of industrial plants)
- [5-31] Hadick, W.; Scharf, T.: A new static back-up protection for ehv systems using zero sequence quantities; IEE Conference on Developments in Power-System Protection, London 1980, Conference manual pp. 226 – 230
- [5-32] Humpage, W. D. and Lewis, D. W.: Distance protection of teed circuits; PROC. IEE, Vol. 114, No. 10, 1967, pp. 1483-1498
- [5-33] Corroyer, C. and Chorel, H.: Protection of multi-terminal EHV-links; CIGRE Conference, Paris 1982, Report 34-01
- [5-34] CIGRE Technical Brochure No. 64: Application Guide on Protection of Complex Transmission Network Configurations; CIGRE Office, Paris, 1992
  
- [6-1] Centralized and remote communication with Siemens protection relays (overview); Siemens AG, Protection Systems Catalog LSA 2.8.1, 1997
- [6-2] DIGSI Relay operating program 7XS5; Siemens AG, Protection Systems Catalog LSA 2.8.2
- [6-3] North American Electric Reliability Council: August 14, 203 Blackout: “NERC Actions to Prevent und Mitigate the Impacts of Future Cascading Blackouts”, February 10, 2004 (www.nerc.com)
- [6-4] Horowitz, S.H., Phadke, A.G.: Third Zone Revised; IEEE Trans. on Power Delivery, Vol. 21, No. 1, January 2006, pp. 23-29
- [6-5] Inglesfield, R.: Rationalised Policy for Application and Setting of Back-up Protection; 4<sup>th</sup> IEE DPSP Conference, Edinburgh, 1989, IEE Conference Publication No. 302, pp. 301-305
  
- [8-1] Portable test set 7VP15 (Omicron CMC156); Siemens AG, Protection Systems Catalog LSA 2.6.1
- [8-2] Omicron electronics GmbH: Literature: End-to-End test (www.omicron.at)
  
- [9-1] Prüfeempfehlungen für digitale Schutzeinrichtungen mit Selbstüberwachung. Herausgegeben vom VDEW-Arbeitsausschuß “Relais- und Schutztechnik”, April 1995  
(Test recommendations for numerical protection equipment, published by the German Utility Board)

## 10.2 Books

- [1] Herrmann, H.-J.: Digitale Schutztechnik; VDE-VERLAG, Berlin und Offenbach, 1997 (in German)  
(Book on numerical protection: Fundamental principles, software, implementation examples.)
- [2] Johns, A.T. and Salman, S.K.: Digital Protection for Power Systems; IEE Power Series 15, Peter Peregrins Ltd., 1995
- [3] Phadke, A.G. and Thorp, J.S.: Computer Relaying for Power Systems; Research Studies Press Ltd., London, 1995
- [4] Wright, A. and Christopoulos, C.: Electrical Power System Protection; Chapman & Hall, London, 1993
- [5] VWEV-Verlag: VDEW-Ringbuch Schutztechnik, 1988; (in German)  
Recommendations of the German Utility Board on system protection.
- [6] Clemens, H. und Rothe, K.: Schutz in Elektroenergiesystemen; Verlag Technik GmbH Berlin, 1991 (in German)  
(Book on protection of power systems)
- [7] Cook, V.: Analysis of Distance Protection; Research Studies Press Ltd. Letchworth, Hertfordshire, England, 1985
- [8] Blackburn, J. L.: Protective Relaying: Principles and Applications, Marcel Dekker, Inc., New York, Basel, Hong Kong, 1987
- [9] Blackburn, J. L.: Symmetrical Components for Power Systems Engineering; Marcel Dekker, Inc., New York, Basel, Hong Kong, 1993

### **Out of print books (history and fundamental principles):**

- [10] Roeper, R.: Short-circuit currents in three-phase systems; Siemens AG, 1985
- [11] Walter, M.: Der Selektivschutz nach dem Widerstandsprinzip, Verlag Von Oldenbourg, 1933 (in German)  
(Book on distance relaying)
- [12] Neugebauer, H.: Selektivschutz; Springer-Verlag Berlin/Göttingen/Heidelberg, 1958 (in German)  
(Book on protective relaying)
- [13] Erich, M.: Relaisbuch (VDEW); Franckh'sche Verlagshandlung, Stuttgart, 1959 (in German);  
Book on protective relaying, issued by the German utility board
- [14] Warrington, A.R.C.: Protective Relays. Their Theory and Practice Verlag Chapman and Hall, Band 1, London, 1962
- [15] Mason C.R.: The Art & Science of Protective Relaying, Verlag John Wiley & Sons, Inc. New York, London, Sydney, 1956 (sixth re-edition 1967)
- [16] Clarke, E.: Circuit Analysis of A-C Power Systems, Vols. I and II, General Electric Co., Schenectady, N.Y., 1943 und 1950



---

# 11 Appendix

## A.1 Distance measurement algorithms

### A.1.1 Principle

The fault loop is defined by the first order line differential equation:

$$u_L(t) = R_L \cdot i_L(t) + L_L \cdot \frac{di_L(t)}{dt} \quad (\text{A.1-1})$$

To determine the unknowns  $R_L$  and  $L_L$ , two equations are required. Theoretically they are arrived at by measuring  $u_L(t)$ ,  $i_L(t)$  and  $\frac{di_L(t)}{dt}$  at two successive instants in time and compiling the equations with these values:

$$u_L(t_1) = R_L \cdot i_L(t_1) + L_L \cdot \frac{di_L(t)}{dt} \quad (\text{A.1-2})$$

$$u_L(t_2) = R_L \cdot i_L(t_2) + L_L \cdot \frac{di_L(t_2)}{dt} \quad (\text{A.1-3})$$

By solving the set of equations, the following is obtained:

$$L_L = \frac{u_{L(1)} \cdot i_{L(2)} - u_{L(2)} \cdot i_{L(1)}}{\frac{di_{L(1)}}{dt} \cdot i_{L(2)} - \frac{di_{L(2)}}{dt} \cdot i_{L(1)}} \quad (\text{A.1-4})$$

$$R_L = \frac{u_{L(1)} \cdot \frac{di_{L(2)}}{dt} - u_{L(2)} \cdot \frac{di_{L(1)}}{dt}}{\frac{di_{L(1)}}{dt} \cdot i_{L(2)} - \frac{di_{L(2)}}{dt} \cdot i_{L(1)}} \quad (\text{A.1-5})$$

The grading plan and relay settings could be done in the usual manner with the reactance  $X_L = \omega_N \cdot L_L = 2\pi \cdot f_N \cdot L_L$ , where  $f_N$  is the nominal frequency of the power system.

In practice, transient oscillations and interference signals arise, which are not considered by the R-L replica of the line:

- line or cable charging oscillations due to the capacitance between phases and earth of cables or long lines

- subharmonic oscillation (series resonance) in the case of series compensated lines
- distortion of the measured values by the instrument transformers (e.g. due to saturation of the current transformers, or by transient oscillation in capacitive voltage transformers)

For this reason, filtering of the measured signals is required.

In the 7SA relays, digital FIR (finite impulse response) filters are employed for this purpose. The measurement is therefore not done with an instantaneous value from a single time instant, but by evaluation of  $n + 1$  samples in a time window with the length  $n \cdot \Delta t$ , where  $\Delta t = 1$  ms (based on 50 Hz) is the sampling interval for the measured value determination.

The initial data window after fault inception is kept short (5 ms in case of relay 7SA522) to achieve subcycle tripping times in case of close-in faults. It is then gradually increased as the fault continues with new samples up to the full length of one period to achieve high accuracy with faults near zone limits.

Fourier filtering techniques are used for this purpose. The distance measuring technique employed, evaluates the fundamental frequency components.

For the general principles of numerical protection technology, the technical literature is referred to [A1.1, A1.2, A1.3, A1.4].

### A.1.2 Fourier analysis based technique

The sampled currents and voltages are initially transformed into phasor quantities (respective real and imaginary components) by means of orthogonal filters and from this the short-circuit impedance R and X-values are calculated.

In this context, the principle is discussed using a Fourier-filter with full period integration length (data window of one period). The following equations produce the real and imaginary part of the fundamental component of the measuring quantity (current as an example).

$$\text{Re}\{\underline{I}\} = \frac{1}{T_N} \cdot \int_{-T_N/2}^{+T_N/2} i(t) \cdot \cos(\omega_N \cdot t) dt \quad (\text{A.1-6})$$

$$\text{Im}\{\underline{I}\} = \frac{1}{T_N} \cdot \int_{-T_N/2}^{+T_N/2} i(t) \cdot \sin(\omega_N \cdot t) dt, \quad (\text{A.1-7})$$

where  $\omega_N = 2\pi \cdot f_N$  is the fundamental angular velocity and  $T_N$  the fundamental period.

The complex value of the phasor is then:

$$\underline{I} = \text{Re}\{\underline{I}\} + j \text{Im}\{\underline{I}\}. \quad (\text{A.1-8})$$

The data window starts at  $t_A = -T_N/2$  and ends at  $t_E = +T_N/2$ .

If the instant of fault inception is designated by  $t_0$ , and the measured values are integrated over one period, the phasor quantity  $\underline{I}$  is consequently obtained at the instant  $t = t_0 + T_N/2$ .

The time instant  $t$  corresponds to the phase angle  $\varphi = \omega_N \cdot t$ .

In general terms, we get for the current phasor in polar notation:

$$\underline{I} = I \cdot e^{j(\omega_N \cdot t + \varphi_1)} = I \cdot [\cos(\omega_N \cdot t + \varphi_1) + j \sin(\omega_N \cdot t + \varphi_1)] \quad (\text{A.1-9})$$

Corresponding formulae are valid for voltages.

The calculation is repeated in defined time intervals, e.g. every quarter period (every 5 ms at  $f_N = 50$  Hz), so that updated phasor values and impedances are available at these instances.

For the differential equation of the short-circuit loop:

$$u_L(t) = R_L \cdot i_L(t) + L_L \cdot \frac{di_L(t)}{dt} \quad (\text{A.1-10})$$

a corresponding equation with phasor quantities in the frequency domain results:

$$\begin{aligned} \underline{U} &= R_L \cdot \underline{I}_L + j \cdot X_L \cdot \underline{I}_L \\ \text{with } X_L &= \omega_N \cdot L_L = 2\pi \cdot f_N \cdot L_L. \end{aligned} \quad (\text{A.1-11})$$

Only the fundamental frequency is evaluated. DC-components or superimposed harmonics are therefore filtered out.

Equation (A.1-11) in terms of real and imaginary components is:

$$\text{Re}\{\underline{U}_L\} + j\text{Im}\{\underline{U}_L\} = (R_L + jX_L) \cdot (\text{Re}\{\underline{I}_L\} + j\text{Im}\{\underline{I}_L\}). \quad (\text{A.1-12})$$

or

$$\begin{aligned} \text{Re}\{\underline{U}_L\} + j\text{Im}\{\underline{U}_L\} &= \\ &= R_L \cdot \text{Re}\{\underline{I}_L\} - X_L \cdot \text{Im}\{\underline{I}_L\} + j(X_L \cdot \text{Re}\{\underline{I}_L\} + R_L \cdot \text{Im}\{\underline{I}_L\}) \end{aligned}$$

The equation can now be separately solved for real and imaginary components:

$$\text{Re}\{\underline{U}_L\} = R_L \cdot \text{Re}\{\underline{I}_L\} - X_L \cdot \text{Im}\{\underline{I}_L\} \quad (\text{A.1-13})$$

$$\text{Im}\{\underline{U}_L\} = X_L \cdot \text{Re}\{\underline{I}_L\} + R_L \cdot \text{Im}\{\underline{I}_L\} \quad (\text{A.1-14})$$

Accordingly, two equations are available for the calculation of  $R_L$  and  $X_L$ .

The solution is:

$$X_L = \frac{\text{Im}\{\underline{U}_L\} \cdot \text{Re}\{\underline{I}_L\} - \text{Re}\{\underline{U}_L\} \cdot \text{Im}\{\underline{I}_L\}}{\text{Re}\{\underline{I}_L\}^2 + \text{Im}\{\underline{I}_L\}^2} \quad (\text{A.1-15})$$

and

$$R_L = \frac{\operatorname{Re}\{\underline{U}_L\} \cdot \operatorname{Re}\{\underline{I}_L\} + \operatorname{Im}\{\underline{U}_L\} \cdot \operatorname{Im}\{\underline{I}_L\}}{\operatorname{Re}\{\underline{I}_L\}^2 + \operatorname{Im}\{\underline{I}_L\}^2} \quad (\text{A.1-16})$$

The phasor quantities are defined as follows:

$$\underline{U}_L = U_L \cdot e^{j(\omega \cdot t + \varphi_U)} = U_L \cdot [\cos(\omega \cdot t + \varphi_U) + j \sin(\omega \cdot t + \varphi_U)] \quad (\text{A.1-17})$$

$$\underline{I}_L = I_L \cdot e^{j(\omega \cdot t + \varphi_I)} = I_L \cdot [\cos(\omega \cdot t + \varphi_I) + j \sin(\omega \cdot t + \varphi_I)] \quad (\text{A.1-18})$$

If the values of (A.1-17) and (A.1-18) are inserted in (A.1-15), the result is:

$$\begin{aligned} X_L = & \frac{U_L \cdot \sin(\omega \cdot t + \varphi_U) \cdot I_L \cdot \cos(\omega \cdot t + \varphi_I)}{[I_L \cdot \cos(\omega \cdot t + \varphi_I)]^2 + [I_L \cdot \sin(\omega \cdot t + \varphi_I)]^2} - \\ & - \frac{U_L \cdot \cos(\omega \cdot t + \varphi_U) \cdot I_L \cdot \sin(\omega \cdot t + \varphi_I)}{[I_L \cdot \cos(\omega \cdot t + \varphi_I)]^2 + [I_L \cdot \sin(\omega \cdot t + \varphi_I)]^2} \end{aligned} \quad (\text{A.1-19})$$

By applying the sum and difference trigonometric functions, the following is obtained:

$$X_L = \frac{U_L \cdot \sin(\varphi_U - \varphi_I)}{I_L} \quad (\text{A.1-20})$$

In the same manner, the following is obtained from (A.1-16):

$$R_L = \frac{U_L \cdot \cos(\varphi_U - \varphi_I)}{I_L} \quad (\text{A.1-21})$$

We can now apply this measuring method to the real fault loops:

*Phase-to-earth measuring loop:*

For the phase-to-earth fault loop the following equation applies:

$$\underline{U}_{\text{ph-E}} = \underline{I}_{\text{ph-E}} \cdot R_L + j \underline{I}_{\text{ph}} \cdot X_L - \underline{I}_E \cdot \frac{R_E}{R_L} \cdot R_L - j \underline{I}_E \cdot \frac{X_E}{X_L} \cdot X_L \quad (\text{A.1-22})$$

We introduce the composed currents:

$$\underline{I}_R = \underline{I}_{\text{ph}} - \frac{R_E}{R_L} \cdot \underline{I}_E \quad \text{and} \quad \underline{I}_X = \underline{I}_{\text{ph}} - \frac{X_E}{X_L} \cdot \underline{I}_E \quad (\text{A.1-23})$$

where  $R_E/R_L = k_{RE}$  and  $X_E/X_L = k_{XE}$  correspond to the earth current compensation factors to be set in the relay.

Segregation of (A.1-22) into real and imaginary parts results in two equations for the unknowns  $R_L$  and  $X_L$ :

$$\operatorname{Re}\{\underline{U}_{\text{ph-E}}\} = \operatorname{Re}\{\underline{I}_R\} \cdot R_L - \operatorname{Im}\{\underline{I}_X\} \cdot X_L \quad (\text{A.1-24})$$

and

$$\operatorname{Im}\{\underline{U}_{\text{ph-E}}\} = \operatorname{Im}\{\underline{I}_R\} \cdot R_L + \operatorname{Re}\{\underline{I}_X\} \cdot X_L \quad (\text{A.1-25})$$

The solutions are:

$$R_{\text{ph-E}} = \frac{\operatorname{Re}\{\underline{U}_{\text{ph-E}}\} \cdot \operatorname{Re}\{\underline{I}_X\} + \operatorname{Im}\{\underline{U}_{\text{ph-E}}\} \cdot \operatorname{Im}\{\underline{I}_X\}}{\operatorname{Re}\{\underline{I}_R\} \cdot \operatorname{Re}\{\underline{I}_X\} + \operatorname{Im}\{\underline{I}_R\} \cdot \operatorname{Im}\{\underline{I}_X\}} \quad (\text{A.1-26})$$

and

$$X_{\text{ph-E}} = \frac{\operatorname{Im}\{\underline{U}_{\text{ph-E}}\} \cdot \operatorname{Re}\{\underline{I}_R\} - \operatorname{Re}\{\underline{U}_{\text{ph-E}}\} \cdot \operatorname{Im}\{\underline{I}_R\}}{\operatorname{Re}\{\underline{I}_R\} \cdot \operatorname{Re}\{\underline{I}_X\} + \operatorname{Im}\{\underline{I}_R\} \cdot \operatorname{Im}\{\underline{I}_X\}} \quad (\text{A.1-27})$$

Fault voltage and current phasors have in this case the following shape:

$$\underline{U}_{\text{ph-E}} = U_{\text{ph-E}} \cdot e^{j\varphi_U} = U_{\text{ph-E}} \cdot (\sin \varphi_U + j \cos \varphi_U) \quad (\text{A.1-28})$$

$$\underline{I}_L = I_L \cdot e^{j\varphi_L} = I_L \cdot (\sin \varphi_L + j \cos \varphi_L) \quad (\text{A.1-29})$$

$$\underline{I}_E = I_E \cdot e^{j\varphi_E} = I_E \cdot (\sin \varphi_E + j \cos \varphi_E) \quad (\text{A.1-30})$$

With (A.1-22), (A.1-23), (A.1-26) and (A.1-27), and some trigonometric transformations, we finally arrive at the following formulae for the measured fault resistance and reactance:

$$R_{\text{ph-E}} = \frac{U_{\text{ph-E}}}{I_L} \cdot \frac{\cos(\varphi_U - \varphi_L) - \frac{I_E}{I_L} \cdot k_{\text{EX}} \cdot \cos(\varphi_U - \varphi_E)}{1 - \left( \frac{I_E}{I_L} \cdot k_{\text{EX}} + \frac{I_E}{I_L} \cdot k_{\text{ER}} \right) \cos(\varphi_E - \varphi_L) + \frac{R_E}{R_L} \cdot \frac{X_E}{X_L} \cdot \left( \frac{I_E}{I_L} \right)^2} \quad (\text{A.1-31})$$

$$X_{\text{ph-E}} = \frac{U_{\text{ph-E}}}{I_L} \cdot \frac{\cos(\varphi_U - \varphi_L) - \frac{I_E}{I_L} \cdot k_{\text{ER}} \cdot \sin(\varphi_U - \varphi_E)}{1 - \left( \frac{I_E}{I_L} \cdot k_{\text{EX}} + \frac{I_E}{I_L} \cdot k_{\text{ER}} \right) \cos(\varphi_E - \varphi_L) + \frac{R_E}{R_L} \cdot \frac{X_E}{X_L} \cdot \left( \frac{I_E}{I_L} \right)^2} \quad (\text{A.1-32})$$

### Compensation of the parallel line zero-sequence coupling

The influence of this effect on distance measurement and the basic principle of its compensation is discussed in paragraph 3.5.3.

The parallel line earth current  $I_{EP}$  must in this case be added to the relay measuring current with a weighting factor considering the zero-sequence mutual impedance. The composed current of (A.27) is then extended by a corresponding compensation term:

$$\underline{I}_R = \underline{I}_L - \frac{R_E}{R_L} \cdot \underline{I}_E - \frac{R_{OM}/3}{R_L} \cdot \underline{I}_{EP} = \underline{I}_L - k_{ER} \cdot \underline{I}_E - k_{EPR} \cdot \underline{I}_{EP} \quad (\text{A.1-33})$$

and

$$\underline{I}_X = \underline{I}_L - \frac{X_E}{X_L} \cdot \underline{I}_E - \frac{X_{OM}/3}{X_L} \cdot \underline{I}_{EP} = \underline{I}_L - k_{EX} \cdot \underline{I}_E - k_{EPX} \cdot \underline{I}_{EP} \quad (\text{A.1-34})$$

Using again (A.1-26) and (A.1-27), we can calculate the impedance, this time with compensation of the mutual coupling.

The voltage and current phasors (A.1-28) to (A.1-30) are completed by the additional phasor for the parallel line earth current:

$$\underline{I}_{EP} = I_{EP} \cdot e^{j\varphi_{EP}} = I_{EP} \cdot (\sin \varphi_{EP} + j \cos \varphi_{EP}) \quad (\text{A.1-35})$$

Herewith, we get the trigonometric form of (A.1-26) and (A.1-27) for impedance calculation with compensation of mutual coupling:

$$R_{ph-E} = \frac{U_{ph-E}}{I_L} \cdot \left[ \frac{\cos(\varphi_U - \varphi_L) - k_{EX} \cdot \frac{I_E}{I_L} \cdot \cos(\varphi_U - \varphi_E) - k_{EPX} \cdot \frac{I_{EP}}{I_L} \cdot \cos(\varphi_U - \varphi_{EP})}{DN} \right] \quad (\text{A.1-36})$$

$$X_{ph-E} = \frac{U_{ph-E}}{I_L} \cdot \left[ \frac{\cos(\varphi_U - \varphi_L) - k_{ER} \cdot \frac{I_E}{I_L} \cdot \cos(\varphi_U - \varphi_E) - k_{EPR} \cdot \frac{I_{EP}}{I_L} \cdot \cos(\varphi_U - \varphi_{EP})}{DN} \right] \quad (\text{A.1-37})$$

with the denominator

$$\begin{aligned} DN = & 1 - (k_{EX} - k_{ER}) \cdot \frac{I_E}{I_L} \cdot \cos(\varphi_E - \varphi_L) - (k_{EPX} - k_{EPR}) \cdot \frac{I_{EP}}{I_L} \cdot \cos(\varphi_{EP} - \varphi_L) + \\ & + (k_{ER} \cdot k_{EPX} - k_{EX} \cdot k_{EPR}) \cdot \frac{I_E}{I_L} \cdot \frac{I_{EP}}{I_L} \cdot \cos(\varphi_E - \varphi_{EP}) + \\ & + k_{ER} \cdot k_{EX} \cdot \left(\frac{I_E}{I_L}\right)^2 + k_{EPR} \cdot k_{EPX} \cdot \left(\frac{I_{EP}}{I_L}\right)^2 \end{aligned}$$

*Phase-to-phase measuring loop:*

We take the L2-L3 fault as an example.

In this case, the loop equation is:

$$\underline{U}_{L2} - \underline{U}_{L3} = \underline{I}_{L2} \cdot R_L + j\underline{I}_{L2} \cdot X_L - \underline{I}_{L3} \cdot R_L - j\underline{I}_{L3} \cdot X_L \quad (\text{A.1-38})$$

We introduce the composed quantities:

$$\underline{U}_{L2-L3} = (\underline{U}_{L2} - \underline{U}_{L3}) \quad \text{and} \quad \underline{I}_{L2-L3} = \underline{I}_{L2} - \underline{I}_{L3} \quad (\text{A.1-39})$$

Segregation of (A.1-31) into real and imaginary parts results in:

$$\text{Re}\{\underline{U}_{L2-L3}\} = \text{Re}\{\underline{I}_{L2-L3}\} \cdot R_L - \text{Im}\{\underline{I}_{L2-L3}\} \cdot X_L \quad (\text{A.1-40})$$

and

$$\text{Im}\{\underline{U}_{L2-L3}\} = \text{Im}\{\underline{I}_{L2-L3}\} \cdot R_L + \text{Re}\{\underline{I}_{L2-L3}\} \cdot X_L \quad (\text{A.1-41})$$

The solution is here:

$$R_{L2-L3} = \frac{\text{Re}\{\underline{U}_{L2-L3}\} \cdot \text{Re}\{\underline{I}_{L2-L3}\} + \text{Im}\{\underline{U}_{L2-L3}\} \cdot \text{Im}\{\underline{I}_{L2-L3}\}}{[\text{Re}\{\underline{I}_{L2-L3}\}]^2 + [\text{Im}\{\underline{I}_{L2-L3}\}]^2} \quad (\text{A.1-42})$$

and

$$X_{L2-L3} = \frac{\text{Im}\{\underline{U}_{L2-L3}\} \cdot \text{Re}\{\underline{I}_{L2-L3}\} - \text{Re}\{\underline{U}_{L2-L3}\} \cdot \text{Im}\{\underline{I}_{L2-L3}\}}{[\text{Re}\{\underline{I}_{L2-L3}\}]^2 + [\text{Im}\{\underline{I}_{L2-L3}\}]^2} \quad (\text{A.1-43})$$

Insertion of the voltage and current phasor quantities results in the corresponding formulae for the impedance calculation of phase-to-phase faults:

$$R_{L2-L3} = \frac{\underline{U}_{L2-L3} \cdot [\underline{I}_{L2} \cdot \cos(\varphi_{UL2-L3} - \varphi_{IL2}) - \underline{I}_{L3} \cdot \cos(\varphi_{UL2-L3} - \varphi_{IL3})]}{I_{L2}^2 - 2 \cdot I_{L2} \cdot I_{L3} \cdot \cos(\varphi_{IL2} - \varphi_{IL3}) + I_{L3}^2} \quad (\text{A.1-44})$$

$$X_{L2-L3} = \frac{\underline{U}_{L2-L3} \cdot [\underline{I}_{L2} \cdot \sin(\varphi_{UL2-L3} - \varphi_{IL2}) - \underline{I}_{L3} \cdot \sin(\varphi_{UL2-L3} - \varphi_{IL3})]}{I_{L2}^2 - 2 \cdot I_{L2} \cdot I_{L3} \cdot \cos(\varphi_{IL2} - \varphi_{IL3}) + I_{L3}^2} \quad (\text{A.1-45})$$

This result is further discussed in paragraph 3.2.3.

### A.1.3 Transient behaviour

The equations derived above apply to the steady state condition.

To evaluate the transient behaviour, the complete numerical measuring algorithm must be modelled and subjected to the digitised measured values. Siemens utilises a simulation software which provides an accurate and realistic replica of the relay behaviour.

The fault transient (short circuit history) must be provided in the form of a digitised data file. It may be the result of a transient simulation (EMTP, NETOMAC), or of a recorded disturbance. The recording format should in any event be COMTRADE<sup>1</sup>.

#### A.1.4 Practical application

Relays of the Siemens 7SA series use a sampling interval of  $18^{\text{Oel}}$  for impedance calculation corresponding to 20 sampled values per period. The sampling rate is therefore 1000 Hz (1200 Hz) at 50 Hz (60 Hz) nominal system frequency. The actual sampling rate can be higher (over-sampling) allowing a degree of pre-filtering.

The Fast Fourier Transform (FFT) method is used for processing the discrete instantaneous values derived from the A/D conversion.

The full cycle Fourier analysis described above, applies to the steady state fault condition. During the transfer from load to short-circuit condition, shorter data windows with correspondingly modified filter characteristics are automatically applied to achieve short operating times. In the case of sinusoidal signals, there is no loss of accuracy as in this case the Fourier integrals also apply for shorter data windows when a corresponding correction factor is each applied. The efficiency of the filters in respect of superimposed interferences is however reduced. Accordingly, the zone reach is reduced when shorter data windows are used shortly after fault inception. (Special impedance estimation methods used for short data windows below one half period are beyond the scope of this book and are not treated here.)

The Fourier analysis based impedance calculation method is also applied with distance to fault calculation (integrated fault locator function in 7SA relays). In this case, however, a data window of more than one period is generally available and the fault impedance can be estimated more accurately out of a number of calculated values using error correction (averaging) methods.

Formulae (A.1-26) and (A.1-27) or (A.1-31) and (A.1-32) can further be used to calculate impedances off-line with data from fault records or short-circuit calculations. The phasor quantities are in general provided by the corresponding programs.

For example, the SIGRA fault analysis program also uses them. The data window for impedance calculation has in this case a length of one period and can be shifted by cursor to any time instant of the oscillographic fault record.

Also, the locus of measured impedances from pre-fault load to fault clearance can be displayed in the impedance plane. The loop impedances are in this case calculated at one ms time intervals with a data window of one period. This provides a very valuable tool for fault analysis and judging of the distance relay behaviour.

---

<sup>1</sup> IEEE standard "Common Format for Transient Data Exchange (COMTRADE) for power systems".



*Hint:*

The traditional impedance calculation method uses the following formulae for resistance and reactance calculation of the phase-to-earth loops:

$$\underline{Z}_{\text{ph-E}} = \frac{\underline{U}_{\text{ph-E}}}{\underline{I}_{\text{ph-E}} - k_0 \cdot \underline{I}_E}$$

$$R_{\text{ph-E}} = \text{Re}\{\underline{Z}_{\text{ph-E}}\}$$

and

$$X_{\text{ph-E}} = \text{Im}\{\underline{Z}_{\text{ph-E}}\}$$

These formulae produce the same results as the above presented calculation method with formulae (A.1-26) and (A.1-27) respectively (A.1-31 and A.1-32) only for the true fault loop (faulty line) with a dead fault ( $R_F = 0$ ).

The fault resistance has different influence on both calculation methods and leads to dissimilar results as shown in paragraph 3.5.1. The difference is small with OH-lines where the angles of positive sequence impedance  $\underline{Z}_L$  and zero sequence impedance  $\underline{Z}_{L0}$  are not too far away. But with cables larger differences may appear because the angle of  $\underline{Z}_{L0}$  can be rather low compared to that of  $\underline{Z}_L$ .

In particular relays on healthy lines, which do not measure in a true fault loop, but get a mixture of fault and load currents, would show larger differences depending on the used calculation method.

The impedance calculation of phase-to-phase loops produces the same values with both calculation methods, see paragraph 3.2.3.

### A.1.5 Literature

- [A1.1] Herrmann, H.-J.: Digitale Schutztechnik (Grundlagen, Software, Ausführungsbeispiele); VDE-VERLAG, Berlin und Offenbach, 1997
- [A1.2] IEEE Tutorial Course: Computer Relaying; Course Text 79 EH0148-7-PWR
- [A1.3] Phadke, A.G. and Thorp, J.S.: Computer Relaying for Power Systems; John Wiley & Sons Inc. New York - Chichester - Toronto - Brisbane - Singapore Research Studies Press Ltd. Taunton, Somerset, England
- [A1.4] Johns, A.T. and Salman S.K.: Digital Protection for Power Systems; IEE Power Series 15, 1995

## A.2 Calculation with phasors and complex quantities

In the protection practice, and also in this book, phasors (vectors) and complex quantities are generally used with fault and relay performance analysis. The notation can either be in polar coordinates with magnitude (r.m.s. value) and angle or in the complex number area (Cartesian coordinates) with real and imaginary part. Often it is necessary to change from the one into the other notation.

In the following, the basic calculation rules are presented.

### A.2.1 Definitions

The sinusoidal course of a.c. quantities (currents and voltages) corresponds to a turning phasor which is defined as follows:

$$\underline{A}(\omega t) = A \cdot e^{j(\omega t + \varphi)} = A \cdot [\cos(\omega t + \varphi) + j \sin(\omega t + \varphi)]$$

where:

$\underline{A}$	Phasor (vector)
$\omega$	Circular frequency $\omega = 2\pi f$
$A$	Amplitude
$j$	Phase angle at the time instant $t = 0$

As all phasors of fundamental frequency (50/60 Hz quantities) turn with the same speed, and because only the relation between the phasors is of interest, we can dispense with the time dependence and calculate with steady state phasors.

Herewith, we get the definition of the phasor as used in the relaying practice:

$$\underline{A}(\omega t) = A \cdot e^{j\varphi} = A \cdot [\cos \varphi + j \sin \varphi]$$

where:

$\underline{A}$	Phasor (vector)
$A$	Amplitude as r.m.s. value
$j$	Phase angle against a common reference axis

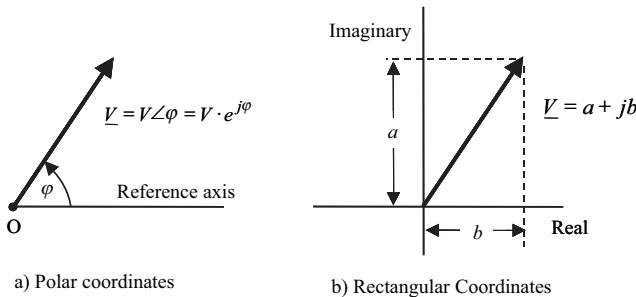


**Figure A.2-1** Phasor coordinates

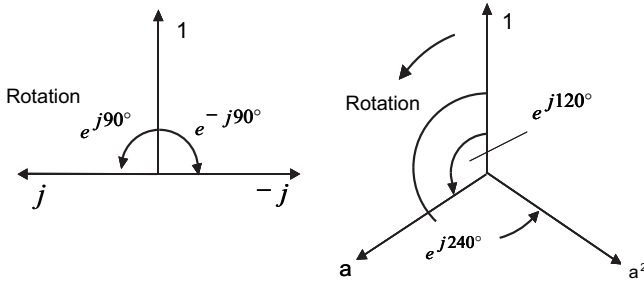


**Figure A.2-2** Familiar operators

*Operators* are phasors of unit magnitude. An operator is used to rotate a phasor by an angle without changing its magnitude.

Two special operators are frequently used:

#### *Operator $j$*

It rotates the phasor to which it is attached by  $90^\circ$ :

$$j = 1 \angle 90^\circ = 1 \cdot e^{j90^\circ} = 0 + j = j$$

$$j^2 = 1 \angle 180^\circ = 1 \cdot e^{j180^\circ} = -1 + j0 = -1$$

#### *Operator $a$*

It rotates the phasor by  $120^\circ$  or in power by a multiple of it.

This operator is used with three-phase systems and with symmetrical components.

$$a = 1 \angle 120^\circ = 1 \cdot e^{j120^\circ} = -0,500 + j\frac{\sqrt{3}}{2} = -0,500 + j0.866$$

$$a^2 = 1 \angle 240^\circ = 1 \cdot e^{j240^\circ} = -0,500 - j\frac{\sqrt{3}}{2} = -0,500 - j0.866$$

### **A.2.2 Calculation with phasors and complex quantities**

*Addition of phasors:*

$$\begin{aligned} \underline{A} + \underline{B} &= A \cdot e^{j\alpha} + B \cdot e^{j\beta} = A \cdot (\cos \alpha + j \sin \alpha) + B \cdot (\cos \beta + j \sin \beta) \\ &= A \cdot \cos \alpha + B \cdot \cos \beta + j(A \cdot \sin \alpha + B \cdot \sin \beta) \end{aligned}$$

*Subtraction of phasors:*

$$\begin{aligned}\underline{A} - \underline{B} &= A \cdot e^{j\alpha} - B \cdot e^{j\beta} = A \cdot (\cos \alpha + j \sin \alpha) - (B \cdot (\cos \beta + j \sin \beta)) \\ &= A \cdot \cos \alpha - B \cdot \cos \beta + j(A \cdot \sin \alpha - B \cdot \sin \beta)\end{aligned}$$

*Multiplication of phasors:*

$$\underline{A} \cdot \underline{B} = A \cdot e^{j\alpha} \cdot B \cdot e^{j\beta} = A \cdot B \cdot e^{j(\alpha+\beta)}$$

*Division of phasors:*

$$\frac{\underline{A}}{\underline{B}} = \frac{A \cdot e^{j\alpha}}{B \cdot e^{j\beta}} = \frac{A}{B} \cdot e^{j(\alpha-\beta)}$$

*Transition from polar to complex notation:*

$$\underline{A} = A \cdot e^{j\varphi} = A \cdot [\cos \varphi + j \sin \varphi] = X + jY$$

Herewith:

$$X = A \cdot \cos \varphi, \quad Y = A \cdot \sin \varphi, \quad \underline{Z} = X + jY$$

*Transition from complex to polar notation:*

$$\underline{Z} = X + jY = A \cdot [\cos \varphi + j \sin \varphi] = A \cdot e^{j\varphi}$$

$$A \cdot \cos \varphi = X, \quad A \cdot \sin \varphi = Y$$

We consider that  $\cos^2 \varphi + \sin^2 \varphi = 1$ , and get:

$$A = \sqrt{X^2 + Y^2}$$

$$\tan \varphi = \frac{Y}{X}, \text{ and herewith } \varphi = \pm \arctan \frac{|Y|}{|X|} \pm 180^\circ$$

The transformation through  $\arctan$  alone is not unambiguous. The sign (+ or -) depends on the quadrant in which the complex quantity  $\underline{Z}$  is located.

Real part	Imaginary part	$\tan \varphi$	Quadrant	Angle range	Calculation rule
+	+	+	I	$0^\circ$ to $+90^\circ$	$+\arctan \frac{ Y }{ X }$
+	-	-	IV	$-90^\circ$ to $0^\circ$	$-\arctan \frac{ Y }{ X }$
-	-	+	III	$-90^\circ$ to $-180^\circ$	$+\arctan \frac{ Y }{ X } - 180^\circ$
-	+	-	II	$+90^\circ$ to $+180^\circ$	$-\arctan \frac{ Y }{ X } + 180^\circ$

*Addition und subtraction of complex quantities*

$$\underline{Z}_1 = X_1 + jY_1, \quad \underline{Z}_2 = X_2 + jY_2$$

$$\underline{Z}_1 + \underline{Z}_2 = X_1 + X_2 + j(Y_1 + Y_2) \quad \text{and} \quad \underline{Z}_1 - \underline{Z}_2 = X_1 - X_2 + j(Y_1 - Y_2)$$

*Multiplication of complex quantities*

We consider that  $j^2 = -1$ , and get:

$$\underline{Z}_1 \cdot \underline{Z}_2 = (X_1 + jY_1) \cdot (X_2 + jY_2) = X_1 \cdot X_2 - Y_1 \cdot Y_2 + j(X_1 \cdot Y_2 + X_2 \cdot Y_1)$$

*Division of complex quantities*

$$\frac{\underline{Z}_1}{\underline{Z}_2} = \frac{X_1 + jY_1}{X_2 + jY_2}$$

We extend the denominator so that it gets real. To achieve this, we consider that  $(a + b) \cdot (a - b) = a^2 - b^2$ :

$$\frac{\underline{Z}_1}{\underline{Z}_2} = \frac{(X_1 + jY_1) \cdot (X_2 - jY_2)}{(X_2 + jY_2) \cdot (X_2 - jY_2)} = \frac{X_1 \cdot X_2 + Y_1 \cdot Y_2}{X_2^2 + Y_2^2} + j \frac{X_2 \cdot Y_1 - X_1 \cdot Y_2}{X_2^2 + Y_2^2}$$

*Example: Calculation of the  $k_0$ -faktor*

Given:

110-kV-Oil cable  $3 \times 185 \text{ mm}^2$  Cu with the following data:

Positive-sequence impedance:  $\underline{Z}_1 = 0.408 \cdot e^{j73^\circ} \Omega/\text{km}$

Negative-sequence impedance:  $\underline{Z}_0 = 0.632 \cdot e^{j18.4^\circ} \Omega/\text{km}$

Searched:

Setting value of the residual compensation factor  $\underline{k}_0$ .

Solution:

$$\frac{\underline{Z}_0}{\underline{Z}_1} = \frac{0.632}{0.408} \cdot e^{j(18.4^\circ - 73^\circ)} = 1.55 \cdot e^{j54.6^\circ}$$

We change over to the corresponding complex value:

$$\frac{\underline{Z}_0}{\underline{Z}_1} = 1.55 \cdot (\cos 54.6^\circ - j \sin 54.6^\circ) = 0.898 - j1.236$$

We calculate the complex value of  $\underline{k}_0$ :

$$\begin{aligned} \underline{k}_0 &= \frac{1}{3} \cdot \left( \frac{\underline{Z}_0}{\underline{Z}_1} - 1 \right) = \frac{1}{3} \cdot [(0.898 - j1.236) - 1] = \frac{1}{3} \cdot (-0.102 - j1.236) \\ &= -0.034 - j0.412 \end{aligned}$$

As the  $\underline{k}_0$  factor is set as phasor value with magnitude and angle, we convert to this notation:

$$k_0 = |\underline{k}_0| = \sqrt{0.034^2 + 0.421^2} = 0.42$$

The complex quantity  $k_0$  is located in the 4th quadrant, therefore

$$\varphi_{k_0} = \arctan\left(\frac{|-0.421|}{|-0.034|}\right) - 180^\circ = -94.6^\circ$$

### A.3 Fundamentals of symmetrical component analysis

Symmetrical components are extensively used in the relaying practice for the analysis of faults and the study of relay performance.

In the following, a short introduction is given to the principles and application of symmetrical components as a reference and for better understanding of the protection examples calculated in this book.

For a more detailed information and study of this subject the reader is referred to the relevant literature (see chapter 10.2, bibliography, reference [9])

#### A.3.1 Calculation procedure

The transformation of a non-symmetrical three-phase system into three symmetrical component systems simplifies the calculation of non-symmetric load or fault cases considerably.

The positive, negative and zero-sequence systems are each three phase. In all three systems, the phasors rotate anti-clockwise, however have different phase sequence and phase displacement. In the positive sequence system, the phasors of the phase voltages and currents are displaced  $120^\circ$  and the phase sequence is a, b, c (L1, L2, L3). This condition corresponds to the symmetrical load or three-phase fault situation. In the negative sequence system, the phase displacement is also  $120^\circ$  but the phase sequence is inverted to a, c, b (L1, L3, L2). The negative sequence system ( $U_2$ ,  $I_2$ ) represents unsymmetrical load and occurs with non-symmetrical faults. In the zero-sequence system ( $U_0$ ,  $I_0$ ), the phase displacement is  $0^\circ$ , which means that the phase quantities are always in phase. The sum of the zero-sequence currents of the three phases corresponds to the earth current, the sum of the zero-sequence voltages to the displacement of the system neutral point.

Figure A.3-1 shows as an example the composition of an unsymmetrical three-phase voltage by symmetrical components.

The sequence quantities corresponding to a given three-phase unbalanced set of phase voltages and currents can be determined from the following fundamental equations:

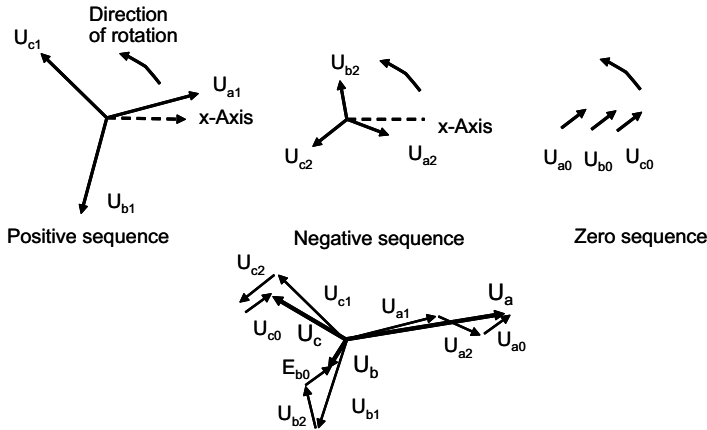


**Figure A.3-1** Phase quantities and their equivalent symmetrical components

Equations of analysis:

$$\begin{aligned}
 U_1 &= 1/3 \cdot (U_a + a \cdot U_b + a^2 \cdot U_c) & I_1 &= 1/3 \cdot (I_a + a \cdot I_b + a^2 \cdot I_c) \\
 U_2 &= 1/3 \cdot (U_a + a^2 \cdot U_b + a \cdot U_c) & I_2 &= 1/3 \cdot (I_a + a^2 \cdot I_b + a \cdot I_c) \\
 U_0 &= 1/3 \cdot (U_a + U_b + U_c) & I_0 &= 1/3 \cdot (I_a + I_b + I_c)
 \end{aligned} \tag{A.3-1}$$

The other way round, the phase voltages and currents corresponding to a given set of sequence component quantities can be determined from the following equations:

Equations of synthesis:

Phase voltages	Phase currents
$U_a = U_1 + U_2 + U_0$	$I_a = I_1 + I_2 + I_0$
$U_b = a^2 \cdot U_1 + a \cdot U_2 + U_0$	$I_b = a^2 \cdot I_1 + a \cdot I_2 + I_0$
$U_c = a \cdot U_1 + a^2 \cdot U_2 + U_0$	$I_c = a \cdot I_1 + a^2 \cdot I_2 + I_0$

(A.3-2)

### Study Procedure

Generally, a short-circuit study would start from a single line diagram of the network part to be considered with the given network data, kind and location fault. The sequence circuits would then be designed accordingly.

Typical system component impedances are given in section A.3. They can be used for estimates when exact data are not available.

The circuits and formulas of the following section A3.2 can be applied to reduce the sequence networks.

The connection of the circuits at the fault point would have to be chosen according to the kind of fault (figure A.3-2).

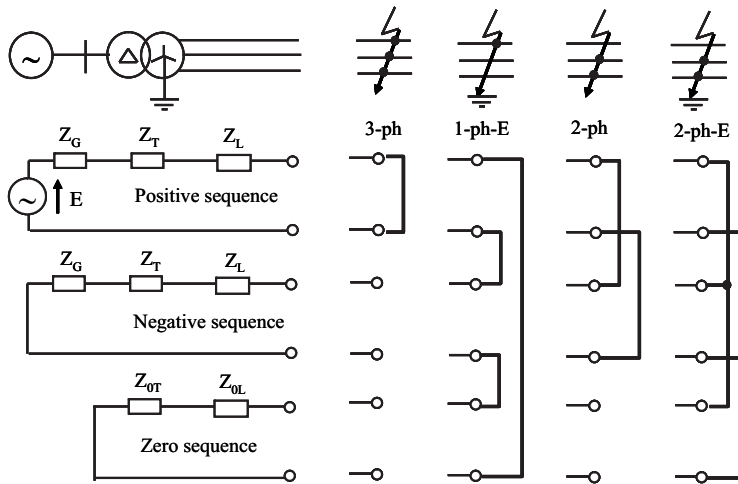


**Figure A.3-2** Connection of the sequence circuits at the fault point

The kind of connections can be derived from the fundamental set of equations (A.3-1) with the fault conditions at the fault point. For example, the Phase a to earth fault is characterised by  $U_{aF} = 0$  and  $I_{bF} = I_{cF} = 0$ , which leads to  $U_{1F} + U_{2F} + U_{0F} = 0$  and  $I_{1F} = I_{2F} = I_{0F}$ . These conditions can only be fulfilled with the shown series connection of the sequence circuits.

The connections shown in Figure A.3-2 are each only valid for a single phase fault a-E (L1-E) and the phase to phase faults a-b (L2-L3) and a-b-E (L2-L3-E) respectively.

For the sake of simplicity, these fault types are generally chosen for calculations, because only in these cases the sequence circuits can be directly connected. Faults between other phases would require phase shifting connections.

With resistance faults, the fault resistances have to be considered in the connection of the sequence circuits. This is shown in Figure A.3-3.

The circuits of the positive and negative system correspond the single-phase equivalent circuit of the usual three-phase system with the generally known short-circuit data. The negative sequence impedances of revolving machines (generators and motors) deviate from the positive sequence values, however, this difference may be neglected in case of network faults.

The zero sequence system needs special consideration:

- The zero sequence impedances deviate partly considerably from the normal positive values, see typical data in section A.3-2.
- Earthed transformer neutrals correspond to a shunt connection with the corresponding zero-sequence impedance of the transformer. At the delta winding side the zero sequence circuit is interrupted (open), that means that it ends at such locations.
- Neutral earthing impedances appear with 3 times their value
- Coupling of zero-sequence circuits of parallel lines must be considered



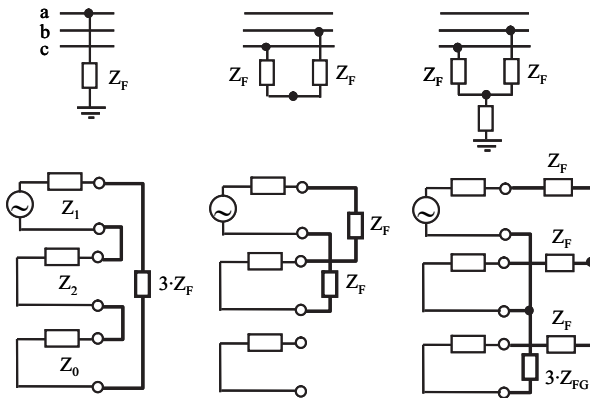


**Figure A.3-3** Connection of sequence networks with fault resistances

Once the equivalent sequence component networks and the connections at the fault point have been completed, the sequence current and voltages can be calculated.

The corresponding phase currents and voltages of the real three-phase system can then be determined by using the synthesis equation sets (A.3-2).

#### *Calculation example: Ph-E line fault*

*Given:*

System configuration according to Figure A.3-4.

System Data:

Infeeding network: 100 kV,  $SCC'' = 1000$  MVA

Transformer: 100/20 kV,  $S_T = 10$  MVA,  $u_K = 10\%$ ,  $X_{0T}/X_{1T} = 0.9$

Line: 20 kV,  $l = 3$  km,  $x_{L1} = 0.4 \Omega/\text{km}$ ,  $x_{0L} = 1.2 \Omega/\text{km}$

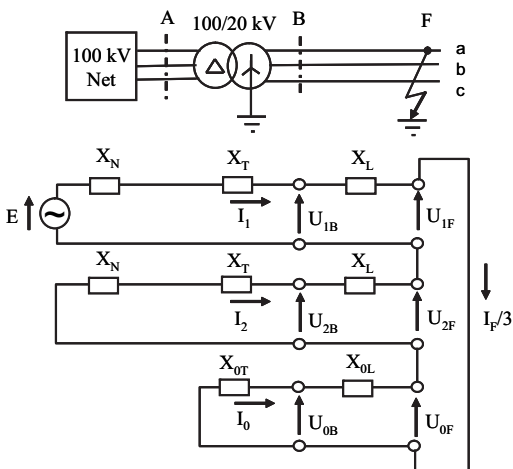


**Figure A.3-4**  
Circuit diagram of  
calculation example

*Searched:*

Currents and voltages at the beginning of the line in B.

*Solution:*

The equivalent symmetrical component circuit diagram is shown in figure A.3-4.

For simplicity, we calculate only with reactance values:

$$X_N = U_N^2 / S_N = 20^2 / 1000 = 0.4 \, \Omega$$

$$X_T = u_K \cdot U_N^2 / S_T = 0.1 \cdot 20^2 / 10 = 4.0 \, \Omega$$

$$X_{0T} = (X_{0T} / X_{1T}) \cdot X_T = 0.9 \cdot 2.0 = 3.6 \, \Omega$$

$$X_L = l \cdot x_L = 3 \cdot 0.4 = 1.2 \, \Omega$$

$$X_{0L} = l \cdot x_{0L} = 3 \cdot 1.2 = 3.6 \, \Omega$$

From the circuit diagram, we get for the sequence currents:

$$\begin{aligned} I_1 = I_2 = I_0 = I_{F/3} &= \frac{\underline{E}}{2 \cdot jX_1 + jX_0} = \frac{\underline{E}_n / \sqrt{3}}{2 \cdot (jX_N + jX_T + jX_L) + jX_{0T} + jX_{0L}} \\ &= \frac{20 / \sqrt{3}}{2 \cdot (j0.4 + j4.0 + j1.2) + j3.6 + j3.6} = -j0.628 \, \text{kA} \end{aligned}$$

The sequence voltages at B are:

$$\underline{U}_{1B} = \underline{E} - (jX_N + jX_T) \cdot I_1 = 20 / \sqrt{3} - (j0.4 + j4.0) \cdot (-j0.628) = 8.78 \, \text{kV}$$

$$\underline{U}_{2B} = -(jX_N + jX_T) \cdot I_2 = -(j0.4 + j4.0) \cdot (-j0.628) = -2.76 \, \text{kV}$$

$$\underline{U}_{0B} = -jX_{0T} \cdot I_0 = -j3.6 \cdot (-j0.628) = -2.26 \, \text{kV}$$

Using the synthesis equations (A.3-2), we can now calculate the phase currents and voltages at location B:

$$\underline{I}_{aB} = \underline{I}_1 + \underline{I}_2 + \underline{I}_0 = 3 \cdot (\underline{I}_F / 3) = 3 \cdot (-j0.628) = -j1.88 \, \text{kA}$$

$$\begin{aligned} \underline{I}_{bB} &= \underline{a}^2 \cdot \underline{I}_1 + \underline{a} \cdot \underline{I}_2 + \underline{I}_0 = (\underline{a}^2 + \underline{a} + 1) = (-0.5 - j\sqrt{3}/2) + \\ &\quad + (-0.5 + j\sqrt{3}/2) + 1 = 0 \, \text{kV} \end{aligned}$$

$$\begin{aligned} \underline{I}_{cB} &= \underline{a} \cdot \underline{I}_1 + \underline{a}^2 \cdot \underline{I}_2 + \underline{I}_0 = (\underline{a} + \underline{a}^2 + 1) = (-0.5 - j\sqrt{3}/2) + \\ &\quad + (-0.5 + j\sqrt{3}/2) + 1 = 0 \, \text{kV} \end{aligned}$$

$$\underline{U}_{aB} = \underline{U}_1 + \underline{U}_2 + \underline{U}_0 = 8.78 - 2.76 - 2.26 = 3.76 \, \text{kV}$$

$$\begin{aligned} \underline{U}_{bB} &= \underline{a}^2 \cdot \underline{U}_1 + \underline{a} \cdot \underline{U}_2 + \underline{U}_0 = (-0.5 - j\sqrt{3}/2) \cdot 8.78 + \\ &\quad + (-0.5 + j\sqrt{3}/2) \cdot (-2.76) - 2.26 = -5.27 - j10.0 \, \text{kV} \end{aligned}$$

$$\begin{aligned} \underline{U}_{cB} &= \underline{a} \cdot \underline{U}_1 + \underline{a}^2 \cdot \underline{U}_2 + \underline{U}_0 = (-0.5 + j\sqrt{3}/2) \cdot 10.0 + \\ &+ (-0.5 - j\sqrt{3}/2) \cdot (-1.6) - 1.3 = -5.27 + j10.0 \text{ kV} \end{aligned}$$

Figure A.3-5 shows the corresponding phasor diagrams.

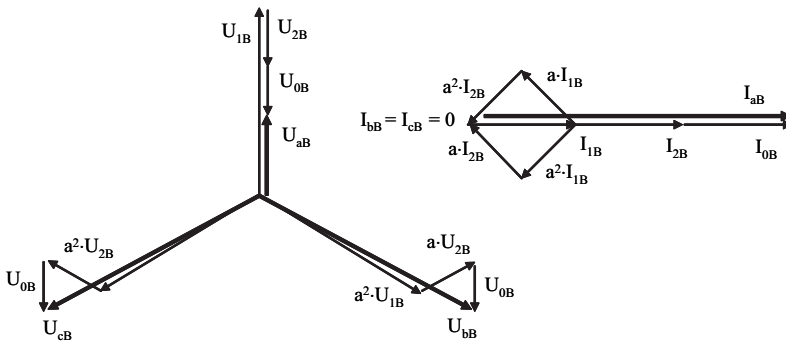


**Figure A.3-5** Phasor diagrams of calculated example

The graphical construction of the phase currents and voltages from the calculate sequence quantities is based on the above equations. The phase shifting operator  $\underline{a}$  is explained in the previous section A.2.

Further calculation examples are contained in the this book.

More complex relaying studies based on symmetrical components are discussed as appendices A.5 and A.6.

### A.3.2 Typical system component data

*Synchronous Generators:*

Type of machine		Turbo-generator	Salient-pole generator (with damper winding)	
			High speed 2p < 16	Low speed 2p > 16
Subtransient reactance	$X_d''$ (%)	9 to 32	14 to 32	15 - 25
Transient reactance	$X_d'$ (%)	14 to 45	20 to 32	22 to 36
Synchronous reactance	$X_d$ (%)	120 to 300	80 to 140	75 to 125
Neg. sequence reactance	$X_2$ (%)	9 to 32	14 to 25	15 to 27
Zero-sequence reactance	$X_0$ (%)	2 to 20	3 to 20	3 to 22
Resistance	$R_G$	0.05 to 0.07 $X_d''$		

*Power transformers with Star-Delta (YNd) connection*

Core	3-limbed			5-limbed
$S_N$ MVA	2 to 5	6.3 to 40	50 to 350	330 to 1000
$u_K$ %	6 to 7	8 to 12	12 to 16	14 to 18
$u_R$ %	1.05 to 0.65	0.7 to 0.5	0.4 to 0.2	0.2 to 0.25
$X_0/X_1$	0.85 to 1.0	0.85 to 1.0	0.85 to 1.0	$\approx 1$
$R_0/R_1$	1.0 to 3.0	1.0 to 3.	1.0 to 3.0	1.0 to 1.1

*Power transformers with Star-Star connection or star-auto connection and delta tertiary winding*

In both cases the values are approximately the same as for the large star-Delta transformers.

*Power transformers with Star-Star connection without tertiary delta winding*

The positive sequence data are also valid for this type of transformer. Those of the zero-sequence system depend very much on the construction and the degree of saturation ( $3 < Z_0/Z_1 \leq 10$ ).

For estimates, we can assume  $X_0 \approx \infty$ .

*Transmission lines and cables*

Typical impedance values are given in table 3.4 of section 3.2.

The calculation of the line parameters based on the tower configuration is outlined in section A.4 of this appendix.

The zero-sequence impedance of cables depends very much on parallel conductors (rails and pipes, etc.) so that standard values normally cannot be used but the actual values have to be measured at the installed cable on site (see section A.4.4).

### A.3.3 Equivalent circuits and formulas for network reduction

*Parallel infeed with partly common path*

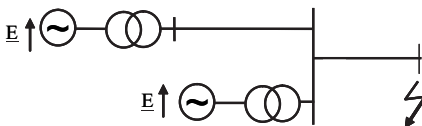


**Figure A.3-6** Single line diagram

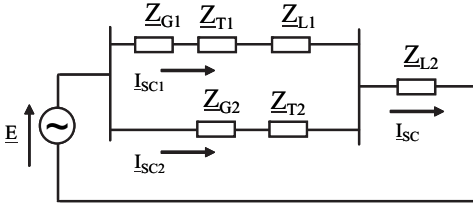


**Figure A.3-7**  
Equivalent circuit diagram

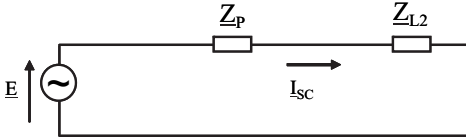


**Figure A.3-8**  
Reduced circuit diagram

$$\underline{Z}_1 = \underline{Z}_{G1} + \underline{Z}_{T1} + \underline{Z}_L \quad (\text{A.3-3}) \quad \underline{I}_{SC} = \frac{\underline{E}}{\underline{Z}_{SC}} \quad (\text{A.3-7})$$

$$\underline{Z}_2 = \underline{Z}_{G2} + \underline{Z}_{T2} \quad (\text{A.3-4}) \quad \underline{I}_{SC1} = \frac{\underline{Z}_P}{\underline{Z}_1} \quad (\text{A.3-8})$$

$$\underline{Z}_P = \frac{\underline{Z}_1 \cdot \underline{Z}_2}{\underline{Z}_1 + \underline{Z}_2} \quad (\text{A.3-5}) \quad \underline{I}_{SC2} = \frac{\underline{Z}_P}{\underline{Z}_2} \quad (\text{A.3-9})$$

$$\underline{Z}_{SC} = \underline{Z}_P + \underline{Z}_R \quad (\text{A.3-6})$$

### Delta-Star and Star-Delta transformation

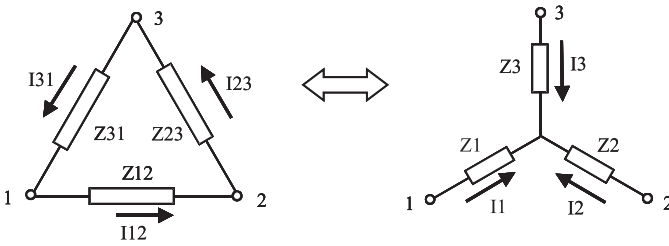


**Figure A.3-9** Delta-Star and Delta-Star transformation

### Delta-Star-transformation:

$$\underline{Z}_1 = \frac{\underline{Z}_{12} \cdot \underline{Z}_{31}}{\underline{Z}_{12} + \underline{Z}_{23} + \underline{Z}_{31}} \quad (\text{A.3-10}) \quad \underline{I}_1 = \underline{I}_{12} - \underline{I}_{31} \quad (\text{A.3-12})$$

$$\underline{Z}_2 = \frac{\underline{Z}_{23} \cdot \underline{Z}_{12}}{\underline{Z}_{12} + \underline{Z}_{23} + \underline{Z}_{31}} \quad (\text{A.3-11}) \quad \underline{I}_2 = \underline{I}_{23} - \underline{I}_{12} \quad (\text{A.3-13})$$

$$\underline{Z}_3 = \frac{\underline{Z}_{31} \cdot \underline{Z}_{23}}{\underline{Z}_{12} + \underline{Z}_{23} + \underline{Z}_{31}} \quad \underline{I}_3 = \underline{I}_{31} - \underline{I}_{23}$$

*Star-Delta transformation:*

$$\underline{Z}_{12} = \frac{\underline{Z}_1 \cdot \underline{Z}_2 + \underline{Z}_2 \cdot \underline{Z}_3 + \underline{Z}_3 \cdot \underline{Z}_1}{\underline{Z}_3} \quad (\text{A.3-14})$$

$$I_{12} = \frac{I_1 \cdot \underline{Z}_1 - I_2 \cdot \underline{Z}_2}{\underline{Z}_{12}} \quad (\text{A.3-17})$$

$$\underline{Z}_{23} = \frac{\underline{Z}_1 \cdot \underline{Z}_2 + \underline{Z}_2 \cdot \underline{Z}_3 + \underline{Z}_3 \cdot \underline{Z}_1}{\underline{Z}_1} \quad (\text{A.3-15})$$

$$I_{23} = \frac{I_2 \cdot \underline{Z}_2 - I_3 \cdot \underline{Z}_3}{\underline{Z}_{23}} \quad (\text{A.3-18})$$

$$\underline{Z}_{31} = \frac{\underline{Z}_1 \cdot \underline{Z}_2 + \underline{Z}_2 \cdot \underline{Z}_3 + \underline{Z}_3 \cdot \underline{Z}_1}{\underline{Z}_2} \quad (\text{A.3-16})$$

$$I_{31} = \frac{I_3 \cdot \underline{Z}_3 - I_1 \cdot \underline{Z}_1}{\underline{Z}_{31}} \quad (\text{A.3-19})$$

*Simplified zero-sequence equivalent circuits of parallel lines*

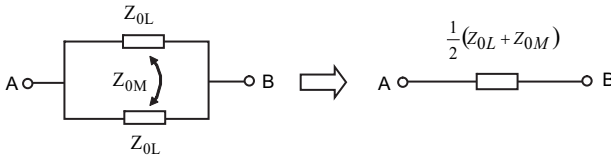


**Figure A.3-10** Parallel line connected at both ends

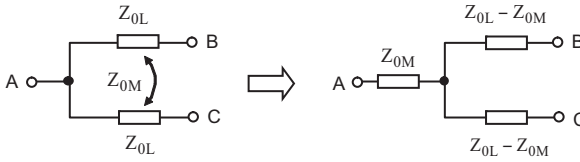


**Figure A.3-11** Parallel line connected at one end only

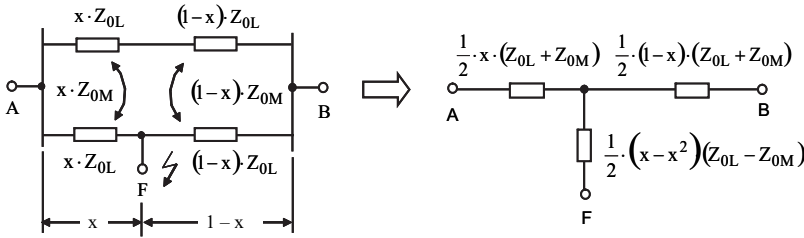


**Figure A.3-12** Faulty parallel line, zero-sequence equivalent circuit

### A.3.4 Equivalent circuits of transformers

The following equivalent symmetrical component circuits allow to include transformers in the short-circuit calculation. Herewith the behavior of distance relays at transformers can be studied and it can in particular be checked how far distance zones reach into transformers or through transformers into coupled other grids or down into connected distribution networks.

### Positive-sequence equivalent circuit of two-winding transformers

The positive sequence impedance of a transformer is equal to its short-circuit impedance which is determined by the leakage flux between the primary and secondary windings. (Figure A.3-13)

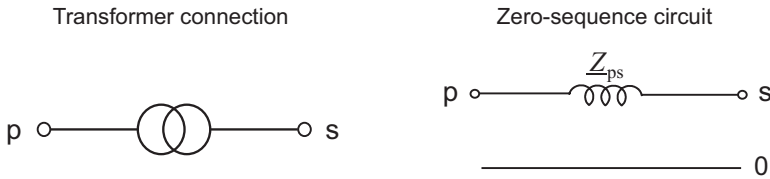


**Figure A.3-13** Equivalent positive sequence circuit for a two-winding transformer

The positive sequence impedance can be calculated from the measured three-phase short-circuit voltage and the power rating of the transformer in relation to the primary or secondary rated voltage:

$$\underline{Z}_{ps} = \underline{Z}_T = R_T + jX_T = I_{F/3} \quad (\text{A.3-20})$$

$$R_T = \frac{u_{TR}}{100} \cdot \frac{U_N^2}{S_T} \quad \text{and} \quad X_T = \frac{u_{TX}}{100} \cdot \frac{U_N^2}{S_T} \quad (\text{A.3-21}) \text{ and } (\text{A.3-22})$$

$S_T$	Transformer rated power in MVA
$U_N$	Transformer rated voltage in kV
$u_T$	Transformer short-circuit voltage
$u_{TX}$	Inductive short-circuit voltage in % (The approximation $u_X \approx u_T$ can be used if $u_T \geq 5\%$ )
$u_{TR}$	Ohmic short-circuit voltage in %

For normal short-circuit calculations (not considering the d.c. component) we can neglect the resistive part of the transformer impedances and calculate with reactances only ( $Z_{ps} = X_{ps}$ ).

### Equivalent zero- sequence circuits of two-winding transformers

The zero-sequence impedance of a three-phase transformer depends on the arrangement of the windings and the nature of the core (three-limb, shell core or single-phase cores). The zero-sequence impedance is only effective in the power system if at least one of the windings is star-connected with the star point earthed.

The equivalent zero-sequence circuits with typical impedance values are shown in figure A.3-14.

Additional impedances in the neutral to ground connection appear in the equivalent zero-sequence circuit with triple value ( $3 \cdot Z_E$ ).

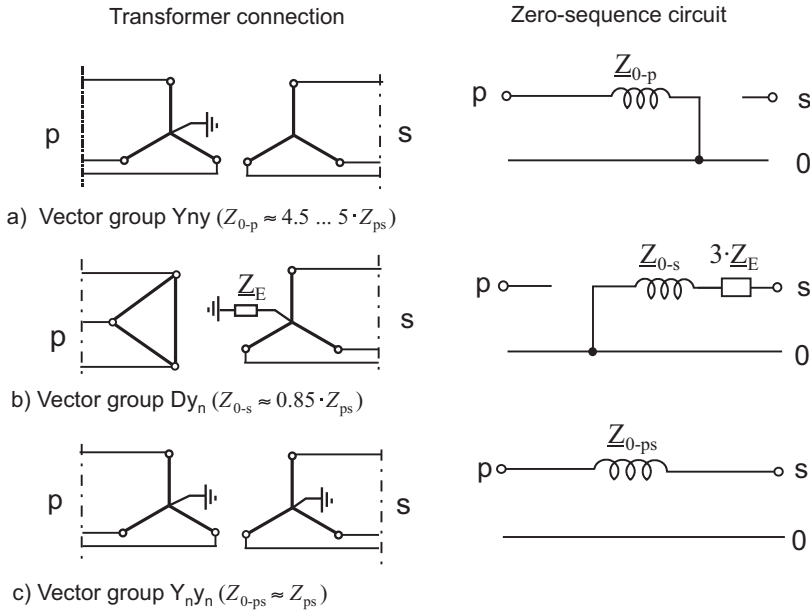


**Figure A.3-14** Equivalent zero- sequence circuits for two-winding transformers

*Equivalent positive- sequence circuits of three-winding- and auto-transformers*

The three- winding transformer is presented in the in the positive and negative sequence system by an equivalent circuit in which the three short-circuit impedances between each pair of windings are incorporated in an equivalent star network (figure A.3-15).

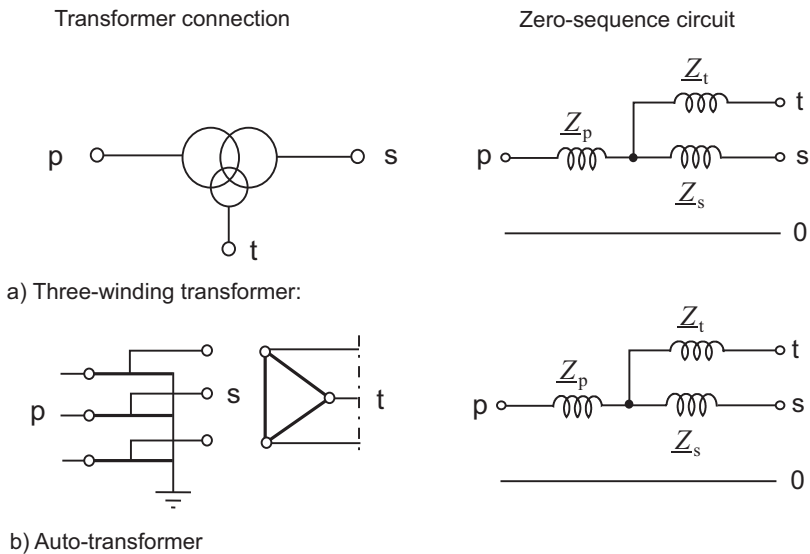


**Figure A.3-15** Equivalent positive- sequence circuits for three-winding- and auto-transformers



The impedances can be calculated from the short-circuit voltages and the associated power ratings referred to one of the three rated voltages of the transformer. Due to the negative term in the equations, one of the three impedances may be zero or even negative.

$$Z_p = \frac{1}{2} \cdot (Z_{ps} + Z_{tp} - Z_{st}) = \frac{1}{2} \cdot \left( \frac{u_{ps}}{S_{ps}} + \frac{u_{tp}}{S_{tp}} - \frac{u_{st}}{S_{st}} \right) \cdot \left( \frac{U_N^2}{100\%} \right) \quad (\text{A.3-23})$$

$$Z_s = \frac{1}{2} \cdot (Z_{st} + Z_{ps} - Z_{tp}) = \frac{1}{2} \cdot \left( \frac{u_{st}}{S_{st}} + \frac{u_{ps}}{S_{ps}} - \frac{u_{tp}}{S_{tp}} \right) \cdot \left( \frac{U_N^2}{100\%} \right) \quad (\text{A.3-24})$$

$$Z_t = \frac{1}{2} \cdot (Z_{tp} + Z_{st} - Z_{ps}) = \frac{1}{2} \cdot \left( \frac{u_{tp}}{S_{tp}} + \frac{u_{st}}{S_{st}} - \frac{u_{ps}}{S_{ps}} \right) \cdot \left( \frac{U_N^2}{100\%} \right) \quad (\text{A.3-25})$$

*Example: Calculation of the equivalent star impedances of a three-winding transformer:*

Given: Autotransformer 230/110/22kV with the following data:

	Primary-secondary	Secondary-tertiary	Tertiary-primary
Rated apparent power	125 MVA	25 MVA	25 MVA
Short-circuit voltage	11.93 %	15.3 %	11.77 %

Related to 230 kV we get:

$$Z_p = \frac{1}{2} \cdot \left( \frac{11.93}{125} + \frac{11.77}{25} - \frac{15.3}{25} \right) \cdot \left( \frac{230^2}{100} \right) = -12.1 \, \Omega$$

$$Z_s = \frac{1}{2} \cdot \left( \frac{15.3}{25} + \frac{11.93}{125} - \frac{11.77}{25} \right) \cdot \left( \frac{230^2}{100} \right) = 62.59 \, \Omega$$

$$Z_t = \frac{1}{2} \cdot \left( \frac{11.77}{25} + \frac{15.3}{25} - \frac{11.93}{125} \right) \cdot \left( \frac{230^2}{100} \right) = 261.2 \, \Omega$$

#### *Equivalent zero- sequence circuits and impedances of three-winding- and auto-transformers*

As with two-winding transformers, the equivalent zero-sequence circuits depend on the neutral earthing conditions (figure A.3-16).

Only a selection of typical connections is shown. For further information refer to [8, 10, 16].

The equivalent star-impedances ( $Z_{0-p}$ ,  $Z_{0-s}$  and  $Z_{0-t}$ ) must be calculated from the measured zero-sequence short-circuit and open-circuit impedances [8, 10].

As a rule the ratios  $Z_{0-p}/Z_p$ ,  $Z_{0-s}/Z_s$  and  $Z_{0-t}/Z_t$  are given. For large transformers it can be assumed as a rough approximation that the positive and zero-sequence impedances are equal ( $Z_{0-p} \approx Z_p$ ,  $Z_{0-s} \approx Z_s$  and  $Z_{0-t} \approx Z_t$ ).

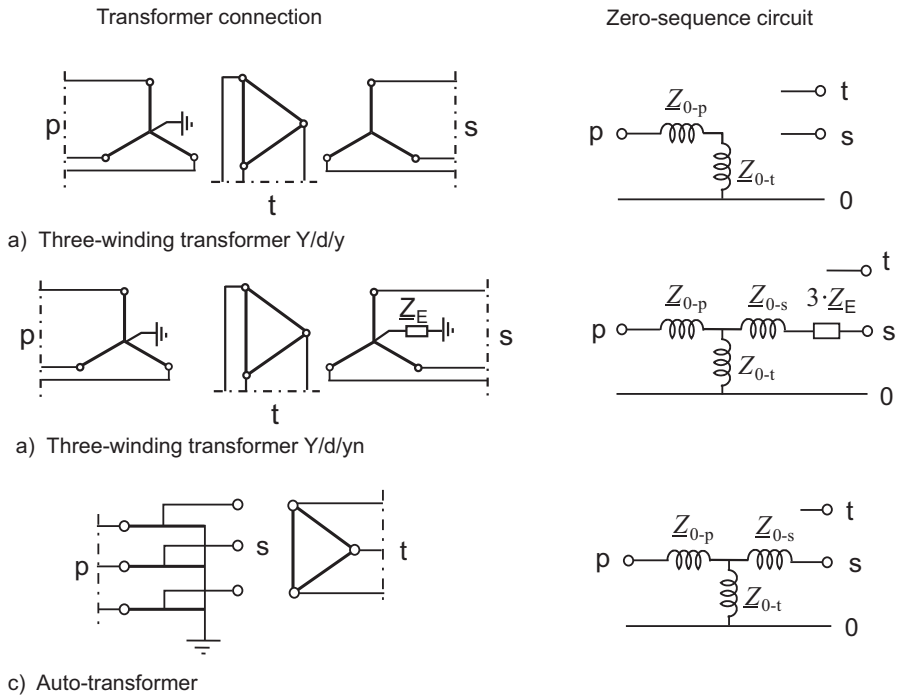


**Figure A.3-16** Equivalent zero- sequence circuits for three-winding- and auto-transformers

## A.4 Impedances of overhead lines and cables

### A.4.1 Single line (transposed)

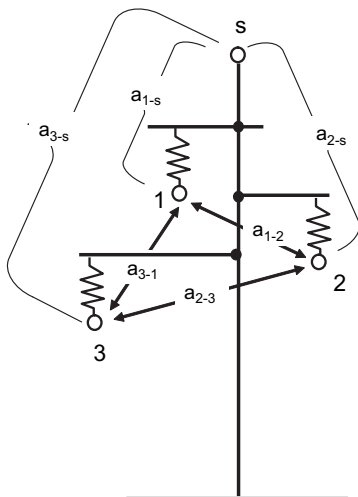


**Figure A.4-1**  
Single line, tower configuration

The mean geometric conductor spacings are:

$$A = \sqrt[3]{a_{1-2} \cdot a_{2-3} \cdot a_{3-1}} \quad \text{und} \quad A_s = \sqrt[3]{a_{1-s} \cdot a_{2-s} \cdot a_{3-s}}$$

Positive sequence impedance

$$\underline{Z}'_1 = R'_L + j\omega \cdot 10^{-4} \cdot \left( 2 \cdot \ln \frac{A}{r} + 0.5 \cdot \eta_1 \right) \quad \Omega/\text{km} \quad (\text{A.4-1})$$

Zero sequence impedance without ground wire:

$$\underline{Z}'_0 = R'_L + 3 \cdot R'_E + j\omega \cdot 10^{-4} \cdot \left( 6 \cdot \ln \frac{\delta}{\sqrt[3]{r \cdot A^2}} + 0.5 \cdot \mu_1 \right) \quad \Omega/\text{km} \quad (\text{A.4-2})$$

Zero sequence impedance with ground wire:

$$\underline{Z}'_{0E} = \underline{Z}'_0 - 3 \cdot \frac{\underline{Z}'_{1s}{}^2}{\underline{Z}'_s} \quad \Omega/\text{km} \quad (\text{A.4-3})$$

$$\text{with } \underline{Z}'_{1s} = R'_E + j\omega \cdot 10^{-4} \cdot 2 \cdot \ln \frac{\delta}{A_s} \quad \Omega/\text{km}$$

$$\text{and } \underline{Z}'_s = R'_s + R'_E + j\omega \cdot 10^{-4} \cdot \left( 2 \cdot \ln \frac{\delta}{A_s} + 0.5 \cdot \mu_1 \right) \quad \Omega/\text{km}$$

where:  $\delta$  Earth penetration depth:  $\delta = 1650 \cdot \sqrt{\rho/\omega}$  in m  
 $R'_E$  Earth resistivity  $R'_E = \pi/2 \cdot \omega \cdot 10^{-4}$  in /km  
 $r$  Specific earth resistance in  $\Omega\text{m}$  (100 for wet and 500 for dry soil)  
 $\mu_1$  Relative permeability (1 for Cu and Al)

#### A.4.2 Double circuit line (transposed)

The conductor allocation at the tower shows Figure A.4-2.

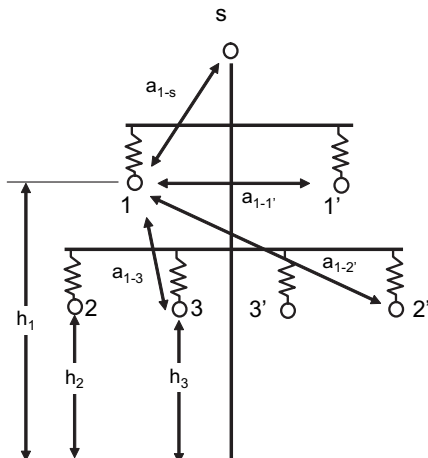


**Figure A.4-2**  
Double circuit line, tower configuration

The following geometric mean conductor spacings result:

$$A = \sqrt[3]{a_{1-2} \cdot a_{2-3} \cdot a_{3-1}}, \quad A' = \sqrt[3]{a_{1-2}' \cdot a_{2-3}' \cdot a_{3-1}'}, \quad \text{and} \quad A'' = \sqrt[3]{a_{1-1}' \cdot a_{2-2}' \cdot a_{3-3}'}$$

$$A_s = \sqrt[3]{a_{1-s} \cdot a_{2-s} \cdot a_{3-s}}, \quad A_L = \sqrt[3]{A'^2 \cdot A''} \quad \text{and} \quad H = \sqrt[3]{h_1 \cdot h_2 \cdot h_3}$$

Zero sequence impedance without ground wire:

$$\underline{Z}'_{00} = \underline{Z}'_0 + \underline{Z}'_{M0} \quad \Omega/\text{km} \quad (\text{A.4-4})$$

$$\underline{Z}'_{M0} = 3 \cdot R'_E + j\omega \cdot 10^{-4} \cdot 6 \cdot \ln \frac{\delta}{A_L} \quad \Omega/\text{km} \quad (\text{A.4-5})$$

Zero sequence impedance of the double circuit line with ground wire:

$$\underline{Z}'_{00E} = \underline{Z}'_{0E} + \underline{Z}'_{M0E} \quad \Omega/\text{km} \quad (\text{A.4-6})$$

Zero sequence coupling impedance of the double circuit line with ground wire:

$$\underline{Z}'_{M0E} = \underline{Z}'_{M0} - 3 \cdot s \cdot 6 \cdot \ln \frac{Z'^2_{1s}}{\underline{Z}'_s} \quad \Omega/\text{km} \quad (\text{A.4-7})$$

#### A.4.3 Bundle conductor

The bundle conductor is replaced by an equivalent conductor defined as follows:

1. The term  $0.5 \cdot \mu_1$  is to replace by  $\frac{0.5 \cdot \mu_1}{n}$
2. The conductor radius  $r$  is to replace by  $r_E = \sqrt[n]{r_s \cdot S}$ ,

where:  $r_s$  Radius of the single conductors  
 $S$  Product of the conductor spacings, one conductor against the others  
 $n$  Number of single conductors  
 Example:  $N = 4$ :  $S = s_1 \cdot s_2 \cdot s_3$  (see figure A.4-3)

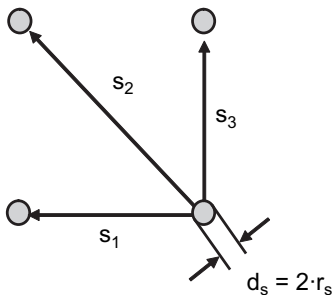


**Figure A.4-3**  
Bundle conductor, data

#### A.4.4 Cable impedances

In principle, the same formulas as for OH lines, also apply for cables. The reactances are however by far lower due to the small conductor spacings.

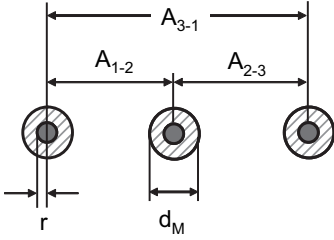


**Figure A.4-4**  
Cable in horizontal installation, dimensions

##### *Positive sequence impedance of cables*

As a rule, the manufacturer will deliver the data.

The following formulas can be used to estimate the impedance:

Mean geometric conductor spacing:

$$A = \sqrt[3]{A_{1-2} \cdot A_{2-3} \cdot A_{3-1}}$$

Positive sequence impedance:

$$\underline{Z}'_1 = R'_L + j\omega \cdot 10^{-4} \cdot \left( 2 \cdot \ln \frac{A}{r} + 0.5 \cdot \mu_1 \right) \Omega/\text{km}$$

*Example:*

20 kV plastic cable 240 mm<sup>2</sup>

Conductor: Cu;  $r = 9,3$  mm;  $d_M = 39,8$  mm;  $A = 110$  mm

$$A = \sqrt[3]{110 \cdot 110 \cdot 2 \cdot 110} = 138,6$$

$$X'_L = 314 \cdot 10^{-4} \cdot \left( 2 \cdot \ln \frac{138,6}{9,3} + 0.5 \right) = 0,185 [\Omega/\text{km}]$$

$$R'_L = \frac{10^3}{q[\text{mm}^2] \cdot \kappa \left[ \frac{\text{m}}{\Omega \cdot \text{mm}^2} \right]} = \frac{10^3}{240 \cdot 58} = 0,072 [\Omega/\text{km}]$$

**Note:** *Cables with conductive shield:*

When the conductive shield is earthed at both cable ends,  $X'_L$  is reduced and  $R'_L$  increased. The coupling impedance between conductor and shield must be considered. Exact values have to be procured from the manufacturer

### *Zero sequence impedance of cables*

A calculation with acceptable accuracy is not possible for the following reasons:

- $Z_0$  depends on the cable environment. Parallel conductors, such as shields of other cables, gas pipes and rails have a strong influence.
- In case of steel armoured cables,  $Z_0$  is also current dependent on the magnetising of steel bands and wires

The zero sequence impedance of cables must therefore be measured on site at the installed cable.

**Table A.4-1** Cable zero sequence impedances, mean values of urban areas<sup>1</sup>

10 kV	Belted cable, AL shield 3×120 mm <sup>2</sup> Cu 0.83 + j0.31 Ω/km	Belted cable, lead shield 3×120 mm <sup>2</sup> Cu 2.11 + j0.62 Ω/km
20 kV	Three phase cable, lead shield 3×150 mm <sup>2</sup> Cu 1.34 + j0.66 Ω/km	Plastic cable 3 conductors in triangle 3×1×150 mm <sup>2</sup> Cu 0.72 + j0.59 Ω/km
110 kV	Compression cable in a steel pipe 3×240 0,36 + j0,27 Ω/km	Single conductor oil cable 3 cables in triangular configuration 3×1×240 mm <sup>2</sup> Cu 0,54 + j0,34 Ω/km

<sup>1</sup> Siemens AG: Handbuch der Elektrotechnik, Verlag Girardet, Essen, 1971 (vergriffen)

## **A.5 Reach of back-up zones on parallel lines**

We refer to the system configuration of the calculation example in section 7.1, figure 7.1 and calculate the impedances that appear at relay D1 for faults along the line L3.

The symmetrical component analysis is used for this study.

### **A.5.1 Phase-to-phase faults**

Here we can restrict the calculation to the three-phase fault. The equivalent circuit diagram is shown in figure A.5-1.

The variable  $x$  designates the fault distance on line 3 as a percentage of the total line length.

#### *Calculation procedure:*

We try to simplify the equivalent circuit diagram and apply at first a delta star transformation to the double line L3/L4 (figure A.5-2).

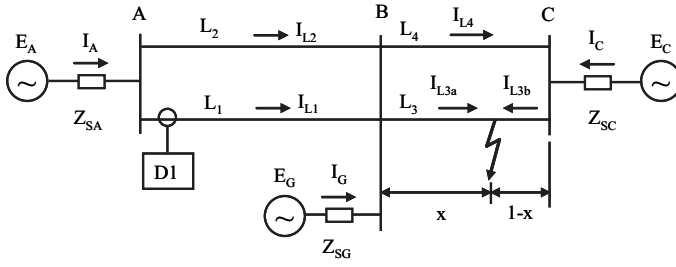


**Figure A.5-1** Three-phase fault equivalent circuit diagram

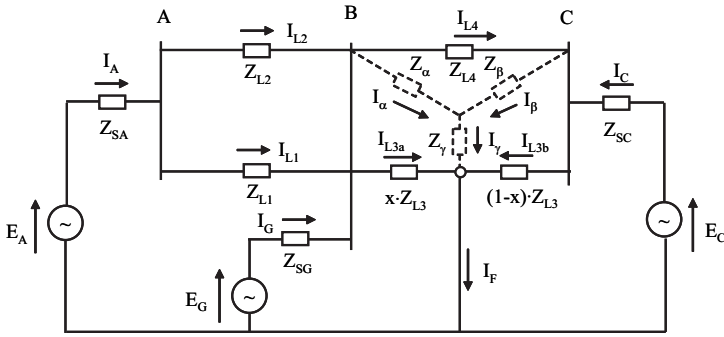


**Figure A.5-2** Network reduction using delta-star transformation

We assume that  $Z_{L3} = Z_{L4}$  (true parallel line) and get:

$$\underline{Z}_{\alpha} = \frac{\underline{Z}_{L4} \cdot x \cdot \underline{Z}_{L3}}{\underline{Z}_{L3} + \underline{Z}_{L4}} = \frac{x}{2} \cdot \underline{Z}_{L3} \quad (\text{A.5-1})$$

$$\underline{Z}_{\beta} = \frac{\underline{Z}_{L4} \cdot (1-x) \cdot \underline{Z}_{L3}}{\underline{Z}_{L3} + \underline{Z}_{L4}} = \frac{(1-x)}{2} \cdot \underline{Z}_{L3} \quad (\text{A.5-2})$$

$$\underline{Z}_{\gamma} = \frac{x \cdot \underline{Z}_{L3} \cdot (1-x) \cdot \underline{Z}_{L3}}{\underline{Z}_{L3} + \underline{Z}_{L4}} = \frac{x \cdot (1-x)}{2} \cdot \underline{Z}_{L3} \quad (\text{A.5-3})$$

We further combine infeed A and the series connected double circuit line with the intermediate infeed G to a common source (figure A.5-3).

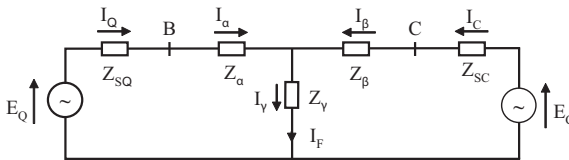


**Figure A.5-3** Final step of network reduction

The equivalent source voltage  $E_Q$  corresponds to the no-load voltage at B with the lines L3 and L4 disconnected:

$$\underline{E}_Q = \frac{\underline{E}_A \cdot \underline{Z}_{SG} + \underline{E}_G \cdot (\underline{Z}_{SA} + \underline{Z}_{PL12})}{\underline{Z}_{SA} + \underline{Z}_{PL12} + \underline{Z}_{SG}} \quad (\text{A.5-4})$$

The corresponding source impedance is derived from the terminal short-circuit condition at B, that means the equivalent source must deliver the same current as the two separate infeeds A and G.

$$\frac{\underline{E}_Q}{\underline{Z}_{SQ}} = \frac{\underline{E}_A}{\underline{Z}_{SA} + \underline{Z}_{PL12}} + \frac{\underline{E}_G}{\underline{Z}_{SG}} \quad (\text{A.5-5})$$

We insert  $E_Q$  from A.5-4, and get:

$$\underline{Z}_{SQ} = \frac{(\underline{Z}_{SA} + \underline{Z}_{PL12}) \cdot \underline{Z}_{SG}}{\underline{Z}_{SA} + \underline{Z}_{PL12} + \underline{Z}_{SG}}, \quad (\text{A.5-6})$$

where  $\underline{Z}_{PL12}$  is the positive sequence impedance of the parallel line circuit L1+L2:

$$\underline{Z}_{PL12} = \frac{\underline{Z}_{L1}}{2} = \frac{\underline{Z}_{L2}}{2} \quad (\text{A.5-7})$$

We consider that  $\underline{I}_\alpha = \underline{I}_Q$ ,  $\underline{I}_\beta = \underline{I}_C$  and  $\underline{I}_\gamma = \underline{I}_\alpha + \underline{I}_\beta$  and set up the following loop equations:

$$\begin{aligned} \underline{E}_Q &= \underline{I}_Q \cdot (\underline{Z}_{SQ} + \underline{Z}_\alpha) + (\underline{I}_Q + \underline{I}_C) \cdot \underline{Z}_\gamma \quad \text{and} \\ \underline{E}_C &= \underline{I}_C \cdot (\underline{Z}_{SC} + \underline{Z}_\beta) + (\underline{I}_Q + \underline{I}_C) \cdot \underline{Z}_\gamma \end{aligned} \quad (\text{A.5-8})$$

Solving this set of equations, we get:

$$\underline{I}_Q = \frac{\underline{Z}_\gamma \cdot \underline{E}_C - (\underline{Z}_{SC} + \underline{Z}_\beta + \underline{Z}_\gamma) \cdot \underline{E}_Q}{\underline{Z}_\gamma^2 - (\underline{Z}_{SQ} + \underline{Z}_\alpha + \underline{Z}_\gamma) \cdot (\underline{Z}_{SC} + \underline{Z}_\beta + \underline{Z}_\gamma)} \quad (\text{A.5-9})$$

Further we derive from the circuit diagrams (figure A.5-2 and A.5-3):

The voltage at B:

$$\underline{U}_B = \underline{E}_Q - \underline{I}_Q \cdot \underline{Z}_{SQ} \quad (\text{A.5-10})$$

The current at infeed A:

$$\underline{I}_A = \frac{\underline{E}_A - \underline{U}_B}{\underline{Z}_{SA} + \underline{Z}_{PL12}} = \frac{\underline{E}_A - \underline{E}_Q + \underline{I}_Q \cdot \underline{Z}_{SQ}}{\underline{Z}_{SA} + \underline{Z}_{PL12}} \quad (\text{A.5-11})$$

The current at the relay location in line 1:



$$I_{L1} = \frac{I_A}{2} \quad (\text{A.5-12})$$

The corresponding voltage at station A:

$$\underline{U}_A = \underline{E}_A - I_A \cdot \underline{Z}_{SA} \quad (\text{A.5-13})$$

We can now finally calculate the impedance measured by the distance relay D1:

$$\underline{Z}_{D1} = \frac{\underline{U}_A}{I_{L1}} \quad (\text{A.5-14})$$

The X-reach would be

$$X_{D1} = \text{Im} \{ \underline{Z}_{D1} \} \quad (\text{A.5-15})$$

The results of the calculation example are shown in figure A.7.3 of section 7.1.

### A.5.2 Phase-to-earth faults

The equivalent symmetrical component diagram for this kind of fault is shown in figure A.5-4. The fault resistance is indicated as  $R_F$ .

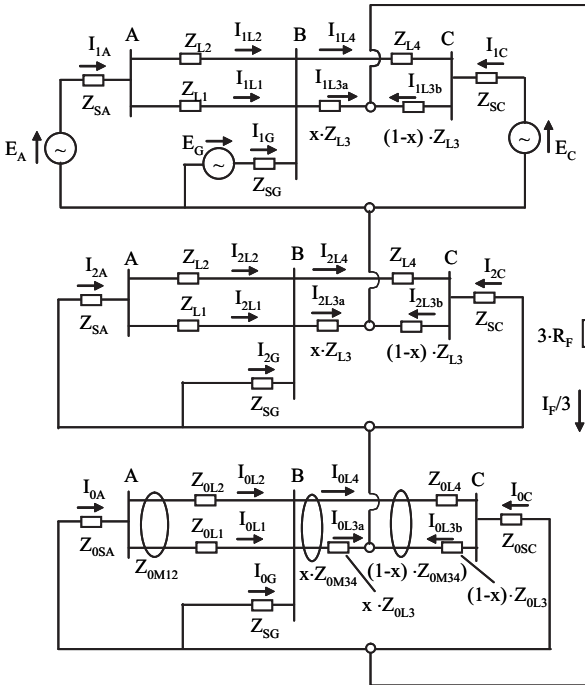


**Figure A.5-4** Equivalent circuit for phase-to-earth faults

The negative and zero-sequence circuits can be reduced to the equivalent impedances  $Z_2$  and  $Z_0$  (see below).

Herewith, we get the reduced circuit diagram shown in figure A.5-5.

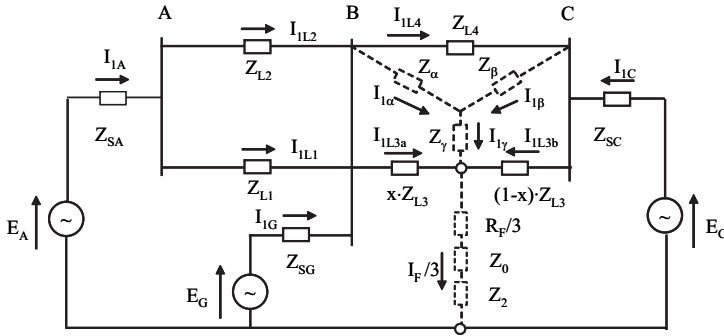


**Figure A.5-5** Reduced circuit diagram for phase-to-earth faults

As above, we apply the delta star transformation to the parallel line L3/L4 and combine the infeed  $E_A$  and the parallel line L1/L2 with the infeed  $E_G$  to an equivalent common infeed  $E_Q$ .

The reduced circuit diagram is shown in figure A.5-6.

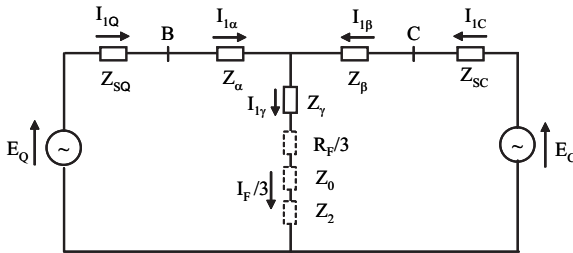


**Figure A.5-6** Final step of network reduction for phase-to-earth faults

The definitions of the impedances  $Z_\alpha$ ,  $Z_\beta$ ,  $Z_\gamma$  and the data of the common infeed  $E_Q$ ,  $Z_Q$  are given above with the formulas (A.5-1) to (A.5-6).

In the next step, we determine the equivalent impedances of the zero-sequence circuit  $Z_0$  and the negative sequence circuit  $Z_2$ .

The zero-sequence circuit diagram is shown in figure A.5-7.

We apply again the delta-star transformation to the parallel line L3/L4 and replace the parallel infeeds on the left side by the equivalent zero-sequence impedance  $Z_{0SQ}$ .

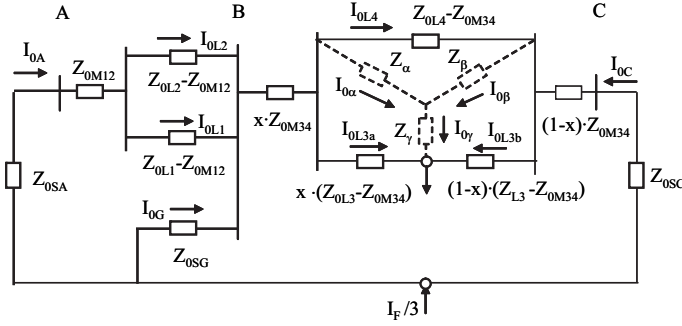


**Figure A.5-7** Equivalent zero-sequence circuit

In this way we get the reduced zero-sequence circuit diagram shown in figure A.5-8.

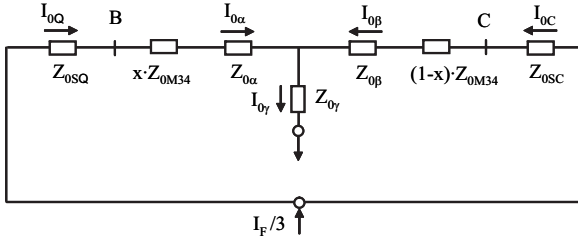


**Figure A.5-8** Reduced zero-sequence circuit

The impedances of the diagram are defined as follows:

$$\underline{Z}_{0SQ} = \frac{(\underline{Z}_{0SA} + \underline{Z}_{0PL12}) \cdot \underline{Z}_{0SG}}{\underline{Z}_{0SA} + \underline{Z}_{0PL12} + \underline{Z}_{0SG}} \quad (\text{A.5-16})$$

In the last equation,  $\underline{Z}_{0PL12}$  represents the zero-sequence impedance of the mutually coupled parallel lines L1 and L2:

$$\underline{Z}_{0PL12} = \frac{1}{2} \cdot (\underline{Z}_{0L1} + \underline{Z}_{0M12}) \quad (\text{A.5-17})$$

$$\underline{Z}_{0\alpha} = \frac{(\underline{Z}_{0L4} - \underline{Z}_{0M34}) \cdot x \cdot (\underline{Z}_{0L3} - \underline{Z}_{0M34})}{\underline{Z}_{0L3} + \underline{Z}_{0L4} - \underline{Z}_{0M34}} \quad (\text{A.5-18})$$

$$\underline{Z}_{0\beta} = \frac{(\underline{Z}_{0L4} - \underline{Z}_{0M34}) \cdot (1-x) \cdot (\underline{Z}_{0L3} - \underline{Z}_{0M34})}{\underline{Z}_{0L3} + \underline{Z}_{0L4} - \underline{Z}_{0M34}} \quad (\text{A.5-19})$$

$$\underline{Z}_{0\gamma} = \frac{x \cdot (\underline{Z}_{0L4} - \underline{Z}_{0M34}) \cdot (1-x) \cdot (\underline{Z}_{0L3} - \underline{Z}_{0M34})}{\underline{Z}_{0L3} + \underline{Z}_{0L4} - \underline{Z}_{0M34}} \quad (\text{A.5-20})$$

The impedance  $\underline{Z}_{0M34}$  designates the zero-sequence coupling impedance of the parallel lines L3 and L4.

With the assumption  $\underline{Z}_{0L3} = \underline{Z}_{0L4}$  (true parallel line), we get:

$$\underline{Z}_{0\alpha} = \frac{x}{2} \cdot (\underline{Z}_{0L3} - \underline{Z}_{0M34}) \quad (\text{A.5-21})$$

$$\underline{Z}_{0\beta} = \frac{(1-x)}{2} \cdot (\underline{Z}_{0L3} - \underline{Z}_{0M34}) \quad (\text{A.5-22})$$

$$\underline{Z}_{0\gamma} = \frac{x \cdot (1-x)}{2} \cdot (\underline{Z}_{0L3} - \underline{Z}_{0M34}) \quad (\text{A.5-23})$$

By corresponding series-parallel-series connection we get the equivalent impedance of the total zero-sequence circuit:

$$\underline{Z}_0 = \frac{(\underline{Z}_{0SQ} + x \cdot \underline{Z}_{0M34} + \underline{Z}_{0\alpha}) \cdot (\underline{Z}_{0SC} + (1-x) \cdot \underline{Z}_{0\beta})}{\underline{Z}_{0SQ} + \underline{Z}_{0SC} + \underline{Z}_{0M34} + \underline{Z}_{0\alpha} + \underline{Z}_{0\beta}} \quad (\text{A.5-24})$$

In the next step we have to find the equivalent impedance of the total negative-sequence circuit.

The circuit diagram is shown in figure A.5-9.

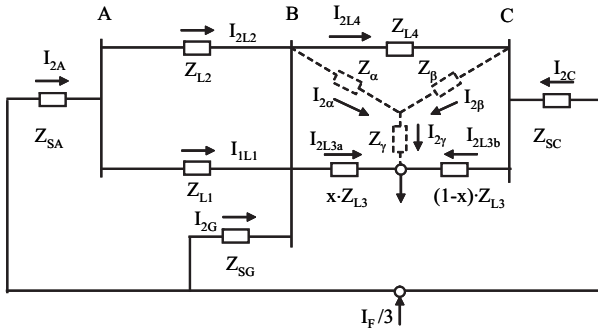


**Figure A.5-9** Equivalent zero-sequence circuit

The values of the star impedances  $Z_{\alpha}$ ,  $Z_{\beta}$  and  $Z_{\gamma}$  are the same as defined for the positive sequence system (A.5-1) to (A.5-3).

Also the impedance of the equivalent left side source is the same as in the positive sequence system (A.5-6).

The correspondingly reduced circuit of the negative sequence system is shown in figure A.5-10.

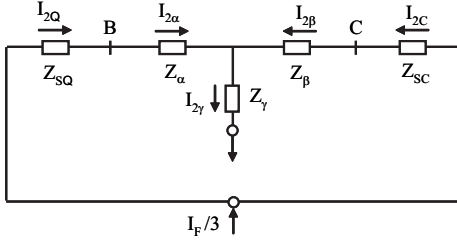


**Figure A.5-10**  
Reduced negative-sequence circuit

After series-parallel-series connection we get the equivalent impedance of the negative sequence circuit.

$$\underline{Z}_2 = \frac{(\underline{Z}_{SQ} + \underline{Z}_{\alpha}) \cdot (\underline{Z}_{SC} + \underline{Z}_{\beta})}{\underline{Z}_{SQ} + \underline{Z}_{SC} + \underline{Z}_{\alpha} + \underline{Z}_{\beta}} + \underline{Z}_{\gamma} \quad (\text{A.5-25})$$

For the calculation of the fault current  $I_F$ , we have to go back to figure A.5-6.

Considering that  $\underline{I}_{1\alpha} = \underline{I}_{1Q}$ ,  $\underline{I}_{1\beta} = \underline{I}_{1C}$  and  $\underline{I}_{1\gamma} = \underline{I}_{1\alpha} + \underline{I}_{1\beta}$ , we can set up the following loop equations:

$$\underline{E}_Q = \underline{I}_{1Q} \cdot (\underline{Z}_{SQ} + \underline{Z}_{\alpha}) + (\underline{I}_{1Q} + \underline{I}_{1C}) \cdot (\underline{Z}_{\gamma} + 3 \cdot R_F + \underline{Z}_0 + \underline{Z}_2) \quad \text{and} \quad (\text{A.5-26})$$

$$\underline{E}_C = \underline{I}_{1C} \cdot (\underline{Z}_S + \underline{Z}_{\beta}) + (\underline{I}_{1Q} + \underline{I}_{1C}) \cdot (\underline{Z}_{\gamma} + 3 \cdot R_F + \underline{Z}_0 + \underline{Z}_2) \quad (\text{A.5-27})$$

We introduce the following abbreviations:

$$\underline{Z}_A = \underline{Z}_{SQ} + \underline{Z}_{\alpha} + \underline{Z}_{\gamma} + 3 \cdot R_F + \underline{Z}_0 + \underline{Z}_2,$$

$$\underline{Z}_B = \underline{Z}_{SC} + \underline{Z}_{\beta} + \underline{Z}_{\gamma} + 3 \cdot R_F + \underline{Z}_0 + \underline{Z}_2 \quad \text{and}$$

$$\underline{Z}_C = \underline{Z}_{\gamma} + 3 \cdot R_F + \underline{Z}_0 + \underline{Z}_2$$

Solving the set of equations (A.5-26) and (A.5-27), we get:

$$\underline{I}_{1Q} = \frac{\underline{Z}_C \cdot \underline{E}_C - \underline{Z}_B \cdot \underline{E}_Q}{\underline{Z}_C^2 - \underline{Z}_A \cdot \underline{Z}_B} \quad (\text{A.5-28})$$

$$\underline{I}_{1C} = \frac{\underline{Z}_C \cdot \underline{E}_Q - \underline{Z}_A \cdot \underline{E}_C}{\underline{Z}_C^2 - \underline{Z}_A \cdot \underline{Z}_B} \quad (\text{A.5-29})$$

The current at the fault point is:

$$\underline{I}_F = 3 \cdot (\underline{I}_{1Q} + \underline{I}_{1C}) \quad (\text{A.5-30})$$

We can now split up the current  $I_F/3$  to the left and right parts of the symmetrical component circuits and then finally to the line L1 where the distance relay D1 is located.

Additionally we have to determine the component voltages at the relay location.

*Positive sequence circuit:*

We refer to figure A.5-6. The positive sequence current  $I_{1Q}$  is given by the above equation (A.5-28).

Further we get:

The positive sequence voltage at B:

$$\underline{U}_{1B} = \underline{E}_Q - I_{1Q} \cdot \underline{Z}_{SQ} \quad (\text{A.5-31})$$

The current at infeed A, which we can derive from the circuit diagram in figure A.5-5:

$$I_{1A} = \frac{\underline{E}_A - \underline{U}_{1B}}{\underline{Z}_{SA} + \underline{Z}_{PL12}} = \frac{\underline{E}_A - \underline{E}_Q + I_{1Q} \cdot \underline{Z}_{SQ}}{\underline{Z}_{SA} + \underline{Z}_{PL12}} \quad (\text{A.5-32})$$

The positive sequence current at the relay location in line 1:

$$I_{1L1} = I_{1A} / 2 \quad (\text{A.5-33})$$

The corresponding positive sequence voltage at station A:

$$\underline{U}_{1A} = \underline{E}_A - I_{1A} \cdot \underline{Z}_{SA} \quad (\text{A.5-34})$$

*Zero sequence circuit:*

We refer to figure A.5-8 and write the following equations for the current  $I_{0Q}$ :

$$I_{0Q} = \frac{\underline{Z}_{0\beta} + (1-x) \cdot \underline{Z}_{0M34} + \underline{Z}_{0SC}}{\underline{Z}_{0SQ} + \underline{Z}_{0SC} + \underline{Z}_{0M34} + \underline{Z}_{0\alpha} + \underline{Z}_{0\beta}} \cdot \frac{I_F}{3} \quad (\text{A.5-35})$$

The current at the infeed A can be derived from the circuit diagram in figure A.5-7:

$$I_{0A} = \frac{\underline{Z}_{0SG}}{\underline{Z}_{0SA} + \underline{Z}_{PL12} + \underline{Z}_{0SG}} \cdot I_{0Q} \quad (\text{A.5-36})$$

Further we get:

The zero-sequence current at the relay location in line 1:

$$I_{0L1} = \frac{I_{0A}}{2} \quad (\text{A.5-37})$$

The corresponding zero-sequence voltage at station A:

$$\underline{U}_{0A} = -I_{0A} \cdot \underline{Z}_{SA} \quad (\text{A.5-38})$$

*Negative sequence circuit:*

We refer to figure A.5-10 and derive the following equation for  $I_{2Q}$ :

$$I_{2Q} = \frac{\underline{Z}_\beta + \underline{Z}_{SC}}{\underline{Z}_{SQ} + \underline{Z}_{SC} + \underline{Z}_\alpha + \underline{Z}_\beta} \cdot \frac{I_F}{3} \quad (\text{A.5-39})$$

The current at the infeed A can be derived from the circuit diagram in figure A.5-9:

$$I_{2A} = \frac{\underline{Z}_{SG}}{\underline{Z}_{SA} + \underline{Z}_{PL12} + \underline{Z}_{SG}} \cdot I_{2Q} \quad (\text{A.5-40})$$

The negative-sequence current at the relay location in line 1 is:

$$I_{2L1} = \frac{I_{2A}}{2} \quad (\text{A.5-41})$$

The corresponding negative-sequence voltage at station A is:

$$\underline{U}_{2A} = -I_{2A} \cdot \underline{Z}_{SA} \quad (\text{A.5-42})$$

*Measured Impedance of relay D1:*

The phase L1 current of line L1 is equal to the sum of the symmetrical component currents in this location:

$$I_{Ph-L1} = I_{1L1} + I_{2L1} + I_{0L1} \quad (\text{A.5-43})$$

The corresponding earth current of line L1:

$$I_{E-L1} = -3 \cdot I_{0L1} \quad (\text{A.5-44})$$

The phase L1 to earth voltage of Line 1 at station A corresponds to the sum of its component voltages:

$$\underline{U}_{Ph-L1} = \underline{U}_{1A} + \underline{U}_{2A} + \underline{U}_{0A} \quad (\text{A.5-45})$$

Finally we get the impedance measured by relay D1:

$$\underline{Z}_{Ph-E} = \frac{\underline{U}_{Ph-L1}}{I_{Ph-L1} - k_0 \cdot I_{E-L1}} \quad (\text{A.5-46})$$

The corresponding measured reactance is:

$$\underline{X}_{Ph-E} = \text{Im} \{ \underline{Z}_{Ph-E} \} \quad (\text{A.5-47})$$

The shown impedance calculation is valid for the sequence of two parallel lines.

In case of other operation conditions (e. g. line 2 switched off or switched off and earthed at both sides), the procedure would have to be adapted accordingly.

The results of the calculation example are shown in figure 7.5 of section 7.1.

Note:

The calculation of the impedances could be made manually by following the above listed sequence of formulas. This however is cumbersome as we would have to use the complex number calculation. Normally one would implement the calculation procedure in a computer program.

The author used the program Mathcad for this purpose. The figure A.5-11 shows as an example the plot of the impedance course for faults on line 3.

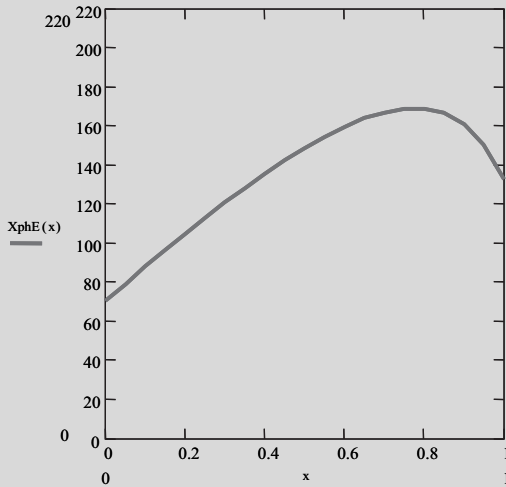


**Figure A.5-11** Impedance plot produced by the Mathcad program

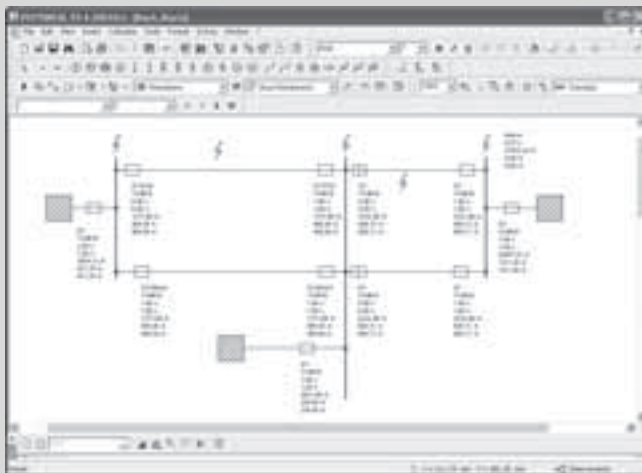


**Figure A.5-12** Use of Program SINICAL for protection studies



For professional purposes, it is recommended to use a state of the art load flow and short-circuit program with add-on functions for relay coordination.

One example is the program SINCAL offered by SIEMENS.

Besides automatic relay coordination and other useful functions for protection studies, it allows to indicate the measured relay impedances for selected fault locations in the network (figure A.5-12 and figure A.5-13).



**Figure A.5-13** SINCAL: Display of measured fault data

## A.6 Tilting of the quadrilateral top line to avoid overreach

The task is to find a suitable setting for the tilting angle of the 1<sup>st</sup> zone top line so that overreach is avoided at the power exporting side, up to the maximum line loading.

First, we have to reduce the network to a “two machine” configuration (figure A.6-1).

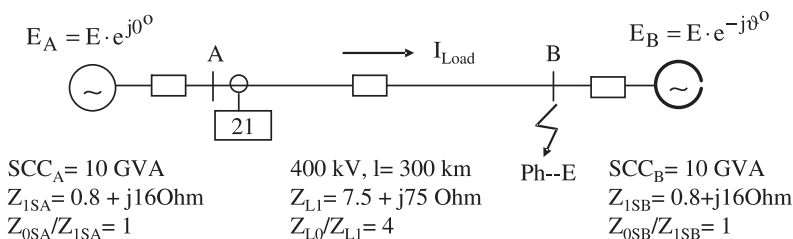


**Figure A.6-1** Transmission line with two side infeed

The needed system data are:

- *Positive and zero sequence line impedances*
- *Equivalent positive and zero sequence source impedances at both sides*  
(These values can be estimated from the three-phase and single phase short-circuit power of the infeeding networks, see paragraph 3.2.1)
- *Electromotive forces  $\underline{E}_A$  and  $\underline{E}_B$ .*  
For the magnitude we can assume  $E = 1.1 \cdot U_N / \sqrt{3}$  as with normal short-circuit calculations.  
 $\underline{E}_A$  can be taken as reference phasor ( $\vartheta = 0$ ). The angle of  $\underline{E}_B$  then corresponds to the transmission angle  $\vartheta$  of the system.
- *Maximum line loading in MW*  
From that we can estimate the transmission angle  $\vartheta$  if not directly available.

In figure A.6-1 a typical example for the technical data is given.

As a sufficiently accurate approximation, we neglect the line capacitances and calculate with lumped line impedances. This results in the voltage diagram of figure figure A.6-2.

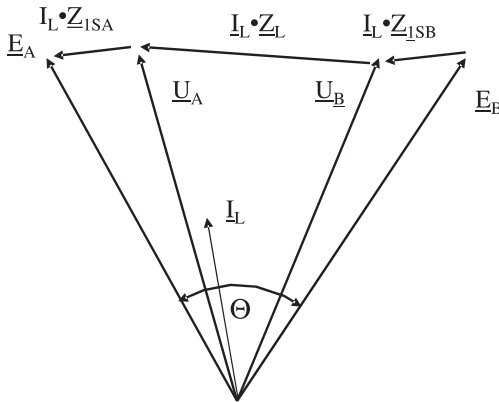


**Figure A.6-2**  
Voltage diagram of  
transmission system

We further assume a loss-free transmission and get the well known formula:

$$P_{\text{active}} = \frac{E_A \cdot E_B}{\Sigma X} \cdot \sin \Theta \quad (\text{A.6-1})$$

By rearranging it, we get:

$$\Theta = a \cdot \sin \left( \frac{P_{\text{active}} \cdot \Sigma X}{E_A \cdot E_B} \right) \quad (\text{A.6-2})$$

For  $P_{\text{active}} = 900 \text{ MW}$ ,  $\Sigma X = 107 \text{ Ohm}$  and  $E_A = E_B = 400 \times 1.1 \text{ kV}$ , we get  $\theta = 30^\circ$ .

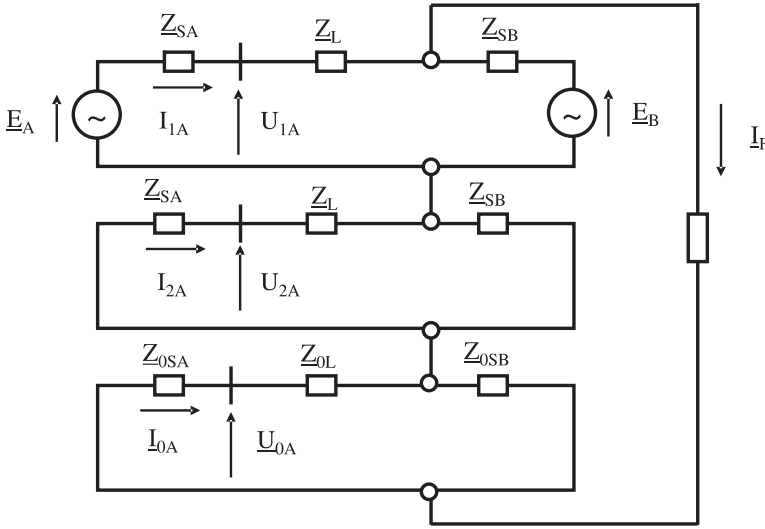


**Figure A.6-3** Symmetrical component equivalent circuit for the single phase to earth fault shown in figure A.6-1

In the next step, we must calculate the voltage and currents appearing in A at the relay location for a fault point at the remote busbar B.

We use the symmetrical component representation (figure A.6-3) und the superposition principle.

The pre-fault load current is:

$$I_{LA} = \frac{E_A - E_B}{Z_{SA} + Z_L + Z_{SB}} \quad (\text{A.6-3})$$

The pre-fault voltage at the fault point is:

$$U_{\text{preF}} = U_B = E_B + I_{LA} \cdot Z_{SB} \quad (\text{A.6-4})$$

The fault current  $I_F$  (1/3 short-circuit current) is driven by the pre-fault voltage at the fault point.

$$I_F = \frac{U_{\text{preF}}}{2 \cdot \frac{(Z_{SA} + Z_L) \cdot Z_{SB}}{Z_{SA} + Z_L + Z_{SB}} + \frac{(Z_{0SA} + Z_{0L}) \cdot Z_{0SB}}{Z_{0SA} + Z_{0L} + Z_{0SB}} + 3 \cdot R_F} \quad (\text{A.6-5})$$

The component currents in A are then:

$$I_{F1A} = \frac{Z_{SB}}{Z_{SA} + Z_L + Z_{SB}} \cdot I_F \quad (\text{A.6-6})$$

$$\underline{I}_{F2A} = \frac{\underline{Z}_{SB}}{\underline{Z}_{SA} + \underline{Z}_L + \underline{Z}_{SB}} \cdot \underline{I}_F \quad (\text{A.6-7})$$

$$\underline{I}_{F0A} = \frac{\underline{Z}_{SB}}{\underline{Z}_{0SA} + \underline{Z}_{0L} + \underline{Z}_{0SB}} \cdot \underline{I}_F \quad (\text{A.6-8})$$

Pure fault current at A:

$$\underline{I}_{FAa} = \underline{I}_{F1A} + \underline{I}_{F2A} + \underline{I}_{F0A} \quad (\text{A.6-9})$$

We get the total current in phase a by superposition of the pre-fault load current and the pure fault current:

$$\underline{I}_{Aa} = \underline{I}_{FAa} + \underline{I}_{LA} \quad (\text{A.6-10})$$

The earth (residual) current is three times zero-sequence current:

$$\underline{I}_{EA} = -3 \cdot \underline{I}_{F0A} \quad (\text{A.6-11})$$

The component voltages in A are:

$$\underline{U}_{1A} = \underline{E}_A - \underline{Z}_{SA} \cdot (\underline{I}_{F1A} + \underline{I}_{LA}) \quad (\text{A.6-12})$$

$$\underline{U}_{2A} = -\underline{Z}_{SA} \cdot \underline{I}_{F2A} \quad (\text{A.6-13})$$

$$\underline{U}_{0A} = -\underline{Z}_{0SA} \cdot \underline{I}_{F0A} \quad (\text{A.6-14})$$

The phase a to earth voltage in A is:

$$\underline{U}_{Aa} = \underline{U}_{1A} + \underline{U}_{2A} + \underline{U}_{0A} \quad (\text{A.6-15})$$

We can now calculate the measured phase to earth loop impedance:

The residual compensation factor is assumed to be set according to the line data:

$$\underline{k}_0 = \frac{\underline{Z}_{0L} - \underline{Z}_L}{3 \cdot \underline{Z}_L} \quad (\text{A.6-16})$$

$$\underline{Z}_{\text{pha-E}} = \frac{\underline{U}_{Aa}}{\underline{I}_{Aa} - \underline{k}_0 \cdot \underline{I}_{EA}} \quad (\text{A.6-17})$$

$$X_{\text{pha-E}} = \text{Im}\left(\frac{\underline{U}_{Aa}}{\underline{I}_{Aa} - \underline{k}_0 \cdot \underline{I}_{EA}}\right) \quad (\text{A.6-18})$$

$$R_{\text{pha-E}} = \text{Re}\left(\frac{\underline{U}_{Aa}}{\underline{I}_{Aa} - \underline{k}_0 \cdot \underline{I}_{EA}}\right) \quad (\text{A.6-19})$$

Note:

The formulae of traditional impedance measurement were used here for simplicity.

For the Fourier based methods (7SA relays) the applicable formulae as outlined in appendix A.1, may be used.

In the example at hand, the results however are the same.

The negative angle shift of the measured fault resistance is given by the following formula:

$$\alpha = a \tan \left( \frac{X_{\text{pha-E}} - X_L}{R_{\text{pha-E}} - R_L} \right) \quad (\text{A.6-20})$$

The angle shift depends on the magnitude of the fault resistance  $R_F$ .

The diagram in figure A.6-4 shows the values calculated for the example of figure A.6-1 with different transmission angles  $\vartheta$ .

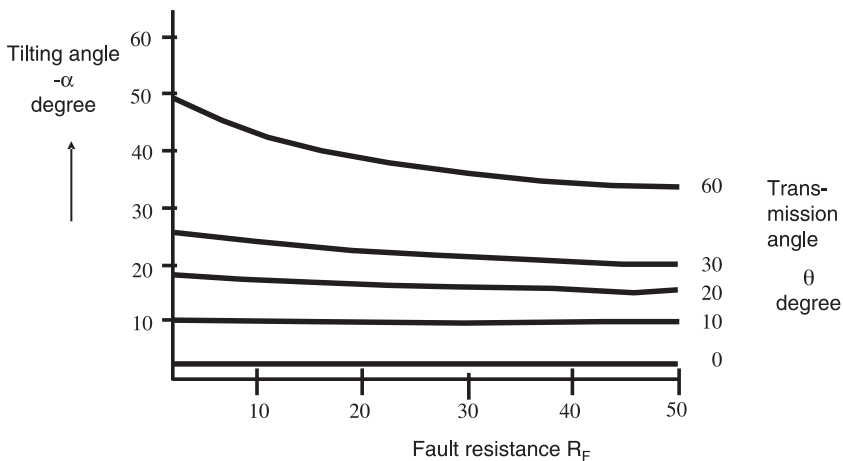


**Figure A.6-4**

Tilting angle for the system data of figure A.6-1 dependent on the fault resistance  $R_F$

For setting the tilt of the zone top line one should calculate the angle shift for the maximum fault resistance to be covered and at least two or three intermediate resistance values. It is then possible to adapt the tilt to the selected reach setting (85 to 90 %  $Z_L$ ) as shown in paragraph 6.3.1, figure 6.7.

---

# Index

1 1/2 circuit-breaker substations 292  
3rd zone 300

## A

Adaptive directional determination 119  
Adaptive measuring techniques 228  
Adaptive polarisation 120  
Angle dependant under-impedance starting 35  
Angle-impedance (OHM) characteristic 15  
Apparent fault resistance 136  
Apparent impedance 18, 36  
Arc compensation 137, 318  
Arc voltage 145  
ARC-cycle 246  
Arc-faults 145  
Arc-influence with double-sided in-feed 146  
Arc-resistance 145  
Automatic reclosure (ARC) 18

## B

Balance point 14  
Bauch's paradox 33, 280  
Blinder characteristic 15  
Blocking of the leading ph 144  
Blocking signal 60  
Blocking techniques 59  
Branched feeders 264

## C

Cable networks 322  
Calculation examples 333  
Capacitive voltage transformers (CVTs) 255  
Circle in the impedance plane 23  
Circular characteristic 41, 120  
Closed iron core CTs 239

Combined protection and control devices 219  
Commissioning 356  
Compensation degree 200  
Connection terminals 212  
Constant 91  
Contour diagram 18  
Conventional measuring technique 132  
Coupling impedance 156  
Cross polarisation 14, 110  
Cross polarised MHO 15  
Cross polarised MHO circle 26  
CT-classes 233  
CT-saturation 244  
Current inversion 206  
Current reversal guard 57  
Current reversal guard for POTT, logic diagram 58  
Current-transformer connection 221  
Current-transformer equivalent circuit 235  
Current-transformers 233  
Current-transformers with air gaps 241  
Cut-off distance 14

## D

Data window 76, 228  
Dead time 68, 70-71  
Dead zone 29  
Delayed auto-reclosure 69  
Delta quantities 206  
De-magnetising 236  
Device design 209  
Device structure 209  
Differential equation 99  
Digital communication networks 52  
Digital distance protection 13  
Digital signal transmission 232  
DIGSI 299

Direct underreaching transfer trip (DUTT) 53  
Directional characteristic 112, 174  
Directional check 358  
Directional comparison blocking 59  
Directional comparison unblocking 61  
Directional determination 108  
Directional fault discrimination 27  
Directional grading 82  
Distance measurement 23, 129  
Distance measuring of double earth-faults 271  
Distance protection 13  
Distance protection blocking mode 16  
Distance protection for transformers 167  
Distance protection in isolated or compensated systems 270  
Distance protection in permissive mode 16  
Distance protection using communication 51  
Distance protection with automatic reclosure 67  
Distance protection with blocking 59  
Distance protection with signalling channels 50  
Distance protection with unblocking 61  
Distance to fault computation 76  
Distance to fault locator 74  
Distance zones 13, 41, 43  
Distribution system 262  
Double (cross-country) earth fault 270  
Double circuit line 192, 293

- DUTT 53
- Dynamic stability 64
- E**
- Earth-current balance 164
- Earth-fault comparison protection 71
- Earth-fault with fault resistance 131
- Echo 56
- Echo-circuit 56
- Effect of intermediate in-feeds 85
- Effective arc-resistance 148
- End zone time 17
- Equal area 64
- F**
- Fault detection 86, 300
- Fault detection problems 267
- Fault detection setting 301
- Fault loop 18, 89, 93
- Fault record 224
- Fault resistance 19, 129
- Faulted loop voltage 18
- Ferraris principle 23
- Ferroresonance filter 260
- Ferroresonance suppression 255
- Full scheme 16
- Full scheme distance protection 50
- G**
- Grading chart 79
- Grading chart programs 89
- Grading for parallel feeders 83
- Grading in a branched radial system 83
- Grading of distance zones in meshed systems 87
- Grading of time delayed fault detector stage 89
- Grading times 17
- H**
- Healthy phase voltage 18
- High-resistance faults 284
- High-voltage overhead lines 287
- I**
- $I_E$ -release 172
- Impedance balance 23
- Impedance characteristic (relay) 14
- Impedance circle 24
- Impedance computation 98
- Impedance diagram 22
- Impedance fault detection 307
- Impedance ratio (SIR) 19
- Impedance relay 14
- Impedance starting 36
- Inductive voltage transformers 254
- Industrial networks 280
- Influence of in-feed from both sides on the fault resistance 135
- Influence of load flow 138
- Influence of load-transfer 138
- Influencing quantities 129
- Instrument transformer requirements 232
- Integrated functions 214
- Intelligent electronic devices (IEDs) 209
- Intermediate infeeds 150
- L**
- Line loading 108
- Line replica impedance 25
- Load angle 22
- Load blocking zone 137
- Load blocking zone (load cut out) 15
- Load compensated (delta) quantities 38
- Load compensation 140
- Load impedance 19, 22
- Load influence 126
- Load influence on a polarised MHO 141
- Load transfer 115
- Loadability of distance relays 15
- Long lines 286
- Loop impedance 94, 100
- Low impedance star-point earthing 277
- M**
- Maintenance strategy 362
- Measured value switching 48
- Measuring element 15
- Measuring error 160
- Measuring system 15
- MHO (Admittance) characteristic (relay) 14
- MHO-circle 120
- Modified or offset impedance-type characteristic 14
- MOV (metal oxide varistor) 208
- Multiple measuring system 16
- Multiple-shot ARC 268
- Mutual inductance 155
- N**
- NERC recommendations 303
- Non-switched 16, 41
- Non-switched distance protection 47
- Non-symmetry of the line 181
- Numerical distance protection 12
- Numerical distance protection (relay) 13
- O**
- Optimised starting characteristics 38
- Out of step protection 62
- Over-current starting 31
- Overreach 13
- Over-reaching stage 21
- Over-reaching zone 44
- P**
- Parallel line compensation 164, 166, 295
- Parallel lines 154
- Permissive intertrip 53
- Permissive overreaching transfer trip (POTT) 55
  - , with pilot wire inter-tripping 58
- Permissive underreaching transfer trip (PUTT)
  - , with starter (fault detector) 53
  - , with zone extension 54
- Phase comparator 27
- Phase preference 273
- Phase selection procedure 39
- Phase selective distance protection 70
- Phase selective tripping 71
- Phase selectors 37
- Phase-current compensation 192
- Phase-earth loops 96, 104
- Phase-phase loops 94, 101
- Phase-selective 30
- Phase-selectivity 304
- Phasor 19
- Ph-Ph-E short-circuit with fault resistances 143

- Pilot protection 16
- PLC 230
- Polarisation 14, 108
- Polarised MHO characteristic 14, 122
- POTT 55, 58
- Power swing 64
- Power swing blocking 62, 65, 328
- Power swing process 65
- Power swing tripping 62
- Power swing vector 66
- Preference circuit 272
- Protection communication system 51
- Protection concepts 287
- Protection data interface 213
- Protection settings 299
- Protection using telecommunication 16
- Protection with information transfer 285
- PUTT 53-54
- Q**
- Quadrature polarisation 14
- Quadrilateral 27
- Quadrilateral characteristic 41
- Quadrilateral characteristic (relay) 15
- R**
- R/X-setting 325
- Radial feeder 79
- Reach of the overcurrent starter 31
- Reactance characteristic (relay) 15
- Recommendation for the CVT lay-out in conjunction with numerical protection 261
- Rectified bridge comparator 24
- Reference voltage 114
- Relay (line) loadability 303
- Relay communications 212
- Relay operation 223
- Remanence 236, 246
- Reset ratio 17
- Reset time 17, 81
- Residual compensation 96
- Residual compensation factor 104, 122
- Resistance coverage 137
- Reverse grading 80
- Ring busbar 293
- R-setting 318
- S**
- Secondary impedance 21
- Security margin 79
- Security of the fault detection 302
- Selective ARC 269
- Self monitoring 361
- Self polarisation 108
- Self polarised MHO 14
- Self-polarised MHO circle 24
- Serial interfaces 212
- Series-compensated line 201, 296
- Series-compensation 200
- Set point 14
- Setting of the distance zones 313
- Short circuit angle 22
- Short-circuit impedance 18, 22, 92
- Short-circuit loop 18, 100
- Short-circuit power 91
- Short-circuit voltage 18
- Shortest line length 226
- SIGRA 224
- Single-phase ARC 69
- SIR 19
- Solid-state 13
- Source impedance 19, 91
- Star/delta transformers 170
- Starting (fault detection) 30
- Starting characteristic 36, 39
- Starting time 17
- Starting zone 43
- Static relay (protection) 13
- Static stability 63
- Steps 41
- Subsidence transient 260
- Substation automation 213
- Switched distance protection 16, 47
- Switching onto faults 284
- System analysis 298
- System/Scada interface 213
- T**
- Tapped line 153
- Teed feeders 346
- Teleprotection channel 16
- Teleprotection scheme 50
- Teleprotection, choice of technique 230
- Terminal connection 220
- Test with load 358
- Testing 356
- Thales-circle 121
- Three terminal line 346
- Three-measuring systems 49
- Three-phase ARC 67
- Three-terminal line 294
- Tilting of the zone 1 top line 314
- Time synchronisation 213
- Tower footing resistance 148
- TP current-transformer classes 238
- TPS 238
- TPX 239, 243
- TPY 239
- TPZ 239, 251
- Transient overreach 14
- Transient response classes 261
- Transmission angle 139
- Transmission networks 282
- Tripping logic 71
- Tripping time 17, 227
- Two-terminal fault locator 77
- Typical impedance values 93
- U**
- $U < \text{and } I >$  32
- Under-impedance 278
- Under-impedance starting 32
- Underreach 13
- Under-reaching stage 21
- Unfaulted 114
- V**
- Varistor 208
- V-connection 223
- Voltage controlled overcurrent 278
- Voltage inversion 204
- Voltage memory 118, 129
- Voltage transformers 253
- Voltage-transformer connection 222
- W**
- Weak infeed supplement 56
- Z**
- Zero-sequence infeed 152
- Zero-sequence system coupling 155
- Zero-volt faults 108
- Zone extension technique 72
- Zone limit 14
- Zone reach limit 87





Gerhard Ziegler

# Numerical Differential Protection

Principles and Applications

2<sup>nd</sup> updated and enlarged edition, April 2011,  
ca. 300 pages, ca. 200 illustrations, hardcover  
ISBN 978-3-89578-351-7, € 59.90

Differential protection is a fast and selective method of protection against short-circuits. It is applied in many variants for electrical machines, transformers, busbars, and electric lines.

Initially this book covers the theory and fundamentals of analog and digital differential protection. Current transformers are treated in detail including transient behaviour, impact on protection performance, and practical dimensioning. An extended chapter is dedicated to signal transmission for line protection in particular modern digital communication and GPS timing.

The emphasis is then placed on the different variants of differential protection and their practical application illustrated by concrete examples. This is completed by recommendations for commissioning, testing and maintenance. Finally the design and management of modern differential protection is explained by means of the latest Siemens SIPROTEC relay series.

A textbook and standard work in one, this book covers all topics, which have to be paid attention to for planning, designing, configuring and applying differential protection systems. The book is aimed at students and engineers who wish to familiarise themselves with the subject of differential power protection, as well as the experienced user, entering the area of digital differential protection. Furthermore it serves as a reference guide for solving application problems.

For this second edition all contents has been revised, extended and updated to the latest state of protective relaying.